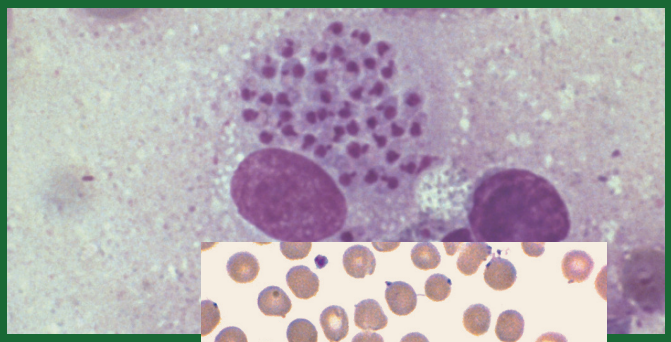
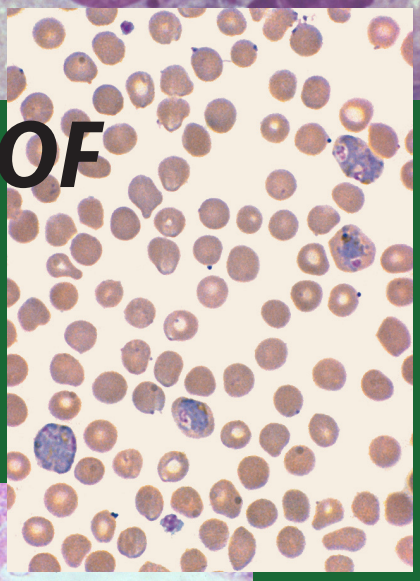
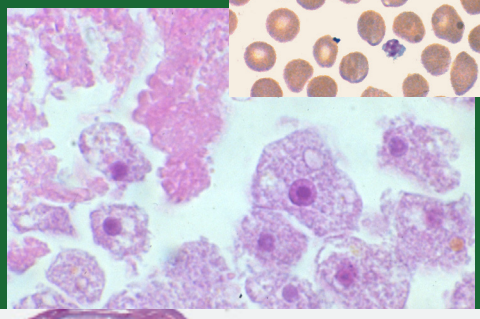
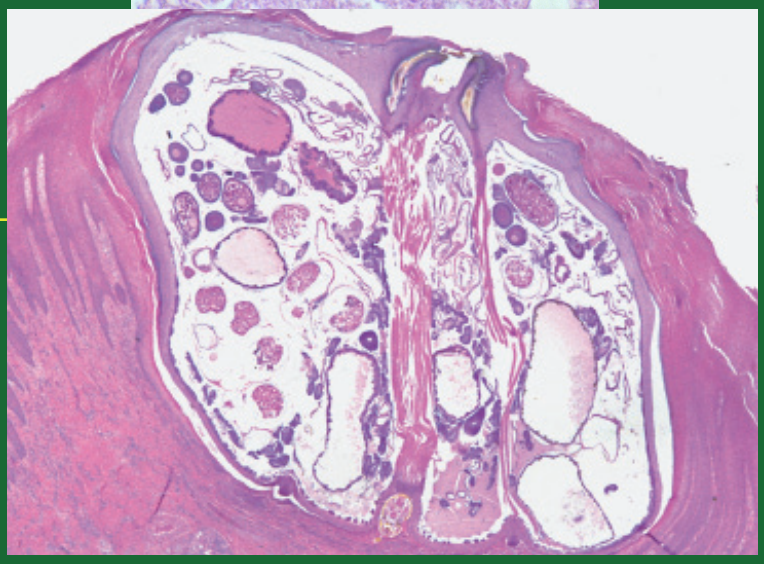








# Topics on the Pathology of Protozoan and Invasive Arthropod Diseases


Series Executive Producer:
Florabel G. Mullick, MD, D.Sc. SES

**Editor:**
**Wayne M. Meyers**
**Coeditors:**
**Adolfo Firpo**
**Douglas J. Wear**



*Armed Forces Institute of Pathology*
*Washington, DC*

# Report Documentation Page

*Form Approved*
*OMB No. 0704-0188*

Public reporting burden for the collection of information is estimated to average 1 hour per response, including the time for reviewing instructions, searching existing data sources, gathering and maintaining the data needed, and completing and reviewing the collection of information. Send comments regarding this burden estimate or any other aspect of this collection of information, including suggestions for reducing this burden, to Washington Headquarters Services, Directorate for Information Operations and Reports, 1215 Jefferson Davis Highway, Suite 1204, Arlington VA 22202-4302. Respondents should be aware that notwithstanding any other provision of law, no person shall be subject to a penalty for failing to comply with a collection of information if it does not display a currently valid OMB control number.

| 1. REPORT DATE | 2. REPORT TYPE | 3. DATES COVERED |
|---|---|---|
| **JUN 2011** | **N/A** | **-** |

| 4. TITLE AND SUBTITLE | 5a. CONTRACT NUMBER |
|---|---|
| **Topics on the Pathology of Protozoan and Invasive Arthropod Diseases** | 5b. GRANT NUMBER |
| | 5c. PROGRAM ELEMENT NUMBER |
| 6. AUTHOR(S) | 5d. PROJECT NUMBER |
| | 5e. TASK NUMBER |
| | 5f. WORK UNIT NUMBER |
| 7. PERFORMING ORGANIZATION NAME(S) AND ADDRESS(ES) **Armed Forces Institute of Pathology Washington DC** | 8. PERFORMING ORGANIZATION REPORT NUMBER |
| 9. SPONSORING/MONITORING AGENCY NAME(S) AND ADDRESS(ES) | 10. SPONSOR/MONITOR'S ACRONYM(S) |
| | 11. SPONSOR/MONITOR'S REPORT NUMBER(S) |

12. DISTRIBUTION/AVAILABILITY STATEMENT
**Approved for public release, distribution unlimited**

13. SUPPLEMENTARY NOTES
**The original document contains color images.**

14. ABSTRACT

15. SUBJECT TERMS

| 16. SECURITY CLASSIFICATION OF: | | | 17. LIMITATION OF ABSTRACT | 18. NUMBER OF PAGES | 19a. NAME OF RESPONSIBLE PERSON |
|---|---|---|---|---|---|
| a. REPORT | b. ABSTRACT | c. THIS PAGE | | | |
| **unclassified** | **unclassified** | **unclassified** | **SAR** | **286** | |

# NOTICE

The use of general descriptive names, registered names, trademarks, etc., in this publication does not imply, even in the absence of a specific statement, that such names are exempt from the relevant protective laws and regulations, and therefore free for general use.

Medicine is ever-changing in all of its aspects - new discoveries, interpretation, recommendations and standards are regularly offered. Thus, the editors, authors, and publishers of this e-book do not accept any legal liability for any claims resulting from errors in misuse of information or accuracy of any and all statements in this e-book. Readers are especially advised to confirm relevant information from other sources; for example recommended use and dosage of drugs in any specific situation.

The views of the authors and editors do not purport to reflect the position of the Department of the Army or the Department of Defense.

Approved for public release, distribution is unlimited.

Armed Forces Institute of Pathology
Washington DC

2011



# DEDICATION

The editors take great pleasure in dedicating this publication

to the memory of

Chapman H. Binford, M.D.

1900-1990

Who, seeing the need, founded
the Geographic Pathology Division of the
Armed Forces Institute of Pathology
in the early 1950s, and
served this unit for decades thereafter
as a volunteer.

The primary objective of this unit was the study of
infectious diseases with emphasis on
collaboration with pathologists in underserved
tropical countries. His selfless devotion to this goal
continues to inspire us and a multitude
of infectious disease specialists worldwide.

# FOREWORD



Rapid advances in technology, particularly over the last decade, has expanded American society and increasingly influenced global economy and society. Advances in travel, the end of the cold war, and the demolition of physical barriers like the Berlin wall and political barriers such as the opening of China, have created opportunities for more intensive and a freer exchange of goods and people. Rapid and increased human travel have also shortened the distance for biologic vectors to travel from their environment to ours, and once in our environment to spread with incredible speed, as we learned during the SARS epidemic. Increased risk is not limited to viral diseases like SARS but also to parasitic diseases which move across geographical frontiers within their human and animal hosts.

It is only fair and appropriate that advances in technology that have increased risk help solve a consequence, the appearance of a non-endemic parasitic agent, by becoming the means whereby the health practitioners make a prompt diagnosis and initiate appropriate treatment. Such is the purpose of this new electronic book, Topics on the Pathology of Protozoan and Invasive Arthropod Diseases. As the last formal educational activity of the Armed Forces Institute of Pathology, it provides a timely and significant contribution to the recognition and understanding of parasitic diseases in humans. The 19 chapters cover a spectrum of protozoan and invasive arthropod-related diseases of growing global importance. Of the 15 contributors to this text, 10 are staff or former staff or fellows at the AFIP. The materials draw upon the Institute's rich collection of over 3 million registered cases and the specimens, slides, and blocks that make up our tissue repository and archives.

For nearly a century and a half, the Armed Forces Institute of Pathology (AFIP) has upheld its reputation as the "people's institute" and fulfilled its mission to provide excellence in consultation, education, and research in pathology. Our goal, as always, is to provide students, clinicians, researchers, and educators with the knowledge they need to address emerging and re-emerging diseases worldwide and through their knowledge make an impact on world health and the global community.

I, as the 38th and final Director of the AFIP have committed myself and the resources of the Institute, in an effort of 21 years, not only to see this electronic book become reality, but also its forerunner, the Pathology of Infectious Diseases, Volume 1: Helminthiases. The Topics on the Pathology of Protozoan and Invasive Arthropod Diseases' electronic design is in response to the needs of local pathology societies worldwide. Practitioners in many countries cannot afford print media or broadband service. The PDF format will enable downloading, printing, and mailing by local organizations to point of need. I specifically want to acknowledge and thank Adolfo Firpo, M.D., who worked incessantly and diligently to see it come to fruition before official termination of all AFIP activities. I take great pleasure in presenting this, our latest and final effort, to provide in the public domain the most up-to-date discussions and almost 1000 illustrations of a selection of protozoan and invasive arthropod-related diseases.

Florabel G. Mullick, MD, ScD, FCAP
Senior Executive Service
The Director, AFIP

# CONTRIBUTING AUTHORS AND EDITORS


Izzat S. Ali CT (ASCP)
Formerly Cytotechnologist, AFIP
e-mail: izzat.s.ali@amedd.army.mil

Ellen M. Andersen, Ph.D, LCDR USN (Ret).
Formerly, Head of Parasitology,
Naval Medical Research Detachment
Lima, Peru
e-mail: wormstress@gmail.com

J Kevin Baird, Ph.D, CAPT USN (Ret),
Director, Eijkman-Oxford Clinical Research Unit,
Jalan Diponegoro No.69
Jakarta 10430 Indonesia
e-mail: kbaird@eocru.org
Centre for Tropical Medicine
Nuffield Department of Clinical Medicine
University of Oxford
Oxford, United Kingdom
e-mail:kevin.baird@ndm.ox.ac.uk

Ann Cali, A.A., B.S., Ph.D.
Professor, Dept. of Biological Sciences
Rutgers University
195 University Avenue, Boyden Hall
Newark, NJ 07102
e-mail: anncali@andromeda.rutgers.edu

Francis (Frank) M. Chiricosta, MD, COL, MC, USA
Department of Environmental & Infectious Disease Science,
Division of Infectious & Tropical Diseases Pathology, AFIP

Adolfo Firpo, MD, MPA, FCAP
Formerly, Staff Pathologist, AFIP
Formerly Registrar of AIDS Pathology,
American Registry of Pathology
Consultant, Office of The Director, AFIP
e-mail: af442@hotmail.com

George D. Imes, Jr, B.S., MS, DVM, COL (Ret), VC, USA
Formerly, Chairman, Department of
Veterinary Pathology
Diplomate, American College of Veterinary Pathologists

Mary K. Klassen-Fischer, MD
Formerly Chief, Division of Infectious and Tropical Diseases Pathology, AFIP
Current: Medical Director, Microbiology,
Inova Central Laboratory
2832 Juniper Street
Fairfax, VA 22031
e-mail: Mary.Klassen-Fischer@inova.org

Alan J. Magill, MD, FACP, FIDSA, COL (Ret), MC, USA
Associate Professor of Medicine and Preventive Medicine
Uniformed Services University of the Health Sciences
4301 Jones Bridge Rd, Bethesda, Maryland
e-mail: alan.magill@us.army.mil

Augusto Julio Martinez, M.D. (Deceased)
Professor of Pathology
University of Pittsburgh School of Medicine,
Neuropathologist
Pathology Department (Neuropathology),
Presbyterian University Hospital
Pittsburgh, PA 15213

Wayne M. Meyers, MD, Ph.D,
Red Cross Volunteer, AFIP;
Formerly Chief, Mycobacteriology Branch,
Division of Infectious and Tropical Diseases Pathology, AFIP

**Ronald C. Neafie, M.S.**
Formerly Chief, Parasitology Branch,
Division of Infectious and Tropical Diseases Pathology, AFIP

Peter M. Takvorian B.S., M.S., Ph.D.
Research Associate Professor
Rutgers University
Dept. of Biological Sciences,
195 University Avenue, Boyden Hall
Newark, NJ 07102
e-mail: petetak@andromeda.rutgers.edu

# CONTRIBUTING AUTHORS AND EDITORS

Govinda S. Visvesvara, Ph.D.
Centers for Disease Control and Prevention,
National Center for Emerging and Zoonotic Infectious Diseases,
Division of Foodborne, Waterborne & Environmental Diseases
Waterborne Disease Prevention Branch
Mailstop D-66
Roybal Campus, 1600 Clifton Road,
Atlanta, GA 30333
e-mail: gsv1@cdc.gov

Douglas J. Wear, M.S., MD, COL (Ret), MC, USA.
Distinguished Scientist, Acting Chair
Department of Environmental and Infectious Disease Science, AFIP.
e-mail: douglas.j.wear@us.army.mil

# PREFACE AND ACKNOWLEDGEMENTS

This e-book, Topics on the Pathology of Protozoan and Invasive Arthropod Diseases, was originally conceived as a companion volume of our earlier book, Pathology of Infectious Diseases, Helminthiases, published in the year 2000. During the production of the current volume, however, administrative circumstances were not conducive to its publication as a hardcover book. We are pleased nevertheless to be able to present this treatise on protozoan and invasive arthropod related diseases electronically. As such, a great advantage is that it will be available freely to a wider audience; not just to the so-called developed world, but to less affluent and more remote areas – in fact to anyone with access to the internet worldwide.

This publication comes at an appropriate time when there is ever increasing attention being given to the neglected tropical diseases of this world, and as world travel is increasing. Pathologists highly experienced in many of the diseases discussed here are often not locally available, increasing the likelihood that accurate diagnoses will be unduly delayed.

We thank, especially, all authors who have waited patiently to see their scholarly writings appear to the public. We are deeply indebted to the following individuals who have made it possible to bring this work to fruition:

- To all authors, particularly for the quality of your effort, and your willingness to update your chapters at least once, but sometimes more than once;
- To Bonnie L. Casey, for your creative guidance in getting the project under way and your superb editorial input, as well as your good humor;
- To Frances W. Card, for your excellent electronic management and layout design;
- To Ken Stringfellow and Douglas Landry, for you professional skills in photographic scanning, photoshop management, and artistic support;
- To our wives, Esther Meyers and Elisabeth Wear;

And finally, this work would not have gone forward without the active interest, support, and total commitment to this project as its executive producer, Florabel G. Mullick, M.D., S.E.S., the Director of the Armed Forces Institute of Pathology.

The Editors

## *Contents*


**1 Introduction to Pathogenic Protozoa**
Mary K. Klassen-Fischer and Ronald C. Neafie

**2 American Trypanosomiasis**
Ellen M. Andersen, Mary K. Klassen-Fischer and Ronald C. Neafie

**3 African Trypanosomiasis**
Mary K. Klassen-Fischer, Wayne M. Meyers, and Ronald C. Neafie

**4 Cutaneous Leishmaniasis**
Alan J. Magill, Wayne M. Meyers, Ronald C. Neafie, and Mary K. Klassen-Fischer

**5 Visceral Leishmaniasis**
Alan J. Magill, Wayne M. Meyers, Mary K. Klassen-Fischer, and Ronald C. Neafie

**6 Giardiasis**
Ellen M. Andersen, Mary K. Klassen-Fischer, and Ronald C. Neafie

**7 Trichomoniasis**
Mary K. Klassen-Fischer and Izzat S. Ali

**8 Amebiasis**
Mary K. Klassen-Fischer, Douglas J. Wear, and Ronald C. Neafie

**9 Amebic Meningoencephalitis and Keratitis**
Govinda S. Visvesvara, A. Julio Martinez, Mary K. Klassen-Fischer, and Ronald C. Neafie

**10 Malaria**
Mary K. Klassen-Fischer, Ronald C. Neafie, and Wayne M. Meyers

**11 Babesiosis**
George D. Imes, Ronald C. Neafie, and Francis M. Chiricosta

**12 Toxoplasmosis**
Ronald C. Neafie, Mary K. Klassen-Fischer, and Wayne M. Meyers

13 Crytosporidiosis, Isosporidiosis, Cyclosporiasis, Sarcocystosis
Mary K. Klassen-Fischer, Ronald C. Neafie, and Wayne M. Meyers

14 Microsporidiosis
Ann Cali, Ronald C. Neafie, and Peter M. Takvorian

15 Balantidiasis
Ronald C. Neafie, Ellen M. Andersen, and Mary K. Klassen-Ficher

16 Pentastomiasis
Wayne M. Meyers and Ronald C. Neafie

17 Tungiasis
J. Kevin Baird, Ronald C. Neafie, and Wayne M. Meyers

18 Myiasis
J. Kevin Baird, Ronald C. Neafie, Mary K. Klassen-Fischer, and Douglas J. Wear

19 Scabies and Demodicosis
J. Kevin Baird, Ellen M. Andersen, Ronald C. Neafie, and Wayne M. Meyers

## *Index of Tables*

**Table 1.1** Classification of parasitic protozoa. 4

**Table 1.2** Morphologic features of selected protozoan trophozoite forms. 6

**Table 1.3** Comparative morphologic features of selected protozoan cyst forms. 8

**Table 1.4** Classification of pathogenic arthropods and pentastomes. 11

**Table 1.5** Comparative morphologic features of selected arthropods in histologic sections. 12

**Table 3.1** African nations within geographic range of trypanosomiasis. 3

**Table 9.1** Morphologic features of *Acanthamoeba* sp that cause meningoencephalitis. 4

**Table 10.1** Morphologic features of *Plasmodium* sp in thin peripheral blood films. 3

**Table 10.2** Clinical features of malaria caused by *Plasmodium* sp infecting humans. 15

**Table 10.3** Temporal features of malaria caused by *Plasmodium* sp infecting humans. 15

**Table 14.1** Interfacial relationships of the microsporidia. 3

**Table 18.1** Dipteran flies whose larvae cause invasive myiasis in humans. 3







1

# Introduction

*Mary K. Klassen-Fischer and*

*Ronald C. Neafie*

## *Introduction*

## *Protozoa*

Protozoa are single-celled eukaryotic animals first discovered by Antonie van Leeuwenhoek as he viewed *Giardia* in a personal enteric specimen through his own invention (above photos). For a summary of the phylogeny of protozoa, see Table 1.1. A recent trend is to replace the term "protozoa" with "protista." For these topics we retain "protozoa" and reserve "protista" for a much larger group of single-celled organisms that include the algae, other single-celled photosynthetic organisms, and some of the water molds (slime molds).

Note that *Pneumocystis jiroveci* (previously called *Pneumocystis carinii*) is not included in this volume.[1] Although this organism had been classified as a protozoon until the late 1980s, it is now considered a fungus.

## *Specimen Preparation*

The diagnosis of most human parasitic infections relies upon the use of appropriate procedures for demonstrating the infecting organisms in feces, blood, urine, other body fluids and tissues. The most commonly applied procedures are briefly reviewed below. For an in-depth presentation of particular procedures, appropriate laboratory guides and atlases may be consulted. [2-4]

### Stool

Fecal specimens may be preserved in 10% formalin, merthiolate-iodine-formalin (MTF) solution, sodium acetate-acetic acid-formalin (SAF) solution, Schaudinn fluid, or polyvinyl alcohol (PVA) combined with Schaudinn fluid. Schaudinn fluid contains mercury, hence it is banned in many laboratories. The quality of the morphology of organisms stained with trichrome or iron hematoxylin suffers when the modified fixative, in which zinc or copper is substituted for mercury, is used. Specimens should be first grossly examined to exclude macroscopic parasites such as roundworms or tapeworm proglottids. Concentration methods may be applied to fresh or preserved fecal specimens to detect light infections. The two most common procedures are zinc sulfate flotation and formalin-ethyl acetate sedimentation.

Wet mount preparations for microscopic examination may be prepared in normal saline or stained with iodine, methylene blue, trichrome or iron hematoxylin. Special

stains may be used to demonstrate specific organisms, such as a modified acid-fast stain or modified safranin stain for *Cryptosporidium parvum* and *Cyclospora cayetanensis*. Ultraviolet fluorescence microscopy demonstrates the autofluorescence of coccidian cysts such as *C. cayetanensis* and *Isospora belli*. Calcofluor white may be used to brighten the fluorescence of coccidian oocysts. Kits for detecting antigens in feces are commercially available for several common parasites.

Important morphologic features of selected trophozoite forms are given in Table 1.2, and a summary of the comparative morphologic features of selected cyst forms is presented in Table 1.3.

### Blood

Identification of most parasites in blood requires the preparation of stained thin or thick blood smears; however, specialized blood concentration techniques and commercial kits are available for the immunodetection of parasites, their antigens, and antibodies. Direct examination of drops of fresh blood or EDTA-preserved blood is useful for the detection of living motile trypomastigotes of *Trypanosoma* species. Preparation of thin or thick blood smears from fresh or EDTA-preserved blood followed by Giemsa, Wright or Dif-Quik® staining is useful for morphologic identification of species of *Plasmodium*, *Babesia*, *Trypanosoma* and *Leishmania*. For more details on blood smear preparation, see Topic 10. Specialized procedures exist for specific protozoans, such as buffy coat concentration for *Trypanosoma* and *Leishmania* species and cytocentrifugation concentration for *Plasmodium* and *Leishmania* species.[5]

### Other fluids

Cytology specimens that may be examined for protozoa include urine, vaginal secretions, cerebrospinal fluid (CSF), aspirates of various tissues, and skin scrapings. Direct examination of the sediment of the first portion of voided urine may detect the motile flagellates of *Trichomonas vaginalis*, especially in male patients. Demonstration of *T. vaginalis* trophozoites in female patients is usually done by preparing wet mounts of vaginal swabs or scrapings. African trypanosomes and pathogenic free-living amebae (such as *Naegleria fowleri*) may be seen in CSF. Motile trypomastigotes of African trypanosomes can be found in aspirates from lymph nodes early in acute disease. Aspirates of bone marrow and spleen can demonstrate *Leishmania donovani*. Duodenal aspirates may be useful in demonstrating *Giardia lamblia*. Sigmoidoscopic material and aspirates of liver or lung abscesses may reveal trophozoites of *Entamoeba histolytica*. Cutaneous leishmaniasis can be diagnosed by finding amastigotes in stained smears prepared from scrapings of an ulcer.[6]

### Tissue

The examination of tissue specimens for protozoan infections may be accomplished in several ways. Fresh, unfixed biopsy material can be used to make touch preparations, to inoculate culture media, or infect experimental animals. Fixed tissue can be examined as stained histologic specimens.

## Arthopods & Pentastomes

Arthropods (phylum Arthropoda) are invertebrates with a chitinous exoskeleton, segmented body and jointed appendages. A summary of the phylogeny of arthropods is given in Table 1.4. This e-book covers diseases caused by arthropods that invade human tissue, including tungiasis (Topic 17), myiasis (Topic 18), and infestation with the non-toxic mites, *Sarcoptes* and *Demodex* species (Topic 19). Arthropods have many other significant relationships to human disease as vectors, or toxin-producers; however, those diseases are not addressed in this volume. The comparative morphologic characteristics of common parasitic arthropods is given in Table 1.5.

Pentastomes, or tongue worms, (Topic 16) are a class of parasitic animals that are similar to arthropods but that lack certain anatomic structures, such as circulatory and respiratory systems. The adults have oral hooks and the larvae have rudimentary legs; otherwise, they lack appendages.

## Pseudoparasites and Artifacts

It is important to be able to distinguish artifacts, contaminants, non-pathogenic protozoa and other microorganisms from pathogenic protozoa. Structures that may mimic pathogenic protozoa vary with the specimen type.

Stool specimens contain a variety of objects that can be mistaken for protozoa, including plant material, especially pollen. Stool may also contain nonpathogenic protozoa, such as *Blastocystis hominis, Retortamonas intestinalis, Chilomastix mesnili, Enteromonas hominis, Endolimax nana, Iodamoeba buetschli, Entamoeba polecki, Entamoeba coli, Entamoeba hartmani* and *Entamoeba gingivalis*. Spores of *Myxobolus plectoplites*, a fish pathogen, have been reported in fecal samples from patients who had recently eaten fish.[7]

In blood films, artifacts, such as platelets superimposed on erythrocytes, staining artifacts, and an array of contaminants, may be mistaken for malarial parasites. Knowledge of the appearance of the normal constituents of blood prevents such errors.

Fluids from non-sterile body sites, such as sputum, are prone to contain foreign objects. Fluids from sterile body sites generally do not contain foreign objects, except in

cases where the fluid has become contaminated during collection or processing.

In tissue sections, one challenge is to distinguish minute protozoa from host cell structures. A common difficulty is discerning nuclear debris from amastigotes of *Leishmania*. Another problem may lie in deciding whether or not pigment deposition is due to *Plasmodium falciparum* infection. Yeast forms of some fungi, such as *Basidiobolus ranarum*, can bear a striking resemblance to amoebae. The intracytoplasmic inclusions of cytomegalovirus may be mistaken for intracellular microorganisms if one does not observe the diagnostic cytoplasmic inclusions of this virus.

## Delusional parasitosis (Morgellons Disease)

Delusional parasitosis is a condition characterized by an isolated delusion by individuals that they are infested by parasites, especially ectoparasites or intestinal parasites. The patient, who usually has no other psychiatric conditions, often describes various symptoms of the skin or near body orifices. It is not uncommon that more than one family member has the same symptoms in a shared delusion (folie à deux). The typical patient collects specimens from skin, feces, clothing or environment. Parasitologists and pathologists are consulted to rule out the presence of actual parasites. The samples often consist of fibers, keratin, scabs, hairs, food particles or flies. Most patients see numerous health care providers and fiercely reject negative findings, and are reluctant to consult a psychiatrist. A dermatologist may be more successful at convincing the patient to begin appropriate psychotropic drugs or other therapy.[8,9]

## References

1. Stringer JR, Beard CB, Miller RF, Wakefiled AE. A new name (*Pneumocystis jiroveci*) for *Pneumocystis* from humans. *Emerg Infect Dis*. 2002;8:891-896

2. Centers for Disease Control and Prevention, Center for Global Health, *Laboratory Diagnosis of Parasites of Public Concern*. http://www.dpd.cdc.gov/dpdx/HTML/DiagnosticProcedures.htm Last modified 07/20/09.

3. Orihel TC, Ash LR. *Parasites: A Guide to Laboratory Procedures and Identification*. Chicago: ASCP Press; 1991.

4. Orihel TC, Ash, LR. *Atlas of Human Parasitology.* 4th ed. Chicago: ASCP Press; 1997.

5. Pethitory JC, Ardoin F, Ash LR, et al. Microscopic diagnosis of blood parasites following a cytoconcentration technique. *Am J Trop Med Hyg.* 1997;57:637-642.

6. Lesho EP, Neafie R, Wortmann G, Aronson N. Nonhealing skin lesinons in a sailor and journalist returning from Iraq. *Cleveland Clinic J Med*. 2005;72:93-94, 96, 98-99, 103-106.

7. Boreham RE, Hendrick S, O'Donoghue PJ, Stenzel DJ. Incidental finding of *Myxobolus* spores (protozoa: myxozoa) in stoll smaples from patients with gastronintestinal symptoms. *J Clin Microbiol*. 1998;36:3728-3730.

8. Koblenzer CS. The current management of delusional parasitosis and dermatitis artefacta. *Skin Therapy Lett*. 2010;15:1-3.

9. Morgellons disease: managing a mysterious skin condition. http://www.mayoclinic.com/health/morgellons-disease/sn00043. Last modified 02/13/2010.

Table 1.1 Classification of Parasitic Protozoa. [a]

**KINGDOM PROTOZOA**

Subkingdom 1 Archezoa

Phylum Metamonada

Class Trepomonadea (intestinal flagellates)

Order Diplomonadida *Giardia lamblia* [b] (Topic 6)

Order Enteromonadida *Enteromonas hominis*

Class Retortamonadea

Order Retortamonadida *Chilomastix mesnili, Retortamonas intestinalis*

Phylum Parabasala (flagellates)

Class Trichomonadea (intestinal and related flagellates)

Order Trichomonadida *Trichomonas vaginalis*
*T. tenax, Pentatrichomonas hominis* (Topic 7)
*Diantamoeba fragilis*

Subkingdom 2 Neozoa

Infrakingdom 1 Discicristata

Phylum Percolozoa (flagellates)

Class Heterolobosea (flagellated amoebae)

Order Schizoprenida *Naegleria fowleri* (Topic 9)

Phylum Euglenozoa (flagellates)

Class Kinetoplastidea (kinetoplastid flagellates)

Order Trypanosomatida *Leishmania donovani, L. tropica* (Topic 4 & Topic 5)*; L. infantum* (Topic 5)*; L. major, L. braziliensis, L. mexicana, L. aethiopica, L. amazonensis, L. garnhami, L. guyanensis* (Topic 4); *L. colombiensis, L. lainsoni, L. naiffi, L. panamensis, L. peruviana, L. pifanoi, L. shawi;*
*Trypanosoma cruzi, T. rangeli* (Topic 2);
*T. brucei gambiense, T. brucei rhodesiense* (Topic 3)

Table 1.1 Classification of Parasitic Protozoa. [a] (Continued)

Infrakingdom 2 Sarcomastigota

Phylum Amoebozoa (amoebae)

Subphylum Lobosa

Class Amoebaea (amoeba)

Order Acanthopodida *Acanthamoeba castellanii, A. culbertsoni, A. hatchetti, A. polyphaga, Balamuthia mandrillaris* (Topic 9)

Subphylum Conosa

Class Entamoebidea (intestinal amoebae)

Order Euamoebida *Entamoeba histolitica, E. coli, E. dispar,E. hartmanni, E. gingivalis, E. moshkoviskii, E. polecki, Endolimax nana, Iodoamoeba bütschlii (Topic 8); E. chattoni*

Infrakingdom 3 Alveolata

Phylum Sporozoa (sporozoans)

Class Coccidea

Order Eimeriida *Cryptosporidium parvum, C. hominis, C. sp, Cyclospora cayetanensis, Isospora belli, Sarcocystis hominis, S. suihominis (*Topic 13*); S. lindemanni; Toxoplasma gondii* (Topic 12)

Order Piroplasmida *Babesia microti, B. divergens, B. gibsoni, Babesia sp* (Topic 11)

Order Haemosporida *Plasmodium falciparum, P. malariae, P. ovale, P. vivax (*Topic 10)

Phylum Ciliophora (ciliates)

Class Litostomatea

Order Vestibulifera *Balantidium coli* (Topic 15)

[a] Adapted from: Cox, FEG. Taxonomy and classification of human parasites. *Manual of Clinical Microbiology,* 9th edition, Volume 2, section X Parasitology, chapter 132, editor in chief PR Murray, editors EJ Barron, JH Jorgensen, ML Landry, MA Pfaller, volume editor MA Pfaller, section editor LS Garcia. Washington DC, ASM Press, 2007. p 1991.

Table 1.2 Morphologic Features of Selected Protozoan Trophozoite Forms

| Trophozoites | Surface features | Shape | Size (μm) | Number of nuclei | Nuclear features | Other features |
|---|---|---|---|---|---|---|
| *Balantidium coli* | Cilia | Ovoid | 50-200 | 1 | Large macronucleus | Well-defined cytostome |
| *Chilomastix mesnili* | 4 flagella, 3 anterior, 1 posterior | Round to pear-shaped | 6-24 | 1 | Large or small karyosome, evenly or irregularly distributed peripheral chromatin | Cytostome bordered by fibrils |
| *Dientamoeba fragilis* | Pseudopodia | Amoeboid | 5-15 | 1 or 2 | Karyosome fragmented into 4-8 pieces, no peripheral chromatin | Finely granular vacuolated cytoplasm, may contain bacteria, no erythrocytes |
| *Endolimax nana* | Pseudopodia | Amoeboid | 6-12 | 1 | Large karyosome, no peripheral chromatin | Coarsely granular cytoplasm, vacuolated, may contain bacteria, no erythrocytes |
| *Entamoeba coli* | Pseudopodia | Amoeboid | 15-50 | 1 | Large non-compact eccentric karyosome, coarse irregular peripheral chromatin | Coarsely granular cytoplasm, vacuolated, may contain bacteria, yeast or other debris, no erythrocytes |
| *Entamoeba dispar* | Pseudopodia | Amoeboid | 20-60 | 1 | Small compact usually central karyosome, fine evenly distributed peripheral chromatin | Finely granular cytoplasm, rarely contain erythrocytes |
| *Entamoeba gingivalis* | Pseudopodia | Amoeboid | 20 | 1 | Small central karyosome, fine granular regular peripheral chromatin | Finely granular cytoplasm, may contain bacteria, no erythrocytes, not found in feces |
| *Entamoeba hartmanni* | Pseudopodia | Amoeboid | 5-12 | 1 | Small compact usually central karyosome, fine evenly distributed peripheral chromatin | Finely granular cytoplasm, may contain bacteria, no erythrocytes |
| *Entamoeba histolytica* | Pseudopodia | Amoeboid | 20-60 | 1 | Small compact, usually central karyosome, fine evenly distributed peripheral chromatin | Finely granular cytoplasm, may contain erythrocytes |

Table 1.2 Morphologic Features of Selected Protozoan Trophozoite Forms (Continued)

| Trophozoites | Surface features | Shape | Size (μm) | Number of nuclei | Nuclear features | Other features |
|---|---|---|---|---|---|---|
| *Entamoeba polecki* | Pseudopodia | Amoeboid | 10-25 | 1 | Minute central karyosome, fine coarse or regular, irregular peripheral chromatin | Cytoplasm may contain bacteria or yeast, no erythrocytes |
| *Enteromonas hominis* | 4 flagella, 3 anterior, 1 posterior | Round to oval | 4-10 | 1 | Large central karyosome | Flattened on one side |
| *Giardia lamblia* | 4 pairs of flagella | Pear-shaped | 10-20 | 2 | Small central karyosome, no peripheral chromatin | Bilaterally symmetrical, median bodies lying transversely, two axonemes, no undulating membrane, ventral sucking disc |
| *Iodamoeba bütschlii* | Pseudopodia | Amoeboid | 8-20 | 1 | Large karyosome, achromic granules between karyosome and nuclear membrane, no peripheral chromatin | Coarsely granular cytoplasm, vacuolated, may contain bacteria, yeast or other debris, no erythrocytes |
| *Pentatrichomonas hominis* | 5 flagella, 4 anterior, 1 posterior | Pear - shaped, oval | 8-20 | 1 | Karyosome usually central | Undulating membrane, axostyle, no median bodies |
| *Retortamonas intestinalis* | 2 flagella, 1 anterior, 1 posterior | Pear-shaped or oval | 4-10 | 1 | Small karyosome, fine peripheral chromatin | Prominent cytostome |

## Table 1.3 Comparative Morphologic Features of Selected Protozoan Cyst Forms

| Cysts | Type of cyst | Surface features | Shape | Size (μm) | Number of nuclei | Nuclear features | Other features |
|---|---|---|---|---|---|---|---|
| *Balantidium coli* | Not oocyst | Cilia within cyst wall | Round to oval | 50-70 | 2 | Large macro-nucleus, small micronucleus | Contractile vacuoles |
| *Chilomastix mesnili* | Not oocyst | No cilia | Round to lemon-shaped | 6-10 | 1 | Large, central karyosome | Hyaline knob or nipple-like protuberance, cytostome with fibrils |
| *Cryptospo-ridium* species | Sporulated oocyst | Modified acid-fast in stool only | Round | 4-6 | Not visible | – | 4 naked sporozoites |
| *Cyclospora cayetanensis* | Unsporu-lated oocyst | Modified acid-fast, double cyst wall | Round | 8-10 | Not visible | – | 2 sporocysts each with 2 sporozoites, greenish central mass, refractile globules |
| *Endolimax nana* | Not oocyst | No cilia | Round, oval or ellipsoidal | 5-10 | 4 | Large central karyosome, no peripheral chromatin | Small granules |
| *Entamoeba coli* | Not oocyst | No cilia | Round, oval, triangular | 15-30 | 8 (mature), 1-4 (immature) | Large non-compact usually eccentric karyosome, coarse irregular peripheral chromatin more uniform than in trophozoites | Chromatoid bodies with splintered ends, central glycogen mass |

Table 1.3 Comparative Morphologic Features of Selected Protozoan Cyst Forms (Continued)

| Cysts | Type of cyst | Surface features | Shape | Size (μm) | Number of nuclei | Nuclear features | Other features |
|---|---|---|---|---|---|---|---|
| *Entamoeba dispar* | Not oocyst | No cilia | Round | 10-20 | 4 (mature), 1-2 *(immature)* | Compact usually central small karyosome, fine evenly distributed peripheral chromatin, | Chromatoid bodies with rounded ends, central glycogen mass |
| *Entamoeba hartmanni* | Not oocyst | No cilia | Round | 5-10 | 4 (mature), 1-2 *(immature)* | Small compact usually central karyosome, fine evenly distributed peripheral chromatin | Grape-like chromatoid bodies with bluntly rounded ends |
| *Entamoeba histolytica* | Not oocyst | No cilia | Round | 10-20 | 4 (mature), 1-2 *(immature)* | Small compact usually central karyosome, fine evenly distributed peripheral chromatin | Chromatoid bodies with rounded ends, central glycogen mass |
| *Entamoeba polecki* | Not oocyst | No cilia | Round, oval | 10-15 | 1 | Small central or eccentric karyosome, fine regular peripheral chromatin | Many grape-like chromatoid bodies or dark-staining inclusion mass |
| *Enteromonas hominis* | Not oocyst | No cilia | Oval or ellipsoidal | 4-8 | 2-4 | 1 or 2 nuclei at each end, small central karyosome, no peripheral chromatin | Intracytoplasmic flagella |
| *Giardia lamblia* | Not oocyst | No cilia | Ovoid to ellipsoidal | 8-19 | 4 (mature) 2 (immature) | 4 nuclei at one end central karyosome, no peripheral chromatin | Axonemes, intracytoplasmic fibrils lying transversely |

Table 1.3 Comparative Morphologic Features of Selected Protozoan Cyst Forms (Continued)

| Cysts | Type of cyst | Surface features | Shape | Size (μm) | Number of nuclei | Nuclear features | Other features |
|---|---|---|---|---|---|---|---|
| *Iodamoeba buetschlii* | Not oocyst | No cilia | Oval, ellipsoidal, triangular | 5-20 | 1 | Large eccentric karysome, no peripheral chromatin | Large glycogen vacuole |
| *Isospora belli* | Unsporulated oocyst contains one immature sporont | Modified acid-*fast* | Elongated | 20-33 | Not visible | – | Mature oocyst contains 2 sporocysts each with 4 sporozoites |
| *E. bieneusi* Microsporidia | Spore | Modified Trichrome stain | Oval | 1-5 | Not visible | - | |
| *Retortamonas intestinalis* | Not oocyst | No cilia | Pear-shaped or oval | 4-9 | 1 | Slightly eccentric, small compact karyosome, variable peripheral chromatin | Fibril and cytostome near nucleus |
| *Sarcocystis* species | Sporulated oocyst | Thin-walled | Elongated | 15-19 | Not visible | – | 2 sporocysts each with 4 sporozoites, single sporozoites from ruptured oocysts |

TABLE 1.4 CLASSIFICATION OF PATHOGENIC ARTHROPODS AND PENTASTOMES

1. Phylum Arthropoda

   a. Subphylum mandibulata
      Class Insecta (fleas, flies, mosquitoes, bees, lice, bugs, beetles, caterpillars, fire ants)

   b. Subphylum Chelicerata
      Class Arachnida (spiders, scorpions, mites, ticks)

   c. Subphylum Onychophora (centipedes, millipedes)

2. Phylum Pentastomida

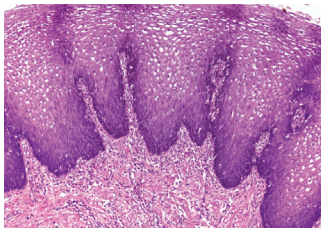
      Class Pentastomata

## Table 1.5 Comparative Morphologic Features of Selected Arthropods in Histologic Sections

| Organism | Anatomic location | Cuticle | | Hypodermis | Eggs (μm) | Legs |
|---|---|---|---|---|---|---|
| | | Thickness (μm) | Features | | | |
| Tick | Above keratin | >50 | Long, thin spurs, striated | Thin | No | Yes |
| *Sarcoptes scabiei* | Stratum corneum | <5 | Sharply pointed spines, striated | Very thin | Yes 150 | Yes |
| *Tunga penetrans* | Stratum corneum | >50 | No spines | Thick | Yes 600 | Yes |
| *Dermatobia hominis* | Dermis, Subcutis | >50 | Spines in rows | Thin | No | No |
| *Cordylobia anthropophagia* | Dermis, Subcutis | >25 | Spines smaller, sparse, irreguarly distributed | Thin | No | No |







2

# American Trypanosomiasis

***Ellen M. Andersen,***
***Mary K. Klassen-Fischer, and Ronald C. Neafie***

## *Introduction*

### Definition

American trypanosomiasis is a zoonosis caused by the flagellate protozoon *Trypanosoma cruzi* (previously *Schizotrypanum cruzi*). In humans, *T. cruzi* can infect parenchymal cells of many different organs, most commonly the heart, brain, esophagus, and colon.

### Synonyms

American trypanosomiasis is commonly known as Chagas' disease or South American trypanosomiasis.

### General Considerations

Carlos Chagas (Fig 2.1) first identified *T. cruzi* in the intestines of reduviid bugs (order Hemiptera, suborder Heteroptera, family Reduviidae, subfamily Triatominae), the arthropod vector, in Brazil in 1909.[1,2] Chagas used infected reduviid bugs to experimentally infect a monkey, from which he subsequently isolated blood-stage parasites. Chagas later identified the same parasites in the blood of a child with an unspecified illness, the only time a human parasite and its arthropod vector have been identified before the disease itself.

## *Epidemiology*

*Trypanosoma cruzi* is enzootic throughout Latin America. Chagas' disease causes significant morbidity and mortality in Argentina, Bolivia, Brazil, Ecuador, Honduras, Paraguay, Peru, and Venezuela. It occurs less frequently in Colombia, Costa Rica, El Salvador, Mexico and Panama. Some indigenous infections have been reported from the southwestern United States, Belize, Guyana, and Trinidad and Tobago.[3]



**Figure 2.1**
Carlos Chagas, Brazilian scientist who identified the cause and described the clinical features of Chagas' disease.

In South America, trypanosomiasis is the most significant endemic disease, particularly among children under 2 years of age. From 1980 to 1985, 16 to 18 million cases of Chagas' disease were reported in Latin America, with at least 120 million people at risk of infection.[4] Two-thirds of reported cases occur in the Southern Cone countries (Argentina, Bolivia, Brazil, Chile, Paraguay, southern Peru and Uruguay) a fact which prompted the development of the Southern Cone Initiative, one of the largest disease control programs ever established.[5] Several other programs concentrating on various geographical areas within Latin America have also been developed. Through the combined efforts of such programs, Chagas' disease transmission has been markedly reduced in endemic areas.[6,7]

*Trypanosoma rangeli*, a related and similarly distributed protozoan, is nonpathogenic. It does not invade and destroy cells and usually causes only a mild parasitemia.



**Figure 2.2**
Trypomastigote of *Trypanosoma cruzi* in peripheral blood of experimentally infected mouse. Note C-shaped configuration, free anterior flagellum, central nucleus, and large spherical kinetoplast at sharply pointed posterior end. Giemsa x1320

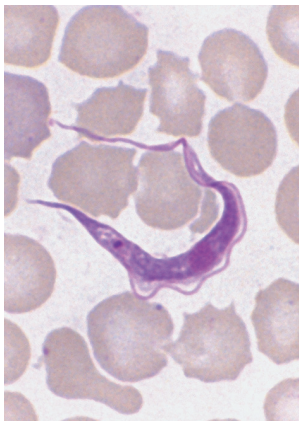


**Figure 2.3**
*Trypanosoma rangeli* trypomastigote in peripheral blood film. Note free anterior flagellum, central nucleus, and small spherical kinetoplast distal to posterior end. Giemsa x1320

## *Infectious Agent*

### Morphologic Description

Two morphologically distinct forms of *T. cruzi*, the trypomastigote and the amastigote, are found in infected humans and other mammalian hosts.

### Trypomastigotes

Trypomastigotes of *T. cruzi* circulate as free organisms in peripheral blood. They are slender, elongate, and 16 to 22 µm long, with a large central nucleus and a prominent round kinetoplast at the sharply pointed posterior end. An undulating membrane arises from the kinetoplast and runs along the cell membrane, terminating in a single free flagellum at the anterior end. On stained blood films, *T. cruzi* trypomastigotes are often C-shaped (Fig 2.2).

There are significant morphologic differences among the trypomastigotes of *Trypanosoma* sp. Trypomastigotes of *T. rangeli* are much longer (25 to 50 µm) than those of *T. cruzi*, have a broader, more prominent undulating membrane, and a much smaller round subterminal kinetoplast (Fig 2.3). *Trypanosoma rangeli* is transmitted to humans directly through the bite, and not through the feces, of a reduviid bug. Trypomastigotes of *T. cruzi* do not divide in peripheral blood in contrast to those of *T. rangeli* and the similar African trypanosomes that do.

### Amastigotes.

Amastigotes of *T. cruzi* are intracellular and primarily infect mesenchymal cells. In histologic sections, amastigotes are readily visible with hematoxylin and eosin stain (Fig 2.4). They are usually spherical and 2 to 4 µm in diameter, with a thin cell membrane, cytoplasm, a large round nucleus, and a rod-shaped kinetoplast (Fig 2.5). The kinetoplast is sometimes more prominent when stained with Brown-Hopps tissue gram stain (Fig 2.5a), Giemsa (Fig 2.5b), or Wilder's reticulum (Fig 2.5c). Amastigotes multiply by binary fission. Amastigotes of *T. cruzi* are slightly larger, but otherwise are morphologically indistinguishable from those of *Leishmania* sp. An amastigote stage has not been described for *T. rangeli*.

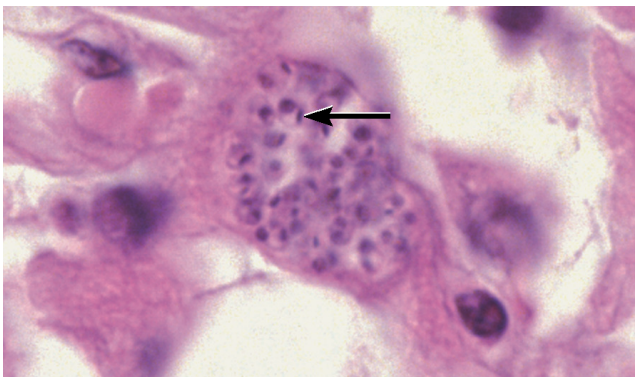


**Figure 2.4**
Cluster of readily observable *Trypanosoma cruzi* amastigotes in myocardial fiber. Note cell membrane, spherical nucleus, and rod-shaped kinetoplast (arrow). x1000

### Life Cycle and Transmission

The life cycle of *T. cruzi* includes a mammalian phase and an arthropod phase (Fig 2.6). Numerous domestic and wild mammals serve as reservoir hosts, including opossums (Fig 2.7), raccoons (Fig 2.8), armadillos, rats, canines, and livestock. Trypomastigotes circulating in the peripheral blood of infected mammals are ingested by a reduviid bug as it takes a blood meal. The now infected bug can remain infective for life serving as a reservoir of infection.

In the triatome midgut, trypomastigotes transform

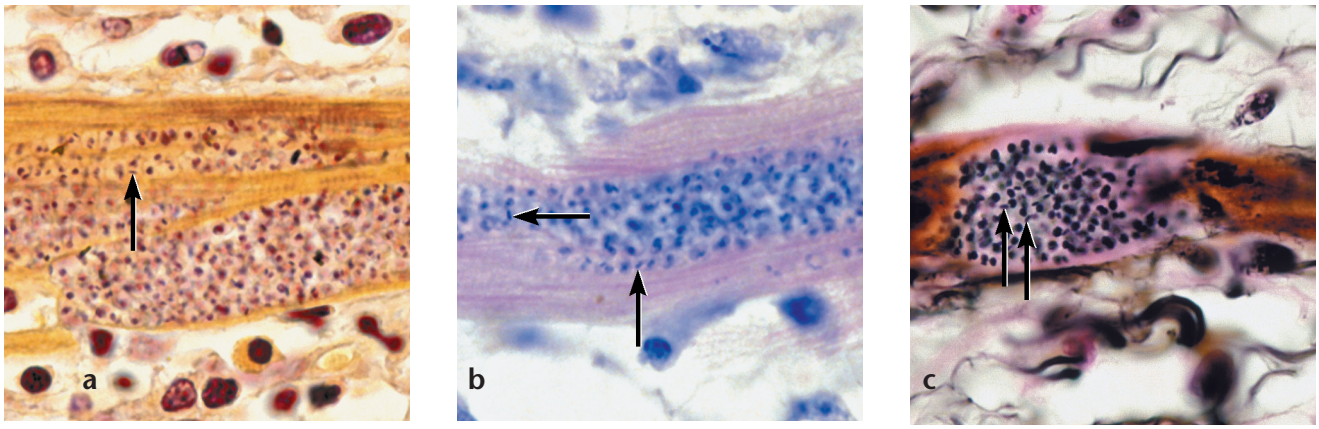



**Figure 2.5 a,b,c**
Amastigotes of *Trypanosoma cruzi* in myocardium in acute Chagas' disease. a. Note dark-staining rod-shaped kinetoplasts (arrows). B-H x375 b. Note dark-staining rod-shaped kinetoplasts (arrows). Giemsa x460 c. Note spherical nucleus and black-staining rod-shaped kinetoplasts (arrows). Wilder's reticulum x450

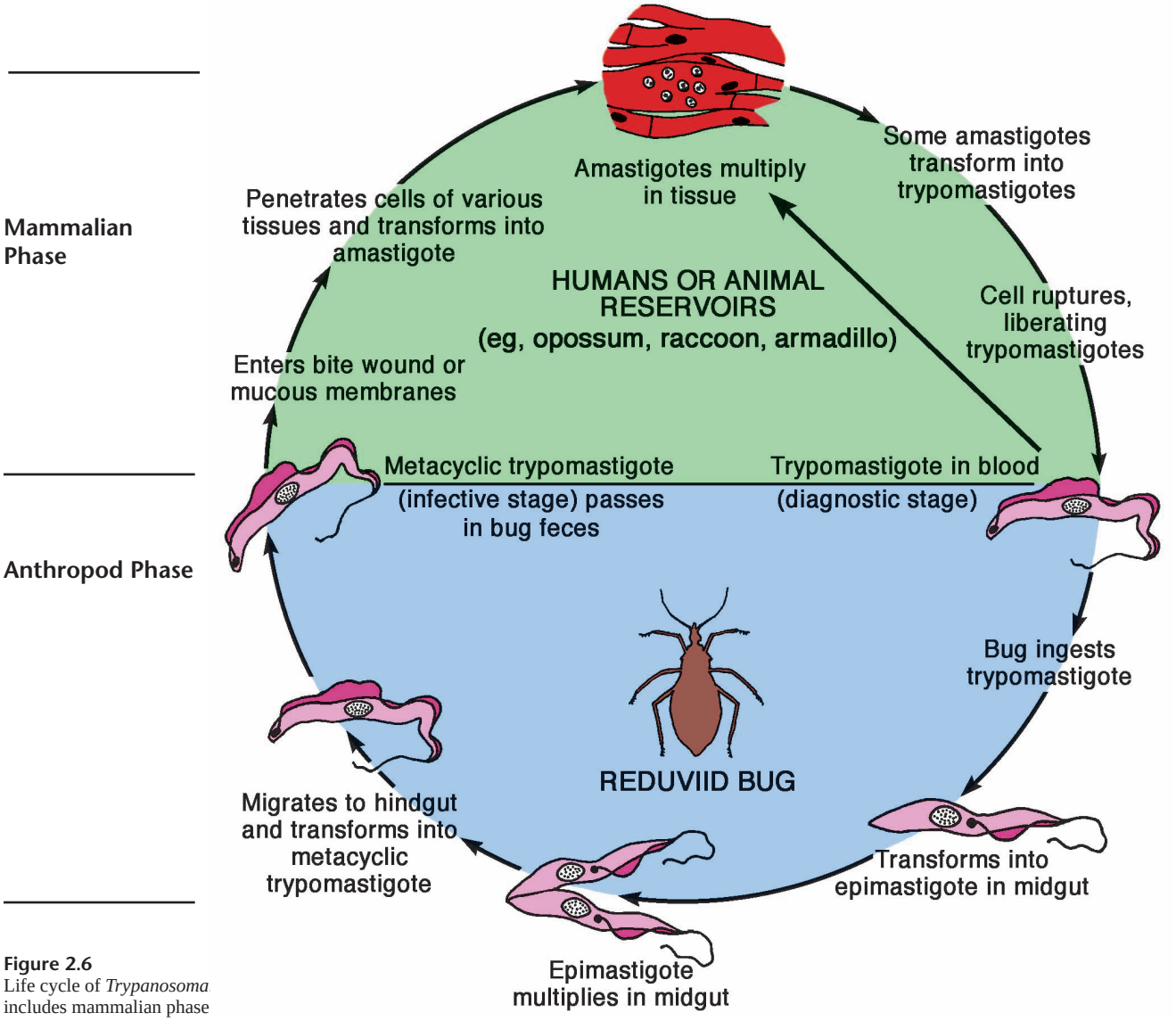



**Figure 2.6**
Life cycle of *Trypanosoma* includes mammalian phase arthropod phase.



**Figure 2.7**
Opossums naturally infected with *Trypanosoma cruzi* are reservoir hosts in southwestern United States and Central and South America.



**Figure 2.8**
Raccoons naturally infected with *Trypanosoma cruzi* are reservoir hosts in southwestern United States.



**Figure 2.9**
*Triatoma infestans*, probably the most important vector of *Trypanosoma cruzi*, is widely distributed in South America.



**Figure 2.10**
*Panstrongylus megistus*, an efficient and important vector of *Trypanosoma cruzi* in southern Brazil. Adults are approximately 2.5 cm long.

into shorter epimastigotes that multiply by binary fission. Daughter epimastigotes migrate to the hind-gut, where they transform into metacyclic trypomastigotes, the infective form for humans. Infective trypomastigotes appear in the feces of reduviid bugs within 20 days after contaminated blood is ingested from an infected mammal. Metacyclic trypomastigotes are excreted in the bug's feces at the bite site during or immidiately after the bug takes a blood meal. Infective metacyclic trypomastigotes deposited on the skin surface during or after a bite are introduced at the bite site or reach neighboring conjuctival or oral mucosae. The trypomastigotes then invade, or are engulfed by, primarily histiocytes within which they transform into amastigotes and multiply by binary fission. Within a few days amastigotes fill and distend the parasitized histiocytes which then rupture releasing the amastigotes to invade other cells. Thus the mammalian phase of the life cycle becomes established. Amastigotes spread throughout the body as parasitized histiocytes disseminate through the blood. Some amastigotes transform into trypomastigotes that also enter the blood and pass through virtually every organ.

It is only during the acute febrile stage of disease, that large numbers of trypomastigotes are present, and that free trypomastigotes are found in peripheral blood smears. Circulating trypomastigotes can invade cells in many different tissues and where they transform into amastigotes. Although cells of any organ may potentially be invaded, amastigotes are most commonly found in the heart, brain, smooth muscle, and striated muscle.

Humans most commonly acquire Chagas' disease from infected reduviid bugs, including *Triatoma* sp, *Panstrongylus* sp, and *Rhodnius* sp (Figs 2.9 & 2.10). These large bugs (sometimes called kissing or assassin bugs) have well-developed wings, cone-shaped heads, and large eyes.

During the day, these large bugs seek shelter and hide in



**Figure 2.11**
Thatched roof of hut in Costa Rica is typical daytime habitat of reduviid bugs. At night, bugs emerge to feed on sleeping humans.

the cracks of trees and houses (Fig 2.11). At night, male and female nymphal and adult stages emerge from their hiding places to feed on sleeping humans. During or immediately after their bite and blood meal, they defecate infective parasites that the host self-inoculates by inadvertently scratching or rubbing the parasite-laden fecal material into the bite wound or a neighboring mucosae, e.g. of the eyes or mouth.

The life cycle of a reduviid bug comprises egg, 5 instars, and adult (Fig 2.12). Molting to the next stage requires a full blood meal, and development from egg to adult may take a year or longer.

*Trypanosoma cruzi* can also be transmitted congenitally, through blood and blood-product transfusions, needle-sharing, organ transplantation, laboratory accident, and through food and drink contaminated by infected triatomes.[8,9,10]

## *Clinical Features and Pathogenesis*

### Primary lesion

The initial lesion develops at the bite site within several days in approximately 50% of patients after a typically painless bite of an infected reduviid bug. The fecal trypomastigotes of the reduviid bug penetrate the skin or neighboring mucosa where they proliferate and induce an inflammatory response characterized by erythema, urticaria, and interstitial edema leading to the formation of the characteristic cutaneous lesion, a chagoma. The chagoma evolves and grows as inflammatory cells proliferate at the bite site and spread to proximal lymph nodes where they cause lymphostasis and regional edema. In young children bites near the eye result in a combination of palpebral and periorbital edema and swelling of the preauricular lymph node known as Romaña's sign (Fig 2.13).

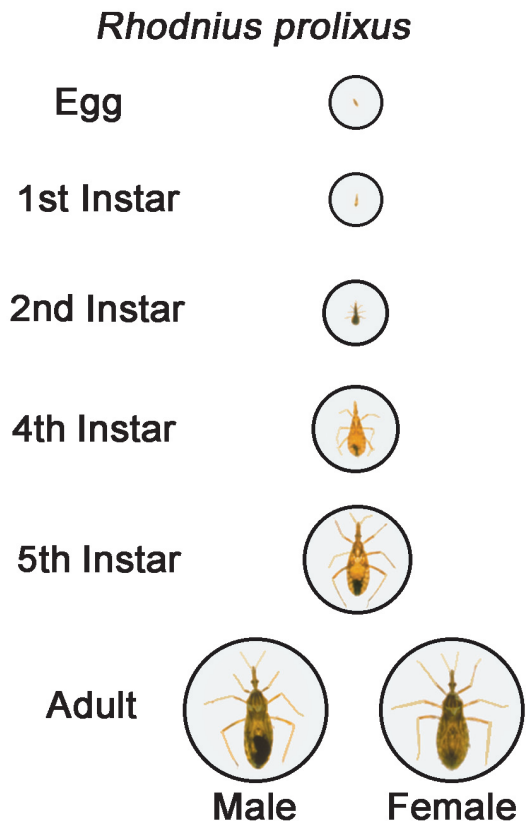



**Figure 2.12**
*Rhodnius prolixus*, a principal vector of *Trypanosoma cruzi* in Central America and northern South America, and principal vector of *Trypanosoma rangeli*.



**Figure 2.13**
Child with classic Romaña's sign: unilateral conjunctivitis, palpebral and periorbital edema, and preauricular lymphadenopathy.

### Acute Chagas' Disease

Only 3% of patients develop acute clinical manifestations of Chagas' disease which is usually mild with fever, malaise, edema of the face and lower extremities, generalized

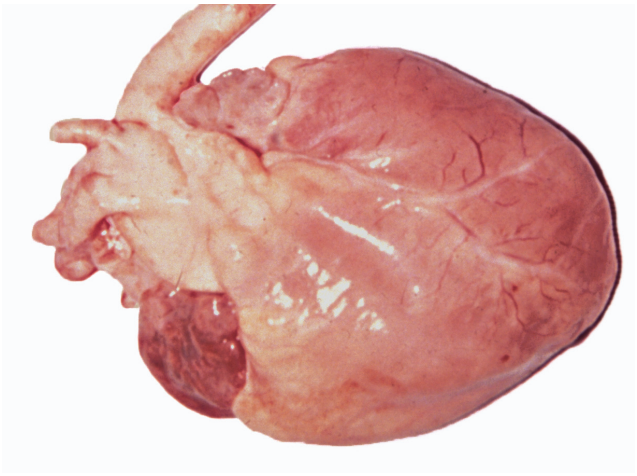


**Figure 2.14**
Anterior aspect of heart of 14-month-old patient who died of acute chagasic myocarditis. Note dilated ventricles and pale myocardium.

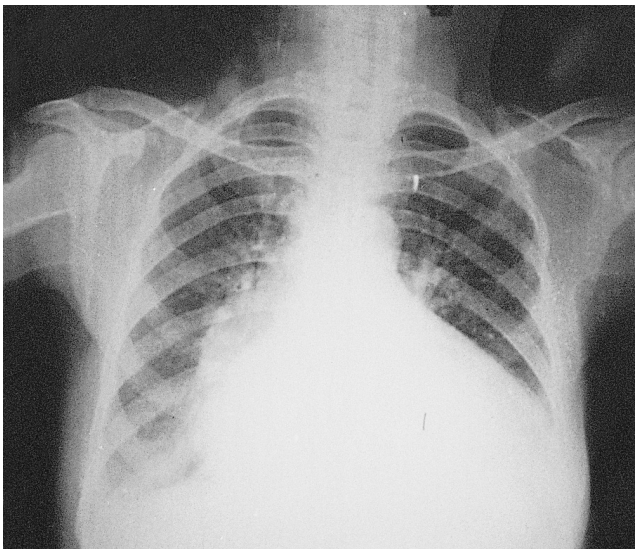


**Figure 2.15**
Chest x-ray of patient with severe cardiomegaly caused by chagasic myocarditis.

lymphadenopathy, hepatosplenomegaly, and leukocytosis.[11] Symptoms usually follow an incubation period which varies according to the mode of infection. For vector-transmitted infection, incubation takes 7 to 14 days; in transfusion-related transmission incubation takes up to 3 to 5 weeks. Severe myocarditis (Fig 2.14) develops in a small proportion of patients and results in electrocardiographic alterations, arrhythmia, hypotension, and cardiomegaly (Fig 2.15). Meningoencephalitis is rare in acute Chagas' disease and may present with nuchal rigidity, paralysis, and coma.

Most patients who develop acute Chagas' disease recover spontaneously in 2 to 4 months, less than 5% die during the acute disease. In some patients the acute phase is followed by an indeterminate, usually asymptomatic, phase of low-grade parasitemia that may last years or decades. In these patients immunosuppression may lead to reactivation of acute Chagas' disease years after infection, which may present as meningoencephalitis or myocarditis. Immunosuppressed patients, such as those with AIDS, hematologic malignancies, organ transplants, or receiving corticosteroids are at highest risk of reactivation disease.[12]

## Chronic Chagas' Disease

Symptomatic chronic infection occurs in only 10 to 30% of infected patients, most are 20 to 50 years old, in which circulating trypomastigotes are rare. The heart is the most commonly affected organ and may take the form of chronic chagasic cardiopathy as a result of severe myocarditis (Fig 2.14). The chronic myocardial damage is probably due, at least in part, to autoimmune mechanisms and continual antigenic stimulation by parasite antigens. Down-regulation of the immune response prevents massive chronic pathological changes in most patients.[13,14] The progressive and cumulative effects of cellular necrosis, inflammatory infiltrates, fibrosis, myocytic hypertrophy, and changes in the microcirculation, together with autoimmune factors, are believed to contribute to the cardiopathy. In patients with symptomatic chronic Chagasic cardiac disease the clinical manifestations vary and may include arrhythmia, cardiac failure, or thromboembolism. Electrocardiographic alterations are evident, especially right bundle branch block, first-degree or total atrioventricular block, and ventricular repolarization.[11]

Two important clinical forms of chronic Chagas' disease involve dilation of the esophagus or the colon either separately or together. These mega syndromes occur in about 10% of patients and vary in prevalence and predominant form by geographic region. Megaesophagus and megacolon have been related to denervation of the ganglia of the myenteric plexus of the intestinal tract, with accompanying disruption of the neural coordination that is necessary for peristalsis. It has been suggested that the degree of neuronal loss beyond a certain threshold causes dilatation of the segment above the affected area and result in the progressive dilation of the viscus, which can be massive. The most common clinical manifestation of megaesophagus is dysphagia and it can be associated with regurgitation, aspiration, pneumonia and death. Up to 25% of patients with megaesophagus also exhibit hypertrophy of the parotid glands. The most common symptom of megacolon is chronic constipation, with some patients reporting complete absence of bowel movements for as long as several weeks. Fecal impaction

or volvulus are common complications in these patients and can lead to infarction or perforation of the intestinal wall and precipitate a surgical crisis.[11] Rarely, patients with either megaesophagus or megacolon also show some form of stomach involvement. Enlargement of other hollow viscera have also been reported in some patients with chronic Chagas' disease.

### Congenital Chagas' Disease

Intrauterine infection by trypanosomes may cause abortion of the fetus or its premature delivery by the infected mother. Congenitally acquired infection may be asymptomatic or it may exhibit clinical features of hepatosplenomegaly, jaundice, cutaneous hemorrhage, and neurologic signs. The mortality rate from congenitally acquired infection is approximately 50%.

## *Pathologic Features*

The initial dermal chagoma is seldom biopsied. Typically, polymorphonuclear cells, monocytes, and lymphocytes infiltrate the dermis and subcutaneous tissue. Infection of myocardial, neuroglial, and smooth muscle cells causes the most serious histopathologic changes in acute systemic Chagas' disease.

### Acute Chagas' Disease

Grossly, the most conspicuous changes are in the heart, which is enlarged and dilated, particularly the right chambers (Fig 2.14). There may be pericarditis and excess serous fluid in the pericardial cavity. The myocardium is soft and pale, with focal hemorrhages and a yellowish tinge in some areas (Fig 2.14). Cardiac failure leads to congestion of the liver, lungs, spleen, and intestine to various degrees, depending on the severity of the cardiac dysfunction. The brain and meninges are also congested, often accompanied by petechiae.

Microscopically, there are trypomastigotes in peripheral blood (Fig 2.2) and amastigotes in the heart (Fig 2.5), smooth muscles, striated muscles, and sometimes the central nervous system.

There is severe myocarditis with degeneration of muscle fibers, and an interstitial inflammatory infiltrate consisting mostly of lymphocytes, monocytes, plasma cells, and sometimes neutrophils (Figs 2.16 & 2.17 ). Fragmentation, vacuolization, hyalinization, destruction of myofibers, and interstitial edema are other manifestations of acute chagasic cardiopathy (Fig 2.16). Transitional forms (Fig 2.18) and amastigotes (Fig 2.19) are found within myocardial fibers. There is usually some degree of pericarditis and endocarditis (Figs 2.20 & 2.21).

In the central nervous system the leptomeninges are infiltrated by mixed inflammatory cells extending into the perivascular space and penetrating the cortex (Fig 2.22). Inflam-

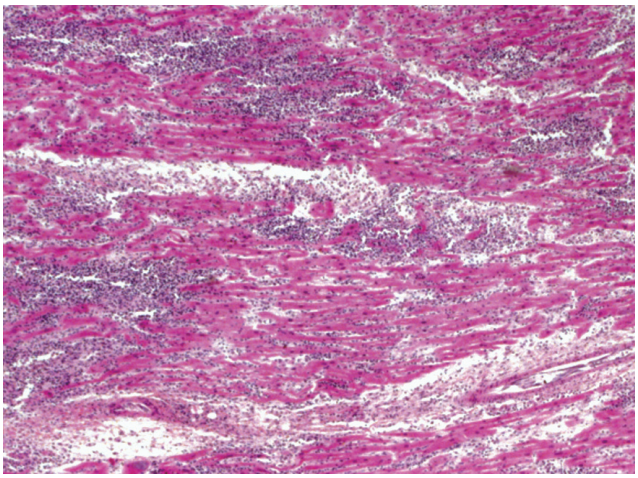


**Figure 2.16**
Fatal acute chagasic myocarditis with inflammatory cell infiltrates, interstitial edema, and ruptured muscle fibers. x30

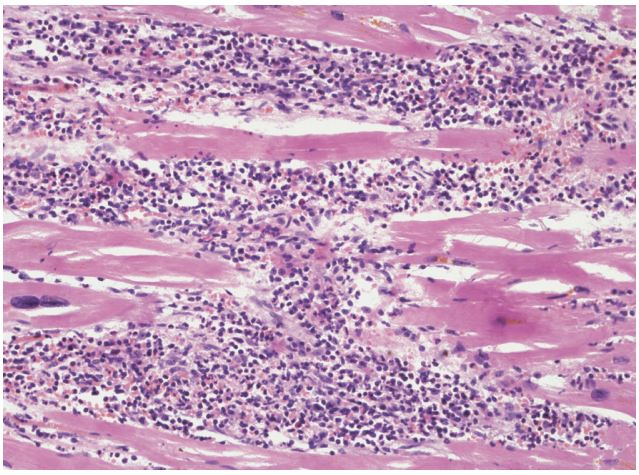


**Figure 2.17**
Fatal acute chagasic myocarditis. Focal accumulations of polymorphonuclear neutrophils may be present in areas of severe degeneration of muscle. x130

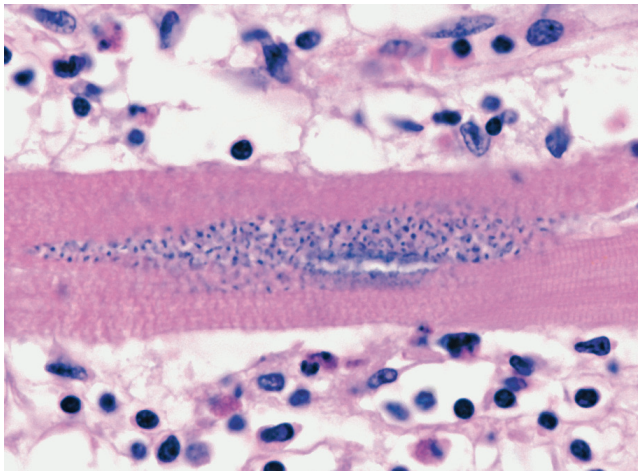


**Figure 2.18**
Transitional forms of *Trypanosoma cruzi* within muscle fibers in fatal acute chagasic myocarditis. Individual cell boundaries are obscured and kinetoplasts are more rounded than rod-shaped. x640

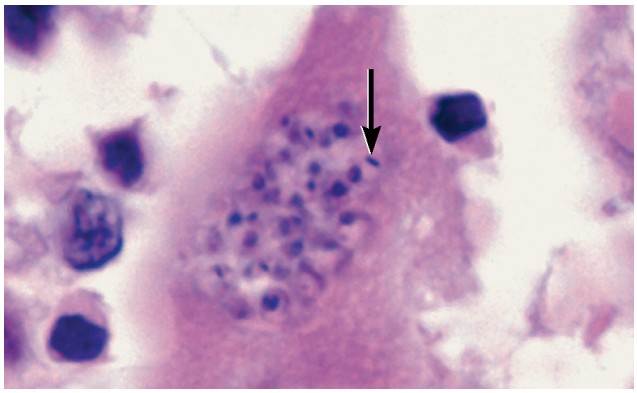


**Figure 2.19**
Cluster of amastigotes within muscle fibers in fatal acute chagasic myocarditis. Note rod-shaped kinetoplast (arrow). x1540

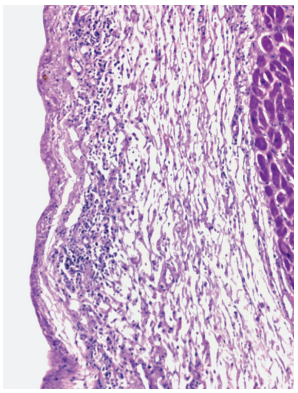


**Figure 2.20**
Pericarditis in fatal acute Chagas' disease. x46

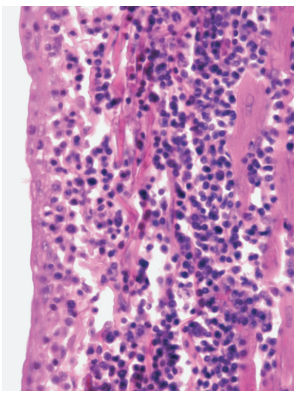


**Figure 2.21**
Endocarditis in fatal acute Chagas' disease. x170

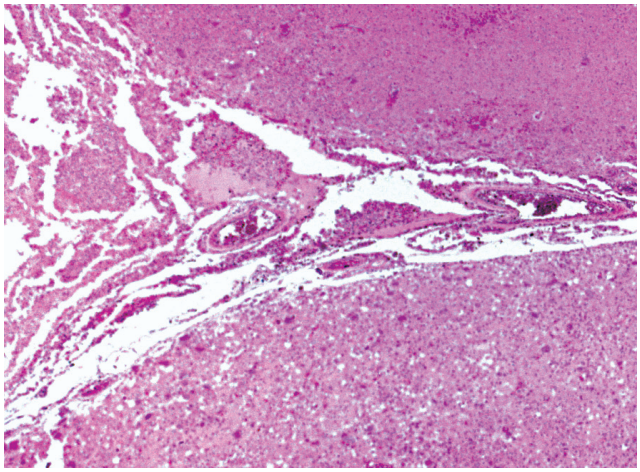


**Figure 2.22**
Brain of 30-year-old Brazilian with Chagas' disease and AIDS. Patient was treated for toxoplasmosis, but became comatose and died 20 days after hospital admission. Note exudate in meninges. x25

mation of the brain parenchyma produces small nodules of glial cells, lymphocytes, and plasma cells (Fig 2.23), and perivascular cuffing by lymphocytes and plasma cells (Figs 2.24a & 2.24b) Parasites invade neurons and glial cells of the brain and spinal cord. Patients with AIDS usually experience severe acute Chagas' disease. Inflammation, necrosis, and numerous amastigotes are seen in various cells of the brain parenchyma and histiocytes (Figs 2.25 to 2.27).

There may be foci of lymphocytes and plasma cells in almost any organ or tissue.[15]

## Chronic Chagas' Disease

The most common findings in chronic Chagas' disease are cardiopathy and megaviscera. Chronic chagasic cardiopathy results from severe myocarditis.

## Chronic chagasic myocarditis

The heart is dilated and heavy (400 to 800 g), and the

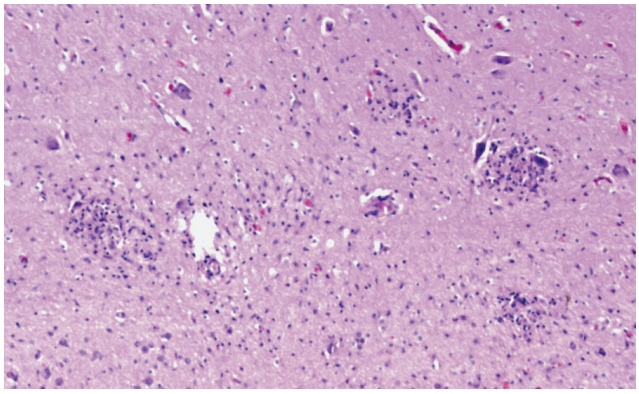
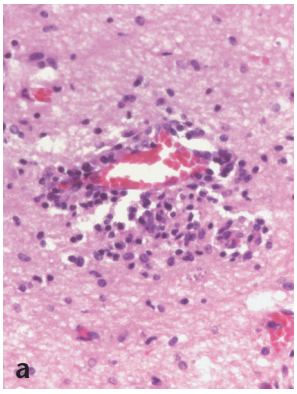


**Figure 2.23**
Several foci of inflammation in brain from autopsy of 3-month-old Venezuelan infant clinically diagnosed with meningoencephalitis. Foci did not contain amastigotes. x72



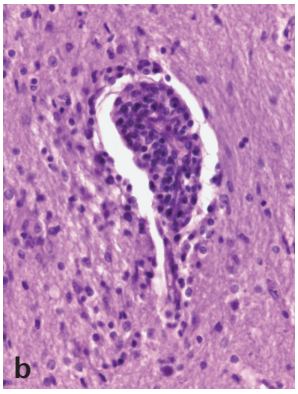




**Figure 2.24 a,b**
a. Perivascular inflammation in patient described in Figure 2.23. x160;
b. Autopsy specimen of brain of Panamanian patient with acute Chagas' disease showing perivascular cuffing by lymphocytes and plasma cells. x185

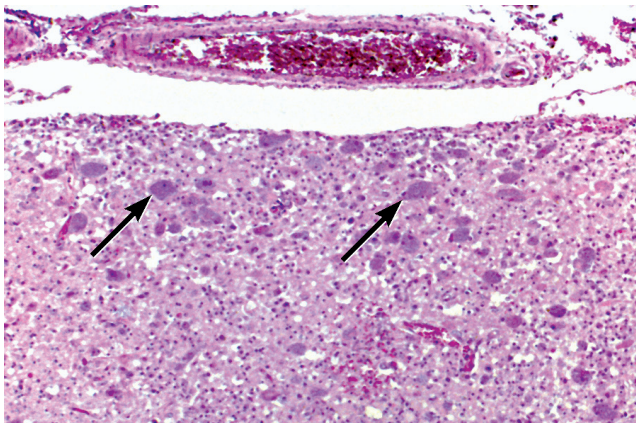


**Figure 2.25**
Brain of patient described in Figure 2.22, showing numerous clusters of amastigotes (arrows). x65

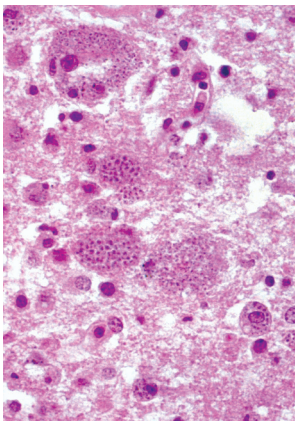


**Figure 2.26**
Brain of patient described in Figures 2.22. Note massive numbers of amastigotes within histiocytes and throughout parenchyma. x230

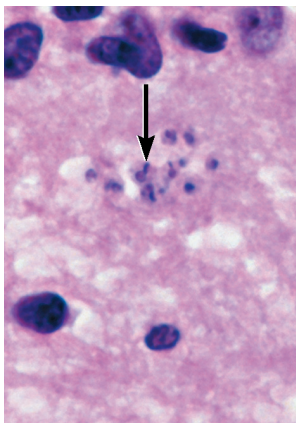


**Figure 2.27**
Brain of patient described in Figure 2.23 with scattered clusters of amastigotes in brain on autopsy. Note odd-shaped kinetoplast (arrow) of amastigote. x975

right ventricular outflow tract is prominent. Valve rings are dilated and atrial walls are fibrotic. The interventricular septum is deviated to the right, which may immobilize the adjacent tricuspid leaflet (Fig 2.28). Rarely, the defect at the apex of the left ventricle forms an aneurysm (Figs 2.29a to 2.29c). Distortion of the papillary muscles of the left ventricle and an increase in trabeculae carneae in the distal parts of the ventricles are common. Coronary arteries are usually normal, but capillaries and small veins are dilated and irregular.

Microscopically, there is marked interstitial fibrosis of the myocardium and rare amastigotes (Figs 2.30 to 2.32), with focal infiltrates of lymphocytes, monocytes, and plasma cells in which multinucleated giant cells are occasionally present (Fig 2.33). Focal accumulations of neutrophils and an occasional eosinophil may also be found. Apical lesions regularly appear as segments of acellular fibrous tissue associated with epicardial vessels and adipose tissue (Fig 2.29c).

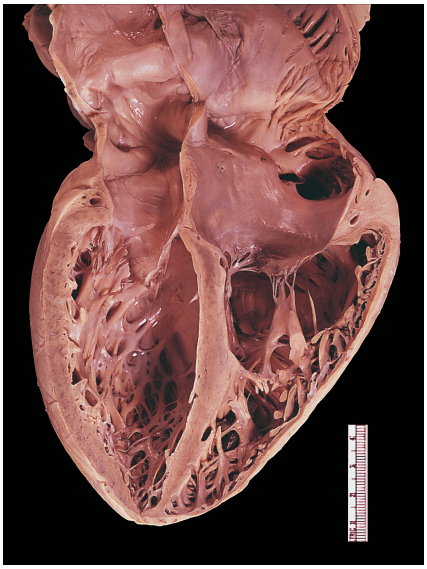


**Figure 2.28**
Posterior half of heart of 36-year-old Brazilian patient who had chronic Chagas disease and died of congestive heart failure. Note thinning of ventricular walls and interventricular septum, left ventricular dilatation, and increased complexity of trabeculae.

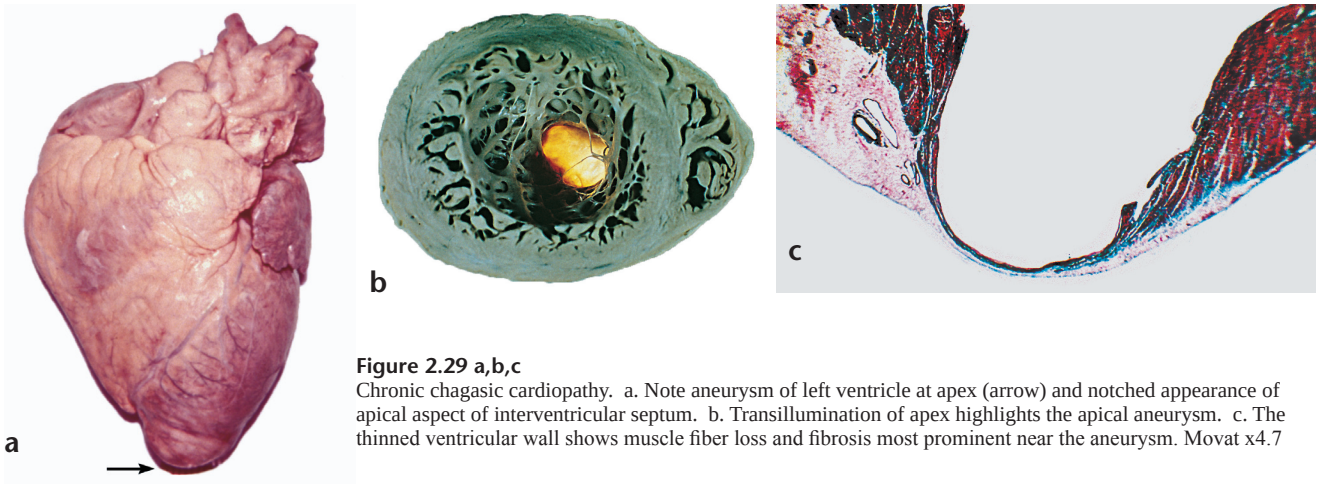



**Figure 2.29 a,b,c**
Chronic chagasic cardiopathy. a. Note aneurysm of left ventricle at apex (arrow) and notched appearance of apical aspect of interventricular septum. b. Transillumination of apex highlights the apical aneurysm. c. The thinned ventricular wall shows muscle fiber loss and fibrosis most prominent near the aneurysm. Movat x4.7

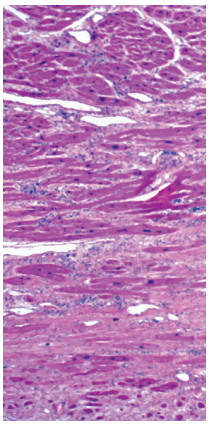


**Figure 2.30**
Chronic chagasic myocarditis in 27-year-old Brazilian farmer who died of congestive heart failure. There is chronic inflammation, edema, and fibrosis. x16

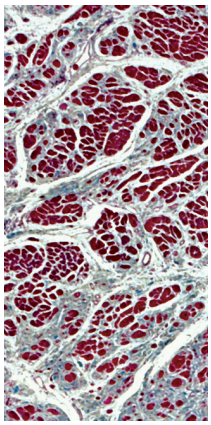


**Figure 2.31**
Chronic chagasic myocarditis in 56-year-old Brazilian patient. Note marked interstitial fibrosis. Movat x20

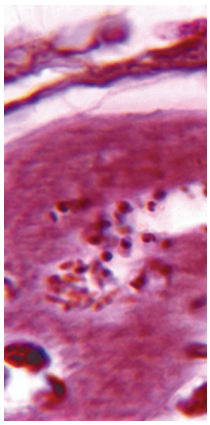


**Figure 2.32**
Chronic chagasic myocarditis with cluster of amastigotes in muscle fiber. Amastigotes are difficult to find in chronic lesions. x1650

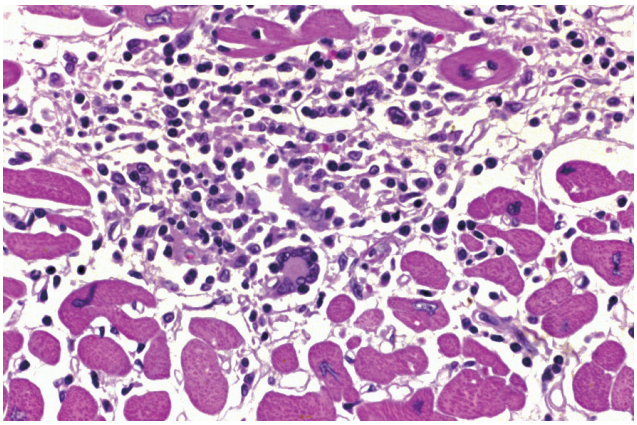


**Figure 2.33**
Rare giant cell in chronic chagasic myocarditis of patient described in Figure 2.30. x240

## Chagasic Megaviscera

In megaviscera of chronic Chagas' disease, the esophagus and colon are most frequently affected (Figs 2.34 and 2.35). In the esophagus, focal round cell infiltrates may be found in the lamina propria (Fig 2.36) and between the muscle layers (Figs 2.37 & 2.38). As megadisease progresses the initially thinned out walls of the esophagus and colon thicken and the smooth muscle fibers become hyperplastic. Along with the hyperplasia of the smooth muscle fibers there is a marked decrease in the number of ganglion cells of the myenteric plexus. Amastigotes are very difficult to find in either the esophagus or colon.

It is possible, though not common, to find amastigotes outside the usual organs. In our experience, a rare finding was chagasic orchitis in a patient from Venezuela. Massive numbers of amastigotes were seen within histiocytes of the testis (Figs 2.39 to 2.41). Unfortunately, the specimen was not accompanied by a clinical history.

## Congenital Chagas' Disease

In pregnant patients, *T. cruzi* infection causes chronic villositis (Figs 2.42a to 2.42c). Babies born with *T. cruzi* infection usually die of chagasic encephalitis within a few days or weeks.



**Figure 2.34**
Megaesophagus in 34-year-old Brazilian patient with chronic Chagas' disease.



**Figure 2.35**
Megacolon in 50-year-old Brazilian patient with chronic Chagas' disease. Colon is saccular and thin-walled.

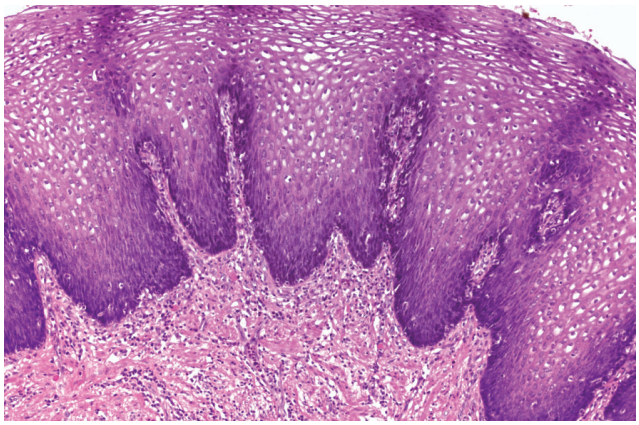


**Figure 2.36**
Megaesophagus in chronic Chagas' disease, with chronic inflammation of lamina propria. x64

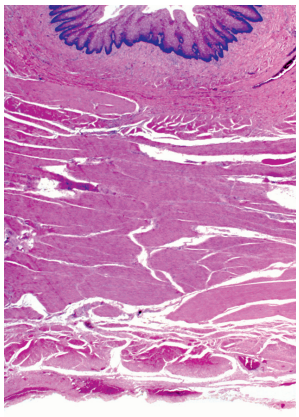


**Figure 2.37**
Megaesophagus in chronic Chagas' disease. Note thickening of smooth muscles. x8

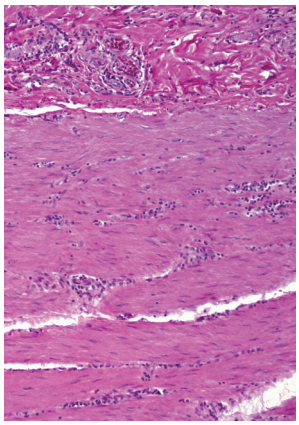


**Figure 2.38**
Megaesophagus in chronic Chagas' disease with chronic inflammatory infiltrate of smooth muscle. x60

## *Diagnosis*

Diagnosis of Chagas' disease during the acute phase, whether primary or due to reactivation associated with immunosuppression, is established by identifying trypomastigotes of *T. cruzi* in peripheral blood films (Fig 2.2). Highly motile trypomastigotes may be observed in wet preparations of blood or buffy coat, and in specimens of cerebrospinal fluid (CSF), bone marrow, mass lesions, and pericardial fluid. With few exceptions, detecting amastigotes in biopsy specimens also confirms a diagnosis of acute Chagas' disease. Autopsy specimens from immunosuppressed patients with Chagas' disease, and patients who die of acute disease usually reveal large numbers of amastigotes.

For chronic Chagas' disease, where parasitemia is much lower, polymerase chain reaction[16], hemoculture, and se-

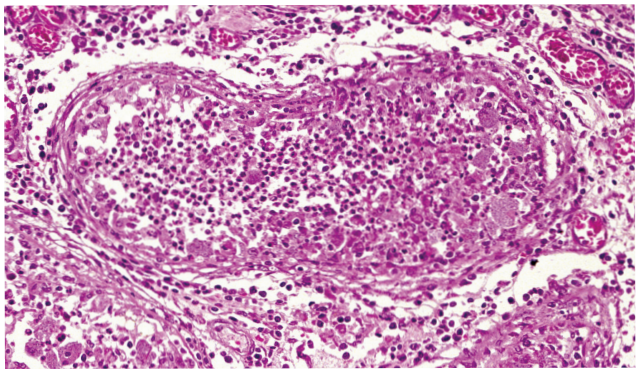


**Figure 2.39**
Rare chagasic orchitis in Venezuelan patient. Note chronic inflammation. x140

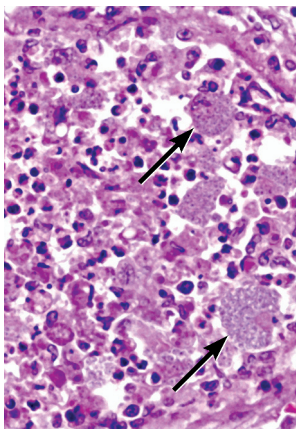


**Figure 2.40**
Higher magnification of testis illustrated in Figure 2.39, showing clusters of amastigotes within histiocytes (arrows). x295

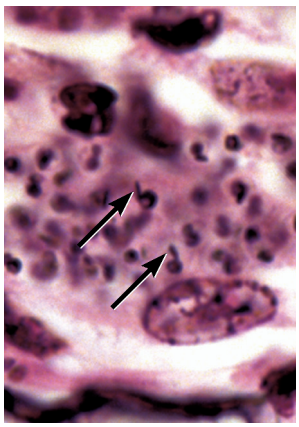


**Figure 2.41**
Cluster of amastigotes in testis of patient described in Figures 2.39 and 2.40. Note black rod-shaped kinetoplasts (arrows) and large spherical nuclei. Wilder's reticulum x1480

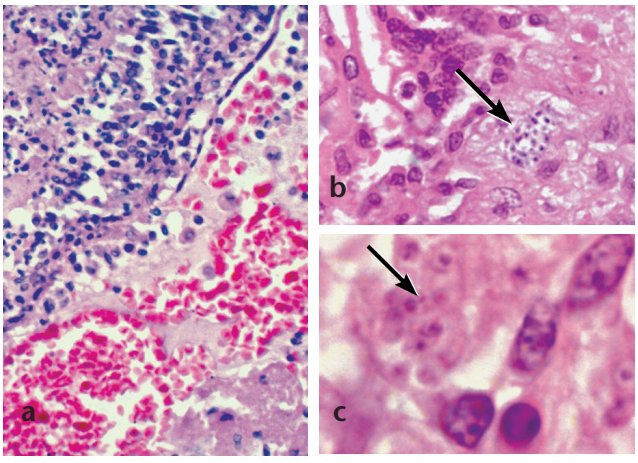



**Figure 2.42 a,b,c**
a. Placenta with chronic villositis in Chagas' disease. x100
b. Placenta with cluster of amastigotes (arrow) in histiocyte in Chagas' disease. x150
c. Higher magnification of amastigotes in placenta in Figure 2.42a and 2.42b. Note rod-shaped kinetoplasts (arrow). x700

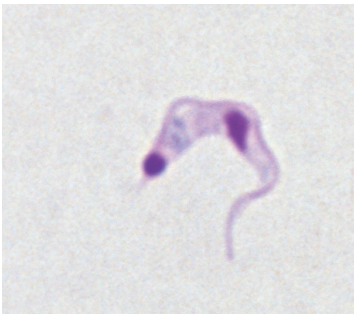


**Figure 2.43**
Trypomastigote of *Trypanosoma cruzi* in CSF, depicting C-shaped configuration and large spherical kinetoplast at posterior tip. Patient was 38-year-old HIV-positive Salvadoran living in Virginia. Patient had not been to El Salvador for more than a year, indicating reactivation of Chagas' disease. Giemsa x2000

rological testing are required to establish a diagnosis. Trypomastigotes do not usually appear in peripheral blood films, and amastigotes are rarely found in biopsy or autopsy specimens. Immunosuppression by HIV can reactivate chronic Chagas' disease and trypomastigotes may appear in CSF (Fig 2.43) and sometimes in peripheral blood samples. The CSF of these co-infected patients may show a mild pleocytosis (predominantly lymphocytes) and increased protein levels.

Hemoculture and xenodiagnosis are highly specific but not very sensitive. Blood cultures with liver infusion tryptose, Warren, or other suitable media must be examined for up to 120 days postinoculation.[16,17] In xenodiagnosis, sterile, laboratory-reared reduviid bugs are allowed to feed on a patient (Fig 2.44). If the patient is infected, the bugs ingest trypomastigotes and a diagnosis is confirmed for the patient 10 to 30 days later when the bugs' feces and hindgut contents are examined for metacyclic trypomastigotes. This very specific procedure is valuable in diagnosing chronic infections where parasites cannot be found in the patient's blood.[18]

PCR techniques for diagnosis of Chagas' disease are under investigation, but none is yet available for routine use.



**Figure 2.44**
Xenodiagnosis technique applied to arm of Costa Rican patient. Procedure is useful in diagnosing chronic Chagas' disease.

## *Treatment and Prevention*

Chemotherapy, which has little apparent effect on chronic Chagas' disease, is reserved for patients diagnosed in the acute phase, accidentally infected laboratory workers, immunocompromised patients, and children with congenital infection. Benznidazole and nifurtimox, both of which are toxic, reduce the duration and severity of acute Chagas' disease, but are curative only for approximately 50% of patients.[19,20] Chronic chagasic cardiopathy is treated with drugs, pacemaker, or transplantation. "Mega" syndromes may require surgery.

With the increasing numbers of serologically positive individuals in the United States, identifying infected blood, tissue and organ donors by exposure questionnaires and screening tests can prevent transmission of Chagas' disease.[21] A few antibody detection screening tests have been approved by the FDA for use in the United States. [22,23] Vector transmission of Chagas' disease can be interrupted through improved housing, community education, and the use of specific insecticides.

## References

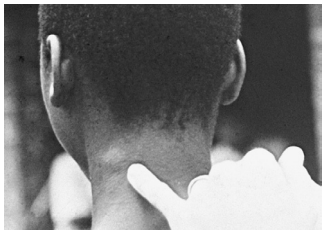

1. Chagas C. Nova tripanozomiase humana. Estudos sobre a morfologia e o ciclo evolutivo do *Schizotrypanum cruzi* n. gen., n. sp., agente etiológico de nova entidade mórbida do homen. *Mem Inst Oswaldo Cruz.* 1909;1:159-218.
2. Lewinsohn R. Carlos Chagas (1879-1934): the discovery of *Trypanosoma cruzi* and of American trypanosomiasis (foot-notes to the history of Chagas's disease). *Trans R Soc Trop Med Hyg.* 1979;73:513-523.
3. Beard CB, Pye G, Steurer FJ, et al. Chagas disease in a domestic transmission cycle in southern Texas, USA. *Emerg Infect Dis.* 2003;9:103-105.
4. Moncayo A. Progress towards interruption of transmission of Chagas disease. *Mem Inst Oswaldo Cruz.* 1999;94:401-404.
5. Pinto Dias JC. Southern Cone Initiative for the elimination of domestic populations of *Triatoma infestans* and the interruption of transfusional Chagas disease. Historical aspects, present situation, and perspectives. *Mem Inst Oswaldo Cruz.* 2007;102(Suppl I):11-18.
6. Moncayo A. Chagas disease: current epidemiological trends after the interruption of vectorial and transfusional transmission in the Southern Cone countries. *Mem Inst Oswaldo Cruz.* 2003;98:557-591.
7. Rassi A Jr, Rassi A, Marin-Neto JA. Chagas Disease. *Lancet.* 2010;375:1388-1402.
8. Kirchhoff LV. American trypanosomiasis (Chagas' disease)–a tropical disease now in the United States. *N Engl J Med.* 1993;329:639-644.
9. Kirchhoff LV. Chagas disease. American trypanosomiasis. *Infect Dis Clin North Am.* 1993;7:487-502.
10. WHO Expert Committee. Control of Chagas disease. *World Health Organ Tech Rep Ser.* 2002;905:1-109.
11. Umezawa ES, Stolf AM, Corbett CE, Shikanai-Yasuda MA. Chagas' disease. *Lancet.* 2001;357:797-799.
12. Ferreira MS, Nishioka SA, Silvestre MT, Borges AS, Nunes-Araujo FR, Rocha A. Reactivation of Chagas' disease in patients with AIDS: report of three new cases and review of the literature. *Clin Infect Dis.* 1997;25:1397-1400.
13. Rossi MA, Bestetti RB. The challenge of chagasic cardiomyopathy. The pathologic roles of autonomic abnormalities, autoimmune mechanisms and microvascular changes, and therapeutic implications. *Cardiology.* 1995;86:1-7.
14. Tarleton RL. Regulation of immunity in *Trypanosoma cruzi* infection. *Exp Parasitol.* 1991;73:106-109.
15. Rocha A, de Meneses AC, da Silva AM, et al. Pathology of patients with Chagas' disease and acquired immunodeficiency syndrome. *Am J Trop Med Hyg.* 1994;50:261-268.
16. Chiari E. Chagas disease diagnosis using polymerase chain reaction, hemoculture and serologic methods. *Mem Inst Oswaldo Cruz.* 1999;94:299-300.
17. Luz ZM. Changes in hemoculture methodology improve the test positivity. *Mem Inst Oswaldo Cruz.* 1999;94:295-298.
18. Schenone H. Xenodiagnosis. *Mem Inst Oswaldo Cruz.* 1999;94:289-294.
19. Bern C, Montgomery SP, Herwaldt BL, et al. Evaluation and treatment of Chagas disease in the United States. *JAMA.* 2007;298:2171-2181.
20. Drugs for Parasitic Infections. *The Medical Letter.* 2010;8(Suppl):e1-20.
21. Leiby DA, Herron RM, Read EJ, Lenes BA, Stumpf RJ. *Trypanosoma cruzi* in Los Angeles and Miami blood donors: impact of evolving donor demographics on seroprevalence and implications for transfusion transmission. *Transfusion.* 2002;42:548-555.
22. Morbidity and Mortality Weekly Report. Blood donor screening for Chagas Disease-United States, 2006-2007. February 23, 2007; 56:141-143.
23. U.S. Food and Drug Administration. FDA approves Chagas disease screening test for blood, tissue and organ donors. FDA News Release, 30 April 2010; http://www.fda.gov/NewsEvents/Newsroom/PressAnnouncements/ucm210429.htm

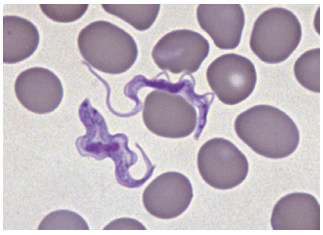

## Acknowledgements


**Figure 2.14**
Contributed by Gorgas Memorial Laboratory, Panama

**Figure 2.29a&b**
Contributed by Gorgas Memorial Laboratory, Panama

**Figure 2.44**
Contributed by Dr. C Lozoni, Pediatric Clinic, Laboratory Hospital, San Juan di Dios







3

# African Trypanosomiasis

***Mary K. Klassen-Fischer,***
***Wayne M. Meyers, and Ronald C. Neafie***

## *Introduction*

### Definition

African trypanosomiasis is infection by protozoan hemoflagellates of the *Trypanosoma brucei* complex, 2 subspecies of which cause disease in humans: *Trypanosoma brucei gambiense* causes Gambian (chronic) trypanosomiasis and *Trypanosoma brucei rhodesiense* causes Rhodesian (acute) trypanosomiasis. A third economically important subspecies, *Trypanosoma brucei brucei*, causes nagana, a fatal disease of animals, but does not infect humans.

### Synonyms

Synonyms include African sleeping sickness, human trypanosomiasis, Gambian sleeping sickness/West African trypanosomiasis (*T. b. gambiense*), Rhodesian sleeping sickness/East African trypanosomiasis (*T. b. rhodesiense*), *maladie du sommeil*, and *sonolencia*.

### General Considerations

The first trypanosomes to be described were nonpathogenic species in the frog (Gruby 1843) and the rat (Lewis 1878). In India in 1880, Evans first attributed a disease to trypanosomes—surra, a disease of horses, mules, camels, and cattle.

African trypanosomiasis has probably played an important role in recorded history from antiquity dating to the 2nd millennium BC. [1]

African sleeping sickness was clearly recognized as early as the 14th century in a Sudanese king.[2] Winterbottom, in his "Account of the Native Africans in the Neighborhood of Sierra Leone" (1803), described the disease incidentally.[3] During his travels in southern Africa (1840-1856), David Livingstone gave a detailed account of a disease afflicting animals bitten by the tsetse fly, noting on one occasion that "we lost forty-three fine oxen by its bite."[4] In 1894 Bruce observed *T. brucei* in the blood of a cow with nagana in Zululand (South Africa), and demonstrated that the disease was transmitted to cattle from big game animals by *Glossina morsitans*, a biting fly. In 1901, Dutton found trypanosomes in the blood of a patient with Gambia fever and named the organisms *T. gambiense*. Two years later, Castellani found identical organisms in the spinal fluid of 5 patients with African sleeping sickness. Bruce and Nabarro demonstrated that the tsetse fly was the vector of the trypanosomes, and that Gambia fever and sleeping sickness were 2 stages of the same disease.[5] In 1910, Stephens and Fantham identified trypanosomes in the blood of a patient in Rhodesia (now Zambia and Zimbabwe). *Trypanosoma rhodesiense* was later determined to be indistinguishable from *T. brucei*.[6]

Three severe epidemics of African trypanosomiasis have been recorded since the late 19th century, the first in Uganda and the Congo Basin between 1896 and 1906. A second epidemic in the 1920s swept through several African countries and was arrested by systematically screening millions of people. African trypanosomiasis practically disappeared between 1960 and 1965, but has reappeared in endemic form in several foci since 1970 as a result of political and socioeconomic instability, diminishing measures for vector control and surveillance for the disease.[7,8] In the Democratic Republic of the Congo (DRC), this lack of active control measures has resulted in a resurgence of sleeping sickness, with rates of infection similar to those of the late 1920s.[9] The importance and impact of sociopolitical factors on the incidence of African trypanosomiasis was investigated quantitatively and qualitatively using data from 35 affected countries in Sub-Saharan Africa.[10] Statistical analytical methods showed an association between civic/political conflicts and changes in the geographical incidence of human African trypanosomiasis.

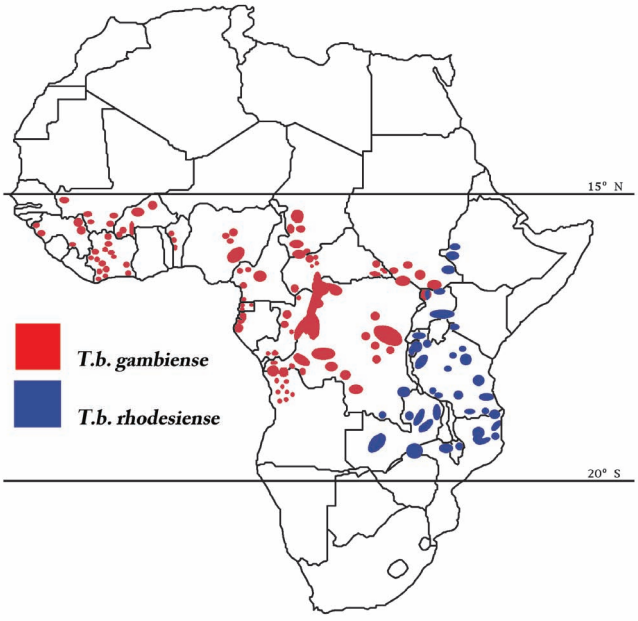



**Figure 3.1**
Focal distribution of African trypanosomiasis in humans. (Modified from WHO Technical Report Series 739, 1986.)

## Epidemiology

*Trypanosoma brucei* is limited to tropical Africa, where it is widely distributed throughout the tsetse-fly belt, a 10-million-square-mile area stretching from 15° N to 20° S of the equator (Fig 3.1) (Table 3.1). *Trypanosoma brucei gambiense* infects humans in foci within a wide range in western and central Africa and Angola. Endemic foci of *T. b. rhodesiense* infections are found in limited areas of eastern and southern Africa. Within this range, the disease is distributed unevenly because the vector is usually confined to rural areas, in dense vegetation along streams and lakes (*T. b. gambiense*) (Fig 3.2), or wooded areas of the savanna (*T. b. rhodesiense*). Moreover, within endemic countries there are many regions where parasite-free tsetse flies are found. A focus of disease can be a single village or an entire region, and the intensity of disease can vary considerably from village to village. Epidemics are typically followed by long periods of endemicity.[11] Occasionally, imported sleeping sickness is reported in a nonendemic country.[12]

At least 60 million Africans are at risk of infection, but only 4 million are under surveillance.[7] Approximately 45 000 cases were reported in 1999, but the World Health Organization estimates that the number of patients was between 300 000 and 500 000. Due to inadequate health care, only 10% of new sleeping sickness patients are diagnosed and treated.[7] Many die before they are diagnosed. African trypanosomiasis is the leading cause of death in some endemic areas, ahead of HIV/AIDS.



**Figure 3.2**
Tributary of Lopori River (1° N lat.) near Bongandanga in Gambian trypanosomiasis-endemic area of northwestern Democratic Republic of the Congo. Note forested terrain with underbrush and grass overhanging riverbank. Tsetse flies bit the photographer many times during the brief ferry crossing.

| Nation | Level of endemicity | Subspecies |
|---|---|---|
| WESTERN AFRICA | | |
| Benin | Low | *gambiense* |
| Burkina Faso | Low | *gambiense* |
| Côte d'Ivoire | High | *gambiense* |
| Ghana | Low | *gambiense* |
| Guinea | High | *gambiense* |
| Guinea Bissau | Low | *gambiense* |
| Liberia | Unknown | *gambiense* |
| Mali | Low | *gambiense* |
| Senegal | Unknown | *gambiense* |
| Sierra Leone | Unknown | *gambiense* |
| Togo | Low | *gambiense* |
| NORTHEASTERN AFRICA | | |
| Chad | High | *gambiense* |
| Ethiopia | Unknown | *rhodesiense* |
| Sudan | Epidemics | *gambiense* |
| CENTRAL AFRICA | | |
| Burundi | Unknown | *rhodesiense* |
| Cameroon | High | *gambiense* |
| Central African Republic | High | *gambiense* |
| Congo | High | *gambiense* |
| Democratic Republic of the Congo | Epidemics | Both |
| Equatorial Guinea | Low | *gambiense* |
| Gabon | Low | *gambiense* |
| Kenya | Low | Both |
| Nigeria | Unknown | *gambiense* |
| Rwanda | Unknown | *rhodesiense* |
| United Republic of Tanzania | High | Both |
| Uganda | High | *rhodesiense* |
| SOUTHERN AFRICA | | |
| Angola | Epidemics | Both |
| Botswana | Unknown | *rhodesiense* |
| Malawi | Low | *rhodesiense* |
| Mozambique | High | *rhodesiense* |
| Namibia | Unknown | Both |
| Zambia | Low | *rhodesiense* |
| Zimbabwe | Low | *rhodesiense* |

**Table 3.1**
African nations within geographic range of trypanosomiasis. Note: Different periods covered account for slight differences in data presented in this table and the map in Figure 3.1.

# *Infectious Agent*

## Morphologic Description

*Trypanosoma brucei gambiense* and *T. b. rhodesiense* are morphologically indistinguishable. In fresh blood or cerebrospinal fluid (CSF), the parasites appear as colorless flagellates. Trypomastigotes, the only stage found in human hosts, are polymorphic and circulate in 3 distinct forms: 1) a long slender form, usually with a blunt posterior end, a subterminal kinetoplast, and a long free anterior flagellum (Fig 3.3); 2) a short stumpy form, usually with a round or pointed posterior end, a terminal kinetoplast, and a short or absent free flagellum (Fig 3.4); and 3) a spectrum of intermediate forms whose morphologic features vary considerably. Stained flagellates are 14 to 33 µm by 1.5 to 3.5 µm. They have a large, oval, centrally placed red or violet nucleus that occupies as much as one quarter of the organism (Fig 3.5). A tiny spherical kinetoplast near the posterior end is composed of a parabasal body and a blepharoplast,



**Figure 3.3**
Trypomastigote of *Trypanosoma brucei rhodesiense* in blood film from American traveler who visited East Africa 10 days previously. Long slender form is characterized by blunt posterior end, tiny spherical subterminal kinetoplast, large centrally placed nucleus, and long free flagellum. Flagellum extends posteriorly along outer border of undulating membrane. Giemsa x1300

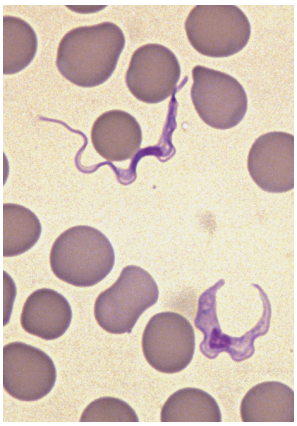


**Figure 3.4**
Long slender form and short stumpy form of *Trypanosoma brucei rhodesiense* in blood film from patient described in Figure 3.3. Note absence of kinetoplast and free flagellum in stumpy form. Giemsa x1240

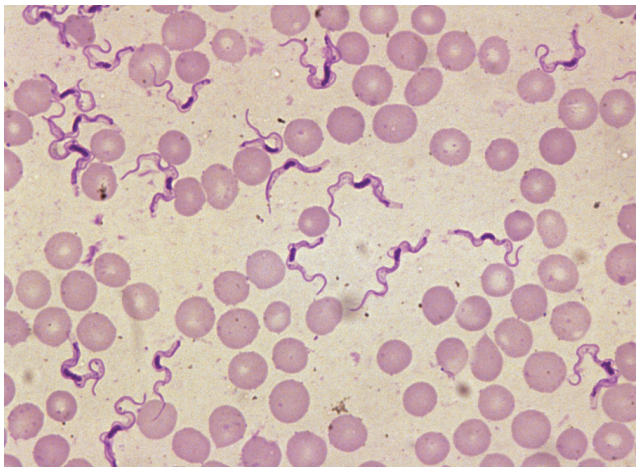


**Figure 3.5**
Trypomastigotes of *Trypanosoma brucei gambiense*, morphologically indistinguishable from *Trypanosoma brucei rhodesiense,* in blood film from experimental infection. Giemsa x725

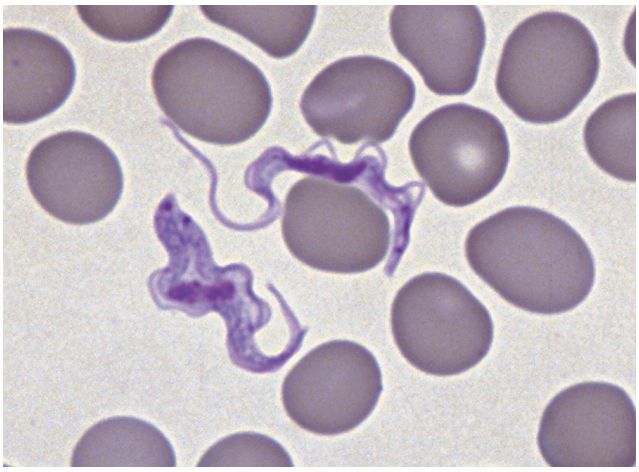


**Figure 3.6**
Two trypomastigotes of *Trypanosoma brucei rhodesiense* dividing by binary longitudinal fission in blood film of patient described in Figure 3.3. Division is more advanced in parasite at bottom. Giemsa s1800

structures rarely identified by light microscopy. Ultrastructural studies show that the kinetoplast is continuous with a single long mitochondrion that occupies much of the core of the parasite, and that it is intimately associated with the blepharoplast. The nucleus and kinetoplast are dark with Giemsa, Romanovsky's, and Wright's stains. Numerous blue or grayish violet granules are usually scattered throughout the pale blue cytoplasm. A rather broad undulating membrane originates on the posterior end of the body and makes several undulations. The axoneme arises from the blepharoplast, continues anteriorly along the outer border of the undulating membrane, and becomes a free flagellum at the anterior end. African trypanosomes divide by binary longitudinal fission (Fig 3.6).

## Life Cycle and Transmission

The life cycle of African trypanosomes is depicted in Figure 3.7. African trypanosomiasis is transmitted by males and females of several species of *Glossina*, the tsetse fly (Figs 3.8 and 3.9). A single fly can be infected with more than one species of trypanosome, and an infected fly remains infected for life.[13] The fly ingests trypomastigotes in a blood meal from an infected mammal. Once inside the fly, parasites have a life cycle of 3 to 5 weeks. Organisms multiply within the insect gut. They penetrate the epiperitropic space where they undergo binary fission, then migrate to the salivary glands where they first become epimastigotes that attach to microvilli of salivary epithelial cells by flagellipodia. While thus attached, epimastigotes develop successively into

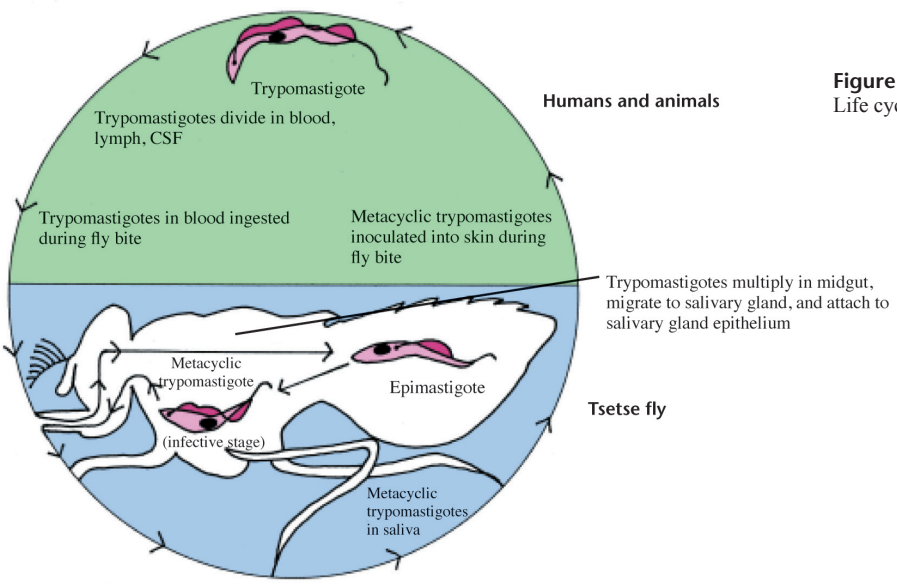



**Figure 3.7**
Life cycle of African trypanosomes.



**Figure 3.8**
Insectary-reared tsetse fly (*Glossina morsitans*) biting skin of rodent. At rest, wings are folded scissor-like over dorsum.

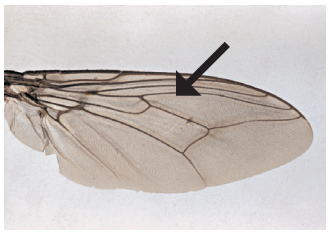


**Figure 3.9**
Tsetse-fly wing showing unique "hatchet" or "cleaver" cell venation (arrow).

premetacyclic, then nascent metacyclic trypomastigotes. In the final stage, mature metacyclic trypomastigotes detach from salivary epithelial cells and are free in the saliva.[14] When the fly takes another blood meal (Fig. 3.8) mature metacyclic trypomastigotes (the infective stage) in the fly's saliva are inoculated into a new host. Infection can be established by as few as 10 trypanosomes. The parasites remain at the bite site for 1 or 2 days, during which time they multiply and begin to spread to the host's blood and extracellular fluids. Some enter interstitial elements of tissues, especially in the lymph nodes and brain, where they multiply rapidly by binary fission. Intracellular forms (amastigotes) similar to those of *Trypanosoma cruzi* have been reported in the choroid plexus of experimentally infected rodents,[15,16] but have never been demonstrated in human tissue.

*Trypanosoma brucei gambiense* can infect domestic animals such as pigs, goats, and sheep, but humans are the most significant host.[17] In humans, *T. b. gambiense* causes a chronic infection that can last for years, allowing infected travelers to introduce sleeping sickness into areas previously free of the disease. Infection with *T. b. rhodesiense* is more rapidly fatal and therefore less likely to spread to nonendemic areas. Wild game animals such as bushbucks and hartebeests are the natural hosts of *T. b. rhodesiense*, although carnivores, cattle, and some other ungulates also serve as hosts.

Trypanosomes can cross the placenta and infect the fetus, causing abortion, stillbirth, or neonatal death.[18] They are rarely transmitted by laboratory accident, blood transfusion, or organ transplantation.

## Clinical Features and Pathogenesis

African trypanosomiasis has been described as a disease of exceptions because its clinical picture is protean. Asymptomatic carriers of both *T. b. gambiense* and *T. b. rhodesiense* have been recorded,[19] but without treatment, virtually all patients with African trypanosomiasis die. Gambian and Rhodesian trypanosomiasis have similar clinical features, but differ significantly in the course of disease. Rhodesian trypanosomiasis becomes symptomatic 1 to 3 weeks after infection, develops rapidly, is more disabling, and often causes death within 3 to 6 months in an untreated patient. Gambian trypanosomiasis causes chronic infection with a more prolonged course (Fig 3.10). Classically, both forms of the disease develop in 3 clinical stages: chancre (Fig 3.11), hemolymphatic invasion, and meningoencephalitis.[20] Chancres are more common in Rhodesian than in Gambian trypanosomiasis, but this stage is often bypassed.

A tsetse-fly bite can be painful and may incite almost immediate inflammation. Between 20% and 50% of patients develop a chancre at the site of inoculation 1 to 2 weeks



**Figure 3.10**
Moribund, emaciated Congolese in terminal stage of Gambian trypanosomiasis.



**Figure 3.11**
Trypanosomal chancre in American who traveled to East Africa. Patient developed severe Rhodesian trypanosomiasis.

after being bitten (Fig 3.11).[21] Initially, the chancre is a cutaneous nodule up to 4 cm in diameter, which may ulcerate and persist for 2 to 3 weeks, then resolve spontaneously. At this stage, differential diagnosis includes various cutaneous nodular lesions, including anthrax or tick bite associated with *Rickettsia conorii* infection.

The chancre is followed by a hemolymphatic stage, during which parasites disseminate through the lymph nodes, lymphatic system, and bloodstream. Symptoms include fever, malaise, generalized rash, headache, myalgia, arthralgia, pruritus, transient (mostly facial) edema, lymphadenopathy (Fig 3.12) splenomegaly, and hepatomegaly. In patients with Rhodesian trypanosomiasis, this stage may be fulminant, following development of the chancre by only a few days. Lymphadenopathy is common in both Rhodesian and Gambian trypanosomiasis, but enlargement of the posterior cervical lymph nodes (Winterbottom's sign) is typical of the Gambian form (Fig 3.12). It is considered a sign of peripheral trypanosomiasis without cerebral involvement; however, there is evidence of a connection between these lymph nodes and the ventricles of the brain.[22] Lymphadenopathy associated with the Rhodesian form is often more generalized and more frequently accompanied by hepatosplenomegaly. Some patients with Rhodesian trypanosomiasis die at this stage, before the central nervous system (CNS) becomes involved; in other patients the hemolymphatic and meningoencephalitic stages overlap.

The meningoencephalitic, or neurologic, stage begins when the parasite crosses the blood-brain barrier into the CNS. Rhodesian trypanosomiasis progresses to this phase 3 weeks to 2 months after infection.[23] Sleep cycle disturbances are a hallmark of the disease and the source of the term sleeping sickness. Other symptoms include headache, sensory disturbances, poor coordination, and mental and physical lethargy. Psychological and behavioral changes may precede clinical neurologic signs such as tremor, fasciculation, athetosis, cerebellar ataxia, and signs of meningitis or encephalitis. There are few focal neurologic signs, such as cranial nerve palsies, and seizures are rare. Patients who do not receive treatment before the onset of the terminal phase of disease experience irreversible neurological damage. Mask-like facies develop and patients become increasingly obtunded. Loss of consciousness, coma, and death follow, often as a result of pneumonia or other complications of coma (Fig 3.10). The fatality rate for patients who receive optimal treatment is approximately 6%.[23]

Adult female patients may experience menstrual disturbances, infertility, and spontaneous abortions; adult male patients may become impotent.[18] Specific trypanosomal myocarditis is more common and more severe in the Rhodesian form, but the diagnosis is usually not established until the patient's tachycardia, hypotension, and congestive heart failure are reversed by specific antitrypanosomal therapy. Some patients have electrocardiographic abnormalities.[24]

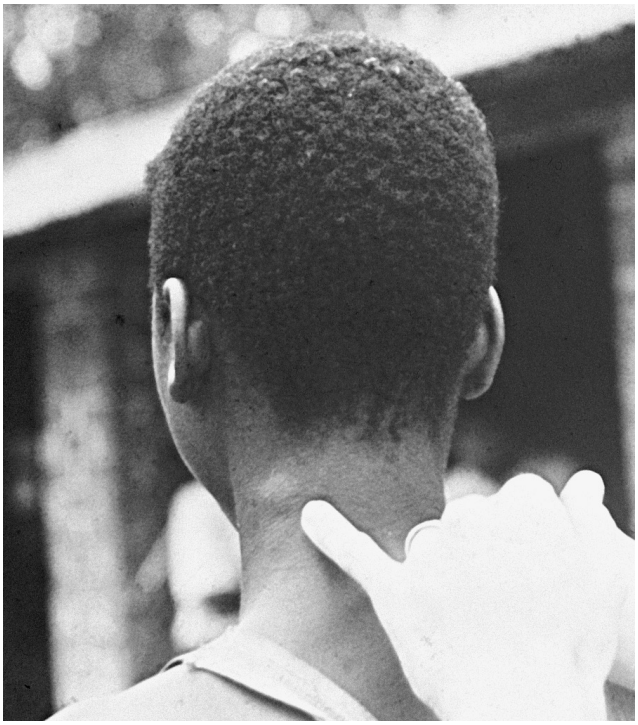


**Figure 3.12**
Cervical lymphadenopathy in Gambian trypanosomiasis (Winterbottom's sign).

Clinical laboratory findings include normochromic normocytic anemia,[25] thrombocytopenia,[26] granulocytopenia, and elevated sedimentation rate and immunoglobulins, especially IgM. The CSF contains increased protein and mononuclear cells (about 5% of which are plasma cells), and often trypanosomes. The majority of lymphocytes in the CSF are B-cells.[27]

Most animal trypanosomes are lysed effectively in the human bloodstream and do not cause disease.[28] A high percentage of trypanosomes that are pathogenic for humans are removed from the bloodstream by macrophages in the liver.

Trypanosomes escape the host immune response by a variety of mechanisms.[29] *Trypanosoma brucei gambiense* and *T. b. rhodesiense* evade the human immune system by periodically changing their variable surface glycoprotein (VSG) through a complex and poorly understood genetically controlled mechanism.[30-32] VSG stimulates a pronounced proliferation of B-lymphocytes, first within lymph nodes and then within the brain and meninges, resulting in marked hypergammaglobulinemia dominated by IgM and antibodies that lyse trypomastigotes. Antigen-antibody complexes circulate and may be deposited in tissues.[20] New insights gained into the role lipids play in various biological processes have shown apolipoprotein L-1 (ApoL-1) as an intracellular trigger of trypanolysis through the formation of anionic pores on lysosomal membranes that allow the massive influx of chloride ions from the blood stream

into the lysosome causing uncontrolled swelling and the ultimate death of the parasite, thus providing an alternative mechanism for the host to reduce the circulating trypanosome burden.[33] Neutralization of the ApoL-1 effect has been shown to be the dominant factor by which *T.b. rhodesiense* resists trypanolysis. In addition the number of organisms in the bloodstream varies in cycles lasting several days, corresponding to changes in the antigenicity of the VSG, which allows trypanosomes to evade the thymus-dependent humoral response. Transfer of VSG from trypanosomes to host cells, such as erythrocytes, may contribute to pathogenic effects such as anemia.[25] The parasite causes generalized host immunosuppression. Thrombocytopenia may be a result of splenomegaly or, in some patients, disseminated intravascular coagulopathy.[26] HIV infection does not appear to have a significant impact on the risk of infection with *T. b. gambiense*.[34]

The immune response produces cytokines and nitric oxide that damage pericytes and break down the blood-brain barrier, allowing inflammatory cells and trypomastigotes to invade perivascular spaces.[35-38] Encephalitis causes demyelinization which, in certain areas of the brain, results in derangement of the internal "clock" that regulates sleeping and waking. The term sleeping sickness refers to this disruption of normal circadian rhythms.[39]

## *Pathologic Features*

Histologic examination of the chancre shows lymphocytic vasculitis involving the dermal blood vessels, plump proliferating endothelial cells, and an intense perivascular mononuclear cell infiltrate with occasional eosinophils. There is marked dermal edema, with necrosis and fibroblast proliferation. In some cases there is mild hyperkeratosis or superficial ulceration of the overlying epidermis. Trypanosomes have been demonstrated in skin biopsy specimens and touch preparations.[40] Rare trypomastigotes may be seen multiplying in the interstitium at the inoculation site.

Although several organs may show gross and microscopic changes, these findings are not pathognomonic. Lymph nodes are grossly enlarged. In the early stages of disease there are prominent germinal centers, follicular hyperplasia, sinus histiocytosis, lymphophagocytosis (Fig 3.13), and numerous plasma cells with occasional Russell bodies, which are globules of immunoglobulin (usually IgM) approximately 3 µm in diameter. There may be focal intranodal hemorrhages. In later stages, lymph nodes may shrink, become fibrotic and lymphocyte-depleted, (Fig 3.14) and demonstrate lymphophagocytosis. Cytologic examination of node imprints may show large numbers of organisms. The spleen may be moderately enlarged. Red pulp is congested and white pulp has foci of histiocytic hyperplasia and lymphophagocytosis, areas of necrosis 2 mm to 5 mm in diameter, and occasional giant cells (Figs 3.15 & 3.16).

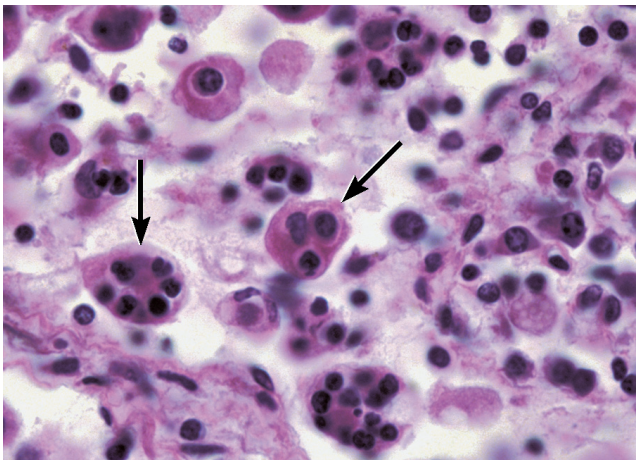


**Figure 3.13**
Lymphophagocytosis (arrows) in histiocytic infiltrate in lymph node from an 18-year-old Zambian female who died of Rhodesian trypansomiasis. x700

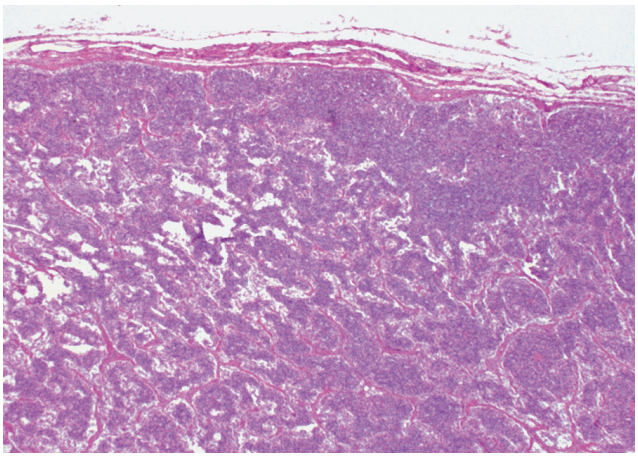


**Figure 3.14**
Follicular atrophy and histiocytic hyperplasia in lymph node from patient described in Figure 3.13. x15

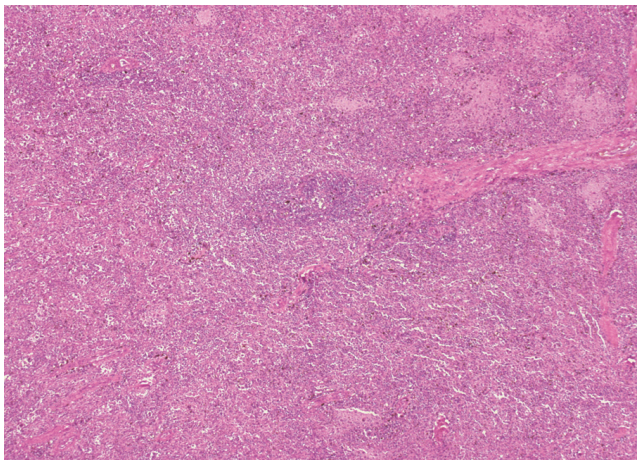


**Figure 3.15**
Spleen of patient described in Figure 3.13. White pulp is reduced and there is histiocytic hyperplasia. x28

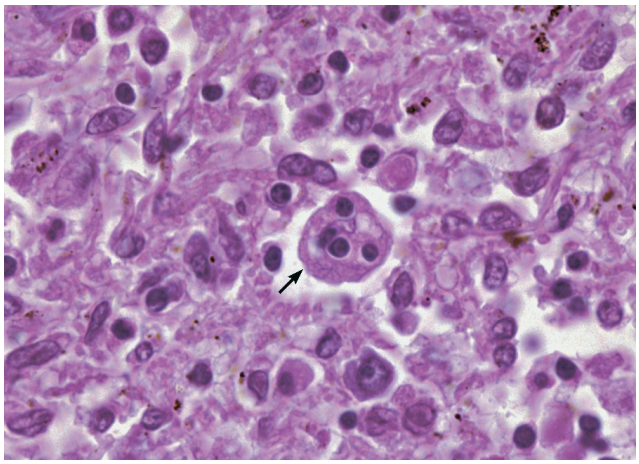


**Figure 3.16**
Lymphophagocytosis (arrow) in spleen shown in Figure 3.15. x700

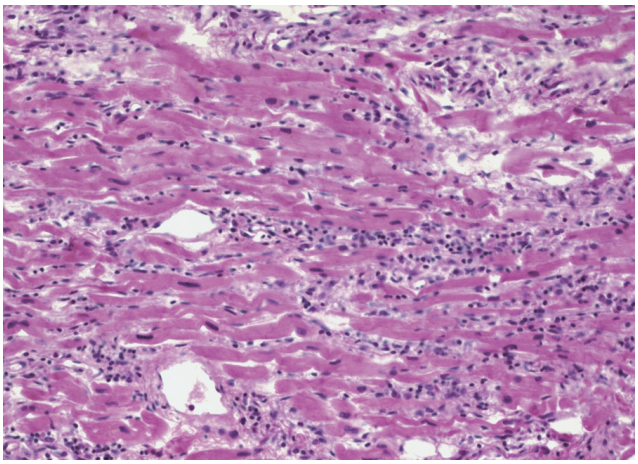


**Figure 3.17**
Myocarditis in patient described in Figure 3.13. Infiltrating cells are lymphocytes, histiocytes, and plasma cells. There are no eosinophils. Scattered areas of myocytolysis are seen. x140

Although trypanosomes are commonly found in blood, they are rarely seen in tissue sections of any organ.

Cardiac changes, more common in Rhodesian trypanosomiasis, may include pericardial and subendocardial petechiae, thickened valves, endocardial thickening, and mild cardiac enlargement. Histologic sections reveal pancarditis with diffuse or focal infiltrates of lymphocytes, macrophages, and plasma cells, with no eosinophils (Fig 3.17). There may be areas of myocytolysis. In advanced infections, there are often irregular areas of fibrosis in the ventricular myocardium. Small endocardial granulomas with necrotic eosinophilic centers have been reported. Inflammation in the conduction system produces electrocardiographic changes and, at times, terminal cardiac insufficiency.[41] Pulmonary lesions specifically related to trypanosomiasis are not recorded, but at autopsy the lungs frequently show hypostatic pneumonia, a common terminal event in African trypanosomiasis. Pleural and pericardial effusions may contain trypanosomes and lymphocytes.

CNS findings are nonspecific and similar to those of viral encephalitis. The brain may be slightly swollen. Gross findings include perivascular sheathing, hyperemia, occasional ecchymoses, small infarcts,[42] expansion of the white matter, decrease in ventricular spaces, and evidence of herniation (Figs 3.18 & 3.19). Long-standing meningoencephalitis may result in ventricular dilatation caused by atrophy of the subcortical white matter, and meningeal thickening and opacification.

Microscopically, leptomeninges, Virchow-Robin spaces, and vessel walls are infiltrated by lymphocytes, plasma cells, and macrophages (Figs 3.20 to 3.23).[43] The cellular infiltrate typically contains scanty eosinophils. Dürck's nodes, which can be seen in sectioned gross specimens, represent compact lymphohistiocytic perivascular infiltration (Fig 3.24). Two cytologic abnormalities suggest Afri-

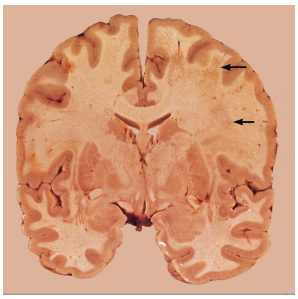


**Figure 3.18**
Coronal section of brain of Ugandan patient showing congestion of white matter and petechial hemorrhages (arrows).

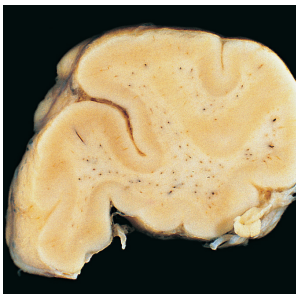


**Figure 3.19**
Section of cerebral cortex of Zambian patient with Rhodesian trypanosomiasis, showing marked congestion and scattered petechial hemorrhaging in white matter.

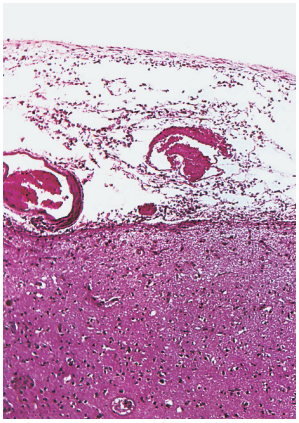


**Figure 3.20**
Cerebrum in Gambian trypanosomiasis showing congestion, edema, and chronic inflammatory cells in leptomeninges. x70

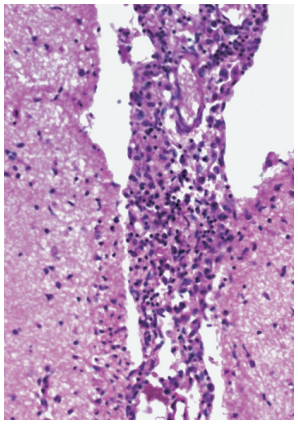


**Figure 3.21**
Chronic leptomeningitis in Rhodesian trypanosomiasis in patient described in Figure 3.13. Lymphocytes and histiocytes infiltrate the pia and arachnoid. x72

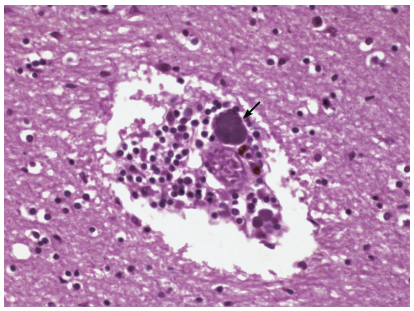


**Figure 3.22**
Rhodesian trypanosomiasis infection, showing Virchow-Robin space around cerebral blood vessel with lymphohistiocytic perivascular infiltration. Note morular cell (arrow) in infiltrate. x180

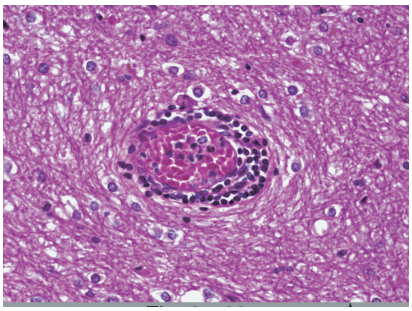


**Figure 3.23**
Lymphohistiocytic infiltration of Virchow-Robin space surrounding blood vessel (perivascular cuffing) in cerebellum in Rhodesian trypanosomiasis. x180

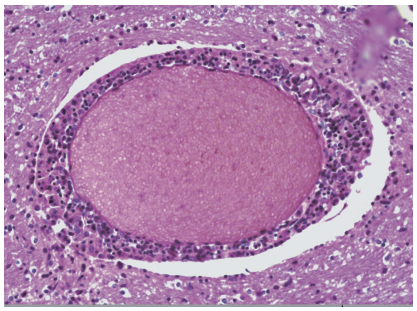


**Figure 3.24**
Compact lymphohistiocytic perivascular infiltration (often called Dürck's nodes) in brain in Rhodesian trypanosomiasis. x100

can trypanosomiasis, although they are not pathognomonic: lymphophagocytosis and morular Mott cells, which are plasma cells whose cytoplasm is distended up to 20 µm in diameter by Russell bodies (Figs 3.22 & 3.25 to 3.27).[44] Gliosis, marked by proliferation of microglial rod cells and gemistocytes, is prominent, especially in the superficial cortex, basal ganglia, and brain stem (Figs 3.28 & 3.29). In contrast, demyelinization with reactive astrocytosis is minimal, focal, and perivascular. In chronic disease, there is focal hemorrhage and destruction of neurons. Careful examination may very rarely reveal organisms in the Virchow-Robin spaces. Involvement of the brain stem, choroid plexus, spinal cord, cranial nerves, and peripheral nerves have been reported.[42]

## *Diagnosis*

Early diagnosis reduces the risk of transmission and irreversible neurologic disorders. Clinical diagnosis of

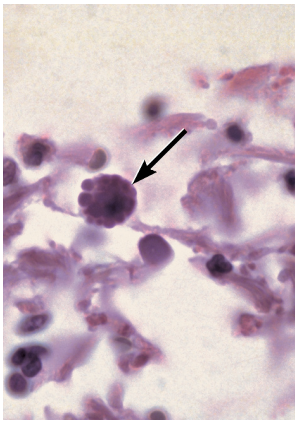


**Figure 3.25**
Morular cell (arrow) in leptomeninges of 16-year-old female from Burundi who died of Rhodesian trypanosomiasis. Nucleus of original plasma cell is visible in morular cell. x640

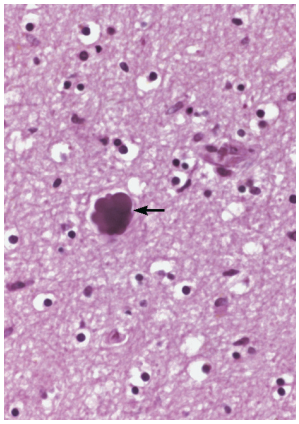


**Figure 3.26**
Morular cell (arrow) in parenchyma of brain of 35-year-old Congolese male who died of trypanosomiasis. x270

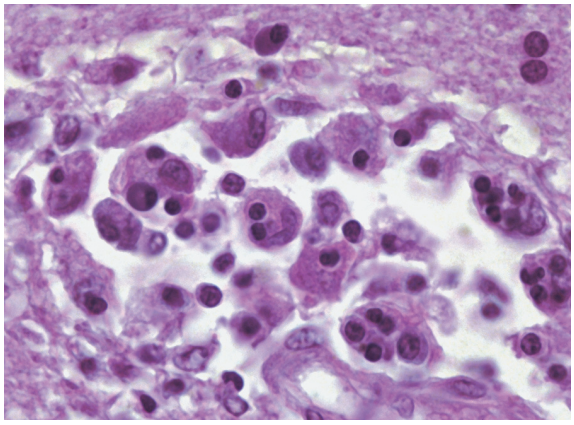


**Figure 3.27**
Focus of histiocytic infiltrate in brain of patient described in Figure 3.13, demonstrating lymphophagocytosis in Rhodesian trypanosomiasis. x625

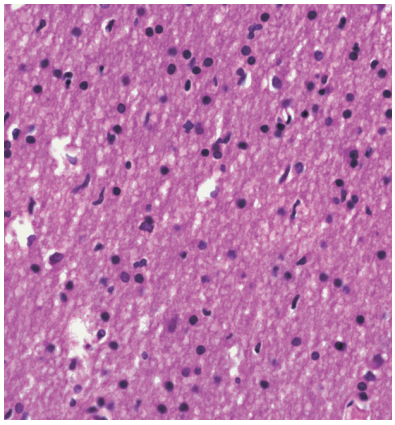


**Figure 3.28**
Microglial proliferation in brain of patient described in Figure 3.13 with Rhodesian trypanosomiasis. x230

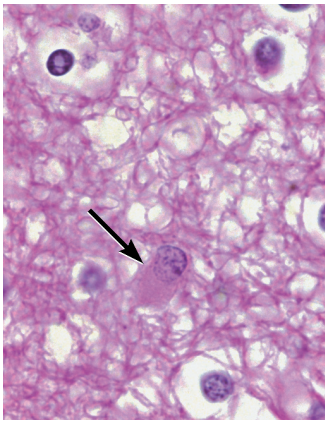


**Figure 3.29**
Gemistocytic astrocyte (arrow) in Rhodesian trypanosomiasis. Note eccentric nucleus and swollen cell body. x630

African trypanosomiasis is based on symptoms and a history of residence in or travel to an endemic area. The long, asymptomatic first phase of Gambian trypanosomiasis makes early diagnosis difficult. Elevated levels of serum IgM are not considered diagnostic; however, increased IgM titers in CSF, a leukocyte count above 5 cells/mm$^3$, and a total protein level greater than 40 mg/100 ml are highly suggestive of CNS involvement.[45-47]

Definitive diagnosis depends on microscopic identification of the parasite. In the early stage of disease, diagnosis is confirmed by demonstrating trypanosomes in films of peripheral blood or in aspirates of the chancre, enlarged lymph nodes, or bone marrow. Because the number of parasites in peripheral blood varies cyclically, several blood samples should be taken at various times. Thick and thin blood films should be studied and smears should be fixed and stained with Giemsa (Figs 3.30 & 3.31). Motile trypanosomes can be identified in an unstained wet preparation. Concentration by centrifugation or ultracentrifugation may increase the yield and simplify the search for parasites. Methods used on centrifuged blood samples include examination of the buffy coat, minianion-exchange column, and the quantitative buffy coat (QBC®) technique.[48,49] Giemsa-stained touch preparations of excised lymph nodes may permit early identification of the parasite. In the late stage of disease, organisms may be observed in the sediment of centrifuged CSF. In vitro culture and animal inoculation techniques have had limited use. Antigen detection and DNA assays are being developed.[46,50,51]

Serologic tests are not clinically useful because of their variable sensitivity and specificity. Cutaneous leishmaniasis or exposure to nonpathogenic trypanosomes may cause false positive serologic findings.[52] A further limiting factor is that, in Rhodesian trypanosomiasis, seroconversion takes place 2 to 4 weeks after the onset of clinical symptoms. Serologic tests are sometimes useful for epidemiologic surveys or screening for Gambian trypanosomiasis. Tests to determine antibody levels in serum and CSF include the card agglutination trypanosomiasis test (CATT), rapid latex agglutination test, indirect immunofluorescence test, and ELISA.[53-55]

Clinical signs and symptoms of African trypanosomiasis must be distinguished from those of reactive arsenical encephalopathy, a complication of treatment with melarsoprol.

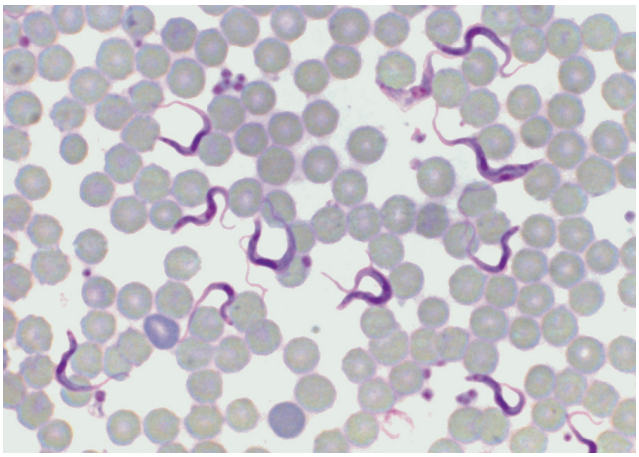


**Figure 3.30**
Giemsa-stained thin blood film from patient with early Gambian trypanosomiasis, demonstrating heavy parasitemia of trypomastigotes. Giemsa x680

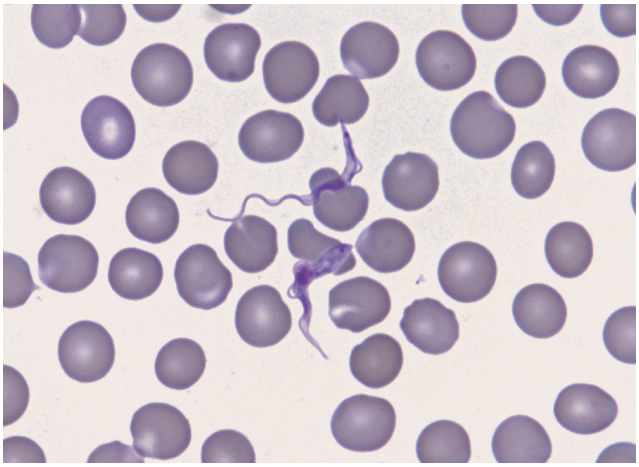


**Figure 3.31**
Giemsa-stained thin blood film from patient with Rhodesian trypanosomiasis, showing long (upper) and short forms of *Trypanosoma brucei rhodesiense*. Giemsa x990

## *Treatment and Prevention*

When diagnosed early, African trypanosomiasis has a high cure rate. The type of treatment depends on the phase of disease. Pentamidine isethionate is used to treat the initial phase of Gambian trypanosomiasis and for chemoprophylaxis or early CNS involvement.[56] Suramin is used for the initial phase of Rhodesian trypanosomiasis. Melarsoprol (Arsobal®, Mel B®), the only available drug that can cross the blood-brain barrier, is used to treat advanced stages of both Gambian and Rhodesian trypanosomiasis. This drug is an arsenical derivative that can have drastic side effects, including seizures associated with acute cerebral edema, rapidly progressive coma without seizures, or acute nonlethal mental disturbances without neurological signs. Reactive arsenical encephalopathy, characterized by acute vasculitis, can occur in either the hemolymphatic or meningoencephalitic stage and is fatal in up to 38% of patients.[43,57] In parts of Central Africa nearly one third of patients are infected with parasites that are resistant to melarsoprol. For Gambian trypanosomiasis, eflornithine (DMFO, Ornidyl®) administered orally or intravenously for 14 days is more effective and has fewer adverse effects than other medications.[58] Nifurtimox – eflornithine in combination has been proposed as an effective regimen for second-stage *Trypanosoma brucei*

*gambiense*.[59] The pharmaceutical industry had suspended production of eflornithine for commercial reasons, but through a cooperative effort between public and private entities, the drug is once again available for distribution in endemic countries.[60] Nifurtimox (Lampit®) is effective against arsenical-resistant Gambian trypanosomiasis.[34]

There is no available vaccine against African trypanosomiasis.[61] Besides vector control, the only preventive measure is to avoid tsetse-fly bites, bearing in mind that the flies feed during the day, are unaffected by insect repellents, and can bite through lightweight clothing.

## References


1. Steverding D. The history of African trypanosomiasis. *Parasit Vectors.* 2008;1:3.
2. Scaravilli F. Parasitic and fungal infections. In: Adams JH, Duchen LW, eds. *Greenfield's Neuropathology*. 5th ed. New York: Oxford University Press; 1992:400-446.
3. Mettler CC. Medicine: nineteenth century. In: Mettler FA, ed. *History of Medicine*. Philadelphia, Pa: Blakiston; 1947:423-476.
4. Livingstone D. *Missionary Travels and Researches in South Africa*. New York: Harper and Bros; 1858.
5. Garrison FH. *An Introduction to the History of Medicine*. 4th ed. Philadelphia, Pa: WB Saunders; 1929:706.
6. Baker JR. The subspecific taxonomy of *Trypanosoma brucei*. *Parasite*. 1995;2:3-12.
7. Control and surveillance of African trypanosomiasis. Report of a WHO Expert Committee. *World Health Organ Tech Rep Ser.* 1998;881:I-VI, 1-114.
8. Seed JR. Current status of African trypanosomiasis. *ASM News*. 2000;66:395-402.
9. Van Nieuwenhove S, Betu-Ku-Mesu VK, Diabakana PM, Declercq J, Bilenge CM. Sleeping sickness resurgence in the DRC: the past decade. *Trop Med Int Health*. 2001;6:335-341.
10. Berrang-Ford L, Lundine J, Breau S. Conflict and human African trypanosomiasis. *Soc Sci Med*. 2011;72:398-407.
11. Hide G. History of sleeping sickness in East Africa. *Clin Microbiol Rev.* 1999;12:112-125.
12. Case records of the Massachusetts General Hospital. Weekly clinicopathological exercises. Case 20-2002. A 37-year-old man with fever, hepatosplenomegaly, and a cutaneous foot lesion after a trip to Africa. *N Engl J Med*. 2002;346:2069-2076.
13. Majiwa PA, Otieno LH. Recombinant DNA probes reveal simultaneous infection of tsetse flies with different trypanosome species. *Mol Biochem Parasitol*. 1990;40:245-253.
14. Noble ER, Noble GA, Schad GA, MacInnes AJ. Introduction to the protozoan group; phylum Zoomastigina. In: *Parasitology: The Biology of Animal Parasites.* 6th ed. Philadelphia, Pa: Lea & Febiger; 1989:25-64.
15. Abolarin MO, Evans DA, Tovey DG, Ormerod WE. Cryptic stage of sleeping-sickness trypanosome developing in choroid plexus epithelial cells. *Br Med J*. 1982;285:1380-1382.
16. Ormerod WE, Venkatesan S. An amastigote phase of the sleeping sickness trypanosome. *Trans R Soc Trop Med Hyg*. 1971;65:736-741.
17. Njiokou F, Nimpaye H, Simo G, et al. Domestic animals as potential reservoir hosts of *Trypanosoma brucei gambiense* in sleeping sickness foci in Cameroon. *Parasite.* 2010;17:61-66.
18. Ikede BO, Elhassan E, Akpavie SO. Reproductive disorders in African trypanosomiasis: a review. *Acta Trop*. 1988;45:5-10.
19. Wurapa FK, Dukes P, Njelesani EK, Boatin B. A "healthy carrier" of *Trypanosoma rhodesiense*: a case report. *Trans R Soc Trop Med Hyg*. 1984;78:349-350.
20. Greenwood BM, Whittle HC. The pathogenesis of sleeping sickness. *Trans R Soc Trop Med Hyg*. 1980;74:716-725.
21. Nadjm B, Van Tulleken C, Macdonald D, Chiodini PL. East African trypanosomiasis in a pregnant traveler. *Emerg Infect Dis*. 2009;15:1866-1867.
22. Ormerod WE. Hypothesis: the significance of Winterbottom's sign. *J Trop Med Hyg*. 1991;94:338-340.
23. Odiit M, Kansiime F, Enyaru JC. Duration of symptoms and case fatality of sleeping sickness caused by *Trypanosoma brucei rhodesiense* in Tororo, Uganda. *East Afr Med J*. 1997;74:792-795.
24. Jones IG, Lowenthal MN, Buyst H. Electrocardiographic changes in African trypanosomiasis caused by *Trypanosoma brucei rhodesiense*. *Trans R Soc Trop Med Hyg*. 1975;69:388-395.
25. Rifkin MR, Landsberger FR. Trypanosome variant surface glycoprotein transfer to target membranes: a model for the pathogenesis of trypanosomiasis. *Proc Natl Acad Sci U S A*. 1990;87:801-805.
26. Robins-Browne RM, Schneider J, Metz J. Thrombocytopenia in trypanosomiasis. *Am J Trop Med Hyg*. 1975;24:226-231.
27. Greenwood BM, Whittle HC, Oduloju KO, Dourmashkin RR. Lymphocytic infiltration of the brain in sleeping sickness. *Br Med J*. 1976;2:1291-1292.
28. Rifkin MR. *Trypanosoma brucei*: some properties of the cytotoxic reaction induced by normal human serum. *Exp Parasitol*. 1978;46:189-206.
29. Zambrano-Villa S, Rosales-Borjas D, Carrero JC, Ortiz-Ortiz L. How protozoan parasites evade the immune response. *Trends Parasitol*. 2002;18:272-278.
30. Rudenko G. Genes involved in phenotypic and antigenic variation in African trypanosomes and malaria. *Curr Opin Microbiol*. 1999;2:651-656.
31. Vickerman K. Antigenic variation in trypanosomes. *Nature*. 1978;273:613-617.
32. Baral TN. Immunobiology of African trypanosomes: need of alternative interventions. *J Biomed Biotechno*. 2010;389153.
33. Pays E, Vanhollebeke B. Mutual self-defence: the trypanolytic factor story. *Microbes Infect*. 2008;10:985-989.
34. Pepin J, Ethier L, Kazadi C, Milord F, Ryder R. The impact of human immunodeficiency virus infection on the epidemiology and treatment of *Trypanosoma brucei gambiense* sleeping sickness in Nioki, Zaire. *Am J Trop Hyg*. 1992;47:133-140.
35. Chimelli L, Scaravilli F. Trypanosomiasis. *Brain Pathol*. 1997;7:599-611.
36. Pentreath VW. Royal Society of Tropical Medicine and Hygiene Meeting at Manson House, London, 19 May 1994. Trypanosomiasis and the nervous system. Pathology and immunology. *Trans R Soc Trop Med Hyg*. 1995;89:9-15.
37. Boda C, Courtioux B, Roques P, et al. Immunophenotypic lymphocyte profiles in human african trypanosomiasis. *PLoS One*. 2009;4(7): e6184. Doi 10.1371/journal.pone.0006184
38. Guilliams M, Movahedi K, Bosschaerts T, et al. IL-10 dampens TNF/inducible nitric oxide synthase-producing dendritic cell-mediated pathogenicity during parasitic infection. *J Immunol*. 2009;182:1107-1118.
39. Buguet A, Bert J, Tapie P, et al. Sleep-wake cycle in human African trypanosomiasis. *J Clin Neurophysiol*. 1993;10:190-196.
40. McGovern TW, Williams W, Fitzpatrick JE, Cetron MS, Hepburn BC, Gentry RH. Cutaneous manifestations of African trypanosomiasis. *Arch Dermatol*. 1995;131:1178-1182.
41. Poltera AA, Cox JN. Pancarditis with valvulitis in endomyocardial fibrosis (= emf) and in human African trypanosomiasis (= hat). A comparative histological study of four Ugandan cases. *Virchows Arch A Pathol Anat Histol*. 1977;375:53-70.
42. Poltera AA, Owor R, Cox JN. Pathological aspects of human African trypanosomiasis (HAT) in Uganda. A post-mortem survey of fourteen cases. *Virchows Arch A Pathol Anat Histol*. 1977;373:249-265.
43. Haller L, Adams H, Merouze F, Dago A. Clinical and pathological aspects of human African trypanosomiasis (*T. b. gambiense*) with particular reference to reactive arsenical encephalopathy. *Am J Trop Med Hyg*. 1986;35:94-99.
44. Mott FW. Observations on the brains of men and animals infected with various forms of trypanosomes: preliminary note. *Proc R Soc*. 1905;76:235-242.
45. Miezan TW, Meda HA, Doua F, Yapo FB, Baltz T. Assessment of central nervous system involvement in gambiense trypanosomiasis: value of the cerebro-spinal white cell count. *Trop Med Int Health*. 1998;3:571-575.
46. Truc P, Jamonneau V, Cuny G, Frezil JL. Use of polymerase chain reaction in human African trypanosomiasis stage determination and follow-up. *Bull World Health Organ*. 1999;77:745-748.
47. Whittle HC, Greenwood BM, Bidwell DE, Bartlett A, Voller A. IgM and antibody measurement in the diagnosis and management of Gambian trypanosomiasis. *Am J Trop Med Hyg*. 1977;26:1129-1134.
48. Bailey JW, Smith DH. The quantitative buffy coat for the diagnosis of trypanosomes. *Trop Doct*. 1994;24:54-56.
49. Camara M, Camara O, Ilboudo H, et al. Sleeping sickness diagnosis: use of buffy coats improves the sensitivity of the mini anion exchange centrifugation test. *Trop Med Int Health*. 2010;15:796-799.
50. Brun R, Blum J, Chappuis F, Burri C. Human African trypanosomiasis. *Lancet.* 2010;375:148-159.

51. Matovu E, Kuepfer I, Boobo A, Kibona S, Burri C. Comparative detection of trypanosomal DNA by loop-mediated isothermal amplification and PCR from flinders technology associates cards spotted with patient blood. *J Clin Microbiol*. 2010; 48:2087-2090.

52. Van Meirvenne N, Le Ray D. Diagnosis of African and American trypanosomiases. *Br Med Bull*. 1985;41:156-161.

53. Jamonneau V, Truc P, Garcia A, Magnus E, Buscher P. Preliminary evaluation of LATEX/T. b. gambiense and alternative versions of CATT/*T. b. gambiense* for the serodiagnosis of human African trypanosomiasis of a population at risk in Cote d'Ivoire: considerations for mass-screening. *Acta Trop*. 2000;76:175-183.

54. Lejon V, Buscher P, Magnus E, Moons A, Wouters I, Van Meirvenne N. A semi-quantitative ELISA for detection of *Trypanosoma brucei gambiense* specific antibodies in serum and cerebrospinal fluid of sleeping sickness patients. *Acta Trop*. 1998;69:151-164.

55. Radwanska M. Emerging trends in the diagnosis of Human African Trypanosomiasis. *Parasitology*. 2010;12:1-10.

56. Doua F, Miezan TW, Sanon Singaro JR, Boa Yapo F, Baltz T. The efficacy of pentamidine in the treatment of early-late stage *Trypanosoma brucei gambiense* trypanosomiasis. *Am J Trop Med Hyg*. 1996;55:586-588.

57. Blum J, Nkunku S, Burri C. Clinical description of encephalopathic syndromes and risk factors for their occurrence and outcome during melarsoprol treatment of human African trypanosomiasis. *Trop Med Int Health*. 2001;6:390-400.

58. Pepin J, Khonde N, Maiso F, et al. Short-course eflornithine in Gambian trypanosomiasis: a multicentre randomized controlled trial. *Bull World Health Organ*. 2000;78:1284-1295.

59. Priotto G, Kasparian S, Mutombo W, et al. Nifurtimox-eflornithine combination therapy for second-stage African *Trypanosoma brucei gambiense* trypanosomiasis: a multicentre, randomised, phase III, non-inferiority trial. *Lancet.* 2009;374:56-64.

60. Stich A, Abel PM, Krishna S. Human African trypanosomiasis. *Br Med J* .2002;325:203-206.

61. Magez S, Radwanska M. African trypanosomiasis and antibodies: implications for vaccination, therapy and diagnosis. *Future Microbio*. 2009;4:1075-1087

## *Acknowledgements*

**Figure 3.3**
Specimen contributed by LA Rosati

**Figure 3.4**
Specimen contributed by LA Rosati

**Figure 3.6**
Specimen contributed by LA Rosati

**Figure 3.9**
Clay-Adams Medichrome Series

**Figure 3.10**
Contributed by Richard P Strong

**Figure 3.11**
National Museum of Health and Medicine #02-0668

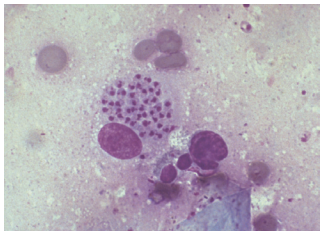
**Figure 3.12**
National Museum of Health and Medicine #54-13845

**Figure 3.14**
Specimen contributed by R Purohit

**Figure 3.30**
Specimen contributed by LR Ash

**Figure 3.31**
Specimen contributed by LA Rosate







4

# Cutaneous Leishmaniasis

*Alan J. Magill, Wayne M. Meyers, Ronald C. Neafie, and Mary K. Klassen-Fischer*

## *Introduction*

### Definition

The cutaneous leishmaniases include a spectrum of self-healing and chronic disease forms caused by protozoan parasites of the genus *Leishmania*. Clinical presentations differ according to parasite burden and host immune response.[1] Although there can be considerable overlap of clinical presentations, 5 distinct cutaneous syndromes are recognized in *Leishmania* infections: 1) simple or localized ulcerative or nodular cutaneous leishmaniasis (CL); 2) mucosal leishmaniasis (ML); 3) leishmaniasis recidivans (LR); 4) diffuse cutaneous leishmaniasis (DCL); and 5) post-kala-azar dermal leishmaniasis (PKDL). Immunocompromised patients may have atypical presentations.[2]

Oligoparasitic (low parasite burden) syndromes are chronic, persistent infections that follow primary ulcerative disease (ML and LR) or drug therapy for kala-azar (early forms of PKDL). Polyparasitic syndromes such as ulcerative and nodular CL, DCL, and late or nodular PKDL are characterized by a high parasite burden.

### Synonyms

The ulcers, nodules, and other cutaneous lesions caused by *Leishmania* sp are known around the world by a variety of descriptive or geographic terms. Cutaneous leishmaniasis (CL) has many colorful names, such as Aleppo sore, Baghdad boil, bouton d'orient, chiclero ulcer, Delhi boil, oriental sore, pian-bois, Sart sore, and uta. Mucosal leishmaniasis (ML) is also called mucocutaneous leishmaniasis and espundia. Leishmaniasis recidivans (LR) is known as chronic leishmaniasis or lupoid leishmaniasis. Diffuse cutaneous leishmaniasis (DCL) is sometimes referred to as disseminated cutaneous leishmaniasis, although disseminated CL is usually reserved for a syndrome described in Brazil.[3]

### General Considerations

In 1903, Wright described the leishmania parasite that causes CL.[4] He outlined the morphology of amastigotes found in the facial lesion of a young Armenian immigrant to the United States. Borovsky, a Russian bacteriologist, had given the first description of the parasite in an ulcerative lesion in 1898, but his report was not translated into English until 1938.[5,6] In 1908, Nicolle isolated the parasite in in-vitro culture from typical cutaneous lesions.[7] His description of the flagellate promastigote form of the parasite established the similarity of the leishmanias of CL and kala-azar. Carini, working in Brazil, first described leishmania parasites in palatal lesions in a patient with ML in 1911.[8] In Venezuela in 1948, Convit and Lapenta reported the first case of DCL.[9]

*Leishmania* sp traditionally carried markers related to clinical syndrome and geographic distribution (*Leishmania*

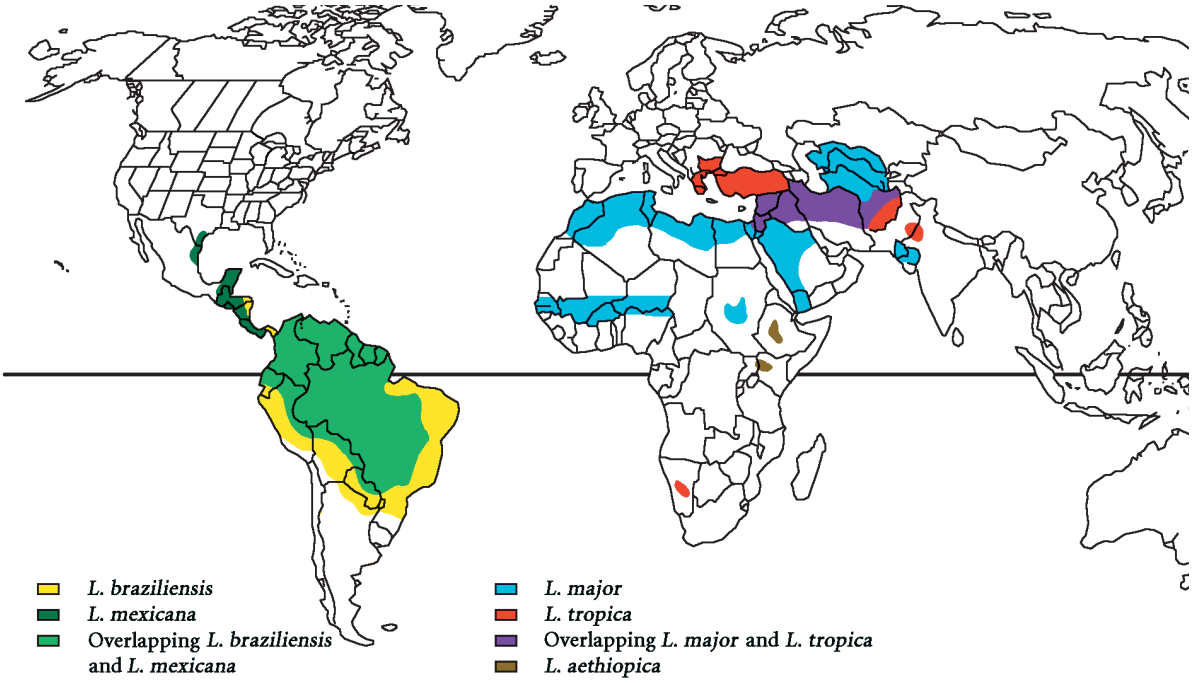



**Figure 4.1**
Geographical distribution of *Leishmania* sp

*braziliensis* as the cause of ML in the New World (Western); *Leishmania tropica* and *Leishmania major* as the cause of CL in the Old World (Eastern). However, beginning in the 1970s, descriptors such as biologic, immunologic, and biochemical characteristics of the parasite significantly changed the classification of leishmaniases. Isozyme electrophoresis has shown that no single *Leishmania* sp is uniquely associated with a clinical syndrome.[10] For example, *Leishmania amazonensis* has been isolated from individuals with ML, CL, DCL, and kala-azar in Brazil.[11] *Leishmania guyanensis* and *Leishmania panamensis* have been isolated from individuals with ML.[12,13] In the Old World, *L. tropica*, a particularly heterogeneous group of parasites,[14] has been isolated from individuals with kala-azar,[15-17] viscerotropic leishmaniasis,[18,19] febrile systemic illness,[20] and isolated lymphadenopathy. Diffuse cutaneous leishmaniasis is associated with parasites of the *Leishmania mexicana* complex in the New World and *Leishmania aethiopica* in the Old world. LR is most commonly associated with *L. tropica*. Post-kala-azar dermal leishmaniasis (PKDL) is seen with the *Leishmania donovani* complex, and ML with the *L. braziliensis* complex. Cutaneous leishmaniasis can be caused by any of the leishmanias.

## Epidemiology

Worldwide prevalence and annual incidence of the cutaneous leishmaniases are unknown with any certainty. The study of Ashford et al suggests that there are approximately 300,000 cases per year from a population of 200 million at risk.[21] Actual prevalence is probably higher because estimates in many countries are obtained by passive notification, not by active surveillance.[22] In endemic areas, small, minimally symptomatic lesions are frequently ignored or treated with traditional therapies such as burning with a hot iron or applying battery acid. When it is available, drug therapy at local clinics can be prohibitively expensive or not available, thus people with CL often do not seek treatment.

Excellent reviews of the geographic distribution of the cutaneous leishmaniases in the New World[23,24] and Old World[25] have been published. The cutaneous leishmaniases are endemic in 82 countries (Fig 4.1).[26] Cutaneous leishmaniasis is widely distributed in the Americas from southern Texas to northern Argentina. ML is most common in the jungles of Amazonia (especially in southern Brazil), but cases have been reported throughout the Americas. Most patients with DCL come from Brazil, the Dominican Republic, Ethiopia and Venezuela, but there are sporadic infections in Bolivia, Colombia, Honduras, Mexico, Peru, Kenya, and southern United States. Leishmaniasis recidivans (LR) is most common in the Middle East. PKDL is seen in India and East Africa (Kenya and the Sudan) following treatment of kala-azar with pentavalent antimony (SbV).

Residents of endemic areas with enzootic cycles between infected sandflies and nonhuman mammalian reservoir hosts are likely to be infected at an early age. Epidemics of

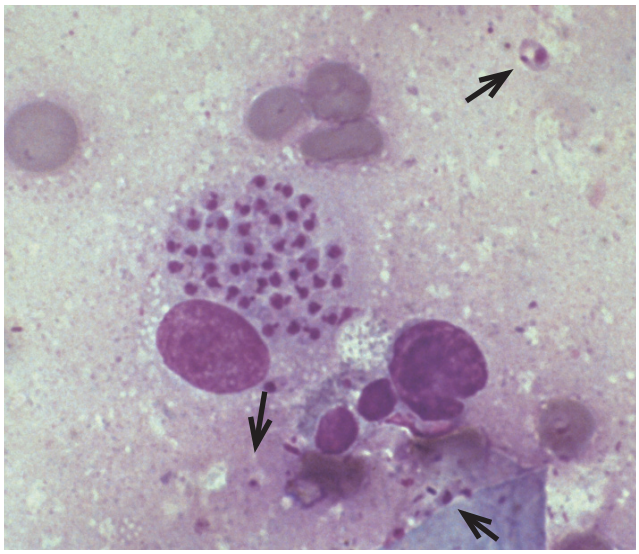


**Figure 4.2**
Smear of skin lesion demonstrating amastigotes within macrophage. Note also a few extracellular organisms (arrows). Giemsa x750



**Figure 4.3**
Female sandfly (*Lutzomyia longipalpis*) taking blood meal from human skin. Except for "V" position of wings over thorax, sandflies assume mosquito-like position while biting. Note erythema around bite site and sandfly's hairy body and wings.

CL frequently occur when a nonimmune population intrudes into a natural enzootic cycle. The population at highest risk for CL is nonimmune expatriates such as tourists, soldiers, new settlers, and construction or agricultural workers.[27,28] New development, construction, or agricultural projects and military operations are commonly accompanied by outbreaks. Socioeconomic factors, population growth, and migration also influence the epidemiology of CL.[29,30]

## *Infectious Agent*

### Morphologic Description

In human tissue, leishmanial parasites are in the amastigote form and multiply within histiocytes. Amastigotes are ovoid or round and 1.5 µm to 3 µm in diameter (Fig 4.2). They have a thin cell membrane, a relatively large nucleus, and a rod-shaped kinetoplast that is not always visible in tissue sections because of its orientation within the parasite.

### Life Cycle and Transmission

Promastigotes of *Leishmania* sp are motile and elongate, with a flagellum at the anterior end. Metacyclic promastigotes, the infective form of the parasite, are carried in the salivary glands of female sandflies (*Phlebotomus* sp in the Old World; *Lutzomyia* sp (Fig 4.3) and *Psychodopygus* sp in the New World) and transmitted to a host during a blood meal (Fig 4.4). Promastigotes attach to mononuclear phagocytes and enter host endosomes, which then fuse with lysosomes. Promastigotes transform into nonmotile, oval amastigotes with no free flagellum. Amastigotes persist and replicate by binary fission within the parasitophorous vacuole. The expanding vacuole nearly fills the cell, leading to lysis and cell death. Released daughter amastigotes attach to and penetrate other cells. When a sandfly ingests an infected cell, amastigotes transform into promastigotes, which live and develop extracellularly in the fly's alimentary tract and then migrate to the salivary glands.

Rarely, transmission is congenital, sexual, occupational, or bloodborne through transfusion or IV drug use.[31-34]

## *Clinical Features and Pathogenesis*

The typical lesion of ulcerative CL starts as a small, erythematous papule at the site where promastigotes are inoculated.[35] The incubation period is usually several weeks to months, but can be a few days or years. In most cases, within a few weeks the papule enlarges, crusts over, and breaks down into a slow-growing ulcer that may be several centimeters in diameter (Fig 4.5). As the ulcer grows, patients develop a delayed hypersensitivity (DH) reaction to leishmanial antigens. The ulcer is shallow and well-defined, with a raised erythematous border and central granulation tissue (Fig 4.6) Very rigorous cleaning and debridement is necessary to get to a clean ulcer base (Fig 4.7). Surrounding inflammation may be minimal or quite marked. The ulcer heals slowly, leaving a depressed, atrophic scar. Nodular presentations of cutaneous leishmaniases are not uncommon (Fig 4.8), Sporotrichoid presentations (Fig 4.9a) and satellite lesions (Fig 4.9b) are common. Hyperkeratotic lesions do not ulcerate. Lymph nodes proximal to lesions

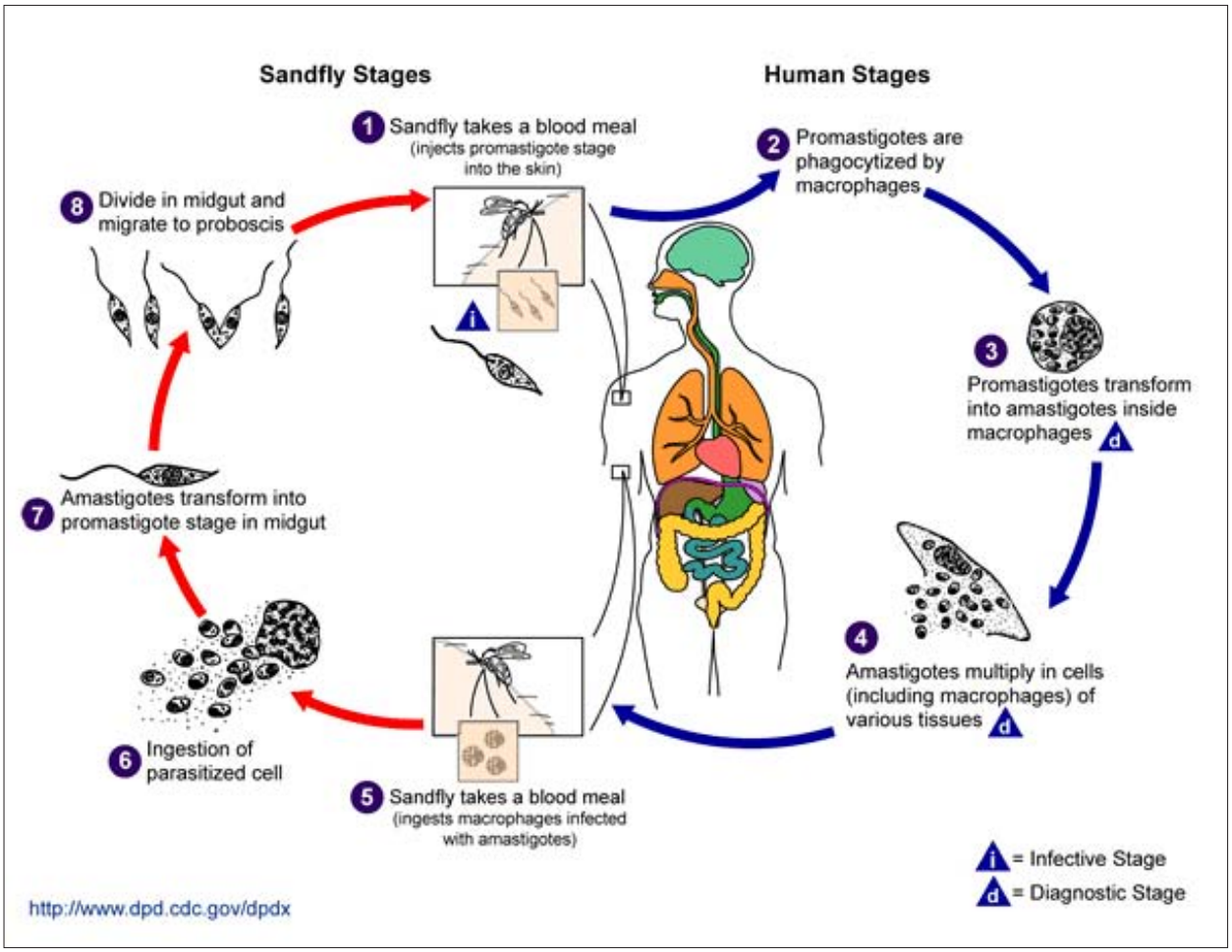



**Figure 4.4**
Life cycle of *Leishmania* sp in humans. Promastigotes enter skin as infected sandfly takes blood meal. Promastigotes transform into amastigotes that reproduce by binary fission in histiocytes. Ruptured histiocytes release amastigotes, which invade other histiocytes that are eventually ingested by a sandfly, repeating the cycle.

may be involved. Macules, papules, plaques (Figs 4.10 to 4.12), nodules (Fig 4.13), and psoriasiform, varicelliform, eczematous, and keloidal (Fig 4.14) lesions are uncommon, but have been reported. Lesions heal by scarring (Fig 4.15).

Mucosal leishmaniasis (ML) is a chronic, oligoparasitic syndrome associated with persistent and enhanced DH reaction to leishmanial antigens. This syndrome develops in up to 5% of individuals following primary ulcerative CL and is almost exclusively associated with *L. braziliensis* infection in the New World. Mucosal leishmaniasis is characterized by metastatic involvement of oro- and nasopharyngeal tissue following a primary ulcerative lesion. Patients may initially experience nosebleed, nasal congestion, and mucopurulent expectoration. Mucosal leishmaniasis progresses slowly over many years, destroying tissues of the nose, palate, uvula, and hypopharynx. Gross changes include septal perforations, irregular vegetative growths, and swelling (Fig 4.16). Crusted, vegetative, heavily infiltrated lessions may involve mucocutanous areas (Fig. 4.17) Leishmaniasis may rarely involve the perineum and adjacent areas (Fig 4.18). Late-stage ML is often accompanied by persistent cough and hoarseness. Extensive tissue destruction can compromise the respiratory tract and lead to pulmonary infections.

Leishmaniasis recidivans (LR) is also a chronic, oligoparasitic syndrome associated with persistent and enhanced DH reaction to leishmanial antigens. It is characterized by painless, recrudescing, brownish-red, lupoid nodules around the periphery of healed primary lesions (Fig 4.19). Leishmaniasis recidivans is most commonly associated with *L. tropica* infection and is seen in the Middle East.

Diffuse cutaneous leishmaniasis (DCL), an uncommon syndrome, is a chronic, polyparasitic syndrome associated with anergy to leishmanial antigen. It is characterized by disseminated nodules which are often prominent about the

head and neck (Figs 4.20 to 4.22a). Because of their gross clinical similarities, DCL and lepromatous leprosy are frequently mistaken for each other. Diffuse cutaneous leishmaniasis, however, lacks many of the cardinal features of lepromatous leprosy, such as madarosis (loss of eyelashes or brows), sensory changes, and changes of the major peripheral nerves. Furthermore, the nodules of lepromatous leprosy are usually firmer than those of DCL.

Post-kala-azar dermal leishmaniasis (PKDL) is a spectrum of dermatologic lesions, including macules, papules, and nodules, that develops during or following treatment of Indian or African kala-azar with SbV (Figs 4.22b & 4.22c) PKDL.[36,37] The initial lesions may resolve spontaneously over a few weeks or months, or develop into chronic papulonodular lesions with heavy parasite burdens. A patient with chronic lesions is a likely reservoir for anthroponotic (human-sand-fly-human) transmission.

Asymptomatic patients with latent infection can develop localized cutaneous lesions at the site of blunt, penetrating, or surgical trauma.[38,39] Immunosuppressed patients may develop disseminated cutaneous lesions.[13,40]



**Figure 4.5**
Chronic ulcer of cutaneous leishmaniasis (CL) in Nigerian boy. Ulcer is shallow with raised edges.

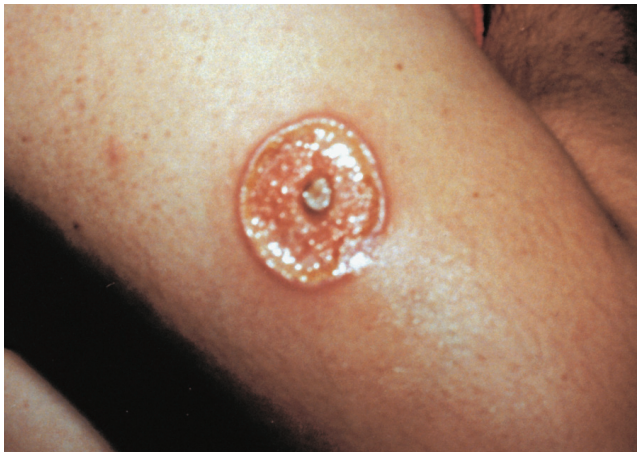


**Figure 4.6**
Early shallow ulcer of cutaneous leishmaniasis (CL) (4.5 cm in diameter) with raised edges and granulating center.



**Figure 4.7**
Shallow ulcer of cutaneous leishmaniasis (CL), 4.5 cm in diameter, with central granulation tissue and raised edges. Most likely this lesion had a crusty exudate on initial presentation.



**Figure 4.8**
Nodular, non-ulcerative presentation of cutaneous leishmaniasis (CL).



**Figure 4.9a**
Sporotrichoid presentation of cutaneous leishmaniasis (CL).



**Figure 4.9b**
Lesions of cutaneous leishmaniasis (CL) with multiple satellite papules on arm of Brazilian patient.



**Figure 4.10**
Plaques of cutaneous leishmaniasis cover nearly entire arm of Brazilian



**Figure 4.11**
Same patient as Figure 4.10, showing widespread papules and plaques of cutaneous leishmaniasis.

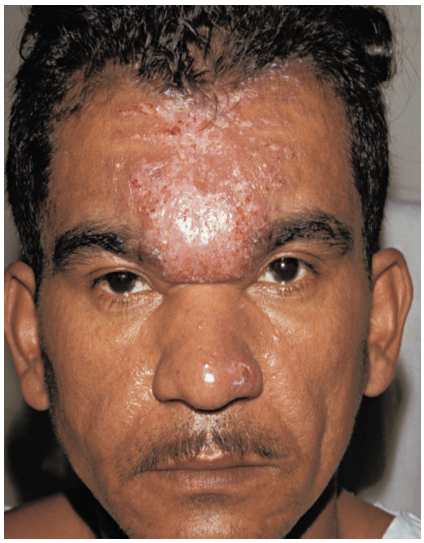


**Figure 4.12**
Maculopapular cutaneous leishmaniasis on forehead of Brazilian patient.



**Figure 4.13**
Ulcerated nodules of cutaneous leishmaniasis on nape of Brazilian patient.

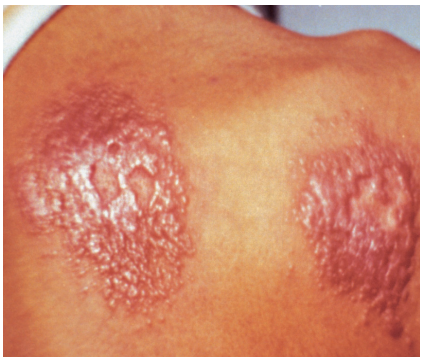


**Figure 4.14**
Yemenite patient with plaques of cutaneous leishmaniasis containing keloids.

## *Pathologic Features*

In early CL, epidermal changes include hyperkeratosis, basal cell degeneration, and epidermal hyperplasia, and may also consist of parakeratosis, pseudoepitheliomatous hyperplasia, follicular plugging, epidermal atrophy, acanthosis, and intraepidermal abscesses (Figs 4.23 to 4.26). In the dermis, where the inflammatory infiltrate consists of histiocytes, lymphocytes, and plasma cells (Fig 4.27), many intra- and extracellular amastigotes may be observed (Figs 4.28 to 4.31). As CL progresses, the epidermis becomes increasingly hyperplastic and ulcerates (Fig 4.32). The dermis becomes necrotic and infiltrated by increasing numbers of vacuolated histiocytes, epithelioid cells,



**Figure 4.15**
Nearly healed cutaneous leishmaniasis (CL) on calf of Brazilian patient.



**Figure 4.16**
Brazilian patient with mucosal leishmaniasis (ML) (espundia) showing ulceration of nasal septum.

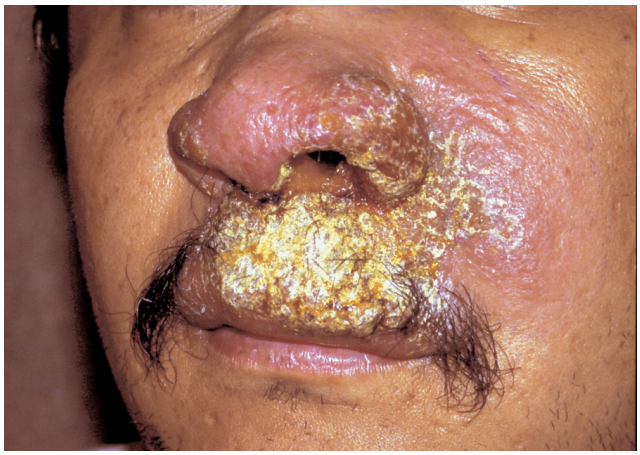


**Figure 4.17**
Mucocutaneous leishmaniasis in Honduran patient. Note crusted, vegetative, and heavily infiltrated lession.

lymphocytes, plasma cells, and giant cells (Figs 4.33 to 4.35). There may be neutrophils in the ulcer bed. As necrotizing (Fig 4.36) or nonnecrotizing (Figs 4.37 to 4.39) granulomas develop, amastigotes decline in number and may be extremely difficult to find.[41] In such instances, biopsies should be taken from the periphery of the ulcer, including the nonulcerated edge. As healing takes place, granulation tissue and fibrosis fill the ulcer crater. Satellite lesions that develop along the course of draining lymphatic channels can cause necrotizing granulomas or histiocytic infiltration in lymph nodes (Figs 4.40 to 4.43).[42]

Mucosal leishmaniasis is characterized by chronic inflammation, necrotizing granulomas, and occasional ulceration (Fig 4.44). The inflammatory infiltrate is made up of numerous lymphocytes, epithelioid cells, and giant cells (Fig 4.45). Early in ML, parasites may be abundant; in chronic ML, they are rarely seen (Fig 4.46).

The histologic features of LR are similar to those of acute and chronic CL. Macrophages, lymphocytes, and plasma cells infiltrate the dermis, and necrotizing granulomas with epithelioid cells develop. Amastigotes vary in number and are usually very difficult to find. Healing is accompanied by fibrosis.

In DCL, numerous macrophages containing multiple amastigotes infiltrate the dermis (Fig 4.47). Although there may be a few lymphocytes and plasma cells, there is usually no necrosis or granuloma formation. The epidermis is atrophic but not ulcerated (Fig 4.48). A clear zone beneath the basal layer of the epidermis is free of inflammatory cells (Fig 4.49).

Histologic features of PKDL often resemble those of DCL. In macular lesions, histiocytes, lymphoid cells, and plasma cells infiltrate the upper dermis and amastigotes are rare. In plaque lesions, the infiltration is denser, consisting of histiocytes, lymphoid cells, and especially plasma cells,



**Figure 4.18**
Brazilian mucocutaneous leishmaniasis patient with rare involvement of perineum and adjacent areas.



**Figure 4.19**
Leishmaniasis recidivans, usually associated with *Leishmania tropica*. Note lupoid satellite nodules.



**Figure 4.20**
Diffuse cutaneous leishmaniasis (DCL) in Venezuelan patient. Clinically, widespread nodules may be mistaken for lepromatous leprosy or cutaneous lymphoma. Madarosis, typical of advanced lepromatous leprosy, is absent.



**Figure 4.21**
Diffuse cutaneous leishmaniasis (DCL) in 24-year-old Mexican patient. Nodules and diffuse infiltrations do not selectively involve central portions of face, as in lepromatous leprosy.




**Figure 4.22**
a. Diffuse cutaneous leishmaniasis (DCL) of pinna, frequently confused with leprosy. b and c. Infiltration and nodules of post-kala-azar dermal leishmaniasis (PKDL) forming a butterfly pattern on face that can become generalized.

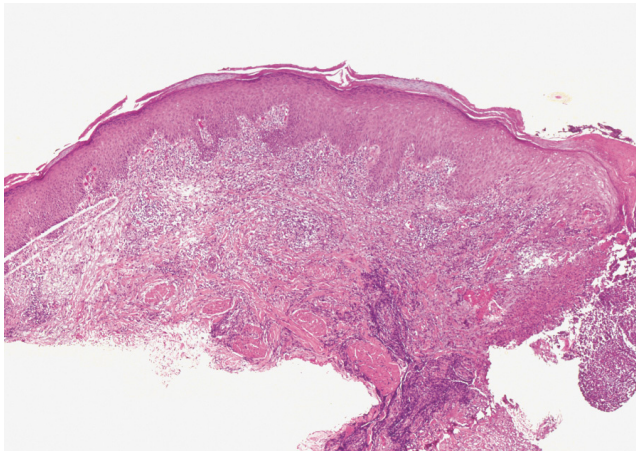


**Figure 4.23**
Ulcer of cutaneous leishmaniasis (CL) in soldier returned from Operation Desert Storm in Middle East, showing inflammation and necrosis. Note epidermal hyperplasia. See also Figure 4.30. x24

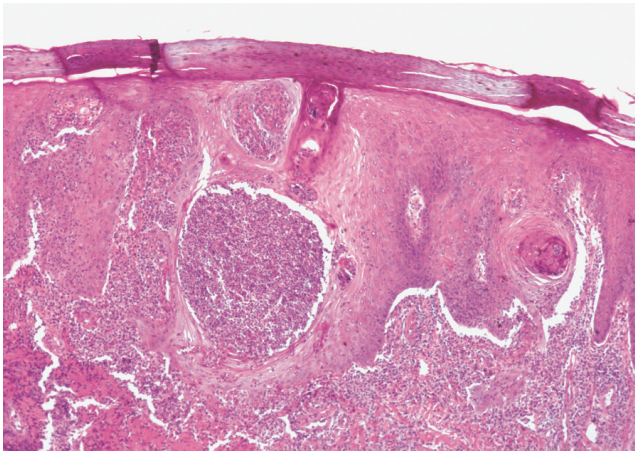


**Figure 4.24**
Early cutaneous leishmaniasis in same patient as Figure 4.26, showing hyperkeratosis, epidermal hyperplasia, and inflammation. x45

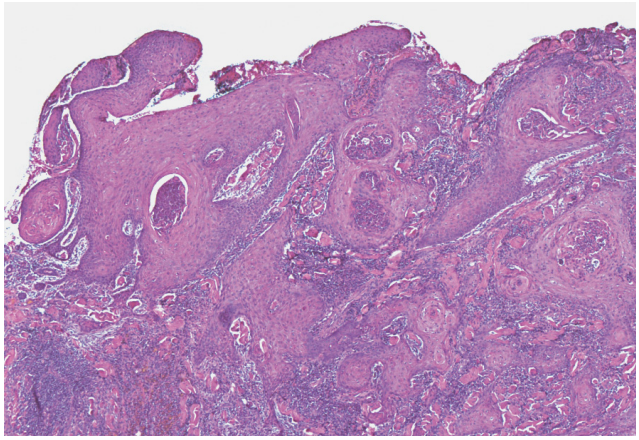


**Figure 4.25**
Cutaneous leishmaniasis in 51-year-old Cuban patient with nonhealing ulcer at site of sandfly bite on leg. Biopsy shows pseudoepitheliomatous hyperplasia and intraepidermal abscess. See also Figures 4.39, 4.51, 4.53, and 4.54. x24

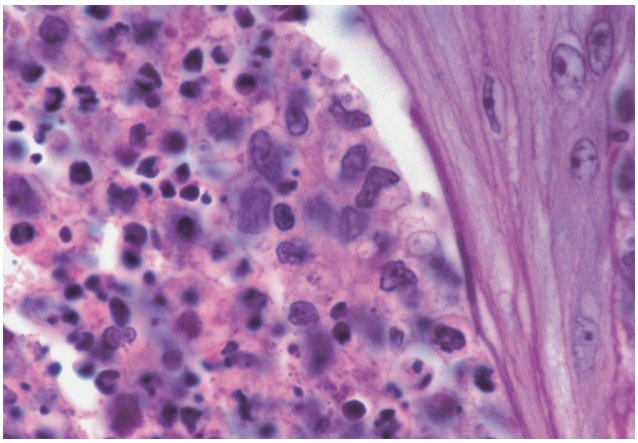


**Figure 4.26**
Higher magnification of intraepidermal abscess in patient described in Figure 4.24. x685

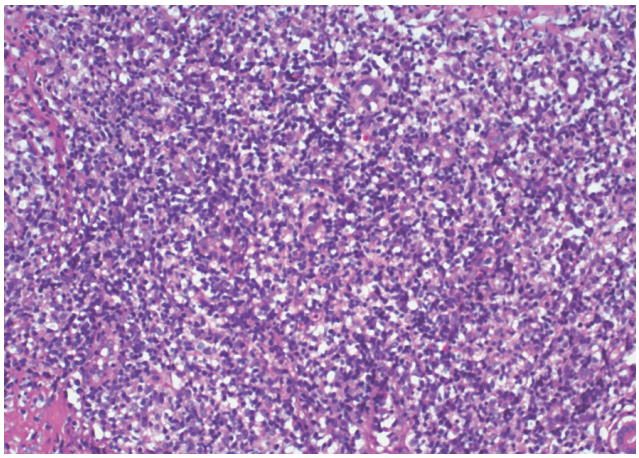


**Figure 4.27**
Dermal infiltration of histiocytes, lymphocytes, and plasma cells in cutaneous leishmaniasis. x125

and amastigotes are more frequent than in macular lesions. In nodular lesions, cellular exudates extend into the subcutis and intracellular amastigotes are usually abundant.

## *Diagnosis*

The different parasitologic techniques for confirming *Leishmania* infection are variously effective, depending on whether the syndrome under examination is oligoparasitic or polyparasitic. A confirmed parasitologic diagnosis is established by any of the following methods:

1) **Visualization of amastigotes in Giemsa-stained smears, aspirates, or histologic sections.** Polyparasitic syndromes such as early-stage CL, DCL, and papulonodular forms of PKDL are easily confirmed with Giemsa-stained smears (Fig 4.2). Oligoparasitic syndromes such as ML, LR, macular PKDL, and late-stage (healing) CL are more

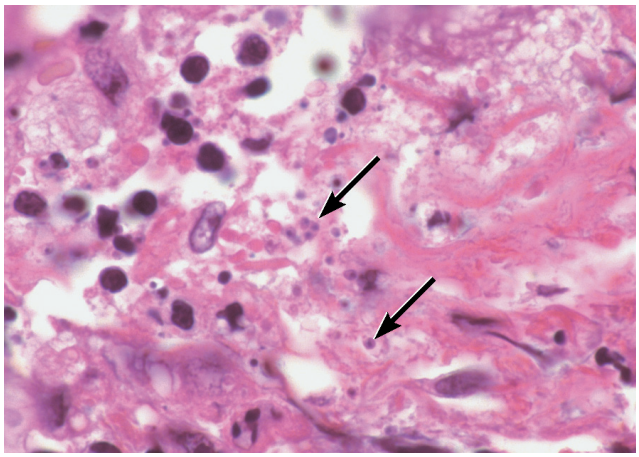


**Figure 4.28**
Biopsy from area near ulcerated epidermis shows several amastigotes (arrows) in dermis. See also Figures 4.32, 4.33, and 4.36. x655

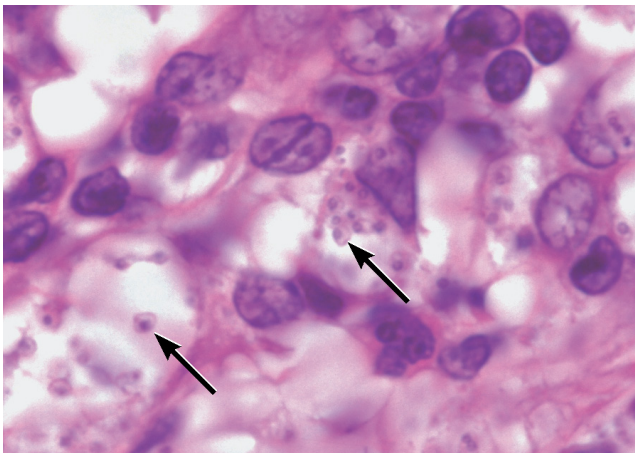


**Figure 4.29**
Multiple amastigotes (arrows) in 44-year-old patient from Dominican Republic. Patient developed multiple skin nodules starting at age 12. See also Figure 4.55. x945

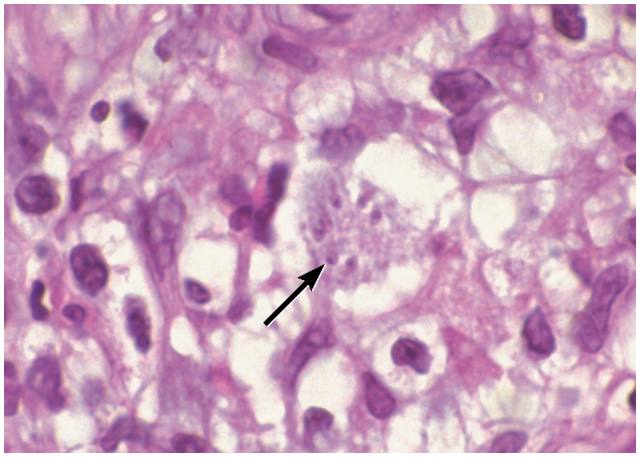


**Figure 4.30**
Amastigotes (arrow) in specimen shown in Figure 4.23. x960

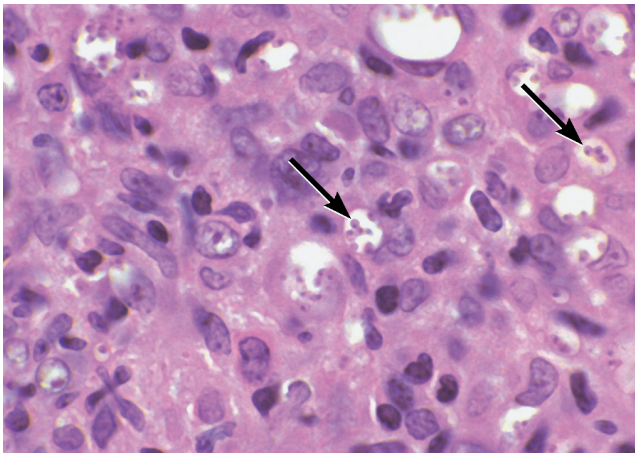


**Figure 4.31**
Amastigotes (arrows) within histiocytes. See also Figure 4.35. x600

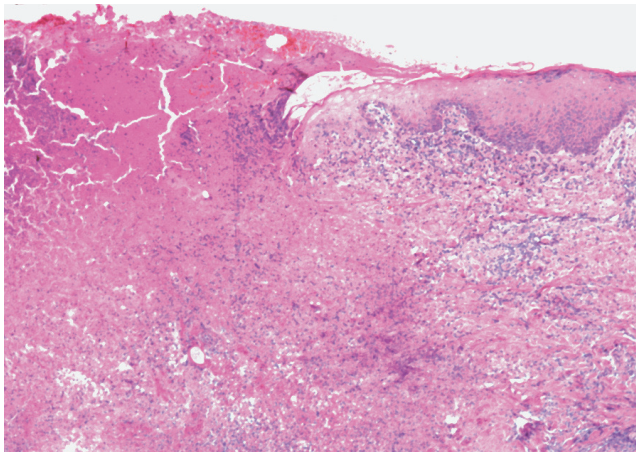


**Figure 4.32**
Ulceration in cutaneous leishmaniasis. Same specimen as Figure 4.28. See also Figures 4.33 and 4.36. x50

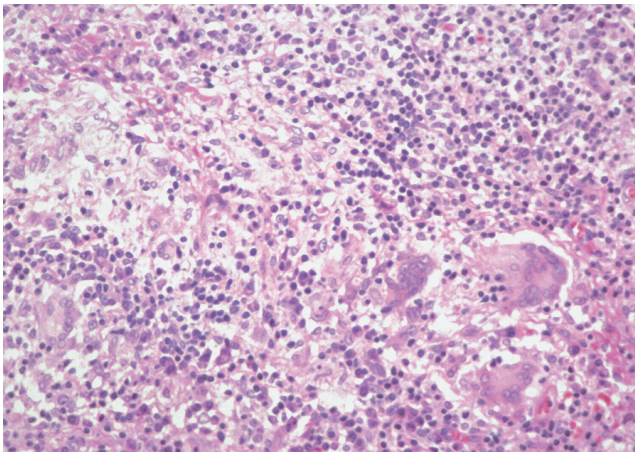


**Figure 4.33**
Later biopsy from same patient as Figure 4.28 showing necrosis and infiltration of dermis by mixed inflammatory cells, including multinucleated giant cells. No amastigotes were found. See also Figures 4.32 and 4.36. x175

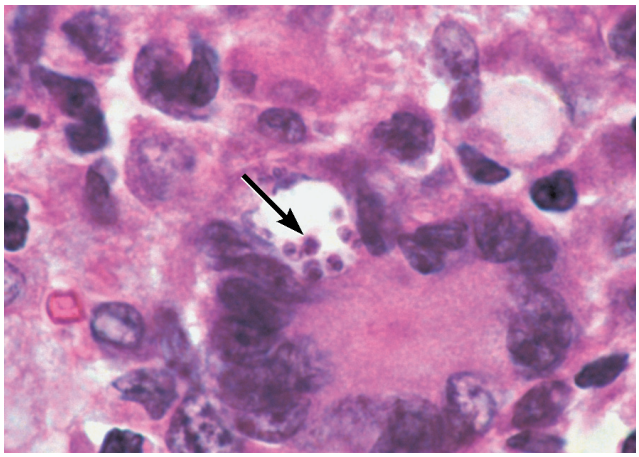


**Figure 4.34**
Multinucleated giant cell containing multiple amastigotes (arrow). Ethiopian patient had large facial lesion involving forehead, eyebrow, nose, and malar area. Three smears and leishmanial cultures were negative. x1115

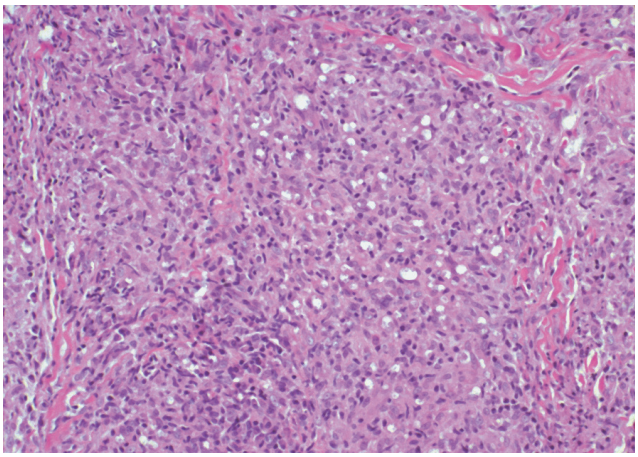


**Figure 4.35**
Diffuse histiocytic infiltration of dermis in cutaneous leishmaniasis . Same patient as Figure 4.31. x120

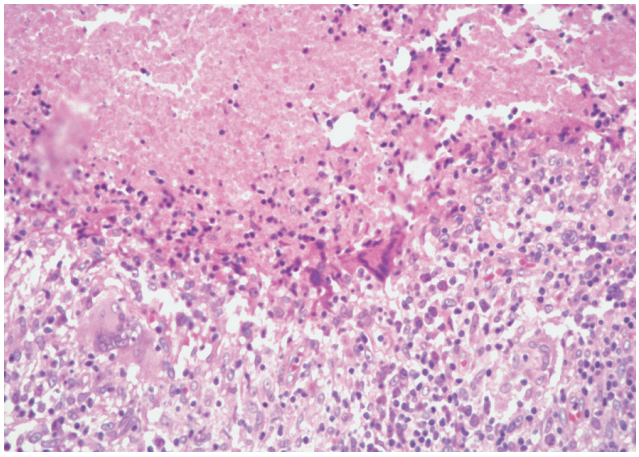


**Figure 4.36**
Necrobiotic granuloma in deep dermis. No amastigotes were found. Same specimen as Figure 4.33. See also Figures 4.28 and 4.32. x170

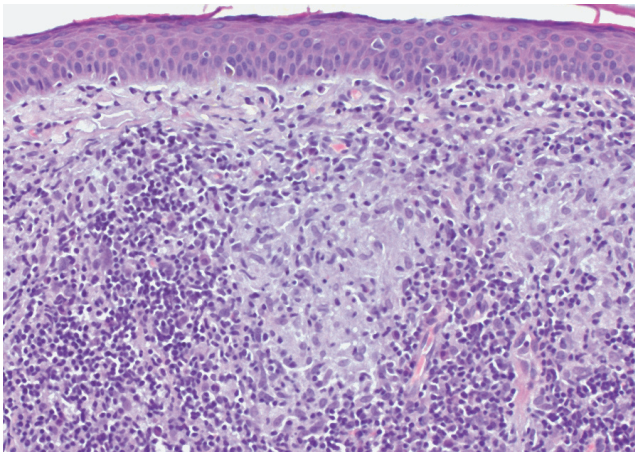


**Figure 4.37**
Noncaseating granulomas in 26-year-old soldier with cutaneous leishmaniasis who had traveled to Panama, Honduras, and Kuwait. For 3 years, patient had slow-growing papule on forehead that was unresponsive to topical steroids. See also Figure 4.38. x120

difficult or sometimes impossible to confirm with standard Giemsa-stained smears. Because factors such as specimen quality, staining methods, and the skill of the microscopist can dramatically affect the sensitivity of this diagnostic procedure, a negative smear does not necessarily exclude a diagnosis of leishmaniasis. In histologic sections, amastigotes stain well with H&E (Fig 4.50) or Brown-Hopps modified tissue gram stain (Figs 4.51 & 4.52). In our experience, the Brown-Hopps stain creates the least amount of background staining and the strongest contrast from surrounding tissue, which makes identifying amastigotes much easier.[43] Other stains sometimes used to identify amastigotes in tissue, including Giemsa (Fig 4.53), Wilder's reticulum (Fig 4.54), PAS (Fig 4.55), and immunoperoxidase (Fig 4.56) stains, offer no advantage over the Brown-Hopps

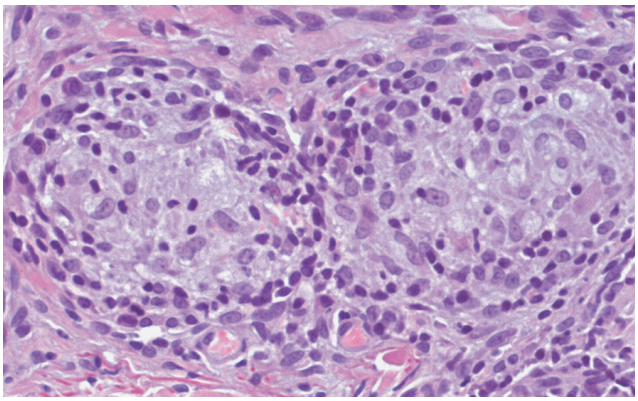


**Figure 4.38**
Two delayed hypersensitivity granulomas in specimen shown in Figure 4.37. x245

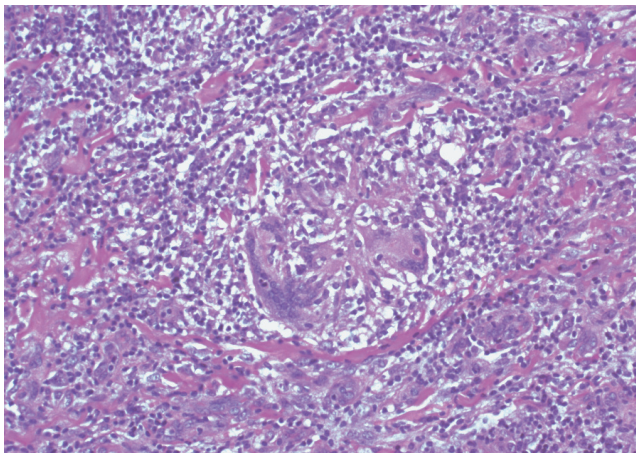


**Figure 4.39**
Granulomatous area of dermis in specimen shown in Figure 4.25. See also Figures 4.51, 4.53, and 4.54. x115

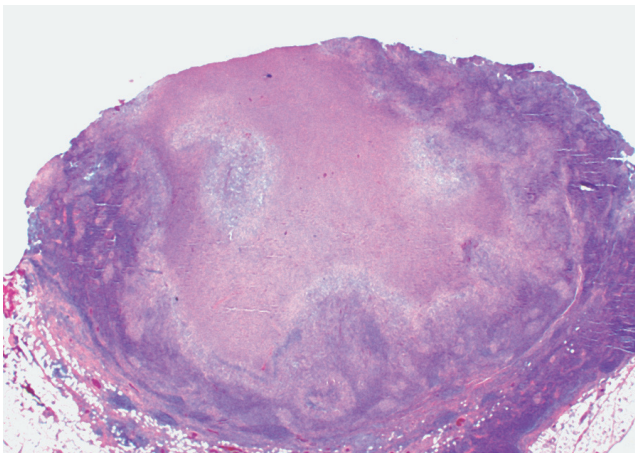


**Figure 4.40**
Caseating granuloma in lymph node from patient with cutaneous leishmaniasis. x8

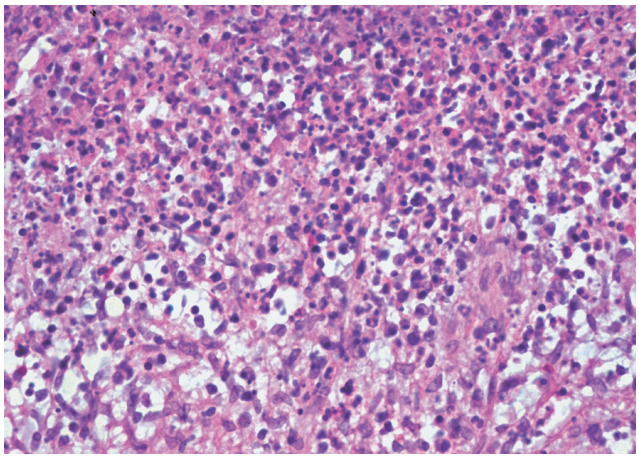


**Figure 4.41**
Necrotic area in lymph node from patient with cutaneous leishmaniasis. x245

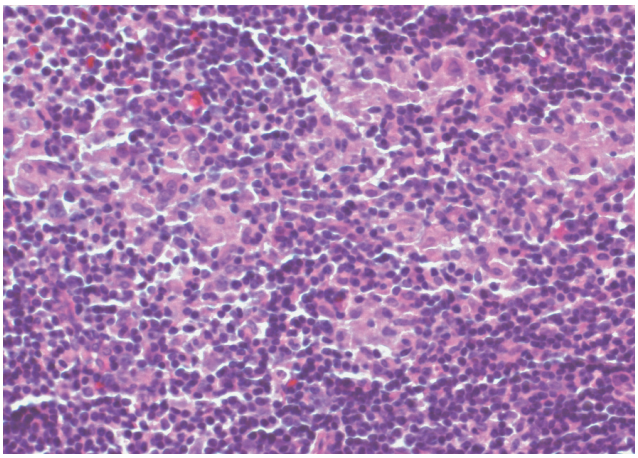


**Figure 4.42**
Histiocytosis in supraclavicular lymph node of 69-year-old patient from Honduras. Patient developed lymphadenopathy following cutaneous leishmaniasis on forehead. x245

stain for efficacy in diagnosis by direct smear examination.

2) **Isolation of promastigotes in in-vitro culture.** This method can be more sensitive than direct smear examination,[44,45] but some parasites, such as *L. braziliensis*, are more difficult than others to culture. Therefore, this method should be complementary to direct smear examination and should be employed whenever possible in clinically suspect cases. The lesion should be debrided to remove overlying exudate and crusting. Scrapings, aspirates, and biopsy specimens may be obtained from both the center and border of the ulcer (scrapings and aspirates are more likely to yield a positive result than tissue specimens). Increasing the number of culture attempts from the same lesion enhances the likelihood of obtaining a positive result.[45]

3) **In-vivo culture**.[46] In vivo culture (animal inoculation with a patient sample) is a sensitive diagnostic technique;

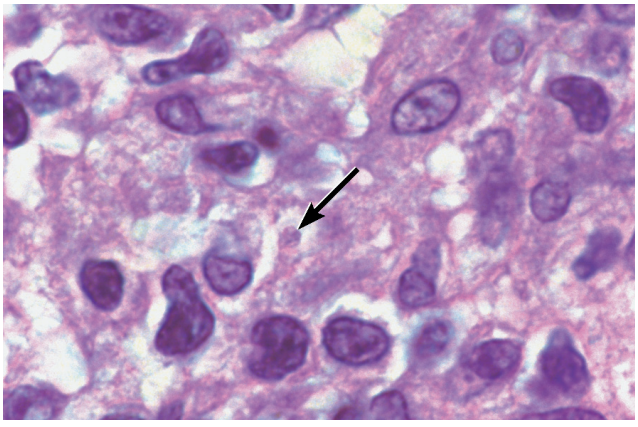


**Figure 4.43**
Amastigote (arrow) in lymph node of patient with cutaneous leishmaniasis. x1070

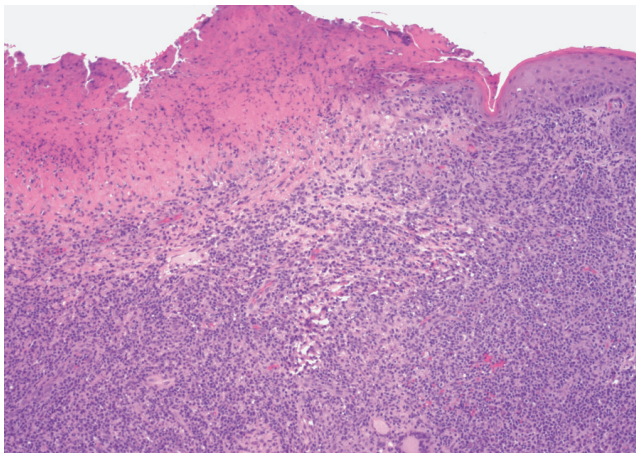


**Figure 4.44**
Ulceration near nares in mucosal leishmaniasis (ML). See also Figure 4.45. x63

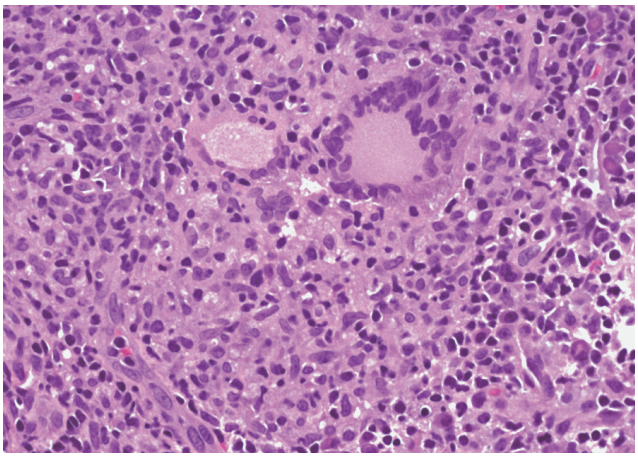


**Figure 4.45**
Granulomatous inflammation in same patient as Figure 4.44. x120

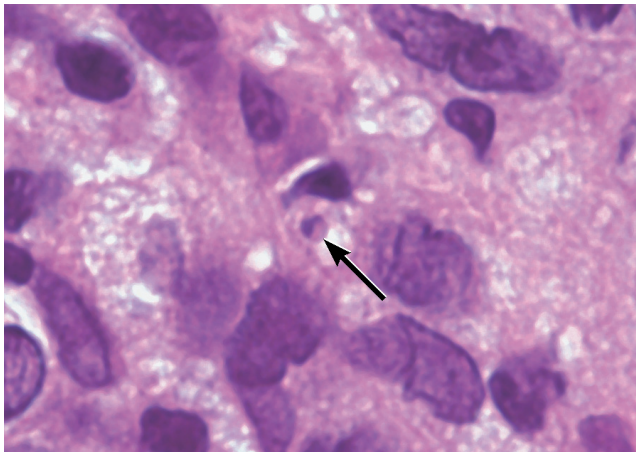


**Figure 4.46**
Single amastigote (arrow) in chronic mucosal leishmaniasis (ML). Note spherical nucleus and rod-shaped kinetoplast. x2000

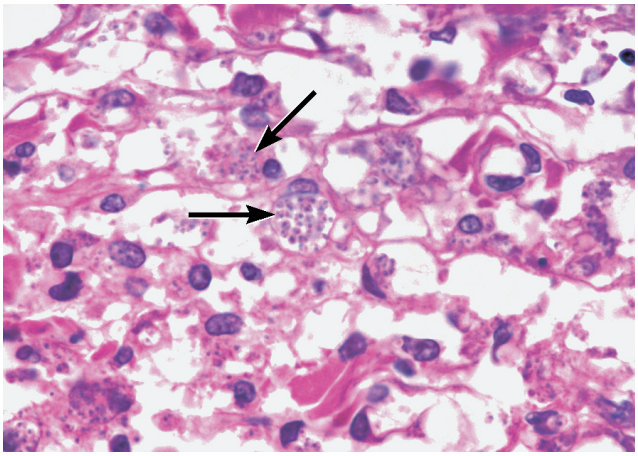


**Figure 4.47**
Macrophages containing multiple amastigotes (arrows) in dermis in diffuse cutaneous leishmaniasis. See also Figures 4.48 and 4.49. x430

many investigators believe a single viable amastigote can initiate infection in a susceptible animal (e.g. the golden hamster). Because the availability of appropriate laboratory animals is limited, this method should be reserved for selected cases when other tests are negative and the diagnosis is in doubt.

4) **Xenodiagnosis**. This technique involves recovering parasites from sandflies that have been allowed to feed on infected patients. Although xenodiagnosis has been used more commonly in patients with visceral leishmaniasis, xenodiagnosis has been successfully employed in cutaneous leishmaniasis, especially in oligoparasitic syndromes and with infecting parasites such as *L. braziliensis* that can be hard to recover in in vitro culture.[47]

5) **Amplification of parasite-specific DNA with polymerase chain reaction (PCR)**. There has been a dramatic proliferation of various polymerase chain reaction based molecular diagnostic tests introduced in the last decade.[48] The perfor-

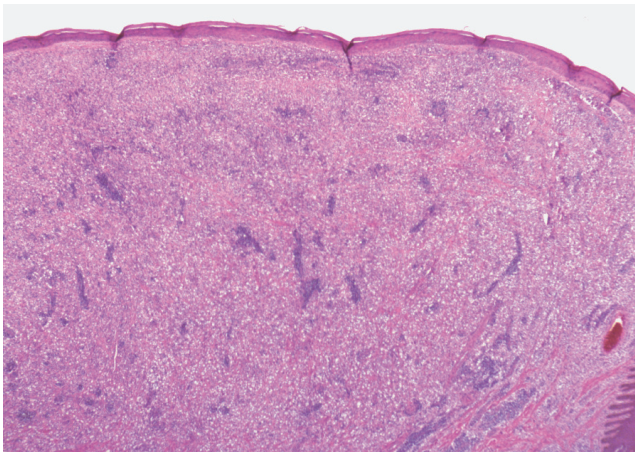


**Figure 4.48**
Atrophic epidermis in diffuse cutaneous leishmaniasis. Same patient as Figure 4.47. See also Figure 4.49. x17

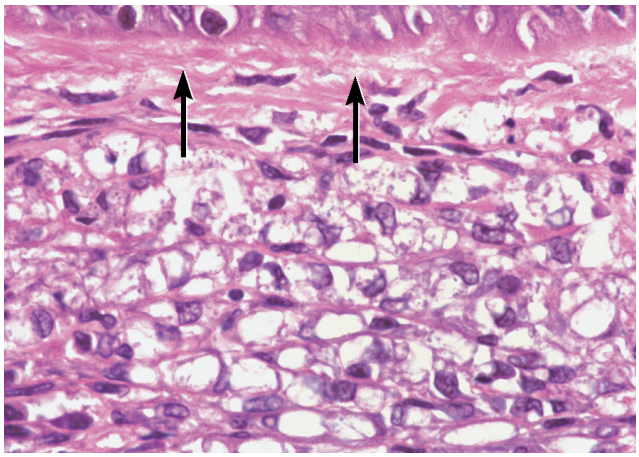


**Figure 4.49**
Narrow subepidermal clear zone (arrows) in diffuse cutaneous leishmaniasis (DCL). Same patient as Figures 4.47 and 4.48. x435

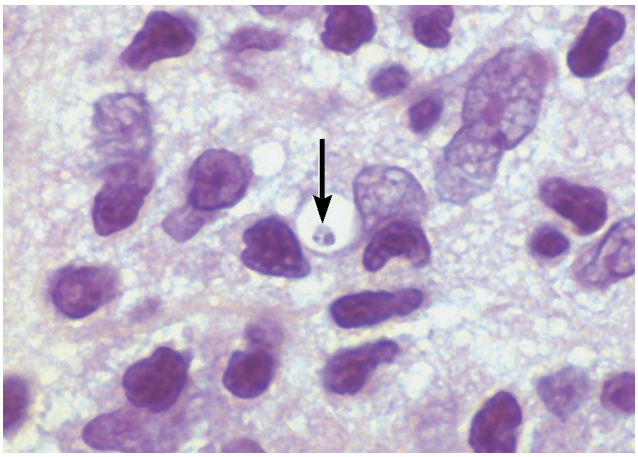


**Figure 4.50**
Single amastigote (arrow) in parasitophorous vacuole of histiocyte stained with H&E. Note spherical nucleus and tiny rod-shaped kinetoplast. x1500

mance characteristics vary significantly, none is commercially available, and their place in routine clinical care is not yet decided. However, locally established centers using PCR can be very useful for the confirmation of leishmaniasis in patients with oligoparasitic syndromes.

Other diagnostic methods may also be useful. In general, polyparasitic syndromes show a detectable humoral polyclonal antibody response to crude antigen, but no cellular immune response. Oligoparasitic syndromes show minimal humoral antibody response to crude antigens, but a marked cellular immune response.

There is currently no sensitive or specific serological assay for detecting *Leishmania*-specific antibody for any of the cutaneous leishmaniases. Development of an antibody-based test has been hindered by the continued use of crude promastigote-derived antigen (whole, disrupted, and solubilized preparations). Since human immune response to *Leishmania* sp is stage-specific, it is likely that amastigote-dominant or amastigote-exclusive antigens will elicit a much more specific response. Production of the antigens as recombinant proteins would allow for an epitope-dense capture antigen.

A skin-test antigen to detect DH (the Montenegro test) can also detect prior infection and corroborate the diagnosis of oligoparasitic syndromes such as ML and LR. Polyparasitic PKDL and DCL are skin test-negative (anergic to *Leishmania* antigens), while ML and LR are positive (Fig 4.57). Currently, no such test is available for use in the United States.

## Treatment and Prevention

A wide variety of treatments for the cutaneous leishmaniases are employed around the world, but few of these therapies have proven consistently effective.[49-52] Recommendations based on randomized, placebo-controlled trials

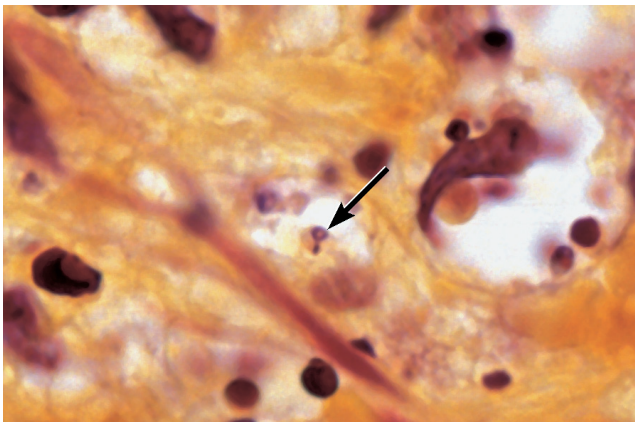


**Figure 4.51**
Single amastigote (arrow) stained with Brown-Hopps tissue gram stain. Note spherical nucleus and rod-shaped kinetoplast. Same patient as Figures 4.25 and 4.39. See also Figures 4.53 and 4.54. B&H x1750

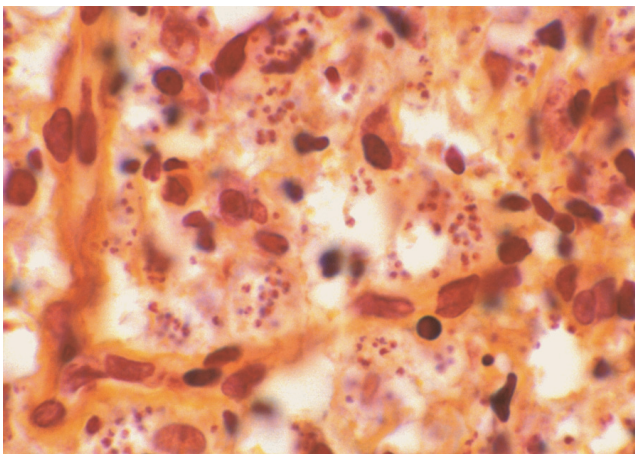


**Figure 4.52**
Amastigotes within histiocytes. B&H x790

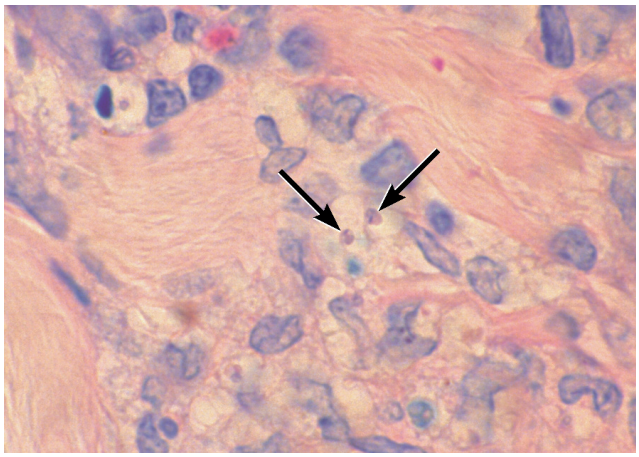


**Figure 4.53**
Amastigotes (arrows) visible on Giemsa-stained section. Same patient as Figures 4.25 and 4.39. See also Figures 4.51 and 4.54. Giemsa x960

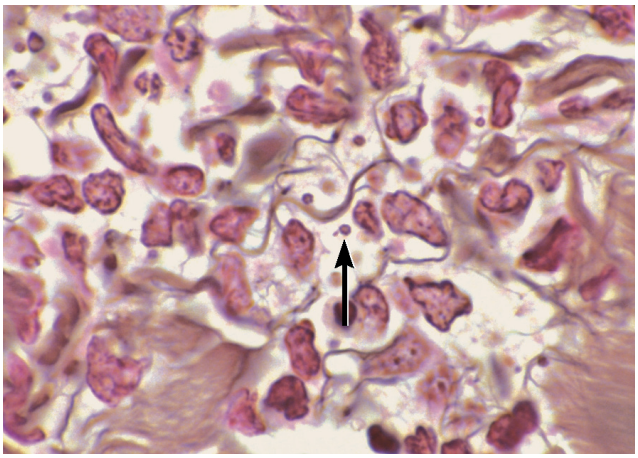


**Figure 4.54**
Reticulum stain demonstrating nucleus and kinetoplast of amastigote (arrow). Same patient as Figures 4.25 and 4.39. See also Figures 4.51 and 4.53. Wilder's reticulum x960

are often lacking because many treatment modalities have been evaluated in small, open-label trials with differing endpoints and insufficient follow-up to detect relapses.[53] In addition, the standard of care in many geographic areas is dictated by local traditions and patient acceptance.

Local therapies include the use of topical agents and physical modalities such as thermotherapy, cryotherapy, surgery, and electrotherapy. Physical modalities are more commonly used in the Middle East and in southwest Asia for Old World cutaneous leishmaniases. Topical use of the aminoglycoside paromomycin (aminosidine) has been extensive in the Middle East, as well as various formulations and concentrations of paromomycin and methylbenzethonium chloride in a variety of regimens.[54] In general, these formulations appear to be moderately effective against *L. major* but ineffective against *L. tropica*. These treatments have not been widely used against New World parasites. Topical antifungal agents are not effective against the cutaneous leishmaniases. Intralesional administration of pentavalent antimonials (SbV) has been used extensively in the Middle East with apparent success, but has been employed only rarely in the New World.[55]

Two SbV compounds (sodium stibogluconate (Pentostam®) and meglumine antimoniate (Glucantime®), first used in the 1940s, are still commonly used drugs for severe or complicated forms of the cutaneous leishmaniases.[2,56,57] Although there have been no clinical trials comparing treatment outcomes for these agents, most authorities consider them to be equally effective. However, systemic SbV therapy requires prolonged parenteral administration (IM or IV) of the compounds at high doses, a difficult and expensive process for health care facilities in endemic developing countries. Ulcerative and nodular CL usually respond to SbV therapy. The persistent syndromes of ML, LR, DCL,

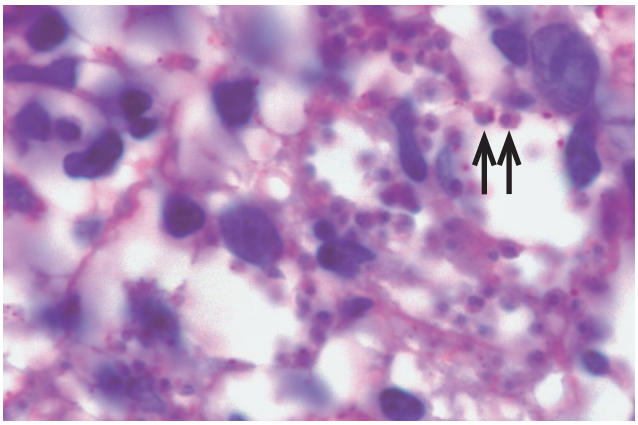


**Figure 4.55**
Amastigotes (arrows) visible on PAS-stained tissue section. Same patient as Figure 4.29. PAS x960

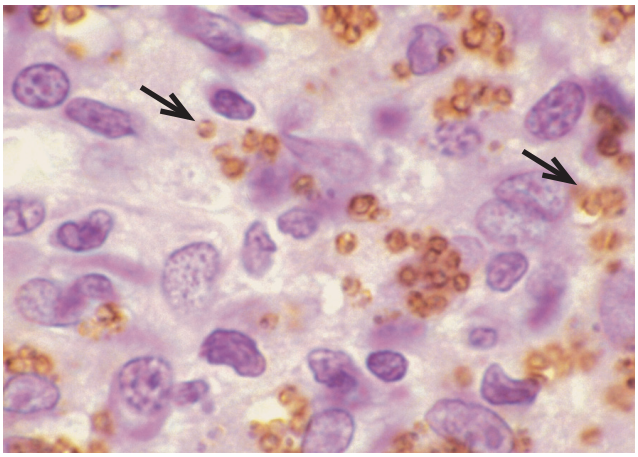


**Figure 4.56**
Immunoperoxidase stain demonstrating brown-stained amastigotes with darker-staining kinetoplasts (arrows). Immunoperoxidase x1140

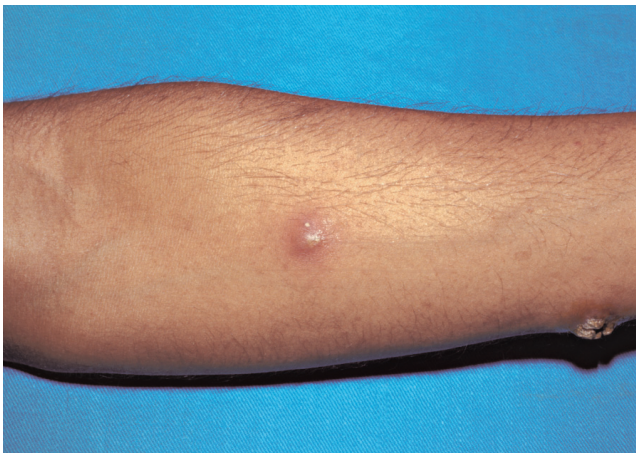


**Figure 4.57**
Positive Montenegro test 7 days after inoculation of leishmanin. Test is positive in oligoparasitic syndromes; negative in patients with polyparasitic disease.

and PKDL do not consistently respond to SbV or any other treatment. In patients coinfected with HIV, responses are often temporary and relapse is common.

No oral agents can be generally recommended for the treatment of any of the cutaneous syndromes. Antifungal agents such as ketoconazole, itraconazole, and fluconazole are antileishmanial in vitro and have been used in numerous uncontrolled trials and a few randomized trials in both the New World and the Old World. Itraconazole and fluconazole are only slightly more effective than placebo. Ketoconazole is modestly effective against *L. major*, *L. panamensis*, and *L. mexicana*, but ineffective against *L. tropica* and *L. braziliensis*. In Guatemala, ketoconazole has proven superior to SbV for CL caused by *L. mexicana*, but markedly inferior for CL caused by *L. braziliensis*.[58] However, it is unusual to have confirmation of the infecting species prior to the start of therapy, so it is not clear how these trial results can be implemented in routine practice.

Amphotericin B, both the deoxycholate salt and newer, less toxic liposomal preparations have been shown to be very effective treatments for many different forms of cutaneous leishmaniasis.[59-61] The cost of liposomal amphotericin B, its requirement for cold chain storage, and intravenous route of administration markedly limit the potential for beneficial impact in endemic areas but liposomal amphotericin B is now considered an acceptable first line treatment for CL in returning travelers. Early-stage ML caused by *L. braziliensis* in the New World usually responds to 20 mg/kg body weight/day of SbV administered for 20 to 40 days. Late-stage ML with extensive anatomic involvement is much less responsive.

There is no approved or effective immunoprophylaxis, chemoprophylaxis, or vaccine against infection or disease. Prevention entails protection against sandfly bites. Control measures in endemic areas are aimed at disrupting the enzootic cycle by eliminating mammalian reservoir hosts and eradicating the sandfly. Such control measures, however, are expensive, difficult to sustain, and potentially environmentally unsound.

## References


1. Convit J, Ulrich M, Fernandez C, et al. The clinical and immunological spectrum of American cutaneous leishmaniasis. Trans R Soc Trop Med Hyg 1993;87:444-448.
2. Magill AJ. Leishmania Species: Visceral (Kala-Azar), Cutaneous, and Mucosal Leishmaniasis. In: Mandell GL, Bennett JE, Dolin R. eds. *Principles and Practice of Infectious Diseases*. 7th ed. Philadelphia (PA): Churchill Livingstone; 2010. p 3463-3480.
3. Vieira-Gonçalves R, Pirmez C, Jorge ME, et al. Clinical features of cutaneous and disseminated cutaneous leishmaniasis caused by *Leishmania (Viannia) braziliensis* in Paraty, Rio de Janeiro. *Int J Dermatol*. 2008;47:926-932.
4. Wright JH. Protozoa in a case of tropical ulcer (Delhi sore). *J Med Res.* 1903;10:472-482.
5. Borovsky PF. On Sart sore. *Voen Med Zh*. 1898;195:925-941.
6. Hoare C. Early discoveries regarding the parasite of oriental sore. *Trans R Soc Trop Med Hyg.* 1938;32:67-92.
7. Nicolle C. Cultivation of the parasite of oriental sore [in French]. *C R Acad Sci*. 1908;146:842-843.
8. Carini A. Leishmaniasis of the naso-oral-pharyngeal mucosa [in French]. *Bull Soc Pathol Exot*. 1911;4:289-291.
9. Convit J, Lapenta P. Report of a case of disseminated leishmaniasis [in Spanish]. *Rev Pol Caracas.* 1948;18:153.
10. Kreutzer RD, Christensen HA. Characterization of *Leishmania* spp. by isozyme electrophoresis. *Am J Trop Med Hyg*. 1980;29:199-208.
11. Barral A, Pedral-Sampaio D, Grimaldi G Jr, et al. Leishmaniasis in Bahia, Brazil: evidence that *Leishmania amazonensis* produces a wide spectrum of clinical disease. *Am J Trop Med Hyg*. 1991;44:536-546.
12. Santrich C, Segura I, Arias AL, Saravia NG. Mucosal disease caused by *Leishmania braziliensis guyanensis. Am J Trop Med Hyg.* 1990;42:51-55.
13. Walton B. American cutaneous and mucocutaneous leishmaniasis. In: Peters W, Killick-Kendrick R, eds. *The Leishmaniases in Biology and Medicine*. Vol 2. London, England: Academic Press; 1987:637-664.
14. Peters W. Heterogeneity of cutaneous leishmaniasis with emphasis on the Old World. *Schweiz Med Wochenschr.* 1993;123:1237-1249.
15. Mebrahtu Y, Lawyer P, Githure J, et al. Visceral leishmaniasis unresponsive to Pentostam caused by *Leishmania tropica* in Kenya. *Am J Trop Med Hyg.* 1989;41:289-294.
16. Sacks DL, Kenney RT, Kreutzer RD, et al. Indian kala-azar caused by *Leishmania tropica. Lancet.* 1995;345:959-961.
17. Schnur LF, Chance ML, Ebert F, Thomas SC, Peters W. The biochemical and serological taxonomy of visceralizing Leishmania. *Ann Trop Med Parasitol.* 1981;75:131-144.
18. Magill AJ, Grogl M, Gasser RA Jr, Sun W, Oster CN. Visceral infection caused by *Leishmania tropica* in veterans of Operation Desert Storm. *N Engl J Med.* 1993;328:1383-1387.
19. Magill AJ, Grogl M, Johnson SC, Gasser RA Jr. Visceral infection due to *Leishmania tropica* in a veteran of Operation Desert Storm who presented 2 years after leaving Saudi Arabia [letter]. *Clin Infect Dis.* 1994;19:805-806.
20. Oren R, Schnur LF, Ben Yehuda D, Mayner V, Okon E, Rachmilewitz EA. Visceral leishmaniasis: a difficult diagnosis and unusual causative agent. *J Infect Dis.* 1991;164:746-749.
21. Ashford R, Desjeux P, de Raadt P. Estimation of population at risk of infection and number of cases of leishmaniasis. *Parasitol Today.* 1992;8:104-105.

22. Copeland HW, Arana BA, Navin TR. Comparison of active and passive case detection of cutaneous leishmaniasis in Guatemala. *Am J Trop Med Hyg.* 1990;43:257-259.
23. Grimaldi G Jr, Tesh RB. Leishmaniases of the New World: current concepts and implications for future research. *Clin Microbiol Rev.* 1993;6:230-250.
24. Grimaldi G Jr, Tesh R, McMahon-Pratt D. A review of the geographic distribution and epidemiology of leishmaniasis in the New World. *Am J Trop Med Hyg* .1989;41:687-725.
25. Griffiths WA. Old World cutaneous leishmaniasis. In: Peters W, Killick-Kendrick R, eds. *The Leishmaniases in Biology and Medicine.* Vol 2. London, England: Academic Press; 1987:617-636.
26. Desjeux P. Human leishmaniases: epidemiology and public health aspects. *World Health Stat Q.* 1992;45:267-275.
27. Herwaldt BL, Stokes SL, Juranek DD. American cutaneous leishmaniasis in U.S. travelers. *Ann Intern Med*. 1993;118:779-784.
28. Melby PC, Kreutzer RD, McMahon-Pratt D, Gam AA, Neva FA. Cutaneous leishmaniasis: a review of 59 cases seen at the National Institutes of Health. *Clin Infect Dis.* 1992;15:924-937.
29. Ashford RW, Kohestany KA, Karimzad MA. Cutaneous leishmaniasis in Kabul: observations on a "prolonged epidemic." *Ann Trop Med Parasitol*. 1992;86:361-371.
30. Reithinger R, Dujardin JC, Louzir H, Pirmez C, Alexander B, Brooker S. Cutaneous leishmaniasis. *Lancet Infect Dis.* 2007;7:581-596.
31. Magill A. The epidemiology of the leishmaniases. In: Weinstock M, ed. *Dermatologic Clinics.* Vol 13:3. Philadelphia, Pa: WB Saunders; 1995:505-523.
32. Herwaldt BL. Laboratory-acquired parasitic infections from accidental exposures. *Clin Microbiol Rev*. 2001 Oct;14(4):659-688.
33. Pineda JA, Martín-Sánchez J, Macías J, Morillas F. *Leishmania* spp infection in injecting drug users. *Lancet*. 2002;360:950-951.
34. Cardo LJ. Leishmania: risk to the blood supply. *Transfusion*. 2006;46:1641-1645.
35. Herwaldt BL, Arana BA, Navin TR. The natural history of cutaneous leishmaniasis in Guatemala. *J Infect Dis.* 1992;165:518-527.
36. Zijlstra EE, Musa AM, Khalil EA, el-Hassan IM, el-Hassan AM. Post-kala-azar dermal leishmaniasis. *Lancet Infect Dis.* 2003;3:87-98.
37. Ganguly S, Das NK, Barbhuiya JN, Chatterjee M. Post-kala-azar dermal leishmaniasis--an overview. *Int J Dermatol*. 2010;49:921-931.
38. Wortmann GW, Aronson NE, Miller RS, Blazes D, Oster CN. Cutaneous leishmaniasis following local trauma: a clinical pearl. *Clin Infect Dis*. 2000;31:199-201.
39. Puig L, Pradinaud R. Leishmania and HIV co-infection: dermatological manifestations. *Ann Trop Med Parasitol*. 2003;97 Suppl 1:107-114.
40. Golino A, Duncan JM, Zeluff B, et al. Leishmaniasis in a heart transplant patient. *J Heart Lung Transplant.* 1992;11:820-823.
41. Azadeh B, Samad A, Ardehali S. Histological spectrum of cutaneous leishmaniasis due to *Leishmania tropica. Trans R Soc Trop Med Hyg*. 1985;79:631-636.
42. Ridley DS, Ridley MJ. The evolution of the lesion in cutaneous leishmaniasis. *J Pathol.* 1983;141:83-96.
43. Abalos FM, Klassen MK, Marty AM, Neafie RC. Brown-Hopps stain for Leishmania amastigotes. *Mod Pathol*. 1998;11:143A.
44. Weigle KA, de Dávalos M, Heredia P, Molineros R, Saravia NG, D'Alessandro A. Diagnosis of cutaneous and mucocutaneous leishmaniasis in Colombia: a comparison of seven methods. *Am J Trop Med Hyg*. 1987;36:489-496.
45. Navin TR, Arana FE, de Merida AM, Arana BA, Castillo AL, Silvers DN. Cutaneous leishmaniasis in Guatemala: comparison of diagnostic methods. *Am J Trop Med Hyg*. 1990;42:36-42.
46. Shatry AM, Oster CN, Mebrahtu YB, Perkins PV, Hendricks LD. Mouse foot-pad inoculation as an aid to the isolation of *Leishmania* spp. from patients. *Trans R Soc Trop Med Hyg.* 1988;82:701-703.
47. Christensen HA, Herrer A. Detection of *Leishmania braziliensis* by xenodiagnosis. *Trans R Soc Trop Med Hyg.* 1972;66:798-799.
48. Reithinger R, Dujardin JC. Molecular diagnosis of leishmaniasis: current status and future applications. *J Clin Microbiol*. 2007;45:21-25.
49. Amato VS, Tuon FF, Siqueira AM, Nicodemo AC, Neto VA. Treatment of mucosal leishmaniasis in Latin America: systematic review. Am J Trop Med Hyg. 2007 Aug;77(2):266-274.
50. González U, Pinart M, Reveiz L, Alvar J. Interventions for Old World cutaneous leishmaniasis. *Cochrane Database Syst Rev*. 2008;4:CD005067.
51. Tuon FF, Amato VS, Graf ME, Siqueira AM, Nicodemo AC, Amato Neto V. Treatment of New World cutaneous leishmaniasis--a systematic review with a meta-analysis. *Int J Dermatol*. 2008;47:109-124.
52. González U, Pinart M, Rengifo-Pardo M, Macaya A, Alvar J, Tweed JA. Interventions for American cutaneous and mucocutaneous leishmaniasis. *Cochrane Database Syst Rev.* 2009;2:CD004834.
53. González U, Pinart M, Reveiz L, et al. Designing and reporting clinical trials on treatments for cutaneous leishmaniasis. *Clin Infect Dis*. 2010;51:409-419.
54. Kim DH, Chung HJ, Bleys J, Ghohestani RF. Is paromomycin an effective and safe treatment against cutaneous leishmaniasis? A meta-analysis of 14 randomized controlled trials. *PLoS Negl Trop Dis.* 2009;3:e381.
55. Solomon M, Baum S, Barzilai A, Pavlotsky F, Trau H, Schwartz E. Treatment of cutaneous leishmaniasis with intralesional sodium stibogluconate. *J Eur Acad Dermatol Venereol*. 2009;23:1189-1192.
56. Herwaldt BL, Berman JD. Recommendations for treating leishmaniasis with sodium stibogluconate (Pentostam) and review of pertinent clinical studies. Am J Trop Med Hyg 1992;46:296-306.
57. Control of the leishmaniasis: report of a meeting of the WHO Expert Committee on the Control of Leishmaniases, Geneva, 22-26 March 2010. (WHO technical report series; no. 949)
58. Navin TR, Arana BA, Arana FE, Berman JD, Chajon JF. Placebo-controlled clinical trial of sodium stibogluconate (Pentostam) versus ketoconazole for treating cutaneous leishmaniasis in Guatemala. *J Infect Dis*. 1992;165:528-534.
59. Solomon M, Baum S, Barzilai A, Scope A, Trau H, Schwartz E. Liposomal amphotericin B in comparison to sodium stibogluconate for cutaneous infection due to *Leishmania braziliensis*. *J Am Acad Dermatol*. 2007;56:612-616.
60. Wortmann G, Zapor M, Ressner R, et al. Lipsosomal amphotericin B for treatment of cutaneous leishmaniasis. *Am J Trop Med Hyg.* 2010;83:1028-1033.
61. Solomon M, Pavlotsky F, Leshem E, Ephros M, Trau H, Schwartz E. Liposomal amphotericin B treatment of cutaneous leishmaniasis due to *Leishmania tropica. J Eur Acad Dermatol Venereol*. 2010 Dec 5. doi: 10.1111/j.1468-3083.2010.03908.x. [Epub ahead of print]


## *Acknowledgements*


**Figure 4.3.**
Contributed by Ed. Rowton

**Figure 4.5**
Contributed by Roy Pfaltzgraff

**Figure 4.9a**
From reference number 2 A.J. Magill.

**Figure 4.12**
Contributed by Lourival Vicente da Silva

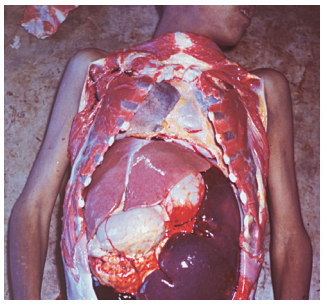
**Figure 4.13**
Contributed by Antonio Lauro Coscina

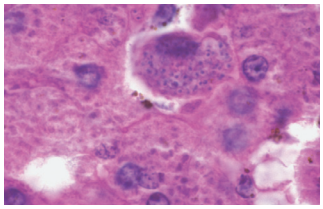
**Figure 4.14**
Contributed by Yasin Al-Qubarti

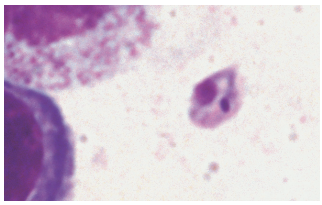
**Figure 4.15**
Contributed by David Purtilo

**Figure 4.18**
Contributed by Jacinto Convit

**Figure 4.22**
Contributed by Bryce Walton







5

# Visceral Leishmaniasis

*Alan J. Magill, Wayne M. Meyers, Mary K. Klassen-Fischer, and Ronald C. Neafie*

## *Introduction*

### Definition

Visceral leishmaniasis (VL), a chronic disease caused by parasites of the *Leishmania donovani* complex, is characterized by irregular fever, enlargement of the spleen and liver, weight loss, pancytopenia, and hypergammaglobulinemia.

### Synonyms

Visceral leishmaniasis is also known as kala-azar, a Hindi word meaning "black sickness", although hyperpigmentation is not a common feature of the disease. Descriptive names for VL, such as Burdwan fever, Dumdum fever, and Shahib's disease, are used infrequently.

### General Considerations

The most common etiologic agents of VL are 3 species of the *L. donovani* complex: *Leishmania donovani donovani* and *Leishmania donovani infantum* in the Indian subcontinent, Africa, China, the Mediterranean littoral, and the Middle East; and *Leishmania donovani chagasi* in South America. (Hereafter, organisms will be identified only by genus and species; eg, *L. donovani* for *L. d. donovani*). Organisms with biochemical characteristics of *Leishmania tropica* have occasionally been isolated from bone marrow cultures of patients with systemic leishmanial infection in Kenya, the Middle East, and India.[1,2,3]

## *Epidemiology*

Visceral leishmaniasis is widely distributed and endemic in 82 countries (Fig 5.1). Estimated incidence of VL worldwide is at least 100,000 per year. Over 90% of patients come from 3 regions: the Ganges River basin in India, Bangladesh, and Nepal; the East African countries of Ethiopia, Sudan, and Kenya; and northeastern Brazil.[4] Since the 1990s, southern Sudan and the Indian state of Bihar have been epidemic centers, with high rates of infection and tens of thousands of deaths. Civil strife, poor nutrition, population movement, and dire poverty are common factors contributing to the spread of disease in these regions.

Subspecies of *L. donovani* are transmitted by sandflies of the genera *Phlebotomus* in the Eastern Hemisphere and *Lutzomyia* in the Western Hemisphere. Epidemiology depends on the interaction of sandflies, reservoir hosts, and susceptible humans.[5,6]

### Reservoir Hosts

**Humans**. In India, where the domestic sandfly vector *Phlebotomus argentipes* feeds solely on humans, large epidemics spread continuously and discontinuously through population migrations. Transmission during the epidemic periods is largely person to person from active cases of visceral leishmaniasis. The contribution of the human reservoir of asymptomatic and oligosymptomatic infections to transmission is not known. Humans appear to be the only reservoir host, but it is possible that an unknown animal

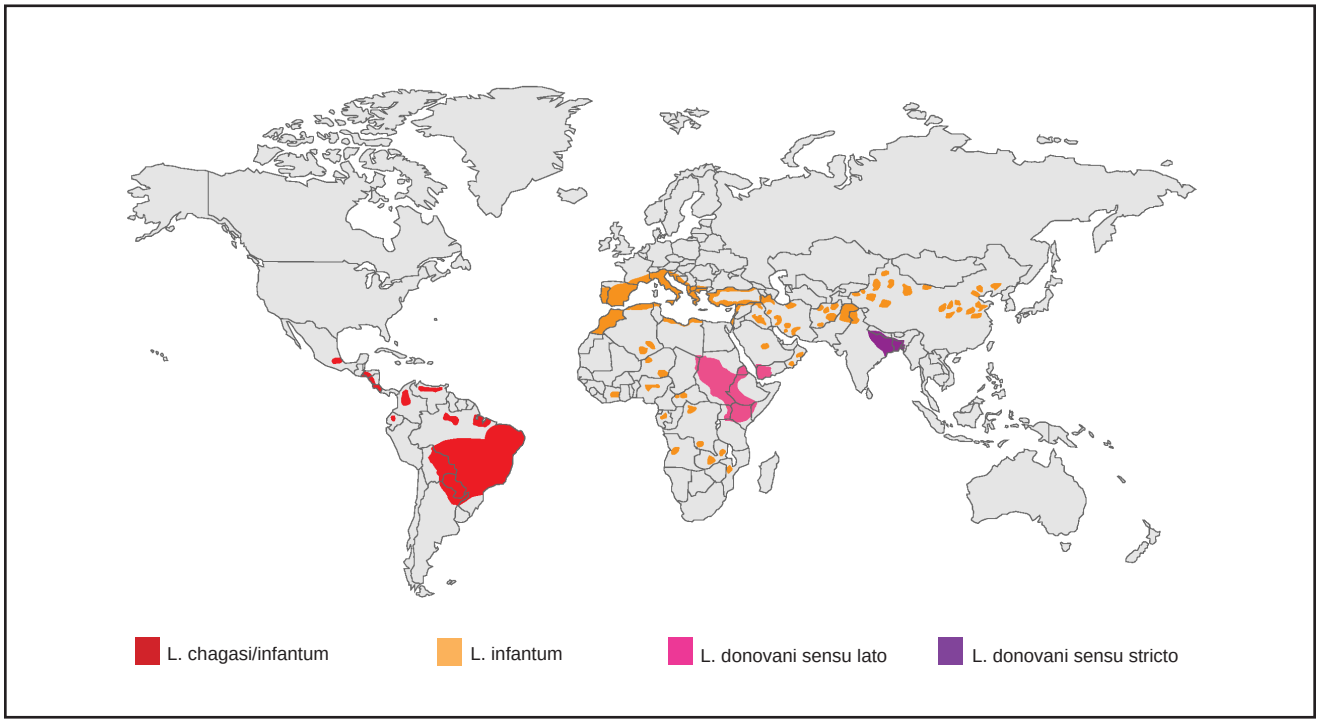



**Figure 5.1 Geographical distribution of leishmaniasis**

reservoir maintains the cycle between epidemics.

**Domestic Canines**. In Mediterranean countries, VL is urban and periurban and transmitted by *Phlebotomus perniciosus*, *Phlebotomus major*, *Phlebotomus simici*, and *Phlebotomus longicuspis*, with dogs as the main reservoir. Infants and young children are most commonly affected. Young dogs and certain breeds such as foxhounds and beagles are especially susceptible to infection with *L. infantum* and develop overt disease that is often fatal. In North America, rare outbreaks among foxhounds have been reported (Fig 5.2).[7,8] Dogs are also important reservoirs in South America, where the main vector is *Lutzomyia longipalpis*.

**Wild Canines**. In southern France and central Italy, VL is primarily a rural disease that affects older children and adults. *Phlebotomus ariasi* and *Phlebotomus perfiliewi* are the vectors, and foxes with no overt disease are the reservoir. Foxes are also reservoirs in Brazil. Jackals are probably an important source of the sporadic, mainly rural outbreaks in the Middle East and Central Asia.

**Multiple Hosts**; ***Rodents***. The epidemiology of VL in Africa is incompletely understood. In Kenya, *Phlebotomus martini* is the probable vector, and epidemics of VL in the 1950s and 1970s suggested a human reservoir. However, domestic dogs in Kenya have occasionally been infected with *L. donovani*. In Sudan, there have been several epidemics of VL since the 1950s, but the disease is usually sporadic in nomads who occupy temporary villages in the dry season near patches of scrub that harbor the vector *Phlebotomus orientalis*. *Leishmania donovani* has been isolated from Nile grass (or Kusu) rats (*Arvicanthis niloticus*) and other rodents in Sudan, which are probably important in maintaining enzootic foci in interepidemic periods. Parasite isolates from Sudan, Ethiopia, and Kenya all appear to be *L. donovani*, albeit a genetically diverse population. [9,10]



**Figure 5.2**
American foxhound, one of the breeds susceptible to visceral leishmaniasis in North America.

## *Infectious Agents*

### Morphologic Description

See chapter 4.

### Life Cycle and Transmission

See chapter 4.

## *Clinical Features and Pathogenesis*

The incubation period for VL is generally 2 to 6 months, although disease occasionally develops many years after exposure. Following inoculation by a sandfly, Leishmania promastigotes enter cutaneous dendritic cells or macrophages through receptor-mediated phagocytosis. The parasites use host complement receptors to enter phagolysosomes, and survive and multiply despite low pH and activated proteinases. Experimental studies in mice have shown that sandfly saliva promotes transmission of *Leishmania* sp through anticlotting and antiplatelet factors, and by vasodilation and immunomodulation. Persistence and propagation of promastigotes and amastigotes in host macrophages are enhanced by the effect of these salivary components on cytokines and by inhibition of nitric oxide killing. These properties of sandfly saliva are the focus of current research on an antileishmania vaccine.[11]

At the site of inoculation, a small granuloma develops, consisting of histiocytes filled with amastigotes and surrounded initially by epithelioid cells and later by giant cells. Parasites spread to local lymph nodes and then, hematogenously within macrophages, to the liver, spleen, and bone marrow. There they either stimulate a granulomatous cellular immune response that results in subclinical disease and spontaneous resolution, or they multiply and cause the clinical syndrome of VL. Pathogenesis depends to some degree on host genetic factors.

In naive adults, onset of disease is frequently acute, with high fever, chills, and malaise that are often mistaken for malaria.[12] Visceral leishmaniasis progresses more gradually in indigenous patients, with intermittent fever, progressive enlargement of the spleen and liver, and vague abdominal/splenic discomfort. Other common symptoms include weight loss, loss of appetite, epistaxis, diarrhea, and nonproductive cough. Patients are often weak and emaciated on initial presentation.

On physical examination and at autopsy, the abdomen is usually distended by a markedly enlarged spleen and a moderately enlarged liver (Figs 5.3 to 5.5). The spleen is smooth, firm, and nontender. In acute VL, the spleen may be scarcely palpable. Femoral and inguinal lymphadenopathy are often noted, especially in African VL. Lymphatic leishmaniasis is frequent, and generalized and regional adenopathy may be present with or without systemic symptoms. Lymph nodes are painless and seldom greater than 2 cm in diameter. Trophic changes of the skin and hair of

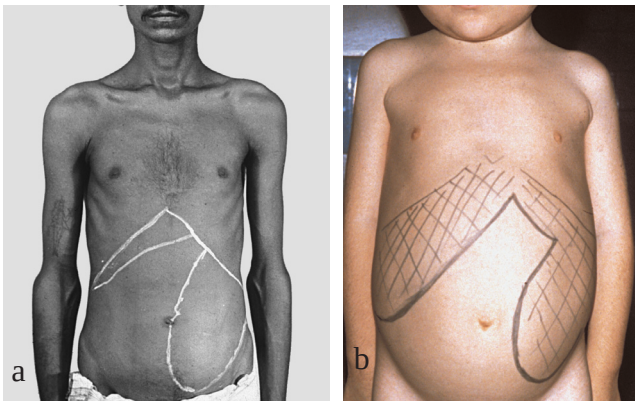



**Figure 5.3 a,b**
Hepatosplenomegaly a. Asian adult patient with visceral leishmaniasis b. Four year-old child from Natal, Brazil.



**Figure 5.4**
Hepatosplenomegaly in siblings from Natal, Brazil.

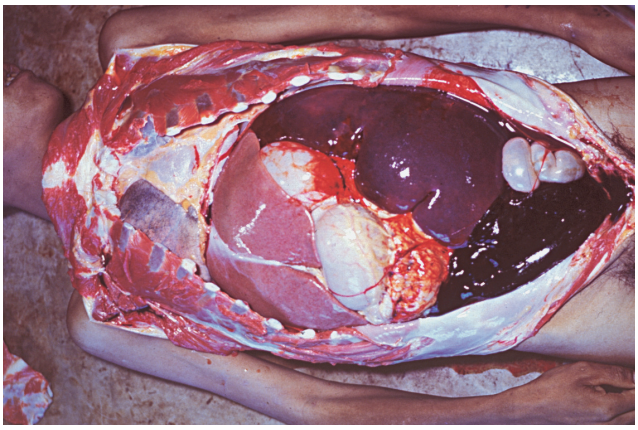


**Figure 5.5**
Autopsy of man with visceral leishmaniasis, hepatosplenomegaly, and intra-abdominal hemorrhage that followed percutaneous needle aspiration of spleen. Note wasting and cutaneous hyperpigmentation

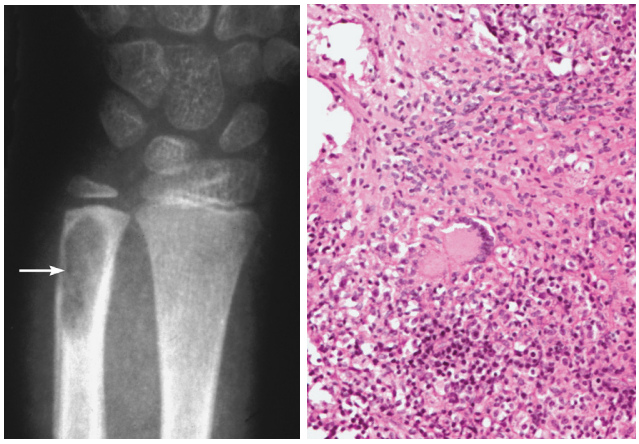


**Figure 5.6. a,b**
a. Radiograph of tender swollen wrist of 9-year-old Iranian patient with no clinical evidence of cutaneous or visceral leishmaniasis. Lesion in distal ulna (arrow) was originally diagnosed as Ewing's tumor.
b. Curettage of the bone lesion revealed visceral leishmaniasis. Note multinucleated giant cells. x110

the lower legs (thinning, dryness, hypopigmentation, loss of curl) are common. Cardiac failure from anemia often causes heart murmurs. Edema of the legs, jaundice, petechiae, and purpura develop in less than 10% of patients. Minor cutaneous, oral, and nasopharyngeal abnormalities are also seen.

Visceral leishmaniasis can be disseminated to virtually any organ or tissue, often mimicking other diseases (Fig 5.6). Uncommon manifestations such as bacteremia, acute hepatitis, and Guillain-Barré syndrome may precede the development of the classic signs and symptoms of VL. Uncommon systemic manifestations associated with classic VL include retinal hemorrhages, massive hepatic necrosis, pancytopenia without splenomegaly, cholecystitis, and paresthesias of the distal extremities.

Laboratory findings typically include hemoglobin concentrations of 5 to 9 g/dl, leukocyte counts of 2,000 to 4,000/mm$^3$, and platelet counts of 50,000 to 200,000/mm$^3$, although lower counts are sometimes seen in advanced disease. Erythrocyte survival time is shortened by hypersplenism and, possibly, by autoimmune mechanisms. Anemia is multifactorial and may result from bone marrow depression, iron deficiency, or a combination of these factors. Coombs' test is usually positive, with both C3 and IgG present on erythrocytes, but does not correlate with the severity of anemia. Neutrophil survival time is shortened, and the leukocyte differential demonstrates neutropenia, relative lymphocytosis, and a near absence of eosinophils. Agranulocytosis is rare.

Liver transaminases are mildly elevated in the majority of patients (ALT more than AST), but elevations of serum bilirubin are uncommon. Prothrombin time is usually 2 to 4 seconds longer than in controls, and serum albumin is generally less than 3 g/dl. A polyclonal hypergammaglobulinemia of 5 to 10 g/dl, most of which is IgG, is usual. Albuminuria is common in some patients; in others, urinalysis and renal function are normal.

**Complications**. Intercurrent illness is common and varies by season and geographic area. Bacterial pneumonia may be present on admission or may develop during treatment. Pulmonary tuberculosis, a common coinfection, should be suspected when response to therapy is unsatisfactory. Severe diarrhea, measles, and malaria can be present. Noma, a necrotizing oral infection, may develop in late stages of VL when neutropenia is severe. Hepatic cirrhosis is an uncommon sequela. Portal hypertension sometimes leads to persistent splenomegaly despite successful treatment. Post-kala-azar anterior uveitis may follow treatment for VL.[13] Other rare ocular complications include retinal hemorrhages, keratitis, central retinal vein thrombosis, and optic neuritis. Disseminated intravascular coagulation, immune complex-mediated glomerulonephritis, and renal amyloidosis with nephrotic syndrome are rare. Death often results from concurrent or intercurrent infections such as tuberculosis, dysentery, measles, or bacterial pneumonia. Severely anemic patients may die from cardiac failure. (See topic 4 for a discussion of post-kala-azar dermal leishmaniasis.)

Differential diagnosis of late-stage VL is limited. Hematologic and lymphatic malignancies, disseminated histoplasmosis, tropical splenomegaly syndrome, and hepatosplenic schistosomiasis can mimic late stage VL. Early disease has a much broader differential, including malaria, African trypanosomiasis, brucellosis, enteric fevers, bacterial endocarditis, generalized histoplasmosis, chronic myelocytic leukemia, Hodgkin's disease and other lymphomas, sarcoidosis, hepatic cirrhosis, and tuberculosis. Multiple myeloma and Waldenström's macroglobulinemia occasionally present with findings suggesting VL.

**Subclinical or Oligosymptomatic Infections.** In endemic areas, inhabitants with no history of overt clinical disease often have a positive leishmanin skin test (Montenegro test). Such individuals appear to be resistant to naturally occurring and experimental infection with *L. donovani*. The difference between true asymptomatic infection and oligosymptomatic disease is difficult to establish in most endemic areas because nonspecific illness is rarely diagnosed and usually not evaluated due to cultural factors and inadequate health care facilities. In a prospective study in Brazil, 33% of children with antibodies to *L. donovani* developed classic VL within a few weeks to 15 months after seroconversion, 23% remained asymptomatic for up to 5 years, and 44% had prolonged, mild constitutional symptoms and intermittent hepatomegaly that resolved without treatment after an average of 35 months. [14]

**Viscerotropic Leishmaniasis**. Viscerotropic leishmaniasis differs from VL in that the infecting organism is *L. tropica* rather than *L. donovani*, and patients do not have the classic signs or symptoms of VL. In the 1990s, 9 cases of

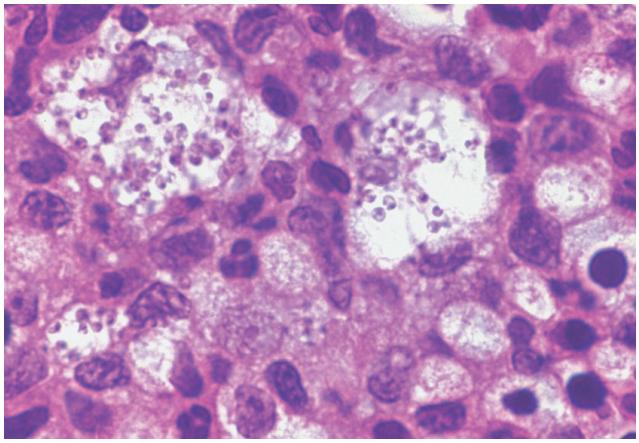


**Figure 5.7**
Bone marrow from 32-year-old AIDS patient who had traveled to Europe and Mexico. Note macrophages containing numerous amastigotes. Specimen also contained mycobacteria. x780

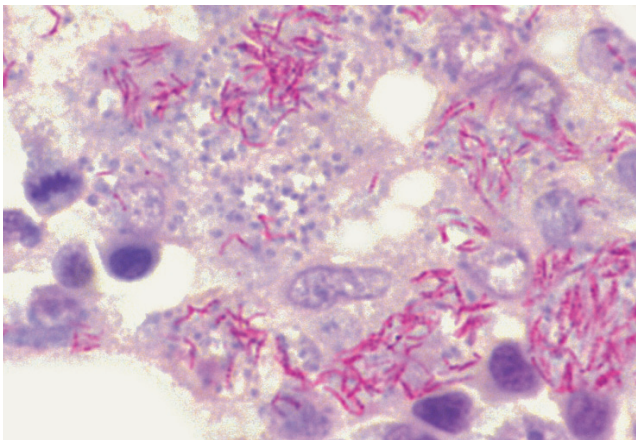


**Figure 5.8**
Acid-fast stain of bone marrow from patient described in Figure 5.20 showing macrophages containing amastigotes and mycobacteria. Ziehl-Neelsen x935

a mild, nonspecific illness characterized by cough, malaise, chronic fatigue, abdominal pain, and intermittent fever and diarrhea were documented in returning American veterans of Operation Desert Storm in the Middle East. All were parasitologically confirmed from bone marrow or lymph node aspirates; 6 of the 9 isolates were characterized as *L. tropica* by isoenzyme analysis.[3] One of the soldiers presented more than 2 years after leaving an endemic area.[15] Nonspecific chronic illness associated with viscerotropic leishmaniasis has also been reported from India and Italy.[16]

**Immunocompromised Hosts**. In the early years of the HIV/AIDs epidemic, visceral leishmaniasis emerged as an important opportunistic infection in HIV-positive patients, especially those with AIDS.[17,18] (Figs 5.7 & 5.8) Coinfection with *Leishmania* sp and HIV is a recognized problem in East Africa, France, Italy, Portugal, and Spain and has been reported in 20 other countries. In the Mediterranean region, it is estimated that up to 70% of cases of VL in adults are associated with HIV, and that approximately 10% of AIDS patients have newly acquired or reactivated VL. In Europe, intravenous drug abuse is thought to be the most significant risk factor for leishmaniasis. As HIV infection spreads in India, Brazil, and East Africa, the number of people at risk for coinfection with VL will increase dramatically.

In coinfected patients, clinical signs and symptoms of VL usually develop in late-stage AIDS. CD4 counts are usually less than 50 and almost always less than 200. In general, AIDS patients with VL have very high parasite burdens but tend to tolerate the coinfection. Many clinicians feel that leishmaniasis does not cause severe symptoms in these patients, but is merely one of many opportunistic infections that plague patients with markedly depressed CD4 counts. Numerous viscerotropic, dermatotropic, and novel *L. infantum* strains (zymodemes) have been isolated from coinfected patients in Europe.[19]

The clinical presentation of VL in AIDS patients is similar to that in non-HIV-infected hosts and includes fever, splenomegaly, and pancytopenia. Involvement of the gastrointestinal tract is more common in AIDS patients. Parasite-laden macrophages are abundant in the submucosa from the esophagus to the rectum. Coinfected patients may have atypical presentations, including a variety of pulmonary radiographic findings such as pleural effusion and pulmonary nodules. Patients with minimal splenomegaly are sometimes afebrile.

Because parasite burdens tend to be higher and serologic tests may be negative in HIV-coinfected patients, classic parasitologic diagnostic methods are preferred. For example, cultures or amplification of parasite specific DNA by PCR of the buffy coat of peripheral blood may be positive in AIDS patients. Fever or hepatosplenomegaly in an HIV-infected patient who has resided in or visited an area endemic for VL should prompt an examination of the bone marrow by both smear and culture for *Leishmania* sp.

Visceral leishmaniasis may occur as an opportunistic infection in patients receiving immunosuppressive drugs or chronic corticosteroids.[20] In solid-organ transplant recipients, VL characterized by fever, splenomegaly, and cytopenia may appear several months following transplantation. Again, in these patients, standard parasitologic diagnostic methods are satisfactory. In endemic areas, VL should never be overlooked in the differential diagnosis of immunocompromised patients.

## *Pathologic Features*

In the less common acute VL, the spleen is smooth and friable and splenic follicles are small. Patients with progressive VL develop marked splenomegaly (Fig 5.5). Splenic infarcts are common. In chronic VL, the spleen is firm, red,

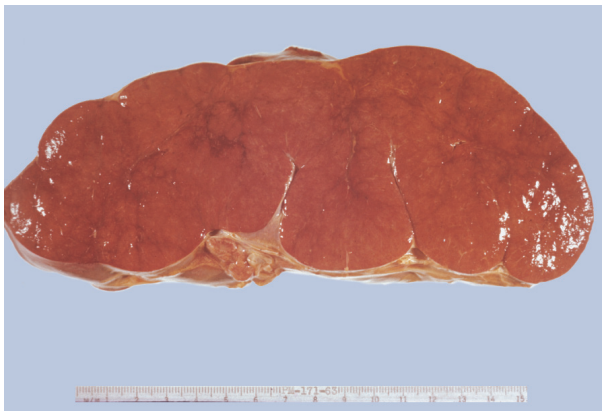


**Figure 5.9**
Splenomegaly in 7-year-old Ugandan patient who died of visceral leishmaniasis after several courses of treatment. Spleen was 970 g and lobulated, with firm red cut surface.

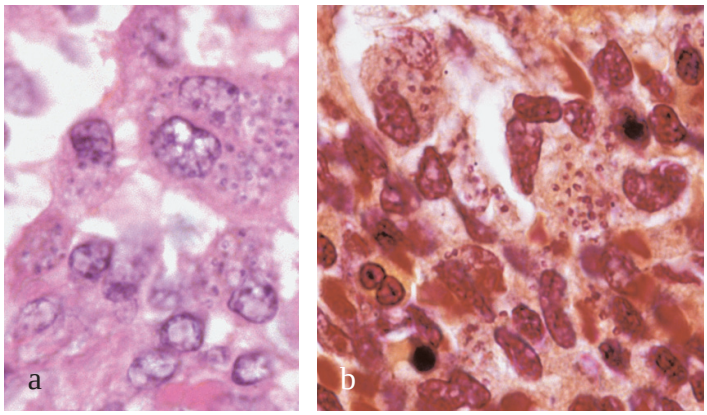



**Figure 5.10 a,b**
Spleen with clusters of amastigotes in phagocytic cells. x720
a. Hematoxylin and Eosin
b. Brown Hopps (B-H).

and lobulated, and has a thickened capsule. The spleen can weigh up to 3 kg even in children (Fig 5.9). Hyperplasia and hypertrophy are caused by parasite-filled reticuloendothelial cells (Fig 5.10a,b). In our experience, amastigotes in VL appear slightly smaller and less distinct than those observed in cutaneous leishmaniasis. Because kinetoplasts are much more difficult to identify, special stains such as Brown-Hopps and Wilder's reticulum are recommended (Fig 5.11b to 5.11d).

The liver is usually enlarged and has a smooth capsule (Fig 5.5). Microscopically, liver sinusoids are dilated, show prominent amastigote-laden Kupffer's cells and little or no cellular reaction (Figs 5.11a & 5.11b). Sections stained by Brown-Hopps and Wilder's reticulum show features of intracellular amastigotes more clearly (Figs 5.11c & 5.11d). In subclinical infections, non-caseating granulomas with few parasites are scattered throughout the liver (Figs 5.12 & 5.13). Lymph nodes may be enlarged and contain macrophages filled with amastigotes, usually with surrounding lymphocytes (Fig 5.14). Tonsillar lymphoid tissue may contain parasites. In subclinical

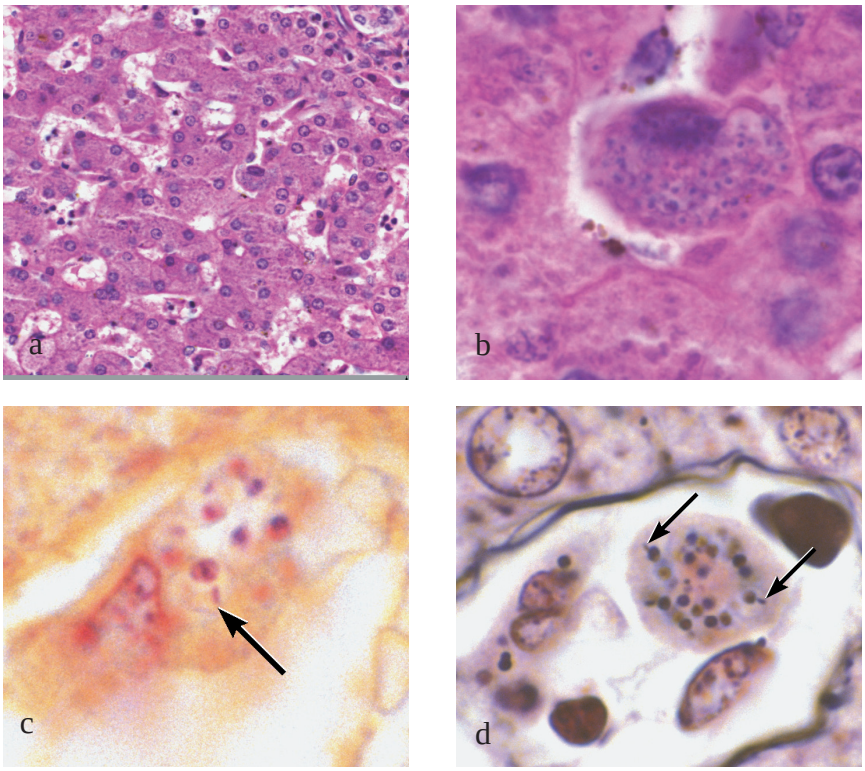



**Figure 5.11 a,b,c,d**
a. Liver with dilated sinusoids and enlarged Kupffer's cells. x250.
b. Numerous amastigotes in Kupffer's cell. x700
c. Amastigotes in Kupffer's cell. Note kinetoplast (arrow). B-H x2200
d. Numerous black amastigotes in Kupffer's cells. Note kinetoplasts (arrows). Wilder's reticulum x1900

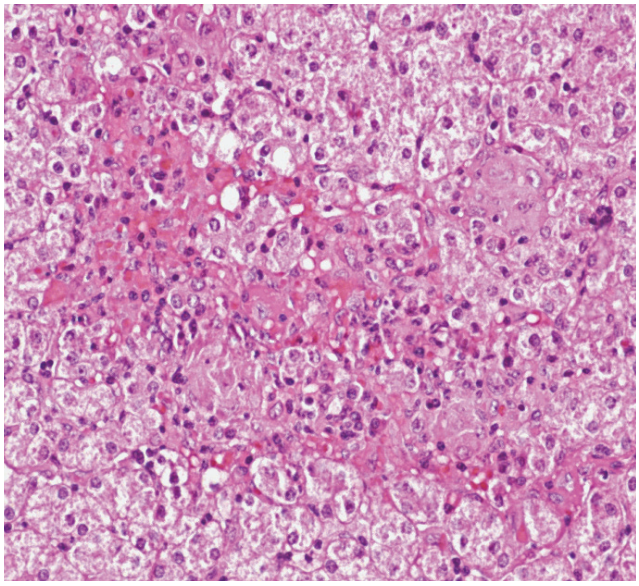


**Figure 5.12**
Nonnecrotizing granuloma in liver. x160.

VL and lymphatic leishmaniasis, there is a granulomatous reaction, with giant cells resembling tuberculosis but without caseation.

Although nasal mucus is an unlikely route of transmission, in Sudan, East Africa, and India, VL sometimes presents with oral and nasopharyngeal lesions. These lesions vary histologically from numerous parasitized histiocytes to granulomas with few parasites. Parasites are less abundant in nasopharyngeal tissues than in oral lesions, but may be demonstrated in secretions from these areas.

In the gastrointestinal tract, there is proliferation of reticuloendothelial cells in the duodenum and jejunum, infiltration of the submucosa with parasitized cells, and, occasionally, villous atrophy with hyperplasia of crypt cells (Fig 5.15). There may be small ulcerations with demonstrable parasites.

The bone marrow is hyperplastic and contains numerous parasite-laden macrophages in acute infections, but few in chronic disease (Fig 5.7). The skin may contain parasites. In fatal VL, all levels beneath the epidermis are often heavily infiltrated, with masses of parasitized cells concentrated around sweat glands and small blood vessels.

Parasites have been identified in virtually all organs, including cardiac muscle (Figs 5.16 & 5.17), adrenals (Figs 5.18a,b), parotid glands, and kidneys (Fig 5.19a,b,c). The kidneys may show an interstitial nephritis (Fig 5.19b) or a mild proliferative glomerulonephritis (Fig 5.19c) and may contain immune complexes. Renal amyloidosis is an uncommon complication of late-stage VL.

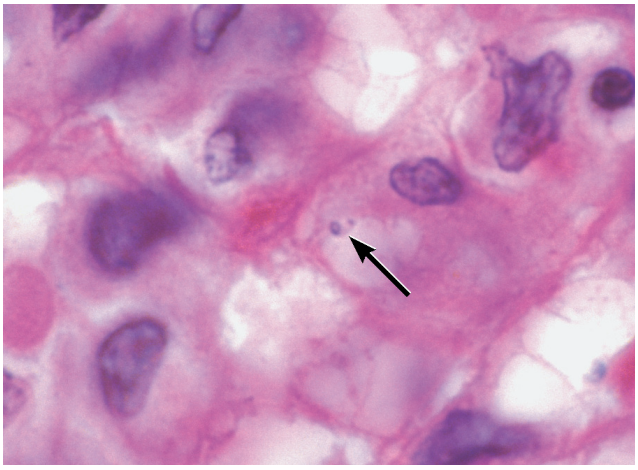


**Figure 5.13**
Higher magnification of liver shown in Figure 5.12 showing rare amastigote in Kupffer's cell (arrow). x1750

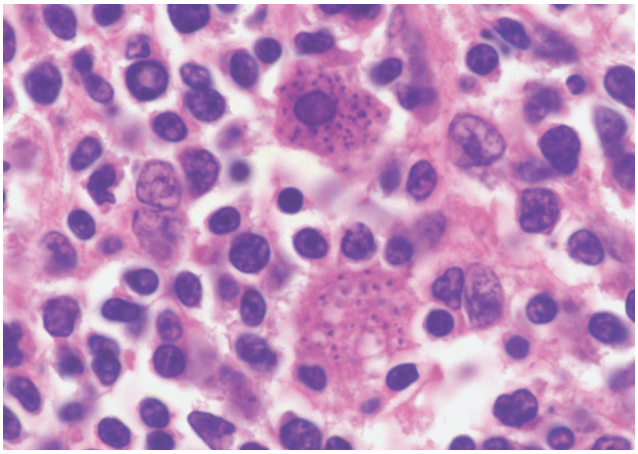


**Figure 5.14**
Lymph node with granular-appearing macrophages containing amastigotes. x620

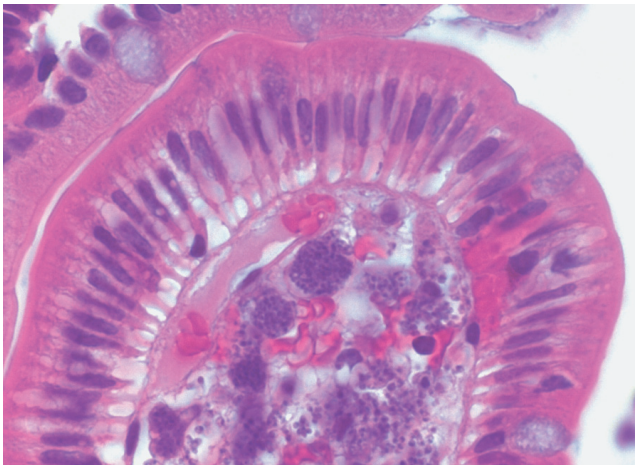


**Figure 5.15**
Numerous amastigotes within histiocytes in lamina propria of duodenum from 46-year-old patient with HIV infection who had traveled to Spain 10 years previously. x600

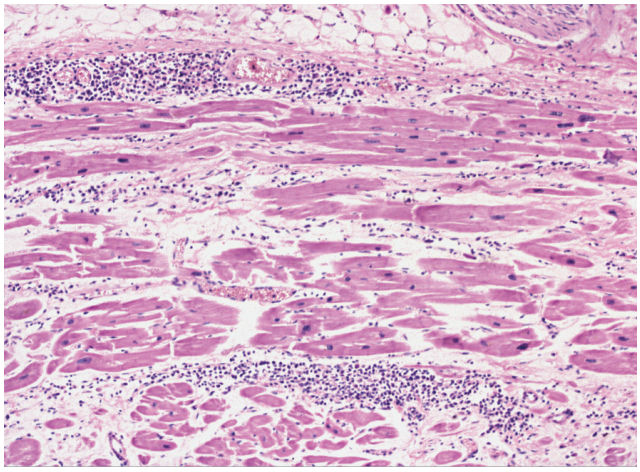


**Figure 5.16**
Chronic myocarditis caused by visceral leishmaniasis. x60

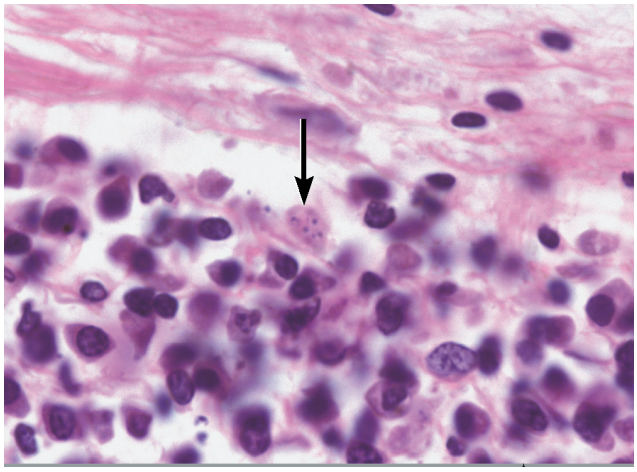


**Figure 5.17**
Amastigotes within histiocyte (arrow) in mycocardium. x730

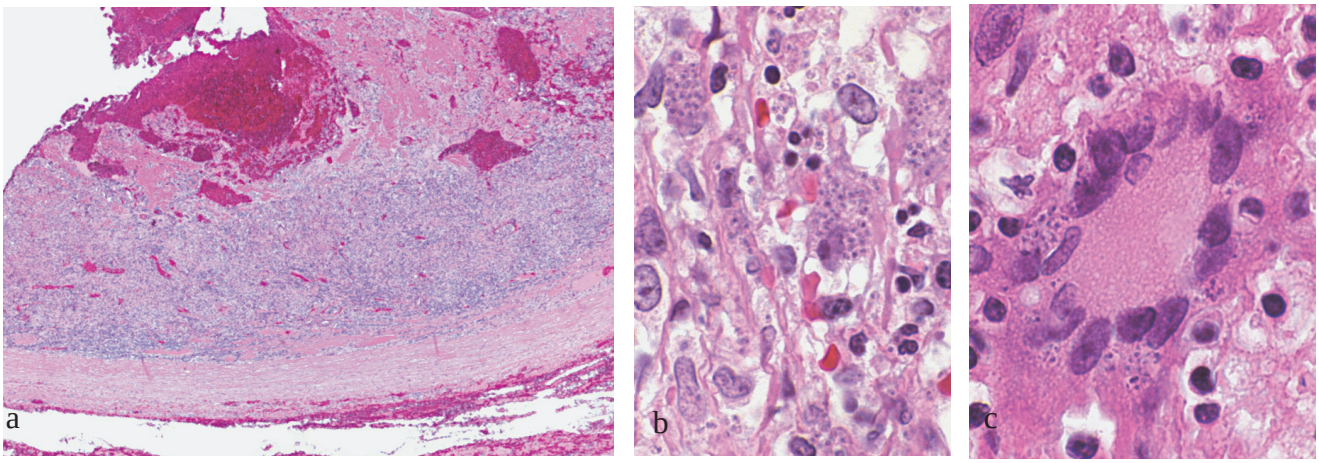



**Figure 5.18 a,b,c**
Adrenal from 69-year-old patient who developed abdominal pain and adrenal enlargement after travel to Greece. a. Note thickened capsule and chronic inflammation. x30 b. Macrophages containing numerous amastigotes. x600 c. A multinucleated giant cell containing amastigotes. x715

## *Diagnosis*

While parasitologic diagnosis and confirmation is always desirable, it is sometimes unfeasible because of the need for invasive procedures, expert microscopy, and adequate health care infrastructure. Depending upon local epidemiological considerations and clinical presentation, VL can be clinically diagnosed with a fair amount of certainty. In an endemic area, the positive predictive value of a clinical diagnosis of late-stage VL with classic signs and symptoms is likely to be high. Clinical diagnosis early in the course of infection when the classic features of disease are not yet established is much less certain. Favorable clinical response to appropriate therapy virtually confirms a clinical diagnosis of VL.

Parasitologic diagnosis is based on demonstrating amastigotes in tissues or clinical specimens, visualizing promastigotes in in vitro cultures, or amplification of parasite specific DNA via the polymerase chain reaction (PCR). Splenic aspiration is the surest method of parasitologic diagnosis, but carries the risk of splenic laceration (Fig 5.5). Careful observation of the patient after the procedure is essential.[21] Giemsa stained splenic smears demonstrate amastigotes in 98% to 100% of patients, and quantitation of splenic smears is helpful in measuring response to therapy.[22] Promastigotes can be seen within 2 to 7 days in Schneider's medium or 7 to 21 days in NNN medium after incubation at 25° C.

For clinicians unfamiliar with splenic aspiration or concerned about its risks, there are satisfactory alternatives. Bone marrow smears usually contain amastigotes, though fewer than in splenic smears; parasites are found in up to 85% of patients.

Amastigotes are frequently found in aspirates or biopsies of liver or lymph nodes. In India and Kenya, buffy coat smears have demonstrated amastigotes in some cases, but this is an uncommon diagnostic method.

A minimally invasive test that would confirm diagno-

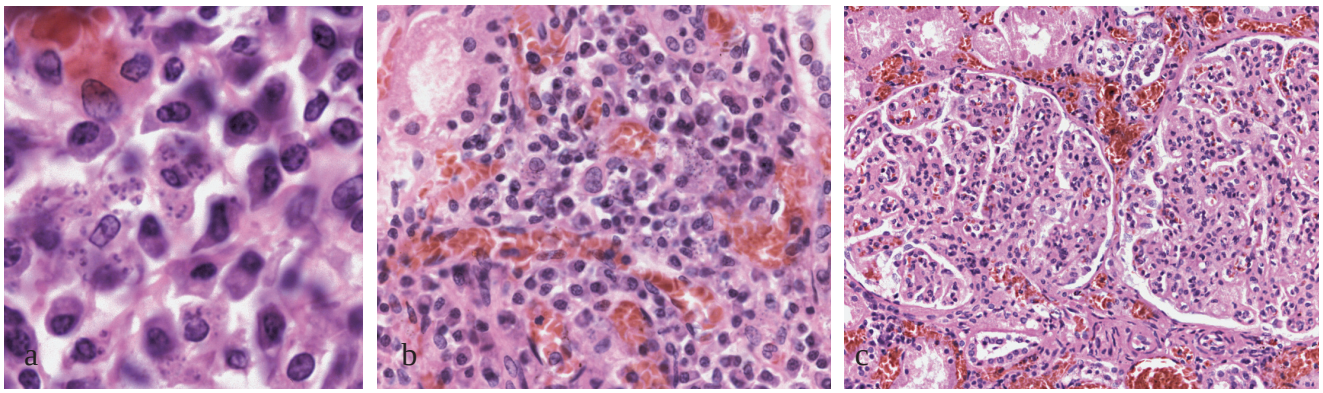



**Figure 5.19 a,b,c**
Kidney. a. Amastigotes in histiocytes. x730 b. Interstitial chronic inflammation. x315 c. Renal glomeruli with features of mesangioproliferative (mesangiocapillary) glomerulonephritis, including thickened basement membrane. x125

sis would be a great asset. Antigen detection assays using whole blood and PCR amplification of *Leishmania* sp DNA from peripheral blood have been used, but these methods are not as sensitive as splenic or bone marrow aspiration.

A variety of serologic tests are available worldwide, many of which however are available only in certain geographic areas. Few have been used extensively enough to compare sensitivity and specificity, but in general, serologic tests for VL currently in use are more than 90% sensitive; specificity tends to be lower. False positive results for VL may be seen in some patients with other infectious diseases. Leishmanial antibodies may also persist for many months following treatment hence are not generally useful to assess response to treatment.

The indirect fluorescent antibody (IFA) test is positive in more than 95% of patients with VL, with titers usually higher than 1:256. These positive IFA tests are readily distinguishable from the low-titer positive tests occasionally seen in malaria, typhoid fever, and other diseases. IFA testing is somewhat subjective and requires expertise and expensive equipment.[23]

Enzyme-linked immunosorbent assay (ELISA) using whole or soluble promastigote antigens appears to be as sensitive and specific as IFA. Economy and convenience make ELISA especially useful for large-scale epidemiologic studies of human and canine leishmaniasis. Both IFA and ELISA can be performed on sera eluted from filter papers impregnated with 50 µl of capillary blood. A direct agglutination test is widely available. Its ease of use, economy, and high sensitivity are offset by poor reproducibility between field sites and the need to establish a cutoff titer for positivity based on local epidemiologic considerations.[24,25]

ELISA and rapid "dipstick" formats for detecting serum antibodies to purified *Leishmania* sp antigens (such as rK39) in patients with VL have improved the sensitivity and specificity of serologic testing for VL. Titers to rK39 decrease following successful chemotherapy and rise during relapse, making this test useful for recognizing treatment failure.[26]

Skin test reactivity is a useful indicator of past infection in epidemiological studies. Intradermal injections of fixed whole promastigotes or a solubilized fraction of parasite antigens (Montenegro or leishmanin test) are negative in symptomatic VL, but become positive in over 90% of patients 6 weeks to a year after recovery. A meta-analysis of the diagnostic performance of the direct agglutination test and rK39 dipstick for visceral leishmaniasis showed comparable sensitivity and specificity of about 95% and 90% respectively.[27]

## Treatment and Prevention

Patients with VL should receive dietary support and antimicrobial agents for concurrent pneumonia, tuberculosis, or other bacterial infections as clinically indicated. Blood transfusion may be indicated in severely anemic patients, and iron or vitamin deficiency may require specific treatment.

Pentavalent antimony compounds (SbV), sodium stibogluconate (SSG) (Pentostam®) and meglumone antimoniate (Glucantime), have been effective drugs for the treatment of VL since the 1930s. SbV is efficacious in East Africa and Brazil and remains one of the first line treatments recommended by the World Health Organization for the treatment of visceral leishmaniasis.[28] However, in the mid-1990s, reports from India of increasing primary treatment failures with SbV led to trials of lipid-associated amphotericin B as initial therapy for Mediterranean and Indian VL.[29] Today, lipid-associated amphotericin B is frequently the first-line therapy for VL.

In the United States, SSG can be obtained from the Centers for Disease Control and Prevention under a clinical protocol by an Investigational New Drug application because

Pentostam is not an approved drug in the United States. The recommended treatment regimen for primary VL is 20 mg/kg body weight/day for 28 days.[30] Longer durations may be required for patients who are slow to respond and for Indian VL.

SSG is safe if used under close medical supervision but can produce side effects such as nausea, anorexia, abdominal pain, malaise, headache, arthralgias, myalgias, and lethargy.[31] These side effects, which frequently appear 3 to 7 days into therapy, are poorly tolerated and more apparent in patients with cutaneous and mucocutaneous leishmaniasis, which have no associated systemic symptoms.[32] Serious adverse events include renal failure, pancreatitis, hepatic failure, and sudden cardiac deaths likely caused by drug induced ventricular dysrhythmias have been documented.

Amphotericin B (either deoxycholate or liposomal encapsulated) has a cure rate of nearly 100% in VL patients who have failed treatment with SbV and pentamidine. It is not widely used, however, because of well documented infusion-related side effects of fever, chills, thrombophlebitis, long-term problems of renal insufficiency, anemia, hypokalemia, and poor tolerability (anorexia, nausea). Furthermore, sudden cardiac death has been reported following the first dose of amphotericin B deoxycholate in patients previously treated with SbV,[33] possibly because conduction abnormalities associated with SbV therapy predispose patients to cardiac events. It is prudent to obtain a baseline ECG and wait until any abnormalities normalize, usually within 10 days of terminating SbV therapy, before administering amphotericin B deoxycholate.

Lipid-associated amphotericin B preparations are the least toxic and best tolerated chemotherapeutic agents for VL. Liposomal amphotericin B (AmBisome®) was approved in 1997 by the United States Food and Drug Administration (FDA) for treatment of VL. A series of trials proved the drug to be safe and active against VL acquired in Brazil, India, Kenya, and Mediterranean countries.[34-36] The current FDA-approved regimen for immunocompetent patients, based on data from Mediterranean countries and Brazil, is 3 mg/kg body weight daily on days 1 to 5, a 6th dose on day 14, and a 7th dose on day 21 (total dose: 21 mg/kg body weight). The overall cure rate with this regimen approaches 100%. The current FDA-approved regimen for immunosuppressed patients is 4 mg/kg body weight daily on days 1 to 5, 10, 17, 24, 31, and 38 (total dose: 40 mg/kg body weight). Even with the higher total dose, relapse is common in those individuals whose immunosuppression cannot be reversed or improved. These regimens have few infusion-related side effects and renal insufficiency is uncommon.

The relatively high cost of AmBisome has limited its adoption and use in resource poor countries and stimulated interest in lower-dose and shorter course regimens, many of which have been shown to be effective in trials in Brazil, India, and Kenya. For example a single 10 mg / kg dose of AmBisome was shown to be > 95% efficacious in Indian VL. [37]

In HIV coinfected patients, the efficacy of SbV is 50%, however the efficacy of liposomal amphotericin B is 100%. Relapse is common after treatment with either drug. The optimal drug, dose, and duration of induction and intermittent maintenance regimens for the various infecting species are not known. Where feasible, the optimal therapy is immune system reconstitution through highly active antiretroviral therapy (HAART). Although data are lacking, it is reasonable to recommend an initial course of induction therapy using liposomal amphotericin B to decrease parasite burden, followed closely by HAART to raise the CD4 cell count.

Infection with *L. donovani* comprises a spectrum of diseases, and spontaneous resolution of subclinical infection is more common than was formerly realized. In contrast, the established syndrome of VL is almost always fatal without specific chemotherapy. With specific chemotherapy, such as SbV or amphotericin B, the death rate is relatively low. For example, in Bihar, India in 1990, mortality from VL was 1%. In war-torn southern Sudan, one of the most difficult environments for VL management, mortality during the VL epidemic of the 1990s was only 11%.[38] Outside of India, failure to respond to initial SbV therapy is uncommon in previously untreated, immunocompetent patients.

Where humans are the reservoir of VL (India and perhaps some areas of East Africa), finding and treating VL patients may interrupt epidemics. In regions where dogs are the reservoir (Mediterranean countries, China, South America), conventional wisdom states that identifying and destroying infected dogs reduces the incidence of VL. Although a recent interventional trial in Brazil failed to support that hypothesis,[39] some authorities strongly recommend continued control of zoonotic VL in Brazil, based on the results of a meta-analysis of the interventional trial.[40] In India in the early 20th century, vector control was maintained by burning houses that were microfocal for *L. donovani*. During malaria eradication campaigns that employed DDT to control the vector, VL virtually disappeared from India. With the termination of these campaigns, incidence has returned to high levels.

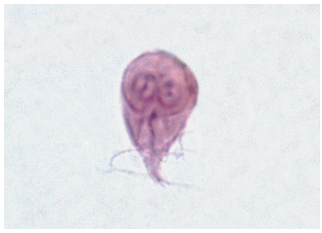
No VL vaccine is currently licensed or commercially available. A variety of vaccine preparations, including killed promastigotes with and without adjuvants, parasite fractions, recombinant antigens, genetically engineered "avirulent" live parasites, and vaccines based on sandfly saliva are in various stages of development and clinical trials.[41-46]

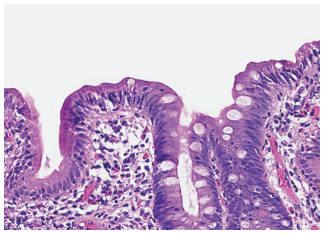
## References

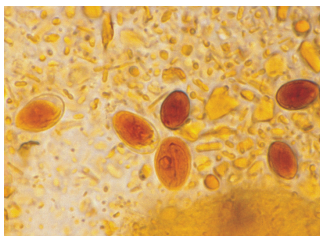

1. Berman JD. Human leishmaniasis: clinical, diagnostic, and chemotherapeutic developments in the last 10 years. *Clin Infect Dis*. 1997;24:684-703.
2. Herwaldt BL. Leishmaniasis [review]. *Lancet*. 1999;354:1191-1199.
3. Magill AJ, Grogl M, Gasser RA Jr, Sun W, Oster CN. Visceral infection caused by *Leishmania tropica* in veterans of Operation Desert Storm. *N Engl J Med*. 1993;328:1383-1387.
4. Desjeux P. Leishmaniasis: current situation and new perspectives. *Comp Immunol Microbiol Infect Dis*. 2004;27:305-318
5. Magill AJ. Epidemiology of the leishmaniases. *Dermatol Clin*. 1995;13:505-523.
6. Sharma U, Singh S. Insect vectors of Leishmania: distribution, physiology and their control. *J Vector Borne Dis*. 2008;45:255-272
7. Gaskin AA, Schantz P, Jackson J, et al. Visceral leishmaniasis in a New York foxhound kennel. *J Vet Intern Med*. 2002;16:34-44.
8. Freeman K. Update on the diagnosis and management of *Leishmania* spp infections in dogs in the United States. *Top Companion Anim Med*. 2010;25:149-154.
9. Jamjoom MB, Ashford RW, Bates PA, et al. *Leishmania donovani* is the only cause of visceral leishmaniasis in East Africa; previous descriptions of *L. infantum* and *"L. archibaldi"* from this region are a consequence of convergent evolution in the isoenzyme data. *Parasitology*. 2004;129:399-409.
10. Gelanew T, Kuhls K, Hurissa Z, et al. Inference of population structure of *Leishmania donovani* strains isolated from different Ethiopian visceral leishmaniasis endemic areas. *PLoS Negl Trop Dis*. 2010;4:e889
11. Titus RG, Bishop JV, Mejia JS. The immunomodulatory factors of arthropod saliva and the potential for these factors to serve as vaccine targets to prevent pathogen transmission. *Parasite Immunol*. 2006;28:131-141
12. Magill AJ. Leishmania Species: Visceral (Kala-Azar), Cutaneous, and Mucosal Leishmaniasis. In: Mandell GL, Bennett JE, and Dolin R. editors. *Principles and Practice of Infectious Diseases*. 7th ed. Philadelphia (PA): Churchill Livingstone; 2010. p 3463-3480.
13. el-Hassan AM, Khalil EA, el Sheikh EA, Zijlstra EE, Osman A, Ibrahim ME. Post kala-azar ocular leishmaniasis. *Trans R Soc Trop Med Hyg*. 1998;92:177-179.
14. Badaro R, Jones TC, Carvalho EM, et al. New perspectives on a subclinical form of visceral leishmaniasis. *J Infect Dis*. 1986;154:1003-1011.
15. Magill AJ, Grogl M, Johnson SC, Gasser RA Jr. Visceral infection due to *Leishmania tropica* in a veteran of Operation Desert Storm who presented 2 years after leaving Saudi Arabia. *Clin Infect Dis*. 1994;19:805-806.
16. Pampiglione S, Manon-Bahr PE, Giungi F, Giunti G, Parenti A, Canestri Trotti G. Studies on Mediterranean leishmaniasis. 2. Asymptomatic cases of visceral leishmaniasis. *Trans R Soc Trop Med Hyg*. 1974;68:447-453.
17. Alvar J, Canavate C, Gutierrez-Solar B. Leishmania and human immunodeficiency virus coinfection: the first 10 years. *Clin Microbiol Rev*. 1997;10:298-319.
18. Alvar J, Aparicio P, Aseffa A, et al. The relationship between leishmaniasis and AIDS: the second 10 years. *Clin Microbiol Rev*. 2008;21:334-359.
19. Jimenez MI, Laguna F, de la Torre F, Solis F, Pratlong F, Alvar J. New *Leishmania (Leishmania) infantum zymodemes* responsible for visceral leishmaniasis in patients co-infected with HIV in Spain. *Trans R Soc Trop Med Hyg*. 1995;89:33.
20. Antinori S, Cascio A, Parravicini C, Bianchi R, Corbellino M. Leishmaniasis among organ transplant recipients. *Lancet Infect Dis*. 2008.8:191-199.
21. Kager PA. Splenic aspiration in visceral leishmaniasis. *Rev Soc Bras Med Trop*. 1992;25:217-223.
22. Chulay JD, Bryceson AD. Quantitation of amastigotes of *Leishmania donovani* in smears of splenic aspirates from patients with visceral leishmaniasis. *Am J Trop Med Hyg*. 1983;32:475-479.
23. Walton BC, Brooks WH, Arjona I. Serodiagnosis of American leishmaniasis by indirect fluorescent antibody test. *Am J Trop Med Hyg*. 1972;21:296-299.
24. Boelaert M, El Safi S, Jacquet D, de Muynck A, van der Stuyft P, Le Ray D. Operational validation of the direct agglutination test for diagnosis of visceral leishmaniasis. *Am J Trop Med Hyg*. 1999;60:129-134.
25. Boelaert M, El Safi S, Mousa H, et al. Multi-centre evaluation of repeatability and reproducibility of the direct agglutination test for visceral leishmaniasis. *Trop Med Int Health*. 1999;4:31-37.
26. Sundar S, Reed SG, Singh VP, Kumar PC, Murray HW. Rapid accurate field diagnosis of Indian visceral leishmaniasis. *Lancet*. 1998;351:563-565.
27. Chappuis F, Rijal S, Soto A, Menten J, Boelaert M. A meta-analysis of the diagnostic performance of the direct agglutination test and rK39 dipstick for visceral leishmaniasis. *BMJ*. 2006;333(7571):723.
28. World Health Organization: Control of the leishmaniasis: report of a meeting of the WHO Expert Committee on the Control of leishmaniases, WHO Tech Rep Ser No 949. 2010, WHO, Geneva.
29. Sundar S, More DK, Singh MK, et al. Failure of pentavalent antimony in visceral leishmaniasis in India: report from the center of the Indian epidemic. *Clin Infect Dis*. 2000;31:1104-1107.
30. Herwaldt BL, Berman JD. Recommendations for treating leishmaniasis with sodium stibogluconate (Pentostam) and review of pertinent clinical studies. *Am J Trop Med Hyg*. 1992;46:296-306.
31. Davidson RN. Visceral leishmaniasis in clinical practice [review]. *J Infect*. 1999;39:112-116.
32. Aronson NE, Wortmann GW, Johnson SC, et al. Safety and efficacy of intravenous sodium stibogluconate in the treatment of leishmaniasis: recent U.S. military experience. *Clin Infect Dis*. 1998;27:1457-1464.
33. Sundar S, Sinha PR, Agrawal NK, et al. A cluster of cases of severe cardiotoxicity among kala-azar patients treated with a high-osmolarity lot of sodium antimony gluconate. *Am J Trop Med Hyg*. 1998;59:139-143.
34. Berman JD. U.S. Food and Drug Administration approval of AmBisome (liposomal amphotericin B) for treatment of visceral leishmaniasis. *Clin Infect Dis*. 1999;28:49-51.
35. Berman JD, Badaro R, Thakur CP, et al. Efficacy and safety of liposomal amphotericin B (AmBisome) for visceral leishmaniasis in endemic developing countries. *Bull World Health Organ*. 1998;76:25-32.
36. Meyerhoff A. U.S. Food and Drug Administration approval of AmBisome (liposomal amphotericin B) for treatment of visceral leishmaniasis. *Clin Infect Dis*. 1999;28:42-48; discussion 49-51.
37. Sundar S, Chakravarty J, Agarwal D, Rai M, Murray HW. Single-dose liposomal amphotericin B for visceral leishmaniasis in India. *N Engl J Med*, 2010.11;362:504-512
38. Seaman J, Mercer AJ, Sondorp HE, Herwaldt BL. Epidemic visceral leishmaniasis in southern Sudan: treatment of severely debilitated patients under wartime conditions and with limited resources. *Ann Intern Med*. 1996;124:664-672.
39. Dietze R, Barros GB, Teixeira L, et al. Effect of eliminating seropositive canines on the transmission of visceral leishmaniasis in Brazil. *Clin Infect Dis*. 1997;25:1240-1242.
40. Palatnik-de-Sousa CB, dos Santos WR, Franca-Silva JC, et al. Impact of canine control on the epidemiology of canine and human visceral leishmaniasis in Brazil. *Am J Trop Med Hyg*. 2001;65:510-517.
41. Handman E. Leishmaniasis: current status of vaccine development. *Clin Microbiol Rev*. 2001;14:229-243.
42. Khalil EA, el-Hassan AM, Zijlstra EE, et al. Autoclaved Leishmania major vaccine for prevention of visceral leishmaniasis: a randomised, double-blind, BCG-controlled trial in Sudan. *Lancet*. 2000;356:1565-1569.
43. Reed SG. Leishmaniasis vaccination: targeting the source of infection. *J Exp Med*. 2001;194:F7-F9.
44. Valenzuela JG, Belkaid Y, Garfield MK, et al. Toward a defined anti-Leishmania vaccine targeting vector antigens: characterization of a protective salivary protein. *J Exp Med*. 2001;194:331-342.
45. Khamesipour A, Rafati S, Davoudi N, Maboudi F, Modabber F. Leishmaniasis vaccine candidates for development: a global overview. *Indian J Med Res*. 2006;123:423-438
46. Silvestre R, Cordeiro-da-Silva A, Ouaissi A. Live attenuated Leishmania vaccines: a potential strategic alternative. *Arch Immunol Ther Exp (Warsz)*. 2008;56:123-126.


## Acknowledgement

**Figure 5.2**
American Foxhound Club







6

# Giardiasis

*Ellen M. Andersen, Mary K. Klassen-Fischer, and Ronald C. Neafie*

## *Introduction*

### Definition

Giardiasis is gastroenteritis caused by the flagellate protozoon *Giardia intestinalis* (syn. *Giardia lamblia*) of the order Diplomonadida, family Hexamitidae.

### Synonyms

Synonyms for *G. intestinalis* include *Giardia duodenalis, Giardia lamblia, Giardia enterica, Lamblia intestinalis, Cercomonas intestinalis,* and *Megastoma enterica*. The name *G. duodenalis* is sometimes followed by the name of the animal from which the parasite was obtained. Lambliasis and lambliosis are also synonyms for giardiasis.

### General Considerations

Until the early 1940s, *G. intestinalis* (syn. G. *lamblia*) was considered a harmless commensal. It is now recognized as a major cause of waterborne enteric disease throughout tropical and temperate regions. In 1682 Leeuwenhoek briefly described an organism that was probably *G. intestinalis*. In 1859 Lambl gave the first comprehensive description of the trophozoite stage, followed by Grassi's description of the cyst stage in 1879. In 1915 Stiles established the name *Giardia lamblia* in honor of Giard, a French biologist and parasitologist (1846-1908), and Lambl.

## *Epidemiology and Transmission*

Giardiasis is cosmopolitan, but infection rates vary regionally from 1% to more than 25%. Rates are higher in warmer climates and in crowded unsanitary environments. Men and women are affected equally, but age is a risk factor. Children under age 5 years are 3 times more susceptible to infection than adults, and prevalence of cyst passage in

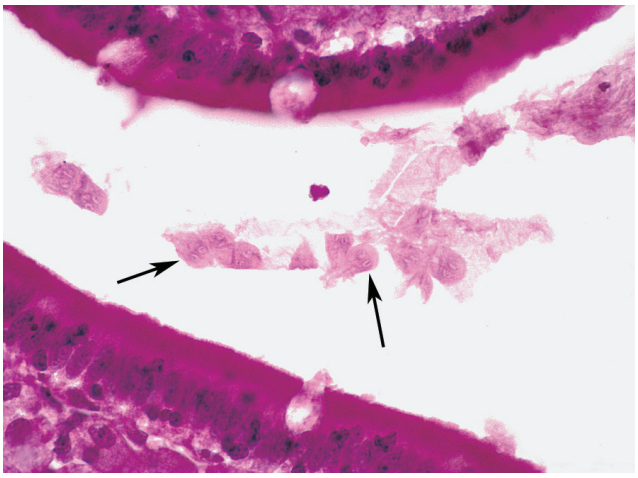


**Figure 6.1**
Multiple piriform *Giardia intestinalis* trophozoites (arrows) in lumen of duodenum demonstrating paired nuclei. x400




**Figure 6.2**
Higher magnification of *Giardia intestinalis* trophozoite in lumen of duodenum from same specimen as in Figure 6.1. Note paired nuclei with large karyosomes, and faintly stained median body (mb) and axonemes (ax). x 1330

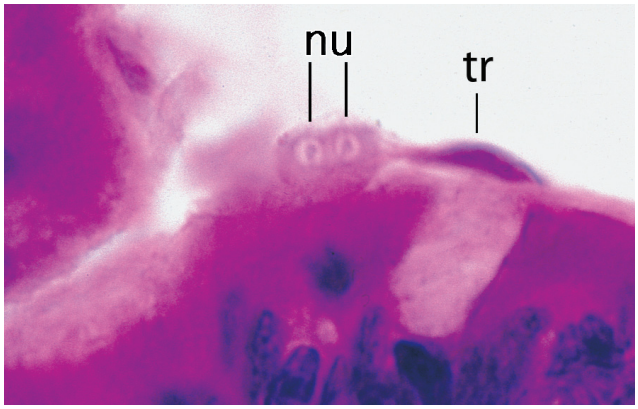



**Figure 6.3**
Two *Giardia intestinalis* trophozoites attached to surface of duodenal epithelium. Note paired nuclei (nu) of trophozoite at left and lateral view of a trophozoite (tr) at right. x1600

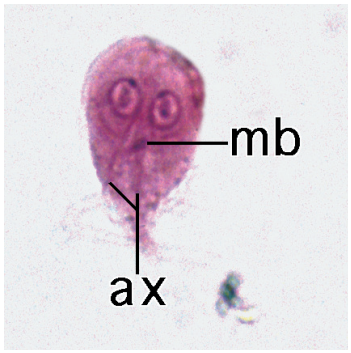



**Figure 6.4**
*Giardia intestinalis* trophozoite in lumen of duodenum. Note pear shape, 2 nuclei with karyosomes, and faintly stained median body (mb) and axonemes (ax). Movat x1800

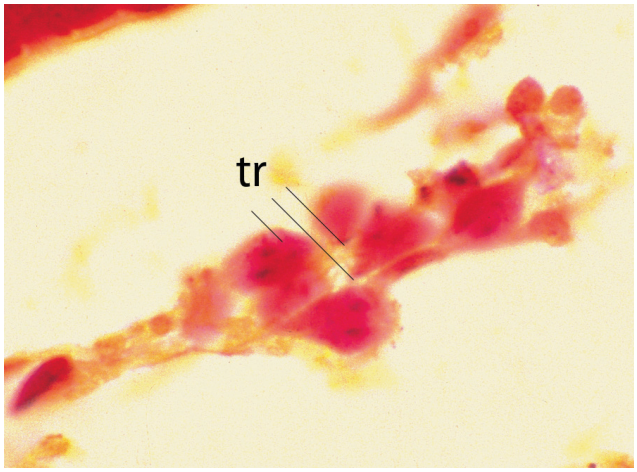



**Figure 6.5**
*Giardia intestinalis* trophozoites (tr) in lumen of small intestine depicting paired nuclei. B&H x1400

children under 3 years can reach 50%. In the United States, although underreporting is likely, approximately 19,000 cases were reported yearly between 2006 and 2008.[1,2]

Humans are infected by ingesting water or food contaminated with *Giardia* cysts or by fecal-oral transmission. Waterborne outbreaks of giardiasis have been linked to unfiltered water from shallow wells, persistent contamination of communal drinking water sources, and ingestion of water from recreational sources such as swimming pools. In the United States, most cases of giardiasis are reported in late summer and early fall, the peak seasons for recreational water sports. Foodborne outbreaks are well-documented, as is person-to-person transmission among homosexual men and among children and staff in day care facilities. The cyst wall of *G. intestinalis* is resistant to chlorine. Before water treatment standards in the United States became more stringent, waterborne transmission of *G. intestinalis* accounted for an estimated 25% of reported cases of giardiasis. In 2002 giardiasis became a nationally notifiable disease in the United States. Enactment of the Surface Water Treatment Rule and the Ground Water Rule by the EPA has decreased the number of ground water associated giardiasis outbreaks.[1]

The importance of giardiasis as a zoonotic disease is controversial, although there has been documented evidence of the zoonotic transmission of *Giardia* sp. Many studies on genotyping of various zoonotic *Giardia* sp have shown that the genotypes found in the zoonotic species (C through G) have not been found in humans. Although there has been documented evidence of *Giardia* sp transmission from animals to humans and humans to animals, zoonotic transmission is generally considered to be of minor consequence .[3-6]

## *Infectious Agent*

### Morphologic Description

*Giardia intestinalis* exists in 2 stages: trophozoite and cyst. Trophozoites, the only stage seen in biopsy and autopsy specimens, are pear-shaped and bilaterally symmetrical. Trophozoites range in size from 10 to 20 µm long, 5 to 15

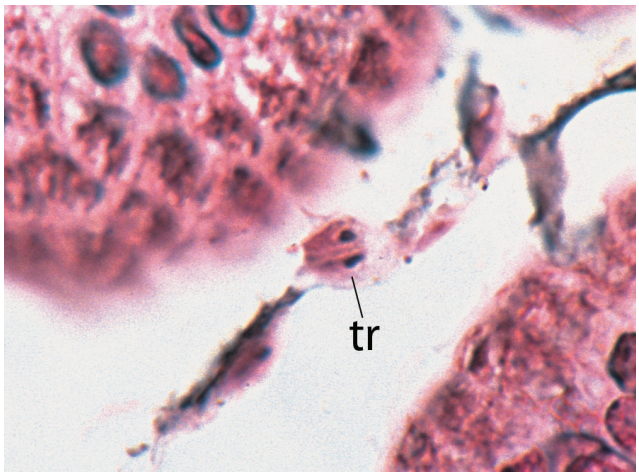



**Figure 6.6**
*Giardia intestinalis* trophozoite (tr) in lumen of small intestine showing paired nuclei and 2 axonemes. Wilder's reticulum x1390




**Figure 6.7**
Same *Giardia intestinalis* trophozoite in lumen of duodenum shown in Figure 6.4, but at a different plane. Note large ventral adhesion disk (ad). Paired nuclei are visible at this level, though slightly out of focus. Movat x1500.

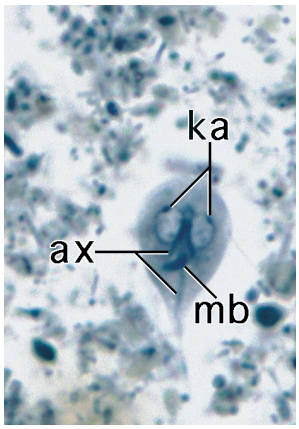



**Figure 6.8**
*Giardia intestinalis* trophozoite in smear of stool specimen. Paired nuclei with karyosomes (ka), median body (mb), and axonemes (ax) are clearly visible. Iron hematoxylin x1630

µm wide, and 2 to 4 µm thick (Figs 6.1 to 6.3). There are 2 nearly identical ovoid nuclei, each having a large central karyosome (Figs 6.2 & 6.4 to 6.6). A large adhesion disk is conspicuous on the anterior ventral surface (Fig 6.7). Pairs of axonemes give rise to 8 long flagella that stain poorly and are rarely observed. Trophozoites typically contain 2 curved rods, called median bodies, that lie posterior to the nuclei near the center of the cell (Fig 6.8). Trophozoites reproduce by longitudinal binary fission and can be cultured from duodenal aspirates (Fig 6.9).

The cyst stage of *G. intestinalis* is usually recovered from stool specimens. Cysts are ovoid to ellipsoid and measure 8 to 12 µm by 5 to 10 µm (Figs 6.10 & 6.11). The cyst wall is 0.3 to 0.5 µm thick. Mature cysts contain 4 nuclei, usually located at one end of the cyst, with each typically containing a spherical karyosome (Figs 6.10 & 6.12). Cysts also have median bodies, an adhesion disk, and retractile flagella in axonemes that appear as fibrils (Fig 6.13).

## Clinical Features and Pathogenesis

As few as 10 to 25 cysts can cause infection in humans.[7] The incubation period can be as long as 10 weeks, but is usually 1 to 2 weeks. Gastric acid and pancreatic enzymes induce excystation of trophozoites. These trophozoites colonize the small intestine, especially the duodenum, by attaching to enterocytes, possibly by specific receptor ligands.[8]

The mechanism by which *G. intestinalis* causes gastrointestinal dysfunction is not completely understood. The number of trophozoites adhering to the gut mucosa directly effects the proper absorptive and enzymatic functions of the intestine. Immune-mediated mechanisms,[9] competition for essential nutrients within the intestinal lumen, bacterial overgrowth, and the formation of a physical barrier to absorption are proposed mechanisms. There may be a significant decrease of brush border enzymes and malabsorption of fat, vitamins A and B12, disaccharides, and protein.[10]

Clinical presentation of giardiasis ranges from asymptomatic infections to fulminant diarrhea, malabsorption and severe malnutrition. In asymptomatic infections only the passage of cysts in stool indicates the presence of parasites. Symptomatic giardiasis can be acute or chronic. The acute stage of infection is marked by the sudden onset of explosive, watery, malodorous diarrhea. Epigastric cramps are accompanied by bloating, flatulence, sulfuric belching,

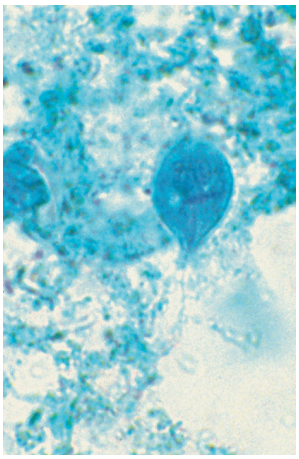


**Figure 6.9**
*Giardia intestinalis* trophozoite in smear from culture. Trichrome x1450

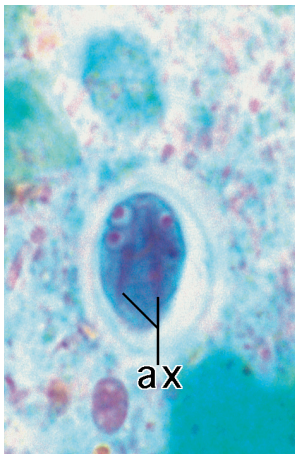



**Figure 6.10**
*Giardia intestinalis* cyst in smear of stool specimen. Axonemes (ax) and 3 of 4 nuclei are visible at this level. Median bodies are barely discernible. Trichrome x2025

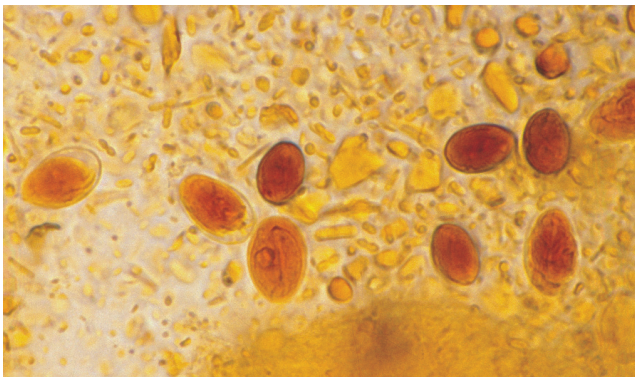


**Figure 6.11**
Several *Giardia intestinalis* cysts in wet mount of stool specimen. Iodine x715

malaise, weight loss, anorexia, and nausea. Continuous or intermittent diarrhea is the cardinal clinical complaint. Stools may be fatty but typically do not contain mucus, blood, or pus. The acute stage lasts from a few days to 2 or 3 months. White blood cell counts are normal and there is no eosinophilia. Persistent symptoms may mimic hiatal hernia, ulcer, or gallbladder disease.[11] Many patients with recurrent diarrhea after treatment are actually experiencing temporary lactose intolerance, not a relapse of infection.[10]

Humoral, cellular, and mucosal responses play a role in immunity to giardiasis.[12] The intestinal IgA response to acute infection is critical, as are the proliferative responses of the mesenteric lymph nodes and Peyer's patches. Nitric oxide synthesized by the intestinal epithelial cells is antiparasitic.[13]

Although asymptomatic infections are more often seen in children, chronic childhood giardiasis can cause malabsorption, weight loss, retarded growth, and zinc deficiency.[14] Persistent diarrhea can produce hypokalemia, especially in elderly hospitalized patients.[15] Rare extraintestinal manifestations such as hepatobiliary disease, and allergic reactions including urticaria, angioedema, and arthropathy have been reported.[16] Patients with AIDS may develop a giardiasis refractory to treatment if they are severely immunosuppressed.[17]

## *Pathologic Features*

Most patients with giardiasis have normal duodenal mucosa (Fig 6.14). It is important to look for *G. intestinalis* in endoscopic biopsies that show normal small intestinal mucosa. Organisms do not invade tissue but are located in the lumen or attached to the epithelial surface of the villi. Laterally oriented organisms, especially when scant, may be easily overlooked (Fig 6.15). Reported cytologic and architectural changes include epithelial cell damage, loss of the brush border, villous atrophy, crypt hyperplasia, increased goblet cells, intraepithelial lymphocytes, increased inflammatory cells within the lamina propria, nodular lymphoid

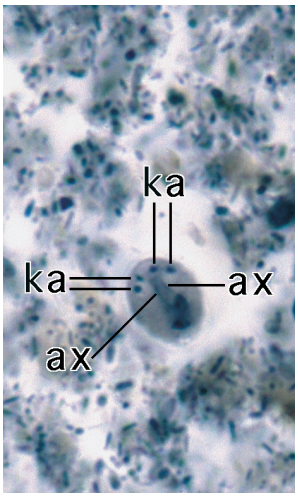



**Figure 6.12**
*Giardia intestinalis* cyst in smear of stool specimen. Axonemes (ax) and 4 karyosomes (ka) are visible at this level. Iron hematoxylin x1405

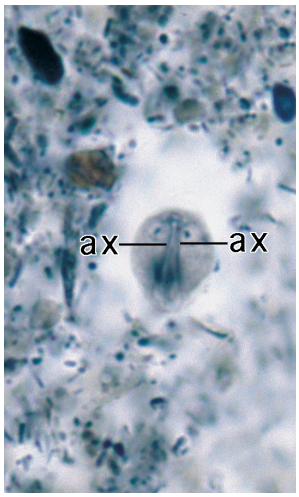



**Figure 6.13**
*Giardia intestinalis* cyst in smear of stool specimen. Axonemes (ax), 2 nuclei with karyosomes, and both median bodies are seen at this level. Iron hematoxylin x1575

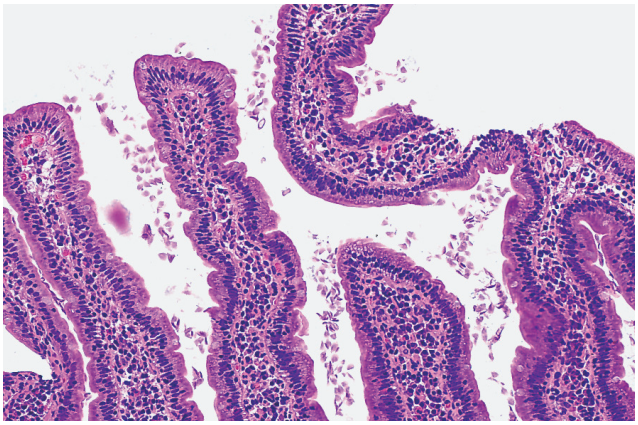


**Figure 6.14**
Many *Giardia intestinalis* trophozoites in lumen of duodenum. Note normal mucosa. x115



**Figure 6.15**
Laterally oriented *Giardia intestinalis* trophozoites (arrows) on surface of duodenal mucosa. x 590

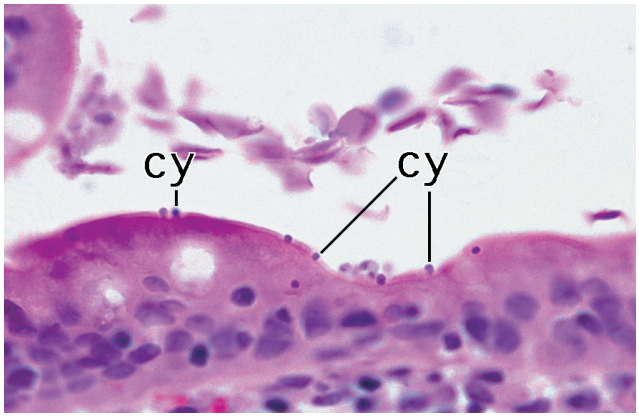



**Figure 6.16**
Biopsy specimen of duodenum from 46-year-old patient with chronic diarrhea and both giardiasis and cryptosporidiosis. *Giardia intestinalis* trophozoites are in the lumen, whereas *Cryptosporidium parvum* cysts (cy) are attahed to the epithelium. x605

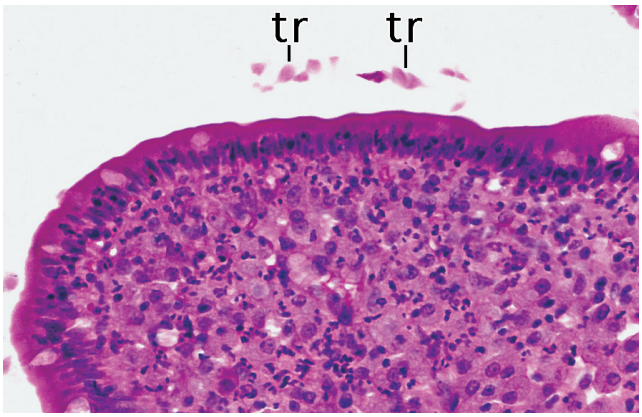



**Figure 6.17**
Biopsy specimen of duodenum from patient with both giardiasis and Whipple's disease. Lumen contains *Giardia intestinalis* trophozoites (tr), but neutrophils and histiocytes in lamina propria are attributed to Whipple's disease. x260

hyperplasia, acute inflammation, and crypt abscesses.[18-20] Some of these features may be seen in small intestinal biopsies from patients with giardiasis and other concomitant diseases such as cryptosporidiosis (Fig 6.16), Whipple's disease (Fig 6.17), or hypogammaglobulinemia (Figs 6.18 and 6.19). The histologic features of giardiasis are similar in immunocompromised and immunocompetent patients. Gastric biopsies from patients with chronic atrophic gastritis with intestinal metaplasia may reveal giardiasis[21], and trophozoites may rarely colonize the biliary tree and gallbladder.

## Diagnosis

Definitive diagnosis is made by demonstrating *G. intestinalis* in stool specimens, duodenal contents, or intestinal biopsy specimens. In most patients, microscopic examination of 3 consecutive stool specimens collected 2 days apart is sufficient to establish or eliminate a diagnosis. Stool specimens usually contain cysts only, but trophozoites may be found in stools from patients with severe diarrhea (Fig 6.8). The parasite can be seen on wet mounts stained with trichrome (Fig. 6.10), iodine (Fig 6.11), or iron hematoxylin (Figs 6.12 & 6.13). In some patients, when stool examination is negative, motile trophozoites may be observed in Giemsa-stained smears of duodenal fluid, collected by the string test or aspiration.

Endoscopic biopsy can reveal other upper intestinal parasites (*Cryptosporidium* (Fig 6.16), *Cyclospora*, or microsporidia) and detect other causes of malabsorptive diarrhea such as celiac disease. *Giardia intestinalis* trophozoites, most numerous in the lumen of the duodenum and upper jejunum, are usually adequately demonstrated in histologic preparations of biopsy specimens stained with hematoxylin and eosin (Figs 6.1, 6.2, & 6.16). Special stains such as

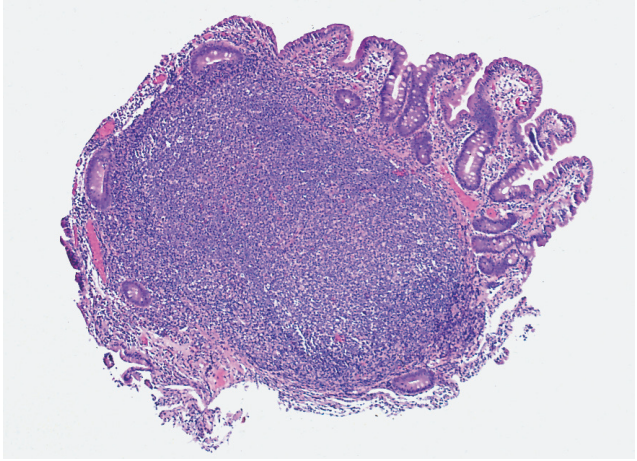


**Figure 6.18**
Lymphoid hyperplasia in duodenum is prominent in patient with hypogammaglobulinemia and associated giardiasis. x40

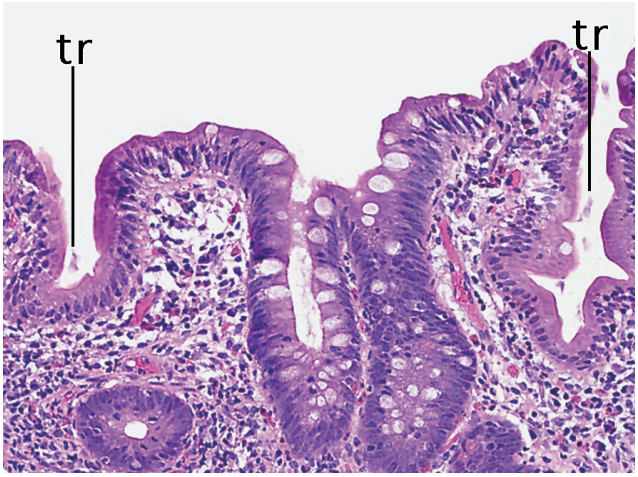



**Figure 6.19**
Higher magnification of duodenum depicted in Figure 6.18. Note several *Giardia intestinalis* trophozoites (tr) in lumen. x160

Movat, Brown and Hopps (Fig 6.5), and Wilder's reticulum (Fig 6.6) may accentuate the paired nuclei. Trophozoites may be demonstrated cytologically by a touch preparation of fresh biopsy specimen stained with Giemsa.

Numerous commercial antigen detection assays are available commercially and are reasonably reliable when compared with stool examination.[22] Immunochromatographic dipstick tests (ICT), direct fluorescent antibody (DFA) assays, and enzyme immunoassays (EIA) are available. Molecular techniques are sensitive and specific but not widely available.

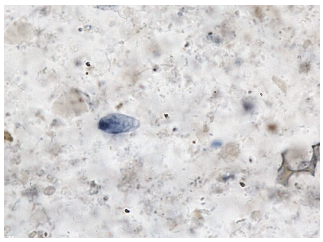
## Treatment and Prevention

Giardiasis is most commonly treated with metronidazole, tinidazole or nitazoxanide. Paromomycin may be used to treat pregnant women as it is poorly absorbed. Alternative medications are albendazole, paromomycin, furazolidone, and quinacrine. Extended treatment may be necessary for immunocompromised patients. A combination of metronidazole and quinacrine has been used in refractory cases.[23]

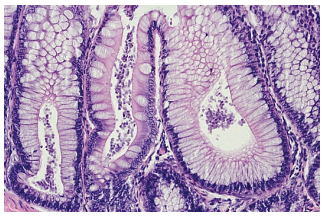
The key to the prevention of giardiasis transmission lies in preventing fecal contamination of food and water, and preventing direct transmission. Drinking untreated water should be avoided. Control measures include removing *Giardia* cysts from water by filtration, flocculation, and sedimentation. Chlorination alone is insufficient. Avoid eating food prepared with untreated water. Adequate personal hygiene, including hand washing, can prevent fecal-oral transmission. Keeping young children with diarrhea away from day care type settings and public recreational water facilities can help prevent waterborne transmission. The proper use of protective barriers during anal-oral sex will prevent sexual transmission of *Giardia* cysts.

## References


1. Yoder JS, Harral C, Beach MJ. Giardiasis Surveillance—United States, 2006-2008. *MMWR CDC Surveill Summ.* 2010;59(SS06):15-25.
2.. Furness BW, Beach MJ, Roberts JM. Giardiasis surveillance—United States, 1992-1997. *MMWR CDC Surveill Summ.* 2000;49:113
3. Palmer CS, Traub RJ, Robertson ID, Devlin G, Rees R, Thompson RC. Determining the zoonotic significance of *Giardia* and *Cryptosporidium* in Australian dogs and cats. *Vet Parasitol.* 2008;154;142-147.
4. Isaac-Renton JL, Cordeiro C, Sarafis K, Shahriari H. Characterization of *Giardia duodenalis* isolates from a waterborne outbreak. *J Infect Dis.* 1993; 167;431-440.
5. Thompson RC, Palmer CS, O'Handley R. The public health and clinical significance of *Giardia* and *Cryptosporidium* in domestic animals. *Vet J.* 2008; 177:18-25.
6. Traub RJ, Monis PT, Robertson I, Irwin P, Mencke N, Thompson RC. Epidemiological and molecular evidence supports the zoonotic transmission of *Giardia* among humans and dogs living in the same community. *Parasitology* . 2004;128:253-262.
7. Rendtorff RC, Holt CJ. The experimental transmission of human intestinal protozoan parasites. IV Attempts to transmit *Endamoeba coli* and *Giardia lamblia* cysts by water. *Am J Hyg.* 1954;60:327-338.
8. Weiland ME, Palm JE, Griffiths WJ, McCaffery JM, Svard SG. Characterisation of alpha-1 giardin: an immunodominant *Giardia lamblia* annexin with glycosaminoglycan-binding activity. *Int J Parasitol.* 2003;33:1341-1351.
9. Faubert G. Immune response to *Giardia duodenalis*. *Clin Microbiol Rev.* 2000;13:35-54.
10. Hill DR. Giardiasis. Issues in diagnosis and management. *Infect Dis Clin North Am.* 1993;7:503-525.
11. Wolfe MS. Giardiasis. *Clin Microbiol Rev.* 1992;5:93-100.
12. Roxstrom-Lindquist K, Palm D, Reiner D, Ringqvist E, Svard SG. *Giardia* immunity: an update. *Trends Parasitol.* 2006;22:26-31.
13. Eckmann L, Laurent F, Langford TD, et al. Nitric oxide production by human intestinal epithelial cells and competition for arginine as potential determinants of host defense against the lumen-dwelling pathogen *Giardia lamblia*. *J Immunol.* 2000;164:1478-1487.
14. Jendryczko A, Sodowska H, Drozdz M. Zinc deficiency in children infected with *Giardia lamblia* [in Polish]. *Wiad Lek.* 1993;46:32-35.
15. Addiss DG, Lengerich EJ. Hypokalemic myopathy induced by *Giardia lamblia* [letter]. *N Engl J Med.* 1994;330:66-67.
16. McKnight JT, Tietze PE. Dermatologic manifestations of giardiasis. *J Am Board Fam Pract.* 1992;5:425-428.
17. Nash TE, Ohi CA, Thomas E, Subramania G, Keiser P, Moore TA. Treatment of patients with refractory Giardiasis. *CID.* 2001;33:22-28.
18. Oberhuber G, Kastner N, Stolte M. Giardiasis: a histologic analysis of 567 cases. *Scand J Gastroenterol.* 1997;32:48-51.
19. Oberhuber G, Stolte M. Giardiasis: analysis of histological changes in biopsy specimens of 80 patients. *J Clin Pathol.* 1990;43:641-643.
20. Ward H, Jalan KN, Maitra TK, Agarwal SK, Mahalanabis D. Small intestinal nodular lymphoid hyperplasia in patients with giardiasis and normal serum immunoglobulins. *Gut.* 1983;24:120-126.
21. Doglioni C, De Boni M, Cielo R, et al. Gastric giardiasis. *J Clin Pathol.* 1992;45:964-967.
22. Weitzel T, Dittrich S, Mohl I, Adusu E, Jelinek T. Evaluation of seven commercial antigen detection tests for *Giardia* and *Cryptosporidium* in stool samples. *Clin Microbiol Infect.* 2006;12:656-659.
23. Drugs for Parasitic Infections. Treatment Guidelines from *The Medical Letter*. 2010;Vol 8(Suppl).







7

# Trichomoniasis

*Mary K. Klassen-Fischer and*
*Izzat S. Ali*

## *Introduction*

### Definition

Trichomoniasis generally refers to infection of the genitourinary tract by the flagellate protozoon *Trichomonas vaginalis*. Trichomoniasis also applies to infection of the intestinal tract by *Trichomonas hominis* (*Pentatrichomonas hominis*) and infection of the oral cavity by *Trichomonas tenax* (*Trichomonas buccalis* and *Trichomonas elongata*). *Trichomonas hominis* and *T. tenax* will be discussed separately at the end of this chapter, since both are usually considered nonpathogenic in humans.

Unusual presentations of *T. tenax* infection have been reported in the lung,[1-3] submaxillary gland,[4] lymph node,[5] and body cavity.[6] Unusual sites of *T. vaginalis* infections have been described in the brochopulmonary tree,[2,7-10] body cavities,[11-12] esophagus,[13] and testes.[14] There appears to be substantial genomic diversity among *T. vaginalis* in the United States.[15]

### General Considerations

Donné first identified *T. vaginalis* in 1836 in a vaginal discharge.[16] He believed the motile organism was the etiologic agent of vaginitis, but other investigators thought it was a commensal. In 1916 Hoehne demonstrated that eradicating *T. vaginalis* alleviated vaginitis.[17] Treatment for trichomoniasis was not widely available until the late 1950s, when Cosar and Jolou discovered that metronidazole was efficacious.[18]

### Epidemiology

In 1995 the World Health Organization estimated that there were 170 million cases of trichomoniasis worldwide, making it the most common nonviral sexually transmitted disease.[19] Incidence is highest among the poor and undereducated, and in individuals who are sexually promiscuous.[1,20] Estimates of the prevalence of *T. vaginalis* vary with geographic location, methods of detection, and study settings (gynecologic clinics, sexually transmitted disease clinics, etc). Frequency rates for unselected female populations in developed countries range from 5% to 15%.[1,21-23]

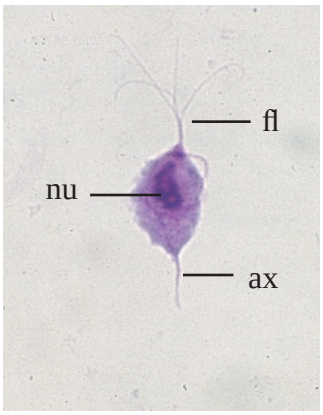



**Figure 7.1**
Whole mount of *Trichomonas vaginalis* trophozoite from culture. Note 4 anterior flagella (fl), nucleus (nu), and axostyle (ax). Giemsa x1030

Frequency rates of up to 70% are reported among low socioeconomic groups and from sexually transmitted disease clinics.[1,24] Epidemiologic studies in the United States indicate that 3 to 5 million women are infected with *T. vaginalis* annually.[25] Some general frequency data follow: 5% (family planning clinics), 13% to 25% (gynecologic clinics), 7% to 35% (sexually transmitted disease clinics), 50% to 75% (female sex workers),[20,26] 4% adolescent females,[27] and 32% incarcerated females.[28]

The prevalence of *T. vaginalis* in males has not been studied as extensively as in females.[29] Estimates vary from 4% to 20% of men with urethritis[30-33] to 20% to 40% of male sexual partners of infected females.[1,33,34] Frequency among males is less than those cited for the respective female populations.[1,28]

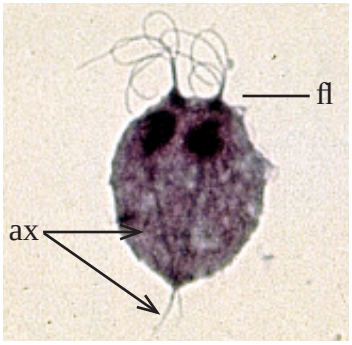



**Figure 7.2**
Whole mount of dividing *Trichmonas vaginalis* trophozoite from culture. Note 2 sets of anterior flagella (fl), 2 nuclei, and 2 axostyles (ax). Giemsa x1320

## *Infectious Agent*

### Morphologic Description

Strains of *T. vaginalis* vary serologically, antigenically, and morphologically. However, differences in size, growth rate, and virulence are insufficient to warrant clinical subdivision.[1,22]

*Trichomonas vaginalis* is the largest trichomonad infecting humans.[35] The infecting form is the trophozoite, the motile feeding stage. *Trichomonas vaginalis* typically has 4 anterior free flagella that originate in a kinetosomal complex (basal body) (Fig 7.1). A fifth flagellum extends posteriorly along the margin of the undulating membrane, and propels the organism. The fifth flagellum and undulating membrane usually do not extend beyond two thirds of the length of the cell. A parabasal body, analogous to a Golgi apparatus, is often attached by fibrils to the kinetosome of the flagella. Remaining organelles include a nucleus, axostyle (supporting structure), costa, and pelta (structural significance unknown). Hydrogesomes are located along the axostyle and costa. The cytoplasm also contains free and membrane-bound ribosomes, glycogen vacuoles, and large vacuoles.[22] Pseudopodia-like extensions are used for attachment and feeding, but not movement.[36]

By light microscopy, *T. vaginalis* is ovoid to spherical or piriform, and approximately the size of a histiocyte (7µm to 23µm by 5µm to 12µm). Flagella are retained in wet mounts (Figs 7.1 & 7.2) but lost in alcohol-fixed, Papanicolaou-stained material (Figs 7.3 and 7.4). In Papanicolaou-stained material, the organism may be hazy and poorly defined. It is gray-green, has a round or elliptical nucleus located centrally or eccentrically, and may have eosinophilic granules in the cytoplasm derived from ingested erythrocytic material (Figs 7.3 & 7.4).[37] Multinucleated forms are occasionally observed.[36,38]

*Trichomonas vaginalis* lacks mitochondria, derives most of its energy from glycolysis, and replicates by binary fission. Hydrogesomes generate hydrogen that combines with oxygen to form an anaerobic atmosphere.[22] Food sources include epithelial cells, yeasts, bacteria, and erythrocytes.[39-41]

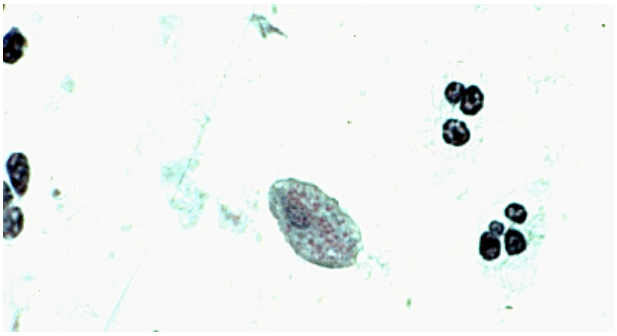


**Figure 7.3**
Single *Trichomonas vaginalis* trophozoite. Note eosinophilic granules and absence of flagella. Pap x1000

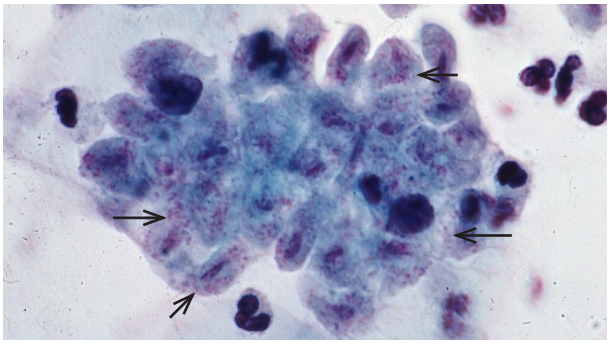


**Figure 7.4**
Aggregate of multiple *Trichomonas vaginalis* organisms. Note eosinophilic granules (arrows) and absence of flagella. Pap x1000

### Transmission

Trichomoniasis is transmitted sexually, although nonsexual transmission is theoretically possible.[42] Newborns are sometimes infected during delivery through the birth canal.[7,10,43] The incubation period is 4 to 28 days in 50% of infected females.[22] Transmission rate is high: 85% of females having sexual contact with infected males and approximately 80% of males having a single sexual exposure to an infected female.[20,33]

## *Clinical Features and Pathogenesis*

Severity of infection depends upon the virulence of the organism, parasite burden, host environment, and host response. *Trichomonas vaginalis* can survive at any vaginal pH, but develops fully at pH 6 to 7. Severity increases during the late secretory phase of the menstrual cycle, during menstruation, and during pregnancy.[44] The exact mechanism of host tissue destruction is not known, but it appears that *T. vaginalis* damages tissue by direct contact and by cytotoxicity.[45,46] Proteins found on *T. vaginalis* but not on *T. tenax* may be key to the pathogenicity and virulence of *T. vaginalis*.[47] Neutrophils are the predominant host response and inhibit deep invasion into host tissue.[48,49] The efficacy of host response in female patients is unknown, but repeated infections do not confer protective immunity.[20]

In females, the organism resides most frequently in the vagina, Skene's glands, and urethra. Cervical mucus acts as a barrier to *T. vaginalis* and inhibits infection beyond the cervix.[1,36,50,51] No evidence links *T. vaginalis* to pelvic inflammatory disease, spontaneous abortion, or sterility, nor is there convincing evidence that *T. vaginalis* causes squamous intraepithelial lesions or cervical carcinoma.[52-57]

*Trichomonas vaginalis* infection in females ranges from asymptomatic (10% to 50%) to severely symptomatic.[58,59] Approximately one third of asymptomatic females become symptomatic within 6 months. Green, foamy vaginal discharge is the most common presentation in symptomatic women.[20,60] Other symptoms include pruritus, red and edematous vulva and vagina, "strawberry" cervix, vaginal bleeding, dyspareunia, and enlarged and tender lymph nodes. Lymphadenopathy is rare.[22] A yellow-green, malodorous vaginal discharge is usually associated with accompanying bacterial infection. In addition to vaginitis and bartholinitis, the lower urinary tract may be infected, resulting in dysuria, urinary frequency, cystitis, urethritis, and infection of Skene's glands.[61] Vaginal trichomoniasis may be associated with bacterial vaginosis, candidiasis, gonorrhea, and syphilis.[46,62,63] Concurrent infections with herpes simplex virus and human papillomavirus are also noted. Respiratory or pharyngeal infections may occasionally be seen. [2,7-10]

In males, the organism resides in the urethra and prostate. Most males infected with *T. vaginalis* are asymptomatic.[46] Reported symptoms include urethral discharge and, less commonly, dysuria, pruritus, prostatitis, orchitis, and epididymitis.[14,31] In a study of trichomoniasis in males, 59% of patients experienced spontaneous regression within 2 weeks; 41% had infections that persisted for 2 weeks or longer. In patients with spontaneous regression of *T. vaginalis*, symptoms were minimal or not apparent, the organism was not evident in large numbers, and the interval between last exposure and detection was relatively long. The reverse was true for male patients with persistent infection.[33]

## *Pathologic Features*

The appearance of *T. vaginalis* in conventional Papanicolaou (Pap) smears varies widely. In nearly a quarter of cases of trichomoniasis, the organism appears without accompanying background and cellular changes.[55] Background milieu and cytologic features may be minimal or marked. The smear background can be clean or "dirty," with relatively uniform proteinaceous debris (Fig 7.5). Inflammatory response may be mild or intense, with numerous neutrophils and few lymphocytes, plasma cells, and histiocytes. Leukocytes may appear singly or in aggregates (sometimes called cannonballs) around epithelial cells (Fig 7.6). Inflammation may cause a spread maturation index, resulting in an increased number of parabasal cells or superficial cells. The increased number of superficial cells, apparently caused by increased epithelial vascularity,[55] can produce a greater number of eosinophils than would normally be expected on a well-stained Pap smear.

Squamous epithelial cells often exhibit inflammatory changes such as slight cellular hypertrophy, slight nuclear enlargement, hyperchromasia, and binucleation (Fig 7.7). Perinuclear halos are often prominent (Fig 7.8). Pyknosis and karyorrhexis, degenerative changes associated with inflammation, may also be noted. These changes affect squamous epithelial cells more often than endocervical cells. Endocervical cells, however, can exhibit slight nuclear and nucleolar enlargement and hyperchromasia (Fig 7.9). Bac-

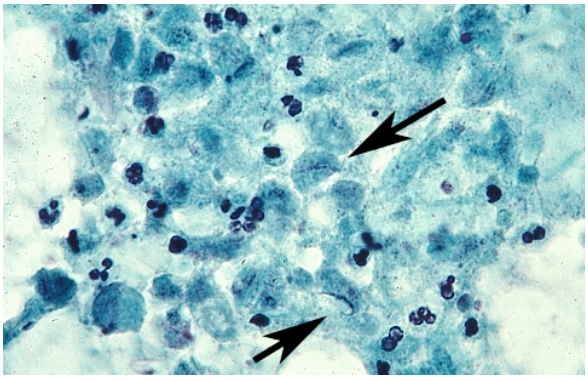


**Figure 7.5**
Numerous trichomonads (arrows) amid proteinaceous debris ("dirty" smear background) sometimes seen in vaginal trichomoniasis. Debris is usually more uniform than in tumor diathesis. Pap x630

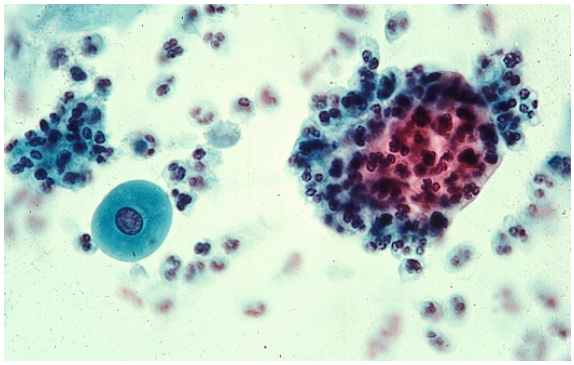


**Figure 7.6**
Acute inflammatory cells aggregating around epithelial cell at right (cannonball appearance). Structures represent nonspecific inflammatory response, but are often associated with trichomoniasis. Pap x630

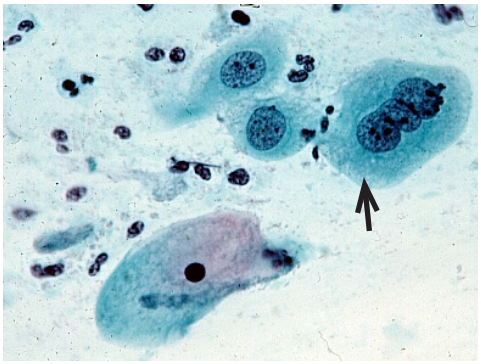


**Figure 7.7**
Cellular hypertrophy, slight nuclear enlargement, hyperchromatism, and bi- or multinucleation in epithelial cells (arrow). Nuclear enlargement is generally within limits of inflammatory cell changes (less than 3 times the size of intermediate cell nucleus). Pap x630

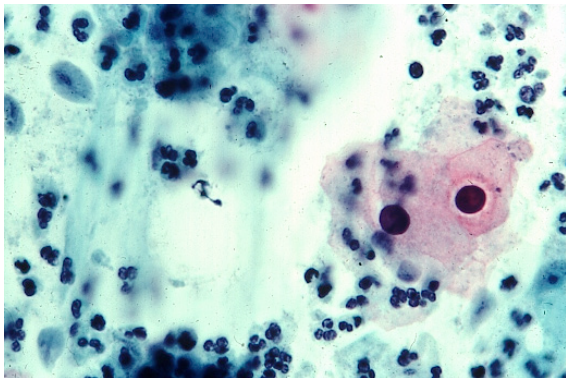
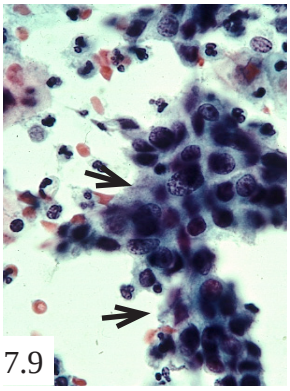
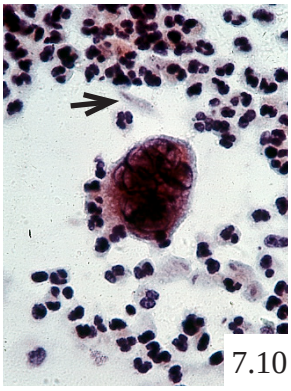


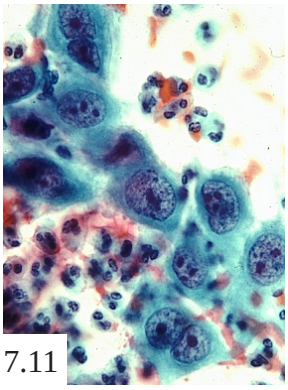
**Figure 7.8**
Slightly enlarged, hyperchromatic nuclei and perinuclear halo associated with vaginal trichomoniasis. Pap x630



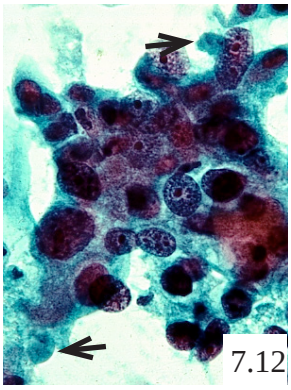
7.9



7.10



7.11



7.12

**Figure 7.9**
Slight nuclear enlargement and hyperchromatism of endocervical cells due to *Trichomonas vaginalis* infection (arrows). Nucleoli may be more prominent than usual. Pap x630

**Figure 7.10**
Concurrent herpes simplex virus inclusion (center) and trichomonads (arrow). Pap x630

**Figure 7.11**
Atypical repair is differentiated from squamous cell carcinoma (see Figure 7.12) by single layer of cells exhibiting well-defined borders. Pap x630

**Figure 7.12**
Squamous cell carcinoma showing characteristic syncytial grouping of cells with loss of polarity (also present in layer of atypical reparative cells) and pronounced nuclear crowding. Note trichomonads (arrows). Pap x630

teria (including *Leptothrix)*, fungi, herpes simplex virus, and human papillomavirus may be evident along with *T. vaginalis* (Fig 7.10). In the vast majority of cases, the cellular changes associated with *T. vaginalis* infection are readily distinguishable from squamous intraepithelial lesions or carcinoma. However, 2 factors should be noted. First, increased cellular maturation in postmenopausal women may simulate increased estrogen levels, requiring a meticulous search for the organism. Second, reparative processes due to epithelial destruction are sometimes cytologically evident on Pap smears. Typical repair is easily identified; atypical repair is more difficult to differentiate from epidermoid or endocervical carcinoma (Figs 7.11 & 7.12). A "dirty" slide background, increased cellular maturation or eosinophilia, aggregates of inflammatory cells, and perinuclear halos all suggest a trichomonal infection.

Histologically, *T. vaginalis* elicits a somewhat generalized inflammatory response in approximately two thirds of infected patients.[55,64] As described by Koss, blood vessels within papillae are often distended, especially in postmenopausal women.[55] Elongation of the papillae is variable,

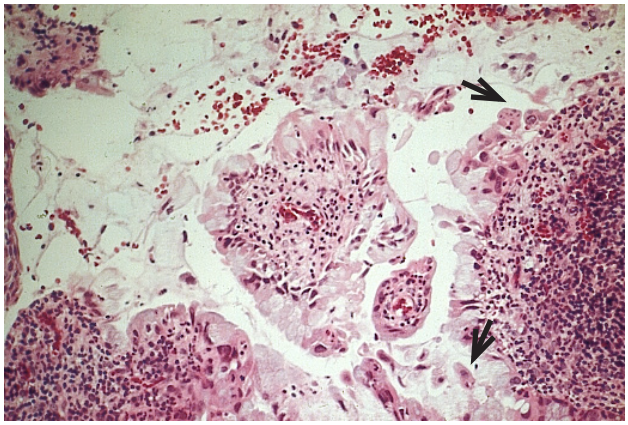


**Figure 7.13**
Histologic section from patient with trichomoniasis (arrows) and nonspecific cervicitis. x300

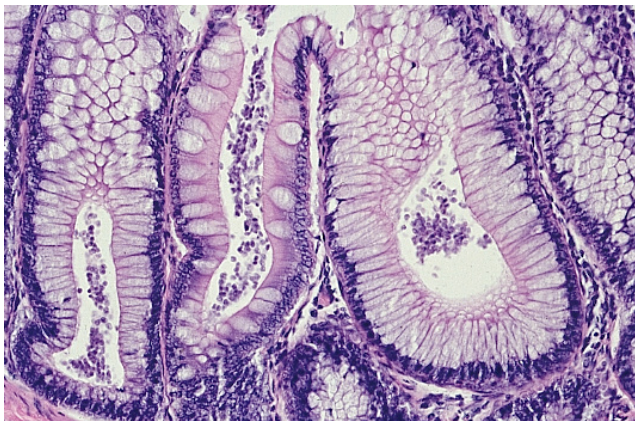


**Figure 7.14**
Trichomonads fill intestinal crypts of monkey. x160

sometimes producing stasis, margination and migration of neutrophils, and papillitis. The strawberry appearance of the cervix is caused by vascular distention and hemorrhage. Edema of the squamous epithelium is accompanied by separation of the epithelial cells. Perinuclear halos, correlative in cytologic material, are characteristically observed in all layers of the epithelium. In nontrichomonal cervicitis, perinuclear halos are less frequently observed and are present only in the basal layer. Layers of squamous epithelium exfoliate, exhibit cytologic features previously described, and become more vulnerable to infection. Necrosis and ulceration can occur, and purulent material may coat the eroded surface. Mild or marked basal-cell hyperactivity is occasionally seen and is exclusive to trichomonal cervicitis. Squamous metaplasia is frequently observed. Because the organism is noninvasive, underlying connective tissue stroma is usually unaffected (Fig 7.13).[65] Trichomonads are rarely observed in tissue sections; Figures 7.14 and 7.15 show trichomonads in the intestinal lumen of an infected monkey.

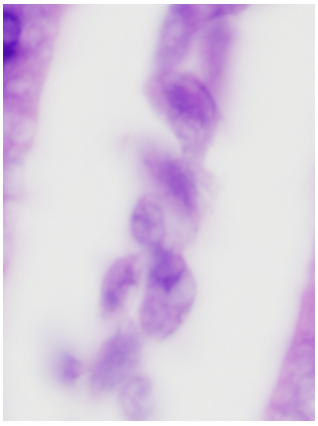


**Figure 7.15**
Trichomonads averaging 8 by 5 µm in intestine of monkey. x800



**Figure 7.16**
Thin Prep® smear of *Trichomonas vaginalis* using liquid-based cytology. Note flagella, nucleus, and clean background compared to Figure 7.3. Pap original magnification x1000.

## *Diagnosis*

Identification of trichomoniasis depends on finding an intact *T. vaginalis* in preparations of wet mount smears of vaginal (Figs 7.16 & 7.17) , cervical, or urethral secretions. Numerous studies have compared the sensitivity and specificity of various diagnostic techniques.[66-73] Culture, antibody-related, and molecular biologic methods can provide up to 95% sensitivity in vaginal specimens.[67] Though not the most sensitive, wet mounts and Pap smears are used in clinical settings because they are cost-effective and easy to collect and evaluate.[74] Wet mounts are most often used to detect *T. vaginalis* in symptomatic patients; Pap smears are useful for asymptomatic patients.[1,66,75] It is important to avoid fecal contamination of specimens because of the possibility of *T. hominis* in stool. FDA-cleared tests for trichomoniasis in women include OSOM® Trichomonas Rapid Test (Genzyme Diagnostics, Cambridge, Massachusetts), an immunochromatographic capillary flow dipstick technology, and the Affirm™ VP III (Becton Dickenson, San Jose, California), a nucleic acid probe test that detects *T. vaginalis*, *Gardnerella vaginalis,* and *Candida albicans*. Each of these tests, which are performed on vaginal secretions, have a sensitivity of >83% and a specificity of >97%. Both tests are considered point-of-care diagnostics. The results of the OSOM Trichomonas Rapid Test are available in approximately 10 minutes, whereas results of the Affirm VP III are available within 45 minutes. Although these tests tend to be more sensitive than those requiring vaginal wet preparation, false positives might occur, espe-

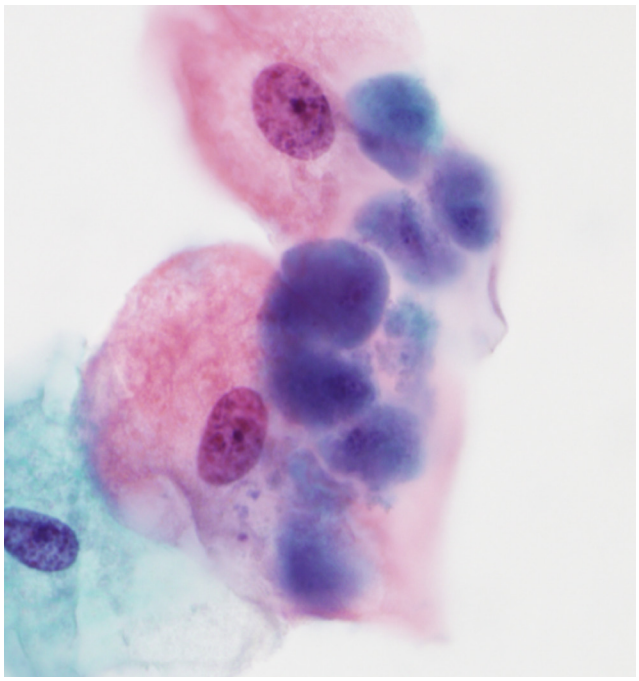


**Figure 7.17**
Thin Prep® smear of *Trichomonas vaginalis.* Note aggregate of multiple organisms attached to vaginal cells. Compare to Figure 7.4. Pap original magnification x1000.

cially in populations with a low prevalence of disease.[60]

## Treatment

The standard treatment for *T. vaginalis* infection is oral administration of metronidazole (Flagyl®), tinidazole, or ornidazole. Of these drugs, only metronidazole and tinidazoe are approved for use in the United States. Metronidazole is administered either by a single 2g oral dose or by a 500 mg oral dose 2 times/day for 7 days. Cure rates for both regimens are essentially the same and are optimized when both sexual partners are treated simultaneously.[60,76] Tinidazole is given 2g orally in a single dose.[60] If treatment failure occurs with metronidazole 2g single dose, and reinfection is excluded, the patient can be treated with metronidazole 500 mg orally twice daily for 7 days. For patients failing this regimen, treatment with tinidazole or metronidazole at 2g orally for 5 days should be considered.[60] In a small percentage of treated patients, metronidazole produces side effects such as nausea, vomiting, diarrhea, darkening of the urine, generalized skin reactions, and an unpleasant or metallic taste.[1,77] Short-term side effects usually peak 72 to 96 hours after administration of the drug.[78] Adverse neurologic reactions have been reported with long-term therapy.

Vaginal trichomoniasis has been associated with adverse pregnancy outcomes, particularly premature rupture of membranes, preterm delivery, and low birth weight. However, metronidazole treatment has not been shown to reduce perinatal morbidity. Although some trials suggest the possibility of increased prematurity or low birth weight after metronidazole treatment, limitations of the studies prevent definitive conclusions regarding risks for treatment.[60] Metronidazole crosses the placenta during pregnancy. Taking metronidazole during the second and third trimesters of pregnancy is controversial because of the drug's carcinogenicity in laboratory animals.[79] Opinions vary as to the drug's safety for nursing mothers. Infected neonates should be treated only if they are symptomatic; dosages of 10 to 30 mg/kg body weight daily for 5 to 8 days have proven curative. Older children with *T. vaginalis* infection should be treated with 15 mg/kg body weight in 3 oral doses daily for 7 to 10 days.[78] There is no conclusive evidence that standard metronidazole regimens are carcinogenic in humans.[78,80,81]

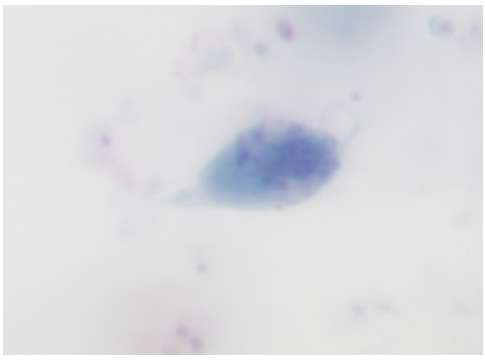


**Figure 7.18**
Fecal smear of intestinal *Trichomonas hominis.* Pap original magnification x1000.

### *Trichomonas hominis* and *Trichomonas tenax*

Trophozoites of the intestinal commensal *T. hominis* are ovoid and 6 to 14 µm by 4 to 7 µm (Fig 7.18). *Trichomonas hominis* has 5 anterior free flagella and is distinguished from *T. vaginalis* by a sixth flagellum that extends beyond the undulating membrane and the cell. It is prevalent in tropical climates, is present in children more than adults, and is transmitted via contaminated food.[1] *Trichomonas tenax,* a commensal of the oral cavity, has 4 anterior flagella, is smaller than *T. hominis*, and is distributed worldwide. It is most commonly found in older adults and is transmitted by kissing.

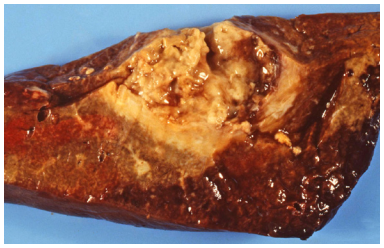
## References

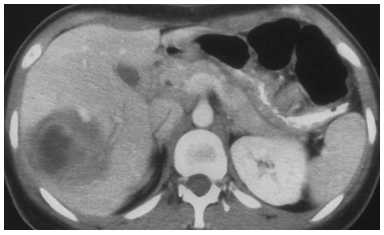

1. Honigberg BM. Trichomonads of importance in human medicine. In: Kreier JP, ed. *Parasitic Protozoa*. Vol 2. New York, NY: Academic Press; 1978:276-454.
2. Hersh SM. Pulmonary trichomoniasis and *Trichomonas tenax*. J Med Microbiol 1985;20:1-10.
3. Shiota T, Arizono N, Morimoto T, Shimatsu A, Nakao K. *Trichomonas tenax empyema* in an immunocompromised patient with advanced cancer. *Parasite* 1998;5:375-377.
4. Duboucher C, Mogenet M, Perie G. Salivary trichomoniasis. A case report of infestation of a submaxillary gland by *Trichomonas tenax*. *Arch Pathol Lab Med*. 1995;119:277-279.
5. Duboucher C, Farto-Bensasson F, Cheron M, Peltier JY, Beaufils F, Perie G. Lymph node infection by *Trichomonas tenax*: report of a case with co-infection by *Mycobacterium tuberculosis*. *Hum Pathol*. 2000;31:1317-1321.
6. Memik F. Trichomonads in pleural effusion. *JAMA*. 1968;204:1145-1146.
7. Temesvari P, Kerekes A, Tege A, Szarka K. Demonstration of *Trichomonas vaginalis* in tracheal aspirates in infants with early respiratory failure. *J Matern Fetal Neonatal Med*. 2002;11:347-349.
8. Wang HK, Jerng JS, Su KE, Chang SC, Yang PC. *Trichomonas empyema* with respiratory failure. *Am J Trop Med Hyg*. 2006;75:1234-1236.
9. Duboucher C, Noel C, Durand-Joly I, et al. Pulmonary coinfection by *Trichomonas vaginalis* and *Pneumocystis* sp. as a novel manifestation of AIDS. *Hum Pathol*. 2003;34:508-511.
10. Carter JE, Whithaus KC. Neonatal respiratory tract involvement by *Trichomonas vaginalis*: a case report and review of the literature. *Am J Trop Med Hyg*. 2008;78:17-19.
11. Hammond TL, Hankins GD, Snyder RR. Transvaginal-peritoneal migration of *Trichomonas vaginalis* as a cause of ascites. A report of two cases. *J Reprod Med*. 1990;35:179-181.
12. Straube E, Ockert G, Koch H, Schneider A, Diener C, Hartmann M. Peritonitis caused by Trichomonas--a preliminary case report. *Zentralbl Bakteriol*. 1991;275:394-396.
13. Borczuk AC, Hagan R, Chipty F, Brandt LJ. Cytologic detection of *Trichomonas esophagitis* in a patient with acquired immunodeficiency syndrome. *Diagn Cytopathol*. 1998;19:313-316.
14. Lloyd GL, Case JR, De Frias D, Brannigan RE. *Trichomonas vaginalis orchitis* with associated severe oligoasthenoteratospermia and hypogonadism. *J Urol*. 2003;170:924.
15. Meade JC, de Mestral J, Stiles JK, et al. Genetic diversity of *Trichomonas vaginalis* clinical isolates determined by EcoRI restriction fragment length polymorphism of heat-shock protein 70 genes. *Am J Trop Med Hyg*. 2009;80:245-251.
16. Kampmeier RH. Description of *Trichomonas vaginalis* by MA Donné. *Sex Transm Dis*. 1978;5:119.
17. Hoehne O. Management of *Trichomonas colpitis* [in German]. *Zentralbl Gynakol*. 1916;40:113-118.
18. Cosar C, Julou L. The activity of 1-(2-hydroxyethyl)-2-methyl-5-nitromidazole (R.P. 8823) aginst experimental *Trichomonas vaginalis* infections [in French]. *Ann Inst Pasteur (Paris)*. 1959;96:238-241.
19. Gerbase AC, Rowley JT, Heymann DH, Berkley SF, Piot P. Global prevalence and incidence estimates of selected curable STDs. *Sex Transm Infect*. 1998;74:S12-16.
20. Sobel JD. Vaginal infections in adult women. *Med Clin North Am*. 1990;74:1573-1602.
21. Sardana S, Sodhani P, Agarwal SS, et al. Epidemiologic analysis of *Trichomonas vaginalis* infection in inflammatory smears. *Acta Cytol*. 1994;38:693-697.
22. Thomason JL, Gelbart SM. *Trichomonas vaginalis*. *Obstet Gynecol*. 1989;74:536-541.
23. Wathne B, Holst E, Hovelius B, Mardh PA. Vaginal discharge–comparison of clinical, laboratory and microbiological findings. *Acta Obstet Gynecol Scand*. 1994;73:802-808.
24. Prins M, Hooykaas C, Coutinho RA, van Doornum GJ, van den Hoek AJ. Incidence and risk factors for acquisition of sexually transmitted diseases in heterosexuals with multiple partners. *Sex Transm Dis*. 1994;21:258-267.
25. Sutton M, Sternberg M, Koumans EH, McQuillan G, Berman S, Markowitz L. The prevalence of *Trichomonas vaginalis* infection among reproductive-age women in the United States, 2001-2004. *Clin Infect Dis*. 2007;45:1319-1326.
26. Sorvillo F, Kovacs A, Kerndt P, Stek A, Muderspach L, Sanchez-Keeland L. Risk factors for trichomoniasis among women with human immunodeficiency virus (HIV) infection at a public clinic in Los Angeles County, California: implications for HIV prevention. *Am J Trop Med Hyg*. 1998;58:495-500.
27. Krashin JW, Koumans EH, Bradshaw-Sydnor AC, et al. *Trichomonas vaginalis* prevalence, incidence, risk factors and antibiotic-resistance in an adolescent population. *Sex Transm Dis*. 2010;37:440-444.
28. Freeman AH, Katz KA, Pandori MW, et al. Prevalence and correlates of *Trichomonas vaginalis* among incarcerated persons assessed using a highly sensitive molecular assay. *Sex Transm Dis*. 2010;37:165-168.
29. Krieger JN. Trichomoniasis in men: old issues and new data. *Sex Transm Dis*. 1995;22:83-96.
30. Giacomini G, Bianchi G, Moretti D. Detection of sexually transmitted diseases by urethral cytology, the ignored male counterpart of cervical cytology. *Acta Cytol*. 1989;33:11-15.
31. Krieger JN, Jenny C, Verdon M, et al. Clinical manifestations of trichomoniasis in men. *Ann Intern Med*. 1993;118:844-849.
32. Ozbilgin A, Ozbel Y, Alkan MZ, et al. Trichomoniasis in non-gonococcic urethritis among male patients. *J Egypt Soc Parasitol*. 1994;24:621-625.
33. Weston TE, Nicol CS. Natural history of trichomonal infection in males. *Br J Ven Dis*. 1963;39:251-257.
34. Latif AS, Mason PR, Marowa E. Urethral trichomoniasis in men. *Sex Transm Dis*. 1987;14:9-11.
35. Noble ER, Noble GA, Schad GA, MacInnes AJ. *Parasitology. The Biology of Animal Parasites*. 6th ed. Philadelphia, Pa: Lea and Febiger; 1989.
36. Jirovec O, Petra M. *Trichomonas vaginalis* and trichomoniasis. In: Dawes B, ed. *Advances in Parasitology*. Vol 6. New York, NY: Academic Press; 1978:117-178.
37. Naib ZM. *Exfoliative Cytopathology*. 2nd ed. Boston, Mass: Little Brown; 1976.
38. Buckner SB, Mikel U. Unusual and giant forms of *Trichomonas vaginalis* [letter]. *Acta Cytol*. 1983;27:549-550.
39. Dailey DC, Chang TH, Alderete JF. Characterization of *Trichomonas vaginalis* haemolysis. *Parasitology*. 1990;101:171-175.
40. Lehker MW, Chang TH, Dailey DC, Alderete JF. Specific erythrocyte binding is an additional nutrient acquisition system for *Trichomonas vaginalis*. *J Exp Med*. 1990;171:2165-2170.
41. Midlej V, Benchimol M. *Trichomonas vaginalis* kills and eats–evidence for phagocytic activity as a cytopathic effect. *Parasitology*. 2010;137:65-76.
42. Pereira-Neves A, Benchimol M. *Trichomonas vaginalis*: in vitro survival in swimming pool water samples. Exp Parasitol. 2008;118:438-441.
43. Trintis J, Epie N, Boss R, Riedel S. Neonatal *Trichomonas vaginalis* infection: a case report and review of literature. *Int J STD AIDS*. 2010;21:606-607.
44. Frost JK. Gynecologic and obstetric cytopathology. In: Novak ER, Woodruff JD, eds. *Gynecologic and Obstetric Pathology*. 6th ed. Philadelphia, Pa: WB Saunders;1967;575-671.
45. Chen WL, Chen JF, Zhong XR, Liang P, Lin W. Ultrastructural and immunohistochemical studies on *Trichomonas vaginalis* adhering to and phagocytizing genitourinary epithelial cells. *Chin Med J (Engl)*. 2004;117:376-381.
46. Schwebke JR, Burgess D. Trichomoniasis. *Clin Microbiol Rev*. 2004;17:794-803.
47. Alderete JF, Garza GE. Identification and properties of *Trichomonas vaginalis* proteins involved in cytadherence. *Infect Immun*. 1988;56:28-33.
48. Styrt B, Sugarman B, Mummaw N, White JC. Chemorepulsion of trichomonads by products of neutrophil oxidative metabolism. *J Infect Dis*. 1991;163:176-179.
49. Ryu JS, Kang JH, Jung SY, et al. Production of interleukin-8 by human neutrophils stimulated with *Trichomonas vaginalis*. *Infect Immun*. 2004;72:1326-1332.
50. Herzberg AJ, Silverman JF. Detection of *Trichomonas vaginalis* in endocervical and ectocervical smears. *Diagn Cytopathol*. 1996;14:273-276.
51. Akarsu GA. Cytotoxic potential of cervical mucus on *Trichomonas vaginalis* to prevent upper genital tract infections. *Saudi Med J*. 2006;27:735-736.
52. Chakrabarti RN, Dutta K, Sarkhel T, Maity S. Cytologic evidence of the association of different infective lesions with dysplastic changes in the uterine cervix. *Eur J Gynaecol Oncol*. 1992;13:398-402.
53. Gram IT, Macaluso M, Churchill J, Stalsberg H. *Trichomonas vaginalis* (TV) and human papillomavirus (HPV) infection and the incidence of cervical intraepithelial neoplasia (CIN) grade III. *Cancer Causes Control*. 1992;3:231-236.

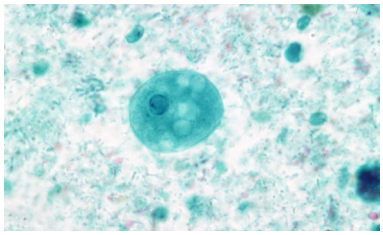
54. Hulka BS, Hulka JF. Dyskaryosis in cervical cytology and its relationship to trichomoniasis therapy. A double blind study. *Am J Obstet Gynecol.* 1967;98:180-187.
55. Koss LG, Wolinska WH. *Trichomonas vaginalis* cervicitis and its relationship to cervical cancer. A histocytological study. *Cancer*. 1959;12:1171-1193.
56. Omer EE, Naeem HA, Ali MH, Catterall RD, Erwa HH. Vaginal and cervical abnormalities associated with trichomonal infection. *East Afr Med J*. 1991;68:455-460.
57. Zhang ZF, Begg CB. Is *Trichomonas vaginalis* a cause of cervical neoplasia? Results from a combined analysis of 24 studies. *Int J Epidemiol.* 1994;23:682-690.
58. Peterman TA, Tian LH, Metcalf CA, Malotte CK, Paul SM, Douglas JM, Jr. Persistent, undetected *Trichomonas vaginalis* infections? *Clin Infect Dis.* 2009;48:259-260.
59. Gatski M, Kissinger P. Observation of probable persistent, undetected *Trichomonas vaginalis* infection among HIV-positive women. *Clin Infect Dis.* 2010;51:114-115.
60. Workowski KA, Berman S. Centers for Disease Control and Prevention (CDC). Sexually transmitted diseases treatment guidelines, 2010. *MMWR Recomm Rep*. 2010;59(RR-12):1-110.
61. Fouts AC, Kraus SJ. *Trichomonas vaginalis*: reevaluation of its clinical presentation and laboratory diagnosis. *J Infect Dis.* 1980;141:137-143.
62. Wisdom AR, Dunlop EM. Trichomoniasis: a study of the disease and its treatment. *Br J Ven Dis.* 1965;41:90-96.
63. Allsworth JE, Ratner JA, Peipert JF. Trichomoniasis and other sexually transmitted infections: results from the 2001-2004 National Health and Nutrition Examination Surveys. *Sex Transm Dis*. 2009;36:738-744.
64. Kaur S, Khurana S, Bagga R, Wanchu A, Malla N. Antitrichomonas IgG, IgM, IgA, and IgG subclass responses in human intravaginal trichomoniasis. *Parasitol Res.* 2008;103:305-312.
65. Kiviat NB, Paavonen JA, Wolner-Hanssen P, et al. Histopathology of endocervical infection caused by *Chlamydia trachomatis*, herpes simplex virus, *Trichomonas vaginalis*, and *Neisseria gonorrhoeae*. *Hum Pathol.* 1990;21:831-837.
66. Lara-Torre E, Pinkerton JS. Accuracy of detection of *Trichomonas vaginalis* organisms on a liquid-based papanicolaou smear. Am J Obstet Gynecol. 2003;188:354-356.
67. Radonjic IV, Dzamic AM, Mitrovic SM, Arsic Arsenijevic VS, Popadic DM, Kranjcic Zec IF. Diagnosis of *Trichomonas vaginalis* infection: The sensitivities and specificities of microscopy, culture and PCR assay. *Eur J Obstet Gynecol Reprod Biol.* 2006;126:116-120.
68. Campbell L, Woods V, Lloyd T, Elsayed S, Church DL. Evaluation of the OSOM Trichomonas rapid test versus wet preparation examination for detection of *Trichomonas vaginalis vaginitis* in specimens from women with a low prevalence of infection. *J Clin Microbiol*. 2008;46:3467-3469.
69. El-Moamly AM, Rashad SM. *Trichomonas vaginalis* antigens in vaginal and urine specimens by immunochromatography, compared to culture and microscopy. *J Egypt Soc Parasitol*. 2008;38:573-584.
70. Bravo AB, Miranda LS, Lima OF, Cambas AV, Hernandez ML, Alvarez JM. Validation of an immunologic diagnostic kit for infectious vaginitis by *Trichomonas vaginalis*, *Candida* sp, and *Gardnerella vaginalis*. *Diagn Microbiol Infect Dis.* 2009;63:257-260.
71. Nye MB, Schwebke JR, Body BA. Comparison of APTIMA *Trichomonas vaginalis* transcription-mediated amplification to wet mount microscopy, culture, and polymerase chain reaction for diagnosis of trichomoniasis in men and women. *Am J Obstet Gynecol.* 2009;200:188 e1-7.
72. Diaz N, Dessi D, Dessole S, Fiori PL, Rappelli P. Rapid detection of coinfections by *Trichomonas vaginalis*, *Mycoplasma hominis*, and *Ureaplasma urealyticum* by a new multiplex polymerase chain reaction. *Diagn Microbiol Infect Dis.* 2010;67:30-36.
73. Noel JC, Engohan-Aloghe C. Morphologic criteria associated with *Trichomonas vaginalis* in liquid-based cytology. *Acta Cytol*. 2010;54:582-586.
74. Krieger JN, Tam MR, Stevens CE, et al. Diagnosis of trichomoniasis. Comparison of conventional wet-mount examination with cytologic studies, cultures, and monoclonal antibody staining of direct specimens. *JAMA*. 1988;259:1223-1227.
75. Lossick JG. The diagnosis of vaginal trichomoniasis [editorial]. *JAMA*. 1988;259:1230.
76. Gatski M, Mena L, Levison J, et al. Patient-delivered partner treatment and *Trichomonas vaginalis* repeat infection among human immunodeficiency virus-infected women. *Sex Transm Dis*. 2010;37:502-505.
77. Hager WD, Rapp RP. Metronidazole. *Obstet Gynecol Clin North Am*. 1992;19:497-510.
78. Lossick JG. Treatment of sexually transmitted vaginosis/vaginitis. *Rev Infect Dis.* 1990;Suppl 6:S665-S681.
79. Wendel KA, Workowski KA. Trichomoniasis: challenges to appropriate management. *Clin Infect Dis*. 2007;44 Suppl 3:S123-129.
80. Beard CM, Noller KL, O'Fallon WM, Kurland LT, Dahlin DC. Cancer after exposure to metronidazole. *Mayo Clin Proc*. 1988;63:147-153.
81. Friedman GD, Selby JV. Metronidazole and cancer [letter]. *JAMA*. 1989;261:866.


## Acknowledgements

The authors thank Sally-Beth A.H. Buckner for her major contributions to this chapter







8

# Amebiasis

***Mary K. Klassen-Fischer, Douglas J. Wear, and Ronald C. Neafie***

## *Introduction*

### Definition

Amebiasis is invasion of human tissues by the protozoon *Entamoeba histolytica*. Infection begins when trophozoites of *E. histolytica* invade the colonic mucosa. The infection may remain localized and be minimal for years, or it may extend to the liver and other organs. What was once thought to be a single species based on morphology is now known to be three genetically distinct species: *Entamoeba histolytica* (pathogen), *Entamoeba dispar* (commensal),[1] and *Entamoeba moshkovskii* (commensal).[2] The free-living amebas that cause meningoencephalitis are discussed in Chapter 9, those infecting other sites are included in this chapter.

### Synonyms

Amebic dysentery, amebic colitis, amoebiasis (British spelling)

### General Considerations

Hippocrates noticed that dysenteries are especially bad "when they are set in with fever, [intestinal] discharges of a mixed character, or with inflammation of the liver". Two thousand years later in 1875, Lösch described trophozoites, which he named "Amoeba coli", in the stool and colonic ulcers in a Russian farmer.[3] Schaudinn distinguished *Entamoeba histolytica* from *Entamoeba coli* in 1903. In 1925, Brumpt proposed that two morphologically identical species of *Entamoeba*, *Entamoeba dysenteriae* (pathogenic) and *E. dispar* (non-pathogenic), can infect humans. During the 1933 Chicago World's Fair, faulty plumbing in a hotel resulted in 1,704 cases of amebic dysentery.[4]

## *Epidemiology*

Amebiasis is the third leading cause of death from parasitic disease worldwide (behind malaria and schistosomiasis), resulting in 40 to 100 thousand deaths annually.[1,5] It is most prevalent in regions where human waste is used as fertilizer. Severity of amebiasis varies greatly among patients and geographic areas. Many people are asymptomatic carriers, and others have sudden severe infections that progress steadily to death.[6,7] There is a spectrum of disease patterns between these extremes.[8] For unknown reasons, some urban populations (particularly in Mexico City, Mexico; Medellin, Colombia; Durban, South Africa; and Kuala Lumpur, Malaysia)[9] are predisposed to severe amebiasis, causing complications and death. Most cases in the United States occur in immigrants from endemic areas and in the states that border Mexico. Some possible contributing factors to the initiation of infection and promotion of severe disease include poor nutrition, tropical climate, decreased host immunocompetence, stress, altered colonic bacterial flora, excessive alcohol ingestion, and heredity. The disease has re-emerged in previously quiescent areas.[1,10]

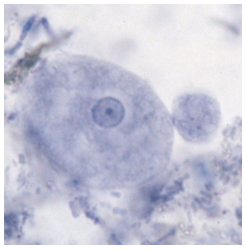


**Figure 8.1**
*Entamoeba histolytica* trophozoite in fecal smear is 24µm in diameter and contains a single, spherical, 5µm diameter nucleus with a discrete, round, centrally placed karyosome. The peripheral chromatin lining the nuclear membrane is uniform. Iron hematoxylin x800

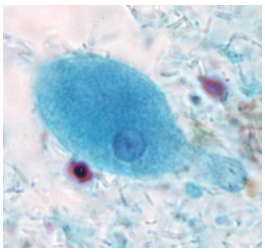


**Figure 8.2**
*Entamoeba histolytica* trophozoite in fecal smear producing pseudopodia. This trophozoite is 35µm long and has a 5µm diameter, spherical, nucleus. The karyosome is centrally placed. The cytoplasm has a finely granular, green appearance. Trichrome x875

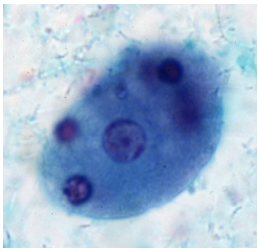


**Figure 8.3**
*Entamoeba histolytica* trophozoite in fecal smear with a large 6µm diameter nucleus and several ingested erythrocytes. The nucleus has irregular peripheral chromatin and a centrally placed karyosome. Trichrome x1000

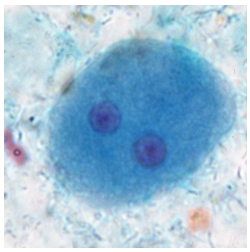


**Figure 8.4**
*Entamoeba histolytica* trophozoite in fecal smear demonstrating rare double nuclei. This trophozoite is 29µm long and nuclei are 5µm in diameter. Trichrome x875

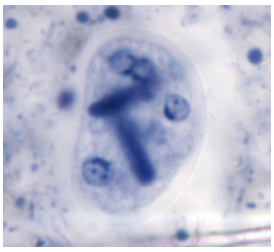


**Figure 8.5**
*Entamoeba histolytica* mature cyst with 4 nuclei and chromatoid bodies in fecal smear and surrounded by halo-like space. The cyst is 19µm long and the nuclei are 3µm in diameter. The nucleus has irregular peripheral chromatin and both centric and eccentric karyosomes are observed. Iron hematoxylin x850

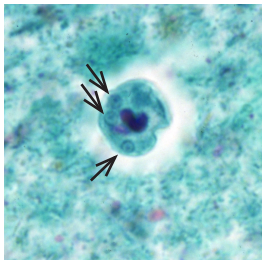


**Figure 8.6**

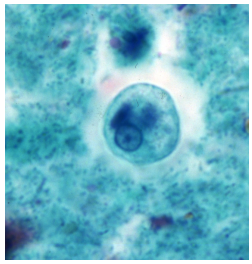


**Figure 8.7**

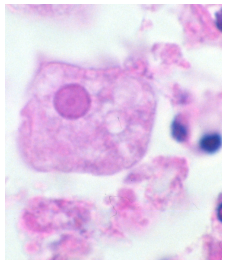


**Figure 8.8**

**Figure 8.6**
Mature *Entamoeba histolytica* cyst in fecal smear. Three of the four nuclei (arrows) are visible as are the red-staining chromatoid bodies. Trichrome x900

**Figure 8.7**
*Entamoeba histolytica* precyst in fecal smear with a single nucleus. Cyst is 12µm in diameter and the nucleus is 4µm in diameter. The peripheral chromatin is uniform and the karyosome is centrally placed. Trichrome x875

**Figure 8.8**
*Entamoeba histolytica* trophozoite in lung abscess. The ameba cytoplasm is eosinophilic, coarse, and vacuolated. The nucleus is 5µm in diameter and there is peripheral chromatin lining the nuclear membrane. The tiny karyosome is centrally placed. H&E x930

## *Infectious Agent*

### Morphologic Description

*Entamoeba histolytica* occurs in humans in two forms: trophozoites and cysts. Trophozoites are in both stool and tissue, but cysts are only in stool. Although cysts form in the lumen of the intestinal tract, they are not observed in biopsy specimens. Stool specimens that contain only trophozoites are usually from patients with acute symptoms.

*Entamoeba histolytica* trophozoites in stool specimens range from 10µm to 60µm (Fig 8.1). Living trophozoites exhibit progressive, sometimes explosive, motility with extrusion of hyaline, finger-like pseudopodia (Fig 8.2). In unstained preparations, the single nucleus is not visible. In stained fecal smears, trophozoites are spherical to elongate and usually range from 12µm to 30µm in diameter. With iron-hematoxylin staining, amebae take on a grayish to black color, blending in with the background (Fig 8.1). The nucleus is spherical and varies from 3.5µm to 6.0µm in diameter. The peripheral chromatin lining the inner surface of the nuclear membrane may be even or uneven (Figs 8.1 & 8.3). The nucleus has a small, compact karyosome (nucleolus) that is usually centrally located, but may occasionally be eccentric. The cytoplasm of the ameba is usually finely granular and green to purple with trichrome staining (Figs 8.2 to 8.4). Amebic trophozoites with pseudopodia are frequently seen as are amebae with ingested erythrocytes (Fig 8.3).

Trophozoites of *E. histolytica* usually do not contain bacteria or debris. Rarely, a trophozoite may contain two nuclei (Fig 8.4). Delays in fixation may cause vacuoles to develop in the cytoplasm and produce variations in nuclear morphology. In trophozoites undergoing degeneration, the nucleus is usually the first structure to undergo changes including fragmentation of the karyosome or alteration of the peripheral chromatin.

*Entamoeba histolytica* cysts in stool specimens are usually spherical and range from 9µm to 20µm in diameter, although most are 12µm to 15µm. The fixation process may cause cysts to shrink resulting in a clear unstained halo-like space, an appearance that is useful in detecting cysts while scanning the fecal smear (Fig 8.5). The mature cyst contains 4 nuclei; rarely 8 (Fig 8.5). It is often difficult to see all 4 nuclei in the same focal plane (Fig 8.6). Immature cysts or precysts contain one or two nuclei (Fig 8.7). The

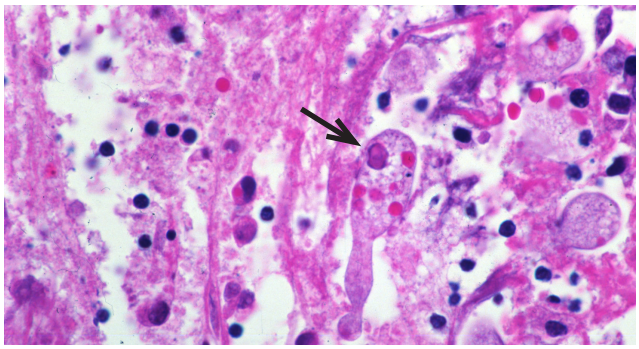


**Figure 8.9**
*Entamoeba histolytica* trophozoite with pseudopodium in colonic ulcer. The ameba has a single nucleus (arrow) and has engulfed several erythrocytes. H&E x480

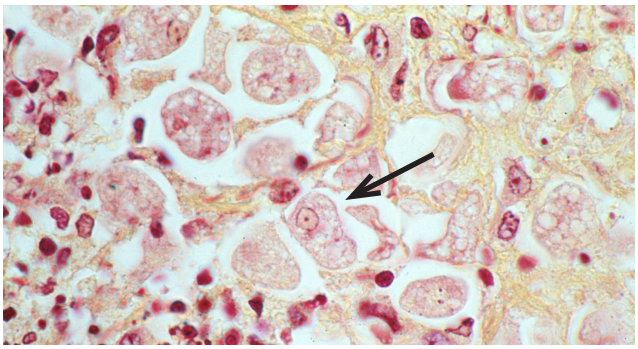


**Figure 8.10**
*Entamoeba histolytica* trophozoites in colonic ulcer demonstrating nucleus with tiny, centrally placed karyosome (arrow). B&H x480

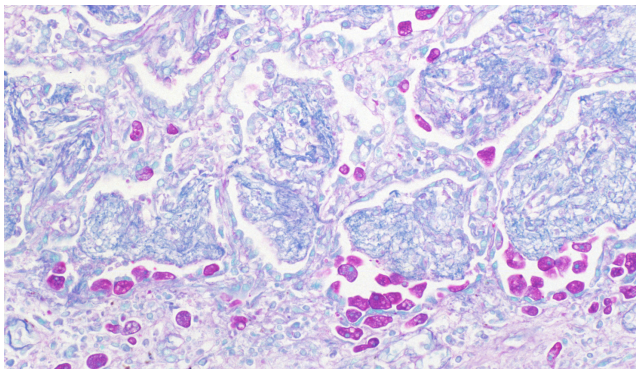


**Figure 8.11**
*Entamoeba histolytica* trophozoites are bright red and are easily distinguished in this PAS stained section of lung. PAS x120

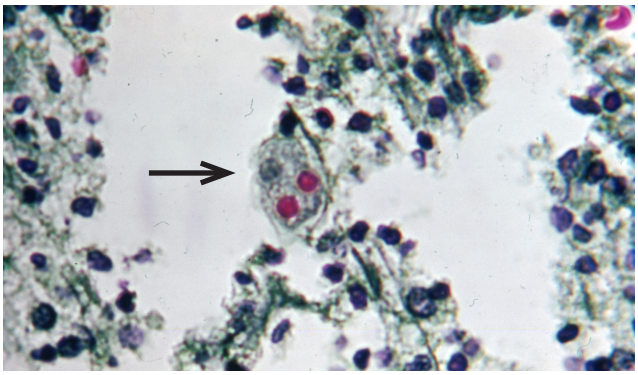


**Figure 8.12**
*Entamoeba histolytica* trophozoite in lumen of appendix. Note gray nucleus (arrow) and two bright red engulfed erythrocytes. Gridley ameba x710

nuclei of cysts vary from 2µm to 4µm, and they are smaller than those of trophozoites, but otherwise morphologically similar. The nuclei of immature cysts are generally larger than those in mature cysts.

Glycogen in mature cysts is usually diffuse, but may be concentrated into a discrete mass in young cysts. Chromatoid bodies, which are ribosomal assemblies, appear as highly refractile, cigar-shaped bars that are bright red with trichrome staining and gray to black with iron hematoxylin staining (Figs 8.5 to 8.7).

In biopsy or autopsy specimens *E. histolytica* trophozoites rarely exceed 35µm in greatest dimension. They are readily visible in H&E stained sections of paraffin embedded tissue and this stain best illustrates their morphologic features (Figs 8.8 & 8.9). They are well demarcated from other surrounding cells and tissue. The nucleus is usually 4µm to 5µm in diameter, has peripheral chromatin lining the nuclear membrane, and contains a tiny centrally placed karyosome (Fig 8.8). Frequently, the nucleus is not observed due to the plane of section. The tiny karyosome is usually difficult to see and is often absent. The Brown-Hopps tissue gram stain sometimes accentuates the karyosome (Fig 8.10).

The cytoplasm of *E. histolytica* trophozoites is eosinophilic, coarse, and vacuolated. Trophozoites occasionally develop pseudopodia and often engulf erythrocytes (Fig 8.9). The amebic cytoplasm usually contains abundant glycogen that stains deeply with PAS, which may help in locating trophozoites (Fig 8.11). However, the PAS stain frequently obscures the morphologic features of the nucleus and sometimes will also deeply stain histiocytes. For these reasons, we prefer the H&E stain for studying *E. histolytica* in tissue sections. The Gridley ameba stain is useful

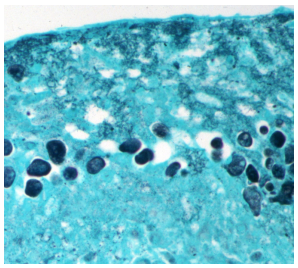


**Figure 8.13**
*Entamoeba histolytica* trophozoites in ulcerated cervix. GMS x190

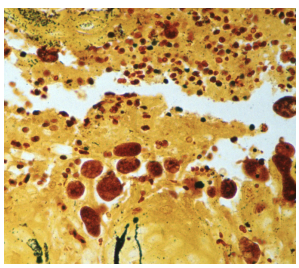


**Figure 8.14**
*Entamoeba histolytica* trophozoites in ulcerated foreskin. WS x190

in demonstrating engulfed erythrocytes (Fig 8.12). Other stains that maybe helpful in demonstrating trophozoites includes GMS and WS (Figs 8.13 & 8.14).

## Life Cycle and Transmission

Although there are 5 stages of the parasite: trophozoite, precyst, cyst, metacyst, and metcystic trophozoite, the life cycle is rather simple (Fig 8.15). Humans usually become infected by ingesting cysts of *E. histolytica* in fecally contaminated water or food. More unusual modes of transmission include oral and anal sex and exposure to contaminated enema apparatus. The ingested cyst passes through the stomach into the small intestine where excystation occurs resulting in the emergence of a 4 nucleated metacyst. The metacyst cytoplasm divides almost immediately resulting in 4 small metacystic trophozoites. The metacystic trophozoites quickly feed and grow into normal-sized trophozoites that pass with the fecal stream into the cecum where colonization occurs. Trophozoites are highly motile and reproduce by binary fission resulting in large numbers of organisms, some of which may invade the intestinal mucosa. Factors controlling invasion may include parasite "quorum sensing," interactions of amebae with colonic bacterial flora, and innate and acquired immune responses of the host.[11] In some patients, trophozoites directly extend or by hematogenous spread involve distant organs such as liver, lung, and brain (Fig 8.16). The reproduction of trophozoites has no sexual cycle. The overall population of *E. histolytica* appears to be clonal.[12] Trophozoites ingest erythrocytes, bacteria and food particles. Under certain undefined conditions, possibly triggered by the parasite's surface galactase/N-acetylgalactosamine (GAL/GALNAC) specific lectin, aggregates of trophozoites in the mucin layer differentiate into precysts and then into cysts that are passed in the stool.[13] The precyst is usually spherical, has a thin wall, and single nucleus. The precyst nucleus undergoes two divisions resulting in the quadrinucleated cyst. Stool specimens may contain trophozoites and uninucleate, binucleate, and quadrinucleate cysts. Tryphozoites cannot survive outside the host, but cysts may survive for days.

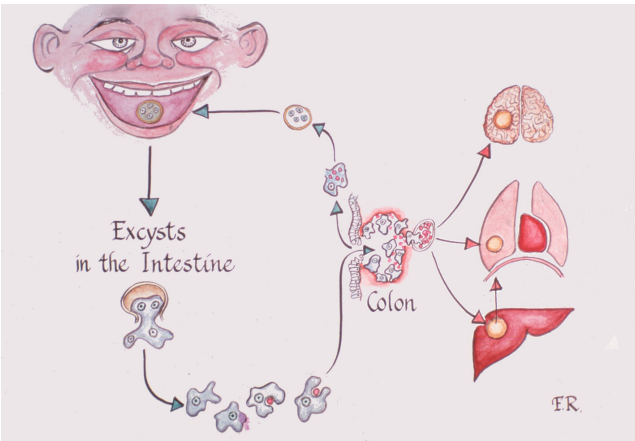



**Figure 8.15**
Life cycle of *Entamoeba histolytica*. Humans are infected by ingesting cysts that transform into metacystic trophozoites that colonize the colonic mucosa. In some patients, amebae disseminate to distant organs including liver, lung, and brain.

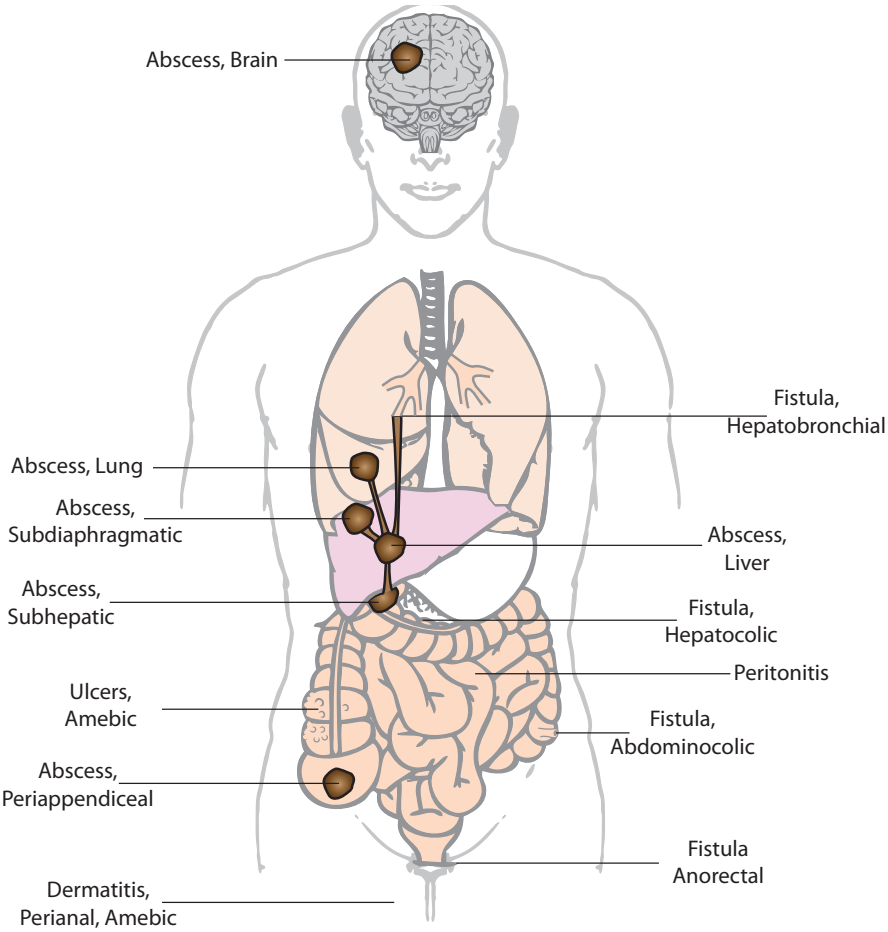



**Figure 8.16**
Schematic representation of complications of amebiasis.

## Clinical Features and Pathogenesis

The specific name "histolytica" refers to the appearance of a clear zone surrounding trophozoites in tissue sections, presumed to be due to parasite toxins or enzymes.[1] The clear zone may be an artifact caused by shrinkage during fixation. Studies by electron microscopy, however, reveal degeneration of epithelial cells as trophozoites approach, supporting the theory that trophozoites elaborate cytolytic substances. Amoebapores, pore-forming peptides, and proteinases secreted by the parasite cleave immunoglobulin and complement components, and may contribute to colonic cell lysis.[5,14] When the parasite Gal/GalNAc-specific lectin attaches to host cell intestinal surface mucin glycoproteins, commensal infection results and leads to host cell apoptosis.[15] The Gal/GalNAc-specific lectin prevents assembly of complement C5b-C9 complex, contributing to evasion of the immune response.[16] Invasion by trophozoites causes secretion of cytokines from host cells, leading to an acute inflammatory response. Recently PATMK, a member of the transmembrane kinase family was found to be a key in human erythrocyte phagocytosis.[17]

The spectrum of amebiasis includes a range of clinical presentations including asymptomatic carriage, diarrhea and liver abscess and may be related to variations in host factors and the parasite genome.[18,19] Patients typically present with a several-week history of gradually increasing cramping lower abdominal pain, weight loss, and recurring bouts of watery, mucoid or bloody diarrhea.[11] The insidious onset, variable signs and symptoms and frequent absence of fever or grossly bloody stool make diagnosis difficult. Other symptoms may include malodorous flatus, intermittent constipation, nausea, vomiting, right-sided cramps, fatigability, loss of appetite and tenesmus. Stools may increase to 25 per day, with weakness and prostration. Any portion of the abdomen may be tender, but maximum tenderness is over the portion of the colon that is most severely involved. Amebic colitis is more severe in patients who are very young, old or receiving corticosteroids.[11] Sometimes the clinical picture is acute, suggesting appendicitis, cholecystitis, intestinal obstruction, diverticulitis, a ruptured viscus, pneumonia, or lung abscess. Stools are occult heme-positive, even if no blood is seen. Rectal bleeding without diarrhea may be seen, especially in children. There may be fecal leukocytosis, although to a lesser degree than that in shigellosis. Circulating leukocytes may rise to 20,000 $mm^3$.

Amebic colitis often persists for weeks, months, or years, and, during intervals between acute attacks, patients may have recurring cramps and soft loose stools, especially after meals. If untreated, those with severe infections become emaciated and anemic. Chronic intestinal amebiasis without dysentery can resemble ulcerative colitis clinically and result in inappropriate treatment with corticosteroids.[5]

The differential diagnosis of diarrhea with hematochezia includes *Shigella, Salmonella, Campylobacter*, and enteroinvasive and enterohemmorhagic *Escherichia coli* infection. Noninfectious causes include inflammatory bowel disease, ischemic colitis, diverticulitis, and arteriovenous malformation.[5]

Unusual manifestations of amebic colitis include acute necrotizing colitis, toxic megacolon, ameboma, perianal ulceration with fistula formation and amebic appendicitis.[11] Fulminant disease is increased in pregnant women, immunocompromised patients and those receiving steroids. Associations with diabetes and alcohol use have been reported. Acute necrotizing colitis is rare (occurring in less than 0.5% of cases) and is associated with a mortality rate of more than 40%.[20] Patients with acute necrotizing colitis typically appear very ill, with fever, bloody mucoid diarrhea, abdominal pain with rebound tenderness, and other signs of peritoneal irritation. Surgical intervention is indicated if there is bowel perforation or if the patient has no response to antiamebic therapy.

Toxic megacolon is rare (occurring in approximately 0.5% of cases) and is typically associated with corticosteroids use.[11] Early recognition and surgical intervention are important, since patients with toxic megacolon usually have no response to antiamebic therapy alone and peritonitis from perforation may occur.

Ameboma (also called amebic pseudotumor) of the colon occurs in 1 to 5% of patients and is a result of annular inflammatory thickening usually in the wall of the cecum or ascending colon. Ameboma may mimic carcinoma by location, symptoms, x-ray examination, and gross appearance.[21]

Extraintestinal complications of amebiasis include hepatic, subdiaphragmic, periappendiceal, and subhepatic abscesses; perianal amebic dermatitis; and hepatobronchial, hepatocolic, abdominocolic or anorectal fistulas (Fig 8.16). Complications of amebic liver abscess may arise from rupture of the abscess with perforation and peritonitis and extension into the peritoneum, pleural cavity or pericardium.[22] Extrahepatic amebic abscesses, presumably from hematogenous spread, have occurred in lung, skin and, very rarely, brain.

Amebic liver abscess (Fig 8.17a) is up to 20 times as common in men as in women and rare in children.[11] The Zulu word for it is "isigwebedhla" meaning "disease of strong young men".[1] Most patients present with symptoms that develop relatively slowly over 2 to 4 weeks, including fever, cough, and constant dull, aching abdominal pain in the right upper quadrant or epigastrium. Usually there is a single abscess in the right lobe. Involvement of the diaphragmatic surface of the liver may lead to right-sided pleural pain or referred shoulder pain. Gastrointestinal symptoms occur in only 10 to 35% of patients, and stool microscopy is often negative for parasites. Hepatomegaly with point tenderness

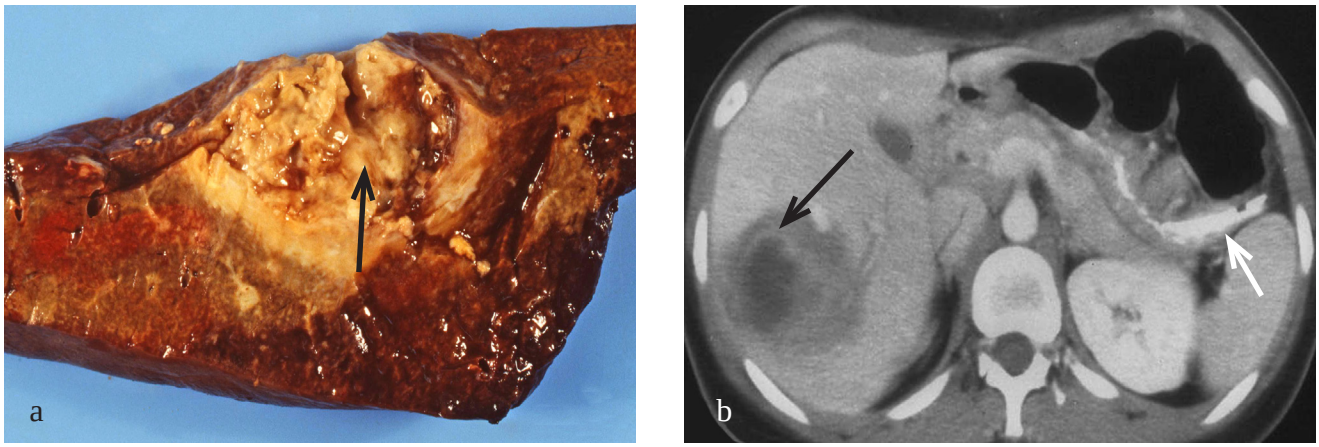



**Figure 8.17 a,b**
44-year-old man with colonic amebiasis complicated by an (a) amebic hepatic abscess (arrow); b. Contrast-enhanced CT shows mural thickening of the transverse colon (white arrow) and peripherally located hepatic abscess (black arrow) that is characterized by central fluid attenuation, an enhancing wall, and a peripheral rim of edema.

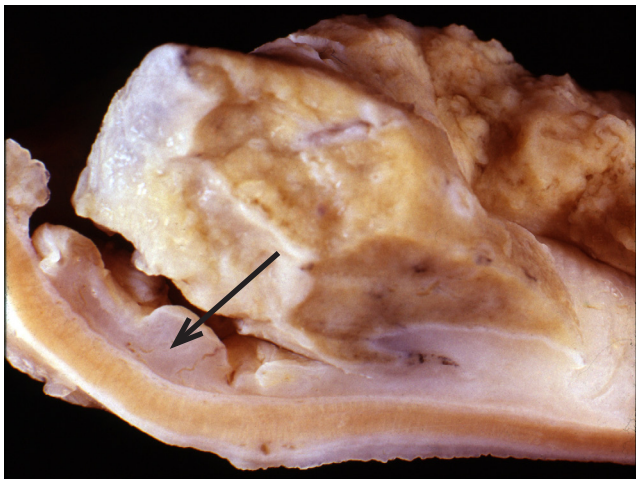


**Figure 8.18**
Amebiasis of lung and pleura (arrow) with attached diaphragm.



**Figure 8.19**
Cutaneous amebiasis involving anus and perianal skin. This is an extension from amebiasis of the rectum and has a cauliflower appearance caused by epithelial hyperplasia. Clinically, this appearance is easily mistaken for squamous cell carcinoma.

over the liver, below the ribs, or in the intercostal spaces is typical. Laboratory studies in patients with amebic liver abscess may reveal a mild to moderate leukocytosis and anemia.[11] Patients with acute amebic liver abscess tend to have a normal alkaline phosphatase level and elevated alanine aminotransferase level; the opposite is true of patients with chronic disease. Ultrasonography, abdominal computed tomography and magnetic resonance imaging are excellent for detecting amebic liver abscess (Fig 8.17b) but are not specific. The differential diagnosis includes bacterial abscess, necrotic hepatocellular carcinoma, and echinococcal cyst.[11] Compared to patients with bacterial liver abscesses, patients with amebic liver abscess are more likely to be male, younger than 50 years-old, immigrants from or travelers to an endemic area, and less likely to have jaundice, biliary disease or diabetes mellitus.

The lung is the second most common extraintestinal amebiasis after the liver. Infection usually spreads to the lungs through the diaphragm by extension of an amebic liver abscess. Pulmonary amebiasis (Figs 8.8 & 8.18) without liver involvement occurs sporadically due to hematogenous spread from the colon. [23,24] The sputum may occasionally contain trophozoites.[24] Pericardial amebiasis is rare and usually due to extension from an amebic abscess of the left lobe of the liver, sometimes from the right lobe of the liver, and rarely from the lungs or pleura. Pericardiocentesis usually confirms the diagnosis and improves the patient's condition.[25]

The skin may be involved by: (1) extension of rectal amebiasis to anus (Fig 8.19), perianal skin and vulva, (2) extension of a liver abscess to the skin of the abdominal wall or flank, or (3) infection of the penile skin (Fig 8.14) from



**Figure 8.20**
African patient with a 6 cm ulcer of the abdomen. Thick grayish pus containing many *Entamoeba histolytica* trophozoites drained from the ulcer, secondary to an amebic liver abscess.



**Figure 8.21**
49-year-old man admitted for cardiac failure found to have an anal lesion consistent with carcinoma with metastasis to the lung. At autopsy there were extensive amebic ulcerations of the colon extending to the rectum, amebic hepatitis, but no pulmonary amebiasis.

anal intercourse. Primary cutaneous amebiasis is extremely rare.[26-28] The initially small well-circumscribed ulcers may extend rapidly (Fig 8.20). They are acutely tender and malodorous with a gray-white necrotic base. In the anogenital area, epithelial hyperplasia causes a thickened cauliflower-like surface appearance that mimics carcinoma (Figs 8.19 & 8.21).

Patients with HIV infection are not at increased risk for amebic colitis. However, an increased incidence of amebic liver abscess among these patients has been reported which suggests that HIV infected patients are more susceptible to invasive disease.[25] *Entamoeba dispar* causes no signs of disease or mucosal invasion even in patients with AIDS.[1]

## *Pathologic Features*

Infection begins as small foci of superficial necrosis in the colonic mucosa. These foci progress to form ulcers. Some ulcers remain small and discrete; others expand or become confluent to form broad geographic patterns (Fig 8.22). Amebic ulcers are usually limited to one region, but may be disseminated throughout the colon. When limited, the cecum is the most common site involved. Less commonly, ulcers are limited to the ascending colon, descending colon, or transverse colon. Rarely, there are amebic ulcers in the ileum near the ileocecal junction. The typical amebic ulcer is flask-shaped, undermined and sharply defined without ragged edges (Figs 8.23 & 8.24). The crater contains heaped up gray necrotic tissue. Sometimes, the exudate raises the undermined mucosa. Mucus may coat the mucosa between ulcers.

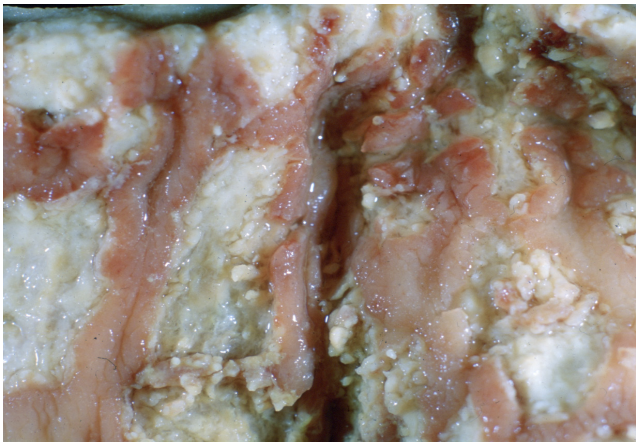


**Figure 8.22**
Colonic amebiasis in a 40 year-old woman from Pennsylvania who recently returned from a trip to Mexico. The ulcers are confluent and filled with exudates. She had chronic diarrhea, thought to have had ulcerative colitis, and was treated with corticosteroids. Ironically, 3 stool specimens were negative for ameba.

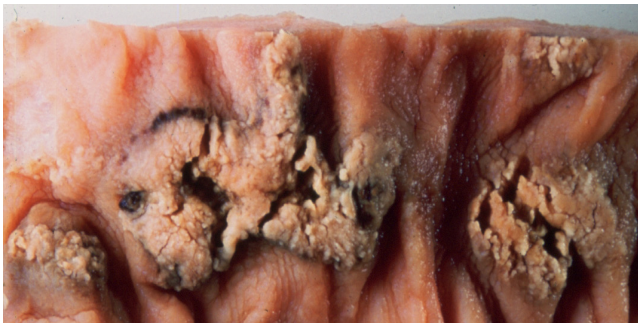


**Figure 8.23**
Colon from adult male Ugandan with fatal amebiasis. The patient was thought to have a plasmacytoma and was treated with corticosteroids and other chemotherapeutic agents. The entire colon is studded with small, confluent ulcers, all covered with a heaped up gray exudates.

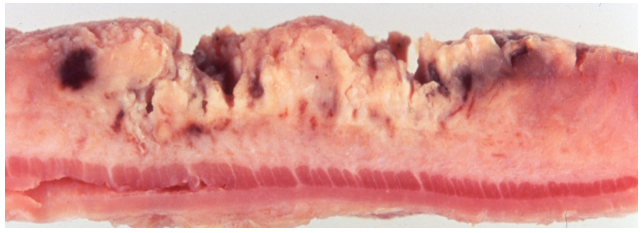


**Figure 8.24**
A vertical section of the specimen shown in Figure 8.23. The ulcer on the left has penetrated the submucosa but not the muscularis.

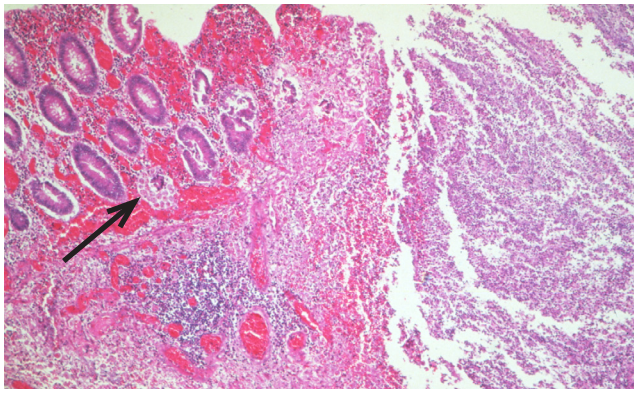


**Figure 8.25**
Ulcerated colon with destruction of the entire thickness of the mucosa. Note congested lamina propria and cluster of trophozoites (arrow). H&E x40

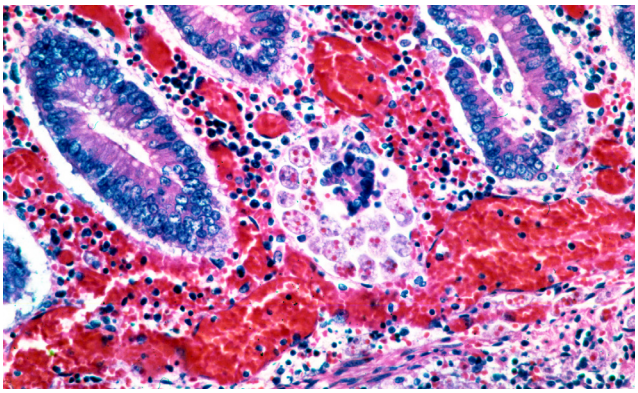


**Figure 8.26**
Higher magnification of trophozoites in Figure 8.25. Most have ingested several erythrocytes. H&E x180

Microscopic examination can reveal a wide range of histopathological findings including diffusely inflamed mucosa, necrosis, acute inflammatory exudate, and ulceration that can extend through the muscularis mucosa into the submucosa (Figs 8.25 & 8.26).[29] The ulcer crater is comprised of fibrin, cellular debris, and trophozoites (Fig 8.27). Trophozoites may also be seen on the surface, in any layer of the colon and rarely in blood vessels. A narrow margin at the edge of the ulcer retains a faint outline of previously viable structures, suggesting that the necrosis may be partly ischemic (Fig 8.28). Early, there is little inflammatory response, but, as ulcers widen, neutrophils, lymphocytes, histiocytes, plasma cells, and sometimes eosinophils, accumulate in the crater and in the viable tissues around it. In well-established ulcers, inflammation may be minimal (Figs 8.29 & 8.30).[30]

The typical histologic pattern is that of chronic crypt destructive colitis with mononuclear inflammatory cells extending into the deep lamina propria and crypt architectural distortion and branching (Fig 8.31).[31] This pattern is not specific and similar to that seen in other conditions including: idiopathic chronic inflammatory bowel disease, common enteric bacteria infections (*Campylobacter, Shigella, Aeromonas,* and *Yersinia*), sexually transmitted diseases (syphilis and chlamydiosis), tuberculosis, fungal infections (histoplasmosis, cryptococcosis, coccidiodomycosis and candidiasis), and chronic nonsteroidal anti-inflammatory drugs use.

Grossly, amebomas are firm, well-defined enlargements of the colon wall. Like some carcinomas of the colon, they tend to cause a "napkin ring" constriction. Microscopically, amebomas are comprised of varying amounts of granulation tissue, fibrosis, chronic inflammatory cells, and clusters of trophozoites that usually concentrate in the submucosa near small points of ulceration (Figs 8.32 & 8.33).

Hepatic amebic abscesses may become very large, sometimes destroying an entire lobe (Fig 8.34). They contain

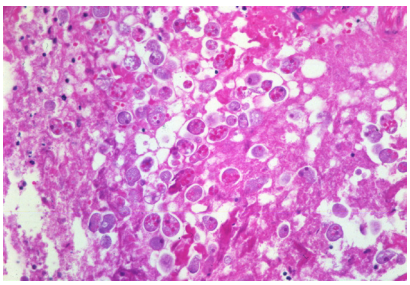


**Figure 8.27**
Ulcerated colon may contain massive numbers of trophozoites. H&E x110

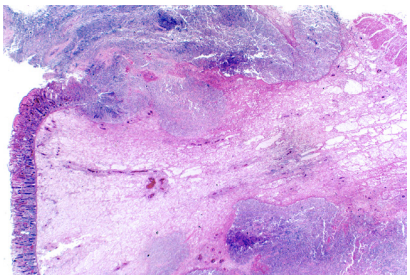


**Figure 8.28**
Narrow margin of ischemic type necrosis at the edge of ulcer. H&E x4.4

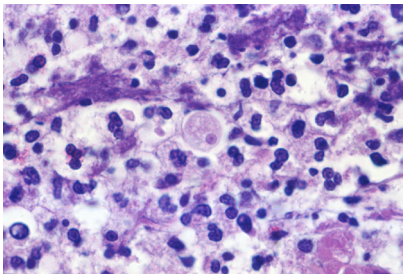


**Figure 8.29**
Neutrophils, lymphocytes, histiocytes and plasma cells join amebae in ulcer's crater. H&E x450

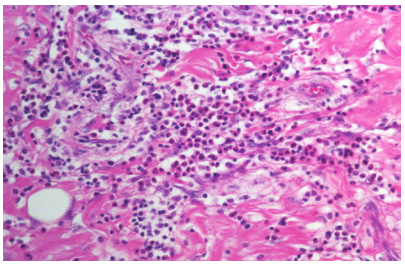


**Figure 8.30**
Amebic colitis in AIDS patient with massive tissue eosinophilia. H&E x110

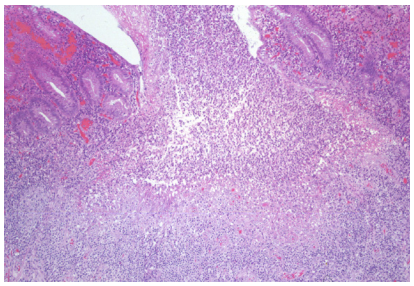


**Figure 8.31**
Typical flask-shaped ulcer in amebic appendicitis. H&E x40

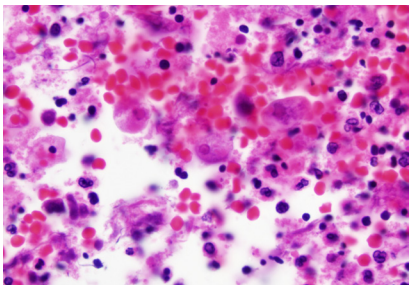


**Figure 8.32**
Ameboma with trophozoites in area of acute inflammation and congestion in colon. H&E x250

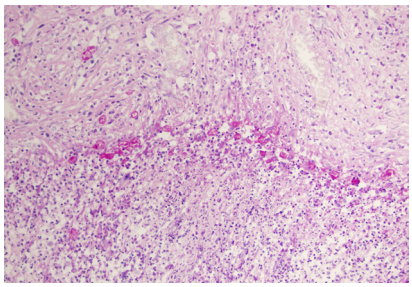


**Figure 8.33**
Ameboma with trophozoites lined up along border of necrotic and more viable tissue in wall of colon. H&E x40

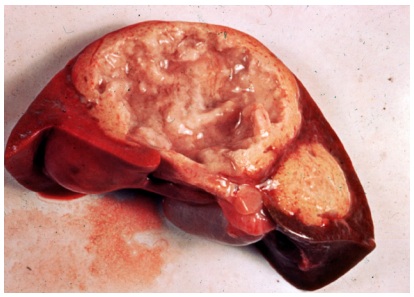


**Figure 8.34**
This large hepatic abscess has destroyed most of the right lobe and a large portion of the left lobe.

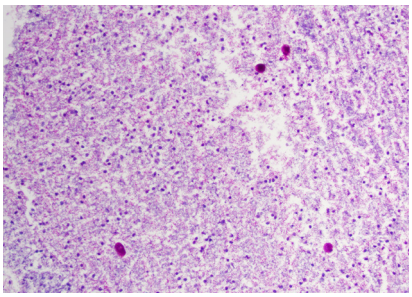


**Figure 8.35**
Liquified center of hepatic abscess is amorphous and necrotic with scattered trophozoites. PAS x40

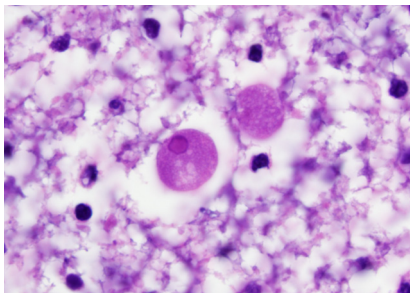


**Figure 8.36**
Viable trophozoites in liquid center of hepatic abscess that lacks neutrophils. H&E x480

yellow or gray, opaque liquid material. The wall is shaggy and fibrinous. Microscopically, the wall contains abundant fibrin. Trophozoites may be abundant or rare and are often clustered in the fibrin near viable hepatic tissue (Figs 8.35 & 8.36). The liquified center is amorphous and necrotic, but does not contain neutrophilic leukocytes as the term "abscess" suggests. The surrounding liver is edematous and may be infiltrated by mixed chronic inflammatory cells. Inflammation surrounding well-established liver abscesses is minimal, given the degree of tissue damage.[30]

In a reported case of fallopian tube amebiasis, microscopic examination showed a poorly formed granuloma composed of large macrophages with many trophozoites in the lumen.[32]

In cutaneous amebiasis, there is benign epithelial hyperplasia that may have a cauliflower appearance grossly, mimicking squamous cell carcinoma (Fig 8.19). Microscopically, there is papillary acanthosis and ulceration of the epithelium (Fig 8.37).[33] The dermis is hyperemic to necrotic and infiltrated by lymphocytes, plasma cells, and, sometimes, eosinophils. Trophozoites are concentrated over the points of ulcer-

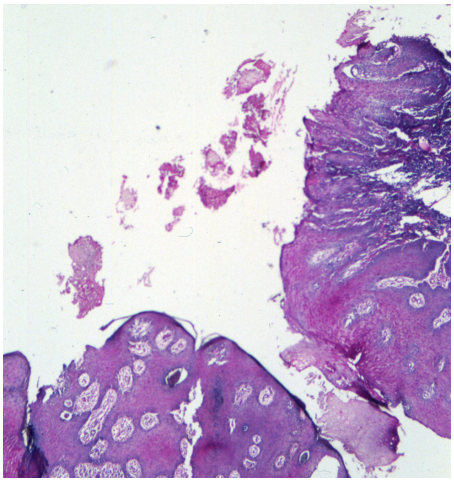


**Figure 8.37**
Amebiasis of anal skin with papillary acanthosis and ulceration. PAS x66

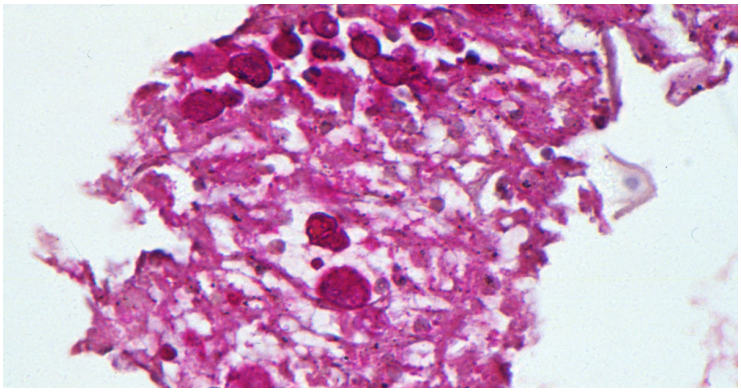


**Figure 8.38**
Clusters of trophozoites concentrated in exudates of ulcer seen in Fig 8.37. PAS x1200

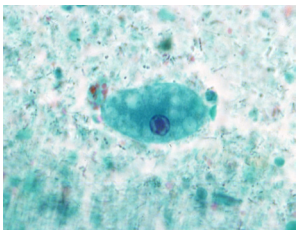


**Figure 8.39**
*Entamoeba coli* trophozoite (32µm diameter) in feces, note large karyosome and vacuoles. Trichrome x350

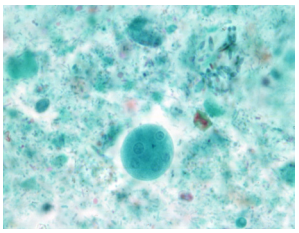


**Figure 8.40**
*Entamoeba coli* cyst (17µm diameter) in feces, note 5 nuclei. Trichrome x350

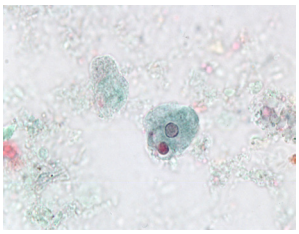


**Figure 8.41**
*Entamoeba polecki* trophozoite (18µm diameter) in fecal smear with ingested RBC and one nucleus. Trichrome x350

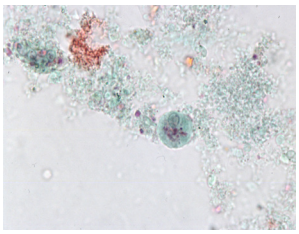


**Figure 8.42**
*Entamoeba polecki* cyst (11µm diameter) in fecal smear with chromatoid body. Trichrome x350

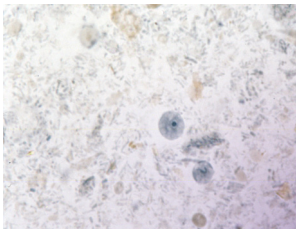


**Figure 8.43**
*Endolimax nana* trophozoite (8µm diameter) with large karyosome in fecal smear. Trichrome x350

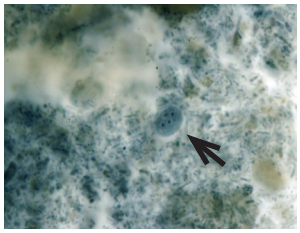


**Figure 8.44**
*Entdolimax nana* cyst (10µm diameter) with 4 nuclei in fecal smear (arrow). Trichrome x350

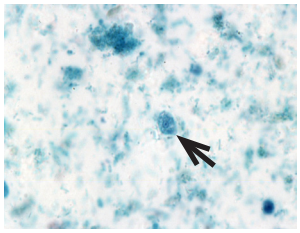


**Figure 8.45**
*Entamoeba hartmanni* trophozoite (8µm diameter) with one central nucleus (arrow). Trichrome x350

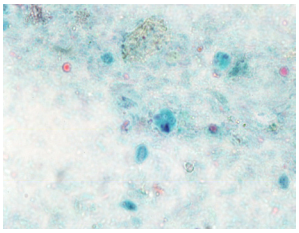


**Figure 8.46**
*Entamoeba hartmanni* cyst (7µm diameter) with two nuclei. Trichrome x350

ation in adjacent epidermis and in the superficial layers of the ulcer (Fig 8.38).

## Diagnosis

Patients presenting with a history of diarrhea or dysentery must first be evaluated to separate cases of invasive diarrhea from cases of secretory diarrhea. Initial diagnostic evaluation includes fecal testing for lactoferrin, leucocytes or occult blood.

Intestinal amebiasis is often diagnosed by identifying cysts or motile trophozoites on a saline wet mount of stool. Only rare patients with symptomatic amebic colitis pass cysts without trophozoites. This method has low sensitivity, and false positive results occur in the presence of nonpathogenic species *E. dispar* or *E. moshkovskii*, which are microscopically identical to *E. histolytica*.[5,34] The presence of erythrophagocytosis by trophozoites in the stool of a patient with bloody diarrhea is considered diagnostic of *E. histolytica* infection. *Entamoeba dispar* rarely contains red blood cells; therefore, in the absence of erythrophagocytosis, *E. dispar* cannot be excluded and bacterial dysentery should be considered. The differential diagnosis of *E. histolytica* in stool, cytologic specimens and tissue sections includes *Entamoeba coli*, *Entamoeba polecki*, *Endolimax nana*, *Entamoeba hartmanni*, *Entamoeba gingivalis*, *Iodamoeba butschlii*, and *Balantidium coli*.[35]

*Entamoeba coli* is a nonpathogenic species.[35] The nucleus of *E. histolytica* may have a large, diffuse, eccentric karyosome and coarse, unevenly distributed peripheral chromatin, resembling that of *E. coli* (Figs 8.39 & 8.40). Although the two species often can be differentiated in iodine stained preparations,[36] a permanent stained smear is necessary for confirmation. The peripheral chromatin of *E. coli* occasionally may appear as a solid dark ring of material. The nucleus of *E. coli* may sometimes contain a central karyosome and uniform peripheral chromatin like that of *E. histolytica*. Immature cysts of *E. coli* containing four or fewer nuclei may be extremely difficult to distinguish from *E. histolytica*, as cyst nuclei frequently have a central karyosome and uniformly distributed peripheral chromatin.

*Entamoeba polecki* is usually considered nonpathogenic but may cause loose stools or diarrhea.[35] Differentiating trophozoites from those of *E. histolytica* may be difficult. Size ranges overlap, and the nucleus of *E. polecki* resembles that of *E. histolytica*, although its peripheral chromatin tends to be more delicate than that of *E. histolytica* (Figs 8.41 & 8.42). Although cysts of *E. polecki* closely resemble the uninucleate cysts of *E. histolytica*, the presence of uninucleate cysts alone should suggest *E. polecki*. A large glycogen vacuole is seldom seen in *E. polecki*. Chromatoid bodies are usually more numerous and pleomorphic in *E. polecki* than in *E. histolytica*.

*Endolimax nana* is a nonpathogenic protozoon that inhabits the colon and is frequently confused with other small amebae.[35] The karyosome of *E. nana* is larger than that of *E. histolytica* (Figs 8.43 & 8.44).

Nonpathogenic *E. hartmanni* was once considered to

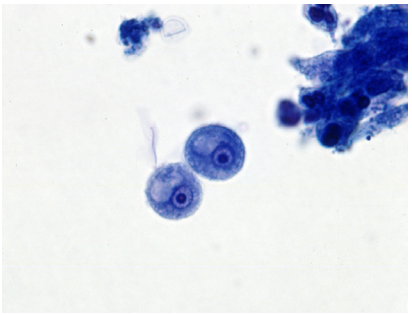


**Figure 8.47**
Two *Iodamoeba butschlii* trophozoites in fecal smear with large nuclei, large karyosome, and large vacuole, PAP x580

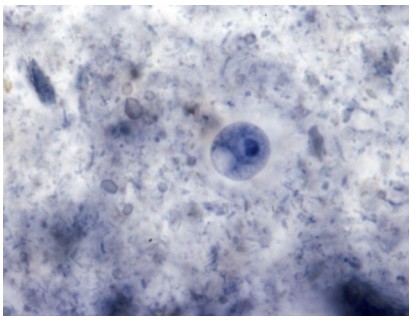


**Figure 8.48**
*Iodamoeba butschlii* cyst (12µm diameter) in fecal smear with karyosome and vacuole. Trichrome x840

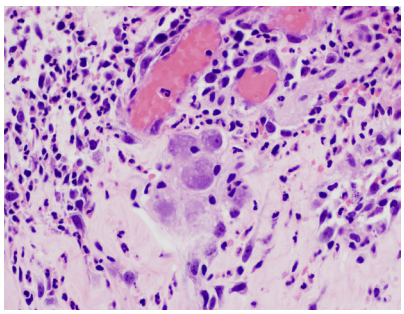


**Figure 8.49**
Ganglion cells in wall of colon lacks karyosomes of amoeba. H&E x130

be the small race of *E. histolytica*, because of its similar morphology.[35] There is some difficulty distinguishing them because the size ranges of the trophozoites and cysts of the two species overlap. The karyosome of *E. hartmanni* usually is smaller and more compact than that of *E. histolytica*, and *E. hartmanni* generally stains more delicately than *E. histolytica* (Figs 8.45 & 8.46).

*Entamoeba gingivalis* is a nonpathogenic ameba that occurs in the oral cavity and lacks a cyst stage.[35] The nucleus of *E. gingivalis* is similar in morphology to that of *E. histolytica*, having a small central karyosome often with delicate chromatin strands extending to the nuclear membrane, which bears fine peripheral chromatin. The cytoplasm often contains ingested leukocytes in varying stages of digestion, bacteria and other detritus but only rarely erythrocytes. Trophozoites of *E. gingivalis* can be found in scrapings from gum tissues, especially from patients with pyorrhea alveolaris. Since *E. histolytica* trophozoites are rarely found in the sputum of patients with pulmonary abscess, it is necessary to be aware of the potential presence of *E. gingivalis* in sputum. There have been rare reports of *E. gingivalis* in vaginal and cervical smears from women with intrauterine contraceptive devices.[37]

The cyst stage of non pathogenic *I. buetschlii* contains a distinct mass of glycogen in the cytoplasm.[35] Occasionally glycogen may occur as a discrete mass in young cysts of *E. histolytica*; however, the two can be distinguished by nuclear structure (Figs 8.47 & 8.48).

*Balantidium coli*, which may cause identical colonic lesions, is discussed in Chapter 15. This ciliated protozoon is several times larger than *E. histolytica* and has a distinctive shape.

The differential diagnosis of amebae in tissue sections includes host cells such as histiocytes and ganglion cells (Fig 8.49). Features that distinguish trophozoites in tissue sections include their sharp cellular outline from the surrounding host cells and the round nucleus with a central karyosome. Macrophages and ganglion cells tend to be less sharply demarcated and have oval nuclei.

Methods of detection of *E. histolytica*-specific antigen in stool or antiamebic antibodies in serum may be more sensitive than microscopy.[11,12,18,38-41] ELISA for detection of fecal lectin antigen is more sensitive method than culture, although antigens are denatured by fixation, limiting testing to fresh or frozen samples.[5,42] Serum antiamebic antibodies are present in 70 to greater than 90% of patients with amebic colitis and 70 to 80% of patients with amebic liver abscess.[16] False-negative serologic tests can occur in the first 7 to 10 days of infection, and serologic tests remain positive for years after infection. A combination of serologic tests with detection of the parasite by antigen detection or PCR may be the best approach, although PCR techniques remain impractical in many developing countries.[5,43,44]

Occasionally, aspiration of a liver abscess is required to rule out bacterial abscess.[16] Amebae are seen in the abscess fluid in a minority of patients. Less than half of patients with amebic liver abscess have parasites detected in their stool by antigen detection. In rare cases of pulmonary amebiasis, amebae are found in aspirated pus or expectorated sputum.

## Treatment and Prevention

Asymptomatic noninvasive infection should be treated with paromomycin because of its potential to progress to invasive disease.[11,45,46] Acute colitis should be treated with a nitroimidazole for trophozoites, followed by a luminal agent for cysts. Although approximately 90% of patients with mild to moderate amebic dysentery respond to nitroimidazole therapy, parasites persist in the intestine in as many as 40 to 60%. Therefore, nitroimidazole treatment should be followed with a luminal agent (paromomycin, iodoquinol or diloxanide furoate) to eradicate colonization.[47-49] Metronidazole (a nitroimidazole) and paromomycin should not be given at the same time, since diarrhea, a common side effect of paromomycin, may make it difficult to assess the patient's response to therapy. In rare cases of fulminant amebic colitis, it is prudent to add broad-spectrum antibiotics to treat intestinal bacteria that may spill into the peritoneum. Surgical intervention is occasionally required for acute ab-

domen, gastrointestinal bleeding, or toxic megacolon.

At one time, amoebic liver abscesses were almost always fatal, but now even large abscesses can be cured by medical therapy.[1,50] Nitroimidazoles, particularly metronidazole (Flagyl), are the mainstay of therapy for invasive amebiasis. Nitroimidazoles with longer half-lives (tinidazole, secnidazole, and ornidazole) are better tolerated and allow shorter periods of treatment. Chloroquine is an alternative treatment but is associated with higher relapse rates.[46] Bacterial infection of amebic liver abscess occasionally occurs spontaneously or as a complication of aspiration; therefore, it is reasonable to use antibiotics in the absence of a prompt response to nitroimidazole therapy.[46]

Imaging-guided percutaneous needle aspiration and catheter drainage of amebic liver abscesses have replaced surgical intervention.[51] Such therapeutic aspiration should be considered in patients in whom pyogenic abscess has been ruled out and in whom there is no response to treatment in three to five days or in those at risk for rupture or pericardial spread.[46] Abscess cavities greater than 5 cm in diameter or in the left lobe are at a higher risk of rupture.

Amebiasis theoretically could be eradicated. Because humans and primates are the only epidemiologically significant reservoirs, herd immunity in humans could interrupt the fecal-oral transmission cycle.[11,52] Potentially, a vaccine could be highly protective.[53,54] Humans acquire partial natural immunity following intestinal infection indicating that a vaccine could stimulate an effective immune response. Improved sanitation could eradicate cyst carriage from a population.[46] Travelers to endemic areas should avoid eating unpeeled fruits and vegetables and should drink bottled or iodine-disinfected water.

## *Free-living Amebas (see also Topic 9)*

Of the four free-living amebas that are medically important, *Acanthamoeba* sp, *Balamuthia mandrillaris*, *Naegleria fowleri*, and *Sappinia diploidea*,, only *Acanthamoeba* and *Balamuthia* produce significant disease outside of the CNS or cornea.[55] Both *Acanthamoeba* and *Balamuthia* cause infections of the lungs and skin.

In immunocompromised hosts *Acanthamoeba* provokes cutaneous lesions such as disseminated nodules,[56,57] pustules, and ulcerations (Fig 8.50). Trophozoites and cysts are numerous (Fig 8.51).[58] Besides skin, *Acanthamoeba* involves the soft palate (Figs 8.52 & 8.53), lung (Figs 8.54 to 8.56), sinuses (Figs 8.57 & 8.58), liver and bone[59] and abdominal organs including kidney.[60]

Diagnosis follows demonstration of cysts and trophozoites (30 µm diameter) in hematoxylin and eosin stained histologic sections often in the dermal-hypodermal junction within polymorphous inflammatory granulomas associated with ischemic necrosis.[58] A polymerase chain reaction (PCR) assay specific for *Acanthamoeba* has been reported positive from formalin-fixed paraffin embedded tissue.[59]

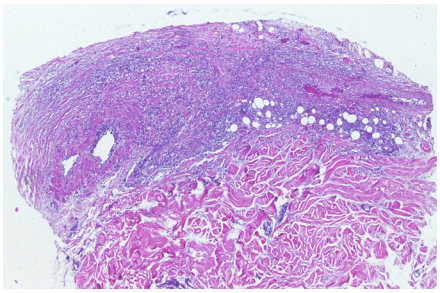


**Figure 8.50**
*Acanthamoeba* infection producing necrosis and inflammation in subcutis of an AIDS patient. H&E x19

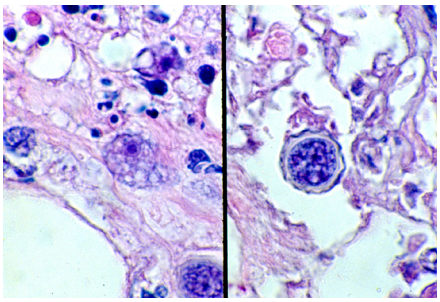


**Figure 8.51**
Side-by-side comparison of *Acanthamoeba* trophozoite (left) and cyst (right) in subcutis of patient in Fig 8.50. H&E x560

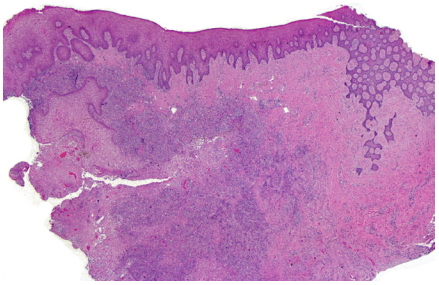


**Figure 8.52**
*Acanthamoeba* infection producing suppuration and granulomas in soft palate. H&E x8

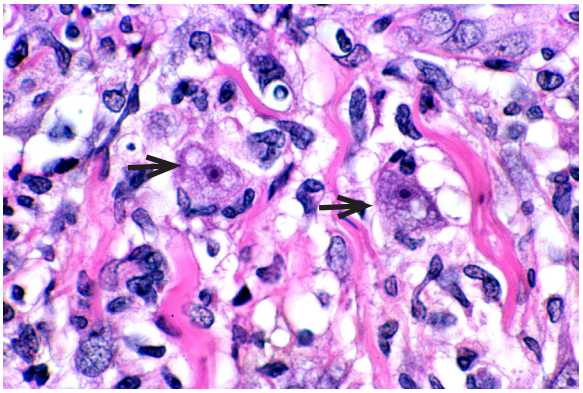


**Figure 8.53**
Two *Acanthamoeba* trophozoites (arrows) with large karyosomes in soft palate. H&E x550

Recommended treatments are pentamidine, itraconazole and flucytosine. Due to the morbidity and mortality of *Acanthamoeba* infection optimal therapy must be defined.[58]

Patients with *Balamuthia* infection may present with lesions of the skin, sinus cavities, or middle ear. Skin lesions are painless, may appear as plaques from one to several centimeters wide and are generally single. Lesions appear most commonly in the centre of the face, less commonly on the trunk, and hands and feet.[55]

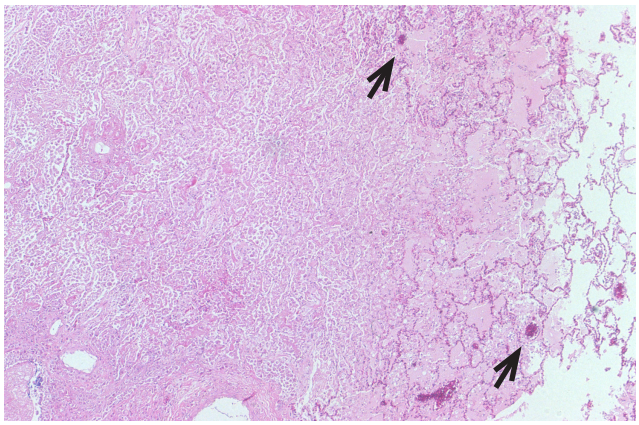


**Figure 8.54**
*Acanthamoeba* (arrows) infection producing necrosis in lung in an AIDS patient. H&E x24

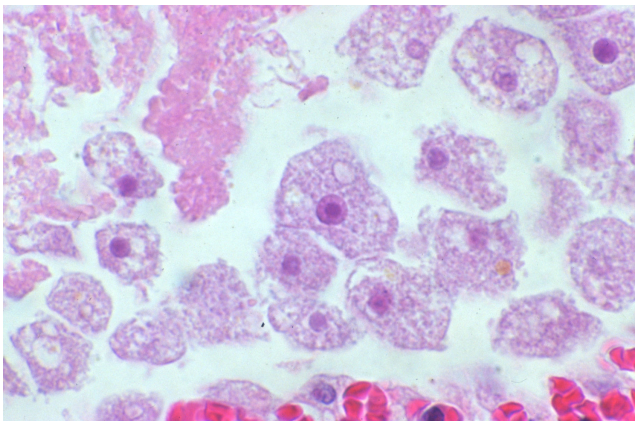


**Figure 8.55**
*Acanthamoeba* trophozoites in lung of patient in Fig 8.54. H&E x600

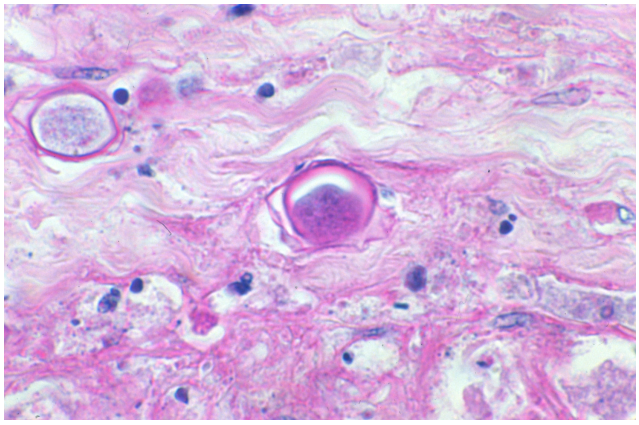


**Figure 8.56**
*Acanthamoeba* cyst with double membrane in lung of patient in Fig 8.54. PAS x600

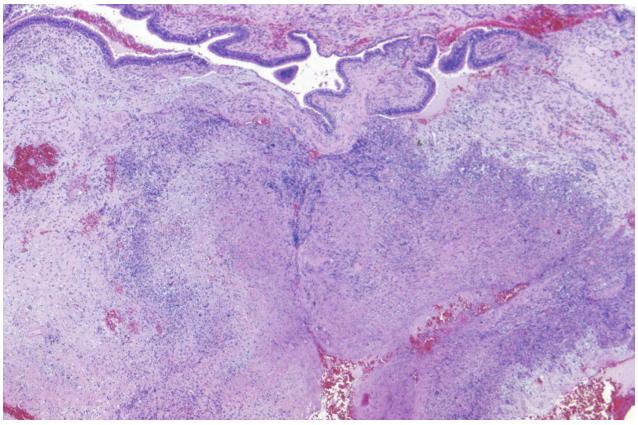


**Figure 8.57**
Maxillary sinusitis of AIDS patient in Fig 8.54. H&E x24

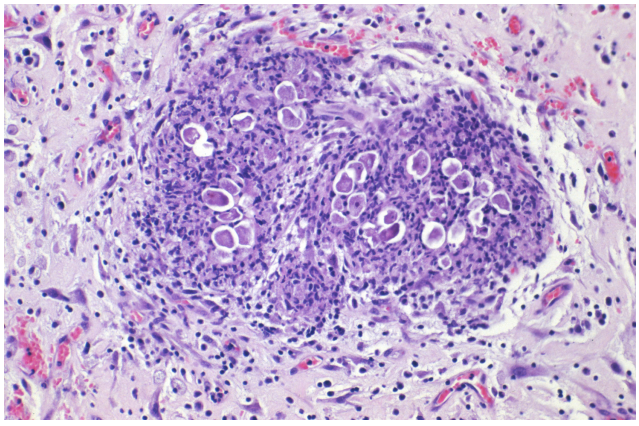


**Figure 8.58**
*Acanthamoeba* trophozoites in granuloma in maxillary sinus of patient in Fig 8.54. H&E x145

## References


1. Stanley SL Jr. Amoebiasis. *Lancet*. 2003;361:1025-1034.
2. Ali IK, Hossain MB, Roy S, et al. *Entamoeba moshkovskii* infections in children, Bangladesh. *Emerg Infect Dis.* 2003;9:580-584.
3. Lösch F. Massenhafte Entwickelung von Amöben im Dickdarm. *Arch F Path Anat.* 1875;65:196-211.
4. Epidemic Amebic Dysentery: The Chicago Outbreak of 1933. U. S. Treasury Department, Public Health Service. National Institute of Health Bulletin No. 166. Washington, D.C.: Government Printing Office, 1936.
5. Tanyuksel M, Petri WA Jr. Laboratory diagnosis of amebiasis. *Clin Microbiol Rev.* 2003;16:713-729.
6. Nisheena R, Ananthamurthy A, Inchara YK. Fulminant amebic colitis: a study of six cases. *Indian J Pathol Microbiol.* 2009;52:370-373.
7. Ali IK, Solaymani-Mohammadi S, Akhter J, et al. Tissue invasion by *Entamoeba histolytica*: evidence of genetic selection and/or DNA reorganization events in organ tropism. *PLoS Negl Trop Dis*. 2008;2:e219. Erratum in: *PLoS Negl Trop Dis*. 2008;2(6).
8. Ali IK, Mondal U, Roy S, Haque R, Petri WA Jr, Clark CG. Evidence for a link between parasite genotype and outcome of infection with *Entamoeba histolytica*. *J Clin Microbiol*. 2007;45:285-289.
9. Farhana F, Jamaiah I, Rohela M, Abdul Aziz NM, Nissapatorn V. A ten year (1999-2008) retrospective study of amoebiasis in University Malaya Medical Centre (UMMC), Kuala Lumpur, Malaysia. *Trop Biomed.* 2009;26:262-266.
10. Petri WA Jr, Mondal D, Peterson KM, Duggal P, Haque R. Association of malnutrition with amebiasis. *Nutr Rev.* 2009;67 Suppl 2:S207-215.
11. Haque R, Huston CD, Hughes M, Houpt E, Petri WA. Amebiasis. *N Eng J Med.* 2003;348:1565-1573.
12. Ghosh S, Frisardi M, Ramirez-Avila L, et al. Molecular epidemiology of *Entamoeba* spp.: evidence of a bottleneck (Demographic sweep) and transcontinental spread of diploid parasites. *J Clin Microbiol.* 2000;38:3815-3821.
13. Eichinger D. A role for a galactose lectin and its ligands during encystment of *Entamoeba*. *J Eukaryot Microbiol.* 2001;48:17-21.
14. Que X, Kim SH, Sajid M, et al. A surface amebic cysteine proteinase inactivates interleukin-18. *Infect Immun.* 2003;71:1274-1280.
15. Petri WA Jr, Haque R, Mann BJ. The bittersweet interface of parasite and host: lectin-carbohydrate interactions during human invasion by the parasite *Entamoeba histolytica*. *Annu Rev Microbiol.* 2002;56:39-64.
16. Braga LL, Ninomiya H, McCoy JJ, et al. Inhibition of the complement membrane attack complex by the galactose-specific adhesion of *Entamoeba histolytica*. *Clin Invest.* 1992;90:1131-1137.
17. Boettner DR, Huston CD, Linford AS, et al. *Entamoeba histolytica* phagocytosis of human erythrocytes involves PATMK, a member of the transmembrane kinase family. *PLoS Pathog*. 2008;4(1):e8.
18. Ali IKM, Hossain MB, Roy S, et al. *Entamoeba moshovskii* infections in children in Bangladesh. *Emerg Infect Dis.* 2003;9:580-584.
19. Okamoto M, Kawabe T, Ohata K, et al. Amebic colitis in asymptomatic subjects with positive fecal occult blood test results: clinical features different from symptomatic cases. *Am J Trop Med Hyg.* 2005;73:934-935.
20. Ellyson JH, Bezmalinovic Z, Parks SN, Lewis FR Jr. Necrotizing amebic colitis: a frequently fatal complication. *Am J Surg.* 1986;152:21-26.
21. Radovanovic ZL, Katic VV, Nagorni AV, Zivkovic VV, Stankovic TD, Trenkic MS. Clinical diagnostic problems associated with cecal ameboma: case report and review of the literature. *Pathol Res Pract.* 2007;203:823-825.
22. Shenoy VP, Vishwanath S, Indira B, Rodrigues G. Hepato-pulmonary amebiasis: a case report. *Braz J Infect Dis*. 2010;14:372-373.
23. Lichtenstein A, Kondo AT, Visvesvara GS, et al. Pulmonary amoebiasis presenting as superior vena cava syndrome. *Thorax.* 2005;60:350-352.
24. Hara A, Hirose Y, Mori H, Iwao H, Kato T, Kusuhara Y. Cytopathologic and genetic diagnosis of pulmonary amebiasis: a case report. *Acta Cytol*. 2004;48:547-550.
25. Shamsuzzaman SM, Hashiguchi Y. Thoracic amebiasis. *Clin Chest Med.* 2002;23:479-492.
26. Parshad S, Grover PS, Sharma A, Verma DK, Sharma A. Primary cutaneous amoebiasis: case report with review of the literature. *Int J Dermatol.* 2002;41:676-680.
27. Kenner BM, Rosen T. Cutaneous amebiasis in a child and review of the literature. *Pediatr Dermatol.* 2006;23:231-234.
28. Al-Daraji WI, Husain EA, Robson A. Primary cutaneous amebiasis with a fatal outcome. *Am J Dermatopathol*. 2008;30:398-400.
29. Prathap K, Gilman R. The histopathology of acute intestinal amebiasis: a rectal biopsy study. *Am J Pathol.* 1970;60:229-246.
30. Brandt H, Tamayo RP. Pathology of human amebiasis. *Hum Pathol.* 1970;1:351-385.
31. Emory TS, Carpenter HA, Gostout CJ, Sobin LH. *Atlas of Gastrointestinal Endoscopy & Endoscopic Biopsies.* Washington DC: Armed Forces Institute of Pathology: 2000, pp289-292.
32. Calore EE, Calore NM, Cavaliere MJ. Salpingitis due to *Entamoeba histolytica*. *Braz J Infect Dis.* 2002;6:97-99.
33. Magaña M, Magaña ML, Alcantara A, Perez-Martin MA. Histopathology of cutaneous amebiasis. *Am J Dermatopathol.* 2004;26:280-284.
34. Nazemalhosseini Mojarad E, Nochi Z, Sahebekhtiari N, et al. Discrimination of *Entamoeba moshkovskii* in patients with gastrointestinal disorders by single-round PCR. *Jpn J Infect Dis*. 2010;63:136-138.
35. Ash LR, Orihel TC. *Atlas of Human Parasitology*, third edition. Chicago, IL: ASCP Press; 1990:31–63.
36. Tan ZN, Wong WK, Nik Zairi Z, et al. Identification of *Entamoeba histolytica* trophozoites in fresh stool sample: comparison of three staining techniques and study on the viability period of the trophozoites. *Trop Biomed.* 2010;27:79-88.
37. Clark CG, Diamond LS. Colonization of the uterus by the oral protozoan *Entamoeba gingivalis*. *Am J Trop Med Hyg.* 1992;46:158-160.
38. Gatti S, Petithory JC, Ardoin F, Pannetier C, Scaglia M. Asymptomatic amoebic infection: *Entamoeba histolytica* or *Entamoeba dispar*? That is the question. *Bull Soc Pathol Exot.* 2001;94:304-307.
39. Zaki M, Meelu P, Sun W, Clark CG. Simultaneous differentiation and typing of *Entamoeba histolytica* and *Entamoeba dispar*. *J Clin Microbiol* 2002;40:1271-1276.
40. *Entamoeba histolytica* infection in female outpatients at a sexually transmitted disease sentinel clinic in Tokyo, Japan. *Jpn J Infect Dis*. 2008;61:175-178.
41. Chen Y, Zhang Y, Yang B, et al. Seroprevalence of *Entamoeba histolytica* infection in HIV-infected patients in China. *Am J Trop Med Hyg.* 2007;77:825-828.
42. Abd-Alla MD, Wahib AA, Ravdin JI. Comparison of antigen-capture ELISA to stool-culture methods for the detection of asymptomatic *Entamoeba* species infection in Kafer Daoud, *Egypt. Am J Trop Med Hyg.* 2000;62:579-582.
43. Hamzah Z, Petmitr S, Mungthin M, Leelayoova S, Chavalitshewinkoon-Petmitr P. Development of multiplex real-time polymerase chain reaction for detection of *Entamoeba histolytica, Entamoeba dispar,* and *Entamoeba moshkovskii* in clinical specimens. *Am J Trop Med Hyg*. 2010;83:909-913.
44. Gutiérrez-Cisneros MJ, Cogollos R, López-Vélez R, et al. Application of real-time PCR for the differentiation of *Entamoeba histolytica* and *E. dispar* in cyst-positive faecal samples from 130 immigrants living in Spain. *Ann Trop Med Parasitol*. 2010;104:145-149.
45. Blessman J, Tannich E. Treatment of asymptomatic intestinal *Entamoeba histolytica* infection. *N Engl J Med.* 2002;347:1384-1384.
46. Petri WA Jr, Singh U. Diagnosis and management of amebiasis. *Clin Infect Dis.* 1999;29:1117-1125.
47. McAuley JB, Herwaldt BL, Stokes SL, et al. Diloxanide furoate for treating asymptomatic *Entamoeba histolytica* cyst passers: 14 years' experience in the United States. *Clin Inf Dis.* 1992;15:464-468.
48. McAuley JB, Juranek DD. Paromomycin in the treatment of mild-to-moderate intestinal amebiasis. *Clin Inf Dis.* 1992;15:551-552.
49. Fujishima T, Nishise S, Ichihara M, Kobayashi S, Takeuchi T. Difficulties in the treatment of intestinal amoebiasis in mentally disabled individuals at a rehabilitation institution for the intellectually impaired in Japan. *Chemotherapy*. 2010;56:348-352.
50. Rossignol JF, Kabil SM, El-Gohary Y, Younis AM. Nitazoxanide in the treatment of amoebiasis. *Trans R Soc Trop Med Hyg.* 2007;101:1025-1031.
51. VonSonnenberg E, Mueller PR, Schiffman HR, et al. Intrahepatic amebic abcesses: indications for and results of percutaneous catheter drainage. *Radiology.* 1985;156:631-635.
52. Stauffer W, Ravdin JI. *Entamoeba histolytica*: an update. *Curr Opin Infect Dis.* 2003;16:479-485.
53. Guo X, Barroso L, Becker SM, Lyerly DM, et al. Protection against intestinal amebiasis by a recombinant vaccine is transferable by T cells and mediated by gamma interferon. *Infect Immun*. 2009;77:3909-3918.
54. Carrero JC, Contreras-Rojas A, Sánchez-Hernández B, et al. Protection against murine intestinal amoebiasis induced by oral immunization with the 29 kDa antigen of *Entamoeba histolytica* and cholera toxin. *Exp Parasitol*. 2010;126:359-365.

55. Visvesvara GS, Moura H, Schuster FL. Pathogenic and opportunistic free-living amoebae: *Acanthamoeba* spp., *Balamuthia mandrillaris, Naegleria fowleri*, and *Sappinia diploidea*. *FEMS Immunol Med Microbiol*. 2007;50:1-26.

56. Galarza C, Ramos W, Gutierrez EL, et al. Cutaneous acanthamebiasis infection in immunocompetent and immunocompromised patients. *Int J Dermatol*. 2009;48:1324-1329.

57. Readinger A, Blumberg M, Colome-Grimmer MI, Kelly E. Disseminated *Acanthamoeba* infection with sporotrichoid nodules. *Int J Dermatol*. 2006;45:942-943.

58. Van Hamme C, Dumont M, Delos M, Lachapelle JM. Cutaneous acanthamoebiasis in a lung transplant patient. *Ann Dermatol Venereol*. 2001;128:1237-1240.

59. MacLean RC, Hafez N, Tripathi S, Childress CG, Ghatak NR, Marciano-Cabral F. Identification of *Acanthamoeba* sp. in paraffin-embedded CNS tissue from an HIV+ individual by PCR. *Diagn Microbiol Infect Dis*. 2007;57:289-294.

60. Barete S, Combes A, de Jonckheere JF, et al. Fatal disseminated *Acanthamoeba lenticulata* infection in a heart transplant patient. *Emerg Infect Dis*. 2007;13:736-738.

61. Martínez DY, Seas C, Bravo F, et al. Successful treatment of *Balamuthia mandrillaris* amoebic infection with extensive neurological and cutaneous involvement. *Clin Infect Dis*. 2010;51:e7-11.

## *Acknowledgements*

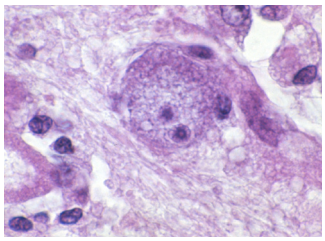
**Figure 8.15**
Contributed by Frank O. Raasch

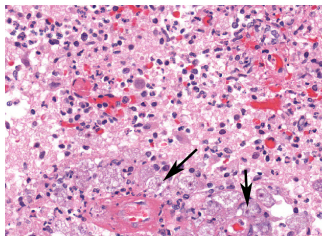
**Figure 8.16**
Adapted from Pathology of Tropical and Extraordinary Diseases (1976) by Douglas Landry

**Figure 8.17**
Contributed by Angela Levy

**Figure 8.34**
Contributed by R. Elson-Dew







9

# Amebic Meningoencephalitis & Keratitis

***Govinda S. Visvesvara, A. Julio Martinez, Mary K. Klassen-Fischer, and Ronald C. Neafie***

## *Introduction*

### Definition

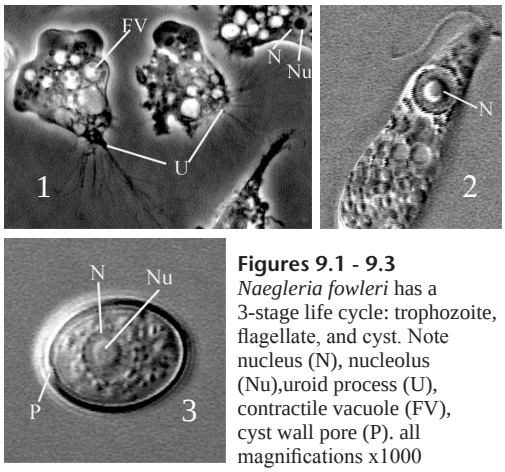
Free-living amebae of the genera *Naegleria*, *Acanthamoeba*, and *Balamuthia* cause fatal diseases of the central nervous system (CNS) of humans.[1-33] *Naegleria fowleri* causes an acute and fulminant primary amebic meningoencephalitis (PAM) in children and young adults with a history of exposure to fresh water leading to death within 5 to 10 days after the onset of symptoms.[4-6,9,10,16,17,19,25,27,30,31,33,34] *Balamuthia mandrillaris*,[2,3,7,8,19-22,24,26,28-31,35,36] and several species of *Acanthamoeba* (*Acanthamoeba castellanii, Acanthamoeba culbertsoni, Acanthamoeba rhysodes, Acanthamoeba polyphaga, Acanthamoeba divionensis, Acanthamoeba healyi*, and *Acanthamoeba lenticulata*) cause a chronic, and usually fatal, granulomatous amebic encephalitis (GAE) that may last for several weeks or months.[1,11,18,19,23,30,31,37-42] *Acanthamoeba* sp also cause an eyesight threatening infection, acanthamoeba keratitis, in humans, especially in persons wearing contact lenses.[12,15,17,19,30,31,40,43-52] Additionally, *N. fowleri*, *Acanthamoeba* sp, and *B. mandrillaris* also infect animals.[12-17, 19,28-31, 53-58] *Sappinia diploidea*, another free-living ameba identified in 2001[59] as an agent of meningitis, was reidentified recently as *Sappinia pedata* based on molecular analysis.[60] So far there is only one case reported due to this ameba.

### Synonyms

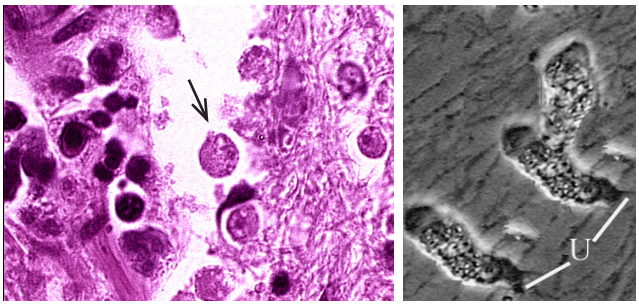
*Naegleria aerobia* and *Naegleria invadens* are not valid synonyms for *N. fowleri*. *Balamuthia mandrillaris* was previously known as leptomyxid ameba.

### General Considerations

In 1958, Culbertson et al isolated an A-1 strain of *Acanthamoeba* identified as a contaminant in a primary monkey kidney cell culture during production of poliomyelitis vaccine.[61] Immunosuppressed animals inoculated with the ameba developed fatal brain lesions containing amebic trophozoites. Culbertson hypothesized that similar strains might exist in nature and may infect humans.[61] Because of taxonomic uncertainties at that time regarding the genera *Hartmannella* and *Acanthamoeba*, Culbertson designated the A-1 strain as *Hartmannella-Acanthamoeba*, or H-A, amebae. It is now well-established that *Hartmannella* and *Acanthamoeba* are distinct genera and that no true hartmannellid ameba causes CNS infection in humans. Culbertson's A-1 strain is now known as *A. culbertsoni*.[11,15,19,30,47] In 1965, Fowler and Carter described a fatal human infection caused by free-living amebae, which they presumed to be *Acanthamoeba* sp, in the brain of an Australian boy.[5] The infection was later attributed to *N. fowleri*.[5,16,19,30] A year later, Butt et al described the first case of *N. fowleri*




**Figures 9.1 - 9.3**
*Naegleria fowleri* has a 3-stage life cycle: trophozoite, flagellate, and cyst. Note nucleus (N), nucleolus (Nu),uroid process (U), contractile vacuole (FV), cyst wall pore (P). all magnifications x1000




**Figures 9.4, 9.5**
Trophozoites are spherical and 10 µm to 18 µm in diameter (arrow). Their slug-like, eruptive movement is produced by smooth hemispheric bulges. The single nucleus has a large, centrally located nucleolus that stains densely with aniline dyes. Note uroid process (U). H&E (left) x400, phase contrast (right). x600

infection in the United States and coined the term "primary amebic meningoencephalitis."[4] Later studies showed that PAM was a recently discovered, rather than a new disease. A study of autopsy records and specimens at the Medical College of Virginia revealed cases of PAM dating back to 1937.[10] Studying museum specimens in England, Symmers discovered a case of human PAM dating from 1909.[25] Of the more than 200 cases of PAM reported worldwide, only a few patients have survived.

Granulomatous amebic encephalitis (GAE) caused by *Acanthamoeba* sp usually occurs in persons with HIV/AIDS or who are otherwise immunocompromised, debilitated, or malnourished. At one time, all cases of GAE were attributed to *Acanthamoeba* sp.[28,29] Although in most cases *Acanthamoeba* sp was identified as the causative agent by immunofluorescence or immunoperoxidase techniques, a few cases could not be confirmed in this way. However, with the isolation of *B. mandrillaris* amebae in the brain of a mandrill (a large baboon) in 1986 and subsequent development of an antiserum and an immunofluorescence test for this organism, *B. mandrillaris* has been definitively identified as the etiologic agent of GAE in a number of human and animal cases.[28,29] Fewer than 100 cases of balamuthia GAE have occurred worldwide, approximately 70 in the United States.[7]

## Epidemiology

*Naegleria* sp and *Acanthamoeba* sp are distributed worldwide and are commonly found in soil, dust, fresh water, household water, sewage, thermal effluents, swimming pools, and hot springs.[12,16,19,30,31,47,62] Recently, *N. fowleri* has also been isolated from drinking water.[16,63] *Acanthamoeba* sp have also been isolated from salt water, ocean sediments, heating and air conditioning units, bacterial, mycotic, and mammalian cell cultures, vegetable matter, contact lens paraphernalia, and human tissue.[12,15,19,30,47] *Balamuthia* mandrillaris has only recently been isolated from nature.[64-66]

## Primary Amebic Meningoencephalitis (PAM)

### Infectious Agent

*Naegleria fowleri* has a 3-stage life cycle: trophozoite, flagellate, and cyst (Figs 9.1 to 9.3). Trophozoites are spherical and 10 µm to 18 µm in diameter. Their slug-like, eruptive movement is produced by smooth hemispheric bulges. In tissue sections, the single nucleus has a large, centrally located nucleolus that stains densely with aniline dyes (Figs 9.4 & 9.5). A contractile vacuole is often seen. The posterior end, or uroid, appears to be sticky and often has several fine, trailing filaments. Clumps of bacteria or debris may attach to the uroid. *Naegleria* sp divide by promitosis, wherein the nucleolus and nuclear membrane persist during division. Under adverse conditions, such as a change in the ionic concentration of the milieu, trophozoites differentiate into a piriform, transient, non-feeding flagellate stage. Flagellates commonly have 2 flagella but may have 3 or more and they usually revert to the trophozoite stage. Trophozoites also differentiate into smooth-walled, spherical cysts 7 µm to 15 µm in diameter. Cyst walls may have 1 or more pores plugged with a mucoid substance.[16,67]

### Clinical Features and Pathogenesis

Primary amebic meningoencephalitis (PAM) is an acute, fulminant infection characterized by severe bifrontal or bitemporal headache, spiking fever of 40°C, nausea, vomiting, nuchal rigidity, positive Kernig's and Brudzinski's signs, photophobia, confusion, delirium, seizures, and coma. Symptoms appear 1 to 14 days after exposure;

most patients die 3 to 7 days after the onset of symptoms. PAM usually occurs in children and young adults who have recently swum in lakes, heated swimming pools with inadequate chlorination, or other bodies of fresh water that harbor amebae. Trophozoites and/or flagellates enter the swimmer's nostrils and invade the subarachnoid space and CNS parenchyma through the olfactory nerves, the cribriform plate, and the olfactory neuroepithelium. The incubation period is usually 3 to 8 days.[4-6,16,17,19,30,33,34]

## Pathologic Features

In its early stages, PAM resembles acute bacterial leptomeningitis. However, the purulent exudate is scant compared to that seen in bacterial leptomeningitis, and the inflammatory reaction in the subarachnoid and Virchow-Robin spaces is less intense.[4-6,16,17,19,30,34] There are no clear differences between PAM and acute pyogenic or bacterial meningoencephalitis. The peripheral white blood count is usually elevated, with a predominance of neutrophils. Cerebrospinal fluid (CSF) appears grayish to yellowish-white and may be tinged with red. CSF pressure is elevated, ranging from 300 to 600 mm $H_2O$. CSF pleocytosis is usually seen, with a predominance of neutrophils, which may be mistaken for bacterial infection. Early in the infection the CSF white cell count may be low, but as the disease progresses it may increase to as much as 26,000 cells/$mm^3$. The CSF glucose level is usually low to normal and CSF protein is high, ranging from 100 to 1,000 mg/dl. Computed tomography (CT) shows obliteration of the cisterns surrounding the midbrain and subarachnoid space. A CT scan of the brain without contrast appears to be normal or may show cerebral edema with obliteration of cisterns surrounding the midbrain and subarachnoid space. However, with intravenous contrast medium marked diffuse enhancement in these regions may be seen.[16,17,19,30]

*Naegleria fowleri* destroys the olfactory neuroepithelium and olfactory bulbs. PAM is characterized by acute hemorrhagic necrosis of both gray and white matter, associated with an acute inflammatory infiltrate consisting mainly of neutrophils, eosinophils, macrophages, and occasional lymphocytes. The cerebral cortex shows evidence of recent superficial hemorrhages in and around the orbitofrontal and temporal lobes, hypothalamus, midbrain, pons, medulla oblongata, cerebellum, and upper portion of the spinal cord. The cortex is most severely affected at the base of the brain, with pockets of amebic trophozoites within edematous and hemorrhagic CNS tissue. Large numbers of amebic trophozoites, some with phagocytosed erythrocytes and myelin fragments, may also be seen deep in the Virchow-Robin spaces and around blood vessels, but with minimal or no inflammatory response. *Naegleria fowleri* generally do not produce cysts in CNS tissue. A focal or diffuse myocarditis has been reported in a few cases of PAM, though microorganisms were not found in myocardial lesions.[16,17,19,30]

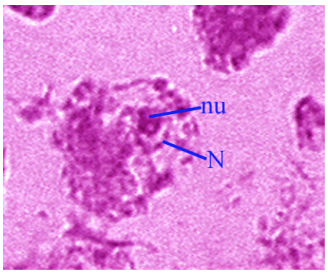



**Figure 9.6**
Trophozoites under reduced bright field light microscopy. Note large, centrally located nucleolus (nu) surrounded by a clear halo within nucleus (N) characteristic of *Naegleria fowleri*. x1250

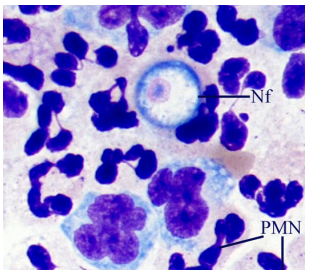


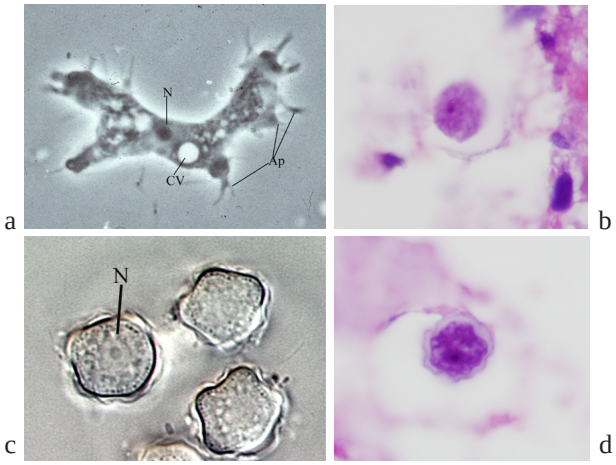

**Fig 9.7**
*Naegleria fowleri* (NF) in wet mount of CSF smear with accompanying polymorphonuclear (PMN) leucocytes. Wright stain x1000

## Diagnosis

Diagnosis of PAM is confirmed by identifying amebic trophozoites in a wet mount of CSF preparation. A light microscope equipped with phase contrast optics is preferable, but the preparation may also be viewed under brightfield illumination with reduced light. *Naegleria fowleri* trophozoites may be distinguished from host cells by their active directional movement and the large, centrally located nucleolus surrounded by a clear halo (Fig 9.6). CSF smears should be stained with Giemsa, Wright, or trichrome (Fig 9.7). Gram stain is not useful in identifying *N. fowleri*. Specimens of CSF or brain tissue should be kept at 24° to 28°C for no more than 24 hours. CSF should be centrifuged at 1,000 rpm for 5 to 8 minutes. After aspirating all but 0.5 ml of the supernatant, the sediment should be inoculated onto the center of an agar plate that has been precoated with bacteria, and incubated at 37°C. Biopsy or autopsy material should be triturated in a small amount of ameba saline (0.5 ml), placed in the center of an agar plate, and incubated in the same way.[16,17,19,30,31]

Under a microscope, *N. fowleri* amebae appear as small, motile blotches. After 2 to 3 days incubation, the amebae begin to encyst. After 4 to 5 days incubation, trophozoites and cysts should be visible.[16,17,19,30] Generic identification is based on characteristic patterns of locomotion, morphologic features of the trophic and cyst forms, and enflagellation experiments.[67] However, specific identification of *N. fowleri* is made by using immunohistochemical techniques using *N. fowleri* monoclonal or polyclonal antibodies[16,68] or molecular techniques such as PCR[16,19,30,69] nested PCR[70] and real-time PCR[71] on the cultured amebae or on infected tissue sections. Recently, a multiplex real-time PCR has been developed at CDC that identifies all three amebae (*Acanthamoeba* sp, *B. mandrillaris* and *N. fowleri)*. The real-time multiplex PCR is a rapid, sensitive, and specific assay which can be performed and results reported within 4 to 5 hours.[71]

Since PAM has a rapid onset and progresses quickly there is little opportunity for an effective humoral response to




a b c d

**Figure 9.8 a,b,c,d**
*Acanthamoeba* sp have a 2-stage life cycle consisting of trophozoite (a & b) and cyst (c & d), nucleus (N), contractile vacuole (CV), retractile projections (P). Phase contrast, a and c. x1000 Hematoxlin-eosin b and d. x1000

develop against the amebae. However, in one case with a successful outcome, *N. fowleri* antibody of the IgM class was demonstrated with a titer of 1:4096.[34]

## Treatment

Two patients, one from the United States and the other from Mexico, are known to have survived PAM.[27,34] Other reports of survival are unconfirmed.[16,17,19,30] The American patient was treated aggressively with intrathecal and intravenous amphotericin B (to which *N. fowleri* is highly sensitive) and miconazole, and with oral rifampin.[34] A Mexican boy was treated early with intravenous amphotericin B and fluconazole, and with oral rifampin.[27] Early identification of the etiologic agent and aggressive therapy appear to be key to patient survival.

# *Acanthamoeba and Balamuthia Granulomatous Amebic Encephalitis (GAE)*

## Infectious Agents

*Acanthamoeba* sp have a 2-stage life cycle consisting of trophozoite and cyst (Figs 9.8a to 9.8d). *Acanthamoeba* sp trophozoites are slightly larger than those of *N. fowleri*, measuring 15 µm to 45 µm in diameter. A contractile vacuole periodically ruptures on the body surface, which is covered with fine, spine-like, retractile projections (acanthopodia). Trophozoites usually have a single nucleus with a large, dense nucleolus.[67]

*Acanthamoeba* sp divide by conventional mitosis, in which the nucleolus and the nuclear membrane disappear during cell division. The organism does not have a flagellate stage, but it differentiates into a cyst under adverse conditions. Cysts are uninucleate and have a proteinaceous, usually wrinkled, ectocyst and an endocyst made of cellulose. At the point of contact between the ectocyst and endocyst there are pores, or ostioles, usually covered by opercula. The cysts are highly resistant to environmental pressures including desiccation.[72] As many as 24 *Acanthamoeba* sp have been described. These species can be divided into 3 groups based on cyst size and morphology as follows: 1) species that produce large cysts (18 µm to 28 µm); 2) species that produce cysts smaller than 18 µm with prominently wrinkled ectocysts and stellate, polygonal, triangular, oval, or round endocysts; and 3) species that produce cysts smaller than 18 µm with slightly wrinkled ectocysts and round or oval endocysts [67] (Table 9.1). However, recent developments in molecular analysis has enabled improvements in the taxonomy of this genus and its phylogenetic relationships. Further, based on the sequencing of the 18S rRNA gene,

Table 9.1 Morphologic features of *Acanthamoeba* sp that cause meningoencephalitis.

| Group | Species | Cyst size | Ectocysts | Endocysts |
|---|---|---|---|---|
| I | *A. astronyxis* | 18 to 28 µm | Nearly circular, gently rippled | Rays if stellate endocyst contact ectocyst in the same plane |
| II | *A. castellani, A. divionensis, A. polyphaga, A. rhysodes* | <18 µm | Prominently wrinkled | Stellate, polygonal, triangular, oval or round |
| III | *A. culbertsoni, A. healyi* | <18 µm | Slightly wrinkled | Round or oval |

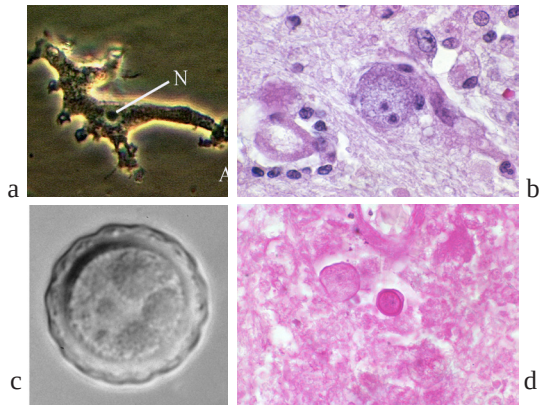



**Figure 9.9a-d**
*Balamuthia mandrillaris* also has a 2-stage life cycle of trophozoite (a & b) and cyst (c & d). In vitro culture under phase contrast, a and c x1000; tissue sections stained with H&E, b and d. x250

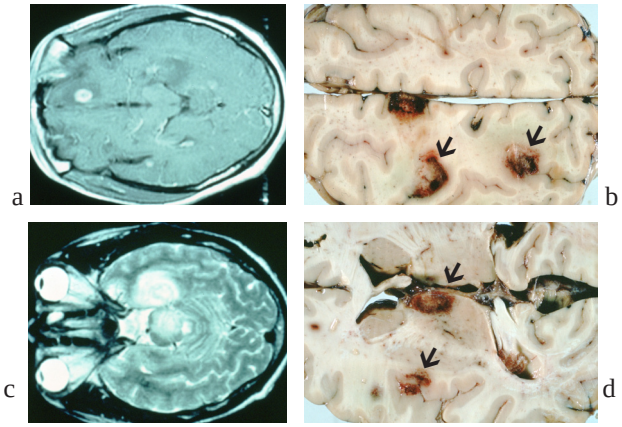



**Figure 9.10 a-d**
Granulomatous amebic encephalitis caused by *Balamuthia mandrillaris*. Cross section of cerebral hemispheres show multiple foci of hemorrhagic encephalomalacia (arrows) involving the cerebral cortex, subcortical white matter, and basal ganglia. CT Scan, a and c; Horinzontal sections of brain after fixation, b and d.

16 genotypes (T1 to T16) have been identified. [12,15,19,30,31,47,73]

*Balamuthia mandrillaris* also has a 2-stage life cycle of trophozoite and cyst (Figs 9.9a to 9.9d). Actively feeding *Balamuthia* trophozoites growing in culture range in size from 12 µm to 60 µm in diameter (average 30 µm). The ameba has a spider-like movement achieved by producing a broad pseudopodium and, sometimes, finger-like determinate pseudopodia. Trophozoites are normally uninucleate, but binucleate forms are occasionally seen. The nucleus usually has a single large nucleolus, but may have up to 2 or 3.[21,28-30]

*Balamuthia mandrillaris* divides by a complex form of mitosis called metamitosis in which the nucleolus and the nuclear membrane are intact during the initial stages. As mitosis progresses, the nuclear membrane breaks down and the nucleolus disappears. Trophozoites differentiate into cysts under adverse conditions. Light microscopy reveals a wrinkled ectocyst and a thick endocyst. However, ultrastructurally there is a third layer consisting of a structureless mesocyst (Fig 9.9b). [29,65]

## Clinical Features and Pathogenesis

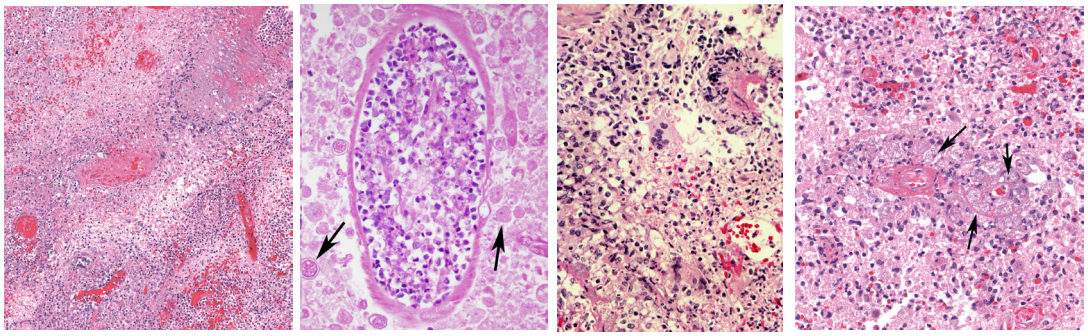
*Acanthamoeba* sp GAE primarily affects immunosuppressed, chronically ill, or otherwise debilitated persons with no history of exposure to bodies of fresh water. There have been a few reported infections in otherwise healthy individuals with no known immunodeficiency or risk factors for HIV.[12,15,17,19,30,47] *Balamuthia mandrillaris* GAE affects the very young or very old, and patients with HIV/AIDS.[17,21,28-30] Whether caused by *Acanthamoeba* sp or *B. mandrillaris*, GAE is a slowly progressive disease of the CNS with no clearly defined incubation period. Onset is insidious, lasting from a few days to several weeks or months. Patients present with focal neurologic deficits, signs of increased intracranial pressure, and neurologic and radiographic features suggestive of an expanding mass. Differential diagnosis includes brain tumor, abscess, or intracerebral hematoma. Common clinical symptoms include headache, irritability, confusion, seizures, dizziness, drowsiness, somnolence, and behavioral changes. Diplopia, aphasia, ataxia, altered mental state, lethargy, and hemiparesis are less common symptoms. Some patients, especially those with HIV/AIDS, develop skin lesions, abscesses, or erythematous nodules.[3,17,21,28-30]

CNS disease is a secondary feature of GAE, probably caused by hematogenous dissemination from a primary site such as a skin lesion or the lower respiratory tract.[17,21,28-30] However, there are a few reported cases of granulomatous skin disease caused by *Acanthamoeba* sp that did not spread to the CNS.[42] *Acanthamoeba* sp and *B. mandrillaris* are known to encyst within such lesions (Fig 9.9d). *Acanthamoeba* and *B. mandrillaris* cysts have also been isolated from airborne dust.[17,21,30,65] In an immunocompromised person who inhales cysts or whose damaged skin surface is contaminated with airborne cysts, amebae may excyst into trophozoites and invade the olfactory mucosa or deeper structures of the skin.

Recently, research efforts have focused on the role of free-living amebae as carriers of pathogenic bacteria, such as *Legionella*, in biofilms.[12,15,17,19,30,47]

## Pathologic Features

Granulomatous amebic encephalitis produces moderate edema of the cerebral hemispheres, with focal hemorrhagic softening of the cerebral cortex. Affected areas may produce a mild purulent exudate.[17] On cross section, cerebral hemispheres show multiple foci of hemorrhagic encephalomalacia involving the cerebral cortex, subcortical white matter, and basal ganglia (Figs 9.10a to 9.10d). Structures of the posterior fossa (cerebellum and brain stem) may be



a b c d

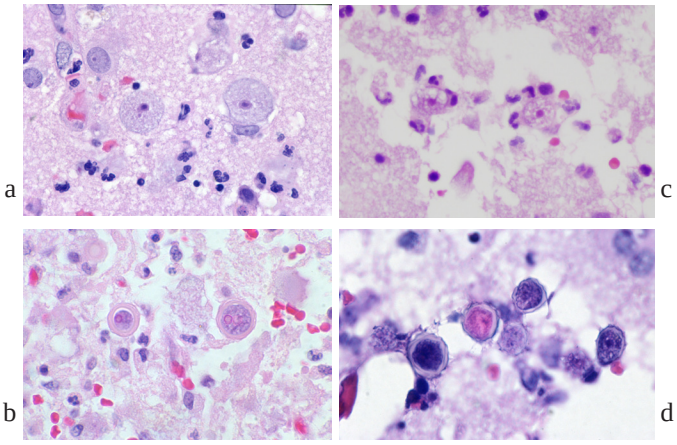
**Figure 9.11 a,b,c,d**
Microscopically, GAE lesions consist of hemorrhagic necrosis of CNS parenchyma, variable subacute and chronic inflammatory reactions, and amebic trophozoites and cysts around and within blood vessel walls (arrows). magnifications: a x35, b x85, c x75, d x90

more severely affected than the cerebral hemispheres.

Microscopically, GAE lesions consist of hemorrhagic necrosis of CNS parenchyma, variable subacute and chronic inflammatory reactions, and amebic trophozoites and cysts around and within blood vessel walls (Figs 9.11a to 9.11d). Multinucleated giant cells may be present, particularly in patients with only mild immunosuppression. Astrocytic gliosis may appear around necrotic areas. There may be panarteritis with perivascular cuffing by lymphocytes, some plasma cells and macrophages, and few eosinophils. Fibrinoid necrosis and thrombosis in arterioles may be present. Trophozoites and cysts may be found in liver, lung, kidney, prostate, lymph nodes, skin, and other organs, suggesting hematogenous dissemination of trophozoites and cysts.[17]

## Diagnosis

*Acanthamoeba* sp and *B. mandrillaris* have been isolated from skin and brain biopsy material. *Acanthamoeba* sp have also been isolated from CSF and lung biopsy material.Until recently, *B. mandrillaris* had never been isolated from CSF. However, *B. mandrillaris* was isolated from the CSF of a patient who developed infection after receiving a kidney transplant.[7] To isolate *Acanthamoeba* sp, specimens should be processed the same as for *N. fowleri*. If amebae are present, trophozoites and cysts will appear on agar plates after 1 or 2 weeks of incubation.[12,15,17,19,30,47] *B. mandrillaris* will not grow on agar plates coated with bacteria.[17,30] However, mammalian cell cultures such as monkey kidney or human lung fibroblasts will support the growth of *B. mandrillaris*. *Balamuthia* sp trophozoites and cysts found in CNS tissue are morphologically similar to those of *Acanthamoeba* sp (Figs 9.12a to 9.12d), making it difficult to differentiate them with light microscopy alone.[17,30] It is sometimes possible to distinguish *Balamuthia* sp from *Acanthamoeba* bsp ased on nuclear morphology; in tissue sections, *B. mandrillaris* trophozoites may have more than 1 nucleolus. In most cases, electron microscopy and/or immunofluorescence assay are necessary to identify *B. mandrillaris* organisms.[2,3,7,17,30,35,36,68] Recent developments in molecular analysis, especially the real-time multiplex PCR has enabled the specific identification of *Acanthamoeba* sp and *B. mandrillaris*



a c b d

**Figure 9.12 a,b,c,d**
*Balamuthia* trophozoites (a) x250 and cysts (b) x250 found in CNS tissue are morphologically similar to those of *Acanthamoeba* sp trophozoites (c) x250 and cysts (d) x800, making it difficult to differentiate them with light microscopy alone.

in the CSF, tissue sections and the cultured amebae.[17,30,74-76] Since *Acanthamoeba* sp are ubiquitous in nature, humans are exposed to them and may produce antibodies to these amebae. Although, indirect fluorescent antibody (IFA) and enzyme immunoassay (EIA) have been developed to detect antibody to *Acanthamoeba* sp in sera of patients as well as infected individuals, they are not routinely used as diagnostic tests.[17,19,30] Similarly IFA, flow cytometry, and ELISA techniques have been developed to identify antibodies to *B. mandrillaris* in the sera of healthy persons as well as patients with *B. mandrillaris* GAE. [21,30,77]

## Treatment

There is no effective treatment for GAE and the prognosis is poor. Athough several patients are known to have survived because of diagnosis antemortem, GAE is most often identified only at death.[7,17,30,76] Several patients with *Acanthamoeba* sp GAE and *Acanthamoeba* sp cutaneous infection have been treated with a combination of several drugs including sulfadiazine, trimethoprim-sulfamethoxazole,[5] fluorocytosine, fluconazole or itraconazole, and topical application of chlorhexidine gluconate on skin ulcers.[15-17,19,21,30,38-42,78] Recently, miltefosine, an analogue of alkyl phosphocholine,

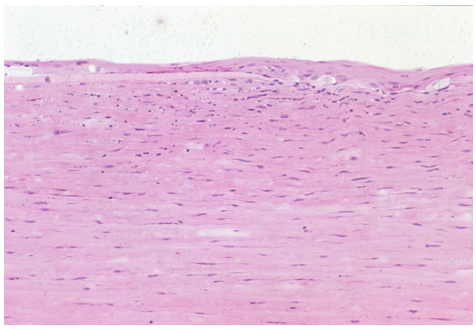


**Figure 9.13**
*Acanthamoeba* keratitis, irregular corneal epithelial breakdown, stromal infiltrative keratitis, and edema. H&E x100

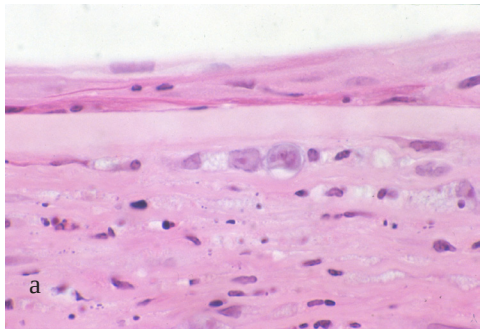






**Figure 9.14 a,b**
Corneal biopsy. a. Early stages of *Acanthamoeba* keratitis showing destruction of the anterior corneal epithelium associated with acute inflammatory cells (mainly neutrophils) into the superficial and middle layers of the corneal stroma. x500 b. Trophozoites and cysts interspersed between the corneal lamellae. x500

has been used succefully to cure an HIV negative man with *Acanthamoeba* sp GAE and disseminated disease.[37] Additionally, voriconazole also has been used successfully to treat a lung transplant patient with cutaneous *Acanthamoeba* sp infection.[79] Experimental in vitro studies indicate that both *Acanthamoeba* sp and *B. mandrillaris* are sensitive to pentamidine isethionate, azithromycin/clarithromycin and miltefosine.[19,30,32,80-83] Several cases of *B. mandrillaris* GAE infection have survived after treatment with pentamidine, clarithromycin/azithromycin, fluconazole, sulfadiazine and 5-fluorocytosine.[3,17,19,21,30,35,36,78,84] Recently, miltefosine has also been used successfully to cure *B. mandrillaris* GAE.[7]

## *Acanthamoeba Keratitis*

*Acanthamoeba* sp keratitis (AK) is a painful, vision-threatening disease of the cornea that, if not treated promptly, can lead to chronic ulceration of the cornea, loss of visual acuity, blindness, and enucleation. [12,17,19,30,43-45,48,50-52,78]

### Infectious Agent

Species reported to cause corneal infections are usually associated with group II and genotype T4 and include, among others, *Acanthamoeba hatchetti, A. polyphaga, A. castellanii, A. culbertsoni*, and *A. rhysodes*, although not all species isolated from the environment are clinically relevant. More than 5,000 cases of *Acanthamoeba* sp keratitis have been reported worldwide, over half of them in the United States. The first case of AK was reported in 1973 in a Texas rancher with a history of trauma to the eye.[46] Trophozoites and cysts of *A. polyphaga* were cultured from corneal scrapings and biopsy specimens. In the 1980s, an in-depth epidemiologic and case-control study revealed that the use of soft contact lenses and homemade saline solution were responsible for an increased incidence of *Acanthamoeba* sp keratitis.[51] A recent outbreak of AK during 2004-2007 occurred in the United States. An in-depth epidemiological study found that it was associated with a particular brand of multipurpose contact lens solution[52] that did not have sufficient activity to kill *Acanthamoeba* sp cysts.[85] Subsequently, this brand of contact lens solution was withdrawn by the company.[52]

AK causes severe ocular pain, a partial or total paracentral stromal ring infiltrate (Fig 9.13), recurrent corneal epithelial breakdown, and a corneal lesion resistant to common ophthalmic antibacterial medications. In its early stages, AK is frequently misdiagnosed as herpetic keratitis because of the irregular epithelial lesions, stromal infiltrative keratitis, and edema common to both forms of the disease. If left untreated, there is a greater risk of corneal perforation and GAE and enucleation. [17,19,30,44,45, 48]

Corneal biopsy reveals that in the early stages of AK there is destruction of the anterior corneal epithelium associated with infiltration of acute inflammatory cells (mainly neutrophils) into the superficial and middle layers of the corneal stroma (Figs 9.14a & 9.14b). As the disease progresses, there is considerable erosion of the corneal stroma, herniation of Descemet's membrane, and perforation of the cornea. Trophozoites and cysts are interspersed between the corneal lamellae.[17, 19,30,44,45,48]

### Diagnosis

Diagnosis is confirmed by finding *Acanthamoeba* sp in corneal scrapings fixed with methanol and stained with Giemsa, Hemacolor®, or trichrome.[17,19,30,44,45,48] *Acanthamoeba* sp can also be isolated into culture on non-nutrient agar plates, as described above. Diagnosis has been established by direct confocal microscopy on the corneal surface.[49]

### Treatment

The current treatment of choice for AK is topical application of a diamide (propamide isethionate or hexamide) and a cationic antiseptic (polyhexamethyl biguanide or chlorhexidine gluconate) for several weeks.[50,53]

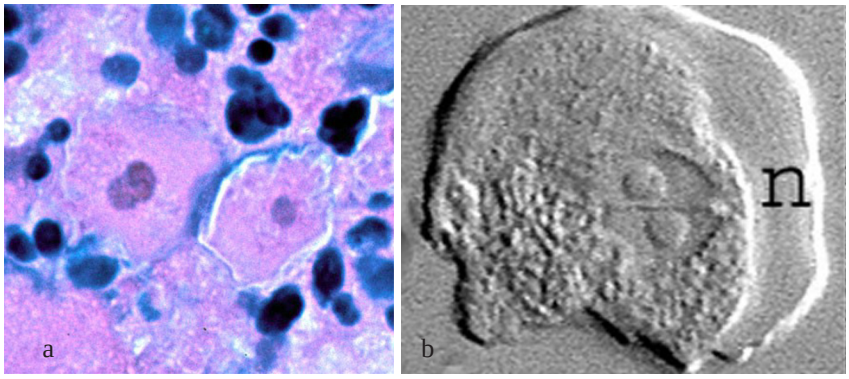



**Figure 9.15 a,b**
*Sappinia* sp, Brain. Amebae are large, usually 40 µm or greater characterized by two nuclei (n) tightly apposed to one another. a. Giemsa. x1250 b. Phase contrast. x1250




**Figure 9.16**
*Sappinia* sp, Brain. Cysts are also binucleate. Two nuclei (N). Phase contrast. x1000

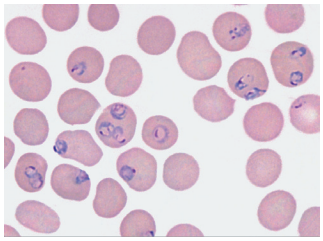
## *Sappinia*

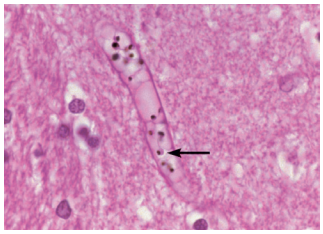
*Sappinia* sp have been previously isolated from feces of humans, elk, bison and cattle. A single case of infection with *Sappinia pedata*, previously described as *Sappinia diploidea*, causing encephalitis in an immunocompetent male occurred in 2001.[59] The patient developed headache, seizure, blurred vision, photophobia and vomiting; an MRI revealed a single space-occupying lesion. On examination of the excised lesion amebic trophozoites but not cysts were seen in the brain tissue. The patient was treated empirically with azithromycin, pentamidine isethionate, itraconazole and flucytosine and recovered with no neurological sequelae. *Sappinia* amebae are large and measure 40 µm or greater and are characterized by the presence of two nuclei tightly apposed to one another (Figs 9.15a & 9.15b). Cysts are also binucleate (Fig 9.16) and can survive adverse conditions in the environment. A recently developed real-time PCR detects both species of *Sappinia* but not other free-living amebae including *Acanthamoeba* sp, *B. mandrillaris* and *N. fowleri* or human DNA.[60]

## References


1. Barete S, Combes A, De Jonckheere JH et al. Fatal disseminated *Acanthamoeba lenticulata* infection in a heart transplant recipient. *Emerg Infect Dis*. 2007; 13:736-738.
2. Bakardjiev A, Azimi PH, Ashouri N et al. Amebic encephalitis caused by *Balamuthia mandrillaris*: Reporty of four cases. *Pediatr Infect Dis*. 2003;22:447-452
3. Bravo FG, Cabreara G, Gottuzo E, Visvesvara GS. Cutaneous manifestations of infections by free-living amebas. In: *Tropical Dermatology*, Tyring SK, Lupin O, Henggae UR, eds. Philadelphia: Elsvier; 2006, pp 49-55.
4. Butt CG. Primary amebic meningoencephalitis. *N Engl J Med*. 1966;274:1473-1476.
5. Carter RF. Primary amoebic meningo-encephalitis. An appraisal of present knowledge. *Trans R Soc Trop Med Hyg*. 1972;66:193-213.
6. Centers for Disease Control and Prevention (CDC). Primary amebic meningoencephalitis-Arizona, Florida, and Texas. 2007. *Morb Mort Wkly Rep*. 2008;57:573-577.
7. Centers for Disease Control and Prevention (CDC). *Balamuthia mandrillaris* transmitted through organ transplantation – Mississippi, 2009. *Morb Mort Wkly Rep*. 2010;59:1165-1170.
8. Centers for Disease Control and Prevention (CDC). Notes from the field: transplant transmitted *Balamuthia mandrillaris* – Arizona, 2010. Morb Mort Wkly Rep. 2010;59:1182.
9. Cogo PE, Scaglia M, Gatti S, et al. Fatal *Naegleria fowleri* meningoencephalitis, Italy. *Emerg Infect Dis.* 2004;10:1835-1837.
10. Gustavo dos Santos Neto. Fatal primary amebic meningoencephalitis. A retrospective study in Richmond, Virginia. *Am J Clin Pathol.* 1970;54:737-742.
11. Kaul DR, Lowe L, Visvesvara GS, et al. *Acanthamoeba* infection in a patient with chronic graft-vs-host disease occurring during treatment with voriconazole. *Transplant Infect Dis.* 2008; 10:437-441.
12. Khan NA. *Acanthamoeba* spp. In: *Emerging Protozoan Pathogens*. Khan NA, ed. New York, NY: Taylor and Francis; 2008, pp 71-118.
13. Kinde H, Read DH, Daft BM et al. Infections caused by pathogenic free-living amebas (*Balamuthia mandrillaris* and *Acanthamoeba* spp) in horses. *J Vet Diagn Invest*. 2007;19:317-322.
14. Lozano-Alarcon F, Bradley GA, Houser BS, Visvesvara GS. Primary amebic meningoencephalitis due to *Naegleria fowleri* in a South American tapir. *Vet Pathol*. 1997;34:239-243.
15. Marciano-Cabral F, Cabral G. *Acanthamoeba* spp. as agents of disease in humans. *Clin Microbiol Rev*. 2003;16:273-307.
16. Marciano-Cabral F, Cabral G. *Naegleria fowleri.* In: *Emerging Protozoan Pathogens*, Khan NA, ed. New York, NY: Taylor and Francis; 2008, pp 119-152.
17. Martinez AJ, Visvesvara GS. Free-living, amphizoic and opportunistic amebas. *Brain Pathol*. 1997;7:583-598.
18. Mckeller M, Mehta L, Greenlee J et al. Granulomatous *Acanthamoeba* encephalitis mimicking a stroke: correlation with sequential MRI and biopsy, in vitro culture, immunofluorescence and molecular analysis. *J Clin Microbiol.* 2006;44:265-269.
19. Schuster FL, Visvesvara GS. Free-living amoebae as opportunistic and non opportunistic pathogens of humans and animals. *Int J Parasitol*. 2004;34:1001-1027.
20. Schuster FL, Glaser C, Honarmand S, et al. *Balamuthia* encephalitis risk, Hispanic Americans. *Emerg Infect Dis.* 2004;10:1510-1512.
21. Schuster FL, Visvesvara GS. *Balamuthia mandrillaris*. In: *Emerging Protozoan Pathogens*, Khan NA, ed. New York, NY: Taylor and Francis; 2008, pp 71-118.
22. Schuster FL, Yagi S, Gavali S,et al. Under the radar: *Balamuthia* amebic encephalitis. *Clin Infect Dis*. 2009;48:879-887.
23. Shirwadkar CG, Samant R, Sankhe M, et al. *Acanthamoeba* encephalitis in a patient with systemic lupus, India. *Emerg Infect Dis.* 2006;12:984-986.
24. Silva-Vergara ML, Da Cunha Colombo ER, Vissoto E de F, et al. Disseminated *Balamuthia mandrillaris* amoeba infection in an AIDS patient from Brazil. *Am J Trop Med Hyg*. 2007;7:1096-1098.
25. Symmers WC. Primary amoebic meningoencephalitis in Britain. *Br Med J*. 1969;4:449-454.
26. Tavares M, Correa da Costa JM, Carpenter S, et al. Diagnosis of first case of *Balamuthia* amebic encephalitis in Portugal by immunofluorescence and PCR. J *Clin Microbiol.* 2006; 44:2660-2663.
27. Vargas-Zepeda J, Gomez-Alcala AV, Vasquez-Morales JA, et al. Successful treatment of *Naegleria fowleri* meningoencephalitis by using intravenous amphotericin B, fluconazole and rifampicin. *Arch Med Res.* 2005;36:83-86.
28. Visvesvara GS, Martinez AJ, Schuster FL, et al. *Leptomyxid ameba*, a new agent of amebic meningoencephalitis in humans and other animals. *J Clin Microbiol.* 1990;28:2750-2756.
29. Visvesvara GS, Schuster FL, Martinez AJ. *Balamuthia mandrillaris*, n. g., n. sp., agent of amebic meningoencephalitis in humans and other animals. *J Eukaryot Microbiol.* 1993;40:504-514.
30. Visvesvara GS, Moura H, Schuster FL. Pathogenic and opportunistic free-living amoebae: *Acanthamoeba* spp., *Balamuthia mandrillaris*, *Naegleria fowleri* and *Sappinian diploidea*. *FEMS Immunol Microbiol*. 2007;50:1-26.
31. Visvesvara GS. Free-living amebae as opportunistic agents of human disease. *J Neuroparastol*. 2010:1:1-13.
32. Walochnik J, Obwaller A, Gruber F et al. Anti *Acanthamoeba* efficacy and toxicity of miltefosine in an organotypic skin equivalent. *Antimicrob Agents Chemother.* 2009;64:539-545.
33. Yoder JS, Eddy BA, Visvesvara GS, et al. The epidemiology of primary amebic meningoencephalitis, 1962-2008. *Epidemiol Infect.* 2010;138:968-975.
34. Seidel JS, Harmatz P, Visvesvara GS, Cohen A, Edwards J, Turner J. Successful treatment of primary amebic meningoencephalitis. *N Engl J Med.* 1982;306:346-348.
35. Cary LC, Mauil E, Porter C, et al. *Balamuthia mandrillaris* meningoencephalitis: survival of a pediatric patient. *Pediatrics*. 2010;125:e699-e703.
36. Deetz TR, Sawyer MH, Billman G, Schuster FL, Visvesvara GS. Successful treatment of *Balamuthia* amoebic encephalitis: presentation of 2 cases. *Clin Infect Dis.* 2003;37:1304-1312.
37. Aichelburg ACV, Walochnik J, Assadian O, et al. Successful treatment of disseminated *Acanthamoeba* sp. infection with miltefosine. *Emerg Infect Dis.* 2008;14:1743-1746.
38. Fung KT-T, Dhillon AP, McLaughlin J, et al. Cure of *Acanthamoeba* cerebral abscess in a liver transplant patient. *Liver Transplantation*. 2008;14:308-312.
39. Martinez MS, Gonzalez-Madiero G, Santiago P, et al. Granulomatous amebic encephalitis in a patient with AIDS. Isolation of *Acanthamoeba* sp Group II from brain and successful treatment with sulfadiazine and fluconazole. *J Clin Microbiol.* 2000;38:3892-3895.
40. Petry F, Torzewski M, Bohl J, et al. Early diagnosis of *Acanthamoeba* infection during routine cytological examination of cerebrospinal fluid. *J Clin Microbiol.* 2006;44:1903-1904.
41. Saxena A, Mittal S, Burman P, Garg P. *Acanthamoeba* meningitis with successful outcome. *Ind J Pediatr.* 2009;1063-1064.
42. Slater CA, Sickel JZ, Visvesvara GS, et al. Brief report:successful treatment of disseminated *Acanthamoeba* infection in an immunocompromised patient. *New Engl J Med.* 1994;331:85-87.
43. Bang S, Edell E, Eghrari AO, Gottsch JD. Treatment with voriconazole in 3 eyes with resistant *Acanthamoeba* keratitis. *Am J Ophthalmol.* 2010;149:66-69.
44. Clarke DW, Niederkorn JY. The pathophysiology of *Acanthamoeba* keratitis. *Trends Parasitol*. 2006;22:175-180.
45. Dart JKG, Saw VPJ, Kilvington S. *Acanthamoeba* keratitis: Diagnosis and Treatment Update 2009. *Am J Ophthalmol.* 2009;148:487-499.
46. Jones DB, Visvesvara GS, Robinson NM. *Acanthamoeba polyphaga* keratitis and *Acanthamoeba uveitis* associated with fatal meningoencephalitis. *Trans Ophthalmol Soc U K*. 1975;95:221-232.
47. Khan NA. Acanthamoeba spp.: In: *Emerging Protozoan Pathogens*, Khan NA, ed. New York, NY: Taylor and Francis; 2008; pp 71-118.
48. Panjwani N. Pathogenesis of *Acanthamoeba* keratitis. *Occul Surf*. 2010;8:70-79.
49. Pfister DR, Cameron JD, Krachmer JH, Holland EJ. Confocal microscopy findings of *Acanthamoeba* keratitis. *Am J Ophthalmol.* 1996;121:119-128.
50. Seal DV. *Acanthamoeba* keratitis update – Incidence, molecular epidemiology and new drugs for treatment. *Eye*. 2003;17:893-905.
51. Stehr-Green JK, Bailey TM, Visvesvara GS. The epidemiology of *Acanthamoeba* keratitis in the United States. *Am J Ophthalmol.* 1989;107:331-336.
52. Verani JR, Lorick SA, Yoder JS, et al. National outbreak of *Acanthamoeba* keratitis associated with use of contact lens solution, United States. *Emerg Infect Dis*. 2009;15:1236-1242.
53. Daft BM, Visvesvara GS, Read DH, Kinde H, Uzal FA, Manzer MD. Seasonal meningoencephalitis in Holstein cattle caused by *Naegleria fowleri. J Vet Diagn Invest*. 2005;17:605-609.

54. Finnin PJ, Visvesvara GS, Campbell BE, Fry DR, Gasser RB. Multifocal *Balamuthia mandrillaris* infection in a dog in Australia. *Parasitol Res*. 2007;100:423-426
55. Morales JA, Chavez AJ, Visvesvara GS, Dubey JP. *Naegleria folwleri* – associated encephalitis in a cow from Costa Rica. *Vet Parasitol.* 2006;139: 221-223.
56. Rideout BA, Gardiner CH, Stalis IH, et al. Fatal infections with *Balamuthia mandrillaris* (a free-living amoeba) in gorillas and other old world primates. V*et Pathol.* 1997;34:15-22.
57. Visvesvara GS, De Jonckheere JF, Sriram R, et al. Isolation and molecular analysis of *Naegleria fowleri* from a cow brain that died of primary amebic meningoencephalitis. *J Clin Microbiol.* 2005;43:4203-4204.
58. Visvesvara GS, Shoff ME, Sriram R, et al. Isolation, morphologic, serologic and molecular identification of *Acanthamoeba* T4 genotype from the liver of a Temminck's tragopan (*Tragopan temminckii*). *Vet Parasitol.* 2010;170:197-200.
59. Gelman BB, Popov V, Chaljub G, et al. Neuropathological and ultrastructural features of amebic encephalitis caused by *Sappinia diploidea*. *J Neuropathol Exp Neurol*. 2003;62:990-998.
60. Qvarnstrom Y, da Silva AJ, Schuster FL, Gelman BB, Visvesvara GS. Molecular confirmation of *Sappinia pedata* as causative agent of amebic encephalitis. *J Infect Dis.* 2009;199:1139-1142.
61. Culbertson CG, Smith JW, Minner JR. *Acanthamoeba*: observations on animal pathogenicity. *Science*. 1958;127:1506.
62. Stockman LJ, Wright CJ, Visvesvara GS, et al. Prevalence of *Acanthamoeba* spp. and other free-living amoebae in household water, Ohio, USA-1990-1992. *Parasitol Res.* 2010;108:621-627.
63. Bright KR, Marciano-Cabral F, Gerba CP. Occurrence of *Naegleria fowleri* in Arizona drinking water supply wells. *J AWWA.* 2009;101:43-50.
64. Dunnebacke TH, Schuster FL, Yagi S, et al. *Balamuthia mandrillaris* from soil samples. *Microbiology*. 2004;150:2837-2842.
65. Niyyati M, Lorenzo-Morales J, Rezaeian M, et al. Isolation of *Balamuthia mandrillaris* from urban dust, free of known infectious involvement. *Parasitol Res*. 2009;106:279-281.
66. Schuster FL, Dunnebacke TH, Booton CG, et al. Environmental isolation of *Balamuthia mandrillaris* associated with a case of amebic encephalitis. *J Clin Microbiol.* 2003:41:3175-3180.
67. Page FC. A New Key to Fresh Water and Soil Gymnamoebae. Cumbria, England: Fresh Water Biological Association; 1985:1-122.
68. Guarner J, Bartlett J, Shieh W-J, Paddock CD, Visvesvara GS, Zaki SR. Histopathologic spectrum and immunohistochemical diagnosis of amebic meningoencephalitis. *Modern Pathol.* 2007; 20:1230-1237.
69. Zhou L, Sriram S, Visvesvara GS, Xiao L. Genetic variation in the internal transcribed spacer and mitochondrial small subunit rRNA gene of *Naegleria* spp. *J Eukaryot Microbiol.* 2003;50:522-526.
70. Reveiller FL, Cabanes PA, Marciano-Cabral F. Development of a nested PCR assay to detect the pathogenic free-living amoeba *Naegleria fowleri. Parasitol Res.* 2002;88:443-450.
71. Qvarnstrom Y, Visvesvara GS, Sriram R, da Silva AJ. A multiplex real-time PCR assay for simultaneous detection of *Acanthamoeba* spp., *Balamuthia mandrillaris* and *Naegleria fowleri. J Clin Microbiol.* 2006;44:3589-3595.
72. Sriram R, Shoff M, Booton CG, et al. Survival of *Acanthamoeba* cysts after desiccation for more than 20 years. *J Clin Microbiol*. 2008;46:4045-4048.
73. Booton GC, Visvesvara GS, Byers TJ, Kelly DJ, Fuerst PA. Identification and distribution of *Acanthamoeba* species genotypes associated with nonkeratitis infections. *J Clin Microbiol.* 2005;43:1689-1693.
74. Booton GC, Carmichael Jr., Visvesvara GS, et al. Genotyping of *Balamuthia mandrillaris* based on nuclear 18S and mitochondrial 16S rRNA genes. *Am J Trop Med Hyg.* 2003;68:65-69.
75. Booton GC, Carmichael JR, Visvesvara GS, Byers TJ, Fuerst PA. Identification of *Balamuthia mandrillaris* by PCR assay using the mitochondrial 16S rRNA gene as a target. *J Clin Microbiol*. 2003;41:453-455.
76. Yagi S, Schuster FL, Visvesvara GS. Demonstration of *Balamuthia* and *Acanthamoeba* mitochondrial DNA in sectioned archival brain and other tissues by the polymerase chain reaction. *Parasitol Res.* 2008;102:211-217.
77. Schuster FL, Yagi S, Wilkins PP, Gavali S, Visvesvara GS, Glaser CA. *Balamuthia mandrillaris*, agent of amebic encephalitis: detection of serum antibodies and antigenic similarity of isolates by enzyme immunoassay. *J Eukaryot Microbiol.* 2008;55:313-320.
78. Visvesvara GS. Amebic meningoencephalitideas and keratitis: challenges in diagnosis and treatment. *Curr Op Infect Dis.* 2010; 23;590-594.
79. Walia R, Montoya JG, Visvesvara GS, et al. A case of successful trteatment of infection of *Acanthamoeba* in a lung transplant recipient. *Transplant Infect Dis*. 2007; 9:51-54.
80. Schuster FL, Visvesvara GS. Axenic growth and drug sensitivity studies of *Balamuthia mandrillaris*, an agent of amebic meningoencephalitis in humans and other animals. *J Clin Microbiol*. 1996;34:385-388.
81. Schuster FL, Visvesvara GS. Efficacy of novel antimicrobials against clinical isolates of opportunistic amebas. *J Eukaryot Microbiol*. 1998;45:612-618.
82. Schuster FL, Guglielmo J, Visvesvara GS. In vitro activity of miltefosine and voriconazole on clinical isolates of free-living amebas: *Balamuthia mandrillaris, Acanthamoeba* spp., and *Naegleria fowleri. J Eukaryot Microbiol*. 2006;53:893-905.
83. Walochnik J, Duchene M, Seifert K, et al. Cytotoxic activities of alkylphosphocholines against clinical isolates of *Acanthamoeba* spp. *Antimicrob Agents Chemother.* 2002;46:695-701.
84. Jung S, Schelper RL, Visvesvara GS, Chang HT. *Balamuthia mandrillaris* meningoencephalitis in an immunocompetent patient: an unusual clinical course and a favorable outcome. *Arch Pathol Lab Med*. 2004;128:466-468.
85. Johnston SP, Sriram S, Qvarnstrom Y, et al. Resistance of *Acanthamoeba* cysts to disinfection in multiple contact lens solutions. *J Clin Microbiol.* 2009;47:2040-2045.







10

# Malaria

*Mary K. Klassen-Fischer, Ronald C. Neafie and Wayne M. Meyers*

## *Introduction*

### Definition

Malaria is an infectious disease caused by coccidian protozoa of the genus *Plasmodium*, and transmitted by infected female anopheline mosquitoes. *Plasmodium* sp infecting humans include *Plasmodium vivax*, *Plasmodium falciparum*, *Plasmodium malariae*, and *Plasmodium ovale*. The 4 species differ in geographic distribution, microscopic appearance, and clinical features.

### Synonyms

Infections with *P. vivax*, *P. falciparum*, *P. malariae*, and *P. ovale* are known respectively as vivax or benign tertian malaria, falciparum malaria, quartan malaria, and ovale malaria. The terms tertian and quartan describe the usual periodicity of the fever.

### General Considerations

In the mid-19th century Meckel and others discovered a black granular substance in the blood and tissues of patients with malaria.[1] In 1847, Meckel observed that the granules lay within protoplasmic masses which Afanasiev, in 1879, suggested were the cause of malaria. In 1880, Laveran, a French army surgeon in Algeria, observed malarial pigment in plasma and leukocytes and clear bodies within erythrocytes. As the irregularly shaped hyaline bodies grew, Laveran noted that the erythrocytes paled and pigment formed within them. Later he observed male gametes form by exflagellation and described the male and female gametes, the trophozoite, and the schizont forms. In 1886, Machiafava and Celli gave the generic name *Plasmodium* to the parasite. Most early observations of malarial parasites were made on unstained specimens since methylene blue and eosin stains were not applied to blood smears until 1891 by Romanovsky; a forerunner of today's Wright stain.

In 1895, Ross, a British medical officer in India, hypothesized that the mosquito is the intermediary host of the malarial parasite and began dissecting various species of mosquitoes. In 1897 he found malarial parasites in the stomach wall of *Anopheles* mosquitoes, and in 1898 described the complete life cycle of the parasite that causes avian malaria, and the *Culex* mosquito vector. For his research Ross received the Nobel prize in 1902. Grassi et al later proved that anopheline mosquitoes transmit malaria to humans.[2]

In 2002, researchers sequenced the genomes of *P. falciparum* [3] and one of its vectors, *Anopheles gambiae*.[4]

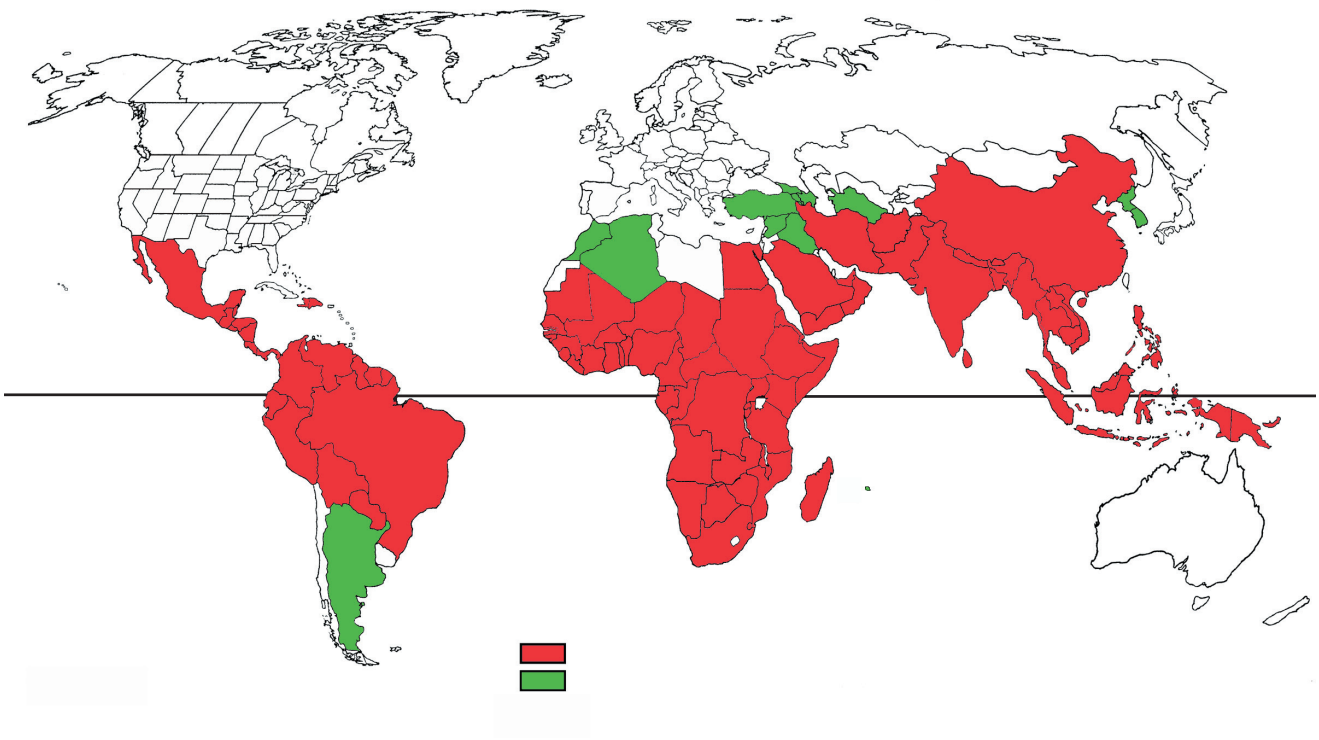


Fig 10.1
Countries endemic for malaria. Regions shown in green are endemic for *Plasmodium vivax* only.

## Epidemiology

Malaria is endemic in tropical and subtropical regions of Africa, Asia, Central and South America, and Oceania, and on the West Indies island of Hispaniola (Fig 10.1).[5,6] Rates of infection vary depending on insect vectors, climate, environmental conditions, the local species of *Plasmodium* and its susceptibility to antimalarial drugs, and the genetic composition, acquired immunity, and behavior of human hosts. Malaria is more prevalent in rural areas, but incidence among urban populations is increasing.

Malaria is one of the most prevalent infectious diseases, with over 40% of the world's population at risk. Approximately 300 million cases of clinical malaria are reported worldwide each year, with more than a million fatalities. Almost 90% of fatalities are in sub-Saharan Africa, where young children are most affected. According to WHO estimates, there are approximately 270 million cases of malaria in Africa per year, and an estimated 5% of African children die of malaria-related illness before their fifth birthday.[6] In areas of the world with high infection rates, children, pregnant women in the second and third trimesters and during the early postpartum period,[7] as well as nonimmune visitors are at greatest risk of fatal malarial infection. In areas where infection rates are lower, the risk is equal for everyone. Although residents of endemic areas acquire some immunity, repeated infections cause tremendous loss of life and productivity. *Plasmodium falciparum* is the second most common species infecting humans, it is found almost exclusively in tropical areas and is the cause of the most severe forms of malaria, and most deaths. *Plasmodium malariae* is rare now but was common in Europe at one time, and *P. ovale*, the rarest species, is found in Africa and Southeast Asia. *Plasmodium vivax* is the most common of all species of plasmodia and has a wide geographical distribution, including some temperate regions, but causes milder disease.

In nonendemic areas, most cases of malaria develop in immigrants and travelers from endemic regions. However, anywhere anopheline mosquitoes are present, the potential exists for reintroduction of malaria, even in temperate climates where the disease has been eradicated. There are rare reports of stowaway mosquitoes transmitting malaria to people who live near airports.[8] Malaria was once common in North America, especially in the Mississippi Valley, but on average, one case per year is now reported in the United States. Most of these patients were infected during travel to

Table 10.1
Morphologic features of *Plasmodium* sp in thin peripheral blood films.

| | *P. vivax* | *P. falciparum* | *P. malariae* | *P. ovale* |
|---|---|---|---|---|
| Erythrocyte | Usually enlarged, pale, irregularly shaped | Normal size | Normal size or slightly smaller | Usually enlarged, frequently oval or fimbriated |
| Stippling (pink-staining granules) | Schüffner's dots | Coarse Maurer's dots rarely observed | Ziemann's dots rarely observed | Schüffner's dots |
| Incidence of multiply infected erythrocytes | Occasional | Frequent | Rare | Occasional |
| Trophozoites | Tenuous and ameboid forms, large, occasional double chromatin dots | Small ring forms frequent, 2 chromatin dots, marginal forms common | Frequent band forms, rare double chromatin dots | Compact, large, sometimes slightly ameboid, occasional double chromatin dots |
| Schizonts | Less numerous than trophozoites, pigment clumped in mature forms | Rare, clumped pigment in immature and mature forms | Often in great numbers, pigment clumped in mature forms | May be frequent, pigment clumped in mature forms |
| Number of merozoites in mature schizont | 16 (12-24) | 8-24 (more if multiply infected erythrocyte) | 8 (6-12) | 8 (4-16) |
| Merozoites | Small, clustered | Very small | Large, frequent rosette pattern around central pigment | Very large, frequent rosette pattern around central pigment |
| Pigment | Yellow-brown | Dark brown | Dark brown | Brown |
| Gametocytes | Usually round, fill most of enlarged erythrocyte | Rare, crescent- or sausage-shaped | Usually round, fill most of normal-sized or slightly smaller erythrocytes | Round or oval, fill most of enlarged erythrocyte |

endemic areas (imported malaria). Occasionally, local mosquitoes become infected by gametocytemic individuals and pass the infection to nontravelers (autochthonous or introduced malaria).

## *Infectious Agent*

### Morphologic Description

In peripheral blood, all species of *Plasmodium* that infect humans are composed of chromatin and cytoplasm, may or may not contain pigment, and are present in 3 forms: trophozoites (growing forms), schizonts (dividing forms), and gametocytes (sexual forms).

Trophozoites range from small young ring forms to mature forms with chromatin that is still undivided. In all four types of malaria, young ring forms, usually indistinguishable among species, may be observed in peripheral blood.

In immature schizonts, division has just begun. In mature schizonts, division of chromatin and cytoplasm is complete, pigment is clumped in a single mass, and cytoplasm is separated into distinct masses. The number of merozoites (asexual components of schizonts) in a mature schizont varies considerably among the different species of *Plasmodium*.

Gametocytes of *P. falciparum* are elongated or sausage-shaped; gametocytes of all other species are round, with a single chromatin mass and compact cytoplasm.

Morphologic features of *Plasmodium*, as seen on thin blood films that allow determination of species, are summarized in Table 10.1.[9,10]

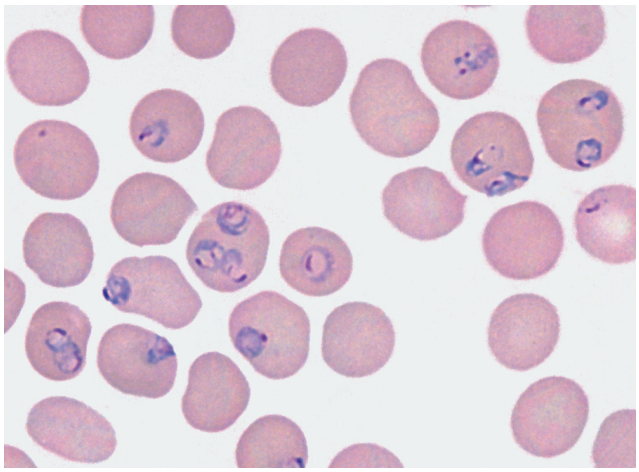


**Figure 10.2**
Heavy parasitemia (30%) in patient who died of falciparum malaria. Infected erythrocytes are normal size. Giemsa. Original magnification x330

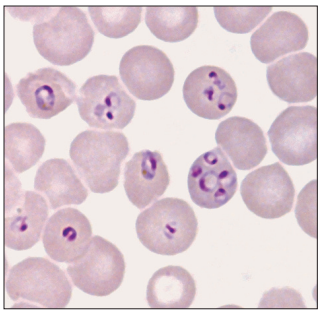


**Figure 10.3**
Five ring trophozoites in single erythrocyte. Multiply infected erythrocytes are very common in *Plasmodium falciparum* infections. Giemsa. Original magnification x330

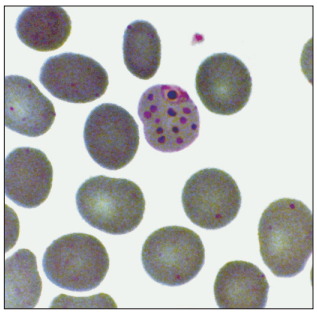


**Figure 10.4**
Pink-staining Maurer's dots in erythrocyte cytoplasm stained at pH 7.4. Giemsa. Original magnification x300

## *Plasmodium falciparum* (Figures 10.2 to 10.10)

Erythrocytes infected with *P. falciparum* are of normal size. Parasitemia is often much greater in falciparum malaria than in the other 3 types. Multiply infected erythrocytes are common, especially in heavy infections (Figs 10.2 to 10.4). Infection by asexual parasites from the older ring trophozoite stage onward causes erythrocytes to be stippled with pink Maurer's dots of various shapes and sizes. Maurer's dots are rarely observed unless they are overstained or stain is alkaline (Fig 10.4).

Young ring trophozoites (Fig 10.5a) of *P. falciparum* are smaller than those of other species (approximately one fifth the diameter of an erythrocyte) and more likely to have double chromatin dots (Fig 10.5b). Three and even 4 chromatin dots may rarely be observed. Young ring trophozoites have delicate, thread-like cytoplasm; very young trophozoites usually contain no pigment. They may be round, rectangular, flame-shaped, or narrow band-shaped (Fig 10.5c). Flattened marginal forms and bridge forms are more common than in other species (Fig 10.5d). Older ring trophozoites are slightly larger and have more cytoplasm and chromatin (Fig 10.5e). Traces of tiny pigment granules may give the cytoplasm a yellowish tinge, and there may be basophilic stippling (blue dots) (Figs 10.5f). It is characteristic in falciparum malaria to observe only ring forms of the asexual cycle, with no older trophozoites or schizonts, in peripheral blood. Mature trophozoites have small, compact, light-staining cytoplasm, a larger chromatin dot, and a small, dense, nearly black clump of pigment (Fig 10.5g). Clumping of pigment at this stage is an exclusive characteristic of *P. falciparum*.

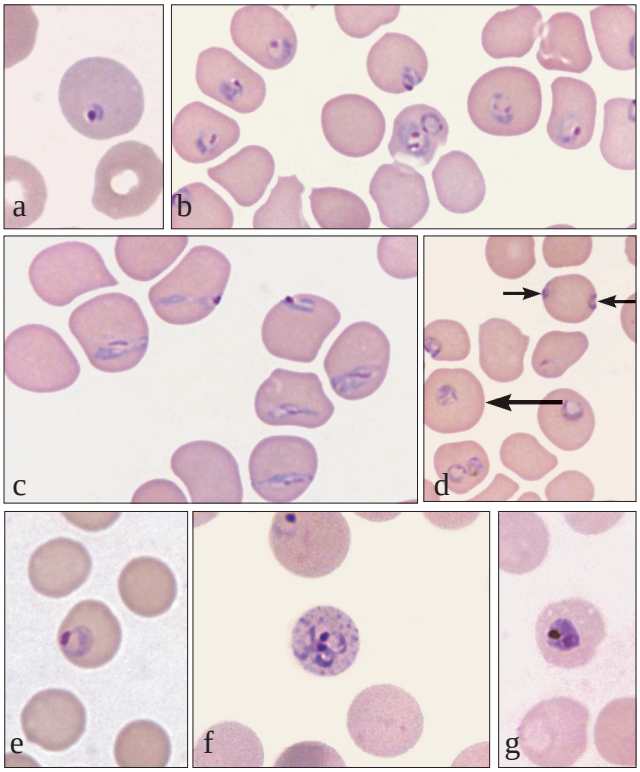



**Figure 10.5 a,b,c,d,e,f,g**
*Plasmodium falciparum* trophpzoites. Giemsa. Original magnifications all x333 except e x290.
a. Small ring trophozoite, no pigment. b. Double chromatin dots. c. Narrow band forms. d. Flattened marginal forms (arrows). e. Older ring trophozoite. f. Erythrocyte basophillic stippling. g. Mature trophozoite with pigment lump in cytoplasm.

Schizonts of *P. falciparum* are rarely observed in peripheral blood, even in heavy infections. During schizogony, the nucleus divides and the cytoplasm breaks apart. In immature schizonts, the chromatin dots and dark brown pigment clumps are dividing and are far more noticeable than the small amount of clear cytoplasm surrounding them (Figs 10.6a & 10.6b). Mature schizonts contain 8 to 24 minute merozoites that are often arranged in a rosette pattern (Fig 10.6c). When more than one schizont infects an erythrocyte, there may be more merozoites. Each schizont in a multiply infected erythrocyte has a separate clump of dark brown pigment. When the schizonts reach maturity, infected erythrocytes burst, releasing merozoites that enter new erythrocytes to begin another generation.

Immature *P. falciparum* gametocytes are seldom observed in peripheral blood (Figs 10.7a & 10.7b). The earliest forms are small, compact, and round. Pigment is scattered throughout the cytoplasm and the nucleus is sometimes stretched along one side. As it matures, the gametocyte becomes elongate, angular, or oval, and the chromatin tends to migrate toward the center. Fully matured gametocytes, which are more commonly seen than younger forms, are usually crescent- or sausage-shaped. Macrogametocytes are usually slightly longer, more slender with pointed ends, and more deeply stained than microgametocytes (Fig 10.7c). Macrogametocytes have dense blue cytoplasm and a small, compact, red or magenta chromatin mass lying in or near the center or near one of the poles. Pigment closely adheres to the chromatin in separate grains, surrounding it or covering it completely. Microgametocytes are sausage-shaped with rounded ends and have pale, often grayish-blue or pink cytoplasm and loose, irregularly scattered chromatin granules (Fig 10.7d). Abundant small, brownish rodlets and granules of pigment occupy the central portion of the parasite. The ends of mature macro- and microgametocytes are usually clear and pigment-free. Infected erythrocytes stretch as gametocytes grow longer. Frequently, the residuum of erythrocytic material filling the concave side of the parasite develops a faint, bowshaped projecting rim. Sometimes the remains of the erythrocyte appear as a red zone around the gametocyte.

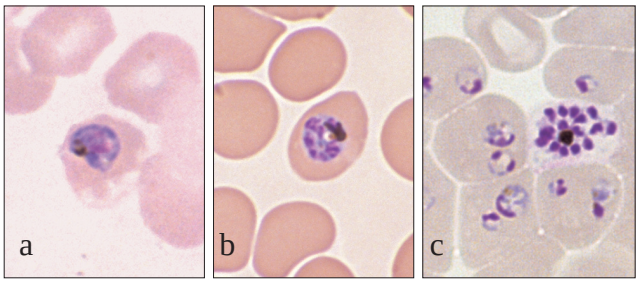



**Figure 10.6 a,b,c**
*Plasmodium falciparum* schizont forms in thin peripheral blood smears, Giemsa. Original magnifications, a & b Immature schizonts. x330 c. Mature schizont with 15 merozoites and central pigment clump. x300

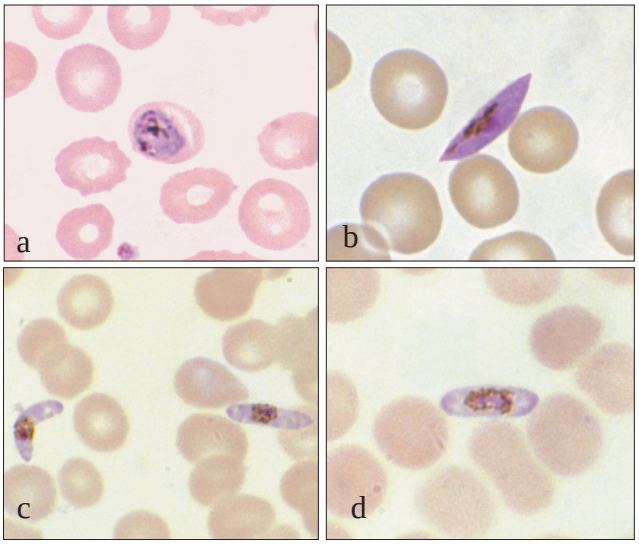



**Figure 10.7 a,b,c,d**
Immature and mature *Plasmodium falciparum* gametocyte forms in thin peripheral smears, Giemsa. Original magnifications. Immature gametocytes (a & b). a. Large round form. x400 b. Elongated shape with pointed ends containing chromatin mass and pigment. x300 c. Sausage-shaped mature macrogametocyte with pointed ends, contains compact chromatin and pigment. x450 d. Sausage-shaped mature microgametocyte has rounded ends and contains diffuse pigment and chromatin. x450

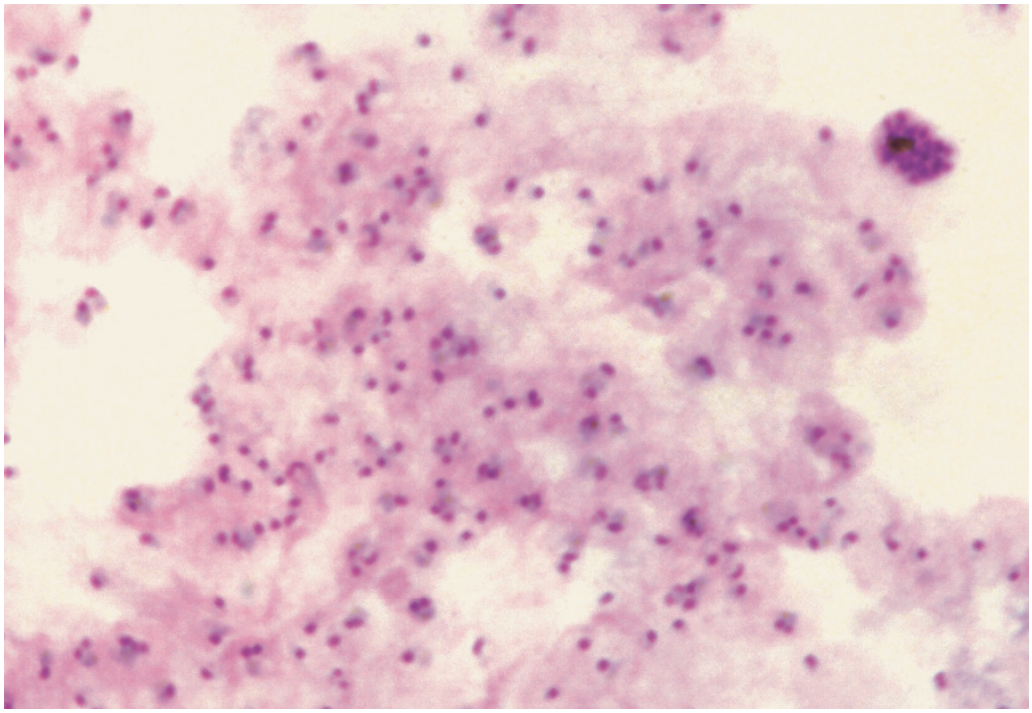


**Figure 10.8**
*Plasmodium falciparum* in thick blood film from patient with 43% parasitemia. Trophozoites have 1 or 2 large chromatin masses and small, compact cytoplasm. Some have faint pigment. Giemsa. Original magnification x290

Thick blood films demonstrate masses of trophozoites (Fig 10.8), a mature schizont with central clumped pigment surrounded by merozoites in rosette pattern (Fig 10.9), and sausage-shaped gametocytes (Fig 10.10).

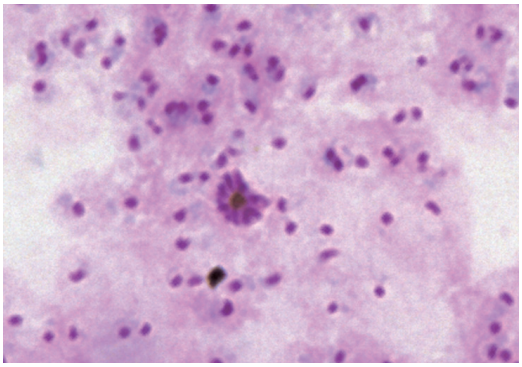


**Figure 10.9**
Mature *Plasmodium falciparum* schizont in thick blood film with clumped pigment in center and merozoites in rosette pattern. Giemsa. Original magnification x330

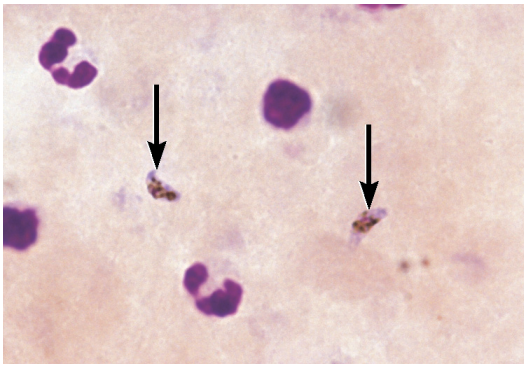


**Figure 10.10**
Two sausage-shaped *Plasmodium falciparum* gametocytes in thick blood film. Giemsa. Original magnification x300

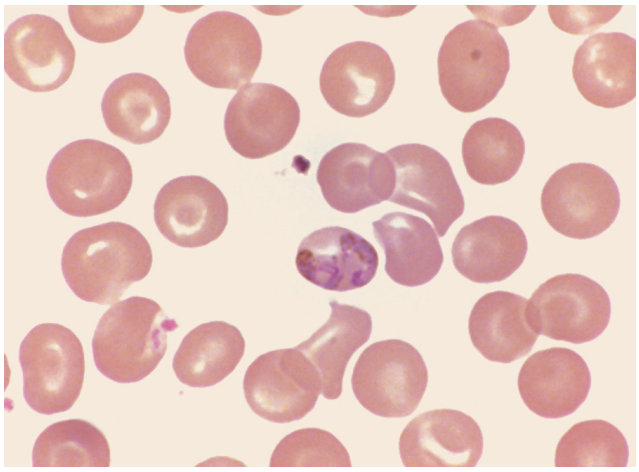


**Figure 10.11**
Erythrocyte with 2 trophozoites, a rare finding in *Plasmodium malariae* infections. Giemsa. Original magnification x290



**Figure 10.12**
Early ring trophozoite (arrow) of *Plasmodium malariae* with red chromatin dot and faintly stained blue cytoplasm in normal-sized erythrocyte. Giemsa. Original magnification x290

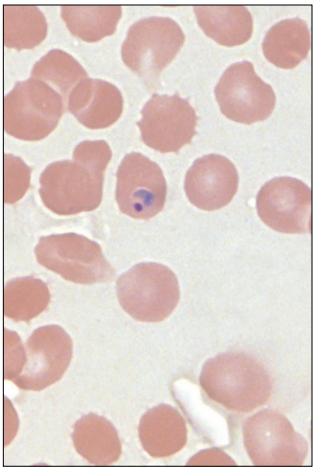


**Figure 10.13**
Ring trophozoite of *Plasmodium malariae* with red chromatin dot and prominent blue cytoplasm in normal-sized erythrocyte. Giemsa. Original magnification x300

## *Plasmodium malariae* (Figures 10.11 to 10.17)

Erythrocytes infected with *Plasmodium malariae* are normal-sized or slightly smaller. Parasitemia in *P. malariae* infections is generally less than 2%. When stained at pH 7.5, stippling with various sizes of pale pink, spherical Ziemann's dots may be seen. However, this stippling is less distinct than in *P. falciparum* and *P. vivax* infections and too rarely observed to be diagnostically significant. Multiply infected erythrocytes are rare (Fig 10.11).

Very young ring trophozoites (Fig 10.12) usually contain no pigment. Young ring trophozoites (Fig 10.13) are roughly the size of *P. vivax* trophozoites, but some are smaller and some have a broader circle of cytoplasm. Double chromatin dots are rare. Some trophozoites contain a vacuole that gives the parasite the appearance of a basket with a handle (Fig 10.14a). Growing trophozoites are usually compact and angular, round, ovoid, or band-shaped. Band forms are more frequently observed in *P. malariae* than in other species (Figs 10.14b & 10.14c). The chromatin in growing or older trophozoites may be round or streaky and frequently looks stretched. The pigment is darker than that of *P. vivax* and is often round and arranged peripherally, sometimes opposite the elongated nucleus. The large pigment granules may have a yellowish edge that gives the blue cytoplasm a greenish hue, a characteristic of *P. malariae* that distinguishes it from *P. vivax*. Trophozoites of *P. malariae* rarely become ameboid like *P. vivax*, but retain their original shape until they mature (Fig 10.14d).

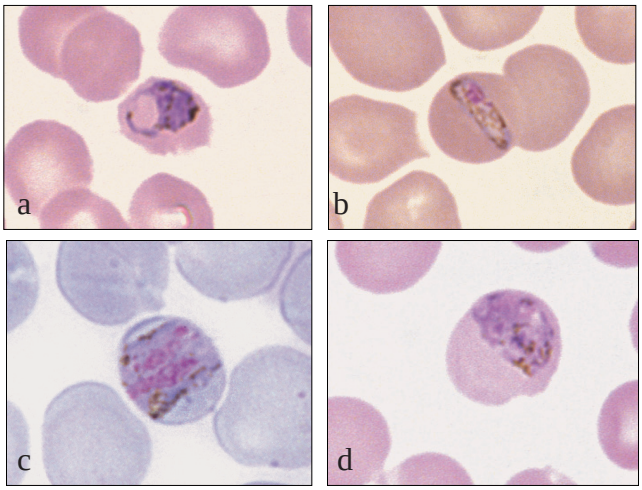



**Figure 10.14 a,b,c,d**
*Plasmodium malariae* trophozoites, thin peripheral blood smear, Giemsa. Original magnifications a. Basket appearance. x330 b. Early band form. x450 c. Mature band form. Blue staining of erythrocyte cytoplasm as seen is unusual. x450 d. Mature rounded compact form. x300

Erythrocytes containing schizonts of *P. malariae* usually do not withdraw from peripheral blood, as they do in vivax malaria. Therefore, erythrocytes with schizonts of P. *malariae* are often observed in great numbers in peripheral blood. Immature schizonts can be so dark and dense that it is difficult to differentiate the divisions of chromatin within the heavily pigmented cytoplasm (Fig 10.15a). The divisions are frequently uneven in size and shape. The pigment remains scattered throughout the cytoplasm until shortly before complete division of the chromatin. Mature schizonts (Figs 10.15b & 10.15c) consist of 6 to 12 (average 8) large merozoites arranged peripherally in a rosette pattern around a central clump of dark brown pigment.

Gametocytes (Fig 10.16a & 10.16b) of *P. malariae* are seldom observed in peripheral blood. It may be difficult to differentiate young gametocytes from round, compact trophozoites. Mature gametocytes of *P. malariae* are spherical or oval, larger than mature trophozoites, but smaller than gametocytes of *P. vivax*. They usually fill or nearly fill a normal-sized erythrocyte. Macrogametocytes (Fig 10.16a) and microgametocytes (Fig 10.16b) are roughly the same size and have the same staining qualities. The chromatin is eccentric in macrogametocytes and central in microgametocytes. The abundant, prominent, dark brown, coarse pigment grains are darker than in *P. vivax*, particularly in macrogametocytes.

Thick blood films demonstrate two trophozoites in Fig 10.17a, an immature schizont in Fig 10.17b, and a mature schizont in Fig 10.17c.

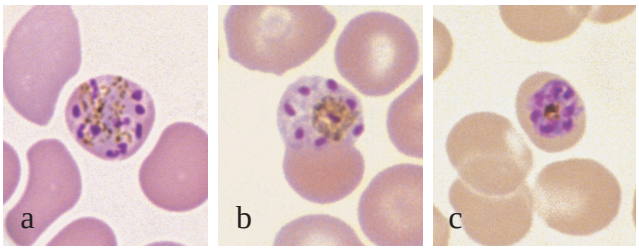



**Figure 10.15 a,b,c**
*Plasmodium malariae* schizont forms in thin peripheral blood smear. Giemsa. Original magnifications. a. Immature schizont. Chromatin and cytoplasm still dividing, light brown granular pigment diffuse. x300 b. Nearly mature schizont with eight merozoites forming rosette. Chromatinc division is complete and pigment is clumped. x330 c. Mature schizont with seven merozoites rosette with clumped central pigment. x330

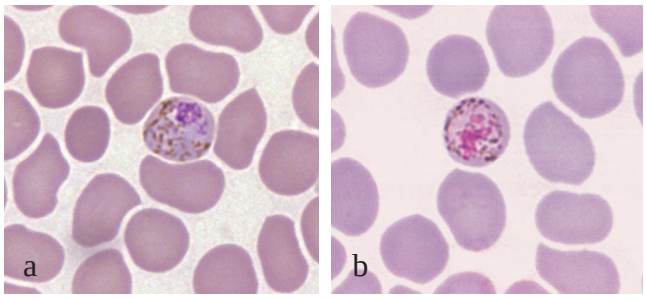



**Figure 10.16 a,b**
*Plasmodium malariae* gametocyte forms in thin peripheral blood smears. Giemsa. Original magnifications. a. Macrogametocyte with eccentric chromatin. x330 b. Microgametocyte with central chromatin. x400

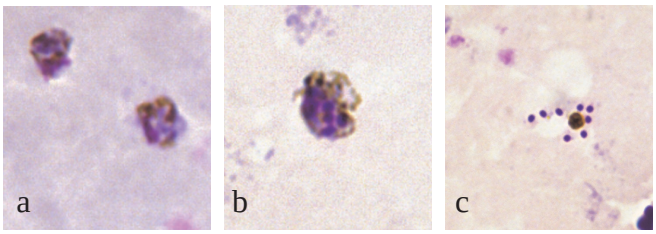



**Figure 10.17 a,b,c**
*Plasmodium malariae* forms in thick peripheral blood smears. Giemsa. Original magnifications x330. a. Two trophozoites with blue cytoplasm, red chromatin and brown pigment. b. Immature schizont with several chromatin masses, undivided cytoplasm and brown pigment. c. Mature schizont with 8 merozoites forming rosette and clumped brown pigment.

## *Plasmodium ovale* (Figures 10.18 to 10.24)

Erythrocytes infected with *P. ovale* are initially normal-sized (Fig 10.18a–10.18c) but eventually enlarge nearly as much as in *P. vivax* infection (Figs 10.19a & 10.19b). Parasitemia in *P. ovale* infections is generally less than 2%. Infected erythrocytes are often oval and fimbriated and may be stippled with Schüffner's dots (Fig 10.19b). Although fimbriated (Fig 10.20a & 10.20b) and elongated erythrocytes (the ovalocytes, for which this species is named) (Fig 10.20) are artifacts that occur in dry, fixed, thin films, they are of great diagnostic value. Multiply infected erythrocytes are occasionally observed (Fig 10.21a).

Very young ring trophozoites of *P. ovale* usually contain no pigment (Fig 10.19a). Young trophozoites are about the same size as *P. vivax* and have a large chromatin dot and a few may have double chromatin dots (Fig 10.18c). Some have a heavy cytoplasmic circle, like *P. malariae*. In growing *P. ovale* trophozoites, the chromatin is solid and compact; the cytoplasm is only slightly ameboid (Fig 10.21b), has few vacuoles and less commonly form bands (Fig 10.21c & 10.21d). Mature trophozoites are round and centrally located. Infected erythrocytes often become oval,

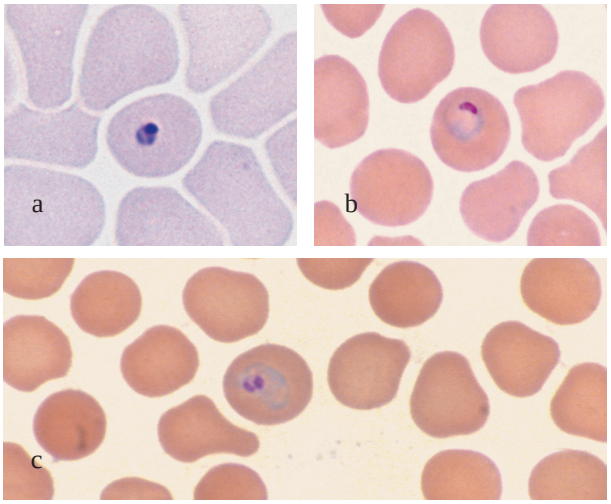



**Figure 10.18 a,b,c**
Ring forms of *Plasmodium ovale* in normal sized erythrocytes. Giemsa. Original magnifications. a. Small early ring trophozoite, chromatin dot, no pigment. x330 b. Older ring trophozoite, red chromatin dot. x290 c. Ring trophozoite with 2 chromatin dots. x290

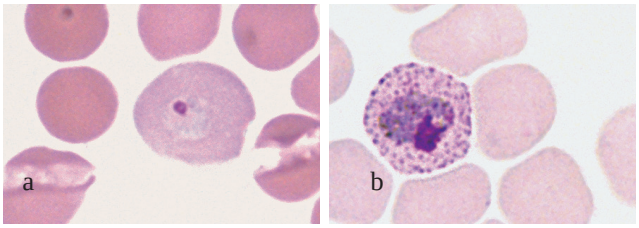



**Figure 10.19 a,b**
Trophozoites of *Plasmodium ovale* in enlarged erythrocytes. Giemsa. Original magnifications x330. a. Ring trophozoite lacks pigment. b. Mature trophozoite contains Schüffner's dots.

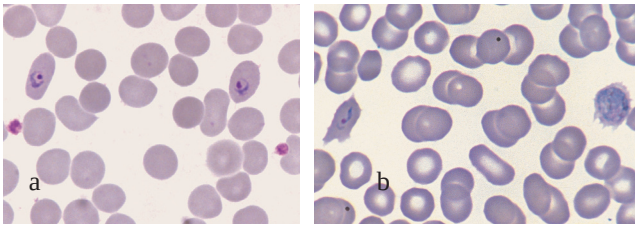



**Figure 10.20 a,b**
Oval and fimbriated erythrocytes infected with *Plasmodium ovale*. Giemsa. Original magnifications. a. Two ring trophozoites in oval erythrocytes. x330 b. Ring trophozoites in fimbriated oval erythrocyte (left) and fimbriated round erythrocyte (right) with macrogametocyte. x290

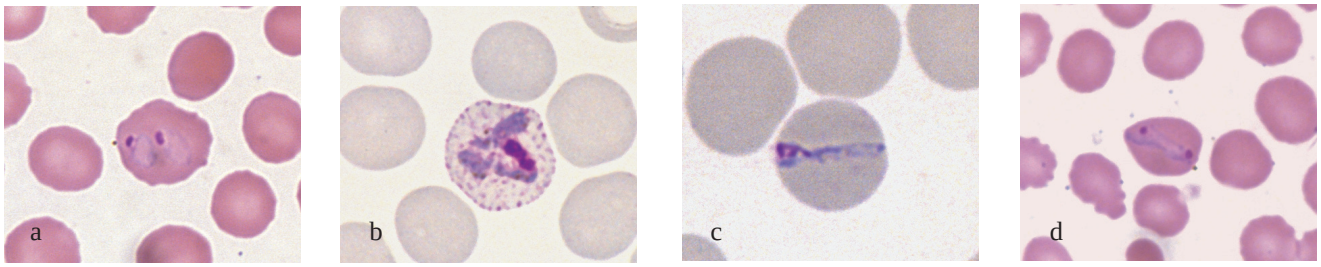



**Figure 10.21 a,b,c,d**
Various forms of *Plasmodium ovale* trophozoites. Giemsa. Original magnifications. a. Multiple infected erythrocytes. x300 b. Slight ameboid configuration with Schüffner's dots. x290 c. Elongate thin band shaped trophozoite. x330 d. Elongate band shaped trophozoite with 2 chromatin dots. x300

spindle-, or pear-shaped, with ragged points or fimbriations on one or both ends. Schüffner's dots may extend to the tips of the fimbriations. In this and later stages, *P. ovale* closely resembles *P. malariae*, except that its pigment is lighter and less conspicuous.

Immature schizonts (Figs 10.22a to 10.22c) of *P. ovale* are usually larger than those of *P. malariae*. Erythrocytes that contain them are frequently fimbriated and oval or elongated. Mature schizonts (Fig 10.22d) consist of 4 to 16 (average 8) very large merozoites, usually in a rosette pattern.

Mature macrogametocytes with eccentric chromatin mass (Fig 10.23a) and mature microgametocyte with central chromatin mass (Fig 10.23b) of *P. ovale* are round and slightly smaller than those of *P. vivax* and contain Schüffner's dots. Pigment rods are brown-black with a greenish tinge, distinctively arranged in a concentric pattern at right angles to the radius. They are more numerous at the periphery. Mature gametocytes fill or nearly fill an enlarged erythrocyte.

Thick blood films demonstrate an ameboid trophozoite in Fig 10.24a, a mature schizont with 8 merozoites in Fig 10.24b, and a gametocyte in Fig 10.24c.

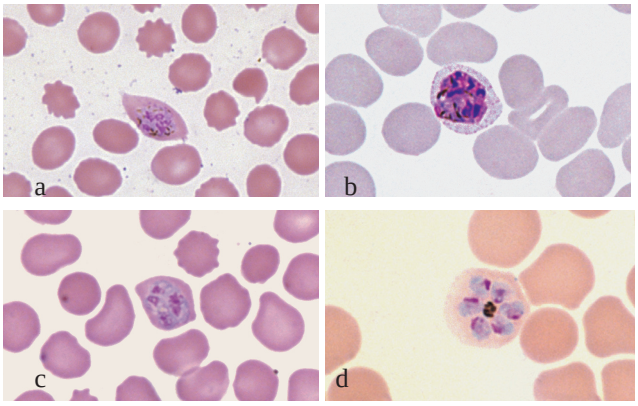



**Figure 10.22 a,b,c,d**
*Plasmodium ovale* schizonts. Original magnifications. a. Immature schizont, chromatin and cytoplasm dividing. x300 b. Pigment beginning to clump, 7 chromatin masses. x330 c. Late immature schizont fills most of erythrocyte. x300 d. Mature schizont in rosette pattern with 6 merozoites. x290

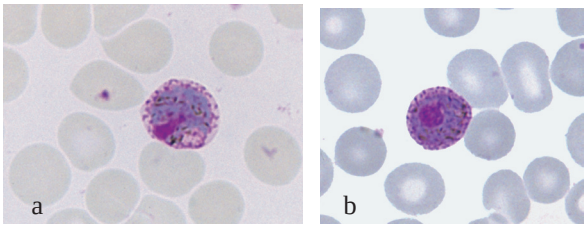



**Figure 10.23 a,b**
Mature *Plasmodium ovale* gametocytes.in thin peripheral blood stains. Giemsa. Original magnification x330. a. Mature macrogametocyte with Schüffner's dots and eccentric chromatin mass. b. Mature microgametocyte with Schüffner's dots and large central mass of chromatin.

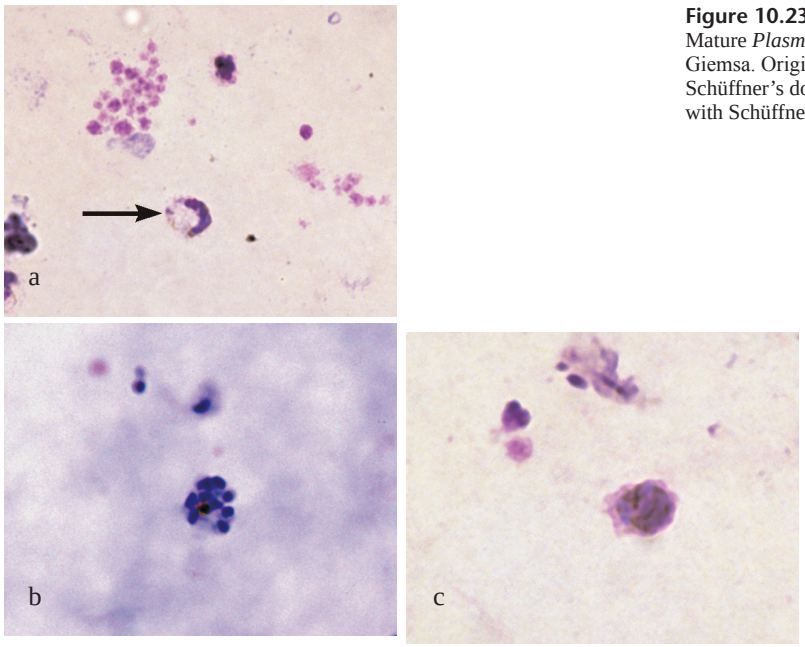



**Figure 10.24 a,b,c**
Thick blood film of *Plasmodium ovale*. Original magnifications. a. Ameboid trophozoite. x300 b. Mature schizont. x330 c. Gametocyte. x300

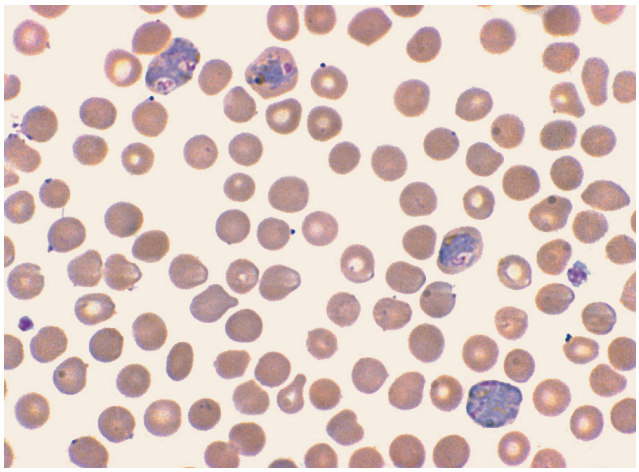


**Figure 10.25**
Heavy parasitemia (approximately 4%) in patient infected with *Plasmodium vivax*. Giemsa. Original magnification x250

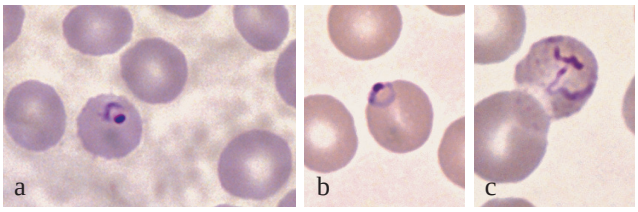



**Figure 10.26 a,b,c**
Young trophozoites of *Plasmodium vivax* in normal sized erythrocytes. Original magnifications. a. Young ring trophozoite, lack pigment. x300 b. Marginal ring trophozoite. x 300 c. Tenuous trophozoite. x330

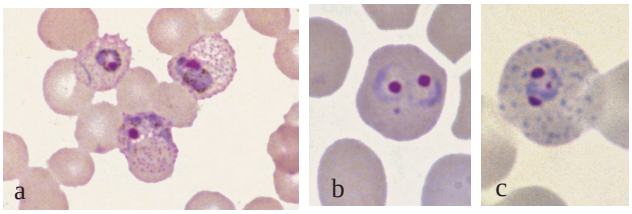



**Figure 10.27 a,b,c**
Multiply infected enlarged erythrocytes with *Plasmodium vivax*. Giemsa pH 7.2. Original magnifications. a. Schüffner's dots in 3 older trophozoites. x290 b. Two ring trophozoites. x450 c. Trophozoite with 2 chromatin dots, cytoplasm of erythrocyte has basophilic stippling. x450

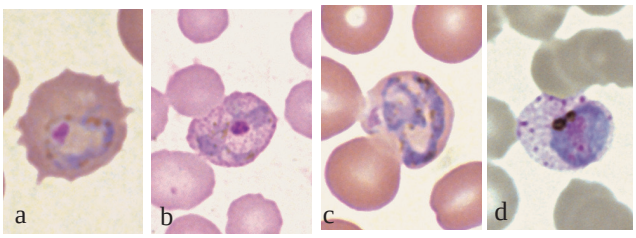



**Figure 10.28 a,b,c,d**
Various forms of *Plasmodium vivax* trophozoites. Original magnifications. a.Older trophozoite in fimbriated erythrocyte. x450 b. Ameboid trophozoite with Schüffner's dots. x300 c. Ameboid trophozoite. x330 d. Mature trophozoite. x300

## *Plasmodium vivax* (Figures 10.25 to 10.31)

Erythrocytes infected with *P. vivax* eventually enlarge, become pale, and irregularly shaped. Parasitemia in *P. vivax* infections is generally less than 2%, but may be higher (4% in Fig 10.25 & 10.26). Parasitized oval erythrocytes are common. The cytoplasm of parasitized erythrocytes may be stippled with small, fairly uniform pink granules called Schüffner's dots which are evenly distributed throughout the part of the erythrocyte that is not occupied by the parasite (Fig 10.27a); Schüffner's dots often become more pronounced and more deeply stained as the parasite grows, and are best demonstrated by careful staining at pH 7.2 preventing prolonged washing which obliterates them. Schüffner's dots are more numerous and less coarse than the Maurer's dots sometimes seen in falciparum malaria. Multiply infected erythrocytes (Fig 10.27b) and double chromatin dots (Fig 10.27c) are occasionally observed, and often different stages of *P. vivax* appear simultaneously because of asynchronous maturation within a brood, and alternate day maturation of separate broods.

Young ring trophozoites of *P. vivax* are large (approximately one third the diameter of an erythrocyte,) consist of blue cytoplasm and a heavy red chromatin dot in the center or at the periphery. Very young ring trophozoites are usually unpigmented (Fig 10.26a). Marginal ring trophozoites may be observed in some erythrocytes (Fig 10.26b). As trophozoites grow their cytoplasm thickens, the chromatin mass enlarges, pigment granules develop, and the host's cytoplasms occasionally fimbriates (Fig 10.28a). Growing trophozoites develop one or more vacuoles; tenuous pseudopodial processes sometimes give them an ameboid appearance (Figs 10.28b &10.28c). In young forms hemozoin (hematin) , pigment granules may be indistinguishable as separate granules or rods due to the yellowish tinge they lend to the cytoplasm. In mature forms pigment granules are small, yellowish-brown, and angular or rod-shaped. At the end of vegetative growth, pseudopodia are drawn in and trophozoites become compact, with an irregular outline and mottled cytoplasm (Fig 10.28d). The single chromatin mass is compact and usually becomes located near the periphery. Full-grown *P. vivax* trophozoites are larger than those of other species and practically fill an enlarged erythrocyte.

Schizonts of *P. vivax* tend to leave peripheral circulation and thus are less frequently found than trophozoites in peripheral blood. Immature schizonts are produced by division of chromatin (Figs 10.29a to 10.29c). When division is complete, the chromatin masses become smaller and more rounded and are surrounded by a mass or circle of cytoplasm. Mature schizonts consist of 12 to 24 small, clustered merozoites (average 16, but as few as 9 have been described) (Figs 10.29d & 10.29e). The yellow-brown pigment clumps (sometimes arranged loosely into a single mass) (Fig 10.29d) are often localized in the center of the cluster of merozoites forming "rosettes" (Fig 10.29e).

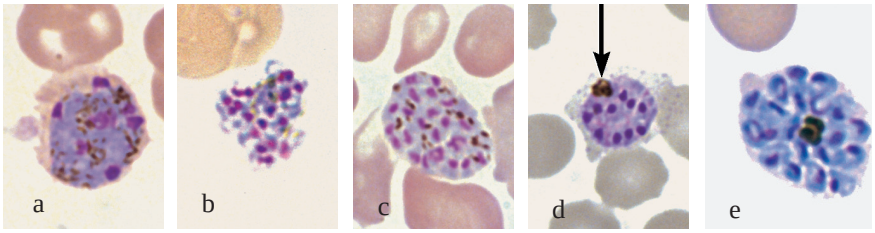



**Figure 10.29 a,b,c,d,e**
*Plasmodium vivax* schizonts. Giemsa. Original magnifications. a. Early immature, 7 chromatin masses. x450 b. Extracellular, immature. x330 c. Late immature with 24 merozoites. x450 d. Mature schizont with 10 merozoites and yellow-brown pigment (arrow). x330 e. Mature schizont with 20 merozoites. x330

Gametocytes of *P. vivax* develop from released merozoites in the circulation of the deep organs before release to the general circulation, for that reason young forms are only infrequently found in the peripheral blood. Immature gametocytes are rounded and have homogeneous cytoplasm, often with a vesicular area around the chromatin mass (Fig 10.30a). They are difficult to distinguish from growing and mature trophozoites whose pseudopodia have drawn in prior to desiccation or with maturation. Mature gametocytes expand the erythrocytes (Figs 10.30b to 10.30e), exhibit pigment granules that become evenly distributed throughout the cytoplasm and are more numerous than in trophozoites. Slightly immature macrogametocytes (female) of *P. vivax* can be distinguished from mature trophozoites by their larger size, circular to ovoid contour, homogenous cytoplasm with larger and darker brown pigment granules (often more numerous than in trophozoites) and lack of vacuoles. Mature macrogametocytes (Figs 10.30b & 10.30c) have densely blue-staining, homogeneous cytoplasm, a compact chromatin mass that is deep red or magenta near the periphery and sometimes surrounded by a colorless vesicular area. Mature microgametocytes (male) (Figs 10.30d & 10.30e) are usually also found in enlarged erythrocytes. Their reticular chromatin mass stains lightly, and is round or stellate and larger than in any other stage, sometimes extending across the body of the parasite in a broad spindle. The reticular chromatin mass of mature microgametocytes of *P. vivax* is centrally located and it is often surrounded by a large unstained vesicular area. Pigment grains and rods are usually lighter than in macrogametocytes.

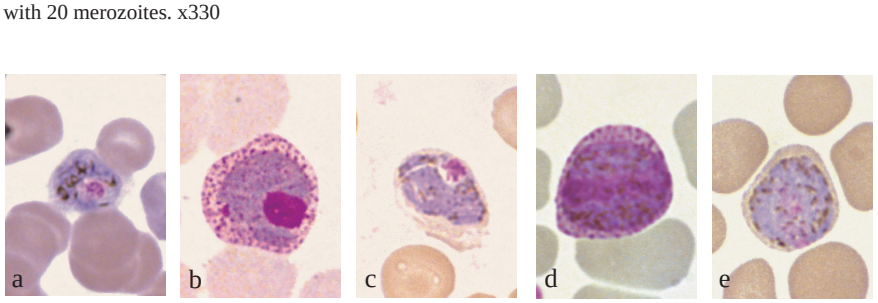



**Figure 10.30 a,b,c,d,e**
*Plasmodium vivax* gametocytes in thin peripheral blood films. Giemsa. Original magnifications. a. Immature gametocyte. x300 b. Mature macrogametocyte. x330 c. Mature oval macrogametocyte. x330 d. Mature microgametocyte. x450 e. Mature microgametocyte. x300

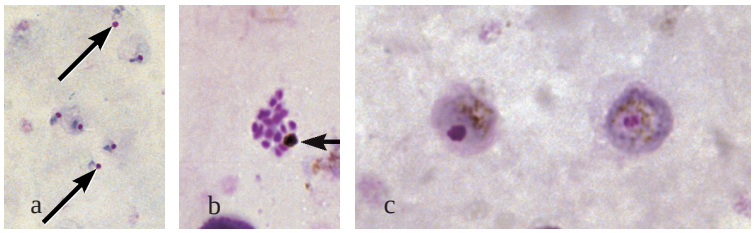



**Figure 10.31 a,b,c**
Thick films of *Plasmodium vivax.* Giemsa. Original magnifications. a. Ring trophozoites (arrows). x290 b. Mature schizont with yellow-brown pigment (arrow). x330 c. Mature gametocyte (left) immature gametocyte (right). x300

Thick blood films demonstrate several ring trophozoites (Fig 10.31a), a mature schizont with 16 merozoites (Fig 10.31b) and a mature gametozoite (left) and an immature gametocyte with vacuole surrounding chromatin mass (right) (Fig 10.31c).

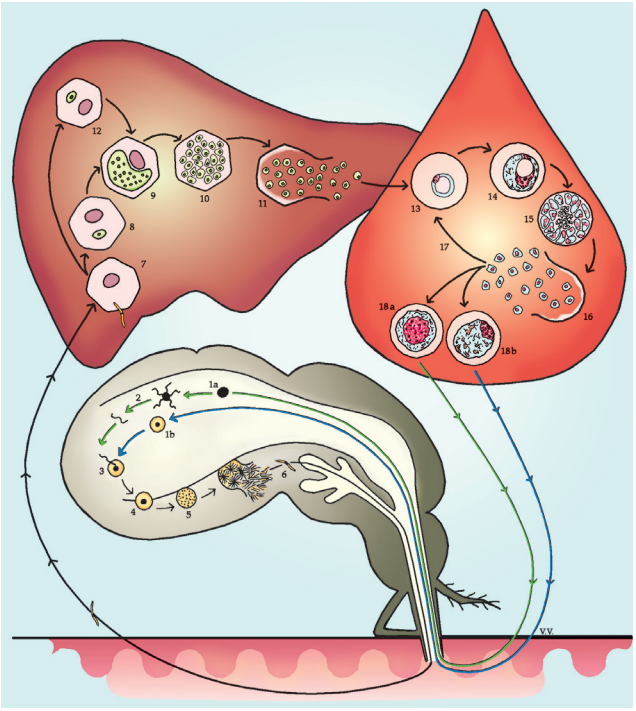


**Figure 10.32**
Life cycle of malarial parasites. Life cycle of *Plasmodium* sp. 1. Mosquito ingests sexual-stage malarial parasites (micro- and macrogametocytes). 2. Microgametocyte exflagellates in mosquito's gut. 3. Exflagellated microgamete fertilizes macrogamete, forming a zygote. 4. Zygote develops into ookinete that penetrates epithelial cells of mosquito's midgut. 5. Ookinete grows into oocyst. 6. Thin motile sporozoites develop, disperse through mosquito's body cavity, lodge in salivary glands, and are inoculated into host during subsequent blood meal. 7. In human host, sporozoites leave blood and infect hepatocytes. 8-10. Sporozoites undergo schizogony, forming tissue schizonts containing many exoerythrocytic merozoites. 11. Hepatocytes rupture and release merozoites into bloodstream. 12. *Plasmodium vivax* and *P. ovale* hypnozoites remain dormant in liver; subsequent schizogony causes relapse. 13. Asexual cycle begins when merozoites from liver invade erythrocytes and develop into young ring form trophozoites. 14. Older mature trophozoites are larger and usually more compact. 15. Mature trophozoite undergoes asexual division (schizogony) to produce mature schizont composed of merozoites. 16. Erythrocyte ruptures, releasing merozoites into bloodstream. 17. Released merozoites invade other erythrocytes and begin new round of asexual reproduction. 18. Some merozoites develop into micro- and macrogametocytes within erythrocytes, which are then ingested by mosquito.

## *Life Cycle and Transmission*

The life cycle of malarial parasites is illustrated in Figure 10.32. The sexual reproductive cycle in the mosquito, called sporogony, takes 8 to 35 days.

A female anopheline mosquito (Fig 10.33) taking a blood meal from an infected host ingests malarial parasites, some of which are in the sexual stage of development (micro- and macrogametocytes). The microgametocyte undergoes a process of exflagellation. The nucleus divides into 4 to 8 nuclei, each of which combines with cytoplasm to form a



**Figure 10.33**
Female Anopheline mosquito.



**Figure 10.34**
Exflagellate form (arrow) of *Plasmodium* in peripheral blood. Giemsa. Original magnification x330

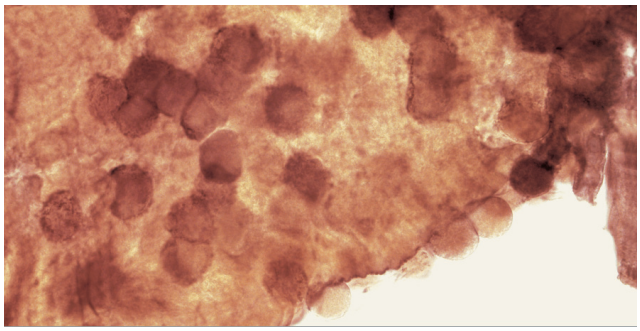


**Figure 10.35**
Spherical oocysts attached to fragment of infected *Anopheles* mosquito gut. Oocysts are approximately 50 µm in diameter. Unstained. Original magnification x120

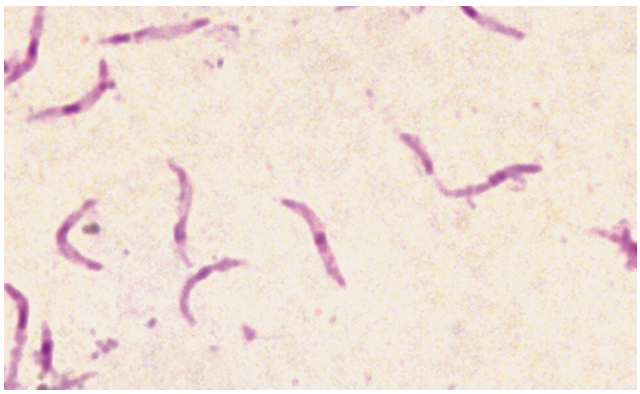


**Figure 10.36**
Elongated sporozoites, approximately 8 µm to 10 µm by 1 µm, from gut of infected *Anopheles* mosquito. Giemsa. Original magnification x300

long, threadlike flagellum. Exflagellation normally occurs in the mosquito's gut, but the process has been observed in peripheral blood films (Fig 10.34).

Gametocytes develop into micro- and macrogametes in the mosquito's gut. An exflagellated microgamete fertilizes a macrogamete, forming a zygote. The zygote develops into an ookinete that penetrates the epithelial cells of the mosquito's midgut. The ookinete grows into a spherical oocyst in which thin, motile sporozoites develop and disperse throughout the mosquito's body cavity (Figs 10.35 & 10.36). An infected mosquito may contain hundreds of oocysts that produce thousands of sporozoites. Sporozoites that reach the mosquito's salivary glands lodge there and are inoculated into a new host when the mosquito takes another blood meal.

In humans, sporozoites leave the blood and infect hepatocytes. In a process called primary exoerythrocytic schizogony, sporozoites divide and mature over a period of 6 to 16 days, forming primary, or tissue, schizonts containing many exoerythrocytic merozoites. The hepatocytes rupture and release the merozoites into the bloodstream, where they invade erythrocytes. In *vivax* and *ovale* malaria, quiescent forms called hypnozoites remain dormant in the liver and may be released into the blood at any time up to 5 years, causing a recurrence of disease called relapse. P*lasmodium falciparum* and *P. malariae* do not develop hypnozoites and therefore do not relapse. In these 2 species, renewed parasitemia, called recrudescence, is caused by erythrocytic parasites that have remained in circulation at subclinical or asymptomatic levels. *Plasmodium falciparum* can recrudesce for 1 to 2 years and *P. malariae* for 30 or more years.

The asexual erythrocytic cycle begins when merozoites released from the liver invade erythrocytes in the bloodstream and develop into trophozoites, the active, motile feeding stage between merozoite and mature schizont. The youngest trophozoites appear as small ring forms. Older mature trophozoites are much larger and usually more compact, and nearly fill the erythrocyte. Within an erythrocyte, the growing trophozoite metabolizes hemoglobin. Pigment granules derived from this process form in the cytoplasm of the growing parasite. In the mature trophozoite, the chromatin mass undergoes asexual division (schizogony), followed by division of the cytoplasm. Complete division of chromatin and cytoplasm produces a mature schizont composed of merozoites and 1 or 2 clumps of pigment. Each merozoite is composed of a small chromatin mass within a tiny fragment of cytoplasm. Eventually, the parasitized erythrocyte ruptures, releasing merozoites into the bloodstream. The released merozoites invade other erythrocytes and commence another round of asexual reproduction.

Not all merozoites that invade erythrocytes evolve into schizonts. Some develop into micro-and macrogametocytes that circulate in the blood until ingestion by a female *Anopheles* mosquito once again triggers the sexual reproductive cycle.

Malaria has 3 known routes of transmission: mosquito-borne, congenital, and blood-borne. When the route of transmission cannot be established, the infection is classified as cryptic malaria. A large majority of infections are transmitted by the bite of an infected female *Anopheles* mosquito (Fig 10.33). Infection can also be acquired in utero or during birth. Blood-borne malaria can be transmitted accidentally through blood-product transfusion, contaminated injection equipment, or organ transplantation. It can also be transmitted intentionally as malariotherapy, widely employed until the 1950s as a treatment for late neurosyphilis. Malariotherapy has recently resurfaced as an unproven alternative treatment for diseases such as AIDS, Lyme disease, and breast cancer.

## Clinical Features and Pathogenesis

Malaria has protean clinical manifestations and may mimic almost any disease (Table 10.2). Proerythrodromal symptoms are vague and include lassitude, myalgia, irritability, anorexia, headache, various gastrointestinal symptoms, and chills. Some of the clinical features of malaria are the same for infections caused by all 4 species of *Plasmodium*. For example, many patients develop splenomegaly (Fig 10.37).



**Fig 10.37**
Child with malarial splenomegaly. Patient was also anemic.

Table 10.2
Clinical features of malaria caused by *Plasmodium* sp infecting humans.

| | *P. vivax* | *P. falciparum* | *P. malariae* | *P. ovale* |
|---|---|---|---|---|
| Complications | Very rare transient cerebral irritation | Severe anemia, frequent cerebral, pulmonary, and renal complications | Rare progressive glomerulonephritis | Milder than *P. vivax* |
| Splenomegaly | Less severe than *P. falciparum*, rupture 2 to 3 months after infection. | Frequent | Less severe than *P. falciparum* | Same as *P. vivax* |
| Hepatomegaly | Less severe than *P. falciparum* | Frequent, with jaundice | Very rare | Same as *P. vivax* |
| Other features | Late-day paroxysms, high fever, nausea, vomiting | High fever, nausea, vomiting, diarrhea | Peripheral edema | Same as *P. vivax* |

In long-standing chronic malaria or with repeated attacks, the spleen may become enormously enlarged, a condition sometimes called tropical splenomegaly syndrome or big spleen disease. Traumatic splenic rupture can cause death. Asplenia results in rapid progression of disease and high parasitemia.

The classic symptom common to all malarial infections is cyclic fever. Fever peaks around the time of schizogony and is more severe in naive patients than in those who have had previous infections. Malarial pyrogens may be products of ruptured erythrocytes or toxic products of the parasites themselves. When parasites develop synchronously, the great majority undergo schizogony at approximately the same time and fever periodicity is determined by the length of the asexual cycle (Table 10.3). Malarial paroxysms are usually sudden, with 3 discernible stages: chills, fever, and sweating. After the paroxysm, the exhausted patient usually sleeps.

Temporal features of malaria vary with factors such as host response and the species of *Plasmodium*. The prepatent period between inoculation and the appearance of parasites in peripheral blood can be lengthened by immunity and prophylactic drugs. The incubation period between inoculation and the appearance of clinical symptoms varies depending on the degree of acquired immunity and the number of sporozoites inoculated. In all forms of malaria, clinical symptoms usually appear 2 or 3 days after parasites appear in peripheral blood. In tertian malaria caused by *P. vivax*, *P. falciparum*, or *P. ovale*, the asexual cycle takes 48 hours, resulting in fever every third day. In quartan malaria caused by *P. malariae*, the asexual cycle takes 72 hours, resulting in fever every fourth day. However, fever periodicity is not a reliable indicator of the species of *Plasmodium* because the cycle may be erratic in patients with repeated or mixed infections, or with 2 or more asynchronous broods.

*Vivax* malaria is very rarely fatal. Erythrocytes infected with *P. vivax* are not sequestered in the microcirculation and thus do not cause the complications associated with

Table 10.3
Temporal features of malaria caused by *Plasmodium* sp infecting humans.

| | *P. vivax* | *P. falciparum* | *P. malariae* | *P. ovale* |
|---|---|---|---|---|
| Prepatent period (days) | 10-13 | 6-12 | 15-21 | 10-14 |
| Incubation period (days) | 8-20 | 12-20 | 18-40 | 8-19 |
| Periodicity of fever (hours) | 48 | 48 | 72 | 48 |
| Time course | Weeks to months, relapses up to 5 years | 1-2 years (untreated) | Several months, relapses up to 30 years | Same as *P. vivax* |

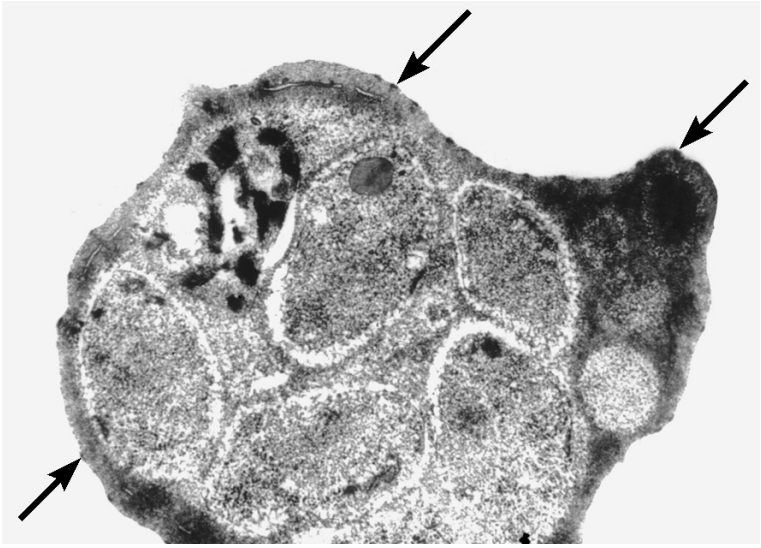


**Figure 10.38**
Transmission electron micrograph of *Plasmodium falciparum* in patient with ocular malaria. Note knobs, conical evaginations, on surface of erythrocyte (arrows).

*falciparum* malaria. *Plasmodium vivax* infects only young erythrocytes; however, hemolysis-induced hematopoiesis can cause significant parasitemia. Relapses of *vivax* malaria occur when merozoites are released into circulation from hepatic hypnozoites. Relapses are usually less severe and of shorter duration than the primary attack, but still create a considerable economic burden for individuals and society. Many Africans are resistant to *P. vivax* infection because they lack the Duffy blood group antigens that are the receptors for the merozoites.

*Plasmodium falciparum* has several unique features that make it the most virulent species and the one that accounts for most deaths due to malaria. It has no secondary exoerythrocytic stage, it parasitizes erythrocytes of any age, and its preerythrocytic schizonts release many more merozoites than other *Plasmodium* sp. Knobs on parasitized erythrocytes facilitate adherence to capillary endothelium (Fig 10.38). Because parasitized erythrocytes are sequestered in the microcirculation, some heavily infected patients have few circulating parasites.

Falciparum malaria often begins with severe gastrointestinal symptoms. Later, patients may develop high fever, hepatomegaly, hepatic tenderness, jaundice due to hemolysis, and splenic tenderness. Laboratory tests may show slightly elevated levels of bilirubin and transaminases. Relapses do not occur because there are no hepatic hypnozoites and because erythrocytic parasites do not persist longer than 1 or 2 years. Fatal complications, usually resulting from microvascular disease, occur more frequently in patients who are very young, immunodeficient, or pregnant, or who have high parasitemia.[7,11] "Algid malaria" describes the clinical findings of clammy skin, cyanosis, and hypotension due to circulatory collapse.[12] Signs and symptoms of cerebral malaria include headache, nuchal rigidity, altered levels of consciousness, seizures, ataxia, aphasia, and dysarthria. Renal involvement may take the form of glomerulonephritis with proteinuria, hemoglobinuria, oliguria, or abnormal urinary sediment. Acute intravascular hemolysis can cause hemoglobinuric nephrosis with renal failure. "Blackwater fever" describes the appearance of dark urine after an acute attack of falciparum malaria. Other complications include gastroenteritis in children, pulmonary edema, severe normocytic anemia, hypoglycemia, and disseminated intravascular coagulopathy. Falciparum malaria during pregnancy increases the risk of maternal anemia, fetal death, prematurity, intrauterine growth retardation, and low birth weight.[7] Falciparum malaria is less severe in heterozygotes for the sickle hemoglobin gene.

In individuals with some acquired immunity to malaria, destruction of pre-erythrocytic stages in the liver by cytotoxic T cells or other mechanisms can prevent the development of disease.[13] If parasites do enter the blood, antibodies may control parasite density and severity of infection.[14] Also, immune responses directed at certain parasite components, such as those involved in fever or adherence to endothelial cells, may help to modify the clinical response.[15] In cerebral malaria there appears to be a complex interaction between pro-inflammatory and anti-inflammatory cytokines affecting sequestration of circulating blood cells[16,17] Parasite-derived molecules—surfaces or soluble—remain necessary but not sufficient to explain the development of cerebral malaria.[18] Persons exposed frequently to malaria have increased immunoglobulin production.[19] Chronic B-cell activation is probably a consequence of immune responses to malarial antigens and of nonspecific B-cell stimulation by toxins and mitogens.[20]

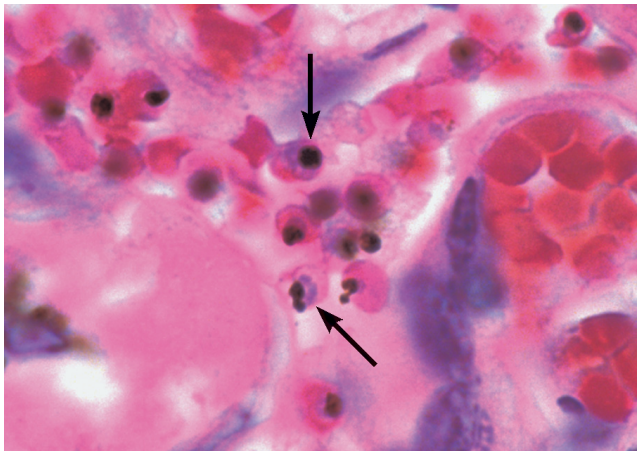


**Figure 10.39**
*Plasmodium falciparum* trophozoites in maternal erythrocytes in placenta. Note pigment and blue cytoplasm (arrows). x1255

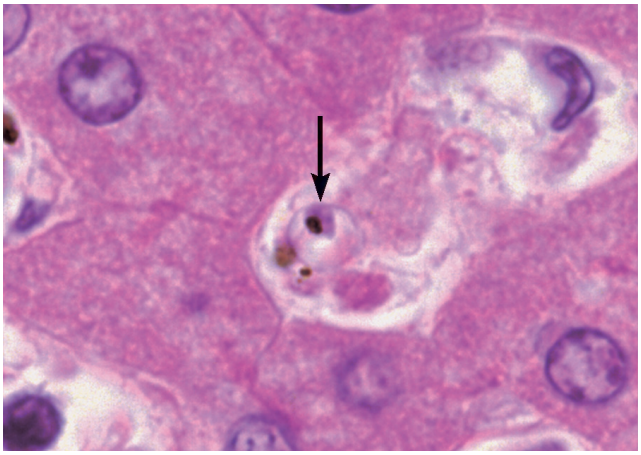


**Figure 10.40**
Trophozoite in Kupffer's cell in liver. Note pigment and cytoplasm (arrow). x1485

AIDS may affect some components of the immune response to *P. falciparum*.[21] After adults leave an endemic area, their protective immunity wanes slowly. It is therefore likely that established antibody responses will be sustained for several years in patients with low CD4 cell counts. In young children, CD4 cells probably play a vital role in the development of immunity to malaria.[22]

Like vivax malaria, *P. malariae* infection is not complicated by microvascular disease. Quartan malaria often has an insidious onset and may cause leukopenia and mild anemia. Relapses do not occur because there are no hepatic hypnozoites. Recrudescence of persistent erythrocytic parasites causes recurrence. Protracted low-grade asymptomatic parasitemia may persist for up to 30 years, making carriers a source of transfusion malaria. Continued antigen stimulation associated with persistent parasitemia may cause immune complex glomerulonephritis. Relapses also occur in ovale malaria due to hepatic hypnozoites.

Clinical features of ovale malaria are similar to those of vivax malaria. Symptoms tend to be mild, and fever often subsides after a few cycles with or without treatment.

## Pathologic Features

Knobs on the surface of erythrocytes parasitized by *P. falciparum* adhere to surface receptors on capillary endothelial cells, believed to be thrombospondin, CD36, and ICAM-1 (Fig 10.38).[15,23] Because *P. falciparum* is the only malarial parasite that becomes sequestered in vessels, it is the only species of *Plasmodium* that we have observed in tissue sections.

In hematoxylin and eosin-stained sections, trophozoites of *P. falciparum* appear as small (2 µm to 4 µm), usually spherical masses of cytoplasm, each containing at least one round clump of dark, birefringent pigment (Figs 10.39 & 10.40). Within an erythrocyte, where trophozoites are most commonly found, the parasite cytoplasm usually stains poorly and may not be visible (Fig 10.41). Infected erythrocytes are frequently depleted of hemoglobin (Fig 10.42), frequently, only malarial pigment can be identified (Fig

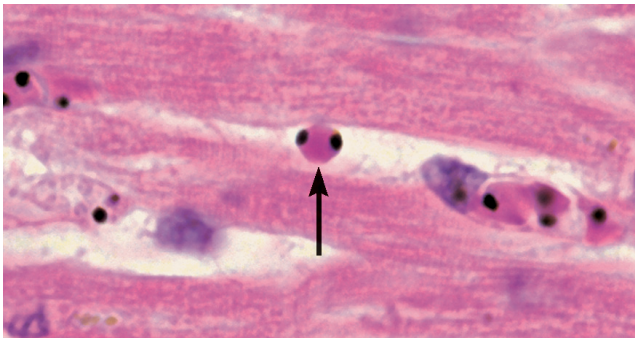


**Figure 10.41**
Two clumps of malarial pigment in erythrocyte (arrow) in myocardium. Parasite cytoplasm not visible in photo. x955

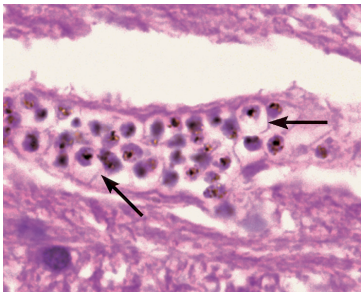


**Figure 10.42**
Trophozoites with cytoplasm and pigment in hemoglobin-depleted erythrocytes (arrows) in cerebral capillary. x960

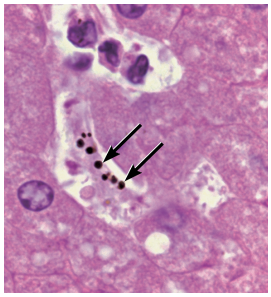


**Figure 10.43**
Spherical clumps of malarial pigment in Kupffer's cell in liver. x870

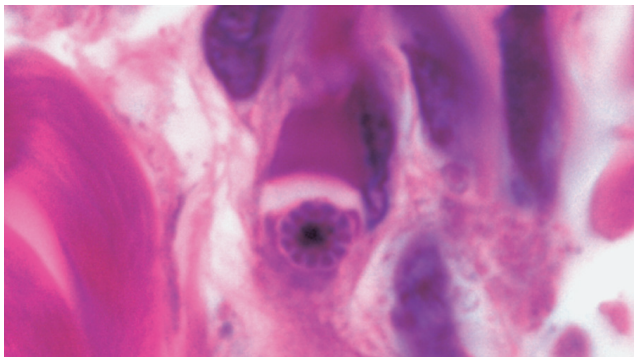


**Figure 10.44**
Schizont in erythrocyte in dermal blood vessel. Note round clump of pigment and merozoites in rosette pattern. Original magnification x500

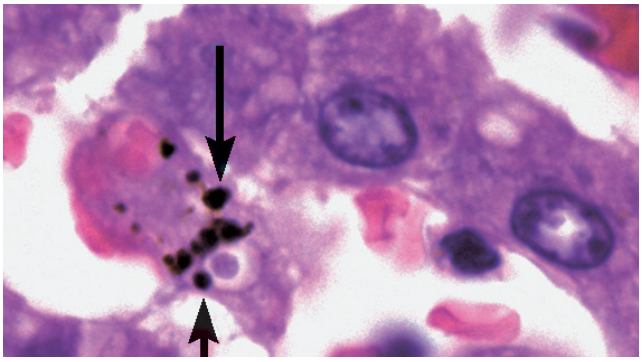


**Figure 10.45**
Round clumps of malarial pigment (arrows) in Kupffer's cell in liver. Elongate aggregate between arrows is also malarial pigment. Original magnification x250

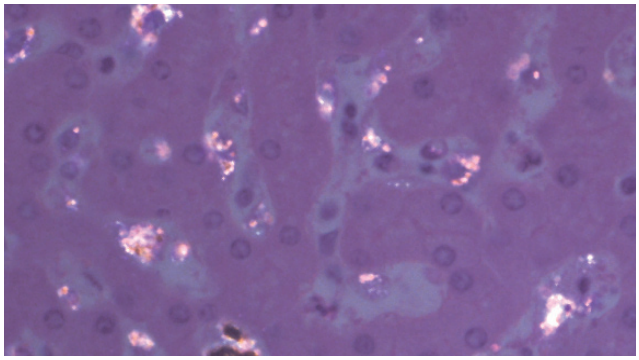


**Figure 10.46**
Birefringent malarial pigment in liver viewed under polarized light. x250

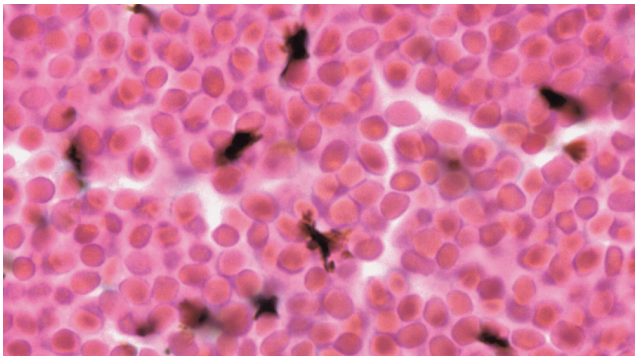


**Figure 10.47**
Large clumps of extracellular nonmalarial pigment in vessel containing erythrocytes. Note that pigment clumps are not round. x800

10.43). Schizonts of *P. falciparum* are occasionally observed in tissue sections. They are usually spherical, 4 µm to 5 µm in diameter, and have a clump of pigment surrounded by tiny merozoites in a rosette pattern (Fig 10.44). Gametocytes are rarely seen in tissue sections.

Malarial pigment is the end product of hemoglobin digestion into a porphyrin conjugated with a protein derived from the globin portion of hemoglobin. Malarial pigment and formalin pigment are morphologically very similar. Both appear microscopically as brown or black crystals that are birefringent under polarized light. However, they can usually be distinguished by certain general characteristics: malarial pigment appears as intracellular round granules (Figs 10.45 & 10.46); formalin pigment is extracellular and frequently rod-shaped (Figs 10.47 & 10.48).

The following steps help to prevent deposition of formalin pigment in congested tissues:

- Trim tissue to less than 3 mm thick.
- Immediately place tissue in phosphate-buffered neu-

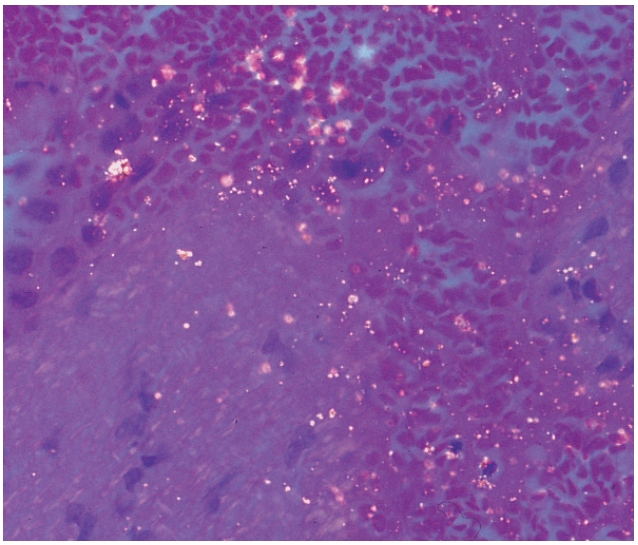


**Figure 10.48**
Birefringent nonmalarial pigment in lung viewed under polarized light. Original magnification x300

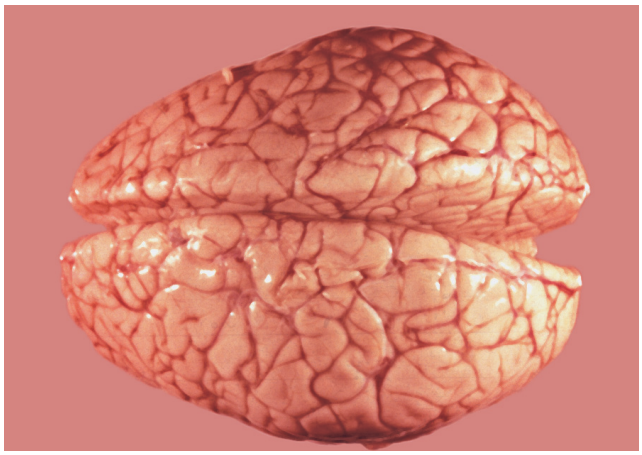


**Figure 10.49**
Brain of child who died of falciparum malaria, showing flat gyri and pink discoloration caused by engorged meningeal vessels.

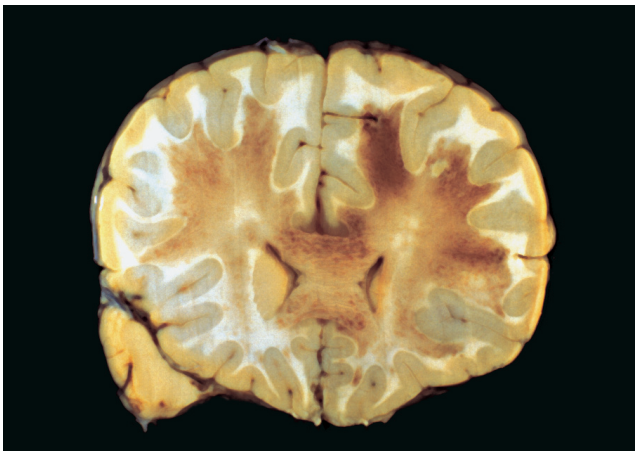


**Figure 10.50**
Brain of patient who died of falciparum malaria, demonstrating congestion and petechial hemorrhage in white matter.

tral formalin.

- Refrigerate fixative and tissues for the first 24 hours.
- Change the formalin whenever it becomes even slightly discolored.

Postmortem findings of falciparum malaria usually include prominent generalized passive congestion. Grossly, there is often gray or brown discoloration of the brain, liver, and spleen caused by malarial pigment.[24]

The brain is edematous with broad, flat gyri (Fig 10.49). Congested arachnoid vessels give it a pinkish cast. When the swollen brain herniates, there may be grooving of the uncinate and cingulate gyri or cerebellar tonsils. The cut surface shows selective congestion and petechial hemorrhage of white matter (Fig 10.50).

Microscopically, masses of erythrocytes fill the lumina of small and medium-sized blood vessels, distending the vessels. Parasitized erythrocytes tend to lie against the endothelial surface of vessels (Fig 10.51). In a ring hemorrhage, a small vessel is occluded by parasitized erythrocytes, surrounded by necrotic parenchyma, then surrounded by hemorrhage of nonparasitized erythrocytes (Fig 10.52).

Dürck's nodes are areas of demyelination and glial proliferation surrounding an occluded vessel (Figs 10.53 & 10.54). Ring hemorrhages and Dürck's nodes are seen in the brains of patients with cerebral malaria of 9 to 10 days duration. Anoxia may result in nonspecific congestion, edema, microinfarcts, and

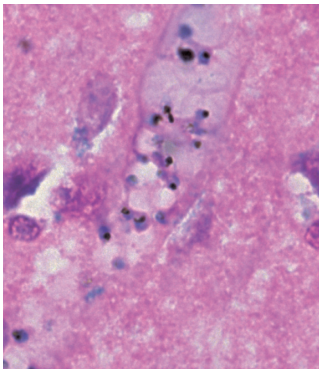


**Figure 10.51**
Trophozoites with blue-staining cytoplasm and black pigment in cerebral capillary. Parasitized erythrocytes tend to lie against capillary endothelium. Thomas x970

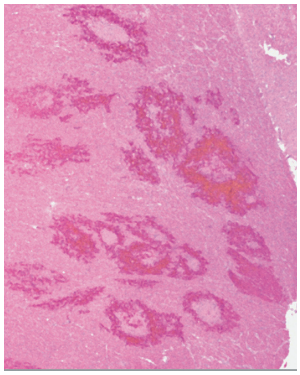


**Figure 10.52**
Multiple ring hemorrhages in brain. x12

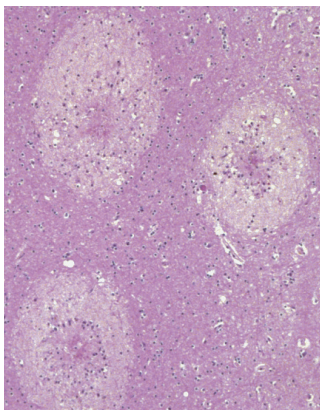


**Figure 10.53**
Dürck's nodes in cerebellum consisting of central occluded vessel surrounded by demyelination and glial proliferation. x40

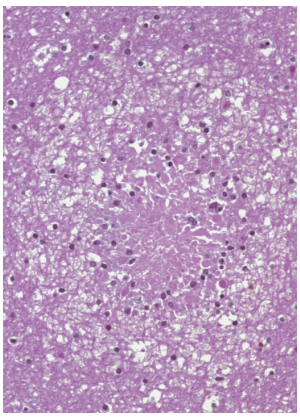


**Figure 10.54**
Dürck's node in cerebellum showing glial proliferation. x150



Figure 10.55
Diffuse slate-gray discoloration in liver caused by accumulation of pigment in Kupffer's cells, characteristic of acute falciparum malaria.

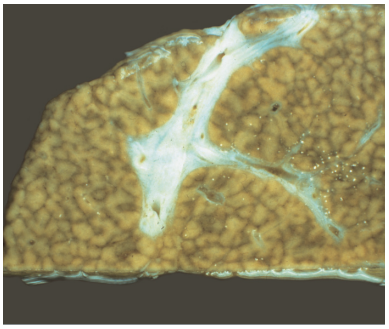


**Figure 10.56**
Well-delineated lobular pattern in liver caused by pigment deposition in portal areas in chronic falciparum malaria.

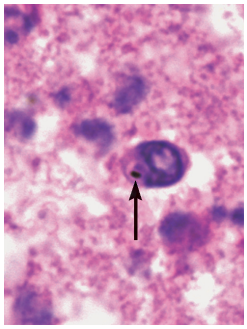


**Figure 10.57**
Malarial parasite in histiocyte in hepatic sinusoid. Note parasite cytoplasm and round clump of pigment (arrow). x1320

focal hemorrhages.

Grossly, the liver appears gray as a result of accumulated malarial pigment (Fig 10.55). There is an increase in Kupffer's cells, which are enlarged and contain malarial pigment, parasites, erythrocytes, and debris from ruptured erythrocytes (Figs 10.40 & 10.43). Pigment deposition extends to portal areas over time (Fig 10.56). Erythrocytes and histiocytes in the sinusoids may contain parasites (Figs 10.45 & 10.57); parasites and malarial pigment are not seen in hepatocytes. Central veins, sinusoids, and portal vein branches may be congested.

In acute malaria, the spleen is enlarged and darkly pigmented (Fig 10.58). Complications of splenomegaly can include rupture, hemorrhage, torsion, and infarction. The red pulp is congested with parasitized erythrocytes, macrophages containing parasites and malarial pigment, and free parasites (Figs 10.59 to 10.63). Malpighian corpuscles are small and indistinct. In chronic malaria, the spleen is even more enlarged and collections of lymphocytes may appear in the sinusoids. Macrophages containing malarial

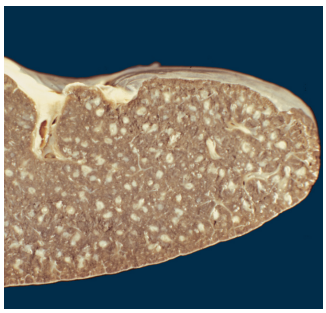


**Figure 10.58**
Spleen of patient with fatal acute falciparum malaria. Gray discoloration is caused by pigment-laden macrophages.

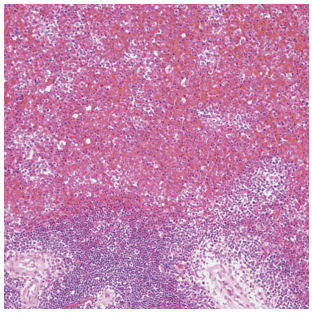


**Figure 10.59**
Congested spleen of patient with falciparum malaria. x60

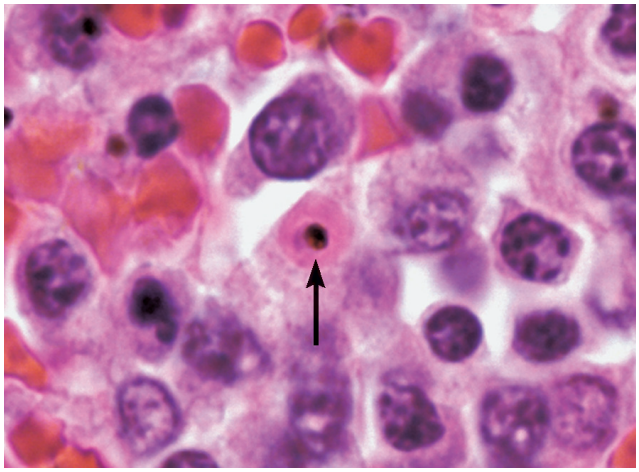


**Figure 10.60**
Trophozoite in splenic erythrocyte in spleen. Note parasite cytoplasm and round clump of pigment (arrow). x1700

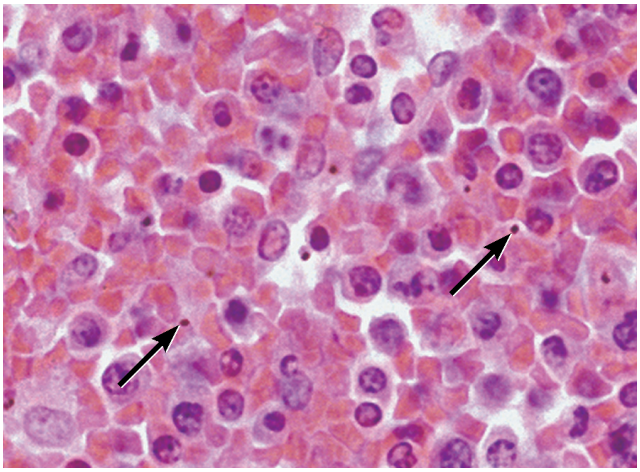


**Figure 10.61**
Congested spleen with tiny clumps of malarial pigment (arrows). x345

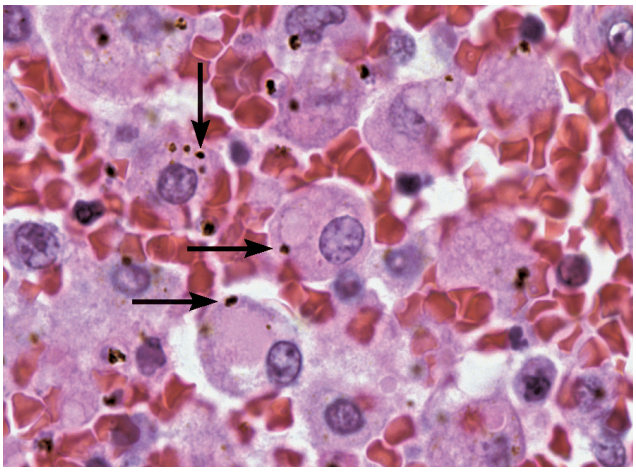


**Figure 10.62**
Macrophages in spleen containing small round clumps of malarial pigment (arrows). x740

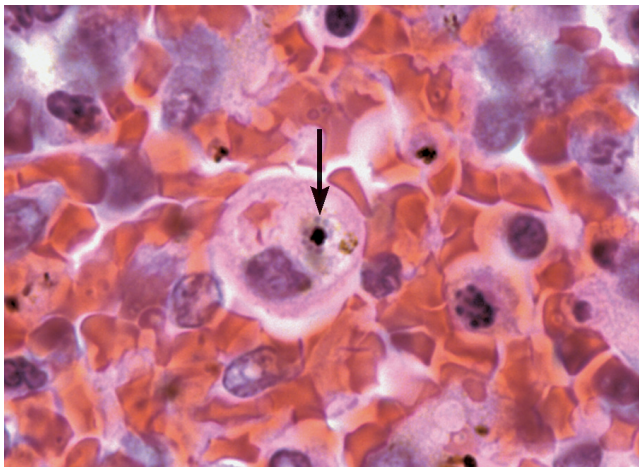


**Figure 10.63**
Macrophage in spleen containing schizont (arrow). Note round clump of pigment and merozoites in rosette pattern. x1140

pigment are increased, and extracellular pigment grains may coalesce and concentrate along arterioles. White pulp may be depleted. Eventually, fibrosis and foci of mineralization called Gamna-Gandy bodies form with iron deposition (Figs 10.64 & 10.65).

Glomerulonephritis can occur in long-standing or recurrent quartan or falciparum malaria. In mesangiopathic glomerulonephropathy caused by quartan malaria, deposition of immune complexes may be demonstrated by electron or immunofluorescence microscopy. In falciparum malaria, renal corticomedullary capillaries may contain parasitized erythrocytes (Fig 10.66). Pigment grains may be seen within glomeruli or phagocytic cells (Fig 10.67). In patients with oliguria, tubular necrosis and hemoglobin casts may be prominent. In patients with blackwater fever, tubules contain hemoglobin casts and erythrocytic debris, and the

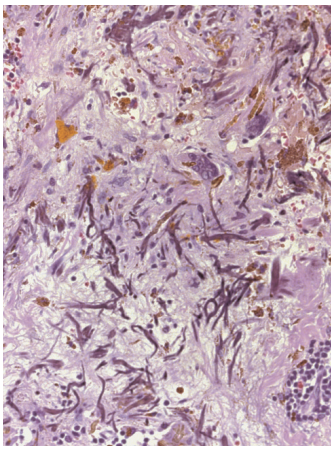


**Figure 10.64**
Gamna-Gandy body in spleen. x125

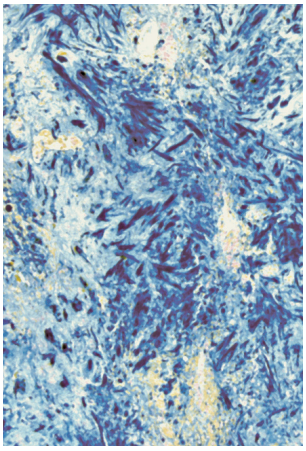


**Figure 10.65**
Iron deposition in Gamna-Gandy body in spleen. Iron x625

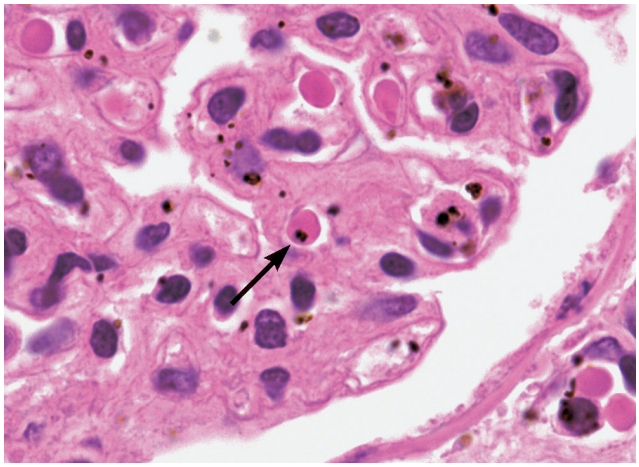


**Figure 10.66**
Malarial pigment in parasitized erythrocyte (arrow) in renal glomerular capillaries. x775

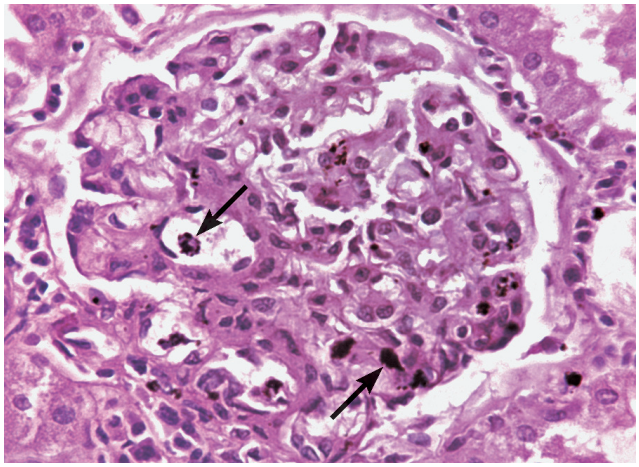


**Figure 10.67**
Renal glomerulus containing malarial pigment (arrows). x440

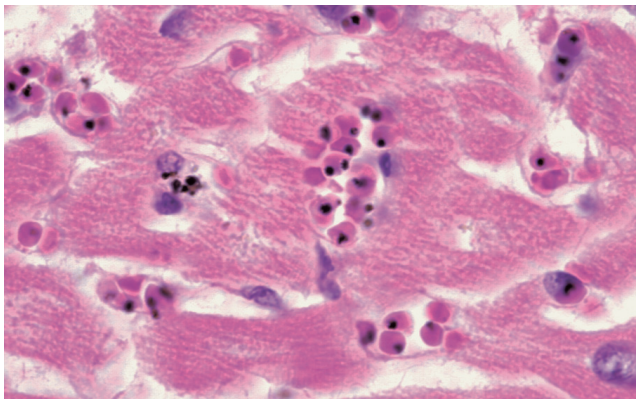


**Figure 10.68**
Capillary in myocardium occluded by parasitized erythrocytes. x480

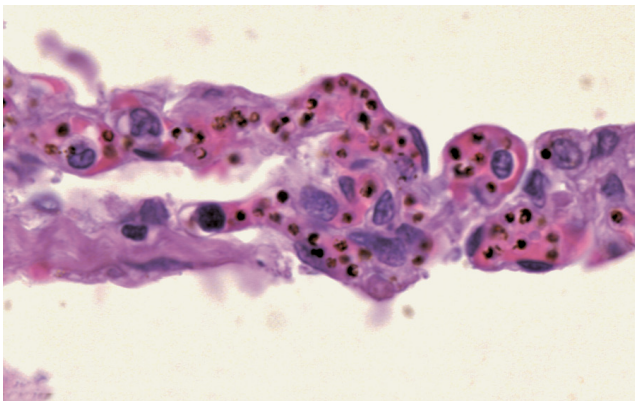


**Figure 10.69**
Parasitized erythrocytes in capillaries of pulmonary alveolar septa. x575

interstitium may contain focal mononuclear cell infiltrates.

Pericardial and endocardial petechiae may be seen in gross specimens. Microscopically, myocardial capillaries are usually congested and occluded with parasitized erythrocytes (Fig 10.68). There may be interstitial edema and focal infiltration by lymphocytes, histiocytes, monocytes, plasma cells, and rare eosinophils.

In the lung, parasitized erythrocytes may be seen within capillaries (Fig 10.69). Alveolar walls may be thickened with chronic inflammatory cells, especially monocytes, lymphocytes, and plasma cells, and alveolar spaces may be filled with proteinaceous fluid, sometimes mixed with erythrocytes.

Involvement of the placenta is more likely in younger women who have had few pregnancies.[11] Possible complications of malarious placenta include decreased placental size, spontaneous abortion, and maternal death. The placenta is severely affected, with numerous sequestered parasites in the intervillous spaces (Fig 10.70). Most parasites are within erythrocytes (Fig 10.71a to 10.71c), but some are found in monocytes (Fig 10.71b) and some are free in the intervillous spaces. Vessels on the fetal side of the placental barrier are usually parasite-free. Rarely, trauma causes mixing of maternal and fetal blood, allowing passage of parasitized cells into fetal circulation, resulting in congenital malaria

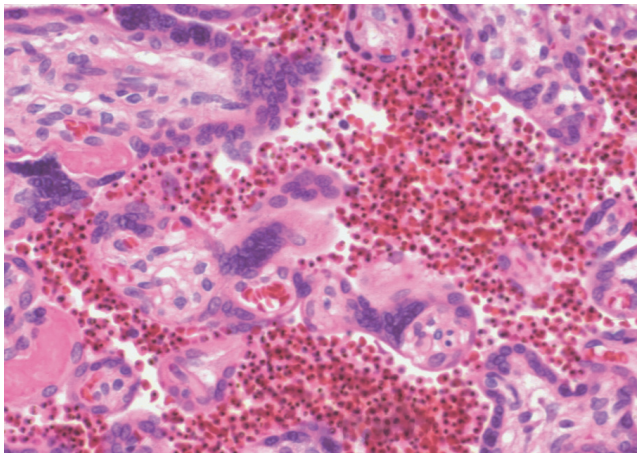


**Figure 10.70**
Placenta from patient with acute falciparum malaria showing massive parasitization of erythrocytes in intervillous spaces. x245

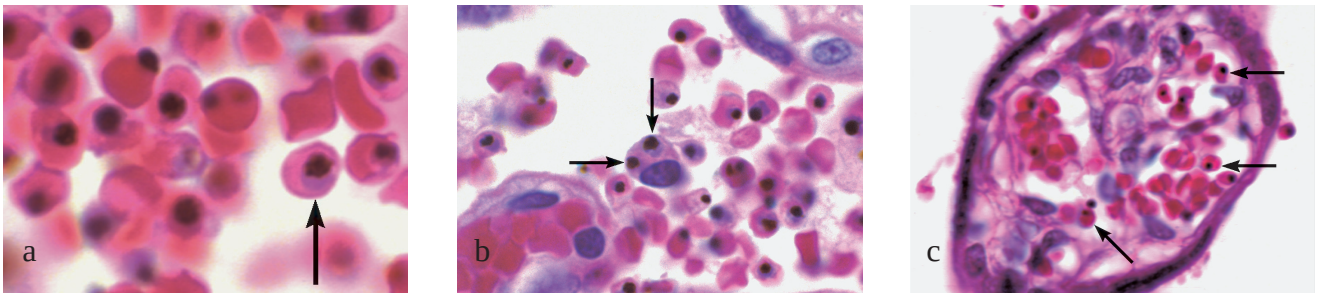



**Figure 10.71 a,b,c**
Placenta with massive parasitization of maternal erythrocytes. a. Parasite pigment is readily visible; faintly stained parasite cytoplasm (arrow) is more subtle. x1500. b. Two trophozoites (arrows) in mononuclear cell in intervillous space. Note absence of parasites in fetal circulation (lower left). x1250. c. Placenta with several parasitized erythrocytes (arrows) in villus of fetal circulation, a rare finding. x810.

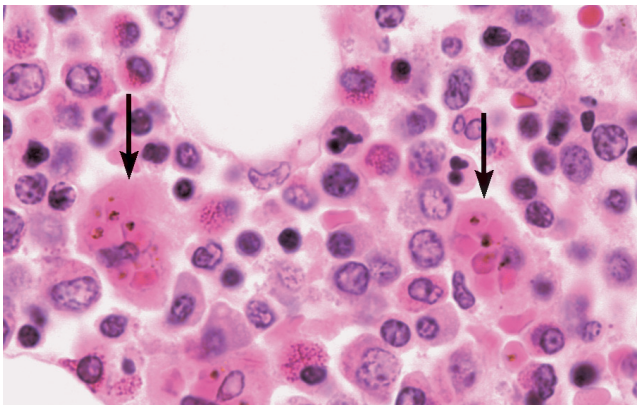


**Figure 10.72**
Macrophages in bone marrow containing parasitized erythrocytes (arrows). x250

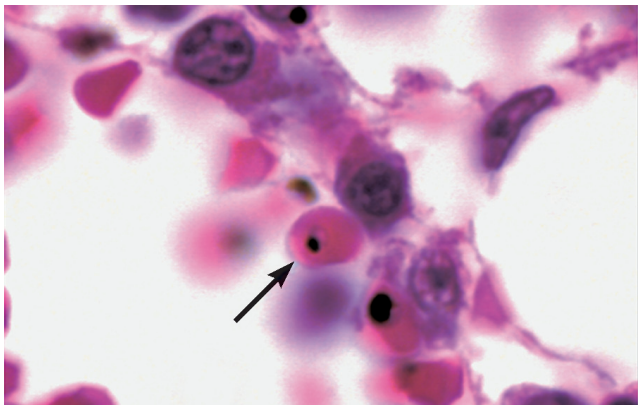


**Figure 10.73**
Bone marrow with parasitized erythrocytes. Note parasite pigment and cytoplasm (arrow). x300

(Fig 10.71c).

Bone marrow may be hypercellular, with hyperplasia of both erythrocytic and leukocytic precursors. Malarial parasites and their pigments are present in phagocytic cells (Fig 10.72), and congested blood spaces may contain large numbers of parasitized erythrocytes (Fig 10.73). Smears of bone marrow may also demonstrate malarial parasites (Fig 10.74).

As in the spleen, lymph nodes are congested with parasitized erythrocytes, but pigment accumulation in macrophages is less than that in the spleen or liver. Lymphoid follicles tend to be inconspicuous, but there is usually prominent histiocytic hyperplasia.

Edema, congestion, hemorrhage, and parasitized erythrocytes within small vessels may be seen in any tissue, including adrenal gland, gastrointestinal tract (Fig 10.75), skin, adipose tissue, retina[25] (Fig 10.76), parathyroid (Fig 10.77), and skeletal muscle, especially in patients with high parasitemia.

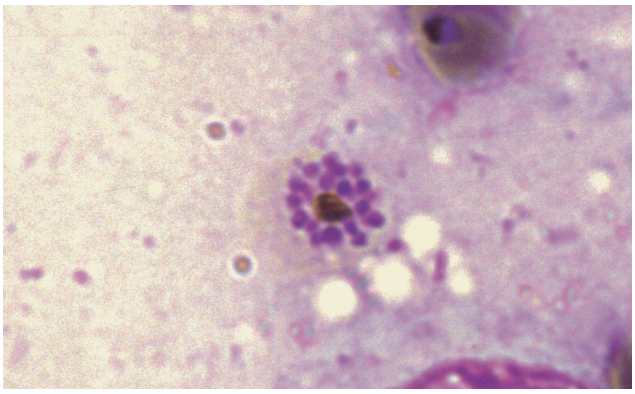


**Figure 10.74**
Smear of bone marrow showing mature schizont with pigment and merozoites in rosette pattern. Dif-Quick x400

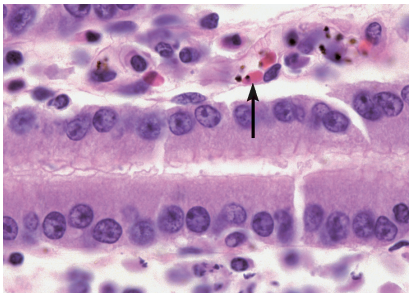


**Figure 10.75**
Mucosal capillaries of stomach occluded by parasitized erythrocytes. Original magnification x250

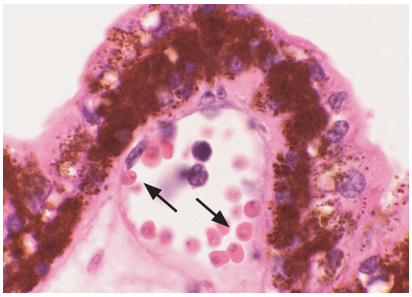


**Figure 10.76**
Parasitized erythrocytes (arrows) in retinal capillary from 53-year-old patient who died of chloroquine-resistant falciparum malaria. x600



**Figure 10.77**
Mature schizont (arrow) in capillary in parathyroid gland .Note dark round clump of pigment and merozoites in rosette pattern. x1550

## Diagnosis

Diagnosis of malaria is usually established in the laboratory by direct examination of thick or thin peripheral blood films (Table 10.1).[26] Microscopic diagnosis is relatively cost-effective and has a sensitivity of approximately 50 parasites per ml of blood. A highly skilled microscopist can estimate the level of parasitemia and identify all species of *Plasmodium*, based on pertinent factors such as morphologic appearance of the parasite and erythrocytes, geographic considerations, and clinical symptoms. Specific diagnosis depends on scrutinizing blood films and accurately identifying all observable forms of the parasite, determining the degree of development of an observed morphologic feature, and how often it occurs.

Because most morphologic forms of malarial parasites and configurations of erythrocytes can be found in all 4 types of malaria, and a given specimen rarely demonstrates all the classic features of a single species, the most useful diagnostic approach combines comparison and exclusion.

For example:

- Erythrocytes enlarged: If a large number of parasitized erythrocytes are oval or fimbriated, the species is likely to be *P. ovale*. A finding of very few oval or fimbriated parasitized erythrocytes suggests *P. vivax*.
- Band erythrocytes enlarged: All 4 species of *Plasmodium* have thin band trophozoites, but only those of *P. malariae* are large enough to occupy 50% to 75% of the erythrocyte.
- Large numbers of ring trophozoites: If the examiner sees only a large number of ring trophozoites, the species is most likely *P. falciparum*.
- If only a few ring trophozoites are observed, it may not be possible to determine the species, and the specimen should be signed out as "malaria, species undetermined."
- In *vivax*, quartan, and *ovale* malaria, parasitemia is usually less than 2%. In *falciparum* malaria, parasitemia may be 40% or higher.
- If parasitized erythrocytes are enlarged, quartan malaria can be excluded, except in mixed infections.
- If gametocytes are round, *falciparum* malaria can be excluded.

Some authorities believe that parasite morphology may be affected by geographic location, parasite strain, and the patient's age, immune status, and treatment.[27] Investigating the patient's travel history may provide clues to the species of *Plasmodium*. Although morphologic features of the parasite are of greater diagnostic value than travel history, a thorough examiner must determine where the patient has been and what species have been reported in those areas.

Mixed infections are probably underdiagnosed. When one species predominates in a blood film, the other species is easily overlooked. Furthermore, upon diagnosing one species of malaria, the microscopist usually looks no further. To diagnose a second species, one of its diagnostic forms must also be identified. All 4 species of *Plasmodium* have diagnostic forms:

- *vivax*: ameboid trophozoite in enlarged erythrocyte with Schüffner's dots.
- *falciparum*: crescent-shaped gametocyte.
- *malariae*: broad band trophozoite.
- *ovale*: oval, fimbriated, enlarged erythrocytes.
- Mature schizonts of all 4 species are usually diagnostic when other stages are also present.

### Preparation and Examination of Peripheral Blood Films

The biggest pitfall in most laboratories in developed countries is leaving too great a delay between taking the blood sample and making the blood films. As blood cools to room temperature, male gametocytes will divide and release microgametes: these are long sinuous filamentous structures that can be mistaken for organisms such as *Borrelia*. If the blood is kept at warmer temperatures, schizonts will rupture and merozoites invading erythrocytes will mistakenly give the appearance of the appliqué form of *P. falciparum*. If *P. vivax* or *P. ovale* is left for several hours in EDTA, the build up of acid in the sample will cause the parasitized erythrocytes to shrink and the parasite will roll up, simulating the appearance of *P. malariae*. This problem is made worse if anticoagulants such as heparin or citrate are used. The anticoagulant that causes the least problems is EDTA. Romanowsky stain or a variant stain is usually used. Some laboratories mistakenly use the same staining pH as they do for routine haematology blood films (pH 6.8): malaria blood films must be stained at pH 7.2, or Schüffner's dots and James's dots will not be seen.

Both thick and thin films should be prepared, preferably on the same slide, from any patient suspected of having malaria (Fig 10.78). Thick films are useful for screening because a larger volume of blood is examined and erythrocytes are hemolyzed, concentrating the parasites and possibly revealing multiple stages. For diagnosis, thick films are significantly more sensitive than thin films because 16 to 30 times as much blood is examined. Thick films can be many

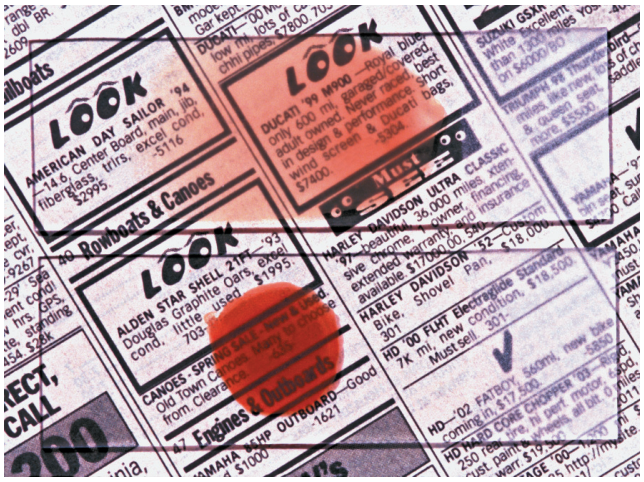



**Figure 10.78**
Thin (top) and thick blood films prepared on separate slides. Newsprint should be readable through feathered edge of properly prepared thin film. (Typically, in most busy clinics, both thin and thick smears are placed on the same slide.)

cell layers thick and are never fixed, since fixation prevents dehemoglobinization. The examiner should use the 100x oil immersion objective to study thick films, and should search for at least 5 minutes (an estimated 100 fields) before reporting a finding of no parasites.

Thin blood films are helpful in species identification because they reveal morphologic details of parasites and erythrocytes not apparent on thick films. On an ideal thin film, the cells are in a single layer and do not overlap. Erythrocytes infected by older parasites are more frequently seen along the feathered edge of the thin film; ring forms are usually evenly distributed. To determine whether parasitized erythrocytes are enlarged or fimbriated, compare them with adjacent uninfected erythrocytes.

Blood films must be carefully prepared and meticulously stained.[28] Slides should be spotlessly clean and free of chemicals, grease, dust, and scratches. Thin films should be fixed in pure methyl alcohol before staining. Ideally, films should be stained within 24 hours, and no later than 72 hours, before the blood loses its affinity for stain. Although Wright's stain can be used for thin films, the most dependable stain for visualizing malarial parasites is Giemsa diluted with distilled water and buffered to pH 7.0 to 7.2. Field's stain is fast and convenient, but the staining process occasionally washes off the entire film.[29]

Erythrocytes on Giemsa-stained thin films should be pale pink and parasites densely stained. Staining artifacts (Fig 10.79) and other structures (Figs 10.80 & 10.81), including platelets (Fig 10.82), may be mistaken for malarial parasites on thin films. To prevent errors, a skilled examiner must

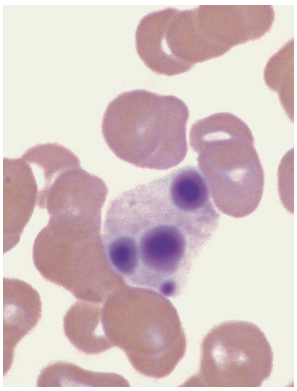


**Figure 10.79**
Staining artifact, not to be mistaken for malarial parasite. Giemsa x1400

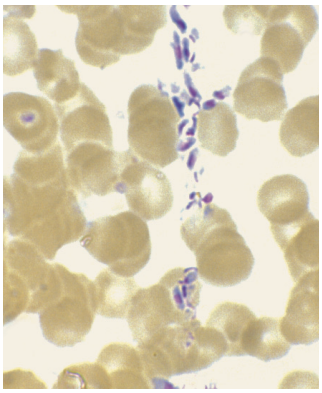


**Figure 10.80**
Unknown structures in thin peripheral blood film, representing no known human pathogen. Giemsa x825

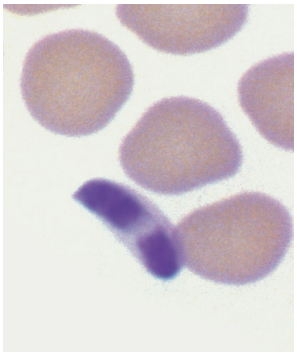


**Figure 10.81**
Unknown pseudoparasite in thin peripheral blood film, representing no known human pathogen. Giemsa x1775

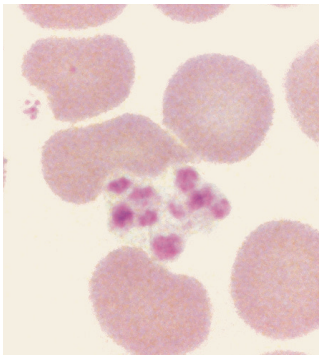


**Figure 10.82**
Blood platelets in thin peripheral blood film. Giemsa x1600

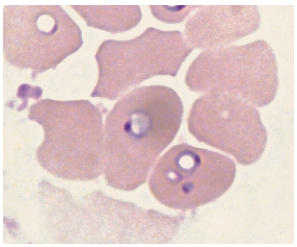


**Figure 10.83**
Ring trophozoites of *Babesia microti* in thin peripheral blood film. Giemsa x780

be familiar with the appearance of normal blood constituents. Because all stages of the erythrocytic cycle may not be visible in a single smear, repeated examinations should be made at different times of day during the course of infection. If the first blood film is negative, additional thick and thin films should be obtained every 6 hours for 24 hours. Examining blood films under polarized light may simplify

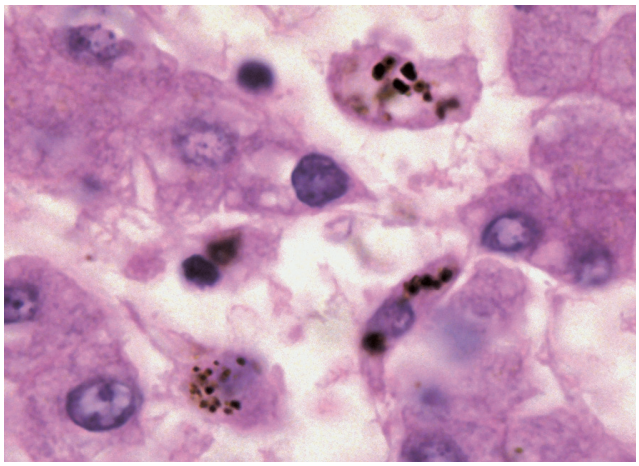


**Figure 10.84**
Section of liver from 21-year-old Vietnam veteran with acute falciparum malaria. Treatment killed malarial parasites; only remnants of infection are round clumps of malarial pigment in Kupffer's cells. Patient died of staphylococcal infection 6 days post-treatment. x965

and accelerate screening for malarial parasites.

*Plasmodium* sp must be differentiated from *Babesia* sp, protozoa that also invade erythrocytes and closely resemble malarial parasites (Fig 10.83). *Babesia* sp are round, rod-shaped, piriform, or ameboid, but lack pigment. Parasitized erythrocytes are normal in size. Patients with babesiosis have no schizonts or gametocytes in peripheral blood (see Topic 11 on Babesiosis).

## Other Methods of Diagnosis

Postmortem, a diagnosis of malaria is made by identifying malarial parasites or their pigment in histologic sections. (Morphologic features are described above and in Figures 10.40 to 10.77.) Adequate treatment for malaria usually eliminates parasites from the patient, but malarial pigment accumulates in the liver and is readily observable at autopsy (Fig 10.84). Absence of malarial pigment in the liver at autopsy suggests that there was no recent attack of acute falciparum malaria.

Electron microscopy is not commonly used for diagnosis, but can reveal characteristic knobs on the surface of an erythrocyte parasitized by *P. falciparum* (Fig 10.38).

The quantitative buffy coat (QBC®) technique identifies malarial parasites by fluorescent dye.[30] A glass capillary tube containing fluorescent stain is filled with blood and a

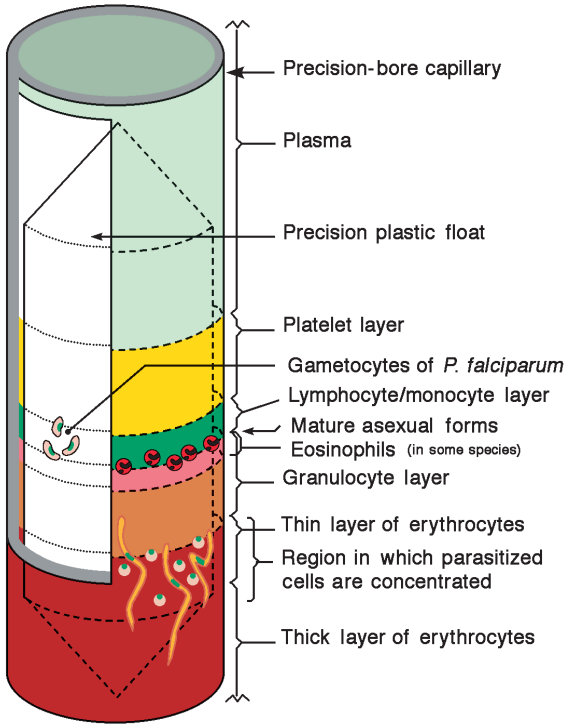



**Figure 10.85**
QBC® tube for detecting malarial parasites.

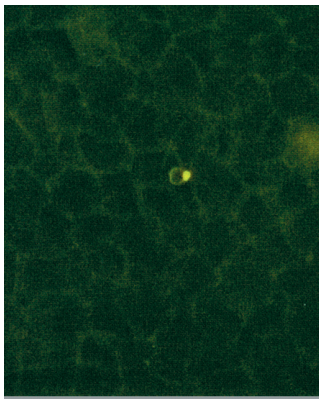


**Figure 10.86**
Trophozoite of *Plasmodium falciparum* detected by QBC® method. Note well-defined, regularly shaped cytoplasm.

plastic float is inserted (Fig 10.85). When the tube is centrifuged, parasitized erythrocytes localize in the upper layer because of their lower density. Parasites are then detectable by ultraviolet or fluorescence microscopy (Fig 10.86).

Enzyme-linked immunosorbent assay (ELISA) and radioimmunoassay (RIA) tests can detect very low densities of malarial antigens in peripheral blood.[31,32] These tests are nearly as sensitive as microscopic techniques and do not require a microscope or an experienced microscopist. Rapid dipstick tests that employ immunochromatographic techniques to detect parasite antigens can provide a crude estimate of the level of parasitemia. These tests have a low turnaround time and do not require skilled personnel or special equipment, but some can detect only one species of *Plasmodium*. Tests targeting histidine-rich protein-2 (ParaSight®-F and ICT Malaria Pf)[29,33,34] detect only *P. falciparum*. OptiMAL® targets lactate dehydrogenase and can distinguish *P. falciparum* from *P. vivax*.[35]

DNA hybridization and PCR methods detect *Plasmodium*-specific DNA sequences in erythrocytes. These assays are often highly sensitive and specific, but may require expensive equipment.[36]

Indirect fluorescent antibody (IFA) test is the preferred method for detecting antimalarial antibodies in serum.[37] Serologic assays cannot distinguish current and prior infections and are used primarily in epidemiological studies.

## Treatment and Prevention

Chloroquine (Aralen®) was once the treatment of choice for malaria but is no longer reliably effective outside the Middle East, the Caribbean, and Central America because of resistant *P. falciparum* strains.[38] *Plasmodium vivax* also is chloroquine-resistant in some endemic areas, particularly Papua New Guinea and Indonesia.[39] Chloroquine-resistant malaria can be treated with a variety of other agents, including mefloquine (Lariam®),[38] atovaquone-proguanil (Malarone®),[40] doxycycline, sulfadoxine-pyrimethamine (Fansidar®), halofantrine, and quinine combined with tetracycline. When atovaquone-proguanil is used to treat vivax malaria, it should be followed by primaquine to eradicate persistent liver hypnozoites. Resistance to mefloquine and sulfadoxine-pyrimethamine has become a significant problem in some parts of Southeast Asia and South America.[39] Combining mefloquine with artemisinin derivatives may decrease resistance.[41] Sulfadoxine-pyrimethamine-resistant malaria has been reported in the Amazon Basin, Southeast Asia, and some countries in eastern and southern Africa.

For complicated falciparum malaria, supportive treatment may include management of hypoglycemia, seizures, pulmonary edema, and renal failure. Exchange transfusion is sometimes recommended for nonimmune patients with high parasitemia.

Oral weekly mefloquine may be the best chemoprophylaxis for travelers in areas endemic for chloroquine-resistant *P. falciparum*.[42] Doxycycline is an effective alternative for travelers who cannot tolerate the side effects of mefloquine. Proguanil taken daily in conjunction with weekly chloroquine is an option for pregnant women traveling in sub-Saharan Africa.[38] Weekly oral doses of chloroquine phosphate are effective prophylaxis in areas with chloroquine-sensitive *P. falciparum*. Oral weekly hydroxychloroquine sulfate (Plaquenil®) is an alternative to chloroquine phosphate, and atovaquone-proguanil is useful as prophylaxis. Long-term travelers who have likely been exposed to *P. vivax* or *P. ovale* may be asymptomatic carriers and at risk for later development of malaria. Primaquine phosphate administered orally once daily for 14 days after departure from an endemic area can eliminate a carrier state.[38]

*Anopheles* mosquitoes bite between dusk and dawn. During waking hours, bites are best prevented by covering most skin with clothing and treating exposed skin with an insect repellent that contains a 30% to 35% concentration of N,N diethyl-meta-toluamide (deet).[38] In sleeping areas that are not screened or air-conditioned, bites can be prevented by sleeping under mosquito netting treated with permethrin or deltamethrin, or by spraying the room with pyrethroid-containing formulas.[43] Other preventive measures include application of environmental mosquito larvicides and drainage of mosquito breeding sites.

Several types of antimalarial vaccine are currently being studied, including cocktails of antigens of asexual blood-stage organisms, DNA recombinant protein, and transmission-blocking vaccines. The search for an effective vaccine is hampered by the parasites' remarkable capacity to vary critical antigenic structures.[44]

## References


1. Ross R. Researches on malaria, Nobel Lecture, December 12, 1902. Available at: http://nobelprize.org/nobel-prizes/medicine/laureates/1902/ross-lecture.html. Accessed March 7, 2011.
2. Grassi GB, Bignami A, Bastianelli G. Report of studies done on malaria during the month of January [in Italian]. *RC Accad Lincei*.1899;8:100-104.
3. Gardner MJ, Hall N, Fung Eula, et al. Genome sequence of the human malaria parasite *Plasmodium falciparum*. *Nature*. 2002;419: 498-511.
4. Holt RA, Subramanian GM, Halpern A, et al. The genome sequence of the malaria mosquito *Anopheles gambiae. Science*. 2002;298:129-149.
5. Roll Back Malaria. Malaria endemic countries [Malaria Foundation International Web site]. Available at http://www.malaria.org/ endemiclist.html. Accessed Mar. 7, 2011.
6. World Health Organization. Rolling back malaria. In: Jamison DT, Creese A, Prentice T, et al, eds. *World Health Report 1999: Making a Difference*. Geneva, Switzerland:WHO;1999:49-63.
7. Diagne N, Rogier C, Sokhna CS, et al. Increased susceptibility to malaria during the early postpartum period. *N Engl J Med.* 2000;343:598-603.
8. El-Bahnasawy MM, Dabbous HKh, Morsy TA. Imported malaria as a threat to Egypt. *J Egypt Soc Parasitol.* 2010;40:773-788.
9. Smith JW, Melvin DM, Orihel TC, Ash LR, McQuay RM, Thompson JH Jr. Atlas of Diagnostic Medical Parasitology. I. Blood and Tissue Parasites. American Society of Clinical Pathologists: 1976.
10. Wilcox A. Manual for the Microscopical Diagnosis of Malaria in Man. Public Health Service Publication No. 796. Washington, DC: US Department of Health, Education and Welfare; 1960.
11. Anagnos D, Lanoie LO, Palmieri JR, Ziefer A, Connor DH. Effects of placental malaria on mothers and neonates from Zaire. *Z Parasitenkd* 1986;72:57-64.
12. Kean BH, Smith JA. Death due to estivo-autumnal malaria: a resume of one hundred autopsy cases, 1925-1942. *Am J Trop Med Hyg* 1944;24:317-322.
13. World Health Organization. 2004 Technical consultation on Malaria and HIV Interactions in Public Health Policy Implications. 23-25 (Geneva, Switzerland).
14. Jouin H, Garraud O, Longacre S, Baleux F, Mercereau-Puijalon O, Milon G. Human antibodies to the polymorphic block 2 domain of the *Plasmodium falciparum* merozoite surface protein 1 (MSP-1) exhibit a highly skewed, peptide-specific light chain distribution. *Immunol Cell Biol.* 2005;83:392-395.
15. Ockenhouse CF, Ho M, Tandon NN, et al. Molecular basis of sequestration in severe and uncomplicated *Plasmodium falciparum* malaria: differential adhesion of infected erythrocytes to CD36 and ICAM-1. *J Infect Dis.* 1991;164:163-169.
16. Coltel N, V. Combes, Hunt NH, Grau GE. Cerebral malaria: a neurovascular pathology with many riddles still to be solved. *Curr Neurovasc Res.* 2004;1(2): 91-110.
17. Couper KN, Blount DG, Wilson MS, Halfalla JC, et al. IL-10 from CD4CD25Foxp3CD127 adaptive regulatory T cells modulates parasite clearance and pathology during malaria infection. *PLoS Pathog.* 2008;4(2): e1000004.
18. Milner DA, Jr. Rethinking cerebral malaria pathology. *Curr Opin Infect Dis.* 2010;23:456-463.
19. Tobie JE, Abele DC, Wolff SM, Contacos PG, Evans CB. Serum immunoglobulin levels in human malaria and their relationship to antibody production. *J Immunol.*1966;97:498-505.
20. Muehlenbachs A, Fried M, Lachowitzer J, Mutabingwa TK, Duffy PE. Genome-wide expression analysis of placental malaria reveals features of lymphoid neogenesis during chronic infection. *J Immunol* 2007;179:557-565
21. UNICEF Malaria Technical Note # 6. Malaria and HIV. 2003 (February) #1c 2470.doc. Accessed January 2011.
22. Stephens R, Langhorne J. Priming of CD4+ T cells and development of CD4+ T cell memory; lessons for malaria. *Parasite Immunol.* 2006;S 25:25-30.
23. Atkinson CT, Aikawa M. Ultrastructure of malaria-infected erythrocytes. *Blood Cells.* 1990;16:351-368.
24. Winslow DJ, Connor DH. Human malaria. *Med Times.* 1967;95:593-608.
25. Hidayat AA, Nalbandian RM, Sammons DW, Fleischman JA, Johnson TE. The diagnostic histopathologic features of ocular malaria. *Ophthalmology.* 1993;100:1183-1186.
26. Moody A. Rapid diagnostic tests for malaria parasites. *Clin Microbiol Rev.* 2002;15:66-78.
27. Gabaldon A, Garnham PCC, Macdonals G, Pampana EJ. Terminology of Malaria and of Malaria Eradication. Geneva, Switzerland: WHO; 1963.
28. Ash LR, Orihel TC. *Atlas of Human Parasitology*. Chicago, Ill: American Society of Clinical Pathologists; 1980:4.
29. Lema OE, Carter JY, Nagelkerke N, et al. Comparison of five methods of malaria detection in the outpatient setting. *Am J Trop Med Hyg.* 1999;60:177-182.
30. Wardlaw SC, Levine RA. Quantitative buffy coat analysis. A new laboratory tool functioning as a screening complete blood cell count. *JAMA.* 1983;249:617-620.
31. Mackey L, McGregor IA, Lambert PH. Diagnosis of *Plasmodium falciparum* infection using a solid-phase radioimmunoassay for the detection of malaria antigens. *Bull World Health Organ.* 1980;58:439-444.
32. Spencer HC, Collins WE, Skinner JC. The enzyme-linked immunosorbent assay (ELISA) for malaria. II. Comparison with the malaria indirect fluorescent antibody test (IFA). *Am J Trop Med Hyg.* 1979;28:933-936.
33. Forney JR, Magill AJ, Wongsrichanalai C, et al. Malaria rapid diagnostic devices: performance characteristics of the ParaSight F device determined in a multisite field study. *J Clin Microbiol.* 2001;39:2884-2890.
34. Singh N, Valecha N, Sharma VP. Malaria diagnosis by field workers using an immunochromatographic test. *Trans R Soc Trop Med Hyg.* 1997;91:396-397.
35. Cooke AH, Chiodini PL, Doherty T, Moody AH, Ries J, Pinder M. Comparison of a parasite lactate dehydrogenase-based immunochromatographic antigen detection assay (OptiMAL) with microscopy for the detection of malaria parasites in human blood samples. *Am J Trop Med Hyg.* 1999;60:173-176.
36. Rubio JM, Benito A, Roche J, et al. Semi-nested, multiplex polymerase chain reaction for detection of human malaria parasites and evidence of *Plasmodium vivax* infection in Equatorial Guinea. *Am J Trop Med Hyg.* 1999;60:183-187.
37. Contreras CE, Pance A, Marcano N, Gonzalez N, Bianco N. Detection of specific antibodies to *Plasmodium falciparum* in blood bank donors from malaria-endemic and non-endemic areas of Venezuela. *Am J Trop Med Hyg.* 1999;60:948-953.
38. Juckett G. Malaria prevention in travelers. *Am Fam Physician.* 1999;59:2523-2530, 2535-2536.
39. Barat LM, Bloland PB. Drug resistance among malaria and other parasites. I*nfect Dis Clin North Am.* 1997;11:969-987.
40. Looareesuwan S, Chulay JD, Canfield CJ, Hutchinson DB. Malarone (atovaquone and proguanil hydrochloride): a review of its clinical development for treatment of malaria. *Am J Trop Med Hyg.* 1999;60:533-541.
41. Bloland PB, Ettling M, Meek S. Combination therapy for malaria in Africa: hype or hope? *Bull World Health Organ.* 2000;78:13781388.
42. Kramer MH, Lobel HO. Antimalarial chemoprophylaxis in infants and children. *Paediatr Drugs.* 2001;3:113-121.
43. Newton P, White N. Malaria: new developments in treatment and prevention. *Annu Rev Med.* 1999;50:179-192.
44. Good MF, Doolan DL. Malaria vaccine design: immunological considerations. *Immunity*. 2010;33:555-566.


## Acknowledgements


*Figure 10.32*
Contributed by Venetia Valiga

*Figure 10.33*
Contributed by Robert W. Gwadz

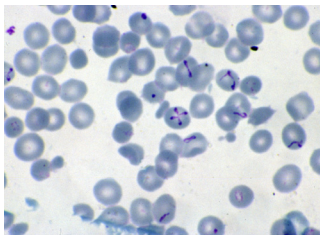
*Figure 10.37*
Contributed by William Gordon

*Figure 10.85*
Contributed by SC Wardlaw

*Figure 10.86*
Courtesy of Becton Dickinson







11

# Babesiosis
## (*Piroplasmosis*)

***George D. Imes, Ronald C. Neafie, and Francis M. Chiricosta***

## Definition

Babesiosis is a malaria-like, zoonotic disease transmitted by ticks and caused by protozoa of the genus *Babesia*, which invade and destroy erythrocytes.

## Synonyms

*Babesia* has been known by other genus names, including *Piroplasma*, *Nuttallia*, *Microbabesia*, *Babesiella*, and *Gonderia*. Babesiosis has been called tick fever, Texas tick fever, Texas cattle fever, red water, bloody murrain, splenic fever, and biliary fever. Because all *Babesia* species are piroplasms, a more inclusive term for human infections caused by these organisms would be piroplasmosis. Development and refinement of methods for identifying and classifying organisms has resulted in some *Babesia* and *Babesia*-like organisms being reclassified to other genera, such as *Theileria*.[1,2] (Fig 11.1)

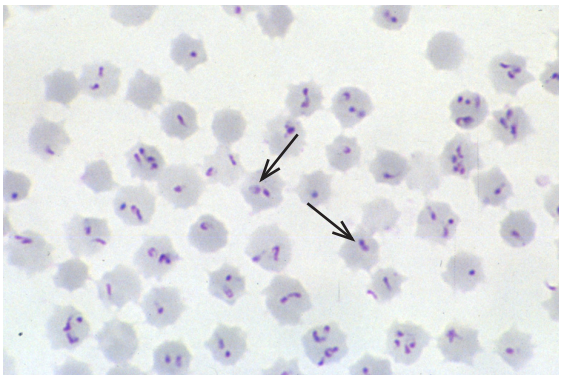


**Figure 11.1**
*Theileria parva* from a cow in Africa. Note numerous small pear or tear-drop shaped piriforms (arrows) in erythrocytes. Giemsa. Original magnification x330

## General Considerations

Babès discovered the organism in Romania in 1888 while studying cattle dying with fever and hemoglobinuria. Believing the organism was a bacterium, be called it *Haematococcus bovis*.[3] In 1889 Smith and Kilborne recognized a protozoon as the cause of Texas cattle fever and called it *Pyrosoma bigeminum* (*Babesia bigemina*) (Fig 11.2). In 1893 they established the role of the tick *Boophilus annulatus*, the first proven arthropod vector of an infectious disease, in the transmission of Texas cattIe fever.[4] They also outlined the transovarial transmission of infection by the female tick to her offspring, an essential element that explained the unusual epizootiology of Texas cattle fever.

In 1904, Wilson and Chowning observed pirosomes that were undoubtedly *Babesia* in the blood of patients who had Rocky Mountain spotted fever in Montana.[5] The first human infection was documented in 1957 in a splenectomized Yugoslavian from an area where cattle were infected with *Babesia bovis* (Fig 11.3).[3] In June of 1966, a 46-year-old splenectomized resident of San Francisco became ill and later diagnosed with babesiosis. This Californian frequented sparsely populated areas. The species of the *Babesia* was not determined, but was thought to be from a wild animal,



**Figure 11.2**
Thin blood film showing 2 piriform *Babesia bigemina*, a parasite of cattle, attached at their ends (arrow). Giemsa. Original magnification x330

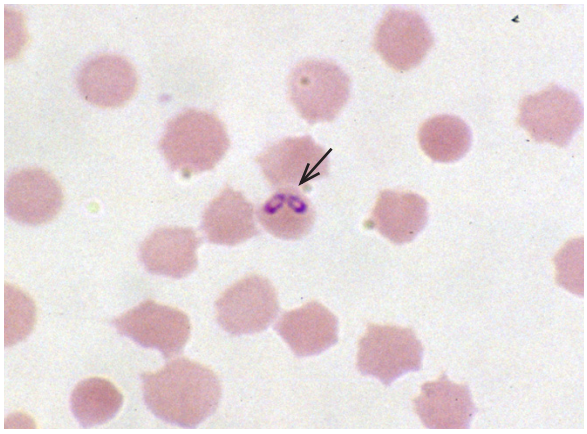


**Figure 11.3**
Thin blood film of *Babesia bovis* (arrow), a parasite of cattle. Note typical paired trophozoites resulting from binary fission. Giemsa. Original magnification x330

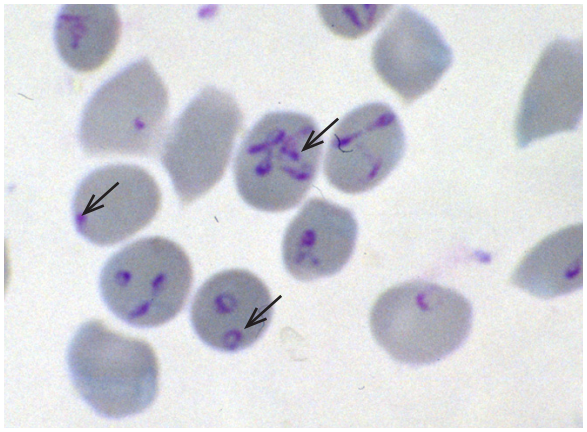


**Figure 11.4**
Thin blood of *Babesia divergens* from human patient, Note erythrocytes infected with multiple parasites in ring forms, divergent forms (forms diverging at a wide angle of up to 180°), piriform, and chromatin dots (arrows). Giemsa. Original magnification x330

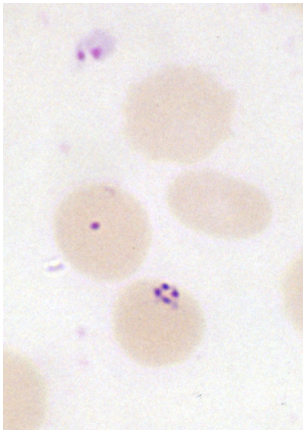


**Figure 11.5**
Thin blood of *Babesia microti* in patient from Fire Island, New York. Note tetrad formation following schizogony. Giemsa. Original magnification x330

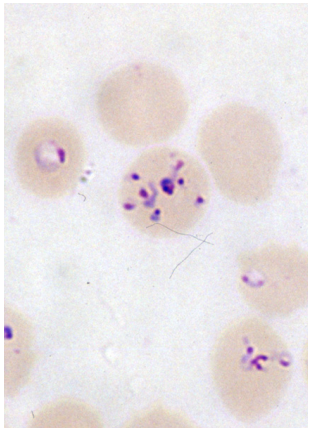


**Figure 11.6**
*Babesia microti* from patient described in Figure 11.5. Note ring forms and pleomorphism. One erythrocyte contains at least 8 parasites.Giemsa. Original magnification x330

most likely a small rodent.[6] In 1968, a third case of human babesiosis was reported in another splenectomized patient.[7] This fisherman from Northern Ireland fell ill August 29, 1967 and died September 5. In this patient the infectious agent was called *Babesia divergens*, another cattle *Babesia* (Fig 11.4). In 1969, human babesiosis developed in a non-splenectomized patient from Nantucket Island. Significantly, this was the first time *Babesia microti* was implicated as a cause of human babesiosis (Figs 11.5 and 11.6).[8]

The first reported transmission by blood transfusion was in 1979.[9] Transfusion transmitted babesiosis is recognized as an increasing problem even outside endemic areas.[10-15] More than 100 transfusion-transmitted cases have been reported, most in the US, but also in Europe and Japan.[16-18] At least 11 deaths following transfussion have been reported in the US.

Approximately 100 species of *Babesia* are currently known and new species are being discovered. *Babesia* infect a wide variety of wild and domestic animals, including cattle,[19] sheep, goats, wild ruminants, horses, donkeys, dogs, cats, swine, raccoons, skunks, fowl, monkeys, and wild rodents. Despite this wide distribution among animals, human infections are not common, probably due to the characteristic host specificity of *Babesia*. Although first documented in humans only about half a century ago, the disease has likely afflicted humans for much longer. Humans are susceptible to infection with: 1) *B. microti*, which infects several wild rodent species and is the cause of most human infections reported in the United States; 2) *B. divergens*, which primarily infects cattle in continental Europe,

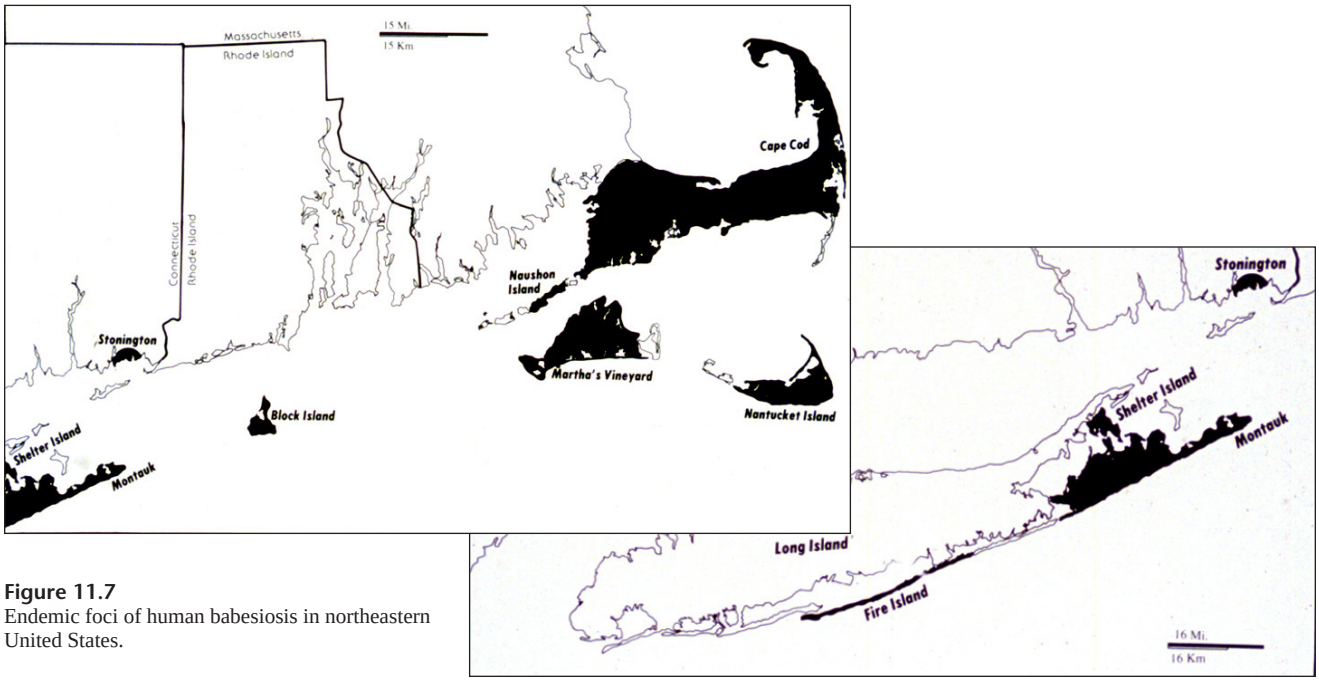



**Figure 11.7**
Endemic foci of human babesiosis in northeastern United States.

the United Kingdom, and Ireland, but also infects splenectomized humans and some rodent species; and 3) novel *Babesia*-like organisms detected by microscopy but with genetic, biologic, and serologic differences from known species. Examples include parasites called WA1, CA1, MO1 and EU1. WA1 and CA1 were the etiologic agents in several human infections in Washington State and California; MO1 has appeared only in Missouri; EU1 was obtained from patients in Italy and in Austria.

## Epidemiology

Incidence of clinical infection with *Babesia* organisms is highly variable from location-to-location. Infection depends on many factors: 1) an animal reservoir; 2) a *Babesia* to which humans are susceptible, or a human host who is asplenic or otherwise immunocompromised; 3) a genus of *Ixodidae* (hard bodied tick) which can transmit the parasite; and 4) a suitable tick habitat. Finally, humans must put themselves at risk by frequenting a tick habitat in an endemic area in the months when infective stages of ticks are feeding. Transfusion transmission can occur anywhere and outside of tick-feeding season, because blood for transfusion can be collected in a different region of the country and asymptomatic donors may carry the parasite. In the US, as of January 2011, babesiosis is a nationally-reportable disease.[20] The systematic collection of these data nationwide should help improve knowledge of the geographic distribution of babesiosis and possibly the spectrum of disease.

Endemic areas in the United States have included islands off the southeastern coast of New England, including Long Island, New York (Fig 11.7),[21,22] and areas of some eastern and upper Midwestern states.[23] Increasing prevalence of tick-borne babesiosis has spread to Rhode Island, New Jersey, and Maryland.[24-26] In the western United States, babesiosis was reported twice prior to the 1990s; both cases involved asplenic patients from California. The protozoon in these infections was a small, unidentified *Babesia* that formed tetrads within erythrocytes.[6,27] The species in these cases was not determined. From 1991 to 1994, six additional cases of babesiosis were diagnosed; four in California[28] and two in Washington State.[11,29,30] One of the cases in Washington was acquired via transfusion. The morphology of these parasites was similar to the earlier reports from California, and to *B. microti*.[31] One of the California infections was suspected to be *Babesia gibsoni* (Fig 11.8), a small *Babesia* of dogs, based on serologic findings.[32] Sequence analysis of the gene for ribosomal RNA showed these and the parasite from the first Washington case to be closely related to *B. gibsoni*.[30,31] The patients who survived their acute illness developed elevated titers of antibody to *B. gibsoni* and to WA1 antigens from the index case in Washington. They did not have cross reacting antibody to *B. microti*.[28,33] These organisms had been termed WA1 and CA1 (the numeral indicating the index case, and applied to the parasite type in general.) The WA1 parasite was later named *Babesia duncani*.[31] Another transfusion-transmitted case of *B. duncani* (WA1) occurred in California in 2000.[34] These seven reported symptomatic infections are insufficient to define the population at risk, but compromised immunity appears to be a significant risk factor for clinical

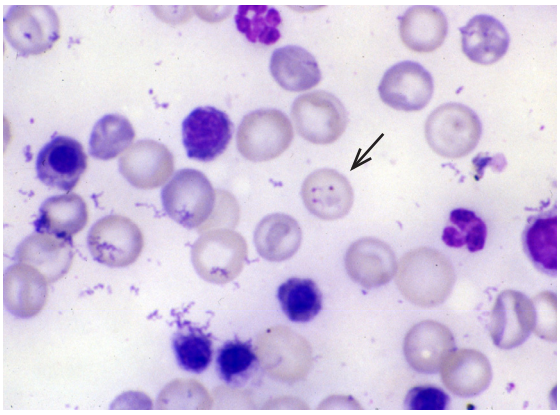


**Figure 11.8**
*Babesia gibsoni* (arrow) from a dog. Giemsa. Original magnification x330

disease. The four patients infected by the CA1-type parasite were splenectomized; one died. The transfusion recipients were an elderly man with megaloblastic anemia and myelodysplasia, and a premature infant. The index patient was young and normosplenic. The two blood donors did not have symptoms of babesiosis. Neither reservoir animals nor vector ticks of *B. duncani* have been identified.[28,29,31]

Though reports of babesiosis on the Pacific coast of the US have been rare, it may be that infection by *B. duncani* is more common than by *B. microti*. Seroprevalence studies in asymptomatic persons have revealed prevalent antibody to *B. duncani* in 3.5%, 16%, 17.8% of local populations in northern California.[28,35] In one reference laboratory, 27% of suspected babesiosis cases from across the US have been positive for antibody to *B. duncani*.[36] These findings suggest that infection by *B. duncani*, or a related organism is common.

In 1992 a piroplasm morphologically and serologically similar to *B. divergens* caused a fatal human infection in Missouri. The patient was asplenic and was taking prednisone for long-standing lupus erythematosus. Serologic testing was positive with *B. divergens* and negative with WA1 and *B. microti*. A relatively small (144bp) DNA sequence had 100% similarity to *B. divergens*. The organism could not be propagated in animals that are competent hosts for *B. divergens*. Thus it appeared related to but distinct from *B. divergens*, and was designated MO1.[37] In 2002, *B. divergens* caused a human infection in Kentucky. The patient was asplenic, with possible exposure during a recent hunting trip. Giemsa stained blood smears (Fig 11.4) revealed ring and divergent forms infecting erythrocytes. Its ribosomal RNA gene was 99.8% similar to *B. divergens*.[38]

At least forty cases of human babesiosis have been reported in Europe. Human babesiosis has usually been attributed to cattle *Babesia* (*B. divergens* and *B. bovis* or related piroplasms) transmitted by *Ixodes ricinus*, the castor-bean tick.[39,40] Transovarial transmission has been confirmed, but a particular tick stage has not been implicated (for *Ixodes scapularis*, nymph and seed-tick have been implicated). Residents of areas with large cattle populations appear to have the greatest risk of infection. Asplenic patients had a nearly 50% fatality rate.[40] Serological surveys in Europe have found from 1.5% to 11.5% prevalence of antibodies to *Babesia;*[41-43] serologic findings in Europe suggest exposure to *B. microti*. In the transfusion transmitted case (recipient and donor), *B. microti* was implicated.[17] Given molecular identification of novel parasite species that resemble the large *Babesia* such as *B. divergens*; thus many of the cases historically attributed to *B. divergens* or *B. bovis* were actually caused by a different species.[37,44,45]

Sporadic reports of human babesiosis have come from Canada,[46] Mexico,[23] Cuba,[47] Portugal,[48] Brazil,[49,50] Japan,[51] Czech Republic,[52] Colombia,[53] Italy,[45] Austria,[45] India,[54] Australia,[55] Taiwan,[56,57] China,[40] South Africa,[58] Egypt,[59] the Commonwealth of Independent States,[23] Yugoslavia,[40] Poland,[33] France,[40] Spain,[23,60,61] Germany,[17,62] Korea,[63] Switzerland,[64] Denmark,[65] Sweden,[66] the UK,[40,67] Finland,[68] and Ireland.[39,67,69]

*Babesia microti* infects children[70,71] and adults at the same frequency, but those with risk factors are more likely to develop clinical, sometimes severe or persistent, disease. Risks include advanced age, asplenism,[21,72] and immunocompromise. Patients with HIV, cancer treatment, immunosuppressive drugs for autoimmune disease, rheumatic disease, or organ transplant have experienced severe babesiosis.[11,21,33,73-81] The incidence of reported *B. microti* infections doubled from more than 200 in 1986 to over 450 by the early 1990s[23,82] and continues to increase in the 2000s.[25] While babesiosis is probably underdiagnosed in all age groups,[83] the increased incidence probably reflects heightened medical and public awareness of the disease and expansion of the endemic range.

Coinfection by *Babesia* and *Borrelia* (Lyme disease agent) have been reported.[84-86] In 1989, a focus of infection emerged in southeastern Connecticut where a large percentage of white-footed mice (*Peromyscus leucopus*) (Fig 11.9) captured near the homes of babesiosis patients were infected with *B. microti.* Some of the mice were also infected with *Borrelia burgdorferi*, the causative agent of Lyme disease.[87] Some of the patients also had serological evidence of recent Lyme disease (IgM to *B. burgdorferi*).

*Babesia*, *Borrelia*, and *Anaplasma* share a tick vector, and coinfection by two or three of these organisms is known. In 1985, Benach et al reported serological evidence of dual infections in 54% of patients initially diagnosed with babesiosis and 66%, of those initially diagnosed with Lyme disease. They determined that babesiosis and Lyme disease do not cross react and concluded that dual infections were acquired from the same tick.[88] Field surveys have confirmed

that dual infections occur in reservoir animals and vector ticks and there is experimental evidence that vector ticks transmit both infections simultaneously.[89-93] A significant factor in the increasing prevalence of human babesiosis and Lyme disease in the northeastern United States is the growing population of white-tailed deer (*Odocoilus virginianus*) with corresponding increases in the vector tick *lxodes scapularis* (the black-legged or deer tick).[94,95]



**Figure 11.9**
White-footed mouse (*Peromyscus leucopus*) reservoir host of *Babesia microti* in northern United States.

## *Infectious Agent*

### Morphologic Description

With Giemsa or Wright's stains, *Babesia* trophozoites appear as a mass of blue cytoplasm, usually with a single red chromatin dot. Cytoplasmic vacuolation occurs in most species. It is common to find multiple organisms in erythrocytes; 16 or more per red blood cell have been seen in dogs infected with *B. canis*. Unlike plasmodia, neither pigment nor gametocytes are seen in mammalian blood infected with *Babesia*. The genus is generally divided into large (over 3 µm long) and small species (less than 3 µm long), but these categories are not rigid. *Babesia bovis*, a small species infecting cattle, is sometimes as large as *B. bigemina*, a large species also infecting cattle. Large species (and some small ones) are piriform (pear-shaped, "tear-drop" forms), whereas most of the small species are elongate, ameboid, or ring-shaped (annulate). In a single smear, the size range of trophozoites can include both the small and the large sizes. The size and morphology may be influenced by host factors including immune response, splenic presence, and partial treatment.

*Babesia microti* exhibits considerable pleomorphism (Fig 11.6). Ring (annulate) forms, elongate forms, and multiple chromatin dots are typical features of *B. microti*. The ring forms and ameboid forms of *B. microti* and some of the other small *Babesia* can be morphologically indistinguishable from those of plasmodia (Figs 11.10 & 11.11), and have been misidentified as malaria. Appliqué forms can also be seen, further lending an appearance similar to *Plasmodium falciparum*. The *B. duncani* and (CA1 type parasite) are morphologically similar to *B. microti*. *Babesia duncani* appears in various forms (Fig 11.12 & 11.13), including the Maltese cross (Fig 11.14). Different proportions of the various forms may be observed in infections by *B. microti* and *B. duncani* (described, but data unpublished).[31] In *B. microti* infections, ameboid forms, often with vacuolated cytoplasm, are more common, and tetrad forms are rare and often asymmetrical. The Missouri parasite MO1 is morphologically similar to *B. divergens*.

*Babesia* that do not produce 4 trophozoites reproduce by binary fission in host erythrocytes. The 2 trophozoites produced in this manner are often seen attached or in close apposition at their narrow ends (Figs 11.2, 11.3, 11.15, & 11.16). Many appear as variously arranged V shapes; *B. divergens* trophozoites are arranged nearly horizontally (Figs 11.4 & 11.17). It is common to find multiple *B. divergens* in a single erythrocyte (Figs 11.4, 11.18, & 11.19). In human erythrocytes, *B. divergens* may appear in ring forms[67] or Maltese cross formations, and are typically located centrally or subcentrally.[96]

### Life Cycle and Transmission

The major animal reservoir of human *B. microti* infection in the United States is the white-footed mouse (*Peromyscus leucopus*) (Fig 11.9). Less important are the meadow vole (*Microtus pennsylvanicus*) and other small rodent species.[97,98] If their habitat of brush land, meadows, and pastures is in an endemic area with a white-tailed deer population (host for adult *I. scapularis*), then the wild rodents are likely to be infested with immature stages of *I. scapularis*. This tick, and related species, serves as a transmission vector to host animal (Figs 11.20 & 11.21).

Ticks have a complex life cycle of egg, larva, nymph, and adult stages that may take 2 or more years to complete. With few exceptions, they are 3-host ticks that spend the feeding portion of each stage on a new animal host. Eggs are laid on the ground, where they hatch into tiny larvae (seed ticks) with 3 pairs of legs. These larvae attach firmly to an animal or human, feed once, drop off, and molt into small nymphs with 4 pairs of legs. A year or more later, the nymphs attach to a new host, feed once, drop off, and molt into adults.

There is considerable variation in the feeding and copulation habits of male and female ticks of different genera and species. In general, females require a blood meal to develop eggs. They attach to a host, engorge with blood, drop to the ground, and deposit eggs. On the other hand, many species of adult male *Ixodes* never feed and do not require a blood meal to become fertile. Those that do feed do not engorge,

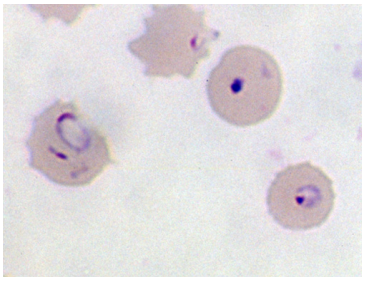


**Figure 11.10**
*Babesia microti* in ring form. Note resemblance to early ring form of *P. falciparum* shown in Figure 11.11. Giemsa. Original magnification x330

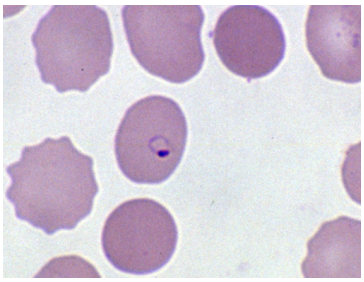


**Figure 11.11**
*Plasmodium falciparum* in early ring form. Note resemblance to *Babesia microti* shown in Figure 11.10, and other *Babesia*. Giemsa. Original magnification x330

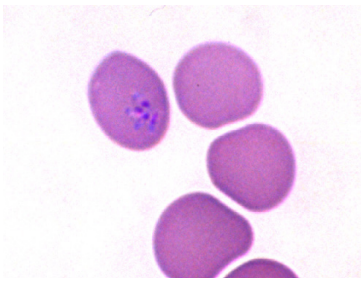


**Figure 11.12**
*Babesia duncani* (WA1) causing human babesiosis in Washington State. Morphologically similar to but serologically distinct from, *B. microti* Giemsa. Original magnification x330

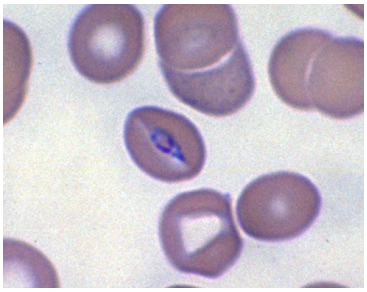


**Figure 11.13**
Single piriform *Babesia duncani* (WA1) with blue cytoplasm. Giemsa. Original magnification x330



**Figure 11.14**
*Babesia duncani* (WA1) in Maltese cross formation. Note dual chromatin dots in each arm of the cross. Giemsa. Original magnification x330

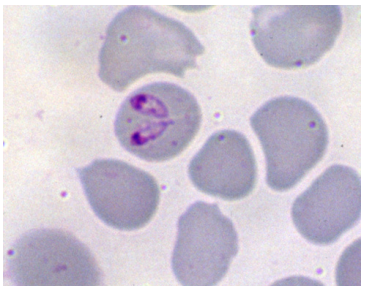


**Figure 11.15**
*Babesia canis* from a dog. Giemsa. Original magnification x330

but may take several small meals and copulate with several different females.[99] The mouth parts of male *I. scapularis* are adapted for semen transfer to the female genital opening more than for attachment to a host animal. A male tick attaches to a female throughout her feeding period (a week or more), but leaves her before she drops to the ground. Male ticks remain on a host throughout the winter.[95]

Only larvae that have received a parasite transovarially from an infected female tick can transmit parasites to an animal or human host. Not all *Babesia* are transmitted transovarially; in general, the small species are not. Some tick stages become infected only by feeding on an infected host; they cannot transmit infection until they develop to the next stage and feed again. Once infected, ticks may remain transstadial (infective from stage to stage) through all following stages or only to the next stage. *Babesia microti* are not transmitted transovarially in *I. scapularis*. Larvae are infected by feeding on reservoir animals from July to September and transstadial infection of nymphs follows.

The nymphal stage of *I. scapularis* is the principal vector of *B. microti* to humans.[100,101] In the late 1970s, the vector of *B. microti* in the northeastern United States was thought to be a new tick species called *Ixodes dammini*, but *I. dammini* was later shown to be a variant of *I. scapularis*.[102] Nymphs harbor *B. microti* through the winter and then transmit the organism when feeding during the late spring and early summer.[58,103] Transstadial infection to adult ticks is insignificant and probably only happens when nymphs have fed on an infected animal.[104] Adult *I. scapularis* are strongly host-specific, preferring to feed on their primary host, the white-tailed deer, or some other large animal, thus reducing the likelihood of humans being infected.[95] Most human infections take place in the summer and fall after the most active feeding period of nymphal *I. scapularis*. Nevertheless, a few human infections have appeared in winter months during adult tick feeding.[105]

In the tick, *Babesia* go through many asexual divisions in the gut epithelium, cells of malpighian tubules, hemolymph, and salivary glands. Some *Babesia* develop in the eggs of the female tick and multiply throughout maturing larval tissue, accounting for transovarial transmission. Sexual reproduction of *Babesia* in ticks is still controversial, though sexual stages in the gut epithelium of ticks infected with *B. equi* have been described.[2] After a few days of feeding, tick salivary glands are filled with differentiated sporozoites which are inoculated into the host.

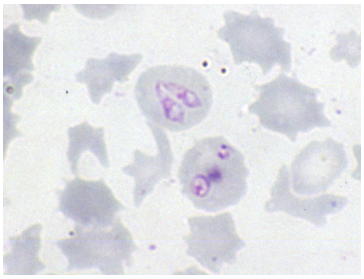


**Figure 11.16**
*Babesia trautmani* from pig in Africa. Parasite is significantly larger than small cattle *Babesia*. Giemsa. Original magnification x330

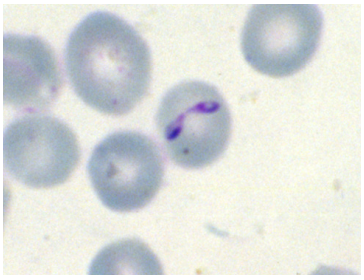


**Figure 11.17**
*Babesia divergens* demonstrating nearly linear apposition of 2 trophozoites following binary fission. Giemsa. Original magnification x330

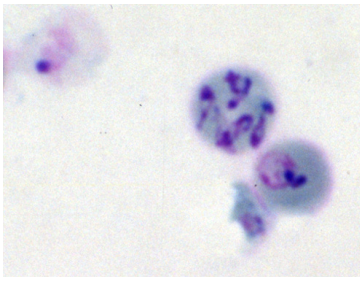


**Figure 11.18**
Multiple *Babesia divergens* in single erythrocyte. Note piriforms, ring forms, and chromatin dots. Giemsa. Original magnification x330

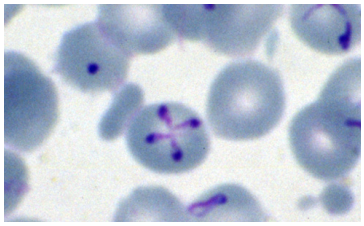


**Figure 11.19**
*Babesia divergens* in Maltese cross formation. Giemsa. Original magnification x330




**Figure 11.20**
*Ixodes scapularis*, vector of *Babesia microti* to humans. (*Right to left*) millet seed, adult female, adult male, nymph, larva. Millimeter scale.




**Figure 11.21 a,b**
Same ticks as in Figure 11.20. Note 4 pairs of legs on nymph and adult (a) and 3 pairs of legs on larval tick (b).

## *Clinical Features and Pathogenesis*

Babesiosis provokes a variety of flu-like symptoms: fever, headache, weakness, myalgia, arthralgia, and malaise are common in moderate infections. Severe infections produce anemia, thrombocytopenia, elevated serum hepatic aminotransferase and lactate dehydrogenase, confusion, depression, night sweats, chills, anorexia, nausea, vomiting, splenomegaly (Fig 11.22), and hepatomegaly. The most severe infections may produce respiratory distress, severe icterus, hemoglobinemia, hemoglobinuria (Fig 11.22), oliguria, anuria, prostration, coma, and death.

Humans develop symptoms of babesiosis one to six weeks after being bitten by an infected tick. One to nine weeks is the usual incubation period for transfusion-transmitted infection.[12,106] Infection can range from subclinical and asymptomatic to severe and fatal disease. Mild and asymptomatic infection is detected in seroprevalence studies in communities and volunteer blood donors who report no history of babesiosis, and by transfusion transmission from asymptomatic parasitemic donors. The proportion of infections that are subclinical is unknown; some may be truly asymptomatic, others may have symptoms that were attributed to the "flu" or other illness. Factors limiting the knowledge on incidence and clinical spectrum include variable experience by clinicians and laboratories in recognizing disease and probable species-related virulence.



**Figure 11.22**
Splenomegaly and hemoglobinuria in a cow (urine shown in sample bottle), nearly pathognomonic findings in enzootic areas of babesiosis.

Much of what is known about the pathogenesis of *Babesia* has been a product of veterinary research on *B. bovis*, a highly virulent cattle *Babesia*,[107,108] but some extrapolation can be made to human babesiosis. Most clinical illness is a direct result of hemolysis and interference with erythrocyte function. Parasitic destruction of red blood cell releases pyrogens, causes severe anemia, and may lead to hemoglo-

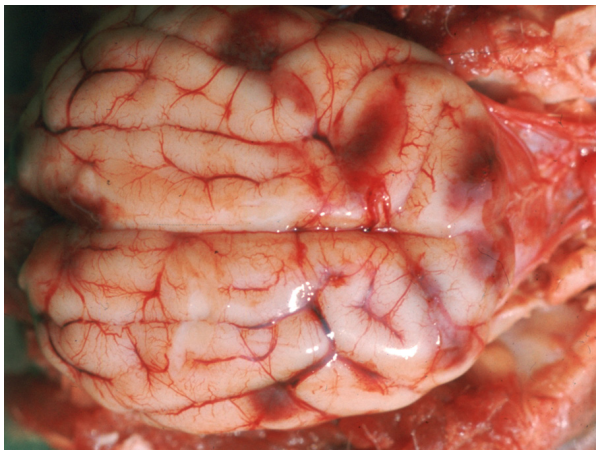


**Figure 11.23**
Hemorrhages and congestion in leptomeninges of dog infected with *Babesia canis.*

binuric nephrosis. Sludging of parasitized erythrocytes and free parasites in capillaries is one of the most significant events of *Babesia* infections, resulting in serious complications including damaged endothelium, capillary fragility (Fig 11.23), tissue anoxia with degeneration, and an accumulation of toxic byproducts from the host and parasite. A wide variety of factors may precipitate sludging: endothelial fibrin and red blood cell bound fibrinogen; strand-type knob-forming membrane changes in parasitized red blood cells; increased plasma viscosity caused by fibrin, fibrinogen, and their complexes; and erythrocyte lipid changes such as externalization of phosphatidylserine. These factors, plus fibronectin, C3, conglutin, parasite antigen, IgG, and cryofibrinogen, have been found in cattle with cerebral babesiosis caused by *B. bovis*.[107,108] The cellular immune system, including production of cytotoxic TNF-alpha, plays an important role in many of these clinical changes. Large amounts of antibody are produced in cattle. *Babesia bovis* produces a more virulent disease in nonsplenectomized adult cattle than in weaned, splenectomized calves, supporting the argument that the most serious symptoms of *B. bovis* infection are related to the immune response.[108]

Cytokine studies in a human patient in the acute stage of babesiosis revealed elevated levels of TNF-alpha, interferon-gamma, IL2, IL6, E selectin, vascular adhesion moIecule-1, and intercellular adhesion molecule-1. CD8+ T cells and natural killer cells were also present.[73,103] A small but growing number of human babesiosis patients have severe respiratory complications.[109,110] Parasite and host-derived proteases, plasma kallikrein, thrombin and thrombin-like enzymes, and anoxia cause alveolar edema and an accumulation of neutrophils and red blood cells in pulmonary capillaries.[108] Increased resistance of erythrocytes to deformation, increased cytoadherence, and perhaps excessive production of TNF and IL-1, may participate in the pathogenesis of respiratory distress in human patients.[109]

Other complications of babesiosis have included retinal infarct, encephalopathy, hepatic failure, renal failure, hemophagocytic syndrome,[111] and autoimmune hemolytic anemia.[112]

The development and severity of human babesiosis is influenced by multiple factors, including virulence of the species of *Babesia*, a compromised immune system, asplenia, corticosteroid or other immunosuppressive therapy, HIV infection, and coinfection with other pathogen.[33,113,114] *Babesia microti* is more likely than other species to produce clinical disease in the elderly. Young adult and middle-aged males (the group with the highest tick exposure) are the usual victims of the more virulent species (*B. bovis* and *B. divergens*). Within this group, asplenic males are at greatest risk of severe or fatal disease. Coinfection with babesiosis and Lyme borreliosis occurs commonly, but triple infection is uncommon. Some reports suggest that the course of Lyme disease is more severe or prolonged with *Babesia* coinfection, others disagree.[86,115,116]

The reticuloendothelial system plays a vital role in nonspecific resistance. Specific resistance depends on both humoral and cell-mediated immunity. *Babesia* infection elevates levels of IgG and IgM in animals and humans. In vitro observations suggest that immunity may be influenced by humoral factors; phagocytosis of infected cells by splenic macrophages requires antibody, complement, and conglutin.[108] In mice, T-cell lymphocytes are responsible for primary resistance to *B. microti*.[117]

## Pathologic Features

In humans, findings at autopsy include congestion of deep organs, occasional hemorrhage, hyperplastic lymph nodes, severe icterus of the skin, mucous membranes, and serosal and visceral surfaces, severe pulmonary edema, enlarged yellow liver, swollen kidneys with reddish brown discoloration of the corticomedullary junction (Fig 11.24), dark urine in the bladder, swelling of the brain, and icteric meninges. Microscopic findings include parasitized erythrocytes in congested capillaries of multiple organs (especially liver sinusoids), acute renal tubular necrosis, hemoglobin casts in tubules, distention of liver canaliculi by bile, immature blood cells in vessels, disseminated intravascular coagulation, and hemophagocytosis.[39,103,111,118] *Babesia* are usually apparent in hematoxylin-eosin stained sections, but are best seen with the Giemsa stain.

## Diagnosis

Babesiosis must be considered in a patient with malaria-like symptoms and a history of travel to regions endemic




**Figure 11.24**
Cut surface of kidney from a dog. Note dark red hemoglobin-stained cortical surface and reddish brown discoloration of corticomedullary junction.

for babesiosis or recent transfusion. Because of the similarity of symptoms and geographic distribution of babesiosis, Lyme disease, and anaplasmosis; suspicion of one disease should prompt testing for all.

The laboratory tests that can be used to diagnose infection by *Babesia* include light microscopy of peripheral blood, serologic identification of anti-*Babesia* antibodies, and detection of *Babesia* nucleic acid. No test kit or device for diagnosis of *Babesia* infection is commercially available. The FDA has not approved any method. Some research and commercial reference laboratories have "home grown" testing capability. The most appropriate test in most settings is light microscopy and it is still the "Gold Standard". WHO and CDC recommend the following:

**Microscopy**.[119] For microscopic examination, peripheral blood is spread on slides in thick and thin smears. At least two of each should be made. Blood smears are useful for detection and identification of a number of different blood parasites. The preferred stain is Giemsa, which can reveal Schüffner's dots of malaria. Other stains (Wright, Wright-Giemsa, Field's stain or other Romanowsky stains) can also be used. The guidelines recommend examining the slide with an oil 100x objective (1000x magnification). Small parasites of either *Babesia* or *Plasmodium* can be easily missed at lower magnification. Examination of a thick smear is approximately 20 times more sensitive than a thin smear. WHO recommends examining at least 100 fields of a thick smear before calling a smear negative.[120] Clinical and Laboratory Standards Institute (formerly NCCLS) standards recommend examining at least 300 fields of a thin smear and a thick smear.[121] The estimated volume of a thick smear examined at 1000x for 100 fields is 0.28 µl.[122] If one parasite is seen, the estimated mean limit of detection is about 4 parasites/µl. The thin smear is often required to provide better visualization of parasite morphology for identification. Malaria and babesia ring forms can be difficult or impossible to distinguish one from the other.

**Serology**

Detection of antibody has traditionally been done by immununofluorescent antibody (IFA) test. The recommended cutoff titres differ by test. However, there is strong cross-reactivity of *B. microti* and several *Plasmodium* sp,[123] so IFA testing in areas endemic for both malaria and babesiosis is inconclusive. More specific tests may be useful in differentiating babesiosis from malaria when microscopic examination and travel history do not support or exclude either parasite. An IFA test has been developed for *B. duncani* (WA1) that has no cross-reactivity with *B. microti* antigen. Serum from patients seropositive to WA1 is cross-reactive with *B. gibsoni* antigen but at significantly lower titers.[28]

The substrate for the IFA has traditionally been obtained by inoculation of susceptible animals (Syrian hamster) and using the infected red cells when high (e.g. 40%) parasitemia is achieved. This can take several weeks. The red cells are washed and concentrated and spread on a slide as a thick smear. Alternatively, relatively purified parasites from the red cells can be used. Recombinant peptides representing specific epitopes have also been tested.[124] Antibody detection using an enzyme-linked detection test (ELISA, EIA) has been performed and may be adaptable to existing platforms used in routine clinical laboratories.

Direct detection of *Babesia* antigens is not available; however, an antigen detection kit for *Plasmodium* (e.g. BinaxNow® rapid diagnostic test) can be useful, since babesia and plasmodia can be morphologically similar. The presence of *Plasmodium* antigen can help differentiate *Babesia* and malaria.[125]

**Fluorescent dye detection.**

Dyes that stain nucleic acids can be used to detect blood parasites. The QBC® test kit described in Topic 10 also detects *Babesia*. It is a nonspecific screening test. Routine light microscopy follows the QBC® test to confirm and identify the parasite.

**Molecular detection**.

An 18S RNA gene sequence has been helpful in identifying species of *Babesia* and related protozoa. Protocols for polymerase chain reactions (PCR) have been used in research and by commercial reference laboratories; however, no commercially available test kits are available. *Babesia*-specific DNA probes have been a significant investigative tool in the study of novel species (e.g. WA1, CA1, MO1, EU1) and phylogenetics.[28-30] DNA probes and PCR tests can be useful in diagnosing low parasitemic infections.[126,127]

Molecular diagnosis is not a primary diagnostic test. Its use should be reserved for the following situations:

- Cases in which organisms are not identified by microscopy and there is a strong clinical suspicion (presumed low parasitemia).[119]
- When *Babesia* and malaria cannot be differentiated by morphology or clinical history, e.g. patient has no known risk for either or has risk for both.[119]
- In recurrent disease after treatment or failure after treatment, to determine if the original diagnosis was incorrect.
- In investigational research of new *Babesia* species or related parasites.[119]
- To reduce risk of transfusion transmission by testing blood donors.[16,128]

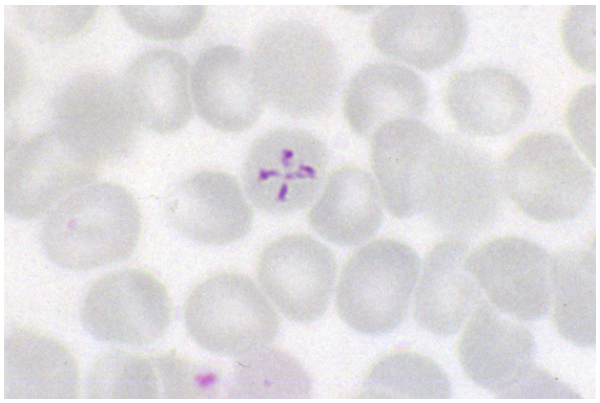


**Figure 11.25**
*Babesia rodhaini* in Maltese cross formation. Formation may be difficult to see in thin thin blood film. Giemsa. Original magnification x330

Identifying species on the basis of morphology is difficult because of similarities among *Babesia* species. In the United States, *B. microti* infection can be diagnosed with certainty if it occurs in a recognized *B. microti* endemic region and the parasite displays a characteristic tetrad formation (Fig 11.5). Finding the Maltese cross formation is helpful but requires meticulous searching (Fig 11.25)

## Treatment and Prevention

The current treatment of choice for most symptomatic human *Babesia* infections is atovaquone plus azityhromycin. Because of a higher rate of adverse drug effects, the combination of clindamycin plus quinine should be reserved for failure by the first line treatment. For severe babesiosis, clindamycin should be given intravenously. Red cell exchange may be considered to reduce parasite burden.[129]

The adult dosage of atovaquone is 750 mg orally every 12 hours; azithromycin is given at 500 to 1000 mg first dose followed by 250 mg daily. Clindamycin is given 300-600 mg every 6 hours (IV) or 600 mg every 6-8 hours orally; quinine, 650 mg, is given every 6-8 hours orally. Higher doses of azithromycin (600 to 1000 mg daily) may be used for immunocompromised patients.[129]

In conjunction with exchange transfusions, this combination of drugs has successfully treated human patients with severe *B. divergens* and *B. microti* infections.[40,75,130] Azithromycin plus quinine cleared *Babesia* parasites from the blood of a Taiwanese patient.[131] Azithromycin and atovaquone, used in combination with or without quinine, have effectively treated babesiosis in adult, infant, asplenic, and HIV-positive patients where clindamycin plus quinine had failed.[22,131-133] Trimethoprim and sulfamethoxazole successfully treated a transplant patient with a *B. microti* infection after other drug therapies had failed.[118] Pentamidine alone has not been successful,[134] but pentamidine plus cotrimoxazole (trimethoprim) and sulfamethoxazole effectively treated a splenectomized patient infected with *B. divergens*. Immunocompetent patients may clear parasitemia without any treatment. In some instances, exchange transfusion is needed to rid patients of persistent parasitemia.[9,74]

There is no vaccine for human babesiosis. The best prevention is to promote public awareness in endemic regions and areas where *Ixodes* ticks (or other competent vectors) are abundant. Simple precautions include using insect repellents, especially in the spring and summer months, checking for ticks after exposure to their habitat, and wearing light-colored clothing to make crawling ticks more visible. Control measures include protecting human habitats by eliminating nesting areas for small reservoir rodents and excluding deer with adequate fencing. Reducing the tick population with acaricides is recommended, especially around lawns and residences.

Blood collectors and regulatory agencies in the US are exploring options for reducing the risk of transfusion transmission of *Babesia*. Proposed strategies include various testing protocols to exclude donations from potentially infected blood donors and modification of the collected blood to destroy pathogens or prevent their replication (pathogen reduction).[16,128]

## References


1. Mehlhorn H, Schein E. Redescription of *Babesia equi Laveran*, 1901 as *Theileria equi Mehlhorn*, Schein 1998. *Parasitol Res*. 1998;84:467-475.
2. Mehlhorn H, Schein E. The piroplasms: life cycle and sexual stages. *Adv Parasitol*. 1984;23:37-103.
3. Skrabalo Z. Babesiosis. In: Marcial-Rojas RA, Moreno E, eds. *Pathology of Protozoal and Helminthic Diseases with Clinical Correlation*. Baltimore, Md: Williams & Wilkins; 1971:225-233.
4. Smith T, Kilbourne FL. Investigations into the nature, causation and prevention of Texas or southern cattle fever. *US Dept Agr Bur Anim Indust*. 1893;Bull 1:1-301.
5. Wilson LB, Chowning WM. Studies in pyroplasmosis hominis (spotted fever or tick fever of the Rocky Mountains). *J Infect Dis*. 1904;1:31-57.
6. Scholtens RG, Braff EH, Healey GA, Gleason N. A case of babesiosis in man in the United States. *Am J Trop Med Hyg*. 1968;17:810-813.
7. Fitzpatrick JE, Kennedy CC, McGeown MG, Oreopoulos DG, Robertson JH, Soyannwo MA. Human case of piroplasmosis (babesiosis). *Nature*. 1968;217:861-862.
8. Western KA, Benson GD, Gleason NN, Healy GR, Schultz MG. Babesiosis in a Massachusetts resident. *N Engl J Med*. 1970;283:854-856.
9. Jacoby GA, Hunt JV, Kosinski KS, et al. Treatment of transfusion-transmitted babesiosis by exchange transfusion. *N Engl J Med.* 1980;303:1098-1100.
10. Dobroszycki J, Herwaldt BL, Boctor F, et al. A cluster of transfusion-associated babesiosis cases traced to a single asymptomatic donor. *JAMA*. 1999;281:927-930.
11. Herwaldt BL, Kjemtrup AM, Conrad PA, et al. Transfusion-transmitted babesiosis in Washington State: first reported case caused by a WA1-type parasite. *J Infect Dis*. 1997;175:1259-1262.
12. Mintz ED, Anderson JF, Cable RG, Hadler JL. Transfusion-transmitted babesiosis: a case report from a new endemic area. *Transfusion*. 1991;31:365-368.
13. Asad S, Sweeney J, Mermel LA. Transfusion-transmitted babesiosis in Rhode Island. *Transfusion*. 2009;49:2564-2573.
14. Tonnetti L, Eder AF, Dy B, et al. Transfusion-transmitted *Babesia microti* identified through hemovigilance. *Transfusion*. 2009;49:2557-2563.
15. Young C and Krause PJ. Editorial: The problem of transfusion-transmitted babesiosis. *Transfusion*. 2009;49:2548–2550.
16. American Association of Blood Banks. Summary of Blood Products Advisory Committee Meeting 7/26 - 7/27/10. http://www.aabb.org/events/government/bpac/Pages/bpacmeeting072610.aspx. Accessed March 7, 2011
17. Hildebrandt A, Hunfeld KP, Baier M, et al. First confirmed autochthonous case of human *Babesia microti* infection in Europe. *Eur J Clin Microbiol Infect Dis.* 2007;26:595-601.
18. Saito-Ito A, Tsuji M, Wei Q, et al. Transfusion-acquired, autochthonous human babesiosis in Japan: isolation of *Babesia microti*-like parasites with hu-RBC-SCID mice. *J Clin Microbiol*. 2000;38:4511-4516.
19. DeVos AJ, Imes GD Jr, Culien JS. Cerebral babesiosis in a newborn calf. *Onderstepoort J Vet Res.* 1976;43:75-78.
20. U.S. Department of Health and Human Services Center for Disease Control. Babesiosis becomes notifiable. http://www.cdc.gov/parasites/features/babesia_notify_9-7-10.html. Page last reviewed: November 2, 2010. Page last updated: November 2, 2010. Accessed March 7, 2011.
21. Meldrum SC, Birkhead GS, White DJ, Benach JL, Morse DL. Human babesiosis in New York State: an epidemiological description of 136 cases. *Clin Infect Dis.* 1992;15:1019-1023.
22. New DL, Quinn JB, Qureshi MZ, Sigler SJ. Vertically transmitted babesiosis. *J Pediatr.* 1997;131:163-164.
23. Healy GR, Ristic M. Human babesiosis. In: Ristic M, ed. *Babesiosis of Domestic Animals and Man*. Boca Raton, Fla: CRC Press, Inc; 1988:209-225.
24. Herwaldt BL, McGovern PC, Gerwel MP, Easton RM, MacGregor RR. Endemic babesiosis in another eastern state: New Jersey. *Emerg Infect Dis.* 2003;9:184-188.
25. Rodgers SE, Mather TN. Human *Babesia microti* incidence and *Ixodes scapularis* distribution, Rhode Island, 1998–2004. *Emerg Infect Dis.* 2007;13:633–635.
26. Weld ED, Eimer KM, Saharia K, Orenstein A, Hess JR. The expanding range and severity of babesiosis. *Transfusion*. 2010;50:290–291.
27. Bredt AS, Weinstein WM, Cohen S. Treatment of babesiosis in asplenic patients. *JAMA*. 1981;254:1938-1939.
28. Persing DH, Herwaldt BL, Glaser C, et al. Infection with a babesia-like organism in northern California. *N Engl J Med*. 1995;332:298-303.
29. Quick RE, Herwaldt BL, Thomford JW, et al. Babesiosis in Washington State: a new species of Babesia? *Ann Intern Med.* 1993;119:284-290.
30. Thomford JW, Conrad PA, Telford SR 3d, et al. Cultivation and phylogenetic characterization of a newly recognized human pathogenic protozoan. *J Infect Dis.* 1994;169:1050-1056.
31. Conrad PA, Kjemtrup AM, Carreno RA, et al. Description of *Babesia duncani* n.sp. (Apicomplexa: Babesiidae) from humans and its differentiation from other piroplasms. *Int J Parasitol*. 2006;36:779-789.
32. Jerant AF, Arline AD. Babesiosis in California. *West J Med*. 1993;158:622-625.
33. Homer MJ, Aguilar-Delfin I, Telford SR 3d, Krause PJ, Persing DH. Babesiosis. *Clin Microbiol Rev.* 2000;13:451-469.
34. Kjemtrup AM, Lee B, Fritz CL, Evans C, Chervenak M, Conrad PA. Investigation of transfusion transmission of a WA1-type babesial parasite to a premature infant in California. *Transfusion*. 2002;42:1482-1487.
35. Fritz CL, Kjemtrup AM, Conrad PA, et al. Seroepidemiology of emerging tickborne infectious diseases in a Northern California community. *J Infect Dis.* 1997;175:1432-1439.
36. Prince HE, Lapé-Nixon M, Patel H, Yeh C. Comparison of the *Babesia duncani* (WA1) IgG detection rates among clinical sera submitted to a reference laboratory for WA1 IgG testing and blood donor specimens from diverse geographic areas of the United States. *Clin Vaccine Immunol*. 2010;17:1729-1733.
37. Herwaldt B, Persing DH, Precigout EA, et al. A fatal case of babesiosis in Missouri: identification of another piroplasm that infects humans. *Ann Intern Med.* 1996;124:643-650.
38. Beattie JF, Michelson ML, Holmes PJ. Acute babesiosis caused by *Babesia divergens* in a resident of Kentucky. *N Engl J Med.* 2002;347:697-698.
39. Clarke CS, Rogers ET. Egan EL. Babesiosis: under-reporting or case-clustering? *Postgrad Med J.* 1989;65:591-593.
40. Gorenflot A, Moubri K, Precigout E, Carcy B, Schetters TP. Human babesiosis. *Ann Trop Med Parasitol*. 1998;92:489-501.
41. Hunfeld KP, Lambert A, Kampen H, et al. Seroprevalence of Babesia infections in humans exposed to ticks in midwestern Germany. *J Clin Microbiol.* 2002;40:2431-2436.
42. Foppa IM, Krause PJ, Spielman A, et al. Entomologic and serologic evidence of zoonotic transmission of *Babesia microti*, eastern Switzerland. *Emerg Infect Dis.* 2002;8:722-726.
43. Genchi C. Human babesiosis, an emerging zoonosis. *Parassitologia*. 2007;49(Suppl 1):29-31.
44. Herwaldt BL. Epidemiology of Babesiosis, Presentation to Blood Products Advisory Committee in July 2010. Document ucm222400. Available at http://www.fda.gov/AdvisoryCommittees/CommitteesMeetingMaterials/BloodVaccinesandOtherBiologics/BloodProductsAdvisoryCommittee/ucm205013.htm. Last Updated: 01/10/2011. Accessed March 17, 2011.
45. Piccaluga PP, Poletti G, Martinelli G, Gherlinzoni F. Babesia infection in Italy. *Lancet Infect Dis*. 2004;4:212
46. Bu Jassoun S, Fong IW, Hannach B, Kain KC. Transfusion-transmitted babesiosis in Ontario: first reported case in Canada. *Can Commun Dis Rep*. 2000;26:9-13.
47. Suarez Hernandez M, Alonso Castellano M, Pelaez Martinez R, Sanchez Perez B, Bravo Gonzalez JR, Sanchez Sibello A. Investigation of Babesia in farm workers and blood donors in the province of Ciego de Avila [in Spanish]. *Rev Cubana Med Trop*. 1997;49:130-135.
48. Centeno-Lima S, do Rosário V, Parreira R,et al. A fatal case of human babesiosis in Portugal: molecular and phylogenetic analysis. *Trop Med Int Health*. 2003;8:760-764.
49. Yoshinari NH, Abrão MG, Bonoldi VL, Soares CO, et al. Coexistence of antibodies to tick-borne agents of babesiosis and Lyme borreliosis in patients from Cotia county, State of São Paulo, Brazil. *Mem Inst Oswaldo Cruz*. 2003;98:311-318.
50. Rech A, Bittar CM, de Castro CG, et al. Asymptomatic babesiosis in a child with hepatoblastoma. *J Pediatr Hematol Oncol*. 2004;26:213.
51. Matsui T, Inoue R, Kajimoto K, et al. [First documentation of transfusion-associated babesiosis in Japan] [Article in Japanese, abstract in English]. *Rinsho Ketsueki*. 2000;41:628-634.
52. Nohýnková E, Kubek J, Měst'ánková O, Chalupa P, Hubálek Z. [A case of *Babesia microti* imported into the Czech Republic from the USA] [Article in Czech, Abstract in English]. *Cas Lek Cesk*. 2003;142:377-381.

53. Ríos L, Alvarez G, Blair S. Serological and parasitological study and report of the first case of human babesiosis in Colombia. *Rev Soc Bras Med Trop*. 2003;36:493-498.

54. Marathe A, Tripathi J, Handa V, Date V. Human babesiosis: a case report. *Indian J Med Microbiol*. 2005;23:267-269.

55. Clark IA, Budd AC, Hsue G, et al. Absence of erythrocyte sequestration in a case of babesiosis in a splenectomized human patient. *Malar J*. 2006;5:69.

56. Shaio MF, Lin PR. A case study of cytokine profiles in acute human babesiosis. *Am J Trop Med Hyg*. 1998;58:335-337.

57. Shih CM, Liu LP, Chung WC, Ong SJ, Wang CC. Human babesiosis in Taiwan: asymptomatic infection with a *Babesia microti*-like organism in a Taiwanese woman. *J Clin Microbiol*. 1997;35:450-454.

58. Bush JB, Isaacson M, Mohamed AS, Potgieter FT, de Waal DT. Human babesiosis -a preliminary report of 2 suspected cases in South Africa. *S Afr Med J*. 1990;78:699.

59. El-Bahnasawy MM, Morsy TA. Egyptian human babesiosis and general review. *J Egypt Soc Parasitol*. 2008;38:265-272.

60. Canas E, de Alarcon A, Regordan C. Viciana P. Babesiosis in an immunocompetent patient [in Spanish] [letter]. *Rev Clin Esp.* 1992;190:45.

61. Moreno Giménez JC, Jiménez Puya R, Galán Gutiérrez M, Ortega Salas R, Dueñas Jurado JM. *Erythema figuratum* in septic babesiosis. *J Eur Acad Dermatol Venereol*. 2006;20:726-728.

62. Häselbarth K, Tenter AM, Brade V, Krieger G, Hunfeld KP. First case of human babesiosis in Germany: clinical presentation and molecular characterization of the pathogen. *Int J Med Microbiol*. 2007;297:197-204.

63. Kim JY, Cho SH, Joo HN, et al. First case of human babesiosis in Korea: detection and characterization of a novel type of *Babesia* sp (KO1) similar to ovine babesia. *J Clin Microbiol*. 2007;45:2084-2087.

64. Loutan L, Rossier J, Zufferey G, et al. Human babesiosis: first case report in Switzerland [in French]. Rev Med Suisse Romande. 1994;114:111-116.

65. Enemark H, Petersen JE. Babesiosis in Denmark [in Danish]. *Ugeskr Laeger.* 1998;160:6225.

66. Uhnoo I, Cars O, Christensson D, Nystrom-Rosander C. First documented case of human babesiosis in Sweden. *Scand J Infect Dis.* 1992;24:541-547.

67. Loutan L, Rossier J, Zufferey G, et al. Imported babesiosis diagnosed as malaria [letter]. *Lancet*. 1993;342:749.

68. Haapasalo K, Suomalainen P, Sukura A, Siikamaki H, Jokiranta TS. Fatal babesiosis in man, Finland, 2004. *Emerg Infect Dis*. 2010;16:1116-1118.

69. Browne S, Ryan Y, Goodyer M, Gilligan O. Fatal babesiosis in an asplenic patient. *Br J Haematol.* 2010;148:494.

70. Esernio-Jenssen D, Scimeca PG, Benach JL, Tenenbaum MJ. Transplacental/ perinatal babesiosis. *J Pediatr.* 1987;110:570-572.

71. Scimeca PG, Weinblatt ME, Schonfeld G, Kaplan MH, Kochen JH. Babesiosis in two infants from eastern Long Island, NY [letter]. *Am J Dis Child*. 1986;140:971.

72. Benach JL, Habicht GS. Hamburger MI. Immunoresponsiveness in acute babesiosis in humans. *J Infect Dis.* 1982;146:369·380.

73. Benezra D, Brown AE, Polsky B, Gold JW, Armstrong D. Babesiosis and infection with human immunodeficiency virus [letter]. *Ann Intern Med.* 1987;107:944.

74. Machtinger L, Telford SR 3d, Inducil C, Klapper E, Pepkowitz SH, Goldfinger D. Treatment of babesiosis by red blood cell exchange in an HlV-positive, splenectomized patient. *J Clin Apheresis.* 1993;8:78-81.

75. Ong KR, Stavropoulos C, Inada Y. Babesiosis, asplenia, and AIDS [letter]. *Lancet*. 1990;336:112.

76. Lux JZ, Weiss D, Linden JV, et al. Transfusion-associated babesiosis after heart transplant. *Emerg Infect Dis*. 2003;9:116-119.

77. Taiwo B, Lee C, Venkat D, Tambar S, Sutton SH. Can tumor necrosis factor alpha blockade predispose to severe babesiosis? *Arthritis Rheum*. 2007;57:179-181.

78. Häselbarth K, Kurz M, Hunfeld KP, Krieger G. Babesiosis in an immunocompromised German patient (Article in German, Abstract in English). *Med Klin (Munich)*. 2008;103:104-107.

79. Cullen G, Sands BE, Yajnik V. Babesiosis in a patient on infliximab for Crohn's disease. *Inflamm Bowel Dis*. 2010;16:1269-1270.

80. Berman KH, Blue DE, Smith DS, Kwo PY, Liangpunsakul S. Fatal case of babesiosis in post liver transplant patient. *Transplantation*. 2009;87:452-453.

81. Perdrizet GA, Olson NH, Krause PJ, Banever GT, Spielman A, Cable RG. Babesiosis in a renal transplant recipient acquired through blood transfusion. *Transplantation*. 2000;70:205-208.

82. Spach DH, Liles WC, Campbell GL, Quick RE, Anderson DE Jr, Fritsche TR. Tick-borne diseases in the United States [review]. *N Engl J Med*. 1993;329:936-947.

83. Krause PJ, Telford SR 3d, Pollack RJ, et al. Babesiosis: an underdiagnosed disease of children. *Pediatr*. 1992;89:1045-1048.

84. Grunwaldt E, Barbour AG, Benach JL. Simultaneous occurrence of babesiosis and Lyme disease [letter]. *N Engl J Med.* 1983;308:1166.

85. Marcus LC, Steere AC, Duray PH, Anderson AE, Mahoney EB. Fatal pancarditis in a patient with coexistent Lyme disease and babesiosis. Demonstration of spirochetes in the myocardium. *Ann Intern Med*. 1985;103:374-376.

86. Krause PJ, Telford SR 3rd, Spielman A, et al. Concurrent Lyme disease and babesiosis. Evidence for increased severity and duration of illness. *JAMA*. 1996;275:1657-1660.

87. Anderson JF, Mintz ED, Gadbaw JJ, Magnarelli LA. *Babesia microti*, human babesiosis, and *Borrelia burgdorferi* in Connecticut. *J Clin Microbiol*. 1991;29:2179-2783

88. Benach JL, Coleman JL, Habitat GS, MacDonald A, Grunwaldt E, Giron JA. Serological evidence for simultaneous occurrences of Lyme disease and babesiosis. *J Infect Dis*. 1985;152:473-477.

89. Anderson JF, Johnson RC, Magnarelli LA, Hyde FW, Myers JE. Prevalence of *Borrelia burgdorferi* and *Babesia microti* in mice on islands inhabited by white-tailed deer. *Appl Environ Microbiol.* 1987;53:892-894.

90. Mather TN, Telford SR 3d, Moore Sl, Spielman A. *Borrelia burgdorferi* and *Babesia microti*: efficiency of transmission from reservoirs to vector ticks (*Ixodes dammini*). *Exp Parasitol.* 1990;70:55-61.

91. Piesman J. Intensity and duration of *Borrelia burgdorferi* and *Babesia microti* infectivity in rodent hosts. *Int J Parasitol*. 1988;18:687-689.

92. Piesman J, Hicks TC, Sinsky RJ, Obiri G. Simultaneous transmission of *Borrelia burgdorferi* and *Babesia microti* by individual nymphal *Ixodes dammini* ticks. *J Clin Microbiol*. 1987;25:2012-2013.

93. Piesman J, Mather TN, Telford SR 3d, Spielman A. Concurrent *Borrelia burgdorferi* and *Babesia microti* infection in nymphal *Ixodes dammini. J Clin Microbiol.* 1986;24:446-447.

94. Piesman J, Spielman A, Etkind P, Ruebush TK 2d, Juranek DD. Role of deer in the epizootiology of *Babesia microti* in Massachusetts, USA. *J Med Entomol.* 1979;15:537-540.

95. Spielman A, Wilson ML, Levine JF, Piesman J. Ecology of *Ixodes dammini*-borne human babesiosis and Lyme disease. *Annu Rev Entomol*. 1985;30:439-460.

96. Brasseur P, Gorenflot A. Human babesiosis in Europe. *Mem Inst Oswaldo Cruz*. 1992;87:131-132.

97. Spielman A, Etkind P, Piesman J, Ruebush TK 2d, Juranek DD, Jacobs MS. Reservoir hosts of human babesiosis on Nantucket Island. *Am J Trop Med Hyg*. 1981;30:560-565.

98. Telford SR 3d, Mather TN, Adler GH, Spielman A. Short-tailed shrews as reservoirs of the agents of Lyme disease and human babesiosis. *J Parasitol*. 1990;76:681-683.

99. Oliver JH Jr. Symposium on reproduction of arthropods of medical and veterinary importance. IV. Reproduction in ticks (Ixodoidea). *J Med Entomol*. 1974;11:26-34.

100. Piesman J, Spielman A. Human babesiosis on Nantucket Island: prevalence of *Babesia microti* in ticks. *Am J Trop Med Hyg.* 1980;29:742-746.

101. Spielman A. Human babesiosis on Nantucket Island: transmission by nymphal Ixodes ticks. *Am J Trop Med Hyg*. 1976;25:784-787.

102. Oliver JH Jr, Owsley MR, Hutcheson HJ, et al. Conspecificity of the ticks *Ixodes scapularis* and *I. dammini* (Acari: Ixodidae). *J Med Entomol*. 1993;30:54-63.

103. Auerbach M, Haubenstock A, Soloman G. Systemic babesiosis. Another cause of the hemophagocytic syndrome. *Am J Med*. 1986;80:301-303.

104. Piesman J, Karakashian SJ, Lewengrub S, Rudzinska MA, Spielman A. Development of *Babesia microti* sporozoites in adult *Ixodes dammini*. *Int J Parasitol*. 1986;16:381-385.

105. Piesman J, Mather TN, Dammin GJ, Telford SR 3d, Lastavica CC, Spielman A. Seasonal variation of transmission risk of Lyme disease and human babesiosis. *Am J Epidemiol*. 1987;126:1187-1189.

106. Leiby DA. Babesiosis and blood transfusion: flying under the radar. *Vox Sang.* 2006;90:157-165.

107. Wright IG, Goodger BV. Pathogenesis of babesiosis. In: Ristic M, ed. *Babesiosis of Domestic Animals and Man.* Boca Raton, Fla: CRC Press, Inc; 1988:99-118.

108. Wright IG, Goodger BV, Buffington GD, Clark IA, Parrodi F, Waltisbuhl DJ. Immunopathophysiology of babesial infections. *Trans R Soc Trop Med Hyg.* 1989;83:11-13.

109. Boustani MR, Lepore TJ, Gelfand JA, Lazarus DS. Acute respiratory failure in patients treated for babesiosis. *Am J Respir Crit Care Med*. 1994;149:1689-1691.

110. Horowitz ML, Coletta F, Fein AM. Delayed onset adult respiratory distress syndrome in babesiosis. *Chest.* 1994;106:1299-1301.

111. Slovut DP, Benedetti E, Matas AJ. Babesiosis and hemophagocytic syndrome in an asplenic renal transplant recipient. *Transplantation.* 1996;62:537-539.

112. Evenson DA, Perry E, Kloster B, Hurley R, Stroncek DF. Therapeutic apheresis for babesiosis. *J Clin Apher*. 1998;13:32-36.

113. Babesiosis-Connecticut. *MMWR Morb Mortal Wkly Rep*. 1989;38:649-650.

114. Rosner F, Zarrabi MH, Benach JL, Habicht GS. Babesiosis in splenectomized adults. Review of 22 reported cases. *Am J Med*. 1984;76:696-701.

115. Swanson SJ, Neitzel D, Reed KD, Belongia EA. Coinfections acquired from Ixodes ticks. *Clin Microbiol Rev*. 2006;19:708–727.

116. Wang TJ, Liang MH, Sangha O, et al. Coexposure to *Borrelia burgdorferi* and *Babesia microti* does not worsen the long-term outcome of lyme disease. *Clin Infect Dis.* 2000;31:1149-1154.

117. James MA. Immunology of babesiosis. In: Ristic M, ed. *Babesiosis of Domestic Animals and Man*. Boca Raton, Fla: CRC Press, Inc; 1988:119-130.

118. Gupta P, Hurley RW, Helseth PH, Goodman JL, Hammerschmidt DE. Pancytopenia due to hemophagocytic syndrome as the presenting manifestation of babesiosis. *Am J Hematol*. 1995;50:60-62.

119. Centers for Disease Control and Prevention. Laboratory Identification of Parasites of Public Health Concern. http://www.dpd.cdc.gov/dpdx/HTML/Frames/A-F/Babesiosis/body_Babesiosis_MolDiag.htm. Last modified 7/20/09. Accessed Mar 6, 2011

120. World Health Organization. Guidelines on Standard Operating Procedures for MICROBIOLOGY, Chapter 18 - Malaria. WHO Regional Office for South-East Asia 2010. Available at http://www.searo.who.int/en/Section10/Section17/section 53/section482_1800.htm. Last updated 04/27/2006. Accessed March 17, 2011.

121. Clinical and Laboratory Standards Institute. Laboratory Diagnosis of Blood-borne Parasitic Diseases; Approved Guideline--NCCLS document M15-A. (ISBN 1-56238-401-5). NCCLS, 940 West Valley Road, Suite 1400, Wayne, Pennsylvania 19087-1898 USA, 2000.

122. Warhurst DC, Williams JE. ACP Broadsheet no 148. July 1996. Laboratory diagnosis of malaria. *J Clin Pathol*. 1996;49:533-538.

123. Chisholm ES, Sulzer Ai, Ruebush TK 2d. Indirect immunofluorescence test for human *Babesia microti* infection: antigenic specificity. *Am J Trop Med Hyg.* 1986;35:921-925.

124. Houghton RL, Homer MJ, Reynolds LD, et al. Identification of *Babesia* microti-specific immunodominant epitopes and development of a peptide EIA for detection of antibodies in serum. *Transfusion*. 2002;42:1488-1496.

125. Rosenblatt JE. Laboratory diagnosis of infections due to blood and tissue parasites. *Clin Infect Dis.* 2009;49:1103-1108.

126. Persing DH, Mathiesen D, Marshall WF, et al. Detection of *Babesia microti* by polymerase chain reaction. *J Clin Microbiol*. 1992;30:2097-2103.

127. Reiter I, Weiland G. Recently developed methods for the detection of babesial infections. *Tran R Soc Trop Med Hyg.* 1989;83:21-23.

128. Gubernot DM, Nakhasi HL, Mied PA, Asher DM, Epstein JS, Kumar S. Transfusion-transmitted babesiosis in the United States: summary of a workshop. *Transfusion*. 2009;49:2759-2771.

129. Wormser GP, Dattwyler RJ, Shapiro ED, et al. The clinical assessment, treatment, and prevention of lyme disease, human granulocytic anaplasmosis, and babesiosis: clinical practice guidelines by the Infectious Diseases Society of America. *Clin Infect Dis.* 2006;43:1089-1134. Erratum in: *Clin Infect Dis.* 2007;45:941.

130. Iacopino V, Earnhart T. Life-threatening babesiosis in a woman from Wisconsin. *Arch Intern Med.* 1990;150:1527-1528.

131. Shih CM, Wang CC. Ability of azithromycin in combination with quinine for the elimination of babesial infection in humans. *Am J Trop Med Hyg.* 1998;59:509-512.

132. Bonoan JT, Johnson DH, Cunha BA. Life-threatening babesiosis in an asplenic patient treated with exchange transfusion, azithromycin, and atovaquone. *Heart Lung.* 1998;27;424-428.

133. Falagas ME, Klempner MS. Babesiosis in patients with AIDS: a chronic infection presenting as fever of unknown origin. *Clin Infect Dis.* 1996;22:809-812.

134. Raoult D, Soulayrol L, Toga B, Dumon H, Casanova P. Babesiosis, pentamidine, and cotrimoxazole [letter]. *Ann Intern Med.* 1987;107:944.

## *Acknowledgements*

**Figure 11.2**
Contributed by Gale G Wagner

**Figure 11.3**
Contributed by Gale G Wagner

**Figure 11.4**
Contributed by Philippe Brasseur

**Figure 11.9**
Contributed by KC Stafford III

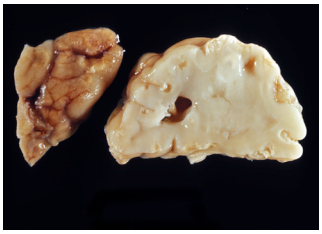
**Figure 11.17**
Contributed by Philippe Brasseur

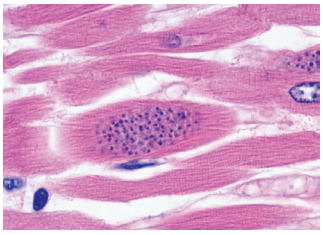
**Figure 11.18**
Contributed by Philippe Brasseur

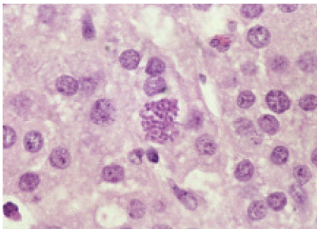
**Figure 11.19**
Contributed by Philippe Brasseur

**Figure 11.20**
Courtesy of Pfizer Central Research, Pfizer Inc.

**Figure 11.21**
Contributed by Dennis White







12

# Toxoplasmosis

*Ronald C. Neafie, Mary K. Klassen-Fischer, and Wayne M. Meyers*

## *Introduction*

### Definition

Toxoplasmosis is infection by *Toxoplasma gondii*, a coccidian protozoan parasite of birds, cats, humans, and other mammals. In humans, infection is usually asymptomatic. Clinical symptoms arise in some congenitally infected infants and in adults whose immune systems have been compromised by, for example, corticosteroids, cytostatic agents, or AIDS.

### General Considerations

The generic name *Toxoplasma* comes from the Greek word "toxon," meaning bow or arc, and refers to the crescent shape of the parasite. The specific name is derived from the gondi, a local rodent used at the Pasteur Institute in Tunisia, in which Nicolle and Manceaux discovered *Toxoplasma* in 1908.[1] In the same year, Splendore identified *Toxoplasma* in a laboratory rabbit in Brazil.[2] In 1923, the organism was recognized in Czechoslovakia in histologic sections of a child's eye.[3] In 1937, Wolf et al suggested placental transmission after finding the parasite in the brains of several babies dying of neonatal encephalitis.[4] A serologic test developed by Sabin and Feldman in 1948 revealed widespread subclinical infection worldwide.[5] Wilder, at the Armed Forces Institute of Pathology (AFIP), identified *Toxoplasma* in eyes previously considered tuberculous or syphilitic.[6] In the 1950s, Jacobs et al at the National Institutes of Health (USA) confirmed that *Toxoplasma* could be transmitted by raw or undercooked meat.[7,8] A coccidian type of sexual development was described in cats in 1970, adding oocysts from cat feces and contaminated sand or soil to the known sources of infection.[9] Lehmann et al characterized 3 subgroups of *T. gondii* by molecular biology for phylogenetic analysis.[10] Subgroup types vary in virulence and geographic distribution, for example, type II predominates in ocular disease in France.[11]

## *Epidemiology*

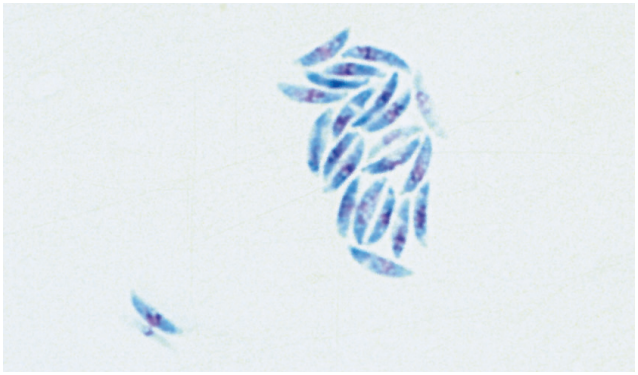


**Figure 12.1**
*Toxoplasma* tachyzoites in smear of cytospin specimen from HIV-positive patient. Each parasite is crescentic and has a prominent nucleus. Giemsa x1250

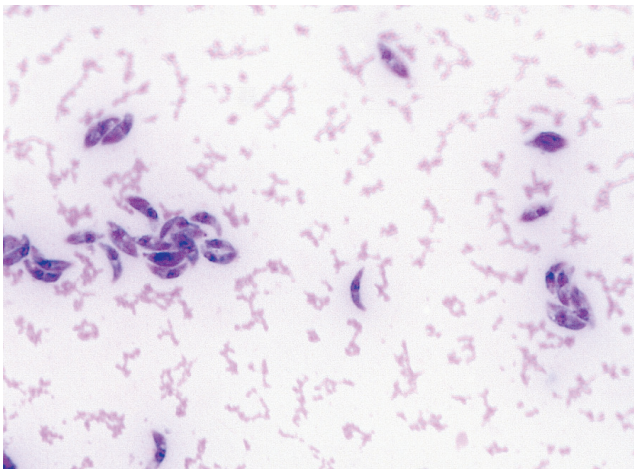


**Figure 12.2**
*Toxoplasma* tachyzoites in smear showing variation in shape and size. Giemsa x1130

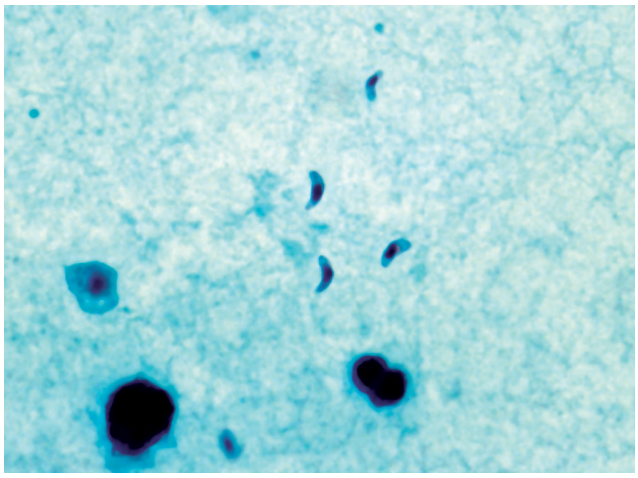


**Figure 12.3**
*Toxoplasma* tachyzoites in Pap smear. Note prominent reddish nucleus in each parasite. Papanicolaou x820

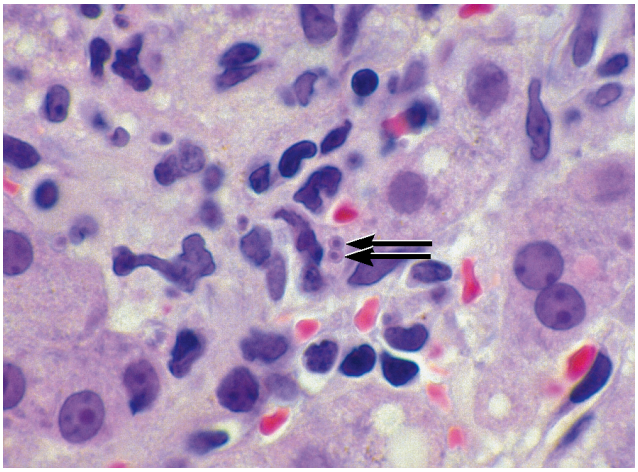


**Figure 12.4**
*Toxoplasma* tachyzoites in biopsy of liver in HIV-positive patient. Note 2 spherical organisms (arrows), each with prominent nucleus. H&E x1460

Toxoplasmosis is one of the most common parasitic infections of humans.[12] Animals and humans on 5 continents show serologic evidence of infection with *Toxoplasma*. Prevalence is highest in warm, humid regions. In the lowlands of Central America, where cats are numerous and shade and moisture favor survival of oocysts in soil, almost all adults have antibodies to *Toxoplasma*. In urban and rural areas of Costa Rica and Panama, where transmission to humans is almost exclusively by oocysts from cats, 25% to 50% of schoolchildren are serologically positive.[12-16] In rain forest areas, where human and feline habitats are less likely to overlap, transmission to humans is irregular.[16] In the United States, infection is most commonly acquired by young adults who have eaten undercooked meat. Viable *T. gondii* can also persist in commercially cured meats, which may be another source of transmission.[17] Pigs raised on small farms in close proximity to cats, rodents, and birds are more likely to be infected with *Toxoplasma* than industrially raised pigs.[18] Sheep are rarely infected on the range, but are likely to be infected when brought to farms where cats are present.[19] Contaminated meat seems to remain the primary source of infection but environmental sources are common. [20,21]

## *Infectious Agent*

### Morphologic Description

Two stages of *T. gondii* occur in human tissues: tachyzoites, the rapidly multiplying form found in acute infection, and bradyzoites, the slowly multiplying form found in chronic infection. Interconversion between rapidly growing tachyzoites and latent encysted bradyzoites is accompanied by numerous morphologic and metabolic adaptations.[22]

Tachyzoites infect many types of cells and multiply asexually by repeated endodyogeny. Daughter cells form within the mother cell until the mother cell ruptures, releasing free tachyzoites that invade new tissue cells.

In fresh preparations and impression films, tachyzoites are crescent-shaped and up to 7µm long and 1µm to 3µm wide, with a well-defined, usually centrally located nucleus (Figs 12.1 to 12.3). They stain well with Giemsa, Wright's, Dif-Quick, and Papanicolaou's stains. In tissue sections prepared from biopsy or autopsy specimens, tachyzoites are best observed in hematoxylin and eosin (H&E) stained sections (Figs 12.4 & 12.5). They are usually round to oval and 2µm to 3µm in greatest dimension, but may be crescentic and 5µm long (Fig 12.6). Tachyzoites sometimes divide by binary fission and occasionally have multiple nuclei (Fig 12.7). Organisms lie free in tissue, unbound by a cyst wall (Figs 12.4 to 12.7), but may aggregate in clusters referred to as groups (Fig 12.8). Hematoxylin and eosin is the preferred stain for identifying tachyzoites in tissue sections, but some special stains may be useful. Tachyzoites are gram-negative by the Brown-Hopps (B&H) modified Gram stain (Fig

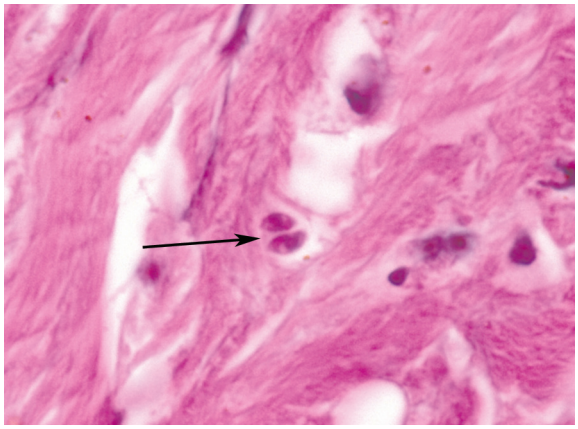


**Figure 12.5**
*Toxoplasma* tachyzoites (arrow) in choroid of enucleated eye of HIV-positive patient. Organisms are oval and each has a prominent nucleus. H&E x1350

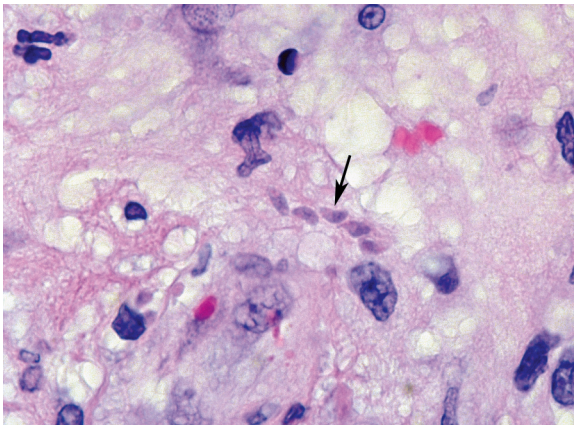


**Figure 12.6**
*Toxoplasma* tachyzoites (arrow) in brain of patient who died of AIDS. Note prominent nucleus within each crescent-shaped organism. H&E x815

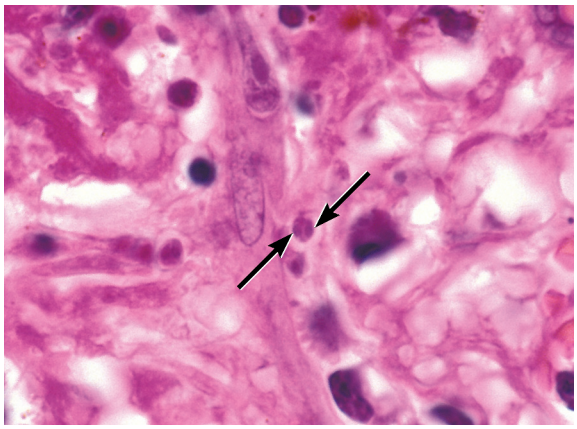


**Figure 12.7**
*Toxoplasma* tachyzoite with 2 nuclei (arrow) undergoing binary fission in choroid of enucleated eye of HIV-positive patient. H&E x1000

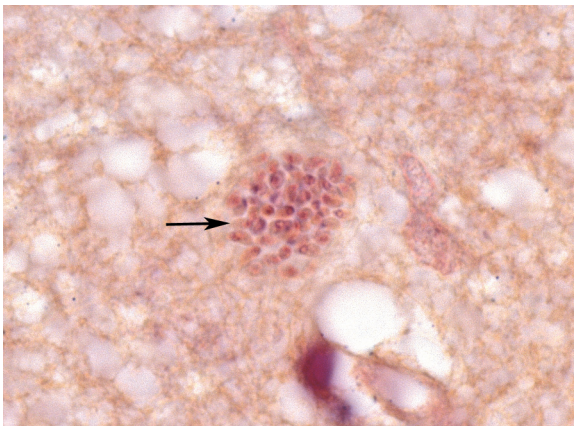


**Figure 12.8**
Group of *Toxoplasma* tachyzoites (arrow) in brain of immunodeficient patient. Note absence of cyst wall. B&H x1000

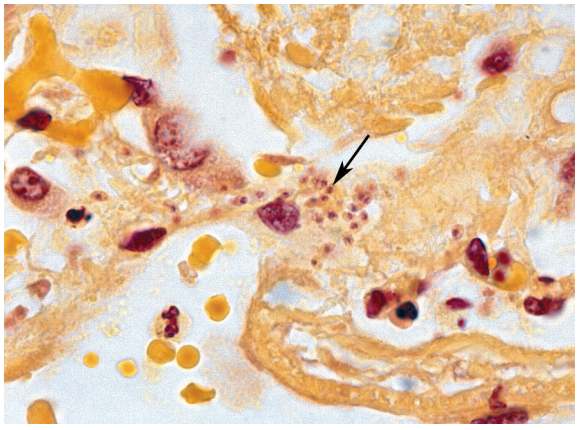


**Figure 12.9**
Section of lung showing gram-negative *Toxoplasma* tachyzoites (arrow), each with prominent nucleus. B&H x1500

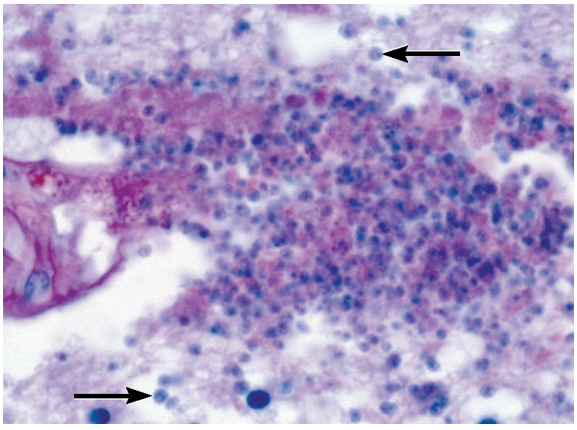


**Figure 12.10**
PAS-negative *Toxoplasma* tachyzoites (arrows) are nonetheless identifiable in this section of brain. PAS x770

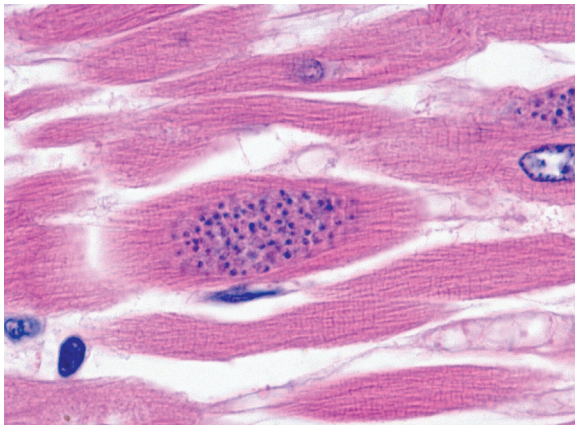


**Figure 12.11a**
Group of *Toxoplasma* tachyzoites in myocardium of HIV-positive patient. Note absence of cyst wall. H&E x860

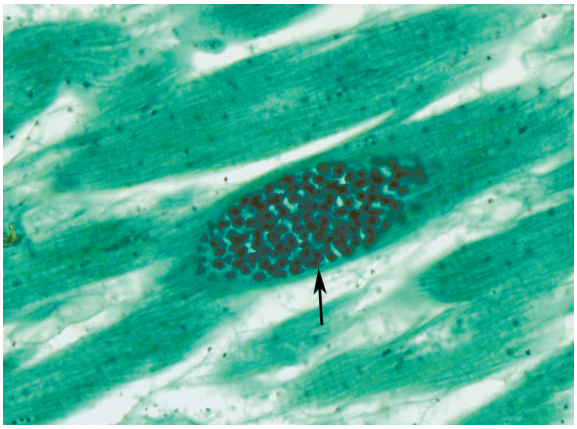


**Figure 12.11b**
Silvered tachyzoites in section (arrow) adjacent to that seen in Figure 12.11A. GMS x875

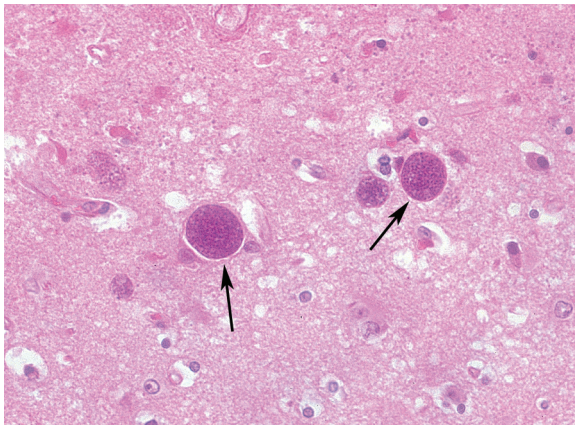


**Figure 12.12**
*Toxoplasma* bradyzoites (arrows) within cysts in brain of immunocompromised patient. Cysts stain well with H&E. H&E x260

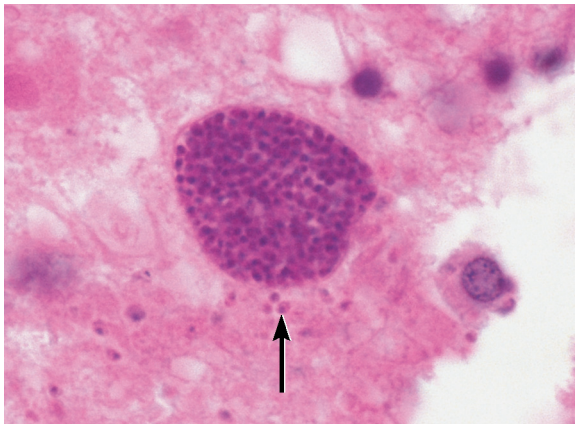


**Figure 12.13**
Single *Toxoplasma* cyst in brain. Note numerous bradyzoites and thin cyst wall, and tachyzoites (arrow) adjacent to cyst. H&E x960

12.9), and PAS-negative by the periodic acid-Schiff (PAS) technique (Fig 12.10). Gomori's methenamine silver (GMS) usually does not stain free tachyzoites, but may stain groups (Figs 12.11a & 12.11b).

Bradyzoites reproduce by both endodyogeny and endopolygeny. They are highly motile and can infect many types of cells. Cysts can proliferate without undergoing an intermediate tachyzoite stage through the process of fission, or by migration of free bradyzoites.[22] Morphologically, individual bradyzoites are nearly identical to tachyzoites; the difference is that bradyzoites are always encysted. Most cysts are less than 50 µm in diameter, but may be up to 100 µm in diameter and contain hundreds of bradyzoites. As with tachyzoites, H&E is the preferred stain for identifying cysts in tissue sections (Figs 12.12 & 12.13), but special stains may be useful, including B&H (Figs 12.14 & 12.15), GMS (Figs 12.16 & 12.17), and PAS (Figs 12.18 to 12.20). It must be emphasized that these special stains vary greatly in their ability to demonstrate *Toxoplasma*.

## Life Cycle and Transmission

In a variety of mammals and birds that act as intermediate hosts, *T. gondii* multiplies asexually in an extraintestinal cycle (Fig 12.21). In domestic and wild cats, the definitive hosts, an enteroepithelial cycle also takes place which, after sexual recombination, leads ultimately to the formation of resistant oocysts eliminated in feces (Fig 12.22). When a cat ingests an animal containing bradyzoites in tissue cysts, the enteroepithelial cycle takes place in the cat's intestine and oocysts appear in feces in 3 to 10 days depending on the quantity of bradyzoites ingested. If a cat ingests sporozoites from oocysts, or an animal with only tachyzoites, a generalized infection with tachyzoites develops first, followed by the development of bradyzoites in tissue cysts, which initiate the enteroepithelial cycle.[23] Oocysts are shed in 21 to 40 days. Enteroepithelial stages of *Toxoplasma* in the intestines of cats include 5 types of multiplicative stages,

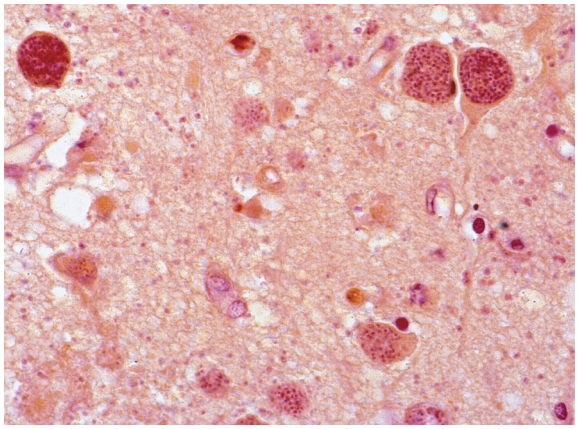


**Figure 12.14**
Numerous bradyzoites within 2 thin-walled cysts in brain. B&H x145

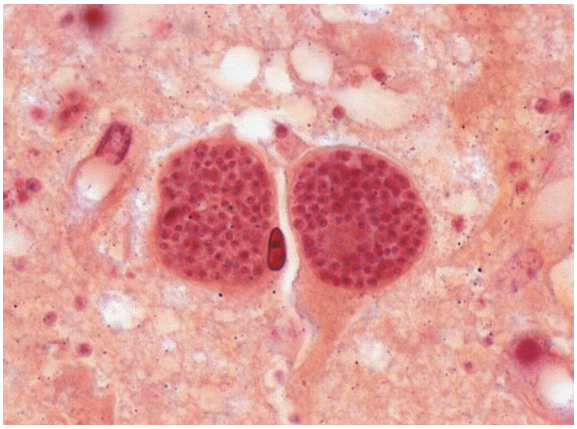


**Figure 12.15**
Several well-stained *Toxoplasma* cysts in brain. B&H x875

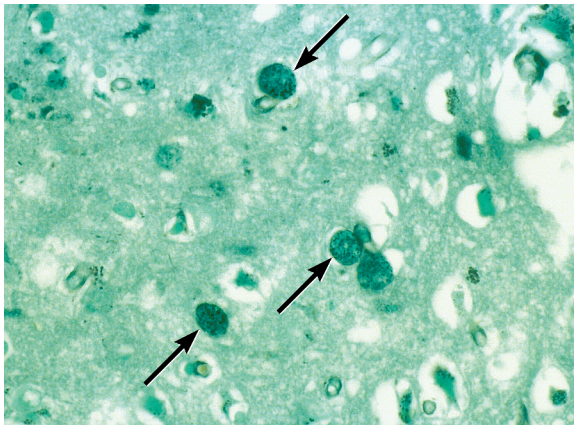


**Figure 12.16**
Several *Toxoplasma* cysts (arrows) in brain. GMS x350

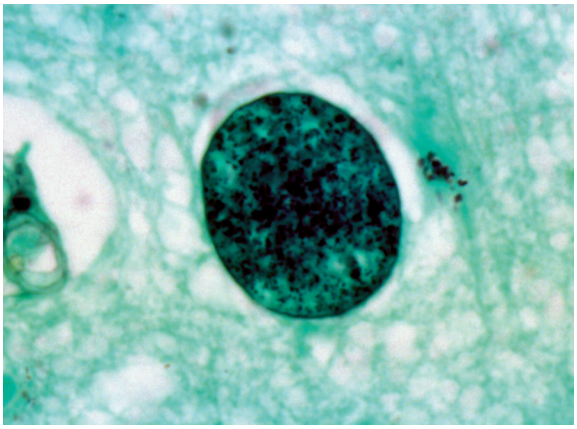


**Figure 12.17**
Single *Toxoplasma* cyst in brain. Note GMS-positive cyst wall and internal amylopectin granules. GMS x900

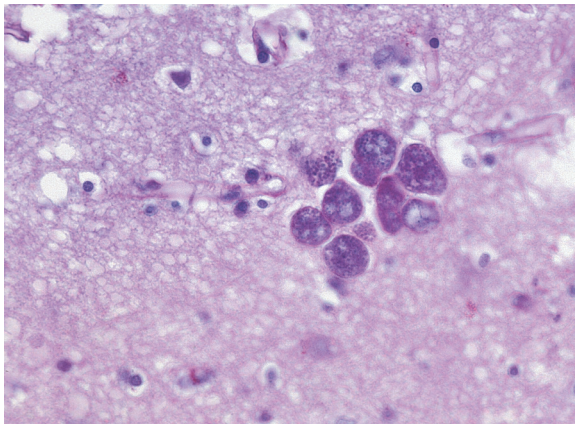


**Figure 12.18**
Several readily identifiable *Toxoplasma* cysts in brain. PAS x320

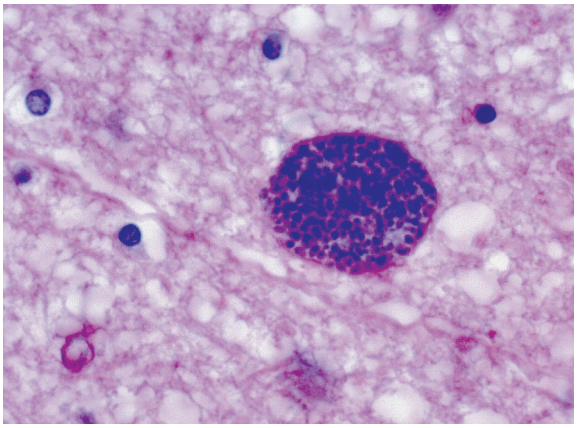


**Figure 12.19**
Single readily identifiable *Toxoplasma* cyst in brain. Cyst wall and amylopectin granules are PAS-negative. PAS x540

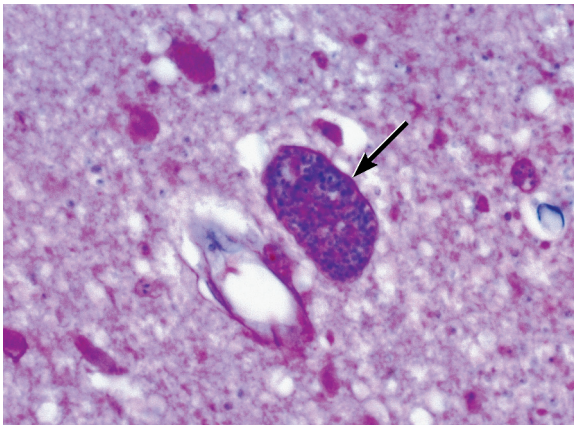


**Figure 12.20**
Single *Toxoplasma* cyst in brain of patient depicted in Figure 12.19. Cyst wall (arrow) and amylopectin granules are PAS-positive. PAS x665

gametocytes, and oocysts.[24]

Transmission to carnivores is mainly by tissue cysts contained in meat, and to herbivores by oocysts ingested with soil or feed contaminated by cat feces. Humans acquire infection by eating meat from chronically infected animals or by ingesting oocysts deposited in soil or sand by cats (Fig 12.21). Mechanical vectors include dogs, flies, cockroaches, and earthworms.[13] The possibility that dogs play a role in transmission through coprophagia and rolling in cat feces was suggested in the 1990s.[13]

## Clinical Features and Pathogenesis

Although most *T. gondii* infections in humans are asymptomatic, there are several clinical patterns of toxoplasmosis: 1) Acute febrile illness, sometimes with pneumonia and myocarditis; 2) Lymphadenopathy, sometimes with or following acute febrile illness; 3) Asymptomatic primary maternal infection with transmission to the fetus; 4) Congenital infection with growth retardation, jaundice, or encephalitis; 5) Acute or chronic encephalitis in an immunosuppressed host; 6) Retinochoroiditis in children or adults, usually without other manifestations.

Acute *Toxoplasma* infection is usually followed by chronic disease. Both are asymptomatic in humans and animals that promptly acquire immunity to the organism. Mammals in Australia and Madagascar that evolved without contact with felines, and neotropical, arboreal primates that have little contact with terrestrial felines, often develop clinically apparent and sometimes fatal toxoplasmosis.[25-27] During acute infection, *Toxoplasma* tachyzoites multiply in many types of cells and tissues. Pathologic changes vary with the number of parasites that are destroying host

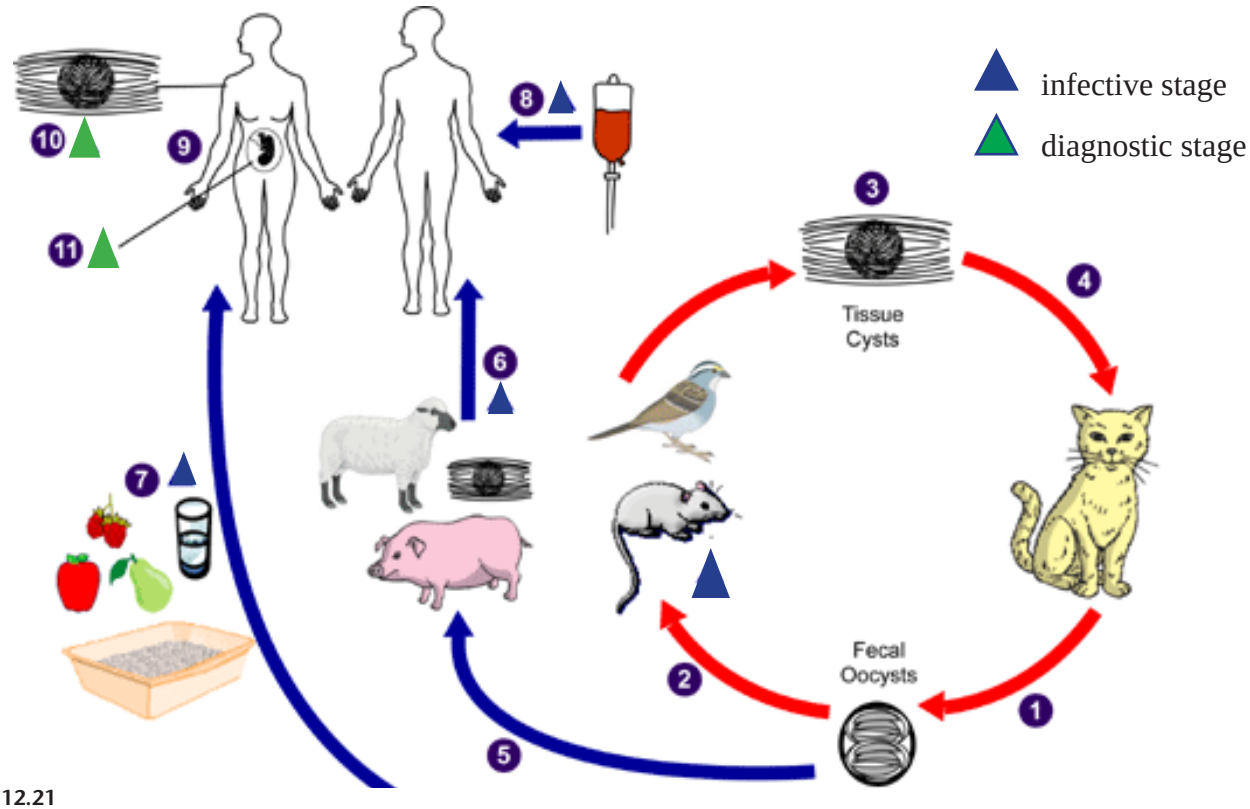



**Figure 12.21**
General *Toxoplasma gondii* life cycle: (1-4) cat to small animal to cat; (5-6) fecal oocysts are eaten by animals that become food sources; (7) fecal oocysts contaminate fruits, water or cat litter; (8) human to human via blood transfusion; and (9-11) risk to fetus.

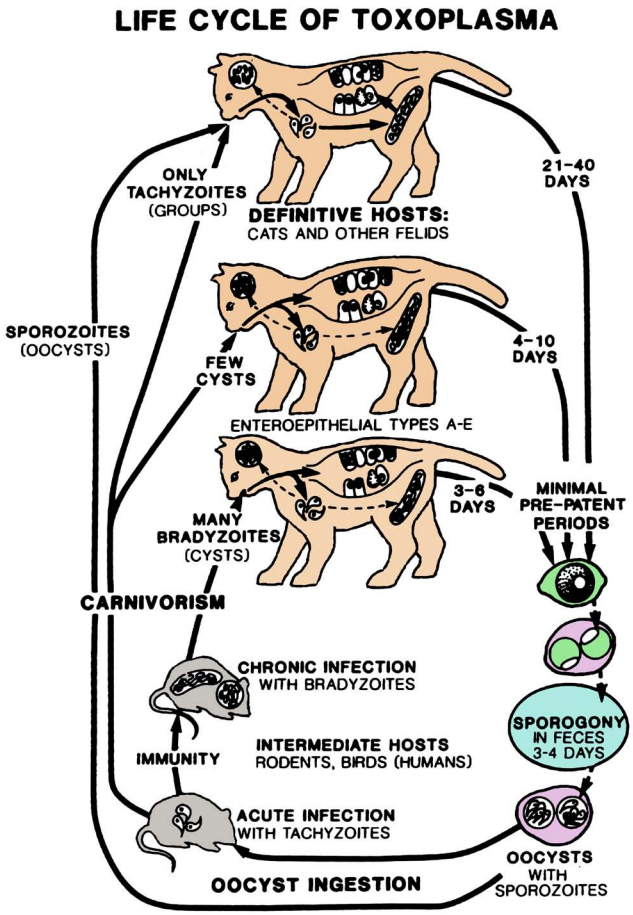



**Figure 12.22**
Life cycle—cat

cells. Tachyzoites enter a host's intestines and disseminate through blood and lymph. Lesions form as a result of cell destruction (Fig 12.23), usually in the lung but sometimes in the heart or other parts of the body. Immunity usually develops during acute infection. High antibody titers develop, but cell-mediated immunity is decisive. With immunity, the number of tachyzoites in the viscera decreases, but bradyzoites persist in many tissues, especially the brain, retina, and placenta. Approximately 30% to 40% of women who become infected during pregnancy transmit infection to the fetus.[28] Maternal infection and placentitis are usually asymptomatic.

While searching for infections predisposing to schizophrenia, several authors noted higher prevalence rates of antibody to *Toxoplasma* in patients with schizophrenia than in normal controls, as well as epidemiologic similarities between the two conditions, and poorer delayed and immediate memory in individuals with *Toxoplasma* antibody than in those without the antibody.[29] Other authors found in individuals who had caused an automobile accident to have more than twice the rate of antibody to *Toxoplasma* than in controls.[30,31] In a study from Istanbul, Turkey, patients with schizophrenia had similarly elevated *Toxoplasma* serologic rates and 59% of this group had contact with cats, compared to 7.5% in controls. Amongst individuals who had contact with cats there was no positive association of schizophrenia with *Toxoplasma* antibody, and of those without cat contact there was a significant negative correlation between schizophrenia and *Toxoplasma* antibody.[32] The effect of toxoplasmosis on risk for schizophrenia disappeared in a complex model analyzed with multivariate logistic regression. Clearly, these provocative findings need further study. In a sample of 20 European countries *T. gondii* infections were positively associated with suicide rates.[33]

Chronic infection is maintained by bradyzoites in tissue cysts, which are relatively nonpathogenic and can survive for long periods in neurons, myocardial and skeletal muscle, and other cells. In children and young adults believed to have been infected in utero, ocular lesions sometimes develop after many years of asymptomatic infection. In such patients optic nerve edema may accompany a concurrent distant active lesion.[34] Another common lesion is juxtapap-

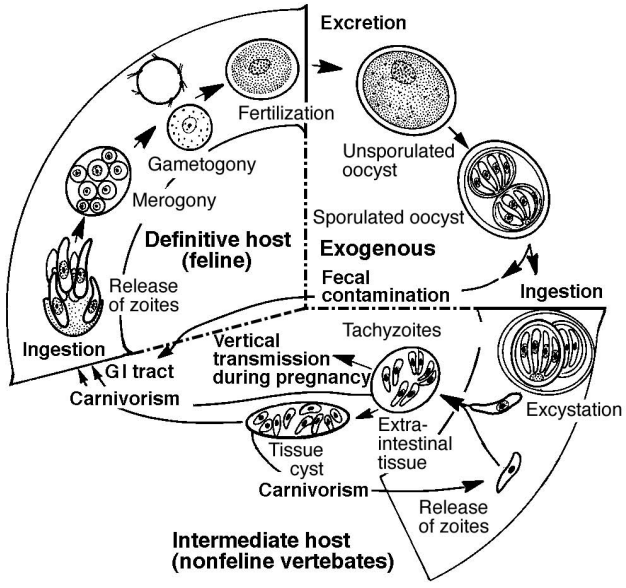



**Figure 12.23**
Diagram of *Toxoplasma gondii* development stages compared to stages in Figures 12.21 and 12.22 : upper left quadrant concerns the cat; upper right quadrant the maturation of the fecal oocyst in the ground or cat box; and the lower half in animals or humans.




**Figure 12.24**
Congenital toxoplasmic encephalitis in 11-day-old infant with focal infarcts (arrows).

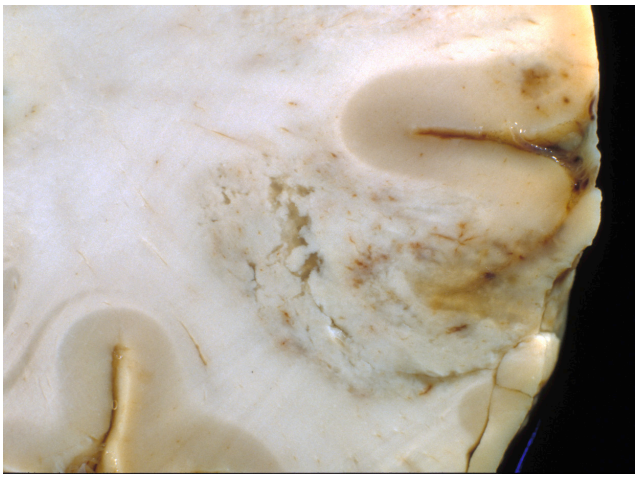


**Figure 12.25**
Focus of cortical necrosis caused by infarction in congenital toxoplasmic encephalitis.

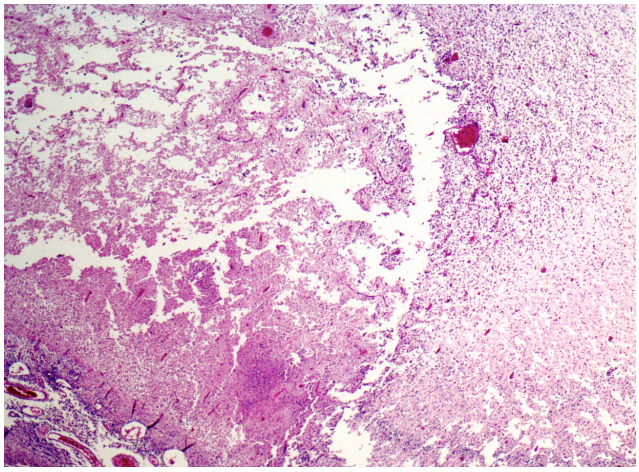


**Figure 12.26**
Section of specimen from patient described in Figure 12.24 showing interface of ischemic necrotic (left) and viable (right) brain tissue with vascular congestion. H&E x19

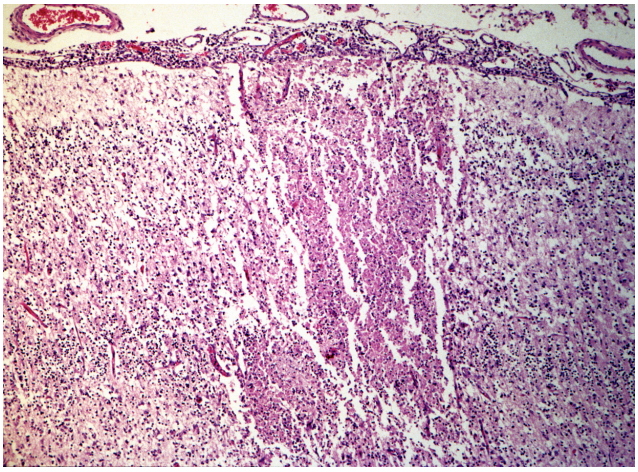


**Figure 12.27**
Meningeal mononuclear-cell infiltrate overlying area of ischemic necrosis in section of specimen from patient described in Figure 12.24. H&E x45

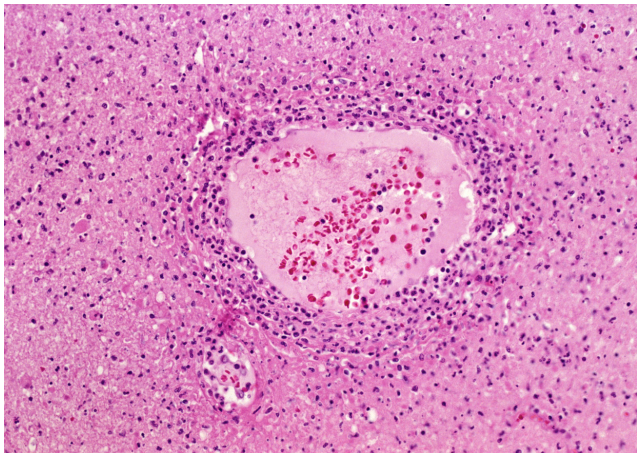


**Figure 12.28**
Primary vasculitis of brain in congenital toxoplasmosis. H&E x135

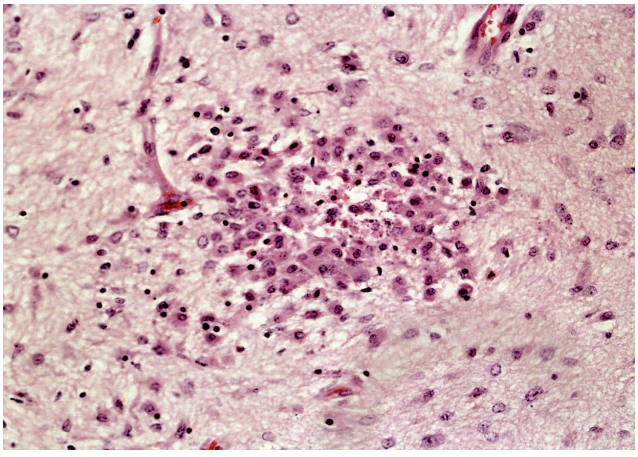


**Figure 12.29**
Glial nodule in patient with congenital toxoplasmosis. H&E x145

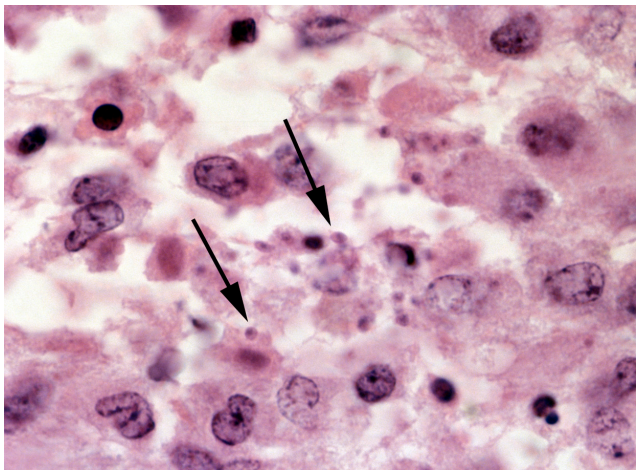


**Figure 12.30**
Tachyzoites (arrows) in higher magnification of glial nodule shown in Figure 12.29. H&E x 780.

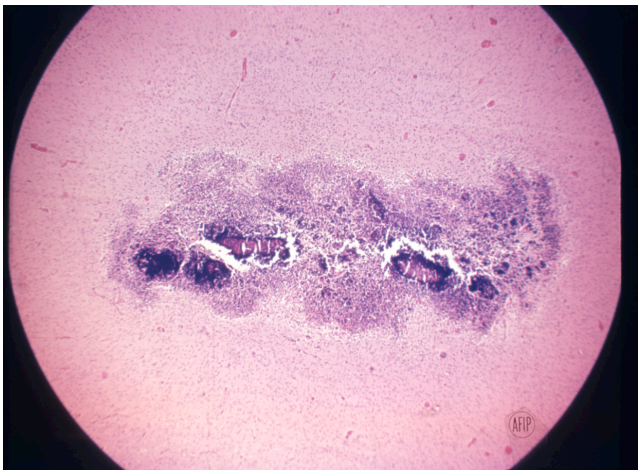


**Figure 12.31**
Calcification in brain of patient with congenital toxoplasmosis. H&E x340

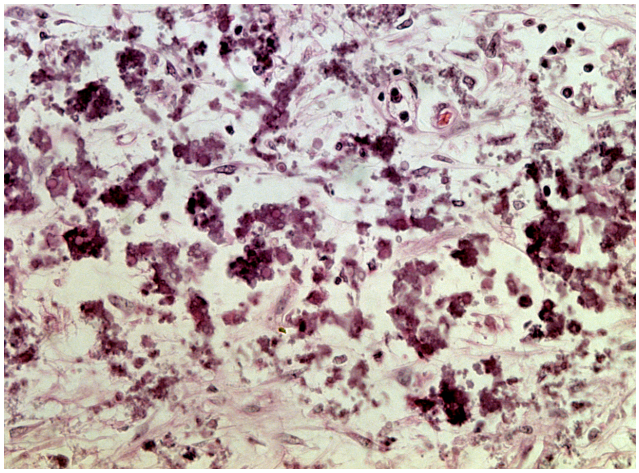


**Figure 12.32**
Calcification in brain of patient with congenital toxoplasmosis. H&E x220

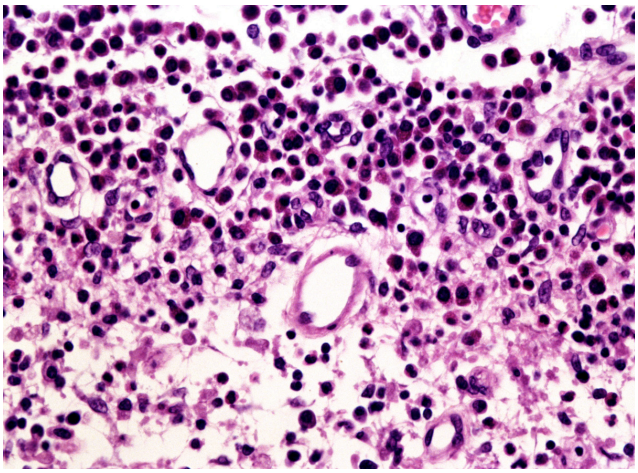


**Figure 12.33**
Prominent eosinophilia in meninges of patient with congenital toxoplasmosis. H&E x260

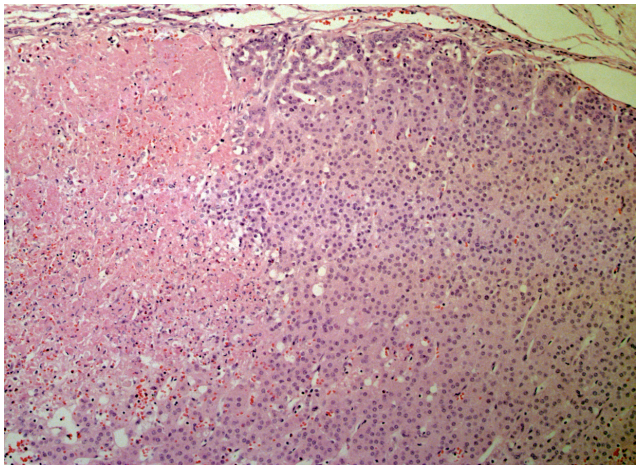


**Figure 12.34**
Necrosis in adrenal gland of patient with congenital toxoplasmosis. H&E x60

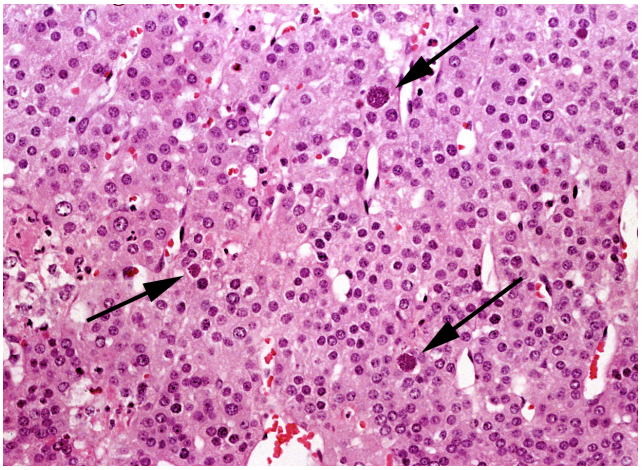


**Figure 12.35**
Several groups of tachyzoites (arrows) in viable adrenal gland of patient with congenital toxoplasmosis. H&E x150

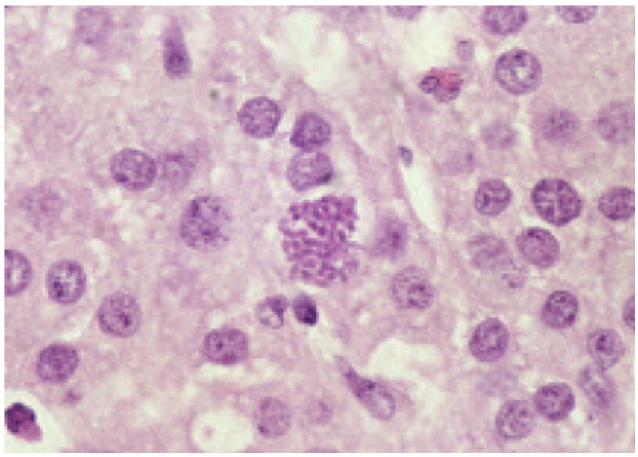


**Figure 12.36**
Group of tachyzoites in viable adrenal gland of patient with congenital toxoplasmosis. Note absence of cyst wall. H&E x590

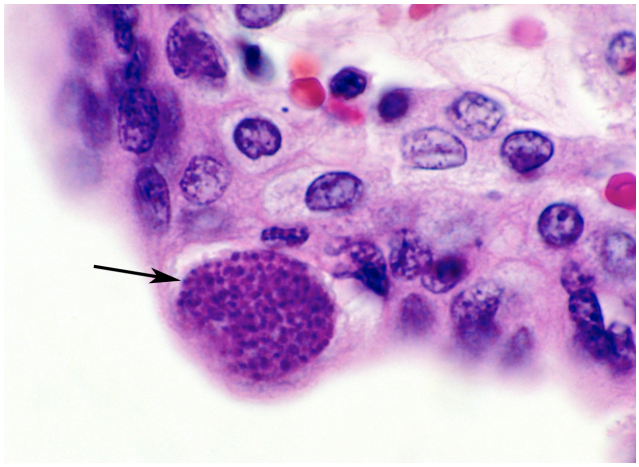


**Figure 12.37**
*Toxoplasma* cyst (arrow) with bradyzoites in viable placental villus. H&E x825

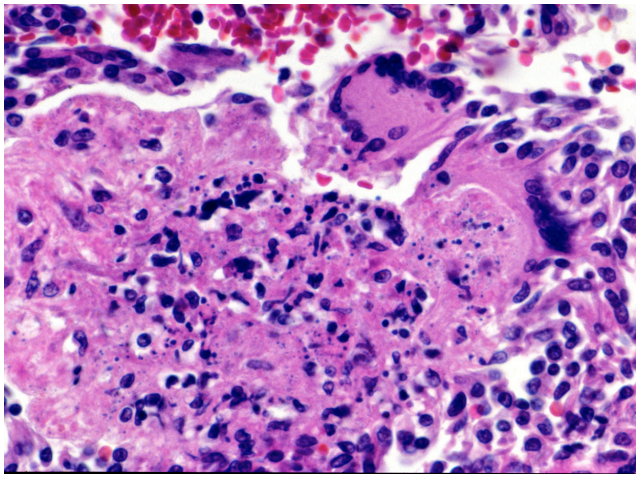


**Figure 12.38**
*Toxoplasma gondii* is presumptive cause of necrotizing granulomatous inflammation in placenta of patient with toxoplasmosis, though careful examination revealed no organisms in specimen. H&E x335

illary retinochoroiditis, which some researchers attribute to disintegration of cysts with resulting inflammatory reaction in a hypersensitive host.[35] Others believe that only proliferation of *Toxoplasma* causes ocular lesions.[36] However, generalized immunity remains effective, as suggested by the self-limiting nature of most untreated lesions. *Toxoplasma gondii* induces production of interleukin-12 by dendritic cells, resulting in a cell-mediated immune response that halts replication of tachyzoites, thus promoting host survival and parasite transmission.[37] Apoptosis is a crucial factor in promoting both a stable host-parasite interaction and persistent infection. Initially, *T. gondii* triggers apoptosis in T lymphocytes and other leukocytes, which suppresses immune response and allows unrestricted parasite replication. *Toxoplasma gondii* can also inhibit apoptosis. Inhibiting apoptosis in nearby uninfected cells modulates the local inflammatory response and facilitates intracellular parasite development.[38] Inflammatory reaction to cyst rupture, with maintenance of immunity, has also been observed in the brain.[39]

Recrudescent toxoplasmosis is increasingly identified in immunocompromised patients with chronic infection. Pregnancy can provoke or be accompanied by the recurrence of ocular toxoplasmosis in an infected patient.[40] Immunosuppressed pregnant women with chronic *Toxoplasma* infection sometimes pass the infection to their fetus.[41] An infected fetus sustains a generalized infection which may be moderated by maternal antibody. Immunity is acquired more slowly in the fetus and newborn than in the generally asymptomatic mother. Active infection of the newborn is liable to persist in the brain and eye and produce significant lesions. In patients treated with corticosteroids and patients with AIDS, lesions progress with proliferation of tachyzoites.[42,43] About 25% of AIDS patients with *Toxoplasma* antibody sustain recrudescent infection, mainly in the brain and retina, but only occasionally in the lungs, stomach, and other parts of the body.[44] Other tissues generally retain immunity. The initiating event is probably a disintegrating tissue cyst from which liberated, surviving bradyzoites develop into tachyzoites that migrate along arterioles and among cells, causing cell destruction.[42] Because some affected arterioles undergo thrombosis, infarcts without *Toxoplasma* can develop. Due to the increased risk of allograft-transmitted toxoplasmosis, serologic evaluation and prophylaxis are standard for donor and recipient in heart and heart-lung transplantation. Screening is not yet routine in transplantation of other solid organs.[45]

## *Pathologic Features*

### Congenital infection

In congenital toxoplasmic encephalitis, there may be gross evidence of infarction, such as focal swelling, necro-

sis, or hemorrhage (Figs 12.24 & 12.25). Histopathologic changes include periventricular ependymal ulcerations, swelling of vessel walls, perivascular inflammation, vascular thrombosis, and necrosis (Figs 12.26 & 12.27). These periventricular lesions, unique to toxoplasmosis, may obstruct the aqueduct and are characterized by vasculitis without major participation of tachyzoites (Fig 12.28).[46] There may be scattered glial nodules with or without tachyzoites (Figs 12.29 & 12.30), and calcium deposits in necrotic areas (Figs 12.31 & 12.32). A prominent tissue eosinophilia may occur in any organ (Fig 12.33). The adrenal gland may be involved, resulting in extensive necrosis and readily identified tachyzoites (Figs 12.34 to 12.36). The placenta, though grossly normal, may nonetheless be infected (Figs 12.37 & 12.38). Placental toxoplasmosis with necrotizing granulomatous villitis has been reported in a patient with acute toxoplasmosis. Granulomas, formed by maternal inflammatory cells, contained rare cysts.[47] Other organs that may be involved in congenital toxoplasmosis include heart, lung, spleen, bone marrow, and eyes (Figs 12.39 to 12.44).

## Infection in Non-immunocompromised Patients

### Lymph node

In acute toxoplasmic lymphadenopathy, although lymph node histologic architecture remains intact, there is prominent reactive follicular hyperplasia. Affected nodes contain clusters of epithelioid histiocytes, principally in perifollicular zones and occasionally within follicles.[48,49] These histiocytes do not form well-defined granulomas or develop multiple nuclei, and are not accompanied by necrosis (Fig 12.45). Monocytoid B cells commonly distend capsular and trabecular sinuses. There may be focal or diffuse infiltrates of plasma cells, but no eosinophilia, fibrosis, or periadenitis. The differential diagnosis includes Hodgkin disease, Whipple disease, infectious mononucleosis, granulomatous lymphadenitis,the lymphoepithelioid cell variant of T-cell (Lennert) lymphoma, smallpox vaccination reaction, HIV-related lymphadenopathy, and sinus histiocytosis with massive lymphadenopathy (Rosai-Dorfman disease).[50] *Toxoplasma* cysts in histologic sections of lymph nodes have been found in less than 1% of cases submitted to the AFIP (Figs 12.46 & 12.47).

## Infection in Immunocompromised Adults

### Brain

In toxoplasmic encephalitis, tachyzoites multiply in neurons, glial and ependymal cells, and vessel walls (Figs 12.48 & 12.49). Tachyzoites tend to migrate along arteriolae, causing vasculitis, thrombosis, and infarction necrosis, mainly in gray matter (Figs 12.50 & 12.51).[42]

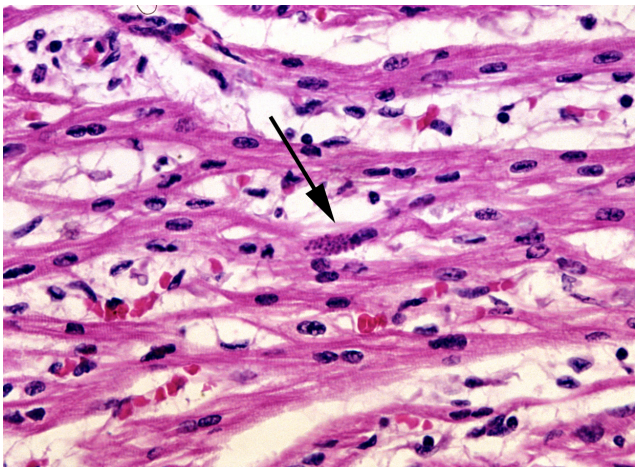


**Figure 12.39**
Group of *Toxoplasma* tachyzoites (arrow) in myocardium of patient with congenital toxoplasmosis. H&E x310

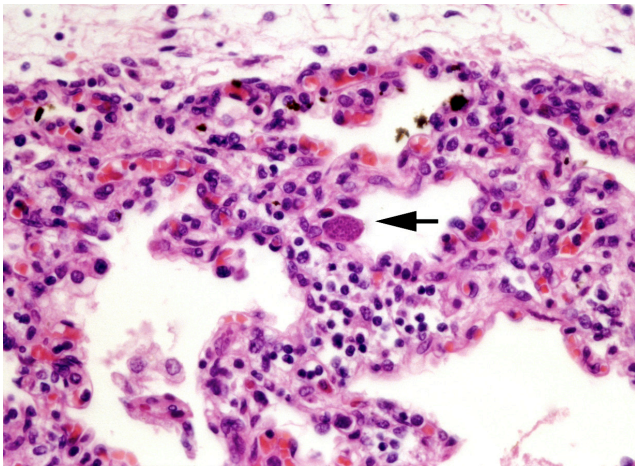


**Figure 12.40**
*Toxoplasma* cyst with bradyzoites (arrow) in lung of patient with congenital toxoplasmosis. H&E x280

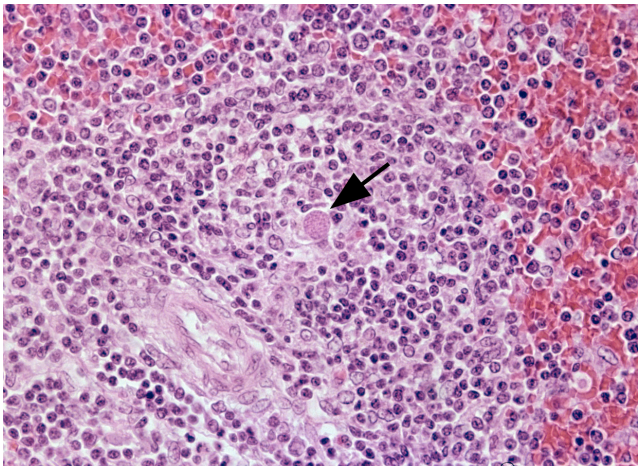


**Figure 12.41**
*Toxoplasma* cyst with bradyzoites (arrow) in white pulp of spleen of patient with congenital toxoplasmosis. H&E x260

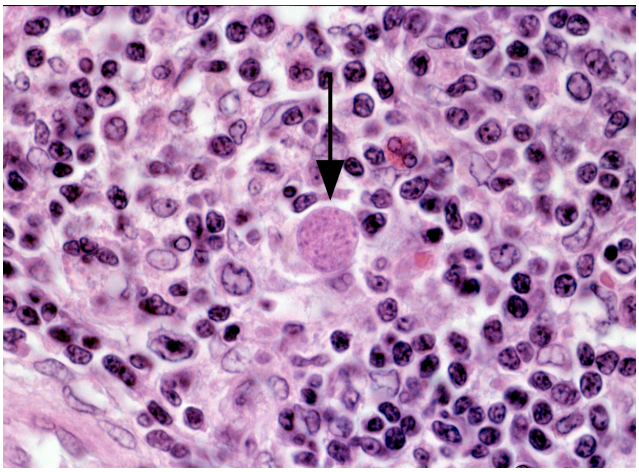


**Figure 12.42**
Higher magnification of *Toxoplasma* cyst in Figure 12.41. Note thin cyst wall (arrow). H&E x660

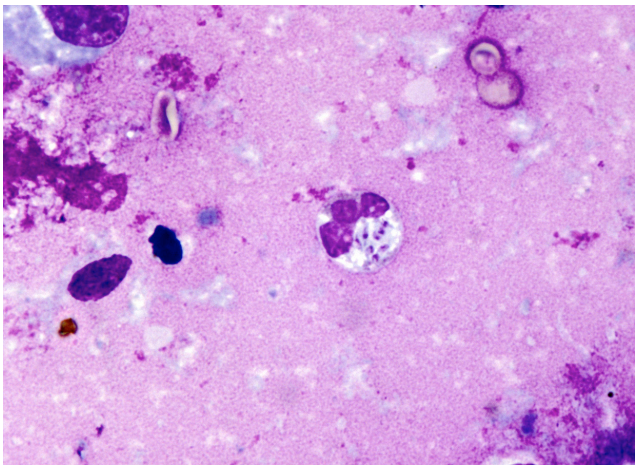


**Figure 12.43**
Smear of bone marrow of patient with congenital toxoplasmosis, demonstrating several *Toxoplasma gondii* organisms in macrophage. Giemsa x1265

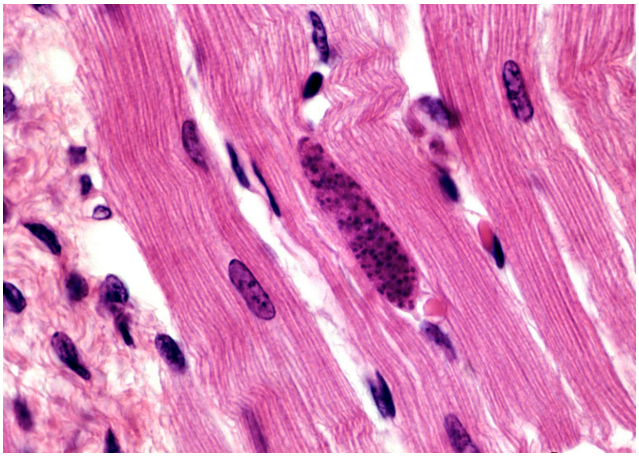


**Figure 12.44**
*Toxoplasma* cyst with bradyzoites in striated muscle of larynx of patient with congenital toxoplasmosis. H&E x660

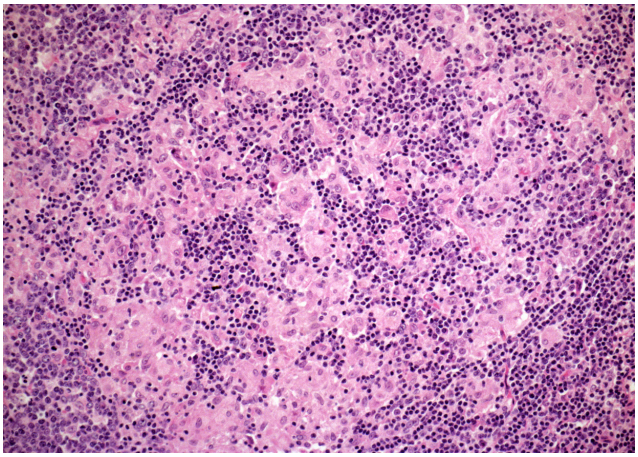


**Figure 12.45**
Toxoplasmic lymphadenitis with characteristic clusters of histiocytes that do not form well-defined granulomas. Note absence of necrosis. H&E x115

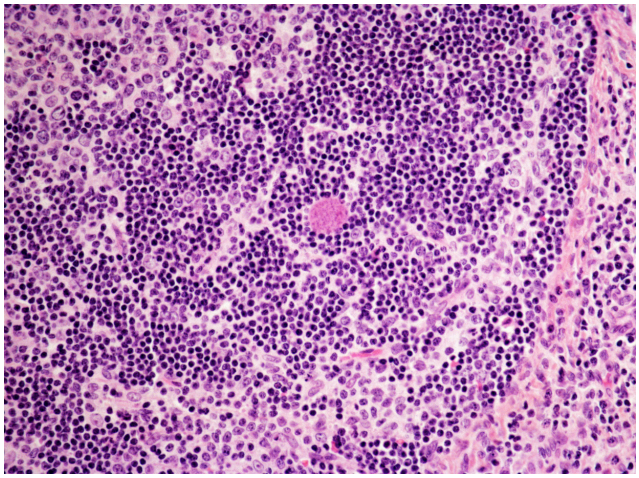


**Figure 12.46**
In lymph node, *Toxoplasma* cyst with bradyzoites is rare finding. H&E x175

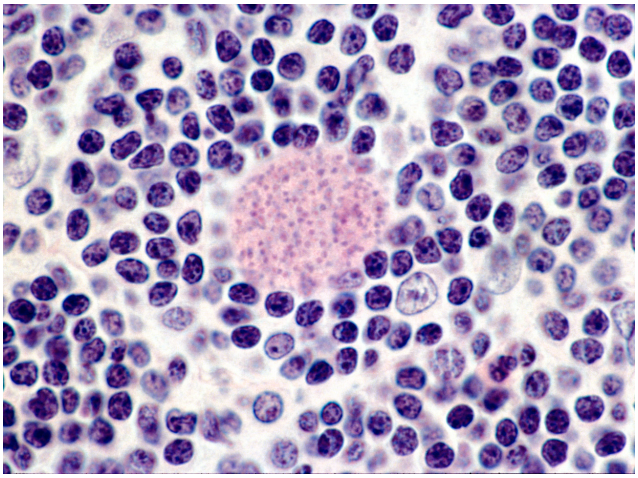


**Figure 12.47**
Higher magnification of bradyzoites within *Toxoplasma* cyst depicted in Figure 12.46. H&E x725

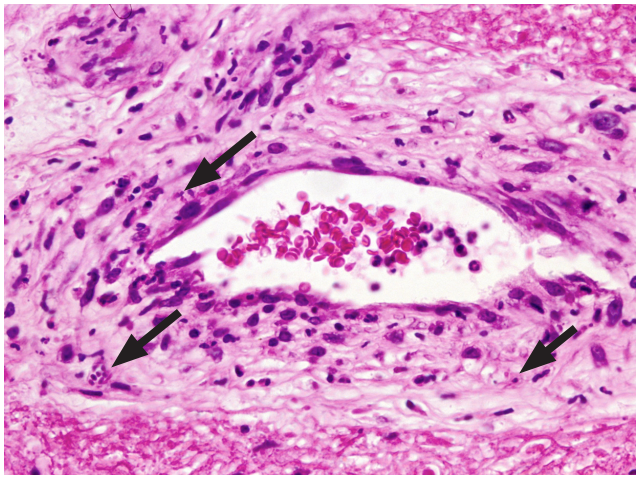


**Figure 12.48**
*Toxoplasma* tachyzoites within vessel wall (arrow) of biopsied brain of 71-year-old male who had been clinically diagnosed with glioma. H&E x235

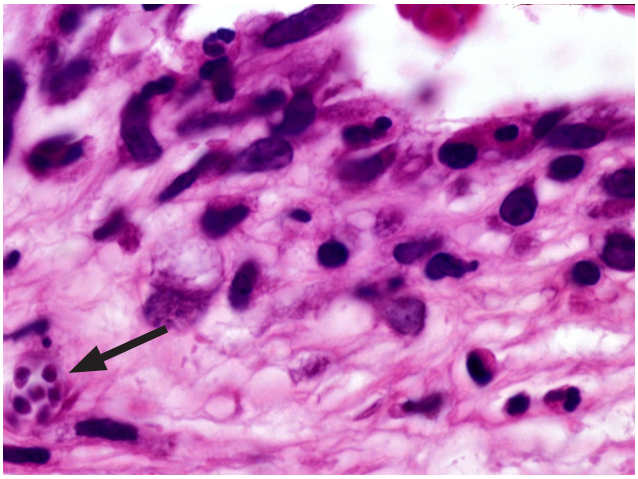


**Figure 12.49**
Higher magnification of vessel wall depicted in Figure 12.48. Note well-stained group of tachyzoites (arrow). H&E x745

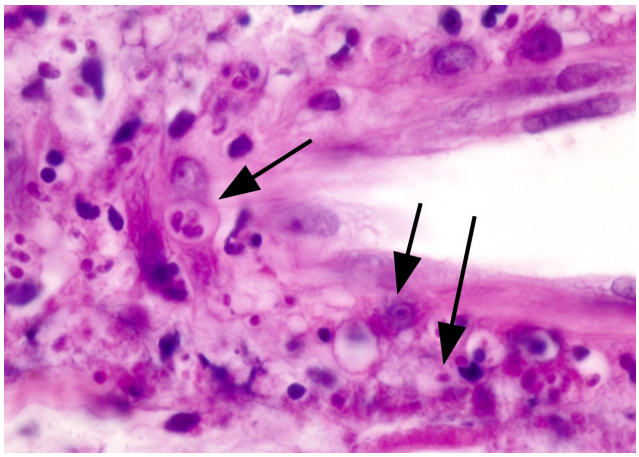


**Figure 12.50**
Primary vasculitis in brain of patient described in Figure 12.48. Vessel wall contains inflammatory cells and numerous tachyzoites (arrows). H&E x785

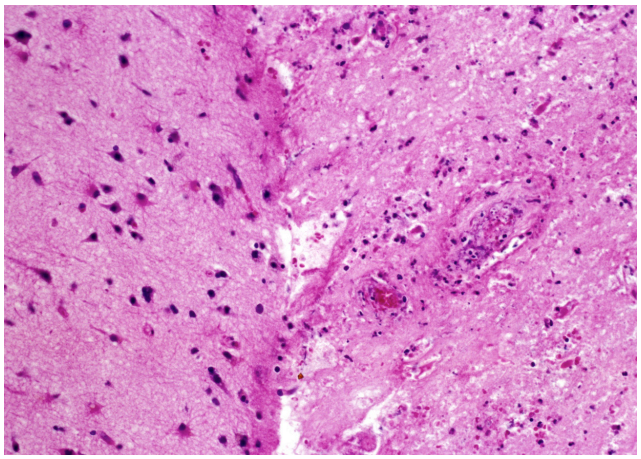


**Figure 12.51**
Interface of viable and necrotic tissue in biopsied brain of patient with toxoplasmosis. H&E x125

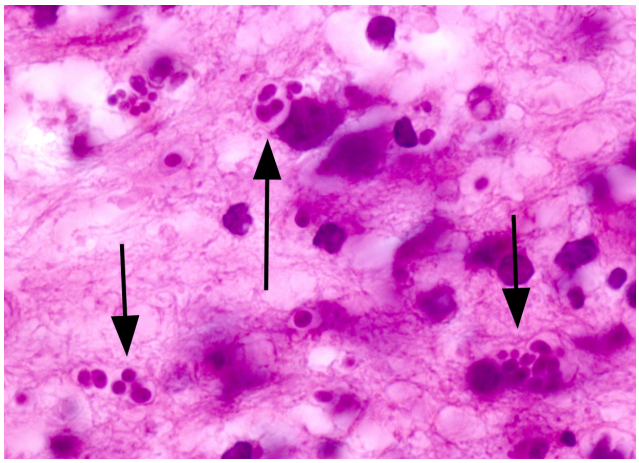


**Figure 12.52**
Clumps of *Toxoplasma* tachyzoites (arrrows) in biopsied brain. H&E x785

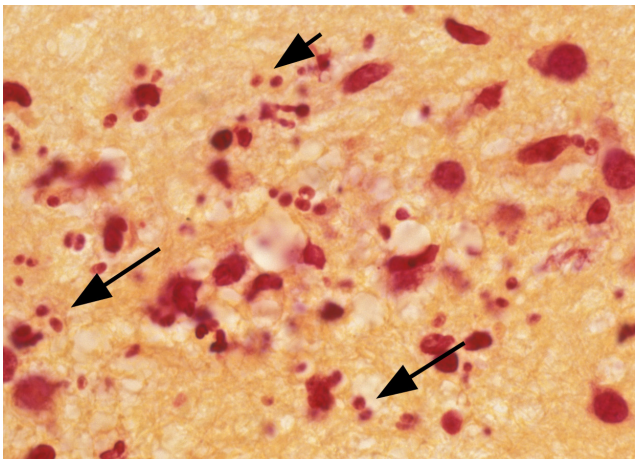


**Figure 12.53**
Many free *Toxoplasma* tachyzoites in biopsied brain. Each tachyzoite is round to oval with well-defined nucleus (arrows). B&H x770

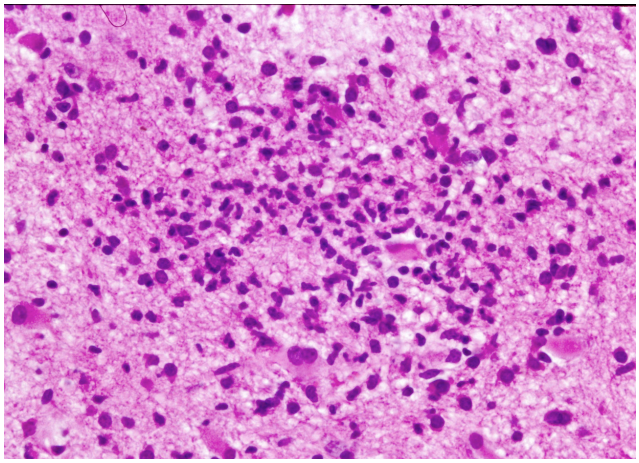


**Figure 12.54**
Focus of neutrophils in biopsied brain of patient with toxoplasmosis. H&E x765

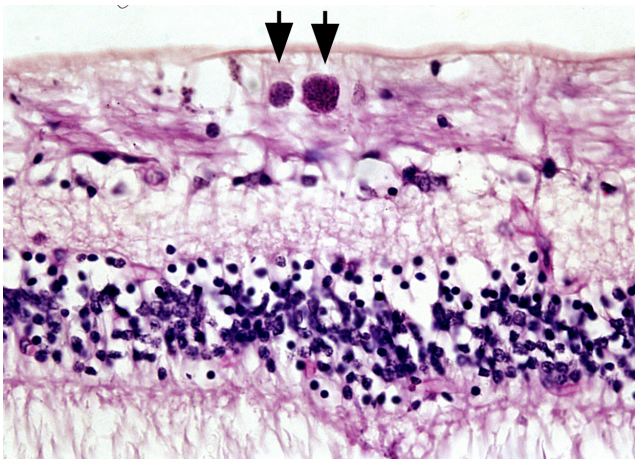


**Figure 12.55**
Two *Toxoplasma* cysts in nerve fiber layer of retina. PAS x260

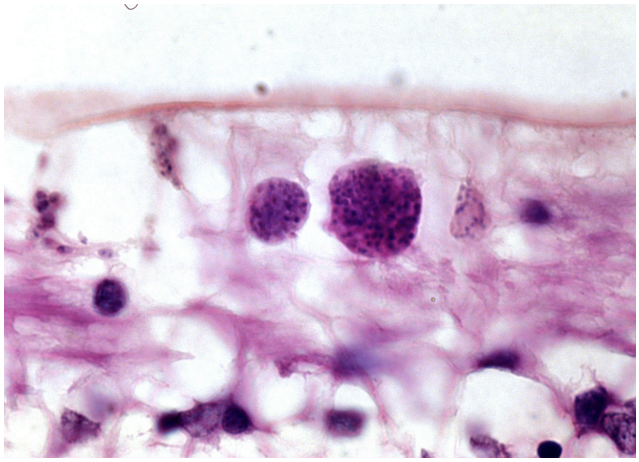


**Figure 12.56**
Higher magnification of *Toxoplasma* cysts in Figure 12.55. PAS x640

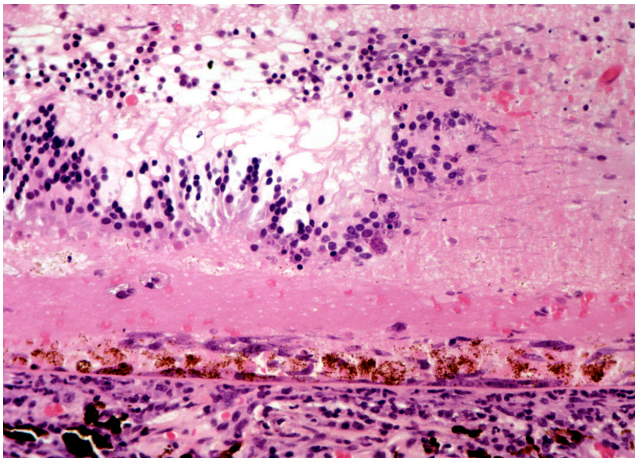


**Figure 12.57**
Acute retinal necrosis caused by toxoplasmosis. H&E x205

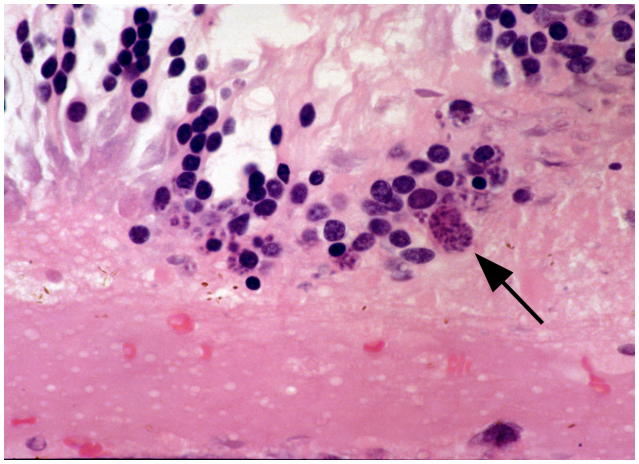


**Figure 12.58**
Higher magnification of retinal necrosis in Figure 12.57, depicting *Toxoplasma* cyst (arrow) and free tachyzoites. H&E x440

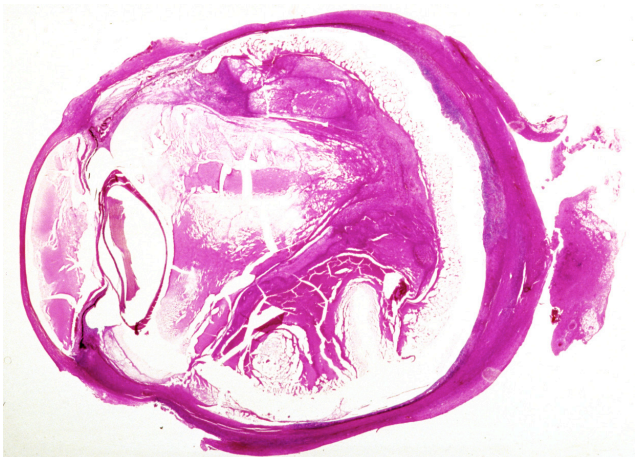


**Figure 12.59**
Enucleated eye from patient with AIDS-related toxoplasmosis, showing detached, necrotic retina and proteinaceous exudate between retina and choroid. H&E x2.8

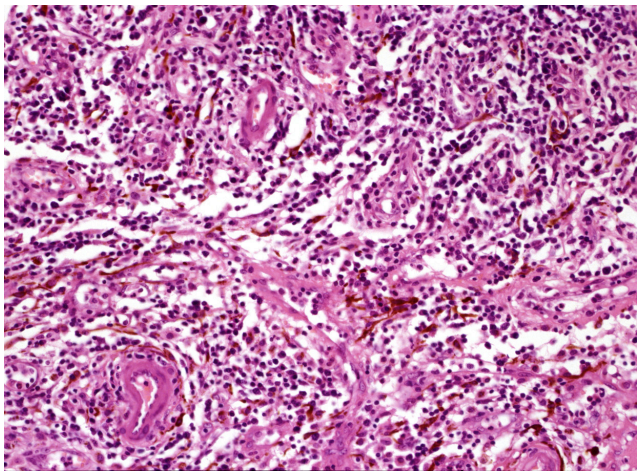


**Figure 12.60**
Chronic choroiditis in enucleated eye from patient described in Figure 12.59. H&E x130

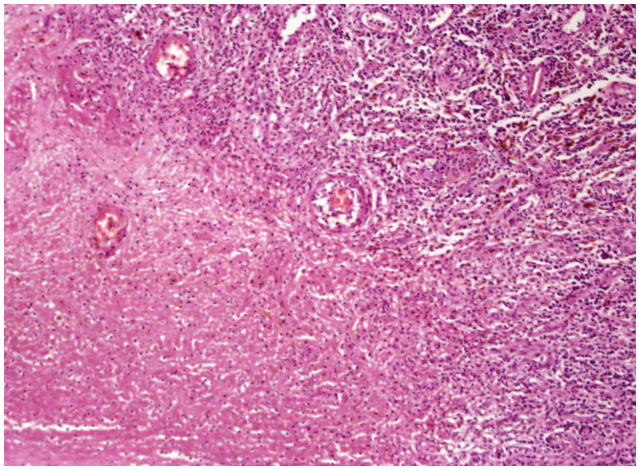


**Figure 12.61**
Interface of viable and necrotic choroid in enucleated eye from patient described in Figures 12.59 and 12.60. H&E x65

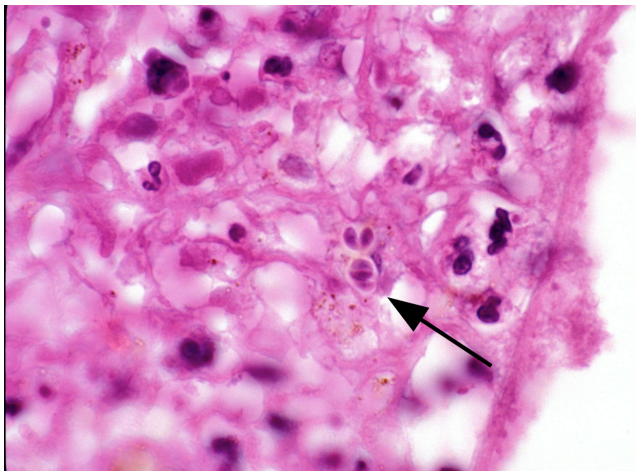


**Figure 12.62**
Several *Toxoplasma* tachyzoites in necrotic choroid (arrow) in enucleated eye from patient described in Figures 12.59 to 12.61. H&E x745

Tachyzoites may be numerous, especially at the periphery of necrotic foci (Figs 12.52 & 12.53), and cysts containing bradyzoites may also be seen (Fig 12.12). Free tachyzoites, disintegrating cysts, and infarction provoke an inflammatory response composed mainly of neutrophils (Fig 12.54). Intracellular tachyzoites and intact cysts do not provoke inflammation. Glial nodules, which are composed of pyknotic nuclei, necrosis, microglial cells, and other inflammatory cells, result from death of parasitized cells. Tachyzoites may be identified in or at the periphery of glial nodules.

## Eye

Examination of enucleated eyes blinded by retinal destruction or glaucoma caused by toxoplasmosis may reveal cysts and/or tachyzoites in the retina (Figs 12.55 to 12.58). In some patients with sporadic retinochoroiditis caused by toxoplasmosis, cysts may persist in the retina for months or years.[51] The anti-inflammatory and immunosuppressive effects of corticosteroids may permit tachyzoites to multiply in the retina; however, liberated tachyzoites are usually inactivated by adequate immunity. Bradyzoites liberated from disintegrating cysts produce intense inflammation and scarring; when tachyzoites destroy parasitized cells, the retinal lesion is more diffuse and inflammation may extend to the vitreous and anterior chamber. The retina is largely necrotic, with pigment-bearing macrophages in its outer layers and in the vitreous. The retina may be detached, with proteinaceous exudate between it and the choroid (Fig 12.59). The choroid is heavily infiltrated with plasma cells, lymphocytes, and mononuclear cells, and may be necrotic (Figs 12.60 & 12.61). The retinal pigment epithelium shows focal proliferation and diffuse necrosis. Tachyzoites and cysts may be seen in all retinal layers and the choroid (Figs 12.62 & 12.63). Panophthalmitis, orbital cellulitis, and hemorrhage are rare (Figs 12.64 & 12.65).[52,53] In AIDS patients with toxoplasmosis, if the full thickness of the retina is involved, miliary toxoplasmic retinitis lesions may become confluent and the retina may detach (Figs 12.59, 12.66, & 12.67).

## Lymph Node

Among AIDS patients with disseminated toxoplasmosis, lymph nodes are rarely involved. Immunocompromised patients who do develop toxoplasmic lymphadenitis show effacement of nodal architecture (Fig 12.68) and areas of massive necrosis that usually contain *T. gondii* cysts and tachyzoites (Fig 12.69).

## Lung

In toxoplasmic pneumonia, the inflammatory reaction is mononuclear and intra-alveolar (Fig 12.70). Vasculitis may be prominent (Fig 12.71). Tachyzoites, groups, and cysts may be diffuse or in foci of coagulation necrosis (Figs 12.72 to 12.74).

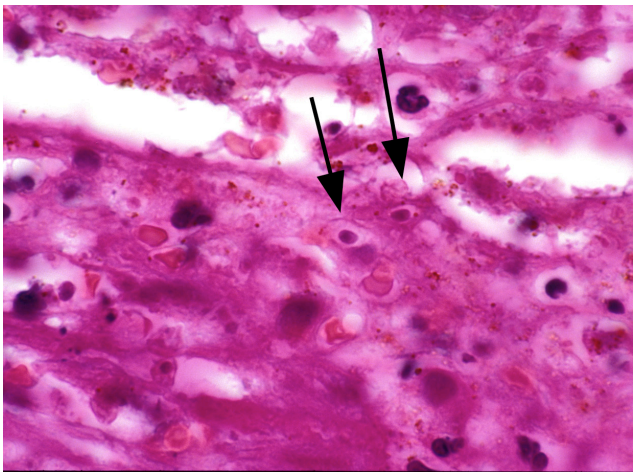


**Figure 12.63**
Two *Toxoplasma* tachyzoites in necrotic choroid (arrows) in enucleated eye from patient described in Figures 12.59 to 12.62. H&E x750

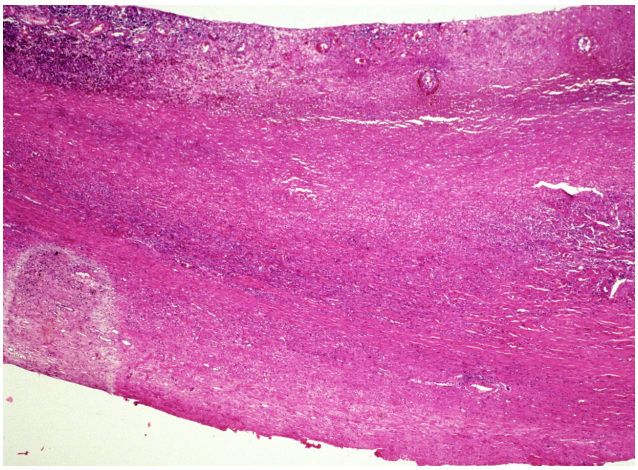


**Figure 12.64**
Panophthalmitis in enucleated eye from patient described in Figures 12.59 to 12.63. Note necrotic sclera. H&E x19

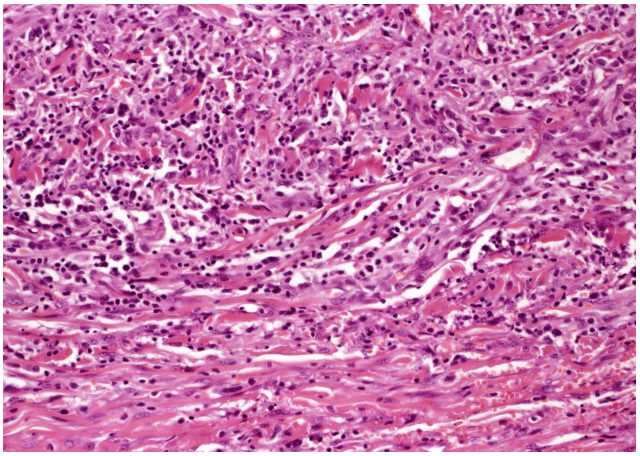


**Figure 12.65**
Panophthalmitis in enucleated eye from patient described in Figures 12.59 to 12.64. Note chronic scleritis. H&E x125

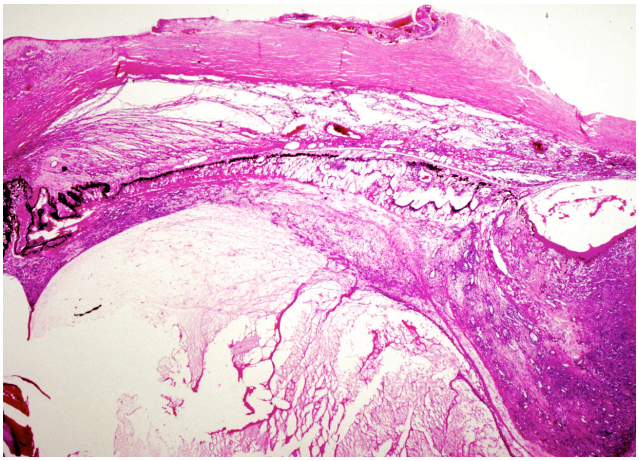


**Figure 12.66**
Panophthalmitis in enucleated eye from patient described in Figures 12.59 to 12.65. Both ciliary body and detached retina are necrotic. H&E x5

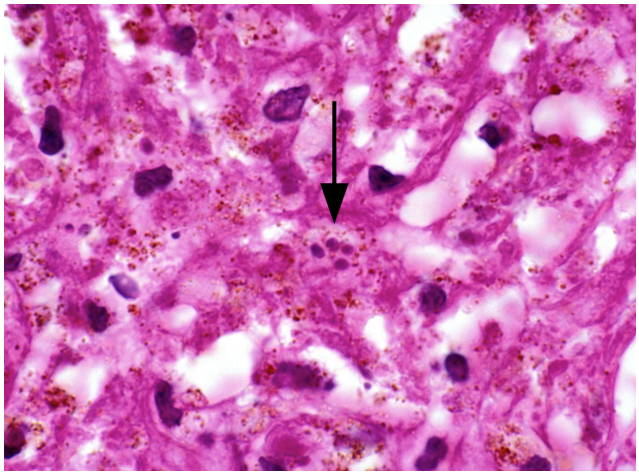


**Figure 12.67**
Four *Toxoplasma* tachyzoites (arrow) in necrotic ciliary body depicted in Figure 12.66. H&E x750

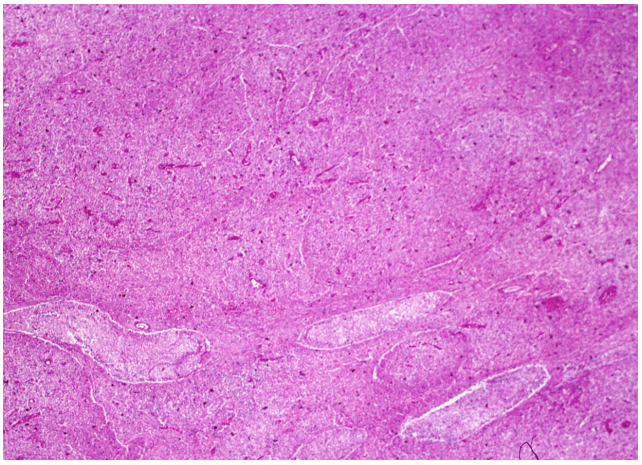


**Figure 12.68**
Massive necrosis in effaced lymph node from immunocompromised patient. H&E x25

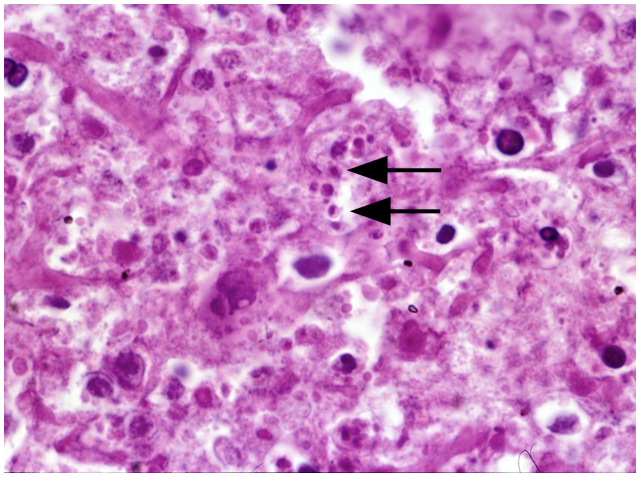


**Figure 12.69**
Several *Toxoplasma* tachyzoites (arrows) in necrotic lymph node shown in Figure 12.68. H&E x800

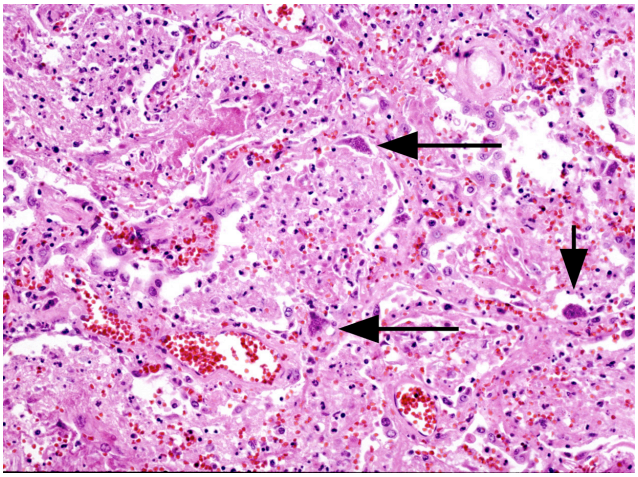


**Figure 12.70**
Toxoplasmic pneumonia with characteristic necrosis, intra-alveolar exudate and cysts (arrows). H&E x125

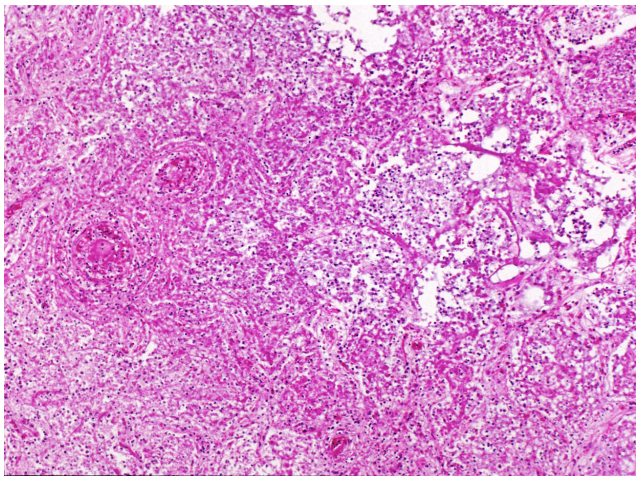


**Figure 12.71**
Toxoplasmic pneumonia with necrosis and prominent vasculitis. H&E x60

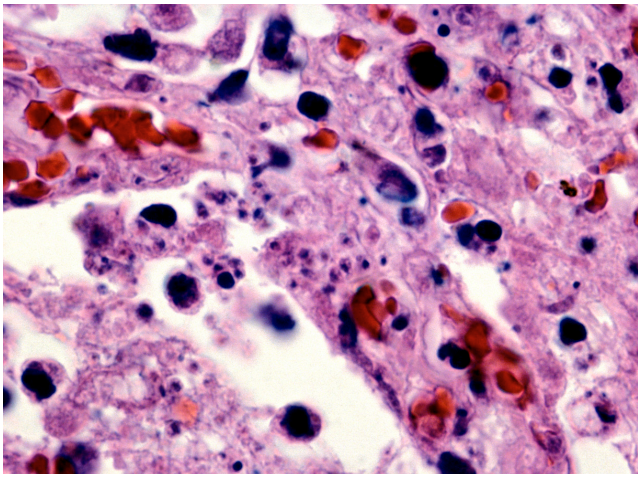


**Figure 12.72**
Intra- and extracellular *Toxoplasma* tachyzoites in necrotic lung. H&E x735

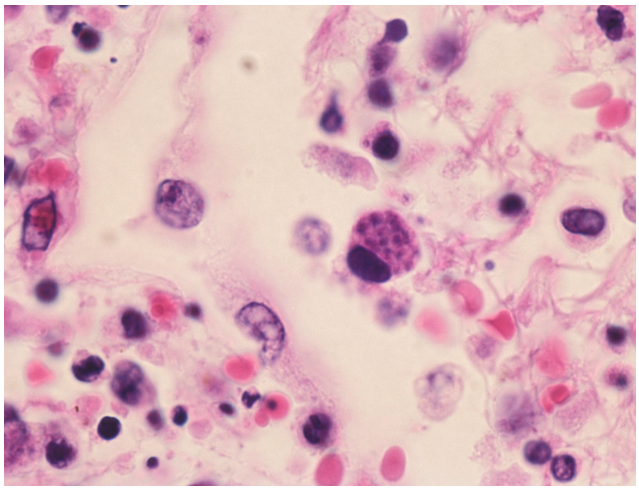


**Figure 12.73**
Group of *Toxoplasma* tachyzoites within histiocyte in lung. H&E x755

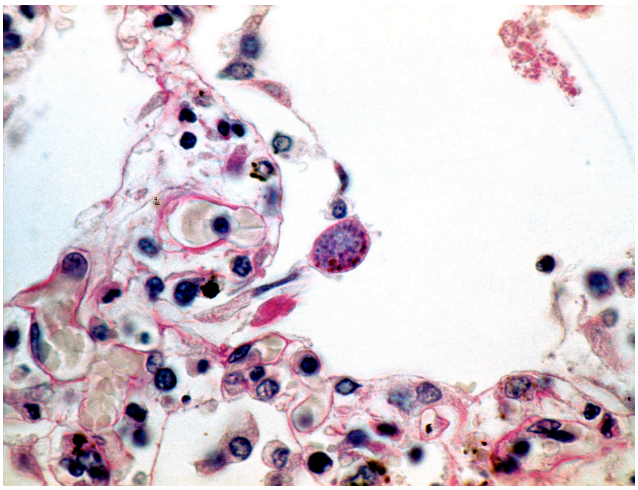


**Figure 12.74**
*Toxoplasma* cyst with bradyzoites in lung. Few organisms are PAS-positive. PAS x450

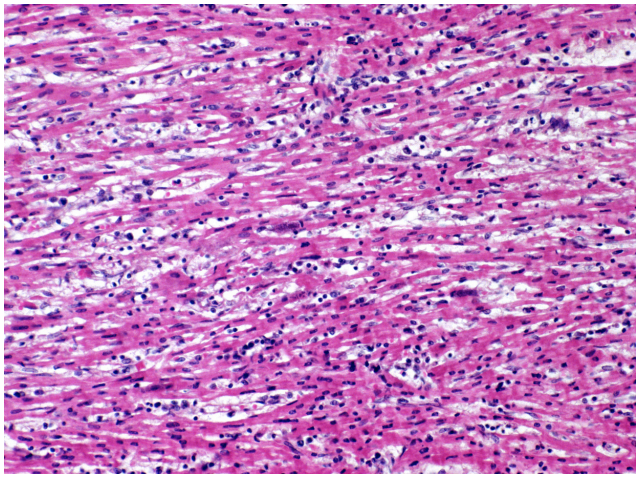


**Figure 12.75**
Toxoplasmic myocarditis characterized by mononuclear inflammatory infiltrate. H&E x130

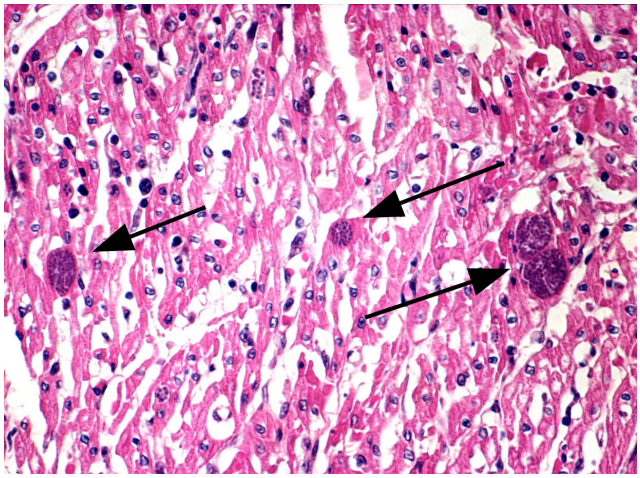


**Figure 12.76**
*Toxoplasma* organisms (arrows) parasitize individual heart muscle fibers. H&E x250

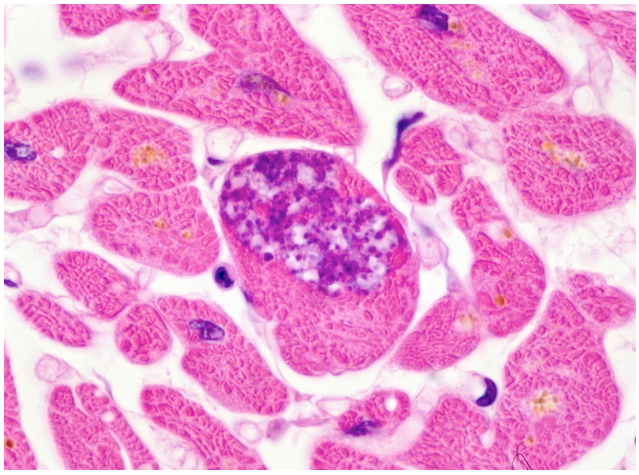


**Figure 12.77**
*Toxoplasma* organisms in heart muscle fiber. Note absence of inflammation. H&E x630

### Heart

Toxoplasmic myocarditis is characterized by a mononuclear inflammatory infiltrate (Fig 12.75). *Toxoplasma* organisms may parasitize individual heart muscle fibers, provoking no inflammatory reaction (Figs 12.76 & 12.77).

### Liver

Liver involvement in toxoplasmosis is rare and generally diagnosed on the basis of abnormal liver function tests and serology. *Toxoplasma* organisms are rarely identified in the liver (Fig 12.4).

## *Diagnosis*

*Toxoplasma* organisms in lesions are best revealed with hematoxylin, immunoperoxidase, or in situ DNA hybridization. PCR tests are highly sensitive and specific for detecting toxoplasmic encephalitis,[54] and are particularly useful when patients have undergone chemotherapy and no organisms are visible in sections.[42] Real-time PCR detection methods for *Toxoplasma* DNA have been developed.[55,56] Used on blood samples, PCR may help to detect recent infections in patients midway through pregnancy.[57] Multicopy sequences specific for *T. gondii*, such as the B1 gene or the 529-bp sequence, are especially useful in molecular tests. Molecular methods are also employed for genotypic characterization of *T. gondii* isolates; analysis of polymorphic sequences determines the precise type.[58] If the patient is immunocompetent, antibody titers should be commensurate with levels usually found in such disease states.[59] Finding tachyzoites in lesions, along with a rising antibody titer, is diagnostic of acute infection. Conversely, finding both *Toxoplasma* cysts and tachyzoites in an enucleated eye may be associated with a low, stable antibody titer indicative of chronic infection.

The most useful serologic tests are the dye test, direct *Toxoplasma* agglutination test, and indirect fluorescent antibody test, each of which is highly sensitive.[60-62] However, interpretation of antibody tests is not dependable in immuno-compromised patients, so diagnosis should be based on identifying the etiologic agent, its antigens, or its DNA.

*Toxoplasma* can be isolated in cell cultures but is best isolated by inoculating suspected material into mice previously shown to be free of *Toxoplasma* antibody. After intraperitoneal inoculation, *Toxoplasma* tachyzoites may be found in the peritoneal exudate that develops after 4 to 6 days. If the mice show no clinical changes on primary inoculation, diagnosis must be based on finding antibody in the mice after 3 to 4 weeks, or finding *Toxoplasma* cysts in the brain after 1 or 2 months. *Toxoplasma* cysts must be differentiated from any *Encephalitozoon* pseudocysts that may be encountered. Because *Toxoplasma* organisms persist through asymptomatic chronic infection, isolation of organisms is not by itself indicative of disease from *Toxoplasma*, but must be correlated with antibody response,

symptoms, and lesions.

In histologic sections, a variety of microorganisms, including those that cause histoplasmosis, pneumocystosis, microsporidiosis, leishmaniasis, American trypanosomiasis, and sarcocystosis, and intracytoplasmic inclusions of cytomegalovirus (CMV) may be mistaken for *Toxoplasma* (Fig 12.78). Intracytoplasmic CMV inclusions stain well with H&E, are round, basophilic to amphophilic, and 1µm to 4µm in diameter; unlike *T. gondii*, however, they have no nucleus (Fig 12.79). *Histoplasma capsulatum* yeast cells are round to oval and frequently contain vacuoles (Fig 12.80), but they reproduce by budding (Fig 12.81), which distinguishes them from *T. gondii*. Microsporidian spores are readily observed with H&E stain (Fig 12.82), but special stains can reveal distinguishing characteristics of some spores, such as a PAS-positive polar granule at the anterior end (Fig 12.83) or a gram-positive band (Fig 12.84).

Amastigotes of *Leishmania* sp and *Trypanosoma cruzi* may be mistaken for *T. gondii* since they stain well with H&E and are about the same size. They can be distinguished from *T. gondii*, however, by the presence of a rod-shaped kinetoplast (Fig 12.85 to 12.89). Brown-Hopps modified Gram stain may help to identify the kinetoplast in tissue sections (Fig 12.86). The kinetoplast stains dark blue by the Giemsa method in smears, scrapings, and imprints (Fig 12.87). *Sarcocystis* sp, which also can mimic *T. gondii*, form sarcocysts that contain various stages of the parasite (Figs 12.90 &12.91), including mature, banana-shaped bradyzoites (Fig 12.92). Distinguishing characteristics of *Sarcocystis* sp include septations in the sarcocyst and bradyzoites that are larger than those of *T. gondii*. Occasionally, unidentified structures that mimic *T. gondii* are found in tissue sections (Figs 12.93–12.96), but careful examination shows none of the pertinent morphologic features. *Toxoplasma gondii* can be cultured and distinguished from other similar microorganisms by their characteristic ultrastructural features (Fig 12.97).

## Treatment and Prevention

Drug therapy of toxoplasmosis is complex considering all the disease forms and status of the patient. Thus the clinician should consult appropriate specialized literature before starting treatment. Following are a few generalized suggestions.

The treatment of choice for toxoplasmosis is chemotherapy with a combination of oral pyrimethamine and sulfadiazine.[63] Pyrimethamine is administered with a loading dose of 75 to 200 mg/day for the first 3 days and 25 to 50 mg/day thereafter. For toxoplasmic encephalitis, the higher dose should be maintained. Sulfadiazine is given as 500 to 1000 mg every 6 hours. Folinic acid (leucovorin, 1 to 20 mg/day) counteracts any hematologic side effects of this drug regimen without significantly impairing therapeutic action.

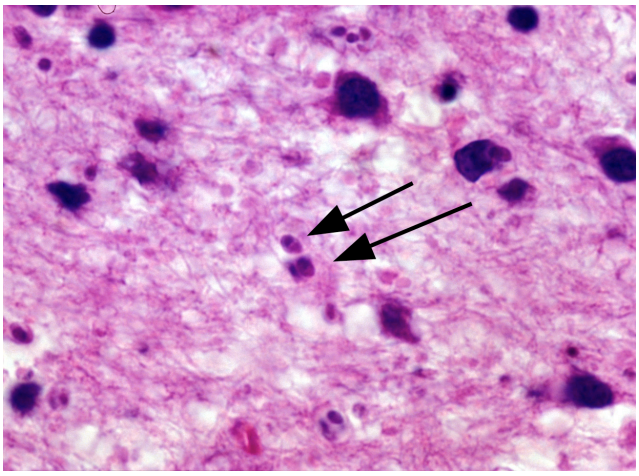


**Figure 12.78**
Typical *Toxoplasma gondii* tachyzoites (arrows), each with prominent nucleus, in biopsy of brain. H&E x780

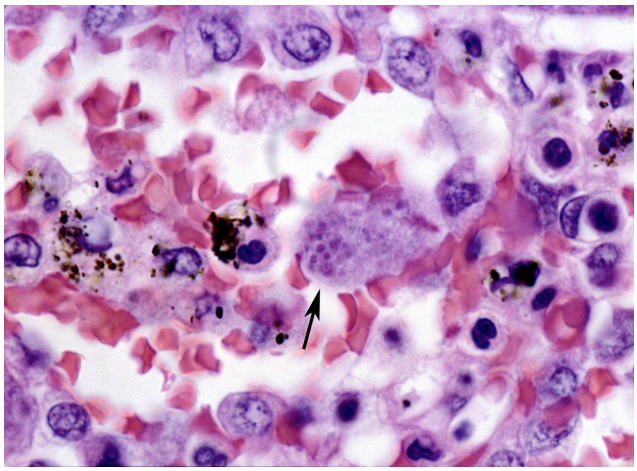


**Figure 12.79**
Intracytoplasmic inclusions of CMV (arrow) in lung are homogeneous and lack nuclei. H&E x710

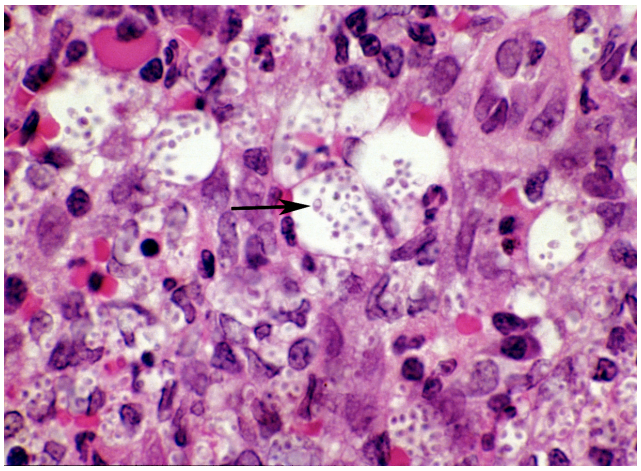


**Figure 12.80**
*Histoplasma capsulatum* yeast cells in cecal mass are round to oval and contain vacuoles (arrow). H&E x780

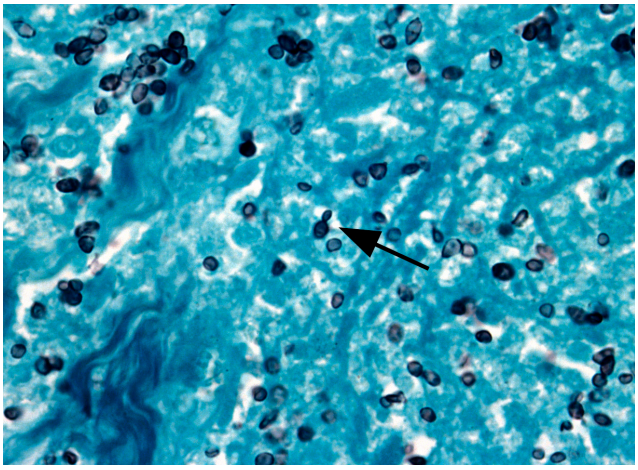


**Figure 12.81**
*Histoplasma capsulatum* yeast cells in necrotic lung, demonstrating narrow-neck budding (arrow) and silver positivity. GMS x590

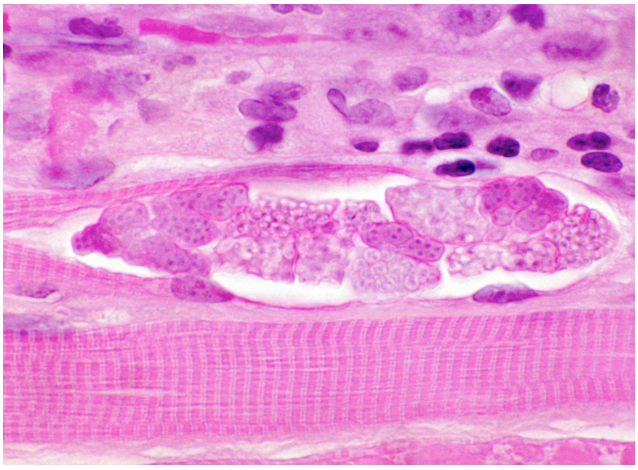


**Figure 12.82**
Microsporidian spores of *Pleistophora ronneafiei* in striated muscle are readily identified by H&E. H&E x800

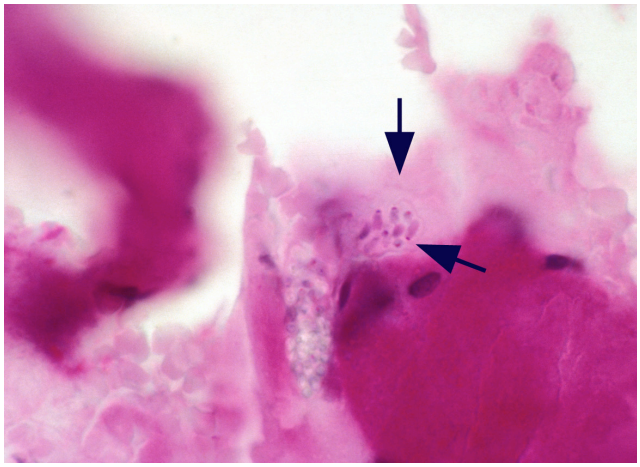


**Figure 12.83**
Microsporidian spores of *Pleistophora ronneafiei* in striated muscle, demonstrating PAS-positive polar granule (arrows) at anterior end of spore. PAS x800

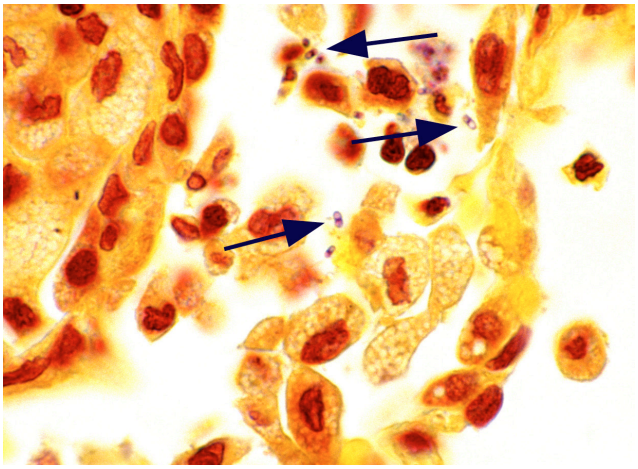


**Figure 12.84**
Microsporidian spores of *Encephalitozoon cuniculi* in lung of AIDS patient. Spores are extracellular and have band of gram-positive material (arrows). B&H x800

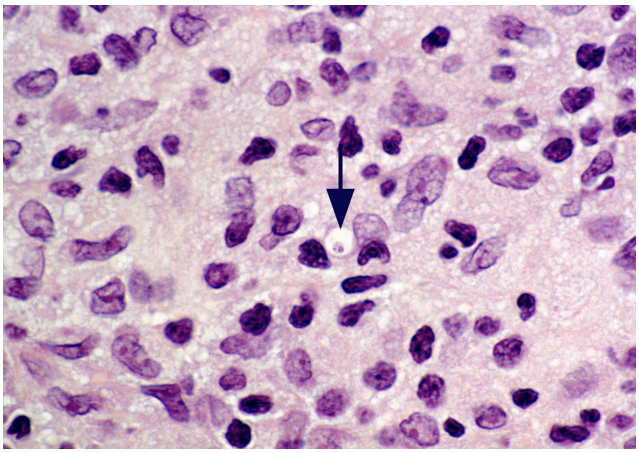


**Figure 12.85**
Single amastigote within vacuolated histiocyte in skin of patient with cutaneous leishmaniasis. Note tiny rod-shaped kinetoplast (arrow) to left of large spherical nucleus. H&E x590

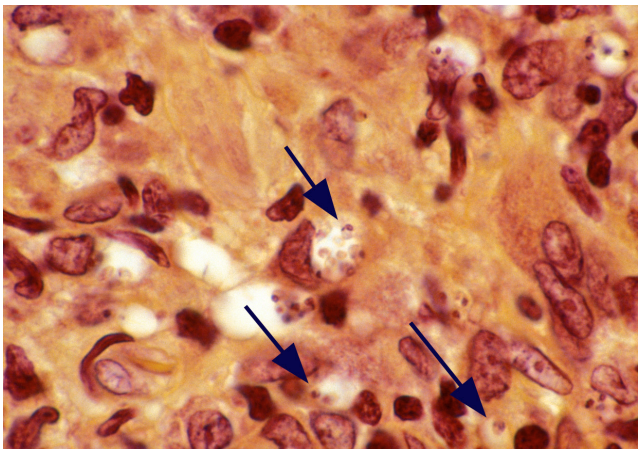


**Figure 12.86**
Several amastigotes of *Leishmania* sp in skin of patient with cutaneous leishmaniasis. Note yellow to pale cytoplasm, large red round nucleus, and tiny black rod-shaped kinetoplast (arrows). B&H x800

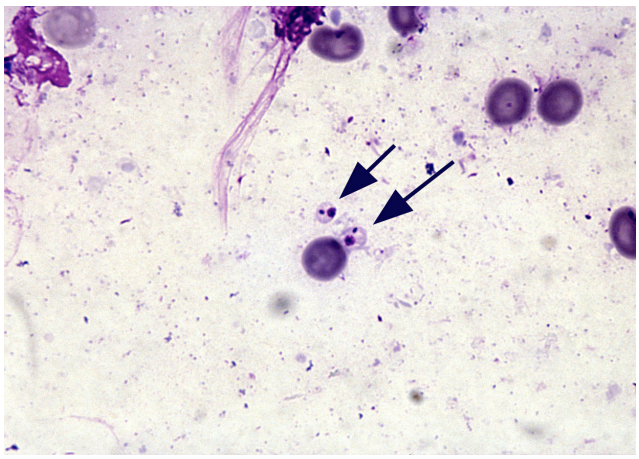


**Figure 12.87**
Smear of skin of patient with cutaneous leishmaniasis shows 2 *Leishmania* sp amastigotes (arrows). Note well-stained large round nucleus and deeply stained rod-shaped kinetoplast. Giemsa x830

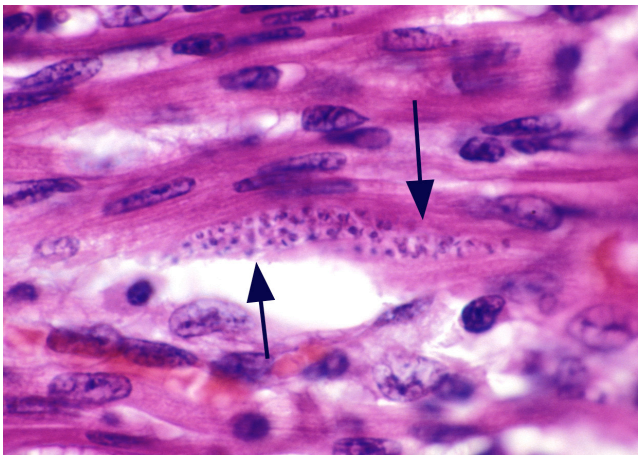


**Figure 12.88**
Cluster of *Trypanosoma cruzi* amastigotes in heart of patient who died of Chagas' disease. Note deeply stained rod-shaped kinetoplasts (arrows). H&E x930

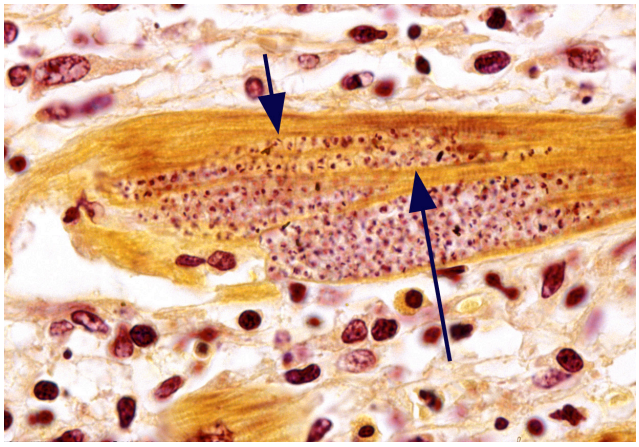


**Figure 12.89**
Cluster of *Trypanosoma cruzi* amastigotes in heart of patient who died of Chagas' disease. Note deeply stained rod-shaped kinetoplasts (arrows). B&H x670

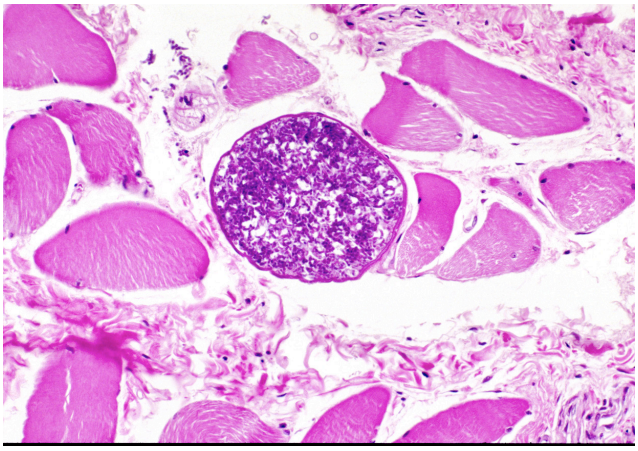


**Figure 12.90**
Mature *Sarcocystis* sp sarcocyst in African patient. Note well-stained bradyzoites and lack of inflammation. H&E x120

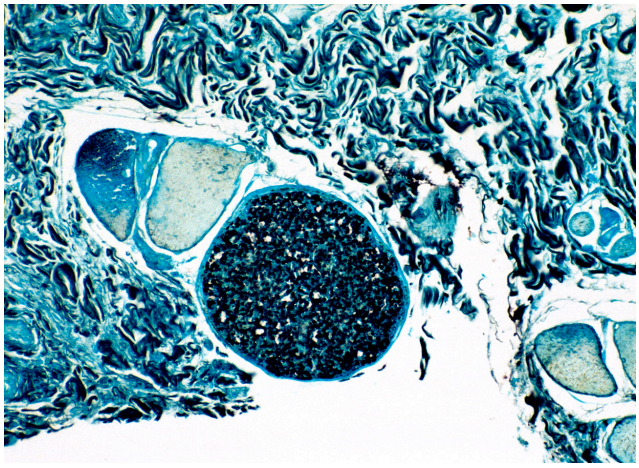


**Figure 12.91**
Same sarcocyst shown in Figure 12.90, demonstrating GMS-positive bradyzoites. GMS x120

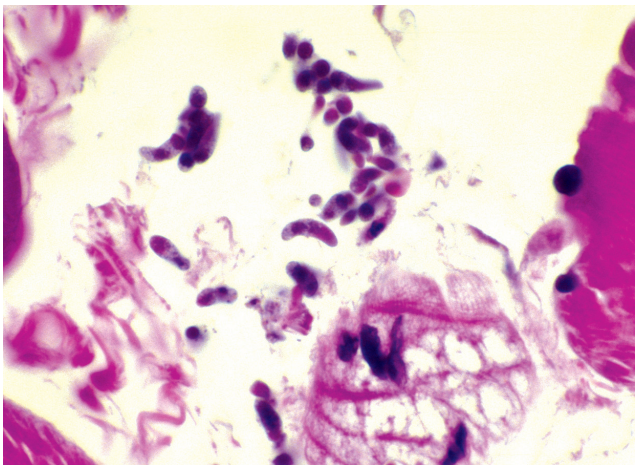


**Figure 12.92**
Extracellular bradyzoites from sarcocyst described in Figures 12.90 and 12.91. Bradyzoites are 9µm to 12µm by 2µm to 4µm and have rounded ends; each organism has prominent nucleus. H&E x650

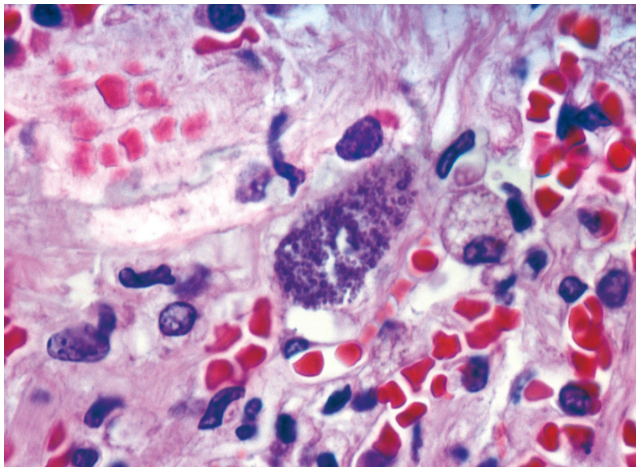


**Figure 12.93**
Calcification in lung mimicking *Toxoplasma gondii* cyst. H&E x830

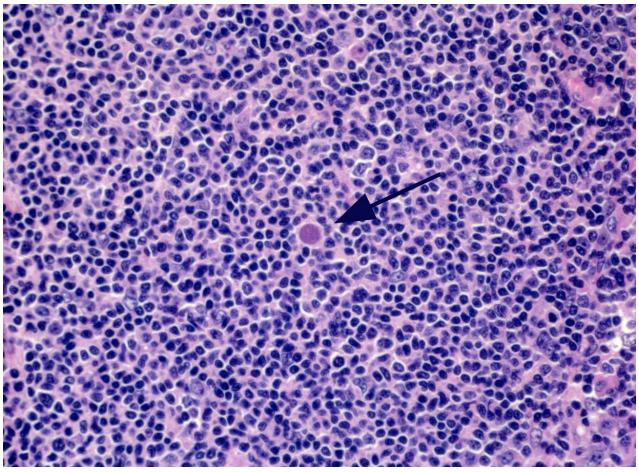


**Figure 12.94**
Unidentified artifact (arrow), initially identified as *Toxoplasma gondii*, in hypertrophic lymph node. H&E x100

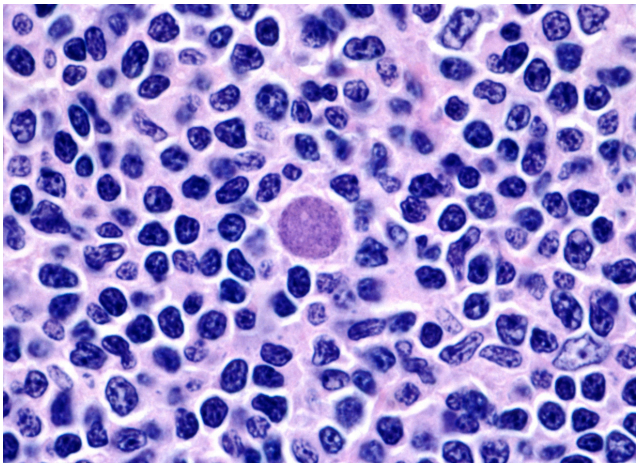


**Figure 12.95**
Higher magnification of structure shown in Figure 12.93. Unidentified artifact is 10 µm in diameter and contains neither bradyzoites nor tachyzoites. H&E x300

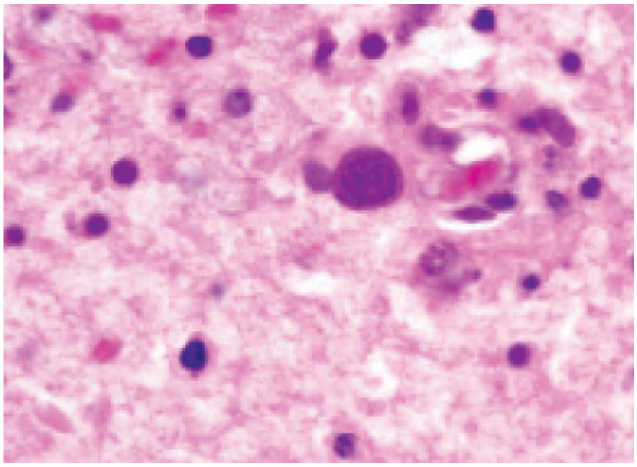


**Figure 12.96**
Unidentified cell in brain of patient with proven toxoplasmic encephalitis. The possibility of an atypical *Toxoplasma* cyst was entertained, but it lacked the pathognomonic features. The cell is 14 µm in diameter. H&E x535




**Figure 12.97**
*Toxoplasma* tachyzoites in cultured cells showing conoid (c), nucleus (n), rhoptries (r), mitochondria (m), and division by endodyogeny (e). x9,430

Because the pyrimethamine-sulfadiazine combination is potentially teratogenic, pregnant patients should be given clindamycin (600 mg every 6 hours). Acute toxoplasmosis in pregnant women should receive speramycin 1 gram orally 3-4 times daily until term delivery. Other drugs with activity against *T. gondii* include, azithromycin, clarithromycin, atovaquone, minocycline, rifabutin, and dapsone. Post-transplant toxoplasmosis can be prevented by prophylaxis with trimethoprim-sulfamethoxazole.[64]

Toxoplasmosis can be prevented by observing a few simple precautions. Because infection is most severe in the perinatal period, pregnant women should avoid contact with outdoor cats that hunt rodents and birds, and soil and sand that may be contaminated with cat feces. Cover children's sandboxes when not in use and do not allow outdoor cats to defecate indoors. Litter boxes used exclusively by indoor cats that do not hunt are not likely to be contaminated. Cook all meat until it is well-done[65] and wash hands thoroughly after contact with any sources of infection.[13] There is no evidence of sexual transmission in humans.[66]

Ultimate control of toxoplasmosis demands an effective vaccine that stimulates both cellular and humoral mucosal immunity. Some vaccines that use attenuated parasites and DNA prime-booster techniques are in development, but have not yet been well-formulated or tested.[67-68] Proteomic research to identify new drug and vaccine targets and produce 2-dimensional gel electrophoresis maps of *T. gondii* tachyzoites is currently under way.[69]

## References


1. Nicolle C, Manceaux L. An infection by Leishman bodies (or closely related organisms) from the gundi [in French]. *C R Acad Sci (Paris).* 1908;147:763-766.
2. Splendore A. A new parasitic protozoan of rabbits. Found in the anatomic lesions of an illness that is similar in many ways to Kala-azar in man [in Italian]. *Rev Soc Sci (São Paulo).* 1908;3:109-112.
3. Janku J. Parasites in coloboma of macula. *Cas Lek Cesk.* 1923;62:1021-1027.
4. Wolf A, Cowen D, Paige BH. Human toxoplasmosis: occurrence in infants as an encephalomyelitis verification by transmission to animals. *Science.* 1939;89:226-227.
5. Sabin AB, Feldman HA. Dyes as microchemical indicators of a new immunity phenomenon affecting a protozoon parasite (*Toxoplasma*). *Science.* 1948;108:660-663.
6. Wilder HC. *Toxoplasma* chorioretinitis in adults. *A M A Arch Ophthalmol.* 1952;48:127-136.
7. Jacobs L, Remington JS, Melton ML. A survey of meat samples from swine, cattle, and sheep for the presence of encysted Toxoplasma. *J Parasitol.* 1957;46:23-28.
8. Weinman D, Chandler AH. Toxoplasmosis in swine and rodents. Reciprocal oral infection and potential human hazard. *Proc Soc Exp Biol Med.* 1954;87:211-216.
9. Frenkel JK. *Toxoplasma* in and around us. *Bioscience.* 1973;23:343-352.
10. Lehmann T, Blackston CR, Parmley SF, Remington JS, Dubey JP. Strain typing of *Toxoplasma gondii:* comparison of antigen-coding and housekeeping genes. *J Parasitol.* 2000;86:960-971.
11. Fekkar A, Ajzenberg D, Bodaghi B, et al. Direct genotyping of *Toxoplasma gondii* in ocular fluid samples from 20 patients with ocular toxoplasmosis: predominance of type II in France. *J Clin Microbiol.* 2011;49:1513-1517.
12. Hill D, Dubey JP. Toxoplasma gondii: transmission, diagnosis and prevention. *Clin Microbiol Infect.* 2002;8:634-640.
13. Frenkel JK, Hassanein KM, Hassanein RS, Brown E, Thulliez P, Quintero-Nuñez R. Transmission of *Toxoplasma gondii* in Panama City, Panama: a five-year prospective cohort study of children, cats, rodents, birds, and soil. *Am J Trop Med Hyg.* 1995;53:458-468.
14. Frenkel JK, Ruiz A. Endemicity of toxoplasmosis in Costa Rica. *Am J Epidemiol.* 1981;113:254-269.
15. Sousa OE, Saenz RE, Frenkel JK. Toxoplasmosis in Panama: a 10-year study. *Am J Trop Med Hyg.* 1988;38:315-322.
16. Etheredge GD, Frenkel JK. Human *Toxoplasma* infection in Kuna and Embera children in the Bayano and San Blas, Eastern Panama. *Am J Trop Med Hyg.* 1995;53:448-457.
17. Warnekulasuriya MR, Johnson JD, Holliman RE. Detection of Toxoplasma gondii in cured meats. *Int J Food Microbiol* 1998;45:211-215.
18. Tenter AM, Heckeroth AR, Weiss LM. *Toxoplasma gondii*: from animals to humans. *Int J Parasitol.* 2000;30:1217-1258.
19. Waldeland H. Toxoplasmosis in sheep. Epidemiological studies in flocks with reproductive loss from toxoplasmosis. *Acta Vet Scand.* 1977;18:91-97.
20. Munoz-Zanzi CA, Fry P, Lesina B, Hill D. *Toxoplasma gondii* oocyst-specific antibodies and source of infection. *Emerg Infect Dis.* 2010;16:1591-1593.
21. Pereira KS, Franco RM, Leal DA. Transmission of Toxoplasmosis (*Toxoplasma gondii*) by foods. *Adv Food Nutr Res.* 2010;60:1-19.
22. Dzierszinski F, Nishi M, Ouko L, Roos DS. Dynamics of Toxoplasma gondii differentiation. *Eukaryot Cell.* 2004;3:992-1003.
23. Freyre A, Dubey JP, Smith DD, Frenkel JK. Oocyst-induced Toxoplasma gondii infections in cats. *J Parasitol* 1989;75:750-755.
24. Dubey JP, Frenkel JK. Cyst-induced toxoplasmosis in cats. *J Protozool.* 1972;19:155-177.
25. Canfield PJ, Hartley WJ, Dubey JP. Lesions of toxoplasmosis in Australian marsupials. *J Comp Pathol.* 1990;103:159-167.
26. Cunningham AA, Buxton D, Thomson KM. An epidemic of toxoplasmosis in a captive colony of squirrel monkeys (*Saimiri sciureus*). *J Comp Pathol* 1992;107:207-219.
27. Frenkel JK. Tissue-dwelling intracellular parasites: infection and immune responses in the mammalian host to *Toxoplasma, Sarcocystis* and *Trichinella*. *Am Zool.* 1989;29:455-467.

28. Remington JS, McLeod R, Desmonts G. Toxoplasmosis. In: Remington JS, Klein JO, eds. *Infectious Diseases of the Fetus and Newborn Infant*. 4th ed. Philadelphia, Pa: WB Saunders; 1995:140-267.

29. Yolken RH, Dickerson FB, Fuller Torrey E. *Toxoplasma* and schizophrenia *Parasite Immunol*. 2009;9:72.

30. Flegr J, Klose J, Novotna M, Berenreitterova M, Havlicek J. Increased incidence of traffic accidents in *Toxoplasma*-infected military drivers and protective effect RhD molecule revealed by a large-scale prospective cohort study. *BMC Infect Dis*. 2009;9:72.

31. Yereli K, Balcioğlu IC, Ozbilgia A. Is *Toxoplasma gondii* a potential risk for traffic accidents in Turkey? *Forensic Sci Int*. 2006;163:34-37.

32. Yuksel P, Alpay N, Babur C, et al. The role of latent toxoplasmosis in the aetiopathogenesis of schizophrenia - the risk factor or an indication of a contact with cat[s]? *Folia Parasitologia*. 2010;57:121-128.

33. Lester D. Brain parasites and suicide. *Psychol Rep*. 2010;107:424.

34. Eckert GU, Melamed J, Menegaz B. Optic nerve changes in ocular toxoplasmosis. *Eye* (London). 2007;21:746-751 .

35. Frenkel JK. Pathogenesis of toxoplasmosis with a consideration of cyst rupture in Besnoitia infection. *Surv Ophthalmol*. 1961;6:799-825.

36. Newman PE, Ghosheh R, Tabbara KF, O'Connor GR, Stern W. The role of hypersensitivity reactions to Toxoplasma antigens in experimental ocular toxoplasmosis in nonhuman primates. *Am J Ophthalmol*. 1982;94:159-164.

37. Aliberti J, Jankovic D, Sher A. Turning it on and off: regulation of dendritic cell function in *Toxoplasma gondii* infection. *Immunol Rev*. 2004;201:26-34.

38. Luder CG, Gross U. Apoptosis and its modulation during infection with *Toxoplasma gondii*: molecular mechanisms and role in pathogenesis. *Curr Top Microbiol Immunol*. 2005;289:219-237.

39. Frenkel JK, Escajadillo A. Cyst rupture as a pathogenic mechanism of toxoplasmic encephalitis. *Am J Trop Med Hyg*. 1987;36:517-522.

40. Kump LI, Androudi SN, Foster CS. Ocular toxoplasmosis in pregnancy. *Clin Experiment Ophthalmol*. 2005;33:455-460.

41. Marty P, Bongain A, Rahal A, et al. Prenatal diagnosis of severe fetal toxoplasmosis as a result of toxoplasmic reactivation in an HIV-1 seropositive woman. *Prenat Diagn*. 1994;14:414-415.

42. Bertoli F, Espino M, Arosemena JR 5th, Fishback JL, Frenkel JK. A spectrum in the pathology of toxoplasmosis in patients with acquired immunodeficiency syndrome. *Arch Pathol Lab Med*. 1995;119:214-224.

43. Frenkel JK. Toxoplasmosis. Mechanisms of infection, laboratory diagnosis and management. *Curr Top Pathol*. 1971;54:28-75.

44. Ganji M, Tan A, Maitar MI, Weldon-Linne CM, Weisenberg E, Rhone DP. Gastric toxoplasmosis in a patient with acquired immunodeficiency syndrome. A case report and review of the literature. *Arch Pathol Lab Med*. 2003;127:732-734.

45. Campbell AL, Goldberg CL, Magid MS, Gondolesi G, Rumbo C, Herold BC. First case of toxoplasmosis following small bowel transplantation and systematic review of tissue-invasive toxoplasmosis following noncardiac solid organ transplantation. *Transplantation*. 2006;81:408-417.

46. Frenkel JK, Friedlander S. *Toxoplasmosis: pathology of neonatal disease. Pathogenesis, diagnosis, and treatment*. Washington, DC: US Public Health Service Publication No. 141; 1951.

47. Yavuz E, Aydin F, Seyhan A, et al. Granulomatous villitis formed by inflammatory cells with maternal origin: a rare manifestation type of placental toxoplasmosis. *Placenta*. 2006;27:780-782.

48. Piringer-Kuchinka A, Martin I, Thalhammer O. Superior cervical-nuchal lymphadenitis with small groups of epithelioid cell proliferation [in German]. *Virchows Arch Pathol Anat*. 1958;331:522-535.

49. Saxen E, Saxen L. The histological diagnosis of glandular toxoplasmosis. *Lab Invest*. 1959;8:386-394.

50. Kara IO, Ergin M, Sahin B, Inal S, Tasova Y. Sinus histiocytosis with massive lymphadenopathy (Rosai-Dorfman's disease) previously misdiagnosed as Toxoplasma Lymphadenitis. *Leuk Lymphoma*. 2004;45:1037-1041.

51. Wakefield D, Cunningham ET, Pavesio C, Garweg JG, Zierhut M. Controversies in ocular toxoplasmosis. *Ocul Immunol Inflamm*. 2011;19:2-9.

52. Elkins BS, Holland GN, Opremcak EM, et al. Ocular toxoplasmosis misdiagnosed as cytomegalovirus retinopathy in immunocompromised patients. *Ophthalmology*. 1994;101:499-507.

53. Moorthy RS, Smith RE, Rao NA. Progressive ocular toxoplasmosis in patients with acquired immunodeficiency syndrome. *Am J Ophthalmol*. 1993;115:742-747.

54. Joseph P, Calderon MM, Gilman RH, et al. Optimization and evaluation of a PCR assay for detecting toxoplasmic encephalitis in patients with AIDS. *J Clin Microbiol*. 2002;40:4499-4503.

55. Buchbinder S, Blatz R, Rodloff AC. Comparison of real-time PCR detection methods for B1 and P30 genes of *Toxoplasma gondii*. *Diagn Microbiol Infect Dis*. 2003;45:269-271.

56. Reischl U, Bretagne S, Kruger D, Ernault P, Costa JM. Comparison of two DNA targets for the diagnosis of toxoplasmosis by real-time PCR using fluorescence resonance energy transfer hybridization probes. *BMC Infect Dis*. 2003;3:7.

57. Nimri L, Pelloux H, Elkhatib L. Detection of *Toxoplasma gondii* DNA and specific antibodies in high-risk pregnant women. *Am J Trop Med Hyg*. 2004;71:831-835.

58. Switaj K, Master A, Skrzypczak M, Zaborowski P. Recent trends in molecular diagnostics for *Toxoplasma gondii* infections. *Clin Microbiol Infect*. 2005;11:170-176.

59. Villard O, Filisetti D, Roch-Deries F, Garweg J, Flament J, Candolfi E. Comparison of enzyme-linked immunosorbent assay, immunoblotting, and PCR for diagnosis of toxoplasmic chorioretinitis. *J Clin Microbiol*. 2003;41:3537-3541.

60. Desmonts G, Remington JS. Direct agglutination test for diagnosis of *Toxoplasma* infection: method for increasing sensitivity and specificity. *J Clin Microbiol*. 1980;11:562-568.

61. Frenkel JK, Jacobs L. Ocular toxoplasmosis: pathogenesis, diagnosis and treatment. *A M A Arch Ophthalmol*. 1958;59:260-279.

62. Suzuki Y, Thulliez P, Desmonts G, Remington JS. Antigen(s) responsible for immunoglobulin G responses specific for the acute stage of *Toxoplasma* infection in humans. *J Clin Microbiol*. 1988;26:901-905.

63. Wong SY, Israelski DM, Remington JS. AIDS-associated toxoplasmosis. In: Sande MA, Volberding PA, eds. *The Medical Management of AIDS*. 4th ed. Philadelphia, Pa: WB Saunders; 1995:460-493.

64. Martina MN, Cervera C, Esforzado N, et al. *Toxoplasma gondii* primary infection in renal transplant recipients. Two case reports and literature review. *Transpl Int*. 2011 Jan;24(1):e6-12. doi: 10.1111/j. 1432-2277.2010.01173.x

65. Centers for Disease Control and Prevention. Update: multistate outbreak of Escherichia coli O157:H7 infections from hamburgers—Western United States, 1992-1993 [comment]. *JAMA* 1993;269:2194-2196.

66. Frenkel JK. Toxoplasmosis: parasite life cycle, pathology, and immunology. In: Hammond DM, Long PL, eds. *The Coccidia: Eimeria, Isospora, Toxoplasma, and Related Genera*. Baltimore, Md: University Park Press; 1973:343-410.

67. Bout DT, Mevelec MN, Velge-Roussel F, Dimier-Poisson I, Lebrun M. Prospects for a human *Toxoplasma* vaccine. *Curr Drug Targets Immune Endocr Metabol. Disord* 2002;2:227-234.

68. Jenkins MC. Advances and prospects for subunit vaccines against protozoa of veterinary importance. *Vet Parasitol*. 2001;101:291-310.

69. Belli SI, Walker RA, Flowers SA. Global protein expression analysis in apicomplexan parasites: current status. *Proteomics*. 2005;5:918-924.

## *Acknowledgements*

The authors thank Dr. JK Frenkel for his major contributions to this chapter

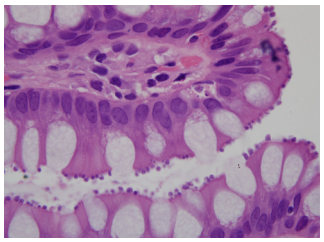
**Figure 12.21**
Courtesy of Centers for Disease Control and Prevention

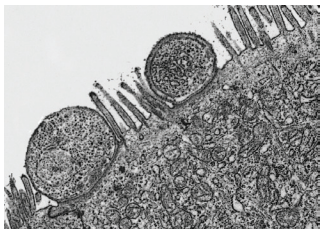
**Figure 12.22**
Courtesy of JK Frenkel

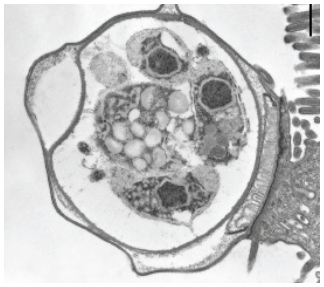
**Figure 2.23**
Gardiner CH, Fayer R, Dubey JP. An Atlas of Protozoan Parasites in Animal Tissues. 2nd edition, Armed Forces Institute of Pathology, American Registry of Pathology, Washington, DC

**Figure 12.24**
Courtesy of Marvin Miller

**Figure 12.97**
Courtesy of Henry Azar







13

# Cryptosporidiosis, Isosporiasis, Cyclosporiasis & Sarcocystosis

*Mary K. Klassen-Fischer, Ronald C. Neafie, Douglas J. Wear and Wayne M. Meyers*

## Introduction

Cryptosporidiosis, isosporiasis, cyclosporiasis, and sarcocystosis are diseases caused by protozoa of the phylum Sporozoa, class Coccidea, order Eimeriida.[1] All are obligate intracellular parasites of intestinal epithelial cells. *Cryptosporidium* sp, *Isospora belli* and *Cyclospora cayetanensis* complete their life cycles within a single host. They cause self-limited or prolonged diarrhea, depending on the host's immune status. In contrast *Sarcocystis* requires two host species. Compared to other coccidia, *Cryptosporidium* sp are less host or organ specific, resist antimicrobial agents and produce auto infection, features more closely related to gregarines.[2]

## CRYPTOSPORIDIOSIS

### Definition and General Considerations

At least 9 species and 4 genotypes of *Cryptosporidium* cause human infection: *C. hominis, C. parvum, C. meleagridis, C. felis, C. canis*, and occasionally *C. muris, C. suis, C. andersoni*, and *Cryptosporidium cervine* sp and, *Cryptosporidium* genotypes in horse, rabbit, skunk, and chipmunk.[3] *Cryptosporidum hominis* and *C. parvum* are morphologically identical and their completely sequenced genomes are 97% identical.[4,5,6.] Although both have 8 chromosomes, the genome of *C. hominis* appears slightly larger, 9.16 Mb to 9.11 Mb and 3,994 to 3,952 genes compared to the genome of *C. parvum*.[5] *Cryptosporidium* was first described in 1895,[7] identified in 1910,[8] and in the 1970s recognized as a cattle pathogen. Some early reported patients had contact with livestock. In the 1980s, *C. parvum* was discovered to be the cause of prolonged diarrhea in patients with acquired immunodeficiency syndrome (AIDS), and is now known also to cause diarrhea in immunocompetent patients.[1]

## Epidemiology

*Cryptosporidium* causes approximately 250 to 500 million cases of diarrhea per year in developing nations of Asia, Africa, and Latin America. *Cryptosporidium* is the most common parasitic cause of diarrhea in the United Kingdom,[9] and infected 28,636 persons in the United States between 2006 and 2008.[10] The asymptomatic carriage rate may be as high as 13% among immunocompetent individuals.[11] Cryptosporidiosis develops in an estimated 10-15% of patients with AIDS in the United States and in 30%-50% of patients with AIDS in the developing world.[12] The serological prevalence of *Cryptosporidium*

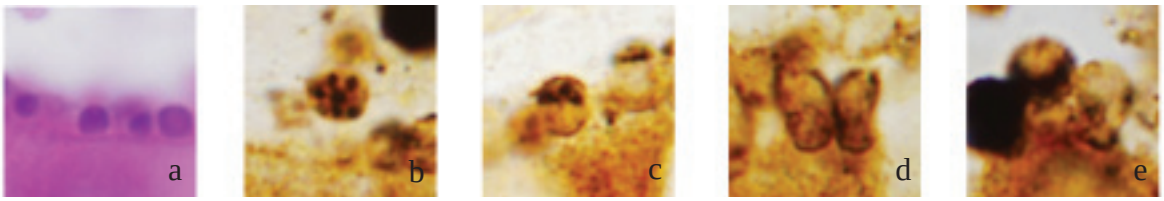



**Figure 13.1**
Spherical or cone-shaped cell stages of *Cryptosporidium* within human cells lining gastrointestinal tracts. x1000. a. Spherical: 4 trophozoites deep in microvilli, H&E; b. Spherical: type I meront with 7 of 8 merozoites, WS; c. Spherical: type II meront with 4 merozoites, WS; d. Cone-shaped: 2 side-by-side macrogamonts, WS; e. Cone-shaped: microgamont with microgametes on right, Spherical: 2 attached oocysts; single-walled oocyst with 4 sporozoites (center); Double-walled, densly stained oocyst on left, WS.

ranges between 30%-60% in industrialized countries and reaches 95% in tropical and developing countries.[12]

## *Infectious Agent*

### Morphologic Description

All four stages of *Cryptosporidium* (trophozoite/type I meront, type II meront, microgamont, and macrogamont/oocyst) form spherical or cone-shaped cells (Fig 13.1) within epithelial cells lining the host's gastrointestinal tract.

Except for unfertilized macrogamonts, each mature stage produces a smaller banana or bullet-shaped penetrating form that is asexual (sporozoite, type I merozoite, type II merozoite) or sexual (microgamete).

Trophozoites are 1 µm to 2.5 µm in diameter[13] (Fig 13.2). Each contains a single nucleus (Fig 13.3),[14] endoplasmic reticulum, and ribosomes, and is surrounded by 5 unit membranes,[15] the outer 2 originating with the host. The parasitophorous vacuole membrane has an electron-dense microfilament network where the host cell membrane apposes the parasite (Fig 13.4). The membrane and the microfilaments form a series of compact folds, called, the feeder organelle, believed to be responsible for nutrient transfer. The parasitophorous vacuole lies in the microvillous border of the cell, just below the plasma membrane. This intracellular but extracytoplasmic location differs from that of related coccidia that reside in intracytoplasmic vacuoles.[1,15]

Type I meronts are 1.5 µm to 2.5 µm in diameter[13] and contain 8 type I merozoites (Figs 13.1b & 13.5). Type II meronts are 3.5 µm in diameter[13] and contain 4 type II merozoites (Fig 13.6). The nuclei of first- or second-generation meronts become smaller during division and migrate toward the periphery. Microgamonts are 2 µm in diameter[13] and contain 14 to 16 peripherally arranged microgametes[1] (Fig 13.7). Macrogamonts are spherical and are 4 µm x 5 µm in diameter[13] (Figs 13.4 & 13.8). They contain a large, eccentrically placed nucleus with a prominent nucleolus.[14] Mature oocysts of *Cryptosporidium* are spherical, refractile (Fig 13.9), 5 µm x 7 µm in diameter,[13] and contain 4 sporozoites (Fig 13.1e). Each of the 4 sporozoites is 2.4 µm x 0.69 µm to 4.5 µm x 0.95 µm and has no sporocyst (Fig 13.10). Merozoites are 0.4 µm x 1 µm in diameter[13] (Figs 13.1 b & 13.1c) and contain a Golgi apparatus, endoplasmic reticulum, and nucleus. Merozoites and sporozoites also contain the organelles comprising the apical complex: rhoptries, micronemes, subpellicular microtubules, polar ring, and conoid. These structures apparently serve as the entry apparatus and disappear in the trophozoite stage.[16] Microgametes are bullet- or rod-shaped not more than 1 µm to 2 µm long (Fig 13.7). Unlike some other members of this phylum, *Cryptosporidium* microgametes have no flagellum.

### Life Cycle and Transmission

The life cycle (Fig 13.11) of *C. parvum* is completed in 3 days in human cell culture[17] and 8 days in cell free culture.[18] Ingested oocysts excyst within a host's stomach, releasing 4 motile sporozoites. The sporozoites are carried along the intestinal tract where they infect epithelial cells, usually in the small intestine. Apposition and invagination of host and parasite membranes mediated by a host receptor result in the formation of a parasitophorous vacuole.[19,20] The sporozoites differentiate into spherical bodies called trophozoites and divide by schizogony (asexual reproduction) to form schizonts (meronts). The outer membranes invaginate deeply around nuclei, forming daughter merozoites. If 2 divisions occur (second-generation schizogony), the result is 4 merozoites or type II meronts. If 3 divisions occur (first-generation schizogony), the result is 8 merozoites or type I meronts. Type I meronts reinfect epithelial cells.[20]

Type II meronts undergo gametogony (sexual reproduction) to produce microgamonts (containing microgametes) and macrogamonts (which become macrogametes). Macrogametes contain polysaccharide and phospholipid amylopectin granule precursors of the oocyst wall. Fertilization occurs when luminal currents or motility of the microgametes carry them near macrogametes. Microgametes attach to and penetrate the cytoplasm of macrogametes, then enter the nucleus where nuclear fusion takes place.[13]

The resulting zygote undergoes schizogony to form an oocyst. Wall-forming bodies coalesce to form oocyst walls.

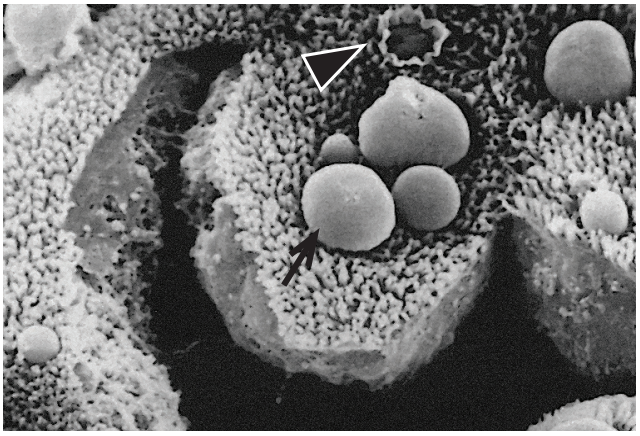


**Figure 13.2**
Scanning electron micrograph showing numerous cryptosporidia on surface of epithelial cells: trophozoites (arrow), crater-like area (arrowhead) is a ruptured parasitophorous envelope. x3500

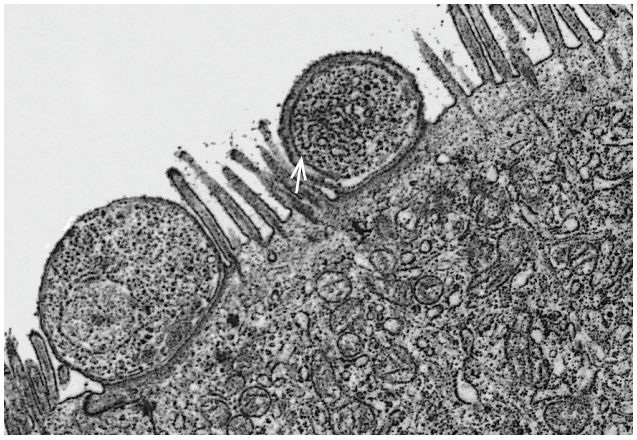


**Figure 13.3**
Transmission electron micrograph of *Cryptosporidium* sp of sheep showing trophozoite with a single nucleus, endoplasmic reticulum and ribosomes deep in microvilli of epithelial cell. Note parasitophorous vacuole (arrow). x5120



**Figure 13.4**
Transmission electron micrograph of a fertilized macrogamete 4.1 µm x 2.5 µm connected to the host cell and surrounded by the parasitophorous vacuole (arrow) and the feeder organelle (arrow head). x25250

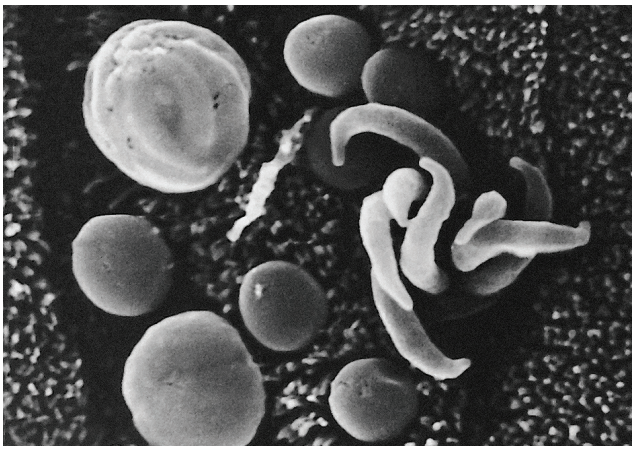


**Figure 13.5**
Scanning electron micrograph showing type I meront releasing 8 merozoites. x18000

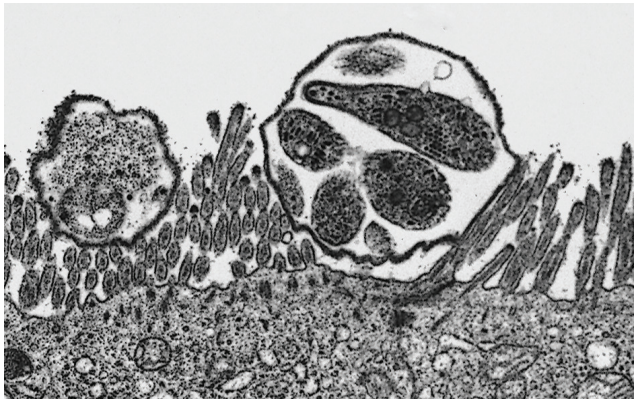


**Figure 13.6**
Transmission electron micrograph showing type II meront containing 4 merozoites. x5720

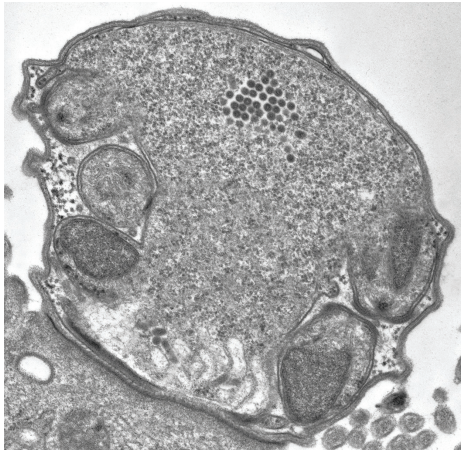


**Figure 13.7**
Transmission electron micrograph showing 5 microgametes in a microgamont. x 24000

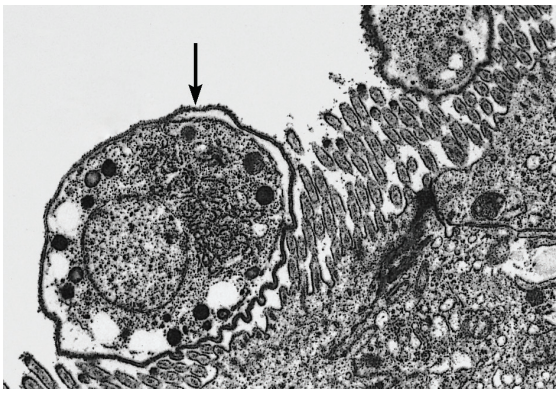


**Figure 13.8**
Transmission electron micrograph showing macrogamont with nucleus and dark bodies. x5720

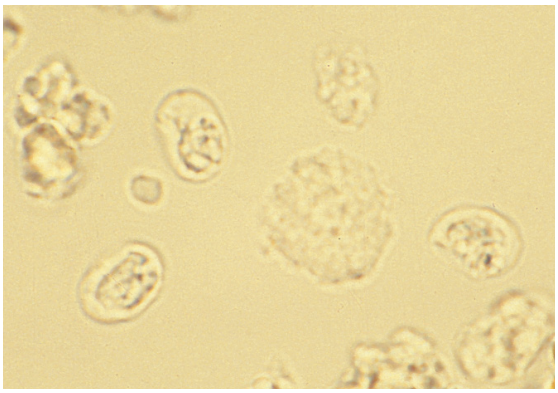


**Figure 13.9**
*Cryptosporidium parvum* of calves. Fecal float with refractile unstained oocysts suspended in water. x500

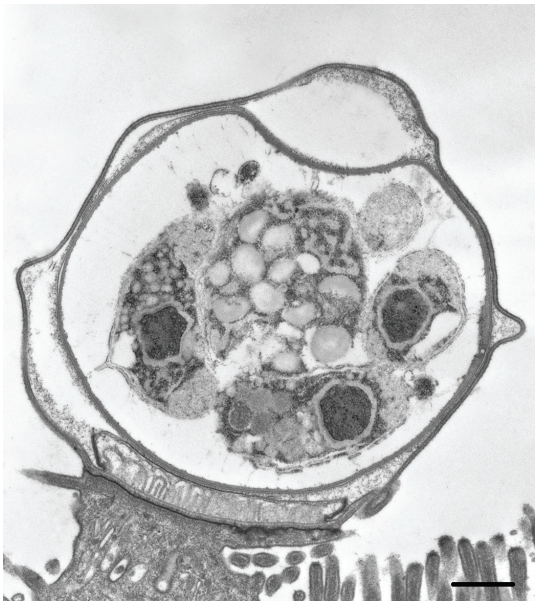


**Figure 13.10**
Transmission electron micrograph showing 3 of 4 naked sporozoites. The oocyst is still within the hosts cell-derived parasitophorous vacuole. Bar, 500 nm

Approximately 20% of oocysts have a thin, single-unit membrane wall and can release their sporozoites in the host before passage, resulting in autoinfection. The remaining 80% have thick-walled, bilayer membranes and are fully sporulated and infectious upon passage from the host.

Cryptosporidiosis spreads from person to person, from animals to people, and from the environment to people by contact with fomites or ingestion of contaminated food or water.[21-24] Factors that contribute to the spread of cryptosporidiosis include travel, overcrowding, malnutrition, early weaning, other infections, use of antibiotics, poor sanitation, and working at or attending health or day-care centers.[25] Waterborne infections have been associated with contamination of reservoirs by pasture runoff and inadequate filtration of swimming pools and water slides. The infective dose is as few as 10 organisms.[26]

## Clinical Features and Pathogenesis

The incubation period for cryptosporidiosis in healthy volunteers is 4 to 22 days after ingestion of oocysts.[27] Most immunocompetent patients have self-limited diarrhea lasting 5 to 14 days. The diarrhea is cholera-like, profuse, watery, and foul smelling, with no leukocytes or blood. Other symptoms include nausea and vomiting, abdominal cramps, low-grade fever, anorexia, dehydration, weight loss, weakness, myalgia, and headache.[27,28] There may be malabsorption of carbohydrates, fats, and vitamins. Rarely, severe disease results in malnutrition and death. Peripheral blood leukocytosis and eosinophilia are infrequent. Characteristic radiographic findings are nonspecific mucosal thickening and disordered small intestinal motility. Endoscopic findings include focal atrophy and small erosions.

Patients with profound immunosuppression, such as in AIDS, may have more severe and prolonged symptoms that may fluctuate with changes in CD4 count and antiretroviral therapy. The 4 patterns of clinical syndromes are chronic diarrhea, cholera-like disease, transient diarrhea, and relapsing illness.[12]

Immunocompromised individuals have a greater incidence of infection in extraintestinal sites, such as the stomach, and the biliary, pancreatic, and respiratory tracts. [29] Although most AIDS patients have no gastric symptoms, stomach involvement is frequent.[30] *Cryptosporidium* has been found in the gallbladder and biliary tree of both immunocompetent and immunocompromised individuals; symptomatic infections of the biliary tract have been seen only in AIDS patients. Up to 15% of AIDS patients with intestinal cryptosporidiosis have hepatobiliary tract infection

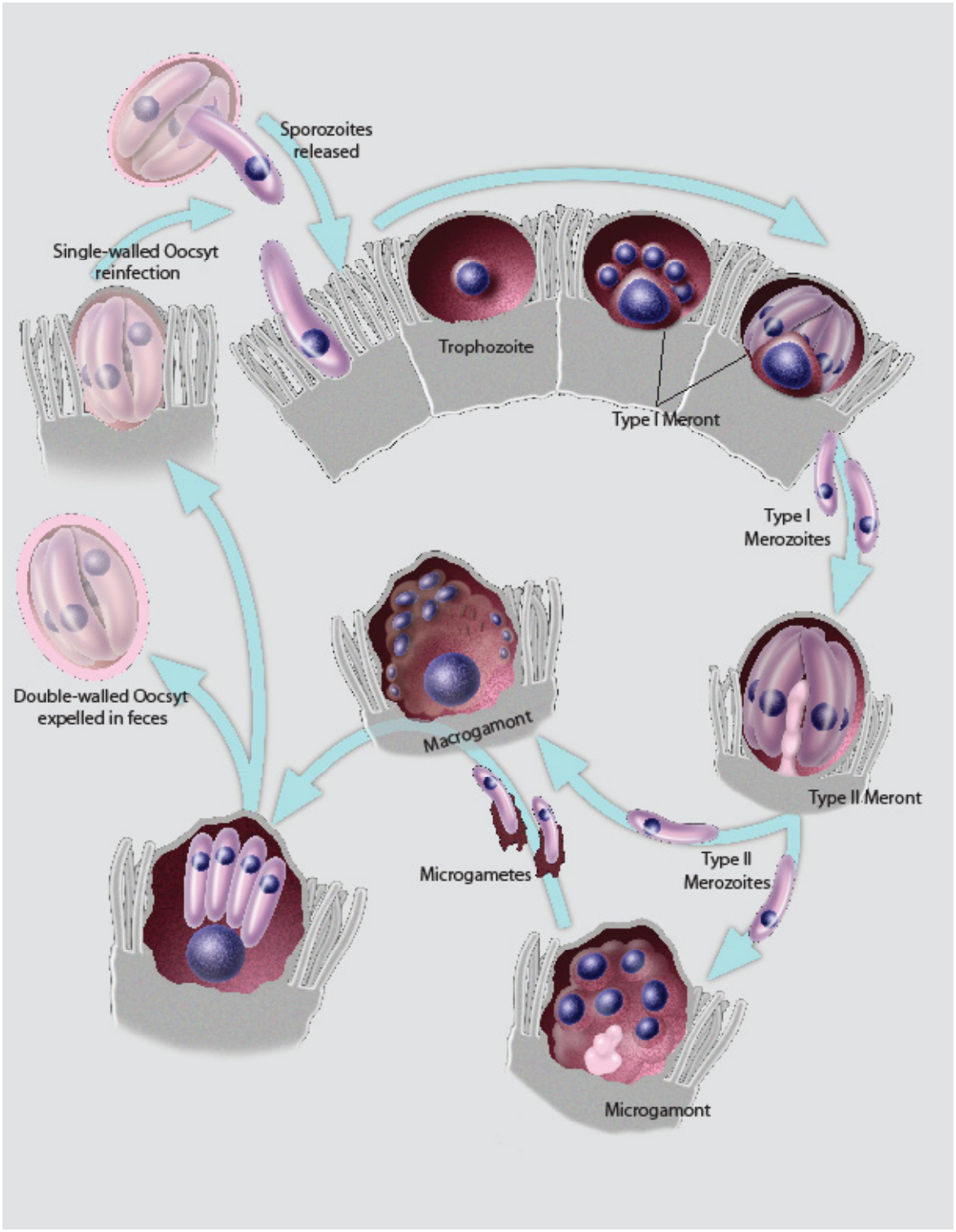



**Figure 13.11**
Life cycle of *Cryptosporidium parvum.* (See text for description).

resulting in fever, right upper quadrant nonradiating pain, nausea, vomiting, and diarrhea. Acalculous cholecystitis and sclerosing cholangitis with obstruction or stenosis of the ampulla of Vater have been reported. These conditions may be found by ultrasound or endoscopic retrograde cholangiography.[20] Respiratory cryptosporidiosis occurs rarely in immunocompetent individuals.[31] Upper respiratory, tracheobronchial, and nasal cryptosporidiosis are common in AIDS patients with severe small intestinal disease. Lower respiratory infection causes interstitial pneumonia.[32]

The pathologic mechanisms of cryptosporidial diarrhea and malabsorption are not well understood. Nutrient transfer through the parasite's feeder organelle may deplete the host cell. A heavy parasite burden may reduce the microvillous absorptive surface area and affect membrane-bound enzymes.[1] Malabsorption and impaired digestion may lead to overgrowth of intestinal flora and influx of fluid, causing diarrhea.

The normal immune response to cryptosporidiosis is both humoral and cell-mediated. When both components are functioning normally, infection is self-limited.[20,33] Cell-mediated immunity in the intestine is important for protection against infection in human volunteers, especially CD4+ T cells and interferon-γ.[34]

Apoptosis may be relevant to the pathogenesis of sclerosing cholangitis. Sporozoites attach to and invade the apical membrane of cholangiocytes, resulting in programmed cell death of bystander uninfected biliary epithelial cells but protect infected cells.[35] In vivo the host cell is killed upon parasite egress; this cell death is necrotic, not apoptotic.[36] The biliary tract may serve as a reservoir of infection. In cultured cells bile acids and bile salts enhance the invasiveness of *Cryptosporidium* sp.[37]

## Pathologic Features

Distribution of cryptosporidiosis in the duodenum, small intestine, and colon is highly variable.[12] In immunocompetent hosts, infection is primarily confined to the jejunum and ileum. The rectum is often involved, while the esophagus and stomach are only occasionally infected. On H&E-stained tissue sections, *Cryptosporidium* parasites appear to bulge from the surface of the epithelial cell (Fig 13.1). Because of their small size and indistinct structure, they may be confused with cellular debris or mucus. Infection is confined to the apical surfaces of enterocytes, from the base of the crypts to the tips of the villi. The numbers of parasites and the degree of inflammation vary, even within a small biopsy. There is no correlation among parasite burden, histopathologic changes, and clinical severity.[12]

In immunocompetent hosts, pathologic changes are relatively mild and nonspecific. Changes in the small intestine include villous architectural abnormalities, crypt elongation, increased inflammatory cells, and occasional crypt abscesses[38] (Fig 13.2). Neutrophils and rare eosinophils infiltrate between epithelial cells and in the lamina propria. Intraepithelial lymphocytes are rare. Enterocyte abnormalities include increased mitotic figures, cellular atypia, necrosis, vesiculation, inconspicuous brush borders, and sloughing. Infected colonic crypts are often dilated, with decreased goblet cells and increased mitotic figures. Immunocompromised hosts may have more severe villous atrophy, heavy colonization throughout the alimentary tract, and dense inflammatory infiltrates (Fig 13.12).

In gastric cryptosporidiosis, organisms are present in the lining epithelium and may extend into the glands. There may be active gastritis, with lymphocytes and plasma cells in the lamina propria.

Organisms probably spread through the pancreatic and biliary ducts to infect epithelial cells of the gallbladder, biliary tract, and pancreatic ducts. Pathologic changes range from acute cholecystitis to necrosis. The gallbladder, bile ducts, and periductal glands become edematous and dilated, and are infiltrated by neutrophils, eosinophils, and chronic inflammatory cells. Organisms may be found in the bile duct epithelium of the liver. Damaged epithelial cells may become flattened, and there may be surface erosions. Organisms in the pancreatic duct epithelium are associated with pancreatitis and periductal inflammation. Unlike the intestinal epithelium, the pancreatic ducts undergo squamous metaplasia.

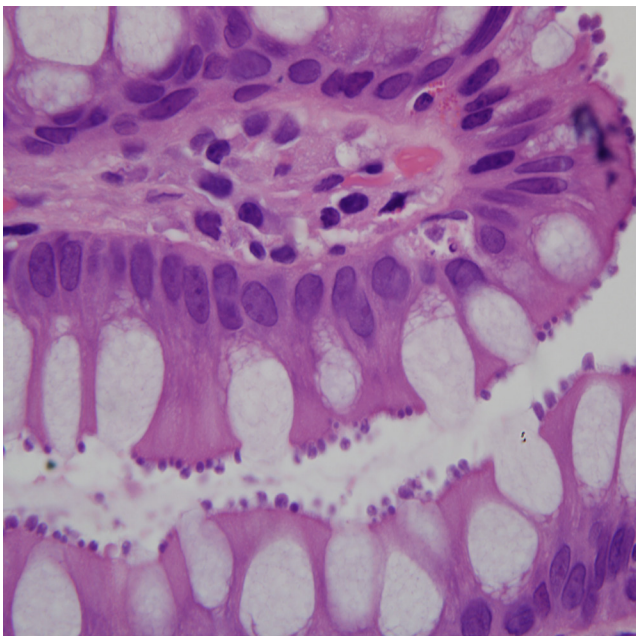


**Figure 13.12**
Large intestine from an immunosuppressed (HIV positive) patient showing flattened epithelial cells supporting heavy protozoan colonization, and an inflammatory infiltrate in the lamina propria with rare eosinophils. H&E. Original magnification x400

In immunocompromised individuals, organisms have been found in tracheal epithelium, macrophages, bronchioles, and alveolar exudates. Infection of columnar epithelial cells may result in squamous metaplasia.

## Diagnosis

Cryptosporidiosis can be diagnosed by stool examination, biopsy, cytology, and serology. The ability to sample oocysts from the entire digestive tract without invasive procedures makes stool examination the preferred method. The number of oocysts passed in feces varies, necessitating multiple sample collections and use of concentration techniques. Stool specimens should be fixed in formalin or sodium acetate-acetic acid-formalin. Oocysts can be concentrated by flotation (Fig 13.9), centrifugation, or sedimentation. Oocysts in stool are stained by a variety of techniques, including modified cold Kinyoun acid-fast (Fig 13.13), Ziehl-Neelsen acid-fast, Safranin-methylene blue, Giemsa, fluorescent acridine orange, and auramine-rhodamine stains. Oocysts are autofluorescent.[39] On phase-contrast microscopy, oocysts are bright, refractile (Fig 13.14), have up to 6 black granules, and often adhere to mucus. They are pink on bright field microscopy (Fig 13.9). Other techniques include ELISA, indirect fluorescent antibody (IFA) tests (Fig 13.15), direct immunofluorescence tests for screening, and fluorescence in situ hybridization (FISH) for verification.[40] The sensitivity of PCR in fecal samples is reduced because of substances that inhibit DNA sequensing.[41] DNA extraction methods for stool samples appears to increase sensitivity.[42]

Some patients require endoscopic intestinal biopsies for diagnosis. Cryptosporidium stains basophilic to amphophilic by H&E, dark blue by Giemsa, and red to purple by Gram stain (Figs 13.16 & 13.17). Acid-fast stains are less effective on tissue sections than on stool or cytology specimens. Electron microscopy has been used to diagnose cryptosporidiosis, but it is impractical and unnecessary in most cases. Cytological diagnosis of cryptosporidiosis has been made by identifying acid-fast organisms in small-intestinal brushing specimens, sputum, bronchoalveolar lavage, bronchial brushings, and tracheal aspirates. Other techniques include indirect immunofluorescence, immunoperoxidase techniques, and molecular diagnostic procedures.[20]

Differential staining, using light microscopy, will identify various stages in the growth cycle of cryptosporidiosis (Figs 13.16 & 13.17). The Grocott's methenamine silver (GMS) stain does not silver any early stage (asexual cycle), i.e. trophozoite or meronts (Figs 13.16m, 13.16r, & 13.16w). In the sexual stages only the microgamonts (Figs 13.17e, 13.17 i, & 13.17 j), not the macrogamonts (Fig 13.17c) stain. Within microgamonts, microgametocytes and the microgamonts' attachment site are silvered. In maturing and mature oocytes, only the sporozoites are silvered (Fig

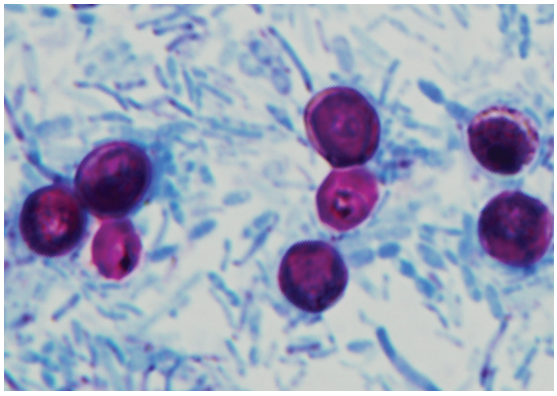


**Figure 13.13**
*Cryptosporidium parvum* in centrifuged human feces stained with modified cold Kinyoun acid-fast. x1000

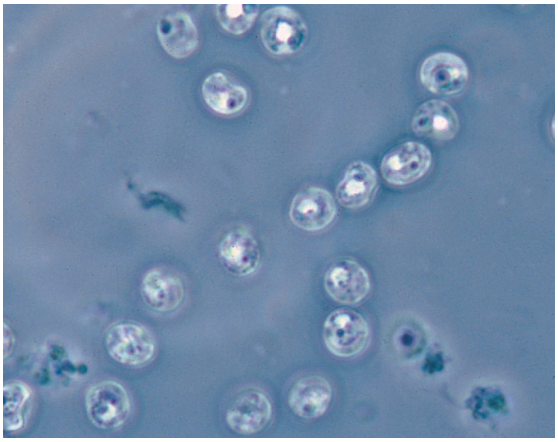


**Figure 13.14**
Fecal float with unstained oocysts suspended in sugar solution and viewed with phase-contrast microscopy. x1500

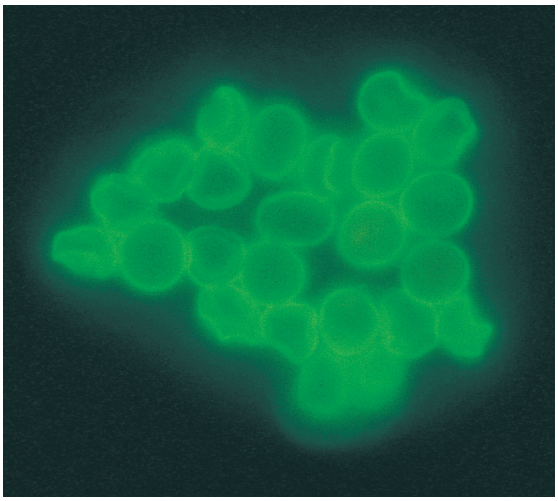


**Figure 13.15**
Fecal float with oocysts stained with monocloanal antibody conjugated with fluorescent isothiocyanate. X750

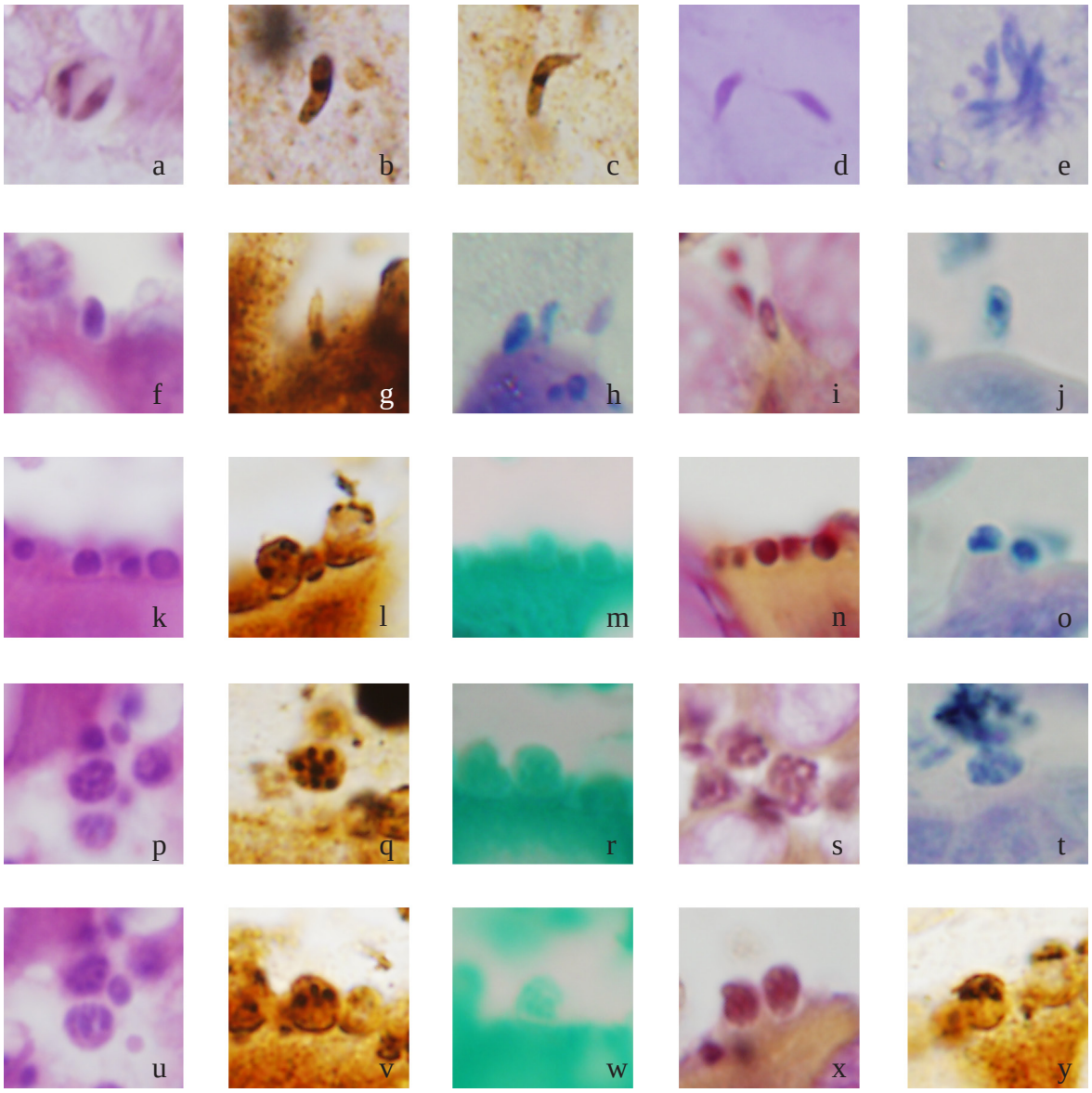



**Figure 13.16**
Differential staining of asexual stages in growth cycle of *Cyptosporidium* sp. x1000
Excysted sporozoities in feces: a. H&E; b. WS; c. WS; d. B&H; e. Type I merozoites (for comparison) ZN.
Early sporozoite attachment: f. H&E; g. WS; h. ZN; i. B&H; j. Giemsa.
Trophozoite: k. H&E; l. WS (in middle); m. GMS; n. B&H; o. Giemsa.
Type I meronts contain 8 type I merozoites: p. H&E; q. WS; r. GMS; s. B&H; t. Giemsa.
Type II meronts contain 4 type II merozoites: u. H&E; v. WS; w. GMS; x. B&H; y. WS.

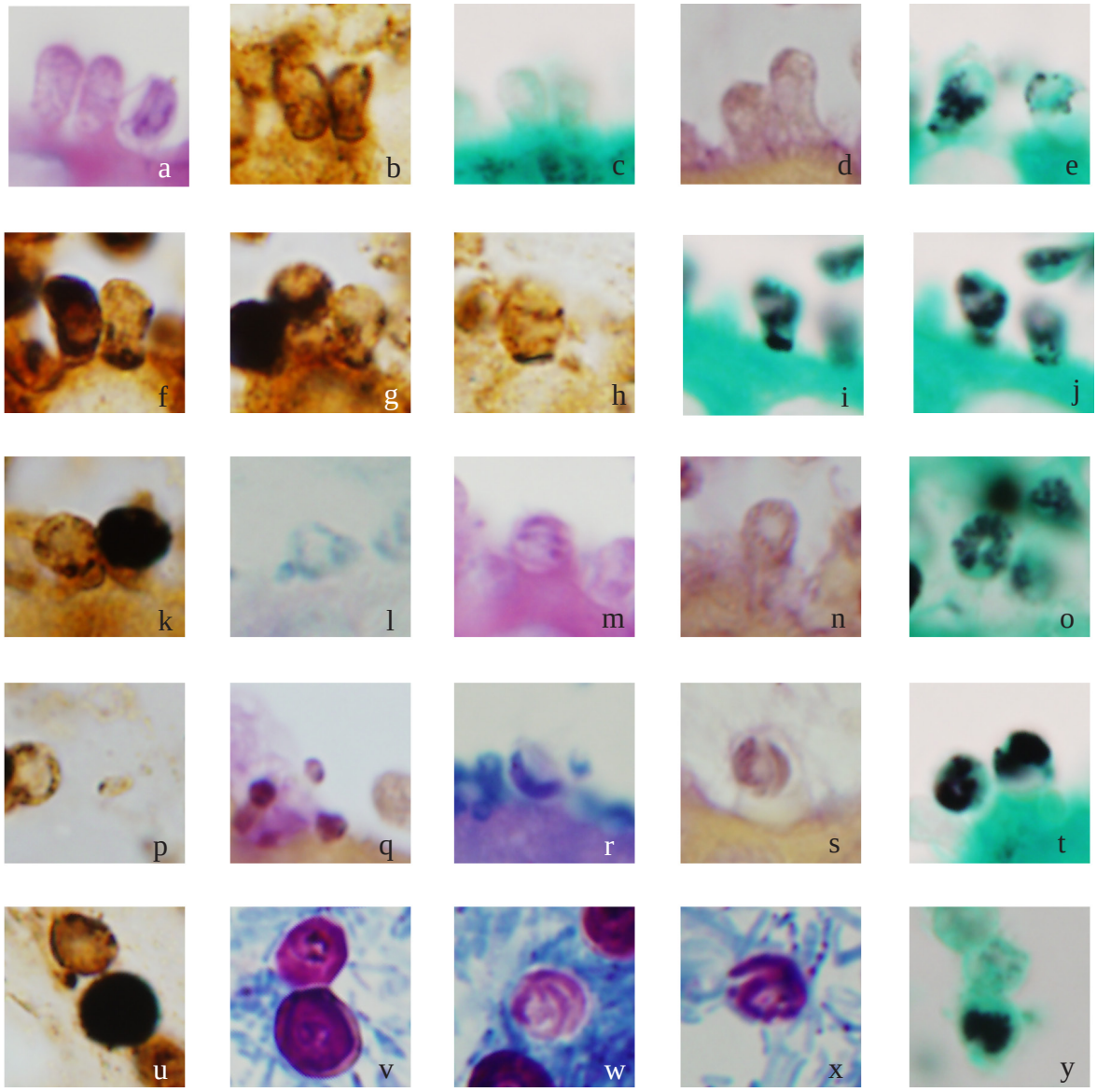



**Figure 13.17**
Differential staining of sexual stages in growth cycle of *Cryptosporidium* sp. x1000
Macrogamonts: a. H&E; b. WS; c. GMS; d. B&H; e. Macrogamete right, microgamete left GMS.
Microgametes; f. Arrow WS; g. Microgamont with micogametes on right WS; h. WS; i. GMS (focus level 1); j. GMS (focus level 2).
Maturing attached oocysts: k. Single walled (left), double walled (right) WS; l. ZN; m. H&E; n. B&H; o. GMS.
Miscellaneous: p. Microgamont with released microgamete (center) WS; q. released microgamete B&H; r. Mature oocyte with sporozoites (center) ZN; s. Mature oocyte with sporozoites B&H; t. Mature oocytes GMS.
Oocytes in feces: u. Single walled (top), double walled (center) WS; v. Kinyoun acid-fast; w. Kinyoun acid-fast; x. Kinyoun acid-fast; y. GMS.

13.17t). The Warthin-Starry silver impregnation stain (WS) silvers the trophozoite's and microgamont's thickened attachment site (Fig 13.16l), but only slightly to moderately stains the attachment sites of meronts (Figs 13.16l, 13.16q, 13.16v, & 13.16y). Merozoites, however, stain well within meronts (Fig 13.17g). In a variety of stains the 8 merozoites in type I meronts tend to appear as a circle around the wall (Figs 13.16 p, 13.16q, 13.16s, & 13.16t) whereas the 4 merozoites of type II meronts tend to present in a row, side-by-side (Figs 13.16u, 13.16v, & 13.16y). The Brown-Hopps (B&H) tissue gram stain demonstrates early trophozoites best (Fig 13.16n). As trophozoites mature, the darker red fades from the attachment site (Fig 13.16x). Merozoites may also stain deep red. In later stages only the microgametocytes stain well.

## *Treatment and Prevention*

In persons with normal immunity, cryptosporidiosis is usually self-limited and requires only fluid replacement. Nitazoxanide is the only drug approved by US FDA in immunocompetent persons.[33] Immunosuppressed patients require treatment with an anti-HIV regime.[33] Paromomycin has shown success in AIDS patients and may be more effective when combined with azithromycin.[43,44] Efforts are ongoing to develop an effective vaccine for cryptosporidiosis.[45]

The Centers for Disease Control and Prevention have established the Waterborne Cryptosporidiosis Working Group to develop guidelines for prevention and early identification of outbreaks of waterborne cryptosporidiosis, now a notifiable disease in the United States. Methods for detecting oocysts in water are improving with new molecular techniques.[46] Oocysts have been found in 17% to 87% of surface drinking-water supplies in the United States. Ozone, chlorine, formaldehyde, and conventional filtration do not eradicate oocysts, making prevention difficult.

# ISOSPORIASIS

### Definition and Synonym

Isosporiasis is acute or chronic enteritis caused by infection with *Isospora belli*. Isosporiasis is also known as isosporidiosis.

### General Considerations

Isospora causes intestinal disease in several mammalian species.[47] Virchow observed *I. belli*, the species that infects humans, in 1860. During World War I *Isospora belli* was detected in the stools of European soldiers stationed in the Middle East; during World War II it was a pathogen among troops in the Pacific. Isosporiasis in the Americas was first reported in the 1960s. *Isospora belli* causes traveler's diarrhea in immunocompetent hosts and is an opportunistic pathogen in patients with AIDS.

## *Epidemiology*

*Isospora belli* is cosmopolitan, but more common in the tropics and subtropics. It is endemic to South Africa [48], South America[49], and the Southwest Pacific islands. In South America, reported infection rates range from 0.1% to 1.8%. Immunodeficiency,[50] malnutrition,[51] and poor hygiene are risk factors. A cross-sectional study conducted in Ethiopia found 12 percent of 214 HIV positive patients infected, while none of 164 HIV negative patients was infected.[52] Isosporiasis is more prevalent in children, but the exact prevalence of the disease is not known.

## *Infectious Agent*

### Morphologic Description

*Isospora* oocysts are ellipsoid and approximately 20 µm to 33 µm by 10 µm to 19 µm (Figs 13.18a to 13.18c) . The smooth, thin cyst wall is composed of 2 layers. The outer layer is tough, impermeable to fluids, and environmentally resistant; the inner layer is membranous.[47] Sporocysts are 12 µm by 7 µm to 9 µm (Fig 13.19). Sporozoites are slender and crescent-shaped (Figs 13.20a & 13.20b). The internal structures of sporozoites and merozoites are similar to those of other coccidians and include polar rings, rhoptries, micronemes, conoids, microtubules, and amylopectin granules. Trophozoites are spherical (Fig 13.21). Macrogamonts contain a single large, centrally located nucleus and wall-forming bodies (Fig 13.22). Microgamonts contain multiple nuclei that migrate to the periphery, elongate and protrude from the surface, and bud into mature flagellated microgametes 5 µm to 6 µm long (Figs 13.23a to 13.23c).

### Life Cycle and Transmission

The life cycle of *Isospora* is similar to that of *Cryptosporidium*, except that oocysts are not sporulated when passed

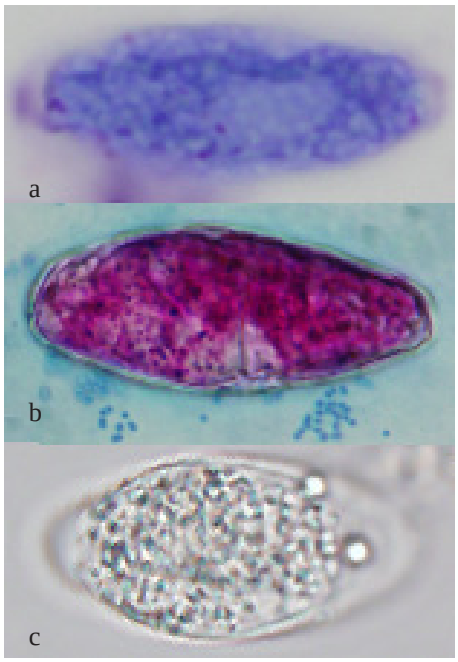



**Figure 13.18 a-c** Unsporulated oocyst (25µm x 8µm) of *Isospora belli*: a. In duodenal aspirate (Giemsa); b. Unspporulated oocyst of *I. belli* in feces (Kinyoun); c. Unsporulated oocyst of *I. belli* in feces. Unstained. Original magnification x400

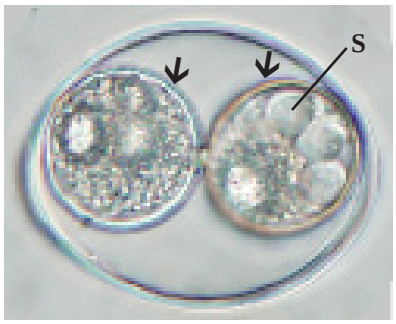



**Figure 13.19** Sporulated oocyst of *Isospora felis* in feces. Oocyst contains two sporocysts (arrows). Each sporocyst contains four sporozoites (S). Unstained. Original magnification x1000

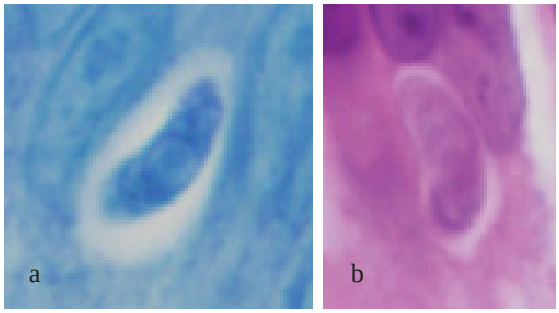



**Figure 13.20 a-b**
Released *Isospora belli* sporozoites (8µm x 3µm) have penetrated enterocyte in duodenum: a. Ziehl-Neelsen; b. H&E x300

in feces (Figs 13.18a to 13.18c). Under appropriate conditions, the 1 or 2 sporoblasts of *Isospora* secrete a wall and become sporocysts (Fig 13.19). Divisions result in 4 sporozoites per sporocyst. Ingested oocysts excyst in the small intestine.

Released sporozoites move about until they penetrate enterocytes in the distal duodenum, proximal jejunum, or other sites (Figs 13.20a & 13.20b). Trophozoites develop in the host-cell cytoplasm (Fig 13.21). By the process of schizogony, (Figs 13.24a to 13.24c) daughter merozoites form within a schizont. When the schizont and its host cell rupture, merozoites move into the gut lumen and penetrate uninfected enterocytes. The organisms either begin another round of merozoite formation or shift to gametogony, the sexual phase. Mature macrogametes develop from macrogamonts and can be differentiated by the multimembranous vacuoles which budded off the nucleus[53] (Figs 13.25a, &13.25b). Mature microgametes bud from a microgamont. Fertilization takes place when microgametes attach to and penetrate macrogametes. Nuclear fusion ensues and wall-forming bodies coalesce to form oocysts.

Infection is acquired by ingesting infective oocysts through contaminated food or water,[54] or from poor personal hygiene.

## Clinical Features and Pathogenesis

Immunocompetent hosts are susceptible to infection, though they may remain asymptomatic, with parasites evident in feces or biopsy specimens for several months or years. Symptoms include diarrhea, steatorrhea, headache, fever, malaise, colicky abdominal pain, vomiting, dehydration, and weight loss. Stools are watery, steatorrheic, and foul smelling, with no blood or pus. Malabsorption can occur in chronic infections. Some patients have peripheral eosinophilia.[47,49,55,56]

Immunocompromised hosts experience more severe infection. Significant damage to the jejunal and ileal mucosa, along with severe alteration of the enterohepatic circulation of bile acids and vitamin B12 absorption may occur. AIDS patients may have a more watery diarrhea. Extraintestinal isosporiasis has been observed in AIDS patients, but not in immunocompetent patients.[47]

On double-contrast radiography, patients with diarrhea lasting a year or less show minimally thickened mucosal folds in the duodenum and proximal jejunum. In patients with long-standing disease (17 to 30 years duration), the duodenum and proximal jejunum have a granular mucosal appearance with effacement of the folds. Radiographic changes seem to reflect the degree of villous atrophy.[57]

The pathologic mechanisms of isosporiasis are not known. Unlike *C. parvum*, *I. belli* does not reside in the microvillous border of the host cell. Destruction of the absorptive surface and digestive enzymes by the parasite is probably not involved in acute infections, nor is an enterotoxin suspected.

## Pathologic Features

Biopsies of the small intestine from individuals with isosporiasis may be normal or show changes of mild to

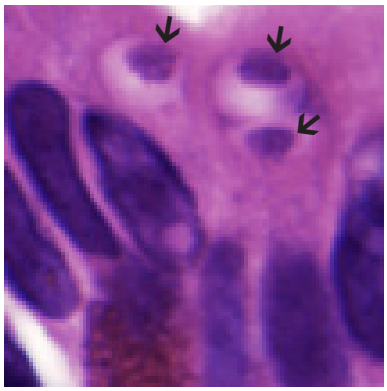


**Figure 13.21**
Spherical *Isospora belli* trophozoites (arrows) (largest 3 µm x2 µm) in duodenal enterocyte. Note eosinophilic granules of Paneth cell. H&E x2300

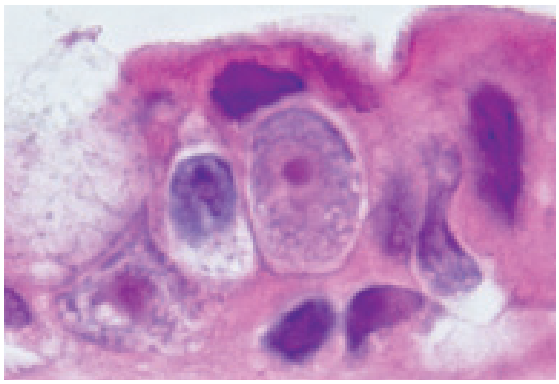


**Figure 13.22**
Macrogamont (12 µm x8 µm) with single large, centrally located nucleus in duodenum. H&E x1750

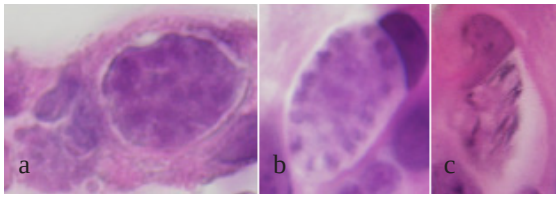



**Figure 13.23 a-c.**
Development of microgametes from microgamont in duodenum: a. Microgamont (12 µm x 8 µm) with multiple nuclei; b. Nuclei have migrated to periphery (12 µm x7 µm); c. Mature flagellated microgametes 5 µm to 6 µm long, (total size 10 µm x 5 µm). Helmes x1500

moderate villous atrophy and crypt hyperplasia with increased inflammatory cells (Fig 13.26). The organisms tend to sit beneath the nucleus, which take on a transverse position in the superficial cytoplasm leading to the so-called 'T sign" (Fig 13.27).[58] Heavily parasitized specimens may have villous blunting or atrophy, crypt hypertrophy, and inflammation of the lamina propria, as seen in cryptosporidiosis. Several stages demonstrate PAS stained granules (Figs 13.28a to 13.28d). Brown-Hopps tissue gram stain also demonstrates the stages (Figs 13.29a to 13.29d). Organisms have rarely been found in mesenteric[59] and tracheobronchial lymph nodes,[60] the bile duct,[61] or in the liver and spleen.[62]

## Diagnosis

Identifying *I. belli* oocysts in stool is the accepted method of diagnosis. Concentration of stool by Sheather's sugar flotation is recommended. *Isospora* oocysts stain well by the Kinyoun acid-fast technique (Fig 13.18b), and auramine-rhodamine[63] staining produces good results. Oocysts stained with carbol-fuchsin fluoresce bright red under green light (546 nm). The oocysts' autofluorescence does not survive staining.[39]

If isosporiasis is suspected but stool examination is repeatedly negative, intestinal biopsy should be performed. Both sexual and asexual stages are readily distinguished in H&E-stained sections (Figs 13.21 to 13.27). Diagnosis by electron microscopy is also possible. DNA analysis of formalin-fixed paraffin-embedded tissue has been successful[61] as well as DNA analysis of stool samples.[64]

## Treatment and Prevention

Trimethoprim-sulfamethoxazole can effect clinical and parasitological cure in approximately 7 days. Low-dose trimethoprim-sulfamethoxazole or weekly pyrimethamine-sulfadoxine is recommended to prevent or treat recurrent infections in AIDS patients.[47,48] Metronidazole and quina-

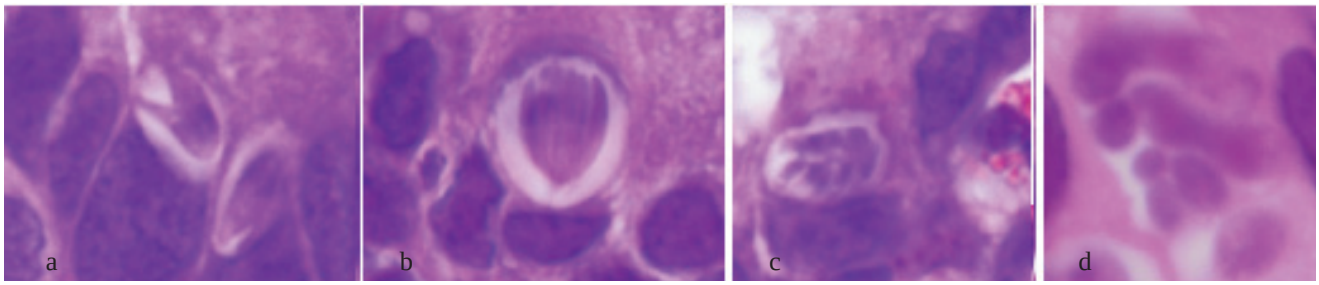



**Figure 13.24 a–d**
Merozoites (7 µm x 1 µm) of *Isospora belli* in duodenum forming within a schizont: a. First division, two merozoites; b. Second division, four merozoites; c. Third division, eight merozoites (total size 6 µm x 5 µm); d. Maturing eight merozoites (total size 10 µm x 6 µm). H&E x2000

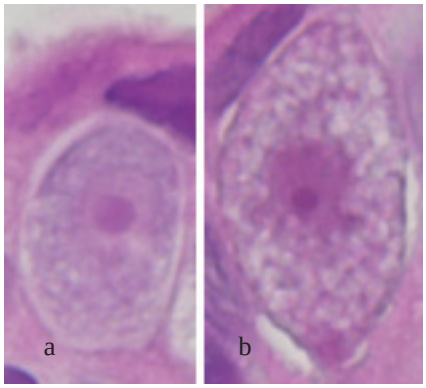



**Figure 13.25 a-b**
Macrogamont differentiate into macrogamete by multimembranous vacuoles which budded off the nucleus: a. Macrogamont (12 µm x 8 µm) H&E x2400; b. Macrogamete (12 µm x 10 µm) H&E x2500

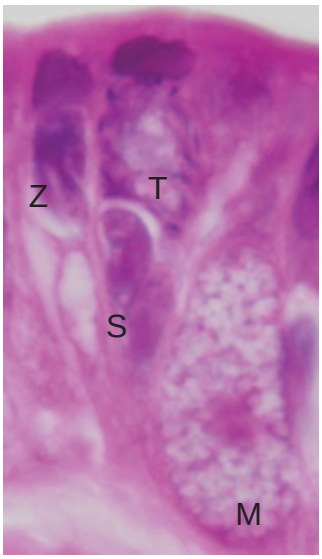



**Figure 13.27**
Heavily parasitized biopsy with sporozoite (S), two merozoites (Z), macrogamete (M) (15 µm x 8 µm), and microgamont (T) with host cell nucleus forming "T" sign and developing microgametes within. H&E x2000

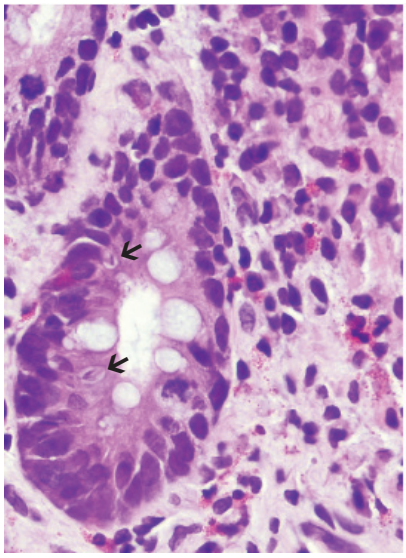


**Figure 13.26**
Heavily parasitized biopsy of duodenum with lymphocytes, plasma cells and eosinophils in lamina propria. Note merozoites (arrows) in enterocytes of gland. H&E x500

crine are also effective. In cases of prolonged, severe diarrhea, hydration therapy may be indicated.

Isosporiasis can be prevented with adequate sanitation, measures to protect food and water supplies, and increased public awareness of the means of transmission.

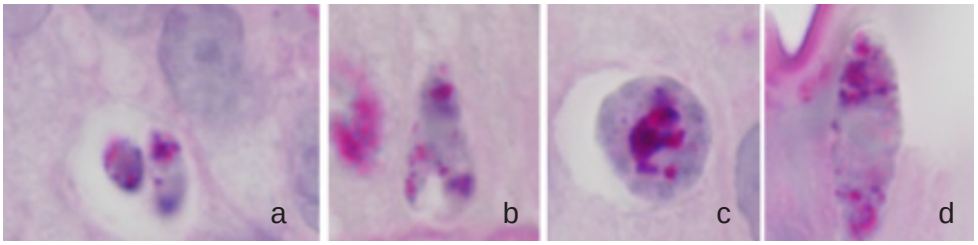



**Figure 13.28**
Developing stages of *Isospora belli d*emonstrate PAS stained granules x2000: a. Trophozoite (smaller 2 µm x 2 µm); b. Merozoite (larger 8 µm x 2 µm); c. Microgamont (8 µm x 8 µm); d. Macrogamete (13 µm x 4 µm).

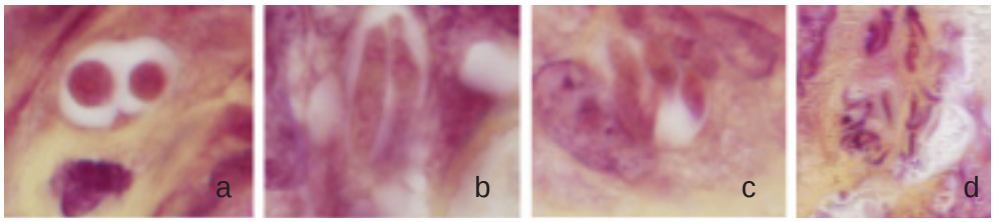



**Figure 13.29**
Developing stages of *Isospora belli* stained by the Brown-Hopps tissue gram stain x2000: a. Trophozoite (largest 4 µm x 4 µm); b. Merozoite (two cell stage larger cell 10 µm x 2 µm); c. Merozoite (four cell stage, individual 7 µm x 2 µm, total 10 µm x 6 µm); d. Microgametes (individuals 3 µm x 0.5 µm).

# CYCLOSPORIASIS

## Definition and Epidemiology

Cyclosporiasis is infection with the protozoon *Cyclospora cayetanensis*. It was first reported in humans in New Guinea in 1977. Several outbreaks occurred in the United States in 1996 and 1997.[65] In 2005, 11.9% of the indigenous people in Bolivar State, Venezuela, were infected.[66]

## *Infectious Agent*

### Morphologic Description

*Cyclospora* oocysts are 8 µm to 10 µm in diameter (Fig 13.30). Hematoxylin-alone stained sections of duodenal biopsies show the intracellular stages.[67] A later report recommends hematoxylin & eosin.[58] All four asexual stages (sporozoite, trophozoite, schizont, and merozoite) have been observed in the enterocyte.[68] Immature schizonts (uninuclear trophozoites) are 2 µm to 3 µm in diameter (Fig 13.31). Budding (ectomerogony) produces the asexual types I and II meronts that contain 8 to12 merozoites (Fig 13.32) and 4 merozoites (Fig 13.33), respectively.[69] Merozoites are banana-shaped and 5 µm to 6 µm long, with a nucleus in the posterior third. Although macrogametocytes and microgametocytes are more easily identified by transmission electron microscopy,[67] a microgamont with developing microgametes is identified. (Fig 13.34) . The organisms lack a PAS-positive sheath. [67]

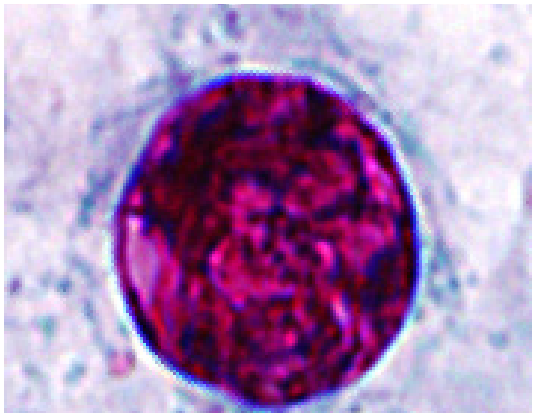


**Figure 13.30**
Spherical *Cyclospora* oocyst (8 µm to 10 µm in diameter). Ziehl-Neelsen acid fast stain x4000

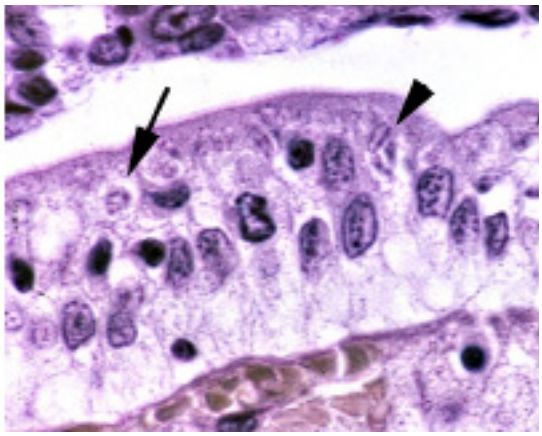


**Figure 13.31**
*Cyclospora* uninuclear trophozoites (2 µm to 3 µm in diameter-long arrow) develop into budding merozoites (arrow head) ending in banana-shaped merozoites (short arrow). Hematoxylin alone, original magnification x420

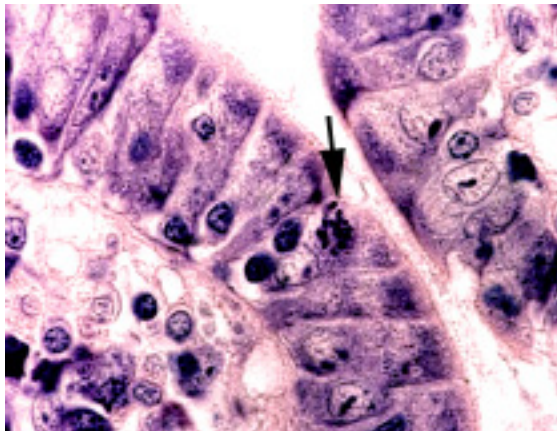


**Figure 13.32**
Asexual type I *Cyclospora* meronts (arrow) in apinuclear location of enterocyte. Hematoxylin alone, original magnification x420

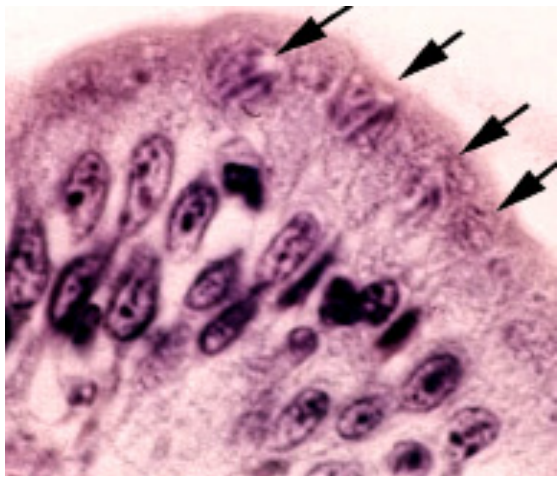


**Figure 13.33**
Asexual type II *Cyclospora* meronts (arrows) in apinuclear location of enterocyte. Hematoxylin alone, original magnification x420

## Life Cycle and Transmission

Ingestion of sporulated oocysts causes infection in humans. Sexual and asexual forms develop within an apical intracytoplasmic parasitophorous vacuole in enterocytes of the small intestine (Fig 13.30).[70] Unsporulated oocysts are excreted in feces (Fig 13.30).

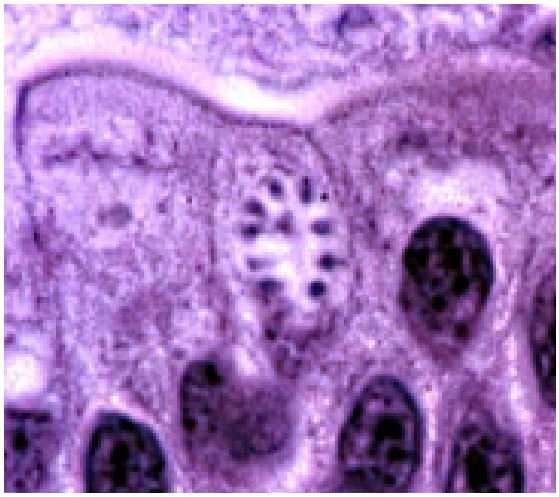


**Figure 13.34**
Microgamont of *Cyclospora* with developing microgametes. Hematoxylin alone, original magnification x420.

*Cyclospora* may be transmitted by contaminated food or water.[54,71] Washing does not easily remove oocysts from fruits and vegetables. The infectious dose is unknown, but is presumed to be low.[70] Animal reservoirs have not been found.

## Clinical Features

The incubation period of *Cyclospora cayetanesis* is 2–22 days.[58] Symptoms include watery diarrhea, nausea, anorexia, abdominal cramping, fatigue, and weight loss.[70] In HIV-positive patients *C. cayetanesis* produces prolonged diarrhea, wasting and weight loss,[58] but was found in only one of 113 HIV-positive patients, 34 of whom had chronic diarrhea.[56]

## Pathologic Features

In infected enterocytes, which are not enlarged, the organisms cluster at the tops of villi.[67] The parasitophorous vacuole is 8 µm to 10 µm in maximum diameter. Jejunal mucosal biopsies show altered architecture with surface epithelial disarray, shortening and widening of villi due to edema, and mild to moderate infiltration of the lamina propria by mixed inflammatory cells, as seen in cryptosporidiosis (Figs 13.31 to 13.34). There is also reactive hyperemia with vascular dilation and congestion of villous capillaries.[69] There are no eosinophils in the inflammatory infiltrate.[67]

## Diagnosis

Oocysts from stool specimens are easily observed by phase-contrast microscopy; the alga-like morula appearance is evident in fresh specimens. Oocysts autofluoresce and stain positively using a modified trichrome method, and stain variably acid-fast using modified Ziehl-Neelsen (Fig 13.30).[34] An oocyst DNA extraction method and PCR screening assay to detect a single oocyst is available to evaluate agriculture produce washes.[72]

## Treatment and Prevention

Treatment consists of supportive care, maintenance of fluid and electrolyte balance, symptomatic relief, and antibiotic therapy. Trimethoprim-sulfamethoxazole effectively eradicates the organism.[73]

# SARCOCYSTOSIS

## Definition and Synonym

Sarcocystosis, also called sarcosporidiosis and sarcocystitis, is infection by protozoa of the genus *Sarcocystis*, which are members of the family Sarcocystidae that also includes *Toxoplasma gondii.* They are heteroxenous, re-

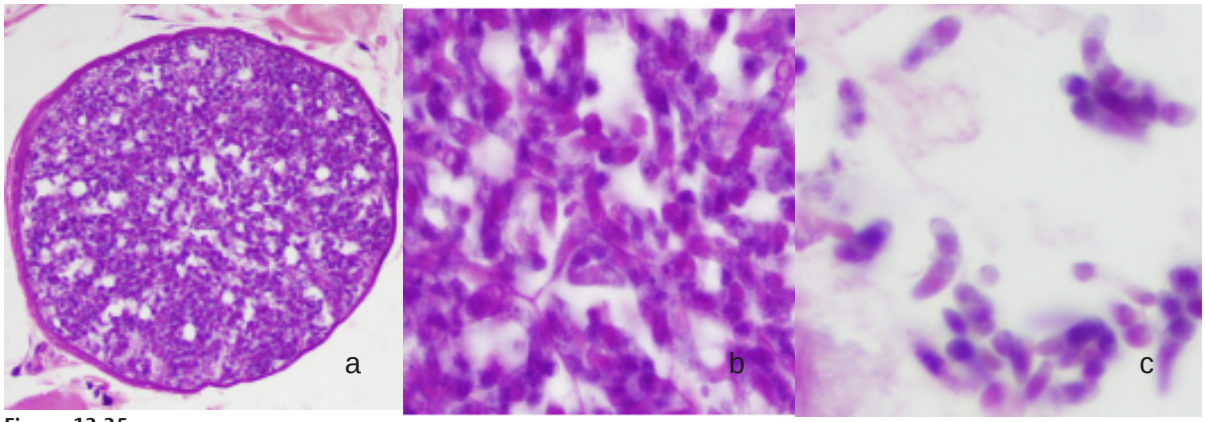



**Figure 13.35a-c**
Mature sarcocyst of *Sarcocystis hominis* in striated muscle from iliac fossa: a. Only a thin band of muscle envelops the sarcocyst (190µm diameter) x270; b. Mature bradyzoites in center of sarcocyst x1000; c. Escaped bradyzoites (9 µm to 12 µm x 2 µm to 4 µm) nearby a sarcocyst. H&E x1000

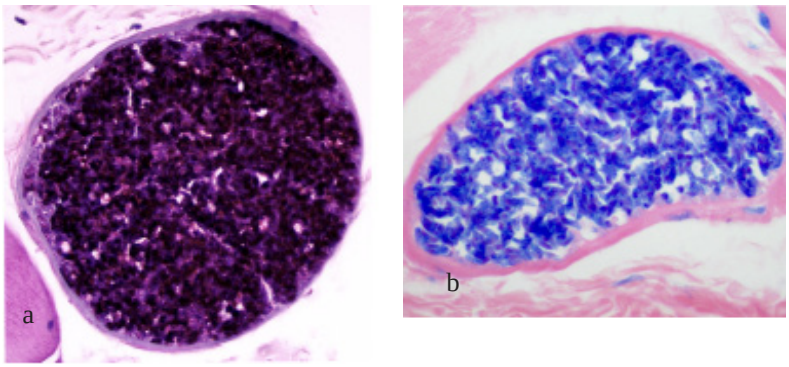



**Figure 36 a,b**
Mature sarcocysts in human muscle: a. Bradyzoites are PAS positive. Original magnification x400
b. Bradyzoites are Giemsa positive. Original magnification x400

quiring 2 host species to complete their life cycle. Asexual development takes place in the muscle of an herbivorous intermediate host; sexual development occurs in the intestine of a carnivorous definitive host. Humans are definitive hosts for *Sarcocystis hominis* and *Sarcocystis suihominis*. Zoonotic species are occasionally found in human muscle. Three types found in skeletal muscle resemble species found in monkeys; another type found in cardiac muscle resembles a species seen in cattle.[74,75]

### General Considerations

*Sarcocystis* was first reported by Miescher in 1843 in mice, and in 1865 in the muscle of swine.[76] In 1970, it was discovered that bradyzoites develop into coccidian gametes in cell culture,[76] and into oocysts when fed to cats.

## *Epidemiology*

*Sarcocystis* is widely distributed but found more frequently in tropical areas.[77] Cases have been reported from the Africa, Central and South America, China, Europe, India, Malaysia, Southeast Asia, and United States.[76]

## *Infectious Agent*

### Morphologic Description

Zoitocysts in muscle are called sarcocysts or Miescher's tubules.[76] The structure of the cyst wall varies in different stages of development. The origin of the cyst wall is unknown, but may be of host origin, parasitic origin, or both. Cysts range from 30 µm to 137.5 µm wide (Figs 13.35a to 13.35c). Cyst walls are smooth and less than 1 µm thick. Numerous merozoites, also called bradyzoites, stain both with PAS and Giemsa (Figs 13.36a & 13.36b) but not with acid-fast and have diameters averaging 1 µm, fill the cyst, and in more immature sarcocysts, form 2 distinct regions (Figs 13.37a to 13.37c).[76,78] The peripheral region is occupied by globular metrocytes that become bradyzoites, which are similar to those of other coccidian merozoites.

Organisms in the sexual stages are within a parasitophorous vacuole bounded by 2 membranes. Gamonts of *S. suihominis* are up to 10 µm in diameter. Microgametes are slender and approximately 4 µm to 5 µm long. Macrogametes are bounded by 2 membranes and contain 2 types of inclusions thought to be wall-forming bodies (Fig 13.38). Each oocyst has a dense outer layer, 4 membranes, and 2 sporocysts, each with 4 sporozoites.[79]

### Life Cycle and Transmission

When an intermediate host consumes infective sporocysts, sporozoites are released from the sporocysts and penetrate the intestinal epithelium (Figs 13.39a & 13.39b). They are distributed throughout the body, invading blood vessel endothelial cells in many tissues, including skeletal

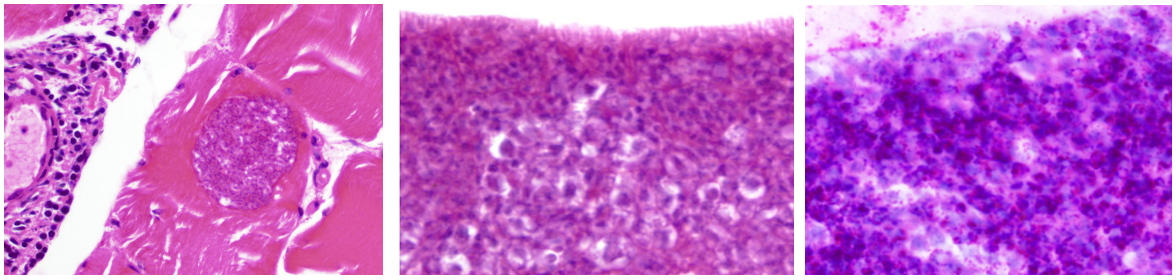


**Fig 13.37**
Immature sarcocysts of *Sarcocystis hominis* in striated musle left leg: a. Spherical form (66 µm diameter) H&E x230; b. Two distinct regions formed by smaller merozoites (1µm) and larger globular metrocytes (2 µm to 4 µm diameter) in a long narrow sarcocyst (50 µm wide) H&E x1000; c. Peripheral globular metrocytes do not stain with PAS, only the bradyzoites stain. PAS: original magnification x1000

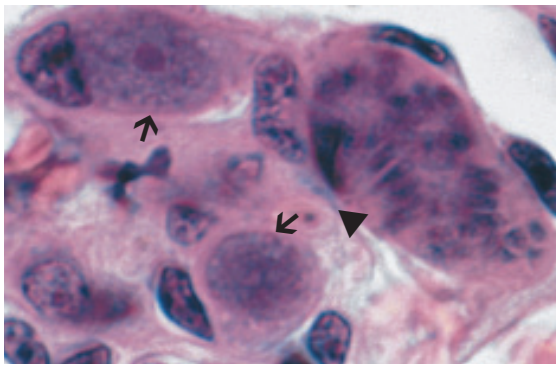


**Figure 13.38**
Renal glomerulus of calf containing three forms of *Sarcocystis cruzi*, two immature macrogamonts (arrows) and a mature meront with merozoites (arrow head). H&E, original magnification x1500

and cardiac muscle, where they undergo schizogony (asexual reproduction). Large accumulations of merozoites form within zoitocysts. After several divisions, metrocytes in the periphery of the zoitocyst give rise to elongated bradyzoites, which are infective in definitive hosts.

Eating meat contaminated with zoitocysts causes infection in a definitive host. The wall of the zoitocyst is digested, and the released bradyzoites penetrate the lamina propria of the small intestine. Within the muscle fiber, they undergo gamogony (sexual reproduction) without an intervening schizogonic generation. The large nucleus of every microgamont gives rise simultaneously to about 20 to 30 microgametes.[79] Male gametes penetrate female gametes, and the resulting oocyst sporulates in the lamina propria. The oocyst wall is thin and is usually ruptured during intestinal passage to form a sporocyst in the stool (Fig 13.40).

## Clinical Features

*Sarcocystis* has been found in muscles of the larynx, diaphragm, chest, abdomen, extremities, heart, and tongue.[76] Conditions associated with sarcocystosis include fever, chronic myositis, muscle soreness, weakness, subcutaneous swelling, sinus drainage, eosinophilia, periarteritis, and polyarteritis nodosa.[74,76,80]

## Pathologic Features

Inflammation is not usually seen.[78] There may be surrounding fibrosis and lymphocytic infiltration with a few eosinophils.[77]

## Diagnosis and Treatment

Sarcocystosis is diagnosed by histologic examination of excised tissue. It may be treated with trimethoprim-sulfamethoxazole or by excision of the involved organ in a life-threatening condition.[77,80]

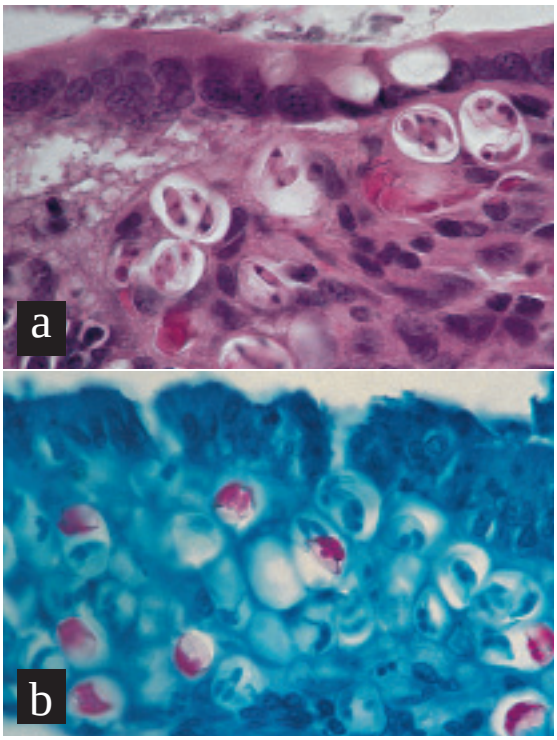



**Figure 13.39 a–b**
Small intestines with numerous sporulated oocysts in subepithelium: a. *Sarcocystis cruzi* in dog. H&E: original magnification x630; b. *Sarcocystis* sp in rattlesnake. Note acid-fastness of mature sporozoites. Acid-fast stain: original magnification x630

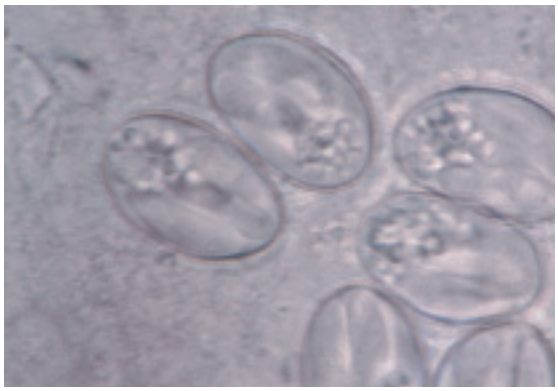


**Figure 13.40**
Feces of dog containing sporocysts of *Sarcocystis cruzi*, each with four sporozoites and granular residuum. Unstained: original magnification x1500

## References


1. Cox FEG. Taxonomy and classification of the human parasites, volume 2 Chapter 132, p 1989-1994. In: *Manual of Clinical Microbiology*. PR Murray, EJ Baron, JH Jrgensen, ML Landry, MA Pfaller, eds. 9th Edition ASM Press, Washington, DC.
2. Barta JR, Thompson RC. What is *Cryptosporidium*? Reappraising its biology and phylogenetic affinities. *Trends Parasitol*. 2006;22:463-468.
3. Xiao L. Molecular epidemiology of cryptosporidiosis: an update. *Exp Parasitol*. 2010;124:80-89.
4. Abrahamsen MS, Templeton TJ, Enomoto S, et al. Complete genome sequence of the apicomplexan, *Cryptosporidium parvum. Science*. 2004;304:441-445.
5. Xu P, Widmer G, Wang Y, et al. The genome of *Cryptosporidium hominis*. *Nature*. 2004;431:1107-1112.
6. Tanriverdi S,Widmer G. Differential evolution of repetitive sequences in *Cryptosporidium parvum* and *Cryptosporidium hominis. Infection, Genetics and Evolution.* 2006;6:113-122.
7. Clarke JJ. A study of coccidia met with in mice. *J Micros Soc*. 1895;37:277-302.
8. Tyzzer EE. An extracellular coccidium, *Cryptosporidium muris* (gen et sp nov.) of the gastric glands of the common mouse. *J Med Res*. 1910;23:487-516.
9. Hunter PR, Chalmers RM, Syed Q, Hughes LS, Woodhouse S, Swift L. Foot and mouth disease and cryptosporidiosis: possible interaction between two emerging infectious diseases. *Emerg Infect Dis*. 2003;9:109-112.
10. Yoder JS, Harral C, Beach MJ; Centers for Disease Control and Prevention (CDC). Cryptosporidiosis surveillance - United States, 2006-2008. *MMWR Surveill Summ.* 2010;59:1-14.
11. Roberts WG, Green PH, Ma J, Carr M, Ginsberg AM. Prevalence of cryptosporidiosis in patients undergoing endoscopy: evidence for an asymptomatic carrier state. *Am J Med.* 1989;87:537-539.
12. Manabe YC, Clark DP, Moore RD, et al. Cryptosporidiosis in patients with AIDS: correlates of disease and survival. *Clin Infect Dis*. 1998;27:536-542.
13. Borowski H, Thompson RC, Armstrong T, Clode PL. Morphological characterization of *Cryptosporidium parvum* life-cycle stages in an in vitro model system. *Parasitology*. 2010;137:13-26.
14. Orenstein JM. Cryptosporididiosis. In: Connor DH, Chandler FW, Schwartz DA, Manz HJ, Lack EE. *Pathology of Infectious Diseases,* Vol II, 1997, Appleton & Lange:Stamford, pp1147-1158.
15. Tzipori S, Griffiths JK. Natural history and biology of *Cryptosporidium parvum. Adv Parasitol.* 1998;40:5-36.
16. O'Hara SP, Huang BQ, Chen XM, Nelson J, LaRusso NF. Distribution of *Cryptosporidium parvum* sporozoite apical organelles during attachment to and internalization by cultured biliary epithelial cells. *J Parasitol*. 2005;91:995-999.
17.. Hijjawi NS, Meloni BP, Morgan UM, Thompson RC. Complete development and long-term maintenance of *Cryptosporidium parvum* human and cattle genotypes in cell culture. *Int J Parasitol.* 2001;31:1048-1055.
18. Hijjawi NS, Meloni BP, Ng'anzo M, et al. Complete development of *Cryptosporidium parvum* in host cell-free culture. *Int J Parasitol*. 2004;34:769-777.
19. Huang BQ. Chen X-M, LaRusso NF. *Cryptosporidium parvum* attachment to and internalization by human bilary epithelia in vitro: a morphologic study. *J Parasitol.* 2004;90:212-221.
20. Chen X-M, Keithly JS, Paya CV, LaRusso NF. Cryptosporidiosis. *N Engl J Med.* 2002;346:1723-1731.
21. Centers for Disease Control and Prevention (CDC). Foodborne outbreak of cryptosporidiosis--Spokane, Washington, 1997. *MMWR Morb Mortal Wkly Rep.* 1998;47:565-567.
22. Pönka A, Kotilainen H, Rimhanen-Finne R, et al. A foodborne outbreak due to *Cryptosporidium parvum* in Helsinki, November 2008. *Euro Surveill*. 2009;14. pii:19269.
23. Mac Kenzie WR, Hoxie NJ, Proctor ME, et al. A massive outbreak in Milwaukee of *Cryptosporidium* infection transmitted through the public water supply. *N Engl J Med.* 1994;331:161-167. Erratum in: *N Engl J Med.* 1994;331:1035.
24. Centers for Disease Control and Prevention (CDC). Outbreak of cryptosporidiosis associated with a splash park - Idaho, 2007. *MMWR Morb Mortal Wkly Rep*. 2009;58:615-8. Erratum in: *MMWR Morb Mortal Wkly Rep*. 2009;58:781. *MMWR Morb Mortal Wkly Rep*. 2009;58:645.
25. Hunter PR, Hughes S, Woodhouse S, et al. Sporadic cryptosporidiosis case-control study with genotyping. *Emerging Infect Dis.* 2004;10:1241-1249.
26. Chappell CL, Okhuysen PC, Langer-Curry R, et al. *Cryptosporidium hominis*: experimental challenge of healthy adults. *Am J Trop Med Hyg*. 2006;75:851-857.
27. DuPont HL, Chappell CL, Sterling CR, Okhuysen PC, Rose JB, Jakubowski W. The infectivity of *Cryptosporidium parvum* in healthy volunteers. *N Engl J Med.* 1995;332:855-859.
28. Fayer R, Ungar BLP. *Cryptosporidium* spp. and cryptosporidiosis. *Microbiol Rev*. 1986;50:458-483.
29. Clark DP. New insights into human cryptosporidiosis. *Clin Microbiol Rev.* 1999;12:554-563.
30. Rossi P, Rivasi F, Codeluppi M, et al. Gastric involvement in AIDS associated cryptosporidiosis. *Gut*. 1998;43:476-477.
31. Mor SM, Tumwine JK, Ndeezi G, et al. Respiratory cryptosporidiosis in HIV-seronegative children in Uganda: potential for respiratory transmission. *Clin Infect Dis.* 2010;50:13661-13672.
32. Travis WD, Schmidt K, MacLowry JD, Masur H, Condron KS, Fojo AT. Respiratory cryptosporidiosis in a patient with malignant lymphoma. *Arch Pathol Lab Med.* 1990;114:519-522.
33. Borad A, Ward H. Human immune responses in cryptosporidiosis. *Future Microbiol*. 2010;5:507-519.
34. Xiao L. Overview of *Cryptosporidium* presentations at the 10th International Workshops on Opportunistic Protists. *Eukaryot Cell*. 2009;8:429-436.
35. Chen XM, Levine SA, Splinter PL, et al. *Cryptosporidium parvum* activates nuclear factor kappaB in biliary epithelia preventing epithelial cell apoptosis. *Gastroenterology*. 2001;120:1774-1783.
36. Elliott DA, Clark DP. Host cell fate on *Cryptosporidium parvum* egress for MDCK cells. *Infect Immun*. 2003;71:5422-5426.
37. Feng H, Nie W, Sheoran A, Zhang Q, Tzipori S. Bile acids enhance invasiveness of *Cryptosporidium* spp. into cultured cells. *Infect Immun*. 2006;74:3342-3346.
38. Lumadue JA, Manabe YC, Moore RD, Belitsos PC Sears C, Clark DP. A clinicopathologic analysis of AIDS-related cryptosporidiosis. *AIDS.* 1998;12:2459-2466.
39. Varea M, Clavel A, Doiz O, Castillo FJ, Rubio MC, Gómez-Lus R. Fuchsin fluorescence and autofluorescence in *Cryptosporidium, Isospora* and *Cyclospora* oocysts. *Int J Parasitol*. 1998;28:1881-1883.
40. Deere D, Vesey G, Milner M, Williams K, Ashbolt N, Veal D. Rapid method for fluorescent in situ ribosomal RNA labelling of *Cryptosporidium parvum. J Appl Microbiol.* 1998;85:807-818.
41. Widmer G. Genetic heterogeneity and PCR detection of *Cryptosporidium parvum. Adv Parasitol.* 1998;40:223-239.
42. Stroup SE, Roy S, Mchele J, et al. Real-time PCR detection and speciation of *Cryptosporidium* infection using Scorpion probes. *J Med Microbiol.* 2006;55:1217-1222.
43. Smith NH, Cron S, Valdez LM, Chappell CL, White AC Jr. Combination drug therapy for cryptosporidiosis in AIDS. *J Infect Dis.* 1998;178:900-903.
44. Meamar AR, Rezaian M, Rezaie S, et al. *Cryptosporidium parvum bovine* genotype oocysts in the respiratory samples of an AIDS patient: efficacy of treatment with a combination of azithromycin and paromomycin. *Parasitol Res.* 2006;98:593-595.
45. Liu K, Zai D, Zhang D, et al. Divalent Cp15-23 vaccine enhances immune responses and protection against *Cryptosporidium parvum* infection. *Parasite Immunol.* 2010;32:335-344.
46. Connelly JT, Nugen SR, Borejsza-Wysocki W, Durst RA, Montagna RA, Baeumner AJ. Human pathogenic *Cryptosporidium* species bioanalytical detection method with single oocyst detection capability. *Anal Bioanal Chem.* 2008;391:487-495.
47. Lindsay DS, Dubey JP, Blagburn BL. Biology of *Isospora* spp. from humans, nonhuman primates, and domestic animals. *Clin Microbiol Rev.* 1997;10:19-34.
48. Guiguet M, Furco A, Tattevin P, Costagliola D, Molina JM; French Hospital Database on HIV Clinical Epidemiology Group. HIV-associated *Isospora belli* infection: incidence and risk factors in the French Hospital Database on HIV. *HIV Med*. 2007;8:124-130.
49. Curry A, Smith HV. Emerging pathogens: *Isospora, Cyclospora* and *microsporidia. Parasitology*. 1998;117 Suppl:S143-159.
50. Koru O, Araz RE, Yilmaz YA, et al. Case report: *Isospora belli* infection in a renal transplant recipent. *Turkiye Parazitol Derg*. 2007;31:98-100.
51. Kochhar A, Saxena S, Malhotra VL, Deb M. *Isospora belli* infection in a malnourished child. *J Commun Dis*. 2007;39:141-143.
52. Assefa S, Erko B, Medhin G, Assefa Z, Shimelis T. Intestinal parasitic infections in relation to HIV/AIDS status, diarrhea and CD4 T-cell count. *BMC Infect Dis.* 2009;9:155.
53. Ferguson DJ, Birch-Andersen A, Hutchison WM, Siim JC. Ultrastructural observations on macrogametogenesis and the structure of the macrogamete of *Isospora felis. Acta Pathol Microbiol Scand B*. 1980;88:161-168.

54. Elshazly AM, Elsheikha HM, Soltan DM, Mohammad KA, Morsy TA. Protozoal pollution of surface water sources in Dakahlia Governorate, Egypt. *J Egypt Soc Parasitol.* 2007;37:51-64.
55. Meamar AR, Rezaian M, Mirzaei AZ, et al. Severe diarrhea due to *Isospora belli* in a patient with thymoma. *J Microbiol Immunol Infect.* 2009;42:526-529.
56. Gupta S, Narang S, Nunavath V, Singh S. Chronic diarrhoea in HIV patients: prevalence of coccidian parasites. *Indian J Med Microbiol.* 2008;26:172-175.
57. Hizawa K, Iida M, Eguchi K, et al. Comparative features of double-contrast barium studies in patients with isosporiasis and strongyloidiasis. *Clin Radiol.* 1998;53:764-767.
58. Field AS. Light microscopic and electron microscopic diagnosis of gastrointestinal opportunistic infections in HIV-positive patients. *Pathology*. 2002;34:21-35. Erratum in: *Pathology*. 2002;34:301.
59. Frenkel JK, Silva MB, Saldanha J, et al. *Isospora belli* infection: observation of unicellular cysts in mesenteric lymphoid tissues of a Brazilian patient with AIDS and animal inoculation. *J Eukaryot Microbiol*. 2003;50 Suppl:682-684.
60. Restrepo C, Macher AM, Radany EH. Disseminated extraintestinal isosporiasis in a patient with acquired immune deficiency syndrome. *Am J Clin Pathol.* 1987;87:536-542.
61. Walther Z, Topazian MD. *Isospora* cholangiopathy: case study with histologic characterization and molecular confirmation. *Hum Pathol*. 2009;40:1342-1346.
62. Michiels JF, Hofman P, Bernard E, et al. Intestinal and extraintestinal *Isospora belli* infection in an AIDS patient. A second case report. *Pathol Res Pract.* 1994;190:1089-1093.
63. Hanscheid T, Cristino JM, Salgado MJ. Screening of auramine-stained smears of all fecal samples is a rapid and inexpensive way to increase the detection of coccidial infections. *Int J Infect Dis.* 2008;12:47-50.
64. ten Hove RJ, van Lieshout L, Brienen EA, Perez MA, Verweij JJ. Real-time polymerase chain reaction for detection of *Isospora belli* in stool samples. *Diagn Microbiol Infect Dis.* 2008;61:280-283.
65. Centers for Disease Control and Prevention. Update: outbreaks of cyclosporiasis–United States, 1997. *JAMA*. 1997;277:1838.
66. Devera R, Blanco Y, Cabello E. [High prevalence of *Cyclospora cayetanensis* among indigenous people in Bolivar State, Venezuela]. *Cad Saude Publica.* 2005;21:1778-1784.
67. Nhieu JT, Nin F, Fleury-Feith J, Chaumette MT, Schaeffer A, Bretagne S. Identification of intracellular stages of *Cyclospora* species by light microscopy of thick sections using hematoxylin. *Hum Pathol.* 1996;27:1107-1109.
68. Sun T, Ilardi CF, Asnis D, et al. Light and electron microscopic identification of *Cyclospora* species in the small intestine. Evidence of the presence of asexual life cycle in human host. *Am J Clin Pathol*. 1996;105:216-220.
69. Ortega YR, Nagle R, Gilman RH, et al. Pathologic and clinical findings in patients with cyclosporiasis and a description of intracellular parasite life-cycle stages. *J Infect Dis*. 1997;176:1584-1589.
70. Sterling CR, Ortega YR. *Cyclospora*: an enigma worth unraveling. *Emerg Infect Dis*. 1999;5:48-53.
71. Dorny P, Praet N, Deckers N, Gabriel S. Emerging food-borne parasites. *Vet Parasitol.* 2009;163:196-206.
72. Lalonde LF, Gajadhar AA. Highly sensitive and specific PCR assay for reliable detection of *Cyclospora cayetanensis* oocysts. *Appl Environ Microbiol.* 2008;74:4354-4358.
73. Brown GH, Rotschafer JC. *Cyclospora*: review of an emerging parasite. Pharmacotherapy. 1999;19:70-75.
74. Beaver PC, Gadgil K, Morera P. *Sarcocystis* in man: a review and report of five cases. *Am J Trop Med Hyg*. 1979;28:819-844.
75. Dubey JP, Lindsay DS. Neosporosis, toxoplasmosis, and sarcocystosis in ruminants. *Vet Clin North Am Food Anim Pract*. 2006;22:645-671.
76. Fayer R. *Sarcocystis* spp. in human infections. *Clin Microbiol Rev*. 2004;17:894-902, table of contents.
77. Liu CT, Roberts LM. Sarcosporidiosis in a Bantu woman. *Am J Clin Pathol.* 1965;44:639-641.
78. Wong KT, Clarke G, Pathmanathan R, Hamilton PW. Light microscopic and three-dimensional morphology of the human muscular sarcocyst. *Parasitol Res.* 1994;80:138-140.
79. Mehlhorn H, Heydorn AO. Electron microscopical study on gamogony of *Sarcocystis suihominis* in human tissue cultures. *Z Parasitenkd.* 1979;58:97-113.
80. Van den Enden E, Praet M, Joos R, Van Gompel A, Gigasse P. Eosinophilic myositis resulting from *sarcocystosis. J Trop Med Hyg*. 1995;98:273-276.


## *Acknowledgements*


Figures 13.2, 13.3, 13.5, 13.6, 13.8, 13.9, 13.14, 13.15, 13.38, 13.39, 13.40

Gardiner CH, Fayer R, Dubey JP. An Atlas of Protozoan Parasites in Animal Tissues (Second Edition). Armed Forces Institute of Pathology, American Registry of Pathology: Washington, DC.

Figures 13.4, 13.7, 13.10

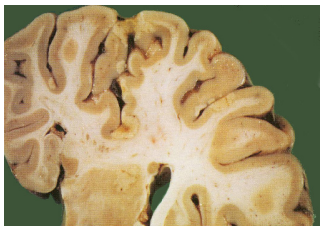
Saul Tzipori, Division of Infectious Diseases, Tufts University, School of Veterinary Medicine, North Grafton, MA as published in Tzipori S, Ward H. Cryptosporidiosis: biology, pathogenesis and disease. *Microbes and Infection* 2002;4:1047-1058. Licensed to the AFIP :Copyright © Elsevier, France.

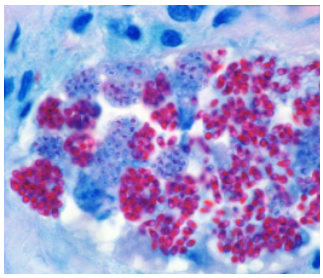
Figures 13.11

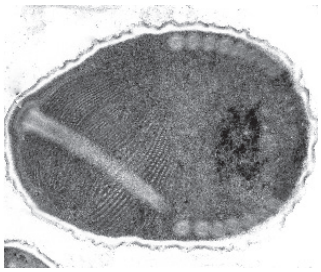
Saul Tzipori, Division of Infectious Diseases, Tufts University, School of Veterinary Medicine, North Grafton, MA as modified from Tzipori S and Widmer G. The biology of *Cryptosporidium*. *Contributions for Microbiology* 2000;6:1-32. Artist: Douglas Landry.

Figures 13.31, 13.32, 13.33, 13.34

Pr Stéphane Bretagne, Laboratoire de Parasitologie-Mycologie, Faculté de Médecine, Créteil Cedex, France as published in Nhieu JT, Nin F, Fleury-Feith J, Chaumette MT, Schaeffer A, Bretagne S. Identification of intracellular stages of *Cyclospora* species by light microscopy of thick sections using hematoxylin. *Hum Pathol* 1996;27:1107-1109.







14

# Microsporidiosis

*Ann Cali, Ronald C. Neafie and Peter M. Takvorian*

## Introduction

### Definition

Microsporidiosis is infection by eukaryotic unicellular protists of the phylum Microsporidia.[1] They are considered most closely related to the fungi,[2] but customarily are discussed among the protozoa. Several genera of microsporidia have been identified in human infections: *Nosema*,[3,4,5] *Brachiola*,[6,7] *Vittaforma*,[8] *Pleistophora*,[9,10] *Trachipleistophora*,[11] *Enterocytozoon*,[12,13] *Encephalitozoon*,[14-16] *Septata*,[17] and *Anncaliia*.[18] All microsporidia are obligate intracellular parasites, but pathologic changes vary with genus and species. In humans, infection may be latent or subclinical until the immune system is suppressed.[19-21] Microsporidia are a significant opportunistic pathogen in patients with AIDS. Clinical features vary with the location and extent of infection. Microsporidia may infect virtually any tissue or organ of the body,[22-25] including muscle,[26-28] intestine,[13,17,29,30] gallbladder,[31] liver,[14,31] kidneys,[28,32,33] eyes,[16,34-38] brain, [28,39] lungs,[4] skin, and nasal sinuses.[33,40,41] Intestinal microsporidiosis is most common, occurring in 30% to 50% of AIDS patients with chronic diarrhea.[42-44] Untreated intestinal, renal, cerebral, hepatic and disseminated infections are usually fatal.

### Synonyms

The phylum Microsporidia[1,45,46] was also known as phylum Microspora,[47,48] formerly subphylum Microspora.[49] *Encephalitozoon* and *Nosema* were considered synonymous[50,51] until 1970, when life cycle features demonstrated that they are separate genera.[52] *Nosema corneum* is now *Vittaforma corneae*,[8] a new genus having been established based on the ultrastructure of this organism's developmental stages and inconsistencies with any established genus. *Septata intestinalis* is also known as *Encephalitozoon intestinalis*[53]. *Nosema algerae* was reclassified as *Brachiola algerae*,[54] and is now *Anncaliia algerae*.[18] *Nosema connori* was *Brachiola connori*,[54] and is now *Anncaliia connori*.[18] Microsporidia with diagnostic spores but no identifiable developing stages are collectively called Microsporidium.[47,48]

The terms nosematosis and encephalitozoonosis are occasionally used to describe microsporidiosis caused by *Nosema* sp or *Encephalitozoon* sp.

## Epidemiology

Microsporidia are ubiquitous in animals (primarily insects, fish, and mammals) in developed and undeveloped, tropical and temperate regions of the world.[28,47,48,55] Human infections have been reported in Africa,[56] Australia,[57] Singapore,[58] Europe,[12] and the United States.[3,19,59,60] Between 1924 and 1985, less than a dozen cases of human microsporidiosis were reported.[61] Since 1985, thousands of cases have been documented, primarily in AIDS patients[62] but also in immunocompetent,[63,64] immunosuppressed[65] and organ

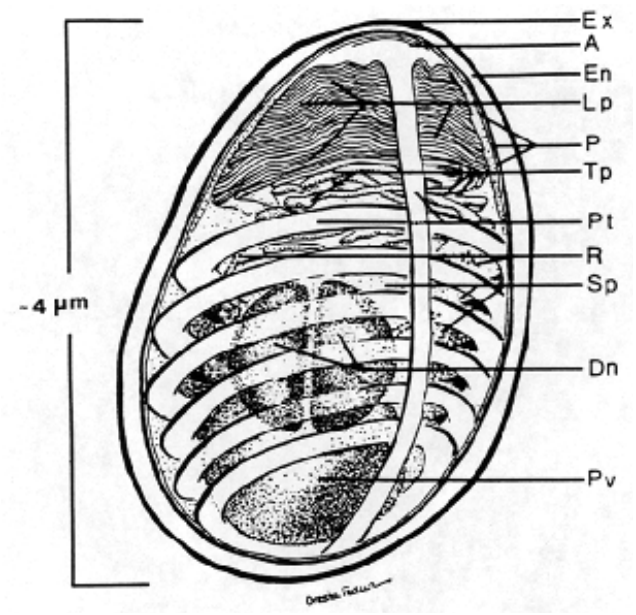



**Figure 14.1**
Diagram of the internal structure of a microsporidian spore. The spore coat has an outer electron-dense region called the exospore (Ex) and an inner thicker electron-lucent region, the endospore (En). A unit membrane (P) separates the spore coat from the spore contents. The extrusion apparatus, anchoring disk (A), polar tubule (Pt), lamellar polaroplast (Lp), spongiform polaroplast (Sp) and tubular polaroplast (Tp), dominates the spore contents and is diagnostic for microsporidian identification. The posterior vacuole (Pv) is a membrane-bound vesicle which sometimes contains a "membrane whirl," a "glomerular-like" structure, flocculent material, or some combination of these structures. The spore cytoplasm is dense and contains ribosomes (R) in a tightly coiled helical array. The nucleation may consist of a single nucleus or a pair of abutted nuclei, a diplokaryon (Dn). The size of the spore depends on the particular species and can vary from less than 1 µm to more than 10 µm. The number of polar tubule coils also varies from a few to 30 or more, again depending on the species observed.



**Figure 14.2**
Electron micrograph of *Anncaliia* (*Brachiola, Nosema) connori* spore in adrenal gland showing the coiled polar filament (arrow) and two nuclei. x30,000

transplant patients.[66,67] With the aid of molecular technology, surveys of humans with no clinical signs of infection have been identified as positive for microsporidia.[63] Additionally, animal reservoir hosts have been identified for the four most common microsporidial organisms found in human infections.[68]

## *Infectious Agents*

Microsporidia are named for the small, resistant spore stage characteristic of this group. The phylum contains more than 170 genera and approximately 1300 species.[28, 69] These diverse eukaryotes have relic mitochondria[70] no centrioles, contain 70S ribosomes, similar to prokaryotes, and have the smallest genome of any eukaryote thus far reported.[71] Their ribosomal sequences are more similar to bacteria than to eukaryotes.[72] However, their histochemically identifiable Golgi organelles indicate that they may be parasitically evolved degenerate protists,[73,74] microtubule gene data[75,76] as well as several enzyme processes, place them closest to the fungi.[2]

Spores infecting humans are 1 to 5 µm in length and ~1 µm in width. All microsporidian spores contain a single long coiled structure called the polar filament, a unique structure attached at the anterior end by a large, mushroom-shaped anchoring disk.[77] Electron microscopy reveals this structure coiled around the single- or double-nucleated sporoplasm inside the thick, resistant and refractile spore coat (Figs 14.1 & 14.2). The straight, anterior portion of the polar filament is surrounded by a polaroplast which may be lamellar, tubular, or both. Light microscopy reveals a PAS-positive granule in the anterior end of the spore (Fig 14.3).

While the spore structures themselves are characteristic of microsporidia, the number of spores produced in sporogony, the manner in which they are produced, and the host-parasite interface (Table 14.1) vary among genera of microsporidia. Host-parasite interface may involve: 1) direct contact with host-cell cytoplasm, 2) indirect contact with host-cell cytoplasm by production of a parasite-secreted envelope (sporophorous vesicle, SPOV), 3) indirect contact by production of a parasite-induced, host-produced envelope (parasitophorous vacuole), or 4) indirect contact by a host-produced envelope (parasitophorous vacuole)[5] and parasite-produced secretions.[28,61,78] These characteristics, along with morphologic features of developmental stages, nucleation, site of infection, and serologic and molecular features, help to identify the genus and species.

Table 14.1. Interfacial Relationships of the Microsporidia

| | |
|---|---|
| Type I. Direct contact | The parasite plasmalemma is in direct contact with the host-cell cytoplasm (hyaloplasm).<br>e.g. *Nosema, Brachiola, Anncaliia* and *Enterocytozoon*. |
| Type II. Indirect contact by host produced isolation. | A. Parasitophorous vacuole-host formed single membrane surrounding the developing parasite cell cluster. This is present during both the proliferative phase and the sporogonic phase, however the parasite relationship to it changes. The developing parasite cells maintain a very close relationship with this envelope until they develop the thickened sporont plasmalemma, then they appear loose within the vacuole.<br>e.g. *Encephalitozoon cuniculi*.<br><br>B. Host endoplasmic reticulum (ER) double membrane, surrounds parasite cells throughout development. In the proliferative phase the host ER double membranes follows the plasmalemma of the dividing cells so that no obvious vacuole is formed. In sporogony, the host ER does not divide with the sporonts and instead forms a double membraned parasitophorous vacuole surrounding the cluster of organisms formed in sporogony.<br>e.g. *Vittaforma* sp, *Endoreticulatus* sp. |
| Type III. Indirect contact by parasite produced isolation: | A. Parasite secreted envelope, surrounds parasite cells throughout development. It becomes a sporophorous vesicle (SPOV) in sporogony when the parasite plasmalemma pulls away from the secreted envelope and then the plasmalemma thickens.<br>e.g. *Pleistophora* sp.<br><br>B. The parasite develops in direct contact with the host cell cytoplasm during early development but then a parasite formed membrane isolates the sporonts from host cytoplasmic contact.<br>e.g. *Vairimorpha* sp. |
| Type IV. Indirect contact by host and parasite produced isolation. | A. Host ER closely abutts the parasite plasmalemma in merogony. Then the parasite produces “blisters” arising from the plasmalemma to form the interfacial envelope. Thus SPOV is formed in sporogony. It may also contain tubules.<br>e.g. *Loma* sp, and *Glugea* sp.<br><br>B. The host and parasite contribute to the formation of a thick interfacial envlope that surrounds all stages of parasite cells.<br>e.g. *Trachipleistophora* sp.<br><br>C. Host formed parasitophorous vacuole surrounds the parasite cluster and parasite secreted material surrounds each parasite cell inside the parasitophorous vacuole.<br>e.g. *Septata* sp. |

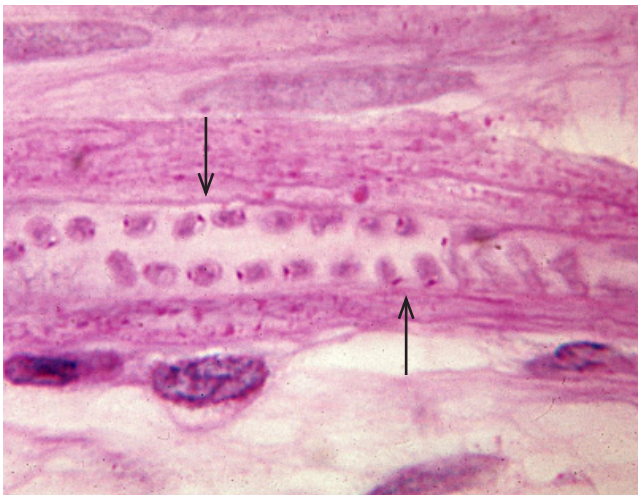


**Figure 14.3**
Section of appendix showing *Anncaliia connori* spores in muscularis. The anterior end of the spore has a PAS positive granule (arrows).
PAS x1,260

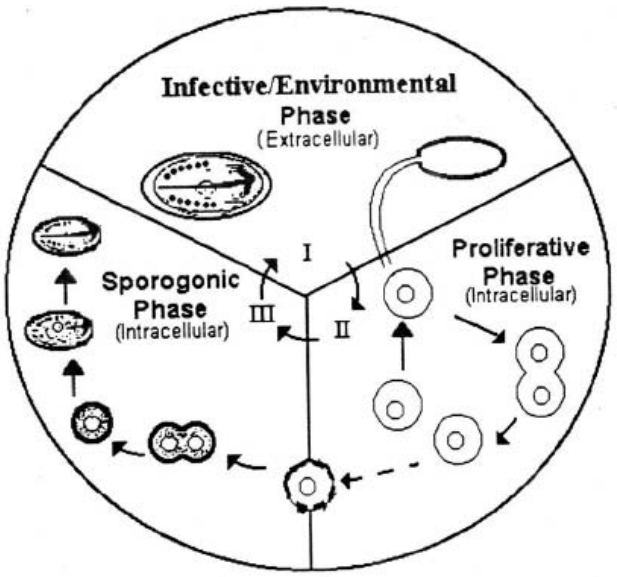



**Figure 14.4**
Life cycle. Diagrammatic illustration of a typical developmental cycle of the microsporidia. The three regions represent the three phases of a microsporidian life cycle. Phase I is the Infective/Environmental phase, the extracellular phase of the cycle. It contains the mature spores in the environment. Under appropriate conditions, the spore is activated (e.g. if the spore is ingested by an appropriate host, it is activated by the gut environment) and triggered to evert its polar filament which becomes a hollow tubule. If the polar tubule pierces a susceptible host cell and injects the sporoplasm into it, phase II begins. Phase II is the proliferative phase. This is the first phase of intracellular development. During the proliferative part of the microsporidian life cycle, organisms are usually in direct contact with the host cell cytoplasm and they increase in number. The transition to phase III, the sporogonic phase represents the organisms' commitment to spore formation. In many life cycles this is morphologically indicated by parasite secretions through the plasmalemma producing the "thickened" membrane. The number of cell divisions that follow varies, depending on the genus in question, and results in spore production.

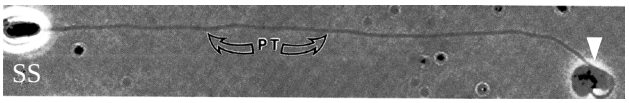



**Figure 14.5**
*Anncaliia algerae.* Spore in germination medium viewed by phase contrast microscopy. Sporoplasm (arrowhead) still connected to its polar tubule (PT) and spore shell (SS).

## Life Cycle and Transmission

The life cycles of microsporidia infecting humans have 3 phases: infective, proliferative, and sporogonic (Fig 14.4). The infective phase begins when a spore has developed fully in a host cell. Whether it remains within the host or passes to the environment through sputum, urine, or feces, the spore must receive the proper stimulus (pH or specific ions) in order to trigger the eversion of the polar filament resulting in the formation of a long polar tubule that emerges with sufficient speed/force to penetrate a new host cell (Fig 14.5).[79] A sporoplasm passes through the tubule and is deposited in a new host cell in less than a second, initiating a new infection.[80] Some spores are autoinfective and will evert their polar tubules, releasing sporoplasms within the same host, establishing additional sites of infection.

The proliferative phase begins when a sporoplasm grows and divides producing many organisms within the host-cell cytoplasm. The beginning of the sporogonic phase, sporogony, is usually signaled by one or more changes: secretions deposited on the surface membrane now called a thickened plasmalemma and/or formation of an isolating envelope (SPOV). Sporonts divide one or more times then become sporoblasts, which metamorphose into spores.

Environmental sources of human exposure to microsporidia are not known definitively, but since many human infections are intestinal and cause severe diarrhea, fecal-oral transmission is likely. In disseminating infections of the renal system, spores are passed in urine, providing another possible source of exposure. A strong correlation between soil exposure and microsporidial keratitis in HIV negative patients has been reported.[58] Municipal drinking water chlorination does not inactivate spores, so this is a possible reservoir for microsporidia as well as spores on food consumed raw (Fig 14.6).[81,82] The use of molecular tools has also led to the identification of human-infecting microsporidia in fecal samples from cats, dogs, primates, cattle, and birds. [83]

## *Families: Nosematidae &Tublinosematidae*

There are over 100 species of *Nosema*, most of which are parasitic in insects. A few *Nosema* species have been described from human ocular infections,[22,58] *N. ocularum*,

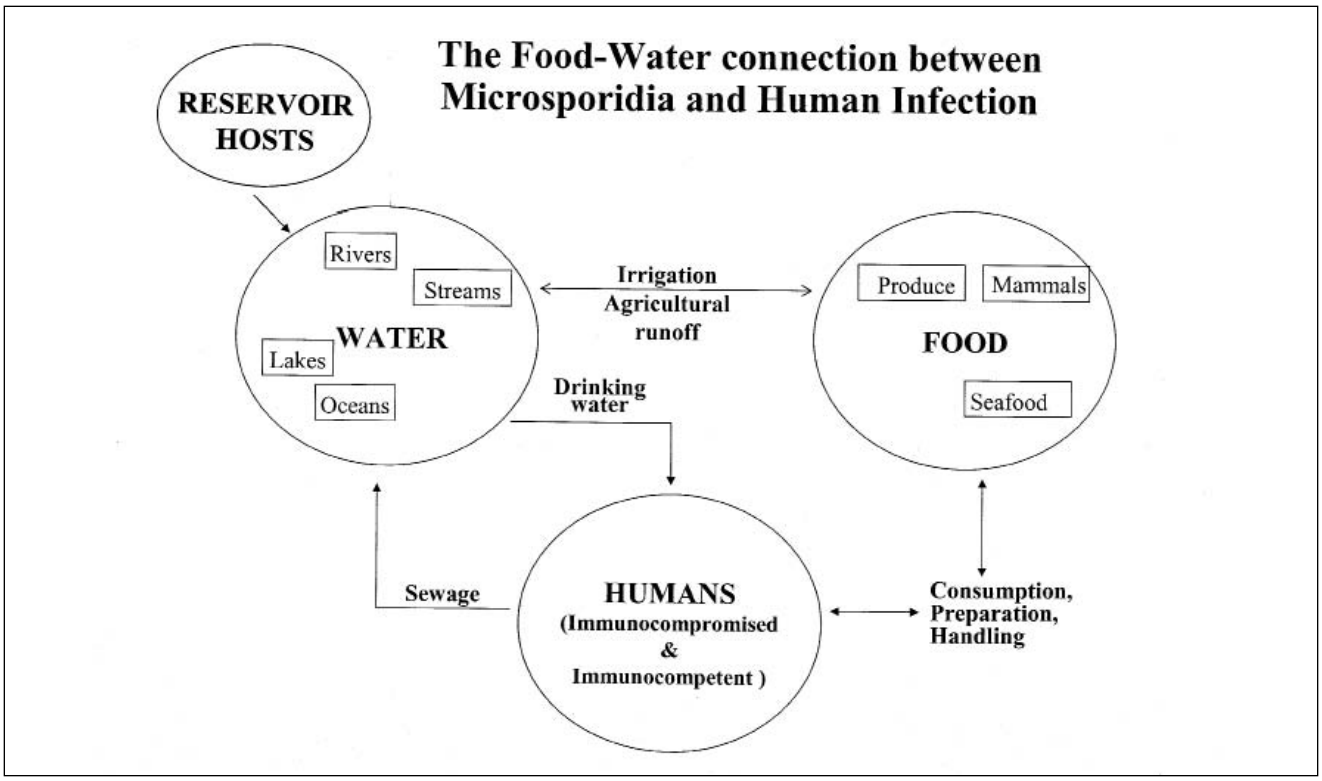



**Figure 14.6**
The food-water connection between microsporidia and human infection.

*Nosema* sp[29,84] and *N. corneum.*[13,17,29,30,85] The genus *Vittaforma* was created for the organism originally named *Nosema corneum*, after Silveira and Canning suggested that the diplokaryotic arrangement of nuclei was the only characteristic indicative of the genus *Nosema*. *Vittaforma corneae,*[8] as it is now known, is polysporoblastic and thus will probably be omitted from family Nosematidae as new molecular sequence data become known. The *Nosema* sp of Curry[84] is accepted in the *Nosema* genus because of the presence and/or absence of features eliminating other possibilities. *Nosema* sp of Ashton[34] lacked definitive generic information and was moved to the "group" Microsporidium with a species designation of *M. celonensis*[55] as was *Nosema* sp of Pinnolis[4] to *M. africanum*.[55] More recently Loh conducted a four year study that confirmed 124 cases of microsporidial keratitis. While the pathology and therapy were described, the generic designations of the organisms were not demonstrated.[58]

Three *Brachiola* spp have been described from human infections and recently moved to a new family, based on molecular and morphologic features.[18]

The new family, Tublinosematidae, was established in 2005 for organisms with many similarities to Nosematidae but with different morphological and molecular features.[86] While the family was established for microsporidia infecting insects, the human as well as the insect infecting *Brachiola* species were subsequently placed here because of the sequence similarity of *B. algerae* and *Anncaliia meligethi*.[18,87] These organisms possess a thickened plasmalemma throughout development and an elaborate surface tubular network that extends into the host cytoplasm. The genus *Anncaliia* was added to this family (2006) and its sequence data so closely resembled *Brachiola algerae* that the genus *Brachiola* became a synonym to the previously described genus *Anncaliia*.[18] However, we retain the genus *Brachiola* in this family, for its type species, *vesicularum,* because of its unique protoplasmic branches that extend into the host cytoplasm, similar to fungal hyphae, not demonstrated in any other microsporidia.[6]

## Morphologic Description

*Nosema* and *Anncaliia* (*Brachiola*) spores are approximately 4 µm in length and have paired abutted nuclei (diplokarya) in every stage of development. The parasite plasmalemma is in direct contact with the host-cell cytoplasm. If there are several nuclear divisions before cytokinesis

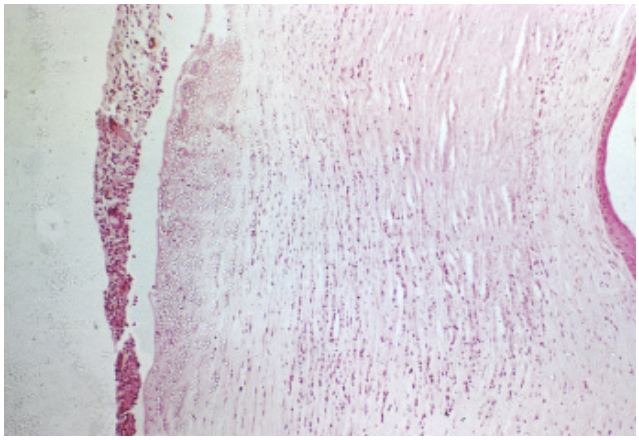


**Figure 14.7**
Microsporidia infection in patient's eye. Central stroma of cornea is necrotic and surrounded by acute inflammatory cells. H&E x210

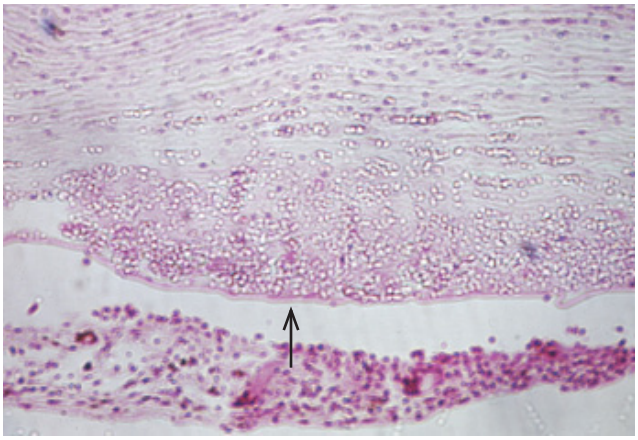


**Figure 14.8**
Refractile microsporidia (arrow) at edge of cornea next to the acute inflammatory cells. H&E x400

takes place, proliferative cells may become elongated. After many cell divisions, large clusters of individual diplokaryotic cells develop. Sporonts produce two sporoblast cells that develop into two spores, all in direct contact with the host-cell cytoplasm.[28,52]

*Nosema* sp form a thickened plasmalemma only in the sporogonic phase. However, all developmental stages of *Anncaliia* (*Brachiola*) sp form a thickened plasmalemma; these stages additionally form elaborate vesiculotubular appendages on the plasmalemmal surface.[81] *Brachiola vesicularum* uniquely forms protoplasmic extensions on elongated cells during the proliferative phase and produces spores that contain one to three rows (usually two) of polar filament coils.[6]

## Clinical and Pathologic Features

Two *Nosema* infections, subsequently changed to *Microsporidium celonensis* and *M. africanum* have been reported in HIV-negative patients with infections of the corneal stroma that led to perforation or blindness, followed by enucleation.[3,4,34,35,85,88] Histologic examination of corneal sections from one patient revealed organisms consistent with microsporidia (Fig 14.7). The central stroma was necrotic and surrounded by acute inflammatory cells. Immediately above Descemet's membrane were abundant refractile spores measuring 3.5 µm by 1.5 µm, some free and some in macrophages (Fig 14.8). No organisms were found in the exudate. In both infections, the genus *Nosema* was suggested but no specific identification could be made.[4,34,89] Two other microsporidia-associated infections of the corneal stroma were reported in the early 1990s in otherwise healthy individuals.[3,88] The first patient was a 39-year-old man from Ohio with a corneal ulcer. Examination of Gram-stained biopsy tissue by electron microscopy revealed microsporidia. Spores were 5 µm by 3 µm, binucleated, and

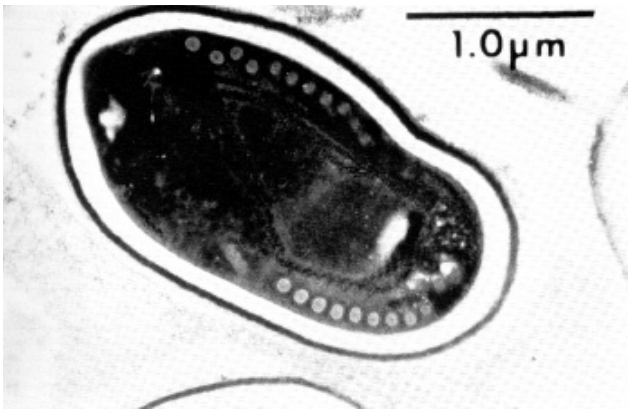



**Figure 14.9**
*Nosema ocularum*. High-power electron micrograph of spore showing 9-12 polar tube cross sections. Bar = 1.0 µm

contained 9 to 12 polar filament coils (Fig 14.9). The parasite was subsequently named *Nosema ocularum*.[3,35] The second patient was a 45-year-old man from South Carolina with no history of prior trauma to the infected eye.[88] Biopsy of the stroma revealed a microsporidium parasite that was isolated and grown in cell culture. The spores were 3.7 µm by 1 µm and contained 5 to 6 polar filament coils. This organism, originally named *Nosema corneum*,[85,88] is now known as *Vittaforma corneae*.[8]

From 1990 to the present, hundreds of microsporidian keratoconjuctivitis cases have been reported, in both HIV negative and positive patients, however, only a few reports have identified the organisms beyond being microsporidia. The pathologic changes, however, have been described from the survey of 124 microsporidia positive patients (134 eyes).[58] "Common features were follicular papillary conjunctivitis and coarse punctuate epithelial lesions in three patterns—diffuse, peripheral, and paracentral—evolving

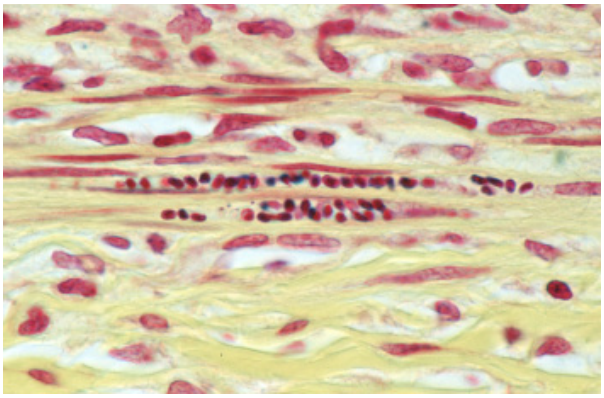


**Figure 14.10**
*Anncaliia connori* (4 µm x2 µm) in bowel of 4-month-old child: Gram-positive microsporidia in smooth muscle of ileum, Brown and Hopps (B&H) x2180

into nummular keratitis before resolution"…(99 percent of the cases were resolved with topical fluoroquinolone monotherapy). "New clinical features were diffuse endotheliitis (19.4%) with corneal edema and limbitis."[58]

The first well documented human infection with a microsporidium was in a 4-month-old male with thymic aplasia, severe diarrhea, and malabsorption (Fig 14.10).[7,89,90] At autopsy, *Anncaliia* (*Brachiola*, *Nosema*) *connori* spores measuring 4 µm by 2 µm were found in the small and large bowel; no other infectious agent was discovered.[7] Infection had disseminated to the lungs, stomach, kidneys, adrenal glands, myocardium, liver, and diaphragm (Figs 14.11 to 14.18).[89]

A *Brachiola* sp infection was reported in a 31-year-old male AIDS patient who had pain and progressive muscular weakness of the lower extremities of five months duration. It was named *B. vesicularum*.[6] The tissue biopsy contained spores measuring 2.5 µm to 2.9 µm by 1.9 µm to 2 µm. Intramuscular infection and cytolysis were observed by light microscopy. Electron microscopy revealed diplokaryotic microsporidia in all stages of development (Figs 14.19 & 14.20). An elaborate array of vesiculotubular appendages emanated from the plasmalemmal surface of most stages (Fig 14.21), and spores presented with variable polar filament arrangements (Fig 14.22). Additionally, protoplasmic extensions develop on some proliferative stages (Figs 14.23 & 14.24) that are unique to this microsporidium. There was loss of muscle striation in surrounding areas.

*Anncaliia* (*Brachiola*, *Nosema*) *algerae*, a parasite of mosquitoes, has been cultured in mammalian cells at 29° to 37°C[54,91] and documented by PCR

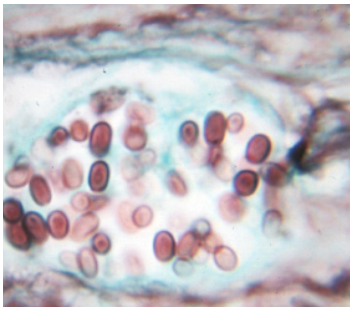


**Figure 14.11**
Silvered *Anncaliia connori* in wall of ileum of patient in Fig 14.10. 90 minute Grocott methenamine silver (GMS) x1300

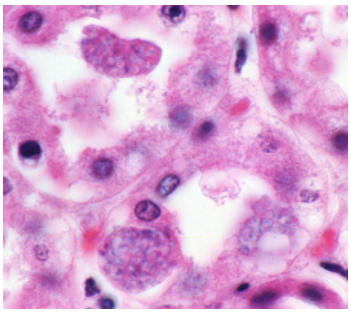


**Figure 14.12**
*Anncaliia connori* (4 µm x2µm) in kidney of patient in Figure 14.10. H&E x1800

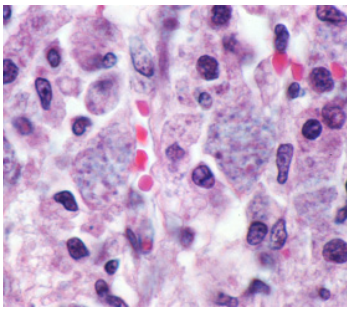


**Figure 14.13**
*Anncaliia connori* in adrenal gland of patient in Figure 14.10. H&E x1475

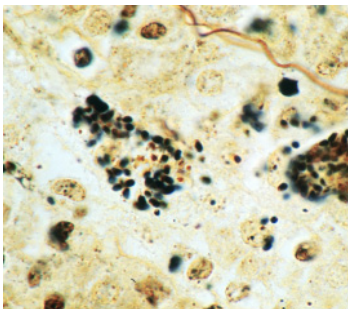


**Figure 14.14**
*Anncaliia connori* in adrenal gland of patient in Figure 14.10. Warthin-Starry (WS) x1860

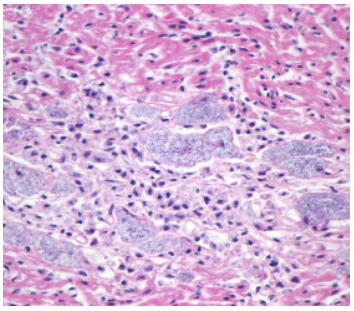


**Figure 14.15**
*Anncaliia connori* in myocardium of patient in Figure 14.10. H&E x450

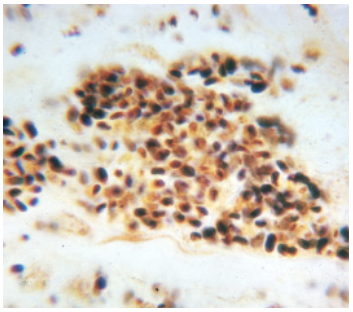


**Figure 14.16**
*Anncaliia connori* in myocardium of patient in Figure 14.10. WS x2260

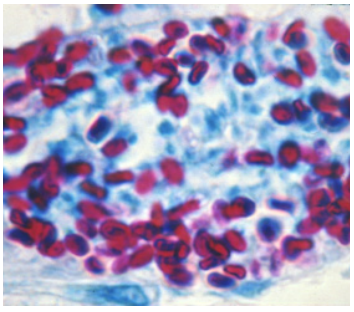


**Figure 14.17**
*Anncaliia connori* in myocardium of patient in Figure 14.10. Ziehl-Neelsen (ZN) x1440

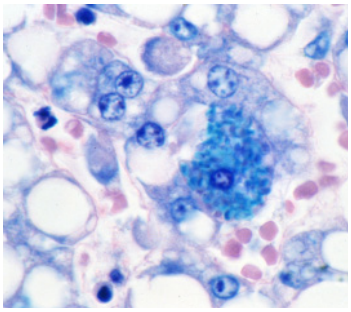


**Figure 14.18**
*Anncaliia connori* in liver of patient in Figure 14.10. Giemsa x1910

techniques in ocular and dermal infections of immunocompetent patients.[38] It has also been documented in deep tissue infections in skeletal muscle from a patient with rheumatoid arthritis being treated with immunosuppressive drugs (Figs 14.24, 14.25a & 14.25b). The infection progressed until the patient died.[65,92] Infection in both epithelial and connective tissue cells of the false vocal chord area (Figs 14.26 a-e & 14.27) was documented in a terminal cancer patient.[93]

## Family: Pleistophoridae

This family was named from the fish parasite *Pleistophora typicalis* (Gurley 1893). Since that time, approximately two dozen species had been described, all of them in fish[55] until 1985 when a human muscle infection with *Pleistophora* sp was identified.[9] This infection from an immunodeficient, but HIV negative male from the USA, was subsequently studied from the original tissue blocks and named *Pleistophora ronneafiei*.[10,92] Two additional *Pleistophora* sp cases were identified in HIV+ males, one in Australia[94] and one from Spain.[95] It was not until 1996, that yet another genus, *Trachipleistophora*, was established for human infection from this family of microsporidia.[11] The first species, *T. hominis* was described from muscle and eye infections in an AIDS patient from Australia.[11,27] A second species, *T. anthropopthera*,[96] was described from two AIDS patients.[97] This species disseminated to multiple organs including the brain, heart, kidney, pancreas, thyroid, parathyroid, liver, bone marrow, lymph nodes, and spleen. The most heavily infected cells were epithelia, cardiac myocytes, and astrocytes.[24]

## Morphologic Description

A thick, parasite-secreted, envelope is produced on the surface of proliferative cells. It separates from the surface and becomes an SPOV in sporogony. *Pleistophora ronneafiei* and *Trachipleistophora* sp develop within the host-cell cytoplasm in this type of parasite produced vesicle. Nuclei are single, even when there are many nuclei (not diplokaryotic) within a plasmodial proliferative cell. In *P. ronneafiei*, proliferative and sporogonic plasmodia divide by multiple fragmentation of large cells. *Pleistophora* is polysporous; 16 to over 100

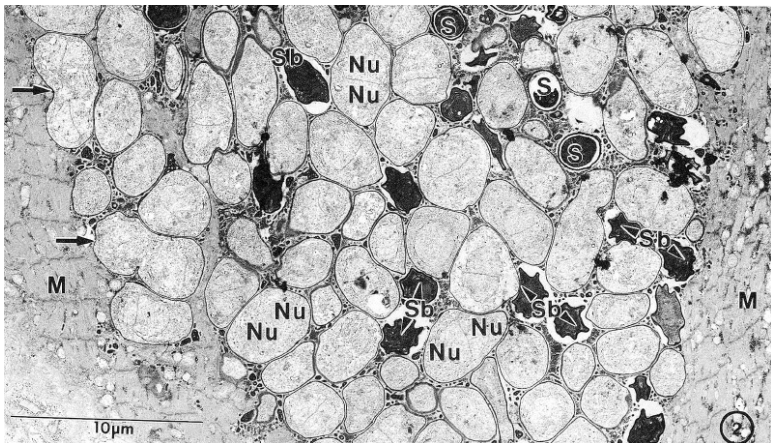



**Figure 14.19**
*Brachiola vesicularum*. Electron microscopic overview of an infected muscle cell. Developmental stages of the parasite appear as clusters surrounded by the striated muscle cell filaments (M). The electron-density variations of the parasite cells are readily observable, represent different stages of parasite development. The most dense stages are sporoblasts (Sb) and spores (S). Diplokaryotic nucleation (Nu) is apparent in the majority of parasitic cells. Some dividing cells contain two diplokarya (arrows) x4,300.

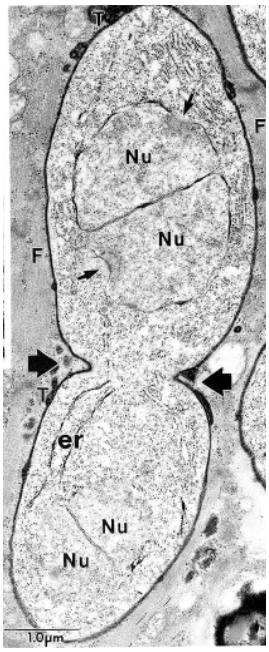



**Figure 14.20**
*Brachiola vesicularum*. A proliferative cell in advanced stage of cytokinesis (broad arrowheads), the spindle plaques (arrows) are still present. The cytoplasm of this proliferative cell is more densely granular and endoplasmic reticulum (er) is more abundant indicating that this cell is also advanced in the parasite developmental cycle. Note the presence of myofilaments (F) and of vesiculotubular material (T).

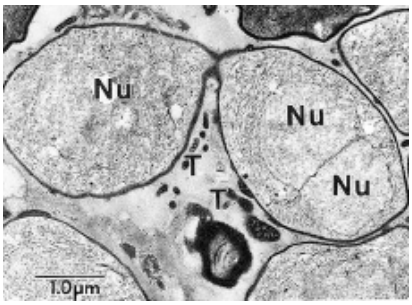
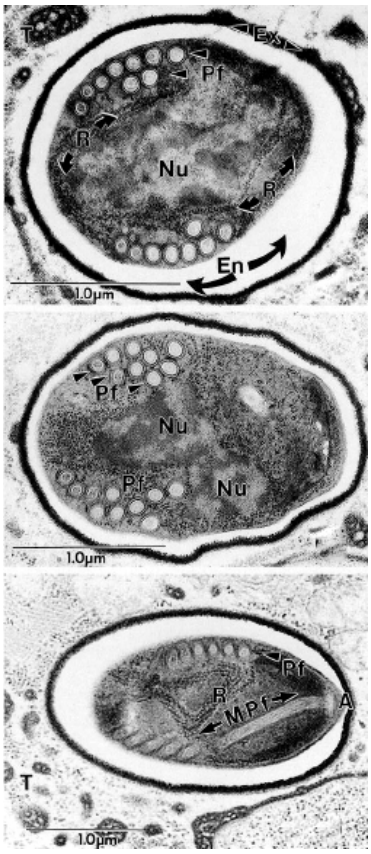



**Figure 14.21**
*Brachiola vesicularum*. A late proliferative/sporont cell completing cytokinesis. The plasmalemmal invagination is almost complete and the diplokaryotic nucleus (Nu) pairs appear to be in interphase. Note the presence of vesicotubular material (T).

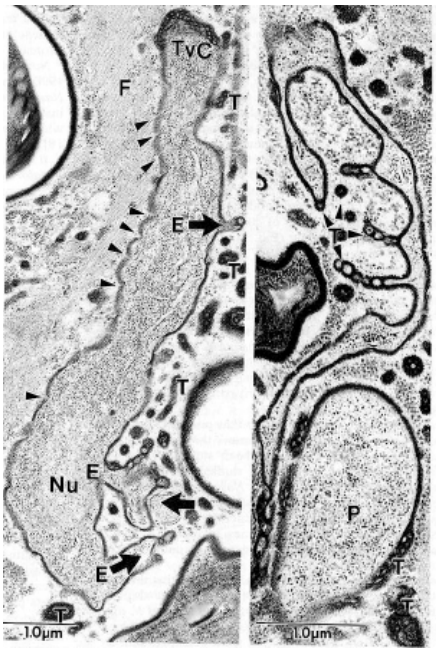



a

b

c

**Figure 14.22 a,b,c**
*Brachiola vesicularum* a. Mature spore containing a fully developed electron-lucent endospore coat (average thickness 90 nm to100 nm). The exospore (62 nm) surface has several vesiculotubular structures (T) on it. Note the presence of nine polar filament (Pf) cross sections arranged in two rows. Ribosomes (R) appear in a spiral-like array forming rows around the nuclear area (Nu). x 41,600; b. Spore containing ten polar filament (Pf) cross sections clustered into three rows. (endospore coat = 82 nm, exospore coat = 63 nm) x 36,800; c. Section through a spore revealing the presence of the anterior anchoring disc complex (A) of the polar filament (Pf) and the manubroid (Mpf) portion of it. The cross sections of the polar filament coils arranged in a single row is visible. Multiple rows of ribosomes (R) are also present. Note the presence of vesiculotubular material (T). x26,000.




a b

**Figure 14.23 a,b**
*Brachiola vesicularum*. Proliferative cells with protoplasmic extensions. a. A very elongated parasite cell (7.1 µm in length and varies between 1.0 µm and 1.2 µm wide) with a vesiculotubular "cap" complex (TvC) at one end and a scalloped thick plasmalemmal surface which contains several channels (arrowheads). Additionally, this cell possesses several protoplasmic extensions (E) of varying lengths, projecting from the cell surface (broad arrows). At the ends of these protoplasmic extensions are vesiculotubular (T) structures with the electron-dense fibrous coating, similar to those previously illustrated on the typical proliferative cells. Note the presence of vesiculotubular (T) structures and myofilaments (F) in the host cytoplasm. x19,300. b. A portion of a parasite cell protoplasmic extension complex measuring 4.80 µm in length and between 0.5 µm to less than 0.3 µm in width. A number of branches of varying lengths, have formed from the cell surface and project into the host cytoplasm. These projections also end in vesiculotubular (T) structures. The surface of the protoplasmic extensions also have some scalloping and shallow indentations present. In the lower third of the figure is a section of a parasite (P) cell with several vesiculotubular (T) structures attached to the cell surface. x 27,000.

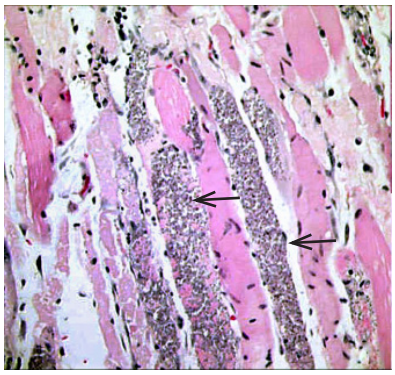
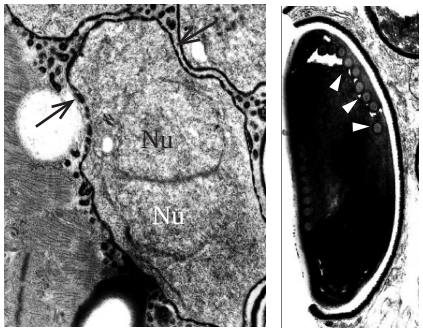


**Figure 14.24**
*Anncaliia algerae* in muscle after the patient presented with myositis and muscle pain showing multiple organisms in the muscle fibers (arrows) with associated cell lysis but little or no inflammation. H&E x100.

spores may be produced from sporonts encased in the parasite-secreted SPOV envelope (Figs 14.28 & 14.29).

In the two species of *Trachipleistophora, T. hominis*[11,98] and *T. anthropophthera*[96], proliferative cells have 2 to 4 nuclei and divide by binary fission. In the sporogony phase, division into sporoblasts is effected by repeated binary fission, producing 2 to 32 spores within the SPOVs, no plasmodial stages are produced (Figs 14.30 to 14.34). Spores of *T. hominis* are approximately 4 by 2 µm (Fig 14.35). *Trachipleistophora anthropophthera* is dimorphic,




a b

**Figure 14.25 a,b**
*Anncaliia algerae* in muscle from patient in Figure 14.24. a. A diplokaryon, a thickened plasmalemma (arrows), and vesiculotubular extensions are evident in proliferative forms. Nu denotes nucleus. x14,000; b. A mature *A. algerae* spore with a single row of nine polar filaments (arrow heads) in cross section. Mature spores in the biopsy specimen had only single rows of 8 to 12 polar filaments in cross section. x18,300

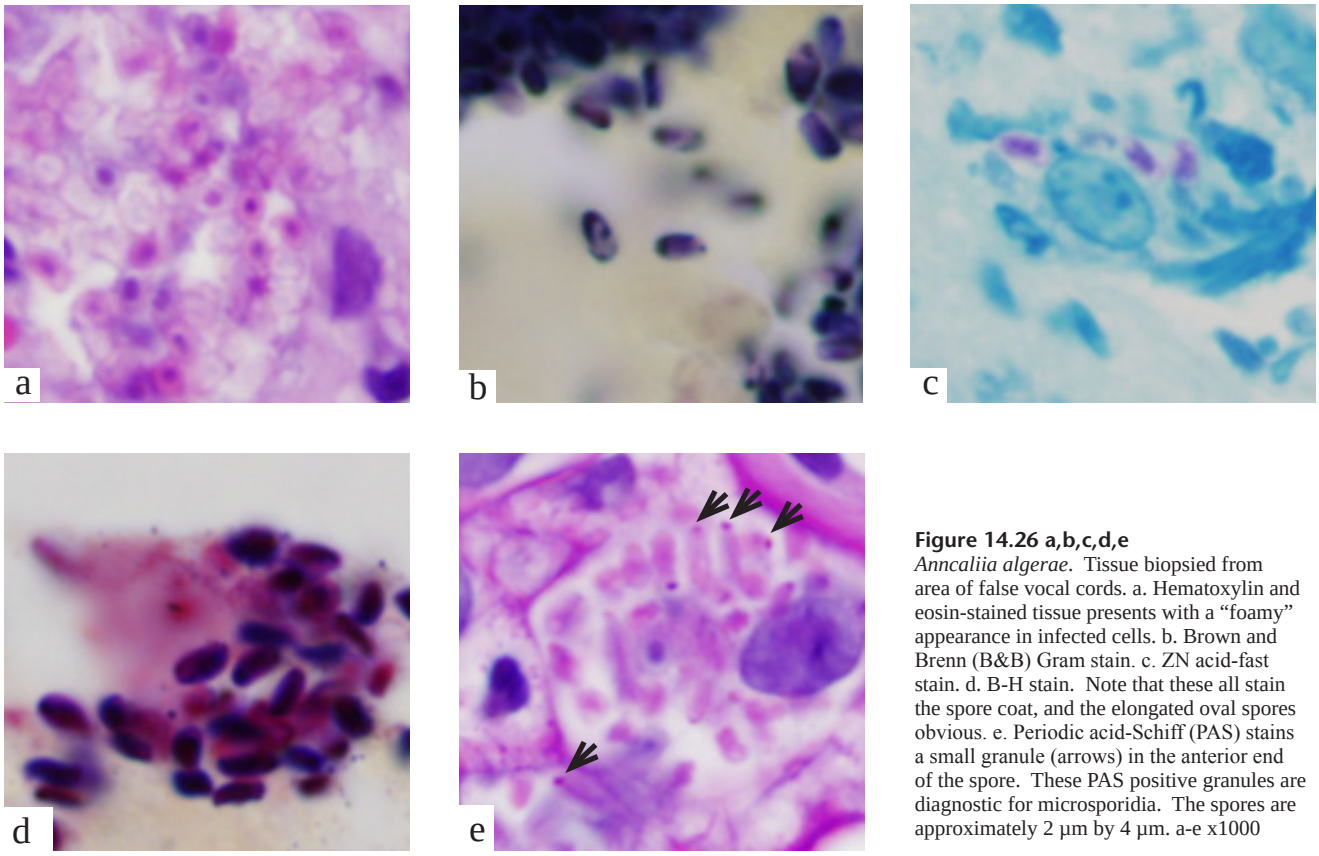



**Figure 14.26 a,b,c,d,e**
*Anncaliia algerae*. Tissue biopsied from area of false vocal cords. a. Hematoxylin and eosin-stained tissue presents with a "foamy" appearance in infected cells. b. Brown and Brenn (B&B) Gram stain. c. ZN acid-fast stain. d. B-H stain. Note that these all stain the spore coat, and the elongated oval spores obvious. e. Periodic acid-Schiff (PAS) stains a small granule (arrows) in the anterior end of the spore. These PAS positive granules are diagnostic for microsporidia. The spores are approximately 2 µm by 4 µm. a-e x1000

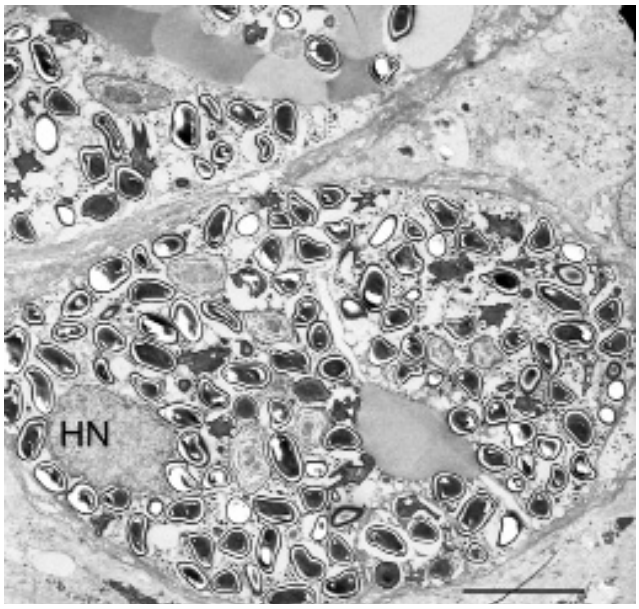



**Figure 14.27**
*Anncaliia algerae*. Tissue biopsied from area of false vocal cords illustrating details of the microsporidial developmental stages. Low magnification of infected host cell. Cell is filled with parasites in various stages of development and in direct contact with host cell cytoplasm. Only remaining discernable organelles are the host nucleus (HN) and the plasmalemma; scale bar = 8 µm.

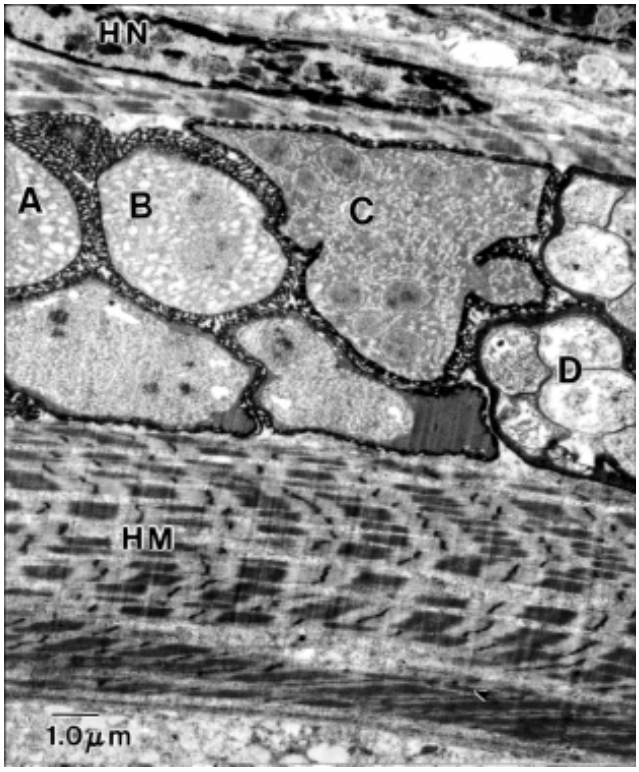
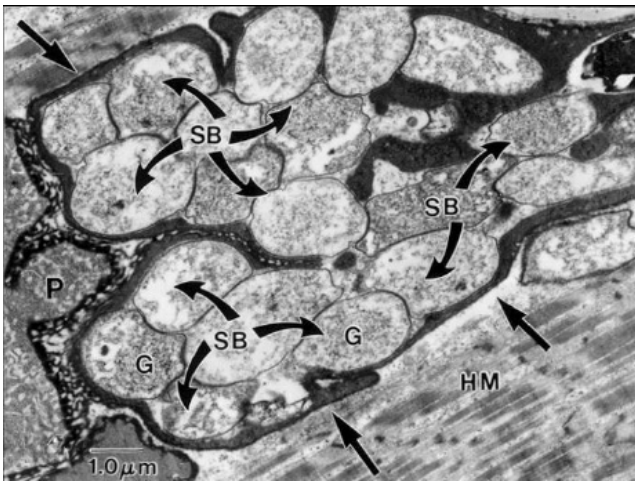
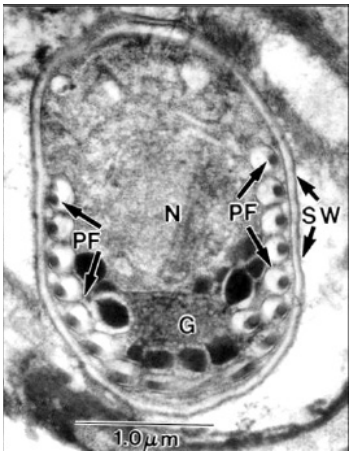



**Figure 14.28**
*Pleistophora ronneafiei*. Developmental stages (A,B,C,D) in human skeletal muscle. Electron micrograph demonstrates the location of the infection, abutting bundles of actin and myosin filaments arranged as normal, functional contractile unit of host muscle (HM) and containing a host cell nucleus (HN). The early stages of parasitic development are each surrounded by parasite-secreted dense material. The vesicle wall is most elaborate in proliferative development as illustrated between proliferative cells A and B. The proliferative cells A and B are probably sister cells, as in early proliferative development, the cells divide with the secretions. In sporogony, multiple parasite cells (cluster D) may be found within each sporophorous vesicle, which becomes more homogeneously dense in sporogony making the elongated oval spores obvious.




a




b

**Figure 14.29 a,b**
*Pleistophora ronneafiei*. Sporoblasts of *Pleistophora* in human skeletal muscle. After sporogonial plasmotomy is completed, the sporophorous vesicles are filled with many uninucleated cells, the sporoblasts. a. Sporophorous vesicle containing early sporoblasts (SB) abutted to a proliferative cell (P) and the lack of projections on the vesicle walls (straight arrows) where it abuts the host cytoplasm (HM). b. Late sporoblast or early spore contains a single nucleus (N), the developing polar filament (PF), the Golgi (G), and the beginning of spore wall (SW) thickening.

in sporogony, 2 types of SPOVs and spores are formed (Figs 14.36). One type of SPOV contains thick-walled spores (approximately 8, measuring 3.7 by 2.0 µm), each containing 9 polar filament coils. The other type contains 2 thin-walled spores with 3 to 5 polar filament coils and measuring 2.2 µm to 5 µm by 1.8 µm to 2.0 µm.[96]

## *Clinical and Pathologic Features*

*Pleistophora* sp primarily infect the muscles of marine and freshwater fish, but three *Pleistophora* infections in human skeletal muscle have been reported.[9,26,94,95] The first, in 1985, was in a 20-year-old immunocompromised man from Florida.[9,99,100] Over a 7-month period, the patient experienced progressive wasting and generalized muscle weakness leading to contractures. Biopsies of skeletal muscle contained large clusters of organisms visible by light microscopy with H&E (Fig 14.37), acid-fast (Fig 14.38) and Giemsa stains (Fig 14.39). Electron microscopy of the same biopsy tissue revealed the diagnostic features of *Pleistophora*.[9] Developmental stages from this case were subsequently described (Fig 14.28 & 14.29) and the parasite named *P. ronneafiei*.[10] The two additional cases of myositis caused by *Pleistophora* in patients with AIDS, in 1993 and in 1996 have not been compared.[94,95]

*Trachipleistophora hominis* was described from an AIDS patient in Australia.[11,27] The infection was primarily (Fig 14.30) muscular[101] but organisms were also found in corne-

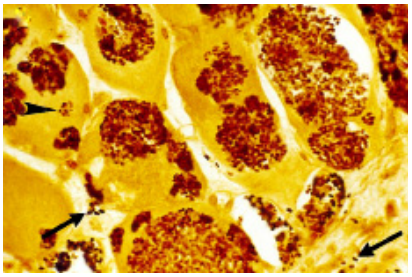


**Figure 14.30**
*Trachipleistophora hominis*. Spores and larger brown spore precursors forming masses within skeletal muscle fibers. Free spores are visible in the adjacent connective tissues (arrow), and discrete early aggregates of spore precursors are visible in fibers (arrowhead). Warthin-Starry x 400.

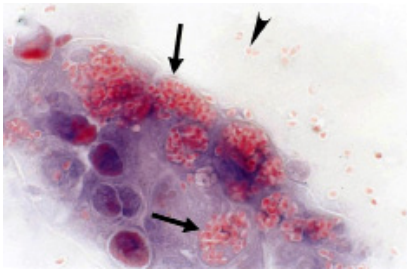


**Figure 14.31**
*Trachipleistophora hominis*. Corneal scraping showing sporophorous vesicles containing spores and spore precursors in epithelial cells (arrows). Note the dispersed spores in the background showing the posterior vacuole (arrowhead). Modified trichrome x1000.

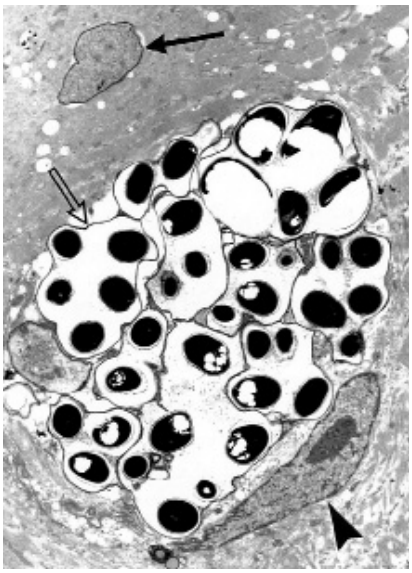


**Figure 14.32**
*Trachipleistophora hominis*. Multiple sporophorous vesicles closely abutting within a skeletal muscle cell (open arrow) with a single meront (arrow). Note the skeletal muscle nucleus (arrowhead). x1,600.

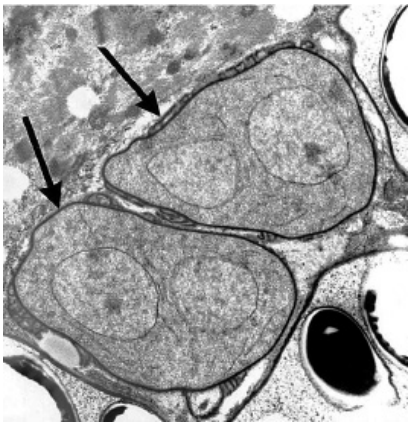


**Figure 14.33**
*Trachipleistophora hominis*. Two adjacent binucleate meronts with thick outer coats (arrow). x3,000.

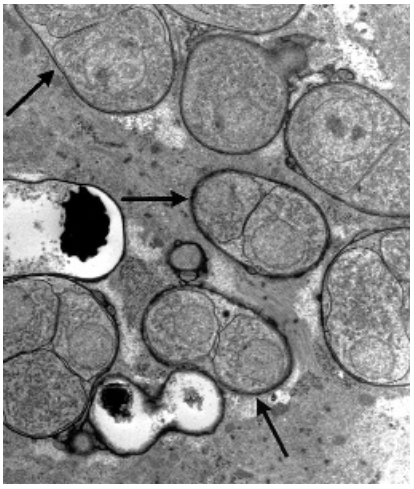


**Figure 14.34**
*Trachipleistophora hominis*. Sporonts undergoing division in a skeletal muscle cell (arrows). x3,000.

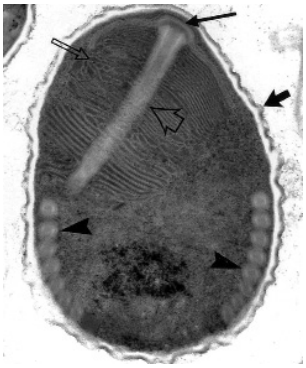


**Figure 14.35**
*Trachipleistophora hominis*. Spore with anchoring disc (arrow), straight portion of polar tube (open short arrow) extending through the polaroplast (open arrow) posterior vacuole, and tangential sections through coils of tube (arrowhead). x12,000.

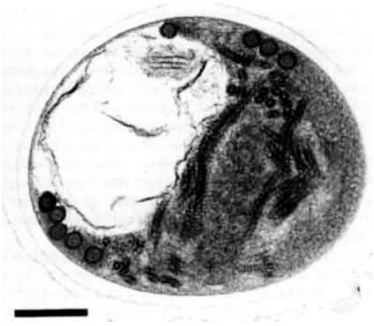


**Figure 14.36**
*Trachipleistophora anthropophthera*. Type I mature spore's polar filament has thicker and inward displaced thinner posterior coils. Bar = 0.5 µm.

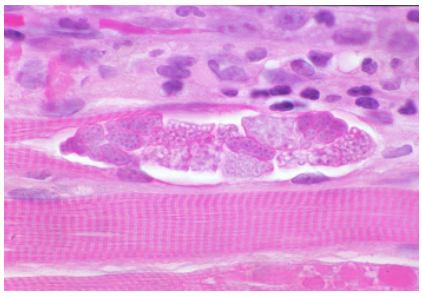


**Figure 14.37**
*Pleistophora ronneafiei* in skeletal muscle showing large clusters of organisms: H&E x560

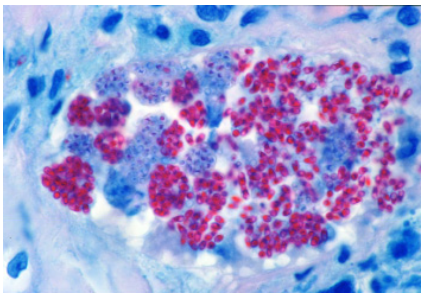


**Figure 14.38**
*Pleistophora ronneafiei* in skeletal muscle showing large clusters of organisms. ZN x490

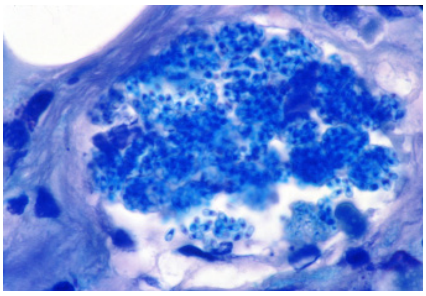


**Figure 14.39**
*Pleistophora ronneafiei* in skeletal muscle showing large clusters of organisms. Giemsa x520

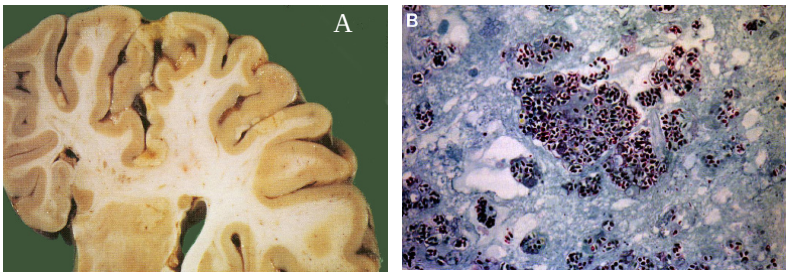



**Figure 14.40**
(A) Gross picture of a brain from a patient with *Trachipleistophora anthropophthera* infection demonstrating multiple necrotic lesions in the gray matter. (B) Light microscopic section from the brain shown in panel A, demonstrating spores in astrocytes and other cells. GMS x400

al epithelium (Fig 14.31) and nasopharyngeal washings. In experimentally inoculated athymic mice, infection spread to tissue of the bladder and large intestine.[11]

*Trachipleistophora anthropophthera* was identified in 2 AIDS patients in the United States. Both had disseminated infections involving the heart, kidneys, and brain (Figs 14.40a & 14.40b), manifesting in seizures and impaired cognition, suggestive of toxoplasmosis.[24,28,96,97]

## Family: Enterocytozoonidae

*Enterocytozoon* was the first genus of microsporidia created for a human infection.[12,30] It has subsequently been found in pigs and cattle.[102] This microsporidium has many unique developmental features[13] and researchers have had only limited success at growing them in culture.

## Morphologic Description

*Enterocytozoon* organisms develop in direct contact with the host-cell cytoplasm. As nuclei multiply, plasmodia enlarge. *Enterocytozoon* forms two unique organelles: electron-lucent inclusions and electron-dense disks. They both form in a multinucleate plasmodial cell in direct contact with the host cell cytoplasm (Fig 14.41).[13] Electron-lucent inclusions appear very early in the development of the proliferative plasmodia, increase in size and number as the plasmodia grow, and are present throughout the life cycle. Electron-dense disks form at the surface of the electron-lucent inclusions, often in small stacks similar to a stack of red blood cells. Plasmodial cells containing these disks have many rounded nuclei. The disks eventually fuse and form the spores' polar filament. Finding several polar filaments within a multinucleate plasmodium is diagnostic for *Enterocytozoon* (Fig 14.42).[13] The presence of these organelles and the development of multiple polar tubules within a multinucleate parasite cell are all unique features of the developmental cycle of *Enterocytozoon*. The plasmodium divides by multiple fission; producing a dozen or more sporoblasts which mature into spores, all in direct contact with the host-cell cytoplasm. Spores are 1.3 µm by 0.8 µm and contain a single nucleated sporoplasm surrounded by approximately 6 polar tubule coils, arranged in a double row (Fig 14.43).[13,24]

## Clinical and Pathologic Features

*Enterocytozoon bieneusi* is one of the most frequently reported microsporidial infection in humans. Incidence in AIDS patients is approximately 7% in Africa,[56] 20% to 30% in the United States and Australia,[43,57,59] and 50% in France.[42] The organism infects the apical portion of enterocytes of the small bowel (Figs 14.44 & 14.45). Endoscopically, infection appears as a slight flattening of the epithelium.[103] Histologically, the only visible pathologic feature is villus atrophy due to more rapid desquamation of infected enterocytes.[12,13,24,30,43,59] The parasite can disseminate to the epithelial lining of the common bile duct, gallbladder epithelium, and biliary and respiratory tracts.[19,31,59,104] *Enterocytozoon bieneusi* most commonly infects male AIDS patients caus-

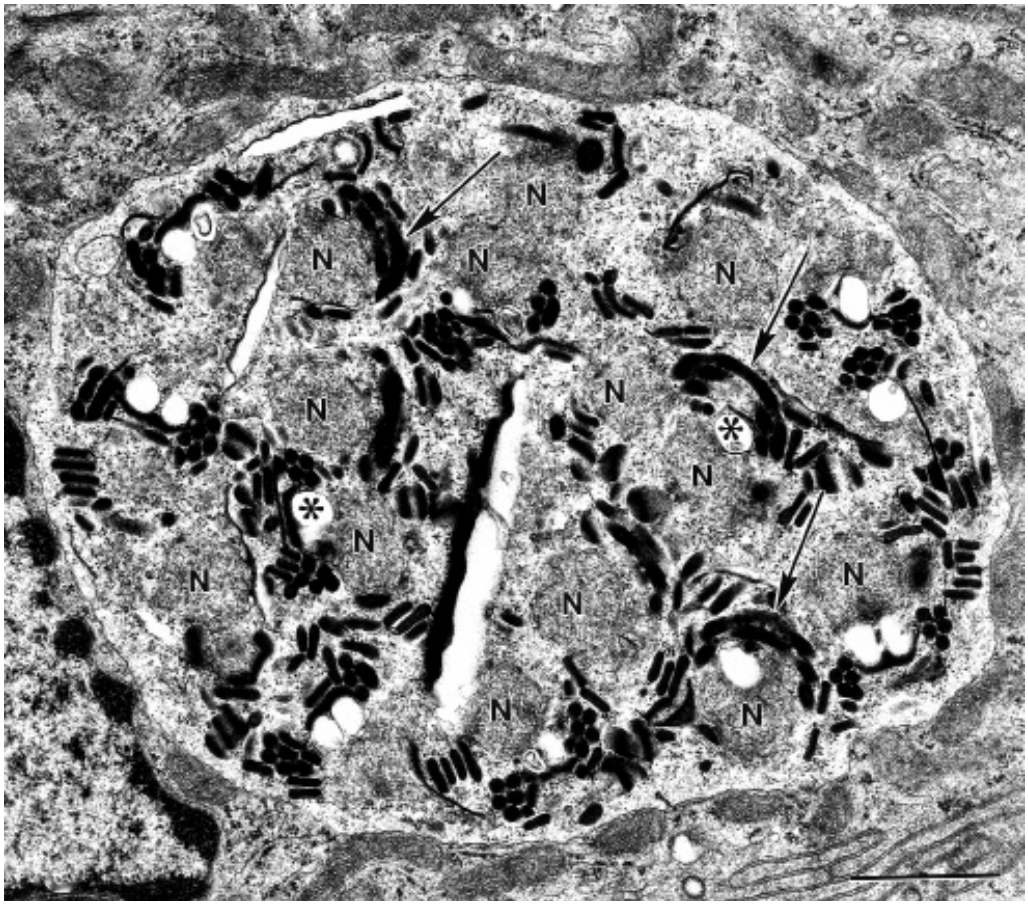



**Figure 14.41**
*Enterocytozoon bieneusi*. Sporogonial plasmodium containing at least 12 nuclei (N) in a single plane of section. The round dense nuclei are each associated with electron dense disc complexes (arrows) and electron lucent inclusions (*). Electron dense discs fuse into arcs forming polar tube coils. Despite the advanced maturation and organelle separation associated with each nucleus, there is not yet any evidence of cytokinesis or plasmalemmal thickening. x25,600. Bar = 1 µm.

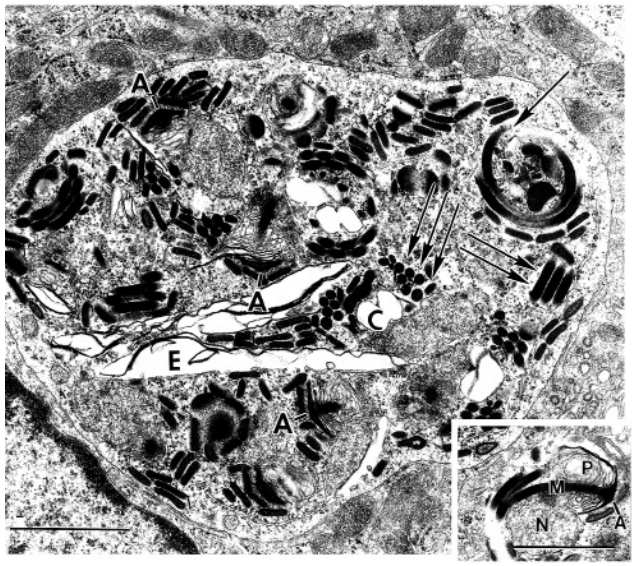



**Figure 14.42**
*Enterocytozoon bieneusi*. Late sporogonial plasmodium with advanced stages of polar tubule formation. Fused electron dense discs are seen in coiled (single arrow), stacked (double arrows) and cross sectional (triple arrows) profiles throughout the cytoplasm. Anterior anchoring discs (A) and associated polaroplast membranes appear at this stage even though individual sporoblast membranes have not yet developed. The electron lucent inclusions are seen in elongated (E) and cross section (C) views. x33,231. Bar = 1 µm. Insert: Connection and arrangement of various structures developing in the plasmodium. Umbrella-shaped anchoring disc (A) and associated polaroplast membranes (P) attached to the manubroid portion of the polar tube (M) which connects with arcs formed by the coiled region of the developing polar tube. This complex of polar tube and associated structures surrounds a single nucleus (N). x28,000. Bar = 1 µm.

ing malabsorption resulting in chronic diarrhea,[12,13,19,30,105,106] and has subsequently been associated with AIDS-related sclerosing cholangitis.[31,104] As awareness of microsporidial infection has grown, *E. bieneusi* has also been reported in HIV-negative[33] and female HIV-positive[107] patients with and without diarrhea,[108] and in tracheal,[32] bronchial,[109] and nasal[110,111] epithelium. *Enterocytozoon bieneusi* can also be diagnosed from stool samples. The spores can be visualized by modified trichrome[112] (Figs 14.46).

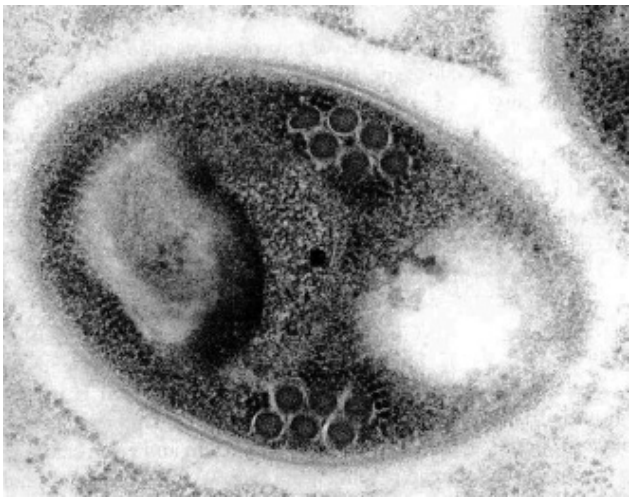


**Figure 14.43**
Spore of *Enterocytozoon bieneusi* demonstrating the characteristic six turns of the polar tubule, which are organized into two tiers of three turns each and which are out of register by 45°. x83,000

## *Family: Encephalitozoonidae*

*Encephalitozoon cuniculi* was first discovered in 1924 in rabbits.[113] It was placed in the microsporidia in 1964 as a junior synonym in the genus *Nosema*.[51] In 1971, it was reclassified as a genus of *Microsporidia*[52] and described from rabbits, mice and hamsters.[114] The family was established in 1989.[115] This parasite has subsequently been reported from over 30 different mammalian hosts[61] and the first human infection with *E. cuniculi* was reported in 1987.[14]

From 1989 to 1991, six cases of microsporidian keratoconjunctivitis were reported in patients with AIDS, four from New York, one from Texas, and one from Ohio.[3, 16,35,36,116,117] All had conjunctivitis, blurred vision, and photophobia. By 1999 over 20 cases were characterized, reported and reviewed.[22] Organisms were observed in corneal epithelial cell scrapings examined by light and electron microscopy.[16,118,119] The organisms were morphologically similar to *E. cuniculi*, but a clearly defined parasitophorous vacuole surrounding the organisms was not always visible.[16] Didier et al. reported that the organism was morphologically the same, but serologically different from *E. cuniculi* and named it *Encephalitozoon hellem*.[15]

First reported in 1991, *Septata* was the second microsporidial genus created for a human infection.[17,29] It was placed in this family as a new genus, based on similarity of some of its morphological features with the type species while presenting some unique features including intestinal infection. Infection with *S. intestinalis* has been reported in the United States,[17,29,59,120] Europe,[23,59,60] and Australia.[57,59,121,122] Subsequent molecular data suggested a closer relationship between the two genera and the species: *S. intestinalis* was moved into the genus *Encephalitozoon*.[53]

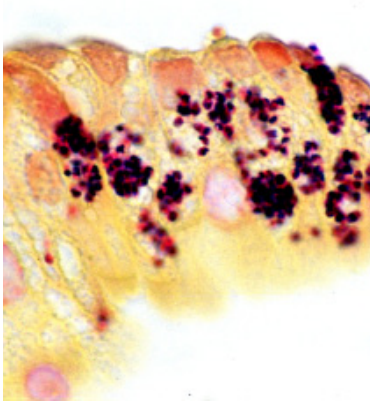


**Figure 14.44**
*Enterocytozoon bieneusi* infects the apical portion of enterocytes of the duodenum: Gram-positive spores (1.5 µm x1.0 µm) B&H x1010

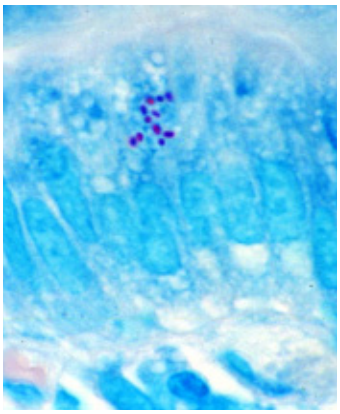


**Figure 14.45**
*Enterocytozoon bieneusi* infects the apical portion of enterocytes of the duodenum containing acid-fast spores ZN x800

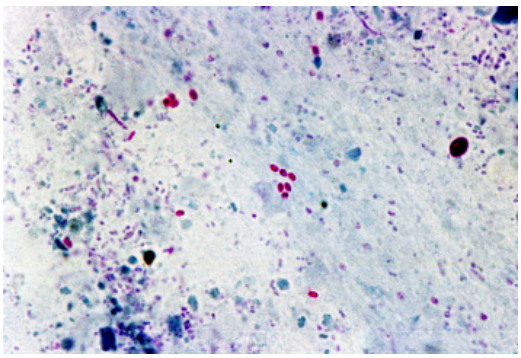


**Figure 14.46**
*Enterocytozoon bieneusi* in feces. Modified trichrome x700

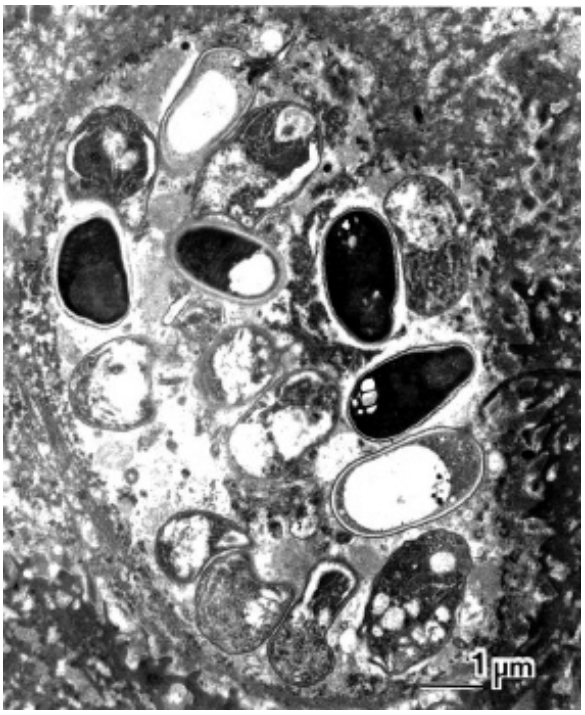



**Figure 14.47**
*Encephalitozoon hellem*. Epithelial cells with large vacuolated area containing oval-shaped organisms and amorphous material. The oval bodies vary in appearance, reflecting different stages of development. X9,100

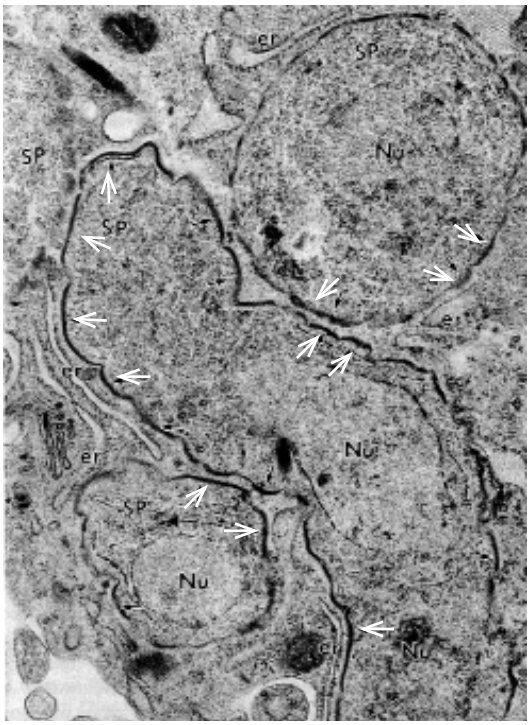



**Figure 14.48**
*Encephalitozoon hellem*. Developing stages of *E. hellem* growing in direct contact with host cell cytoplasm of RK-13 cell line. Four early sporonts (SP) with "thickening membranes" (arrows) are present and the elongated sporont contains at least two nuclei (Nu). Note host rough endoplasmic reticulum (er) in close proximity to sporonts. x23,000

## Morphologic Description

The genus *Encephalitozoon* is characterized by a phagosome-like parasitophorous vacuole that surrounds developing parasites and isolates them from the host-cell cytoplasm. Developing stages (Fig 14.47) may contain one or more nuclei but the nuclei are not attached to each other in diplokaryotic arrangement. Multinucleate cells are long and narrow, not plasmodial (Fig 14.48).[114] Proliferative cells usually abut the vacuole membrane and break free of it in sporogony. Sporonts form a thickened plasmalemma on individual cells. Within the parasitophorous vacuole, each sporont elongates, divides, and produces spores. Spores are 1 µm to 1.5 µm by 0.5 µm and contain a sporoplasm with a single nucleus and approximately 6 polar tubule coils (Fig 14.49), arranged in a single row.[114,123] *Encephalitozoon hellem* is morphologically the same as *E. cuniculi* except that the parasitophorous vacuole is not always present.[124]

*Encephalitozoon* (*Septata*) *intestinalis* is characterized by parasite-secreted material surrounding the developing stages and spores (Fig 14.50) inside the parasitophorous vacuole. Proliferative and sporogonic stages have 1 to 4 nuclei. Cells are rounded when single-nucleate and elongated when they contain 2 to 4 nuclei. In sporogony, the plasmalemma thickens and elongated sporonts are produced. Each sporont divides, producing up to 4 single-nucleate sporoblasts. After a final cell division, sporoblasts develop the polar filament complex and metamorphose into spores. *Encephalitozoon intestinalis* cells develop in clusters. During early development, these clusters appear tightly packed. During sporogony and spore formation, some cells condense, leaving a space between individual developing forms. When this happens, the parasite-secreted fibrillar matrix surrounding the different stages is apparent. Early and late forms develop asynchronously, with parasite secretions surrounding individual cells and a parasitophorous vacuole surrounding the cluster (Fig 14.50). Spores are 2 µm by 1.2 µm, with a single nucleus and 4 to 7 (usually 5) polar tubule coils arranged in a single row.[17,29]

## Clinical and Pathologic Features

*Encephalitozoon cuniculi* is probably the most studied microsporidian. Primarily a parasite of animals, it has been reported in over 30 mammalian hosts.[55,61,114] In 1984, Bergquist et al reported serologic evidence of *E. cuniculi* in AIDS patients with a history of travel to the tropics.[125,126] In 1987, Terada et al. found *E. cuniculi* organisms in the liver of an AIDS patient with hepatitis.[14,127]

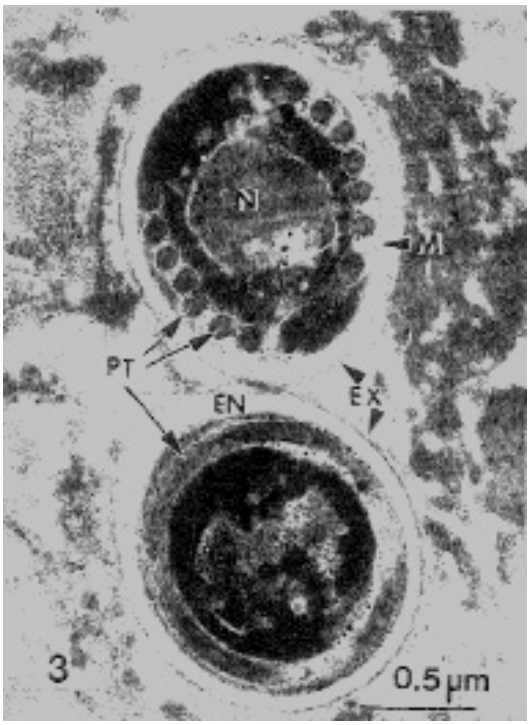



**Figure 14.49**
*Encephalitozoon hellem.* Two spores are cut in longitudinal (upper) and cross section. Both have a thick spore coat including thin dense exospores (EX), thick electron-lucent endospore (EN), and the thin inner spore coat membrane (M). In the organism above, a single, large, rounded nucleus (N) is centrally located. Peripheral to and on each side of the nucleus are seven to eight round dense bodies that are cross sections of the polar tubule (PT) coils, In the organism below, the polar tubule is coiled parallel to the plane of the section and appears as a single dense ring situated adjacent to the inner aspect of the spore coat. x32,500.

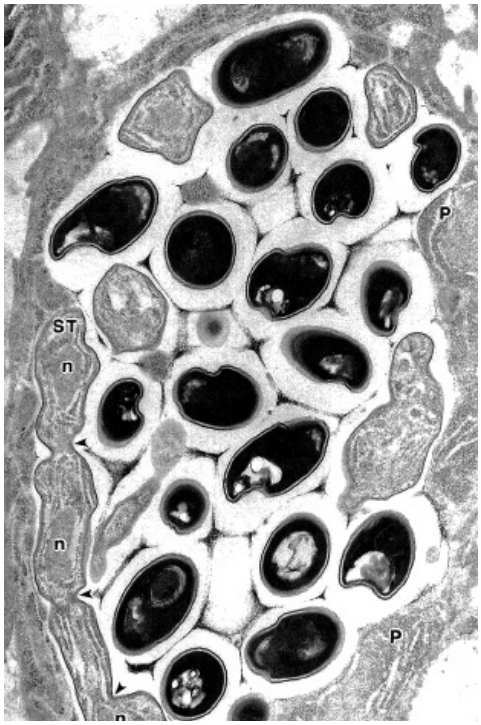



**Figure 14.50**
*Encephalitozoon* (*Septata*) *intestinalis*. Deposition of material results in a uniformly thick plasmalemma surrounding the sporont cells. These sporonts continue to secrete the fibrillar lamina. The sporont (ST) is a tetranucleate (n) elongated cell in the process of cytokinesis (arrowhead). This cluster of parasite cells also contains many mature electron-dense spores, proliferative cells (P), and a dense fibrillar lamina separating the individual parasite cells. x9,000

Since then, *E. cuniculi* has been demonstrated in peritoneal, cerebral, and disseminated infections in AIDS patients (Figs 14.51 & 14.52).[39,128-130]

In cell culture, *E. hellem* may develop with or without a surrounding vacuole (Fig 14.48). *Encephalitozoon hellem*, originally reported from eye infections, has since been associated with disseminated infection and infection of the sinuses,[40] nasal tissue,[131] tongue, respiratory system (Figs 14.53 & 14.54),[132,133] kidneys (Fig 14.55) and male genital tract (Figs 14.56 & 14.57).[109,134,135] Schwartz et al[132] used immunofluorescence and H&E to demonstrate the organisms in tissues (Figs 14.58).

*Encephalitozoon intestinalis* is an intestinal epithelial cell parasite, causing diarrhea, malabsorption, and wasting. Because it can also infect macrophage,[120] fibroblastic, and endothelial cells, it can infect the lamina propria below the enterocytes and disseminate to other parts of the body (Figs 14.59 to 14.61).[103] Infections have been reported in the liver, renal system, colon,[121] gallbladder, lungs, sinuses,[121,136] and conjunctiva.[17,20, 32,37,57,137] It has been misdiagnosed as *Enterocytozoon bieneusi* in the intestine and as *Encephalitozoon hellem* in the eye, sinuses, and urine.[59,138]

Although size, nucleation, and number of polar tubule coils are similar in *Encephalitozoon intestinalis* and *Enterocytozoon bieneusi*, the organisms can be distinguished by the arrangement of polar filaments in the spore stage. In *Enterocytozoon bieneusi*, the polar filament forms a double row of coils; in *Encephalitozoon intestinalis*, they form a single row. Another diagnostic feature is observable in tissue sections. Spores and developing stages of *Encephalitozoon intestinalis* are within individual chambers inside a vacuole in the host-cell cytoplasm. *Enterocytozoon bieneusi* development is in direct contact with the host-cell cytoplasm (Fig 14.53).[17,20,120]

## *Diagnosis*

Identifying the spore stage containing the polar filament is diagnostic for microsporidia. Spores can be seen by light microscopy using stains[139] such as Giemsa,[100,140-142] Ziehl-

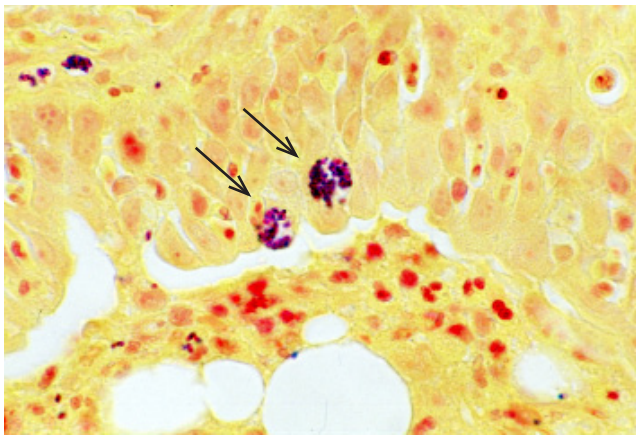


**Figure 14.51**
*Encephalitozoon cuniculi* (arrows) spores in bronchiole epithelium. B&B x650.

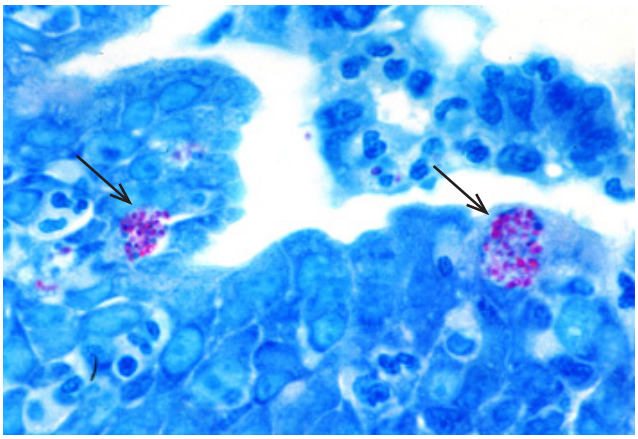


**Figure 14.52**
*Encephalitozoon cuniculi* acid -fast spores (arrows) in bronchiole epithelium. (Not all spores are acid-fast) ZN x875

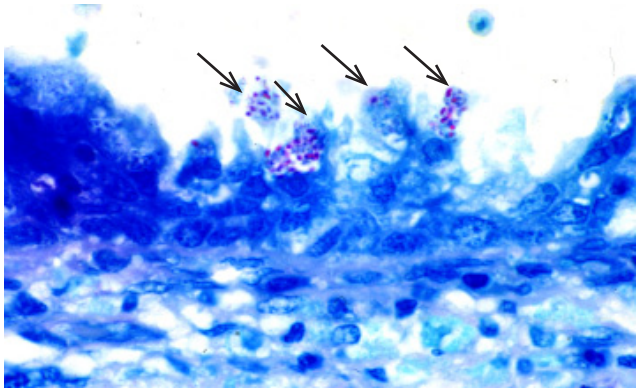


**Figure 14.53**
*Encephalitozoon hellem* spores (arrows) in the trachea: Some acid-fast spores ZN x620

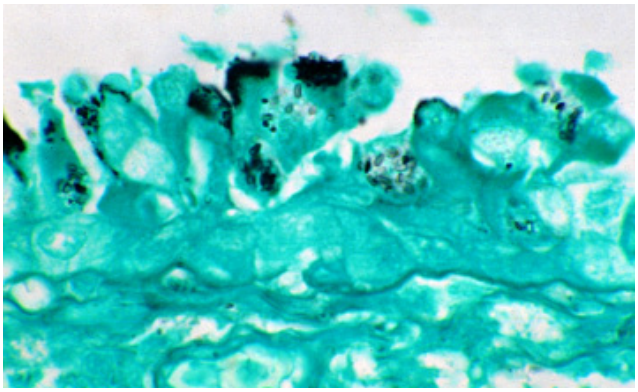


**Figure 14.54**
*Encephalitozoon hellem* spores in the trachea: Silvered spores in mucosa, GMS x800

Neelsen,[89] Brown & Brenn,[103] Brown & Hopps, Weber's trichrome,[112] Warthin-Starry,[57,122,143] and fluorescence.[60, 119,132,144] Hematoxylin-eosin is not particularly useful for identifying microsporidia. Spores are birefringent and can be seen with polarized light (Fig 14.8). A PAS-positive granule in the anterior end of the spore is diagnostic for larger microsporidia such as *Nosema*, *Anncaliia* and *Pleistophora* (Fig 14.3), but trying to identify the granule in the smaller, more common human-infecting microsporidia, *Encephalitozoon* and *Enterocytozoon*, is impractical.

Touch preps and smears can be made from biopsy materials, eye scrapings, tissue specimens (Fig 14.31) and aspirates stained with Giemsa or Gram's stain. Spores can be identified in urine, fecal samples (Fig 14.46), or duodenal fluid by light, fluorescence,[132,144] or electron microscopy.[3,61,132] Where available, immunologic technology (such as ELISA,[145] Western blot,[15,146] monoclonal and polyclonal an-

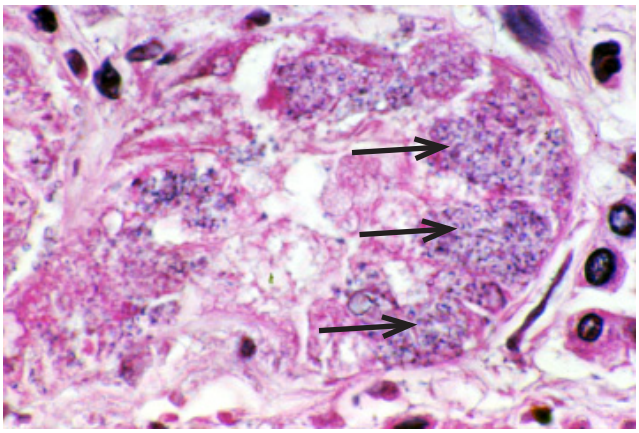


**Figure 14.55**
Cluster of *Encephalitozoon hellem* spores (arrows) in kidney. H&E x850

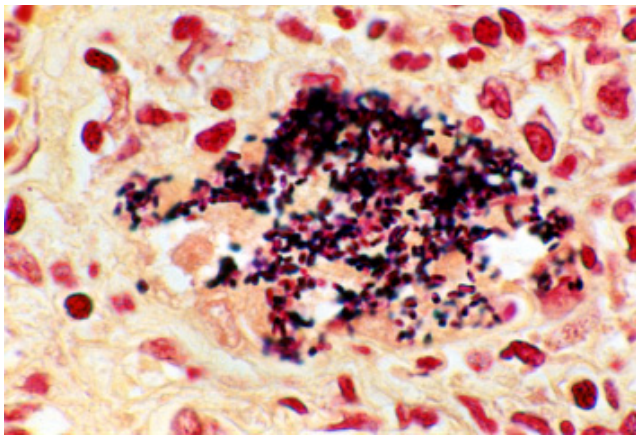


**Figure 14.56**
Cluster of *Encephalitozoon hellem* spores in kidney. Black bodies are Gram-positive spores. B&H x875

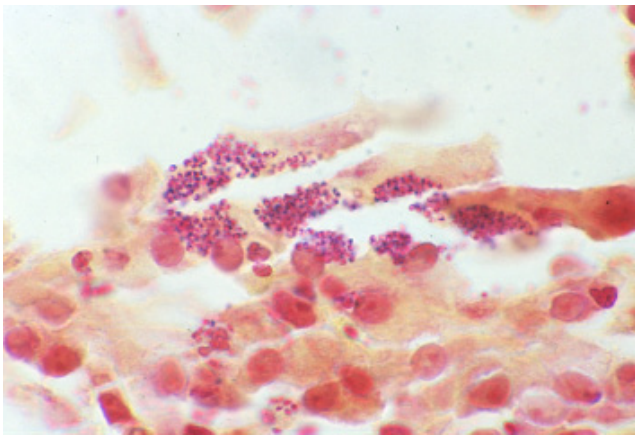


**Figure 14.57**
*Encephalitozoon hellem* spores in bladder exudates. B&H x650

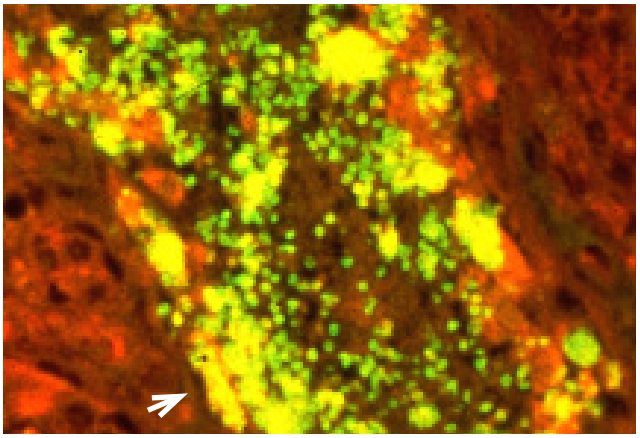


**Figure 14.58**
Tubular epithelium of the kidney infected with *Encephalitozoon hellem.* Immunofluorescence staining reveals brightly staining clusters of intra-epithelial spores (arrow). x750

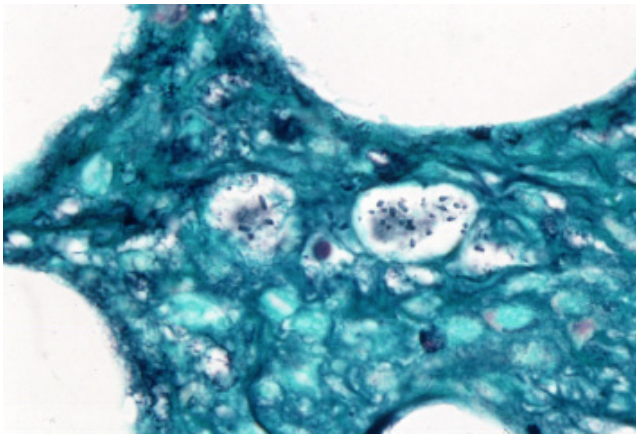


**Figure 14.59**
*Encephalitozoon* (*Septata*) *intestinalis* cells in tightly packed clusters in skin: Silvered 3 µm x1 µm spores. GMS x790

tibody,[147,148] fluorescent antibody,[132,135,144,149]) and PCR[150,151] techniques are significant diagnostic aids.[28,63,152-156]

Electron microscopy is the preferred method for identifying microsporidia.[19,55,61] It can be used to identify the presence of a polar filament in the spore. Additionally the polar filament arrangement and number of coil cross sections may aid in identification of organisms. Example: a double row of polar filament coils distinguishes spores of *Enterocytozoon bieneusi* from those of *Encephalitozoon intestinalis* in fecal or other samples. In tissue biopsies, microsporidial families can be identified by the host/parasite interface (Table 14.1). For example: there is no separation from host cytoplasm (Nosematidae, Enterocytozoonidae) by vacuole (Encephalitozoonidae) or SPOV (Pleistophoridae).

For histologic examination of tissue sections, glutaraldehyde fixation and plastic embedding are highly recommended, even if electron microscopy is unavailable. Parasites are often masked by the host tissue in 6 µm paraffin-embedded preparations. One-micrometer-thick plastic sections, heat-fixed to a glass slide and stained with toluidine blue, provide better visualization of microsporidia, even by light microscopy, because of the thinness of the section (Fig 14.36). Plastic embedding provides a permanent tissue specimen that can be re-evaluated by electron microscopy if the need or opportunity arises. Additionally, paraffin-embedded tissue can be deparaffinized and reprocessed for plastic embedding.[10]

The most common microsporidia that infect humans are able to disseminate. Therefore, if they are found in a single location, other locations to which they are known to disseminate should be examined/tested.



**Figure 14.60**
Nodular Cutaneous Microsporidiosis of the leg caused by *Encephalitozoon intestinalis* in an HIV positive patient

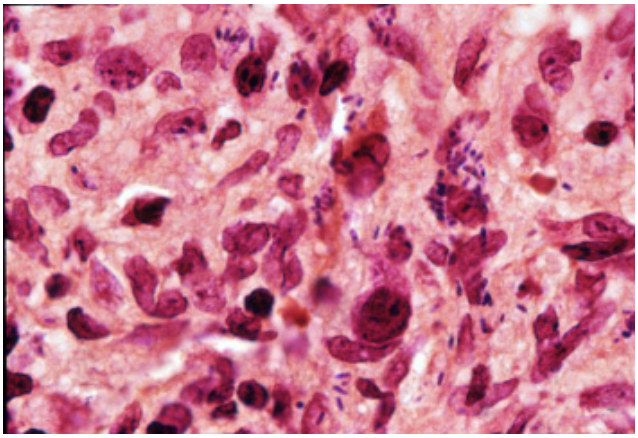


**Figure 14.61**
*Encephalitozoon intestinalis* cells in skin from patient in Figure 14.60 demonstrating gram-positive spores with bipolar staining and central band. B&H x900

## Treatment

Several drugs have been used to treat microsporidiosis in humans, with varying results. Fumagillin, a compound that inhibits microsporidiosis in honeybees, inhibits replication of *Encephalitozoon cuniculi* in human tissue culture.[157] Although not recommended or approved for internal use in humans, it has been used topically to treat *Encephalitozoon hellem* infections of the eye with some success.[158] Topical fluoroquinolone monotherapy resulted in resolution of 99% of 124 cases of keratitis.[58]

Albendazole is the most effective treatment for microsporidiosis in humans. The usual regimen is 400 mg administered orally twice a day for 4 to 6 weeks. Albendazole was first used against *Enterocytozoon bieneusi* infection in HIV-positive patients with AIDS, chronic diarrhea, and wasting. After 4 weeks of treatment with albendazole, all patients regained continence and either gained weight or stopped losing weight. Within a month after stopping treatment, most patients had a recurrence of symptoms but responded well to further albendazole treatment.[159]

Albendazole is more effective against *Encephalitozoon intestinalis* than against *Enterocytozoon bieneusi*.[137,160] Parasites are cleared from the urine and intestinal tract within 6 weeks, with no recurrence after treatment. Biopsy reveals normal enterocyte morphology with only disintegrating spore remnants in macrophages.[160] Albendazole is also effective against other *Encephalitozoon* sp[128,161-164] and *Brachiola* sp,[6] clearing infections with no recurrence. It has proven effective against *Vittaforma corneae* in culture.[165-167] The effects of albendazole, fumagillin, and TNP-470 on microsporidian replication in culture has also been studied.[168]

## References


1. Sprague V, Becnel JJ, Hazard EI. Taxonomy of phylum Microspora. *Crit Rev Microbiol.* 1992;18:285-395.
2. Weiss LM. The First United Workshop on Microsporidia from Invertebrate and Vertebrate Hosts. *Folia Parasitol (Praha)*. 2005;52:1-7.
3. Bryan R, Cali A, Owen R, Spencer H. Microsporidia: newly recognized opportunistic pathogens in patients with AIDS. In: Sun T, ed. *Progress in Clinical Parasitology*. Vol 2. Blue Bell, PA: Field and Wood, Inc Pub; 1990:1-26.
4. Pinnolis M, Egbert PR, Font RL, Winter FC. Nosematosis of the cornea. Case report, including electron microscopic studies. *Arch Ophthalmol.* 1981;99:1044-1047.
5. Cali A. Comparison of the biology and pathology of microsporidia from different host groups. In: Samson RA, Vlak JM, Peters D, eds. *Fundamental and Applied Aspects of Invertebrate Pathology*. 1986;356-359. Netherlands, Fourth International Colloquium of Invertebrate Pathology; 1986:356-359.
6. Cali A, Takvorian PM, Lewin S, et al. *Brachiola vesicularum*, n. g., n. sp., a new microsporidium associated with AIDS and myositis. *J Eukaryot Microbiol.* 1998;45:240-251.
7. Margileth AM, Strano AJ, Chandra R, Neafie R, Blum M, McCully RM. Disseminated nosematosis in an immunologically compromised infant. *Arch Pathol.* 1973;95:145-150.
8. Silveira H, Canning EU. *Vittaforma corneae* n. comb. for the human microsporidium *Nosema corneum* Shadduck, Meccoli, Davis and Font, 1990, based on its ultrastructure in the liver of experimentally infected athymic mice. *J Eukaryot Microbiol*. 1995;42:158-165.
9. Ledford DK, Overman MD, Gonzalvo A, Cali A, Mester SW, Lockey RF. Microsporidiosis myositis in a patient with the acquired immunodeficiency syndrome. *Ann Intern Med*. 1985;102:628-630.
10. Cali A, Takvorian PM. Ultrastructure and development of *Pleistophora ronneafiei* n. sp., a Microsporidium (Protista) in the skeletal muscle of an immune-compromised individual. *Journal of Eukaryotic Microbiology.* 2003;50:77-85.
11. Hollister WS, Canning EU, Weidner E, Field AS, Kench J, Marriott DJ. Development and ultrastructure of *Trachipleistophora hominis* n.g., n.sp. after in vitro isolation from an AIDS patient and inoculation into athymic mice. *Parasitology*. 1996;112:143-154.
12. Desportes I, Le Charpentier Y, Galian A, et al. Occurrence of a new microsporidian: *Enterocytozoon bieneusi* n. g., n. sp., in the enterocytes of a human patient with AIDS. *J Protozool*. 1985;32:250-254.
13. Cali A, Owen RL. Intracellular development of Enterocytozoon, a unique microsporidian found in the intestine of AIDS patients. J Protozool. 1990;37:145-155.

14. Terada S, Reddy KR, Jeffers LJ, Cali A, Schiff ER. Microsporidan hepatitis in the acquired immunodeficiency syndrome. *Ann Intern Med.* 1987:107:61-62.
15. Didier ES, Didier PJ, Friedberg DN, et al. Isolation and characterization of a new human microsporidian, *Encephalitozoon hellem* (n. sp.), from three AIDS patients with keratoconjunctivitis. *J Infect Dis.* 1991;163:617-621.
16. Cali A, Meisler DM, Rutherford I, et al. Corneal microsporidiosis in a patient with AIDS. *Am J Trop Med Hyg.* 1991;44:463-468.
17. Cali A, Kotler DP, Orenstein JM. *Septata intestinalis*, n. g., n. Sp., an intestinal microsporidian associated with chronic diarrhea and dissemination in AIDS patients. *J Eukaryot Microbiol.* 1993;40:101-112.
18. Franzen C, Nassonova ES, Schölmerich J, Issi IV. Transfer of the members of the Genus Brachiola (Microsporidia) to the Genus Anncaliia based on ultrastructural and molecular Data. *J Eukaryot Microbiol.* 2006;53:26-35.
19. Weber R, Bryan RT, Schwartz DA, Owen RL. Human microsporidial infections. *Clin Microbiol Rev.* 1994;7:426-461.
20. Cali A. Cytological and taxonomical comparison of two intestinal disseminating microsporidioses. *AIDS.* 1993;7(suppl 3):S12-S16.
21. Sak B, Kasicková D, Kvác M, Kvetonová D, Ditrich O. Microsporidia in exotic birds: intermittent spore excretion of *Encephalitozoon* spp. in naturally infected budgerigars (*Melipsittacus undulatus*). *Vet Parasitol.* 2010;168:196-200.
22. Friedberg DN, Ritterband DC. Ocular microsporidiosis. In: Wittner M, Weiss LM, eds. *The Microsporidia and Microsporidiosis*. Washington, DC: ASM Press; 1999:293-314.
23. Gunnarsson G, Hurlbut D, DeGirolami PC, Federman M, Wanke C. Multiorgan microsporidiosis: report of five cases and review. *Clin Infect Dis.* 1995;21:37-44.
24. Kotler DP, Orenstein JM. Clinical syndromes associated with microsporidiosis. In: Wittner M, Weiss LM, eds. *The Microsporidia and Microsporidiosis*. Washington, DC: ASM Press; 1999:258-292.
25. Orenstein JM, Gaetz HP, Yachnis AT, Frankel SS, Mertens RB, Didier ES. Disseminated microsporidiosis in AIDS: are any organs spared? *AIDS.* 1997;11:385-386.
26. Cali A, Takvorian PM, Keohane E, Weiss LM. Opportunistic microsporidian infections associated with myositis. *J Eukaryot Microbiol.* 1997;44:86S.
27. Field AS, Marriott DJ, Milliken ST, et al. Myositis associated with a newly described microsporidian, *Trachipleistophora hominis*, in a patient with AIDS. *J Clin Microbiol.* 1996;34:2803-2811.
28. Wittner M, Weiss LM, eds. *The Microsporidia and Microsporidiosis.* Washington, DC: ASM Press; 1999.
29. Cali A, Orenstein JM, Kotler DP, Owen RL. A comparison of two microsporidian parasites in enterocytes of AIDS patients with chronic diarrhea. *J Protozool.* 1991;38:96S-98S.
30. Modigliani R, Bories C, Le Charpentier Y, et al. Diarrhea and malabsorption in acquired immune deficiency syndrome: a study of four cases with special emphasis on opportunistic protozoan infestations. *Gut.* 1985;26:179-187.
31. Pol S, Romana CA, Richard SR, et al. *Enterocytozoon bieneusi* infection in acquired immunodeficiency syndrome-related sclerosing cholangitis. *Gastroenterology.* 1992;102:1778-1781.
32. Orenstein JM. Pathology of intestinal microsporidiosis in HIV-infection [abstract]. AIDS: Workshop on Intestinal Microsporidioses in HIV Infection. 1993;7(suppl 3).
33. Sandfort J, Hannemann A, Gelderblom H, Stark K, Owen RL, Ruf B. *Enterocytozoon bieneusi* infection in an immunocompetent patient who had acute diarrhea and who was not infected with the human immunodeficiency virus. *Clin Infect Dis.* 1994;19:514-516.
34. Ashton N, Wirasinha PA. Encephalitozoonosis (nosematosis) of the cornea. *Br J Ophthalmol.* 1973;57:669-674.
35. Cali A, Meisler DM, Lowder CY, et al. Corneal microsporidioses: characterization and identification. *J Protozool.* 1991;38:215S-217S.
36. Didier ES, Shadduck JA, Didier PJ, Millichamp N, Vossbrinck CR. Studies on ocular microsporidia. *J Protozool.* 1991;38:635-638.
37. Lowder CY, McMahon JT, Meisler DM, et al. Microsporidial keratoconjunctivitis caused by *Septata intestinalis* in a patient with acquired immunodeficiency syndrome. *Am J Ophthalmol.* 1996;121:715-717.
38. Visvesvara GS, Belloso M, Moura H, et al. Isolation of *Nosema algerae* from the cornea of an immunocompetent patient. *J Eukaryot Microbiol.* 1999;46:10S.
39. Weber R, Bryan RT. Microsporidial infections in immunodeficient and immunocompetent patients. *Clin Infect Dis.* 1994;19:517-521.
40. Lacey CJ, Clarke AM, Fraser P, Metcalfe T, Bonsor G, Curry A. Chronic microsporidian infection of the nasal mucosae, sinuses, and conjunctivae in HIV disease. *Genitourin Med.* 1992;68:179-181.
41. Schwartz DA, Cali A, Visvesvara GS, Roseberger D, Hewan-Lowe KO, Bryan RT. A nasal microsporidian with unusual features from a patient with AIDS. *Abstracts of International Conference on AIDS.* 1993;1:384.
42. Molina JM, Sarfati C, Beauvais B, et al. Intestinal microsporidiosis in human immunodeficiency virus-infected patients with chronic unexplained diarrhea: prevalence and clinical and biological features. *J Infect Dis* 1993;167:217-221.
43. Orenstein JM, Chiang J, Steinberg W, Smith PD, Rotterdam H, Kotler DP. Intestinal microsporidiosis as a cause of diarrhea in human immunodeficiency virus-infected patients: a report of 20 cases. *Hum Pathol.* 1990;21:475-481.
44. Verre J, Marriot D, Hing M, Field A, Harkness J. Evaluation of light microscopic detection of microsporidia spores in feces from HIV-infected patients [abstract]. *AIDS: Workshop on Intestinal Microsporidioses in HIV Infection.* 1993;7(suppl 3).
45. Issi IV. Microsporidia as a phylum of parasitic protozoa. *Protozoology (Leningrad).* 1986;10:1-136.
46. Sprague V, Becnel JJ. Note on the name-author-date combination for the taxon *Microsporidies Balbiani*, 1882, when ranked as a phylum. *J Invertebr Pathol.* 1998;71:91-94.
47. Sprague V, Vavra J. Biology of the Microsporidia. In: Bulla LA, Cheng TC, eds. *Comparative Pathobiology.* Vol 1. New York, NY: Plenum Press; 1977:1-371.
48. Sprague V, Vavra J. Systematics of the Microsporidia. In: Bulla LA, Cheng TC, eds. *Comparative Pathobiology*. Vol 2. New York, NY: Plenum Press; 1977:1-510.
49. Levine ND, Corliss JO, Cox FE, et al. A newly revised classification of the protozoa. *J Protozool.* 1980;27:37-58.
50. Lainson R, Garnham PC, Killick-Kendrick R, Bird RG. Nosematosis, a microsporidial infection of rodents and other animals, including man. *Br Med J.* 1964;5407:470-472.
51. Weiser J. On the taxonomic position of the genus *Encephalitozoon Levaditi*, Nicolau and Schoen, 1923 (Protozoa: Microsporida). *Parasitology.* 1964;54:749-751.
52. Cali A. Morphogenesis in the genus *Nosema*. Proceedings of the IVth International Colloquium on Insect Pathology. College Park, Md: 1970;431-438.
53. Hartskeerl R., Van Gool T, Schuitema AR, Didier ES, Terpstra WJ. Genetic and immunological characterization of the microsporidian *Septata intestinalis* Cali, Kotler and Orenstein, 1993: reclassification to *Encephalitozoon intestinalis*. *Parasitology.* 1995;110:277-285.
54. Lowman PM, Takvorian PM, Cali A. The effects of elevated temperatures and various time-temperature combinations on the development of *Brachiola (Nosema) algerae* N. Comb. in mammalian cell culture. *J Eukaryot Microbiol.* 2000;47:221-234.
55. Canning EU, Lom J, Dykova I. *The Microsporidia of Vertebrates.* London, England: Academic Press; 1986.
56. Lucas SB, Papadaki L, Conlon C, Sewankambo N, Goodgame R, Serwadda D. Diagnosis of intestinal microsporidiosis in patients with AIDS [letter]. *J Clin Pathol.* 1989;42:885-890.
57. Field AS, Canning EU, Hing MC, Verre J, Marriott DJ. Microsporidia in HIV-infected patients in Sydney, Australia: a report of 37 cases, a new diagnostic technique and the light microscopy and ultrastructure of a disseminated species. *AIDS: Workshop on Intestinal Microsporidioses in HIV Infection* 1993;7(suppl 3):S27-S33.
58. Loh RS., Chan CM , Ti SE, Lim L, Chan KS, Tan DT. Emerging prevalence of microsporidial keratitis in Singapore: epidemiology, clinical features, and management. *Ophthalmology.* 2009;116:2348-2353.
59. Desportes-Livage I, Levy JP. Intestinal microsporidia and HIV Infection. *AIDS 1993: 7(Suppl 3); S1-S2.* Editorial, Workshop on Intestinal Microsporidia in HIV Infection, 15-16 December 1992, Paris, France
60. van Gool T, Snijders F, Reiss P, et al. Diagnosis of intestinal and disseminated microsporidial infections in patients with HIV by a new rapid fluorescence technique. *J Clin Pathol.* 1993;46:694-699.
61. Cali A, Owen RL. Microsporidiosis. In: Balows A, Hausler WJ Jr, Ohashi M, and Turano A, eds. *The Laboratory Diagnosis of Infectious Diseases: Principles and Practice: Vol I: Bacterial, Mycotic, and Parasitic Diseases.* New York: Springer-Verlag; 1988:928-949.
62. Schwartz DA, Sobottka I, Leitch GJ, Cali A, Visvesvara GS. Pathology of microsporidiosis: emerging parasitic infections in patients with acquired immunodeficiency syndrome. *Arch Pathol Lab Med.* 1996;120:173-188.
63. Sak B, Brady D, Pelikanova M, et al. Unapparent microsporidial infection among immunocompetent humans in the Czech Republic. *J Clin Microbiol.* 2010;PMID: 21191056
64. Microsporidian keratoconjunctivitis in patients with AIDS. *MMWR Morb Mortal Wkly Rep.* 1990;39:188-189.

65. Coyle C, Weiss LM, Rhodes LV, et al. Fatal myostitis due to the microsporidian *Brachiola algerae*, a mosquito pathogen. *N Engl J Med*. 2004;351:42-47.
66. Talabani H, Sarfati C, Pillebout E, van Gool T, Derouin F, Menotti J. Disseminated infection with a new genovar of *Encephalitozoon cuniculi* in a renal transplant recipient. *J Clin Microbiol.* 2010;48:2651-2653.
67. Lanternier F, Boutboul D, Menotti J, et al. Microsporidiosis in solid organ transplant recipients: two *Enterocytozoon bieneusi* cases and review. *Transpl Infect Dis.* 2009;11:83-88.
68. Mathis A, Weber R, Deplazes P. Zoonotic potential of the microsporidia. *Clin Microbiol Rev*. 2005;18:423-445.
69. Cali A, Takvorian PM. Microsporidia. In: *Handbook of Protoctista*, 2nd ed. Margulis L, Chapman M, eds. Jones and Bartlett, Boston. In press. 2011.
70. Williams B, Hirt R, Lucocq JM, Embley TM. A mitochondrial remnant in the microsporidian *Trachipleistophora hominis*. *Nature*. 2002;418:865-869.
71. Katinka MD, Duprat S, Cornillot E, et al. Genome sequence and gene compaction of the eukaryote parasite *Encephalitozoon cuniculi*. *Nature*. 2001;414:450-453.
72. Vossbrinck CR, Maddox JV, Friedman S, Debrunner-Vossbrinck BA, Woese CR. Ribosomal RNA sequence suggests microsporidia are extremely ancient eukaryotes. *Nature.* 1987;326:411-414.
73. Takvorian PM, Cali A. Enzyme histochemical identification of the Golgi apparatus in the microsporidian, *Glugea stephani*. *J Eukaryot Microbiol.* 1994;41:63S-64S.
74. Takvorian PM, Cali A. Polar tube formation and nucleoside diphosphatase activity in the microsporidian, *Glugea stephani*. *J Eukaryot Microbiol.* 1996;43:102S-103S.
75. Edlind T, Katiyar S, Visvesvara G, Li J. Evolutionary origins of Microsporidia and basis for benzimidazole sensitivity: an update. *J Eukaryot Microbiol*. 1996;43:109S.
76. Edlind TD, Li J, Visvesvara GS, Vodkin MH, McLaughlin GL, Katiyar SK. Phylogenetic analysis of beta-tubulin sequences from amitochondrial protozoa. *Mol Phylogenet Evol.* 1996;5:359-367.
77. Cali A. General microsporidian features and recent findings on AIDS isolates. *J Protozool.* 1991;38:625-630.
78. Cali A, Takvorian PM. Developmental morphology and life cycles of the Microsporidia. In: Wittner M, Weiss LM, eds. *The Microsporidia and Microsporidiosis*. Washington, DC: ASM Press; 1999:85-128.
79. Cali A, Takvorian PM. *Brachiola algerae* sporoplasms. *J Eukaryot Microbiol*. 2001;Suppl:81S-82S.
80. Lom J, Vavra J. The mode of sporoplasm extrusion in microsporidian spores. *Acta Protozool.* 1963;1:81-89.
81. Cali A, Takvorian PM. The Microsporidia: pathology in man and occurrence in nature. *Southeast Asian J Trop Med Pub Health.* 2004;35:58-64.
82. Enriquez FJ, Taren D, Cruzlopez A, Muramoto M, Palting JD, Cruz P. Prevalence of intestinal encephalitozoonosis in Mexico. *Clin Infect Dis*. 1998;26:1227-1229.
83. Lobo ML, Teles A, da Cunha MB, et al. Microsporidia detection in stools from pets and animals from the zoo in Portugal: a preliminary study. *J Eukaryot Microbiol.* 2003;50 (Suppl):581-582.
84. Curry A, Hardeep SM, Sumedh D, Canning EU, Wagner BE. A case of bilateral microsporidial keratitis from Bangladesh: infection by insect parasite from the genus *Nosema*. *J Med Microbiol*. 2007;56:1250-1252.
85. Shadduck JA, Meccoli RA, Davis R, Font RL. Isolation of a microsporidian from a human patient. *J Infect Dis*. 1990;162:773-776.
86. Franzen C, Fischer S, Schroeder J, Scholmerich J, Schneuwly S. Morphological and molecular investigations of *Tubulinosema ratisbonensis* gen. nov., sp. nov. (Microsporidia: Tubulinosematidae fam. nov.), a parasite infecting a laboratory colony of *Drosophila melanogaster* (Diptera: Drosophilidae). *J Eukaryot Microbiol.* 2005;52:141-152.
87. Cali A, Weiss LM, Takvorian PM. An Analysis of the microsporidial genus *Brachiola*, with comparisons of human and insect isolates of *B. algerae. J Eukaryot Microbiol.* 2004;51:678-685.
88. Davis RM, Font RL, Keisler MS, Shadduck JA. Corneal microsporidiosis. A case report including ultrastructural observations. *Ophthalmology.* 1990;97:953-957.
89. Strano AJ, Cali A, Neafie R. Microsporidiosis. In: Binford CH, Connor DH, eds. *Pathology of Tropical and Extraordinary Diseases*. Vol 1. Washington, DC: AFIP; 1976:336-339.
90. Sprague V. *Nosema connori* n. sp., a microsporidian parasite of man. *Trans Am Microsc Soc.* 1974;93:400-403.
91. Trammer T, Chioralia G, Maier WA, Seitz HM. In vitro replication of *Nosema algerae* (Microsporidia), a parasite of anopheline mosquitoes, in human cells above 36 degrees C. *J Eukaryot Microbiol.* 1999;46:464-468.
92. Cali A, Weiss LM, Takvorian PM. A review of the development of two types of human skeletal muscle infections from microsporidia associated with pathology in invertebrates and cold-blooded vertebrates. *Folia Parasitologica (Praha).* 2005;52:51-61.
93. Cali A, Neafie R, Weiss LM, et al. Human vocal cord infection with the Microsporidium *Anncaliia algerae*. *J Eukaryot Microbiol*. 2010;57:562-567.
94. Chupp GL, Alroy J, Adelman LS, Breen JC, Skolnik PR. Myositis due to *Pleistophora* (Microsporidia) in a patient with AIDS. *Clin Infect Dis.* 1993;16:15-21.
95. Grau A, Valls ME, Williams JE, Ellis DS, Muntane MJ, Nadal C. Myositis caused by *Pleistophora* in a patient with AIDS [in Spanish]. *Med Clin (Barc)* 1996;107:779-781.
96. Vavra J, Yachnis AT, Shadduck JA, Orenstein JM. Microsporidia of the genus *Trachipleistophora*–causative agents of human microsporidiosis: description of *Trachipleistophora anthropophthera* n. sp. (Protozoa: Microsporidia). *J Eukaryot Microbiol.* 1998;45:273-283.
97. Yachnis AT, Berg J, Martinez-Salazar A, et al. Disseminated microsporidiosis especially infecting the brain, heart, and kidneys. Report of a newly recognized pansporoblastic species in two symptomatic AIDS patients. *Am J Clin Pathol*. 1996;106:535-543.
98. Weidner E, Canning EU, Hollister WS. The plaque matrix (PQM) and tubules at the surface of intramuscular parasite, *Trachipleistophora hominis*. *J Eukaryot Microbiol*. 1997;44:359-365.
99. Macher AM, Neafie R, Angritt P, Tuur SM. Microsporidial myositis and the acquired immunodeficiency syndrome (AIDS): a four-year follow-up [letter]. *Ann Intern Med*. 1988;109:343.
100. Macher AM, Neafie R, Angritt P, Tuur SM, Nelson RP, Cali A. AIDS. Case for diagnosis series, 1988. *Mil Med.* 1988;153:M41-M48.
101. Curry A, Beeching NJ, Gilbert JD, Scott G, Rowland PL, Currie BJ. *Trachipleistophora hominis* infection in the myocardium and skeletal muscle of a patient with AIDS. *J Infect.* 2005;51:e139-e144.
102. Rinder H, Thomschke A, Dengje B, Gothe R, Loscher T, Zahler M.Close genotypic relationship between *Enterocytozoon bieneusi* from humans and pigs and first detection in cattle. *J Parasitol*. 2000;86:185-188.
103. Orenstein JM, Lew E, Poles MA, Dieterich D. The endoscopic brush cytology specimen in the diagnosis of intestinal microsporidiosis. *AIDS.* 1995;9:1199-1201.
104. McWhinney PH, Nathwani D, Green ST, Boyd JF, Forrest JA. Microsporidiosis detected in association with AIDS-related sclerosing cholangitis. *AIDS.* 1991;5:1394-1395.
105. Canning EU, Hollister WS. *Enterocytozoon bieneusi* (Microspora): prevalence and pathogenicity in AIDS patients. *Trans R Soc Trop Med Hyg.* 1990;84:181-186.
106. Orenstein JM, Friedberg DN, Cali A, Kotler DP. Microsporidiosis in AIDS: an update of enteritis caused by *E. bieneusi* and a second species, and *E. cuniculi* as a cause of keratoconjunctivitis. *Abstracts of Sixth International Conference on AIDS.* 1990:Th.B.522.
107. Sun T, Kaplan MH, Teichberg S, Weissman G, Smilari T, Urmacher C. Intestinal microsporidiosis: report of five cases. *Ann Clin Lab Sci.* 1994;24:521-532.
108. Rabeneck L, Gyorkey F, Genta RM, Gyorkey P, Foote LW, Risser JM. The role of Microsporidia in the pathogenesis of HIV-related chronic diarrhea. *Ann Intern Med.* 1993;119:895-899.
109. Weber R, Kuster H, Visvesvara GS, Bryan RT, Schwartz DA, Luthy R. Disseminated microsporidiosis due to *Encephalitozoon hellem*: pulmonary colonization, microhematuria, and mild conjunctivitis in a patient with AIDS. *Clin Infect Dis.* 1993;17:415-419.
110. Eeftinck Schattenkerk JK, van Gool T, Schot LS, van den Bergh Weerman MA, Schot LJ, Dankert J. Chronic rhinosinusitis in HIV-infected patients with microsporidiosis. *AIDS: Workshop on Intestinal Microsporidioses in HIV Infection.* 1993;7(suppl 3):S36-S37.
111. Hartskeerl RA, Schuitema AR, van Gool T, Terpstra WJ. Genetic evidence for the occurrence of extra-intestinal *Enterocytozoon bieneusi* infections. *Nucleic Acids Res.* 1993;21:4150.
112. Weber R, Bryan RT, Owen RL, Wilcox CM, Gorelkin L, Visvesvara GS. Improved light-microscopical detection of microsporidia spores in stool and duodenal aspirates. The Enteric Opportunistic Infections Working Group. *N Engl J Med.* 1992;326:161-166.

113. Levaditi C, Nicolau S, Schoen R. Etiologic agent of epizootic encephalitis in rabbits (*Encephalitozoon cuniculi*) [in French]. *Comp Rend Soc Biol*. 1923;89:984-986.

114. Pakes SP, Shadduck JA, Cali A. Fine structure of *Encephalitozoon cuniculi* from rabbits, mice and hamsters. *J Protozool*. 1975;22:481-488.

115. Voronin VN. Macrotaxonomy of the Microsporidia phylum. *Parazitologiia.* 2001;35:35-44.

116. Friedberg DN, Stenson SM, Orenstein JM, Tierno PM, Charles NC. Microsporidial keratoconjunctivitis in acquired immunodeficiency syndrome. *Arch Ophthalmol*. 1990;108:504-508.

117. Lowder CY, Meisler DM, McMahon JT, Longworth DL, Rutherford I. Microsporidia infection of the cornea in a man seropositive for human immunodeficiency virus. *Am J Ophthalmol.* 1990;109:242-244.

118. Desser SS, Hong H, Yang YJ. Ultrastructure of the development of a species of *Encephalitozoon* cultured from the eye of an AIDS patient. *Parasitol Res.* 1992;78:677-683.

119. Schwartz DA, Visvesvara GS, Diesenhouse MC, et al. Pathologic features and immunofluorescent antibody demonstration of ocular microsporidiosis (*Encephalitozoon hellem*) in seven patients with acquired immunodeficiency syndrome. *Am J Ophthalmol*. 1993;115:285-292.

120. Orenstein JM, Tenner M, Cali A, Kotler DP. A microsporidian previously undescribed in humans, infecting enterocytes and macrophages, and associated with diarrhea in an acquired immunodeficiency syndrome patient. *Hum Pathol*. 1992;23:722-728.

121. Dore GJ, Marriott DJ, Hing MC, Harkness JL, Field AS. Disseminated microsporidiosis due to *Septata intestinalis* in nine patients infected with the human immunodeficiency virus: response to therapy with albendazole. *Clin Infect Dis.* 1995;21:70-76.

122. Fields AS, Hing MC, Milliken ST, Marriott DJ. Microsporidia in the small intestine of HIV-infected patients. A new diagnostic technique and a new species. *Med J Aust.* 1993;158:390-394.

123. Sprague V, Vernick SH. The ultrastructure of *Encephalitozoon cuniculi* (Microsporidia, Nosematidae) and its taxonomic significance. *J Protozool*. 1971;18:560-569.

124. Cali A, Weiss LM, Takvorian PM. Microsporidian taxonomy and the status of *Septata intestinalis. J Eukaryot Microbiol.* 1996;43:106S-107S.

125. Bergquist NR, Morfeldt-Mansson L, Pehrson PO, Petrini B, Wasserman J. Antibody against *Encephalitozoon cuniculi* in Swedish homosexual men. *Scand J Infect Dis.* 1984;16:389-391.

126. Bergquist NR, Stintzing G, Smedman L, Waller T, Andersson T. Diagnosis of encephalitozoonosis in man by serological tests. *Br Med J (Clin Res Ed).* 1984;288:902.

127. Gordon SC, Reddy KR, Gould EE, et al. The spectrum of liver disease in the acquired immunodeficiency syndrome. *J Hepatol.* 1986;2:475-484.

128. De Groote MA, Visvesvara G, Wilson ML, et al. Polymerase chain reaction and culture confirmation of disseminated *Encephalitozoon cuniculi* in a patient with AIDS: successful therapy with albendazole. *J Infect Dis*. 1995;171:1375-1378.

129. Weber R, Deplazes P, Flepp M, et al. Cerebral microsporidiosis due to *Encephalitozoon cuniculi* in a patient with human immunodeficiency virus infection. *N Engl J Med.* 1997;336:474-478.

130. Zender HO, Arrigoni E, Eckert J, Kapanci Y. A case of *Encephalitozoon cuniculi* peritonitis in a patient with AIDS. *Am J Clin Pathol.* 1989;92:352-356.

131. Canning EU, Curry A, Lacey CJ, Fenwick JD. Ultrastructure of *Encephalitozoon sp.* infecting the conjunctival, corneal and nasal epithelia of a patient with AIDS. *Eur J Protistol.* 1992;28:226-237.

132. Schwartz DA, Bryan RT, Hewan-Lowe KO, et al. Disseminated microsporidiosis (*Encephalitozoon hellem*) and acquired immunodeficiency syndrome: autopsy evidence for respiratory acquisition. *Arch Pathol Lab Med*. 1992;116:660-668.

133. Schwartz DA, Visvesvara GS, Leith GJ, et al. Pathology of symptomatic microsporidial *(Encephalitozoon hellem*) bronchiolitis in the acquired immunodeficiency syndrome: a new respiratory pathogen diagnosed from lung biopsy, bronchoalveolar lavage, sputum, and tissue culture. *Hum Pathol*. 1993;24:937-943.

134. Schwartz DA, Visvesvara GS, Weber R, Bryan RT. Male genital tract microsporidiosis and AIDS: prostatic abscess due to *Encephalitozoon hellem. J Eukaryot Microbiol*. 1994;41:61S

135. Visvesvara GS, Leitch GJ, Moura H, Wallace S, Weber R, Bryan RT. Culture, electron microscopy, and immunoblot studies on a microsporidian parasite isolated from the urine of a patient with AIDS. *J Protozool*. 1991;38:105S-111S.

136. Molina JM, Oksenhendler E, Beauvais B, et al. Disseminated microsporidiosis due to *Septata intestinalis* in patients with AIDS: clinical features and response to albendazole therapy. *J Infect Dis.* 1995;171:245-249.

137. Orenstein JM, Dieterich DT, Kotler DP. Systemic dissemination by a newly recognized intestinal microsporidia species in AIDS. *AIDS.* 1992;6:1143-1150.

138. Coyle CM, Wittner M, Kotler DP, et al. Prevalence of microsporidiosis due to *Enterocytozoon bieneusi* and *Encephalitozoon (Septata) intestinalis* among patients with AIDS-related diarrhea: determination by polymerase chain reaction to the microsporidian small-subunit rRNA gene. *Clin Infect Dis.* 1996;23:1002-1006.

139. Luna LG. *Manual of Histologic Staining Methods of the Armed Forces Institute of Pathology*. New York, NY: McGraw-Hill; 1968.

140. Rijpstra AC, Canning EU, Van Ketel RJ, Eeftinck Schattenkerk JK, Laarman JJ. Use of light microscopy to diagnose small-intestinal microsporidiosis in patients with AIDS. *J Infect Dis.* 1988;157:827-831.

141. Simon D, Weiss LM, Tanowitz HB, Cali A, Jones J, Wittner M. Light microscopic diagnosis of human microsporidiosis and variable response to octreotide. *Gastroenterology.* 1991;100:271-273.

142. Weber R, Schwartz DA, Deplazes P. Laboratory diagnosis of microsporidiosis. In: Wittner M, Weiss LM, eds. *The Microsporidia and Microsporidiosis.* Washington, DC: ASM Press; 1999:315-362.

143. Field AS, Marriott DJ, Hing MC. The Warthin-Starry stain in the diagnosis of small intestinal microsporidiosis in HIV-infected patients. *Folia Parasitol (Praha).* 1993;40:261-266.

144. van Gool T, Canning EU, Dankert J. An improved practical and sensitive technique for the detection of microsporidian spores in stool samples. *Trans R Soc Trop Med Hyg*. 1994;88:189-190.

145. Hollister WS, Canning EU. An enzyme-linked immunosorbent assay (ELISA) for detection of antibodies to *Encephalitozoon cuniculi* and its use in determination of infections in man. *Parasitology.* 1987;94:209-219.

146. Weiss LM, Cali A, Levee E, et al. Diagnosis of *Encephalitozoon cuniculi* infection by western blot and the use of cross-reactive antigens for the possible detection of microsporidiosis in humans. *Am J Trop Med Hyg.* 1992;47:456-462.

147. Aldras AM, Orenstein JM, Kotler DP, Shadduck JA, Didier ES. Detection of microsporidia by indirect immunofluorescence antibody test using polyclonal and monoclonal antibodies. *J ClinMicrobiol*. 1994;32:608-612.

148. Keohane E, Takvorian PM, Cali A, Tanowitz HB, Wittner M, Weiss LM. The identification and characterization of a polar tube reactive monoclonal antibody. *J Eukaryot Microbiol*. 1994;41:48S.

149. Alfa Cisse O, Ouattara A, Thellier M, et al. Evaluation of an immuno-fluorescent-antibody test using monoclonal antibodies directed against *Enterocytozoon bieneusi* and *Encephalitozoon intestinalis* for diagnosis of intestinal microsporidiosis in Bamako (Mali). *J Clin Microbiol.* 2002;40:1715-1718.

150. Garcia L. Laboratory identification of microsporidia. *Journal of Clinical Microbiology*. 2002;40:1892-1901.

151. Weiss LM, Zhu X, Cali A, Tanowitz HB, Wittner M. Polymerase chain reaction identification of *Microsporidia* using ribosomal RNA. *AIDS: Workshop on Intestinal Microsporidioses in HIV Infection.* 1993;7(suppl 3):S62-S63.

152. Weiss LM, Zhu X, Cali A, Tanowitz HB, Wittner M. Utility of microsporidian rRNA in diagnosis and phylogeny: a review. *Folia Parasitol (Praha).* 1994;41:81-90.

153. Zhu X, Wittner M, Tanowitz HB, Cali A, Weiss LM. Nucleotide sequence of the small ribosomal RNA of *Encephalitozoon cuniculi*. *Nucleic Acids Res.* 1993;21:1315.

154. Zhu X, Wittner M, Tanowitz HB, Cali A, Weiss LM. Nucleotide sequence of the small subunit rRNA of *Septata intestinalis*. *Nucleic Acids Res.* 1993;21:4846.

155. Zhu X, Wittner M, Tanowitz HB, Cali A, Weiss LM. Ribosomal RNA sequences of *Enterocytozoon bieneusi*, *Septata intestinalis* and *Ameson michaelis*: phylogenetic construction and structural correspondence. *J Eukaryot Microbiol*. 1994;41:204-209.

156. Zhu X, Wittner M, Tanowitz HB, Kotler D, Cali A, Weiss LM. Small subunit rRNA sequence of *Enterocytozoon bieneusi* and its potential diagnostic role with the use of the polymerase chain reaction. *J Infect Dis.* 1993;168:1570-1575.

157. Shadduck JA. Effect of fumagillin on in vitro multiplication of *Encephalitozoon cuniculi*. *J Protozool.* 1980;27:202-208.

158. Yee RW, Tio FO, Martinez JA, Held KS, Shadduck JA, Didier ES. Resolution of microsporidial epithelial keratopathy in a patient with AIDS. *Ophthalmology.* 1991;98:196-201.

159. Blanshard C, Ellis DS, Tovey DG, Dowell S, Gazzard BG. Treatment of intestinal microsporidiosis with albendazole in patients with AIDS. *AIDS*. 1992;6:311-313.

160. Orenstein JM, Dieterich DT, Lew EA, Kotler DP. Albendazole as a treatment for intestinal and disseminated microsporidiosis due to *Septata intestinalis* in AIDS patients: a report of four patients. *AIDS: Workshop on Intestinal Microsporidioses in HIV Infection.* 1993;7(suppl 3):S40-S42.

161. Koudela B, Lom J, Vitovec J, Kucerova Z, Ditrich O, Travnicek J. In vivo efficacy of albendezole against *Encephalitozoon cuniculi* in SCID mice. *J Eukaryot Microbiol*. 1994;41:49S-50S.

162. Lecuit M, Oksenhendler E, Sarfati C. Use of albendazole for disseminated microsporidian infection in a patient with AIDS. *Clin Infect Dis*. 1994;19:332-333.

163. Weiss LM, Michalakakis E, Coyle CM, Tanowitz HB, Wittner M. The in vitro activity of albendazole against *Encephalitozoon cuniculi*. *J Eukaryot Microbiol*. 1994;41:65S.

164. Aarons EJ, Woodrow D, Hollister WS, Canning EU, Francis N, Gazzard BG. Reversible renal failure caused by a microsporidian infection. *AIDS*. 1994;8:1119-1121.

165. Didier ES, Maddry JA, Kwong CD, Green LC, Snowden KF, Shadduck JA. Screening of compounds for antimicrosporidial activity in vitro. *Folia Parasitol (Praha)*. 1998;45:129-139.

166. Silveira H, Canning EU. In vitro cultivation of the human microsporidium *Vittaforma corneae*: development and effect of albendazole. *Folia Parasitol (Praha)*. 1995;42:241-250.

167. Franzen C, Salzberger B. Analysis of the tubulin gene from *Vittaforma corneae* suggests benzimidazole resistance. *Antimicrob Agents Chemother*. 2008;52:790-793.

168. Didier ES. Effects of albendazole, fumagillin, and TNP-470 on microsporidial replication in vitro. *Antimicrob Agents Chemother.* 1997;41:1541-1546.

## *Acknowledgements*

### The following figures are used by permission."Copyright © American Society for Microbiology."

**Figures 14.1, 14.4.**
Cali A, Takvorian PM. Developmental morphology and life cycles of the Microsporidia. In: Wittner M, Weiss LM, eds. The Microsporidia and Microsporidiosis, Washington, DC: ASM Press; 1999:85-128.

**Figures 14.30 to 14.35.**
Field AS, Marriott DJ, Milliken ST, et al. Myositis associated with a newly described Microsporidan, *Trachipleistophora hominis*, in a patient with AIDS. *J Clin Microbiol*. 1996;34:2803-2811.
Licensed to the Armed Forces Institute of Pathology. "Copyright © American Society for Microbiology.

**Figures 14.40a,b and 14.43.**
Kotler DP, Orenstein JM. Clinical syndromes associated with microsporidiosis. In: Wittner M, Weiss LM, eds. The Microsporidia and Microsporidiosis. Washington, DC:ASM Press; 1999:258-292.

### The following figures are used by permission "Copyright © Wiley Publications."

**Figure 14.5.**
Cali A, Takvorian PM. *Brachiola algerae* sporoplasms. *J Eukaryot Microbiol* 2001;Suppl:81S-82S.

**Figures 14.19 to 14.23.**
Cali A, Takvarian PM, Lewin S, et al. *Brachiola vesicularum*, n. g., n. sp., a new microsporidium associated with AIDS and myositis. *J Eukaryot Microbiol*. 1998;45:240-251.

**Figures 14.28, 14.29a,b.**
Cali A, Takvorian PM. Ultrastructure and development of *Pleistophora ronneafiei* n. sp, a Microsporidium (Protista) in the skeletal muscle of an immune-compromised individual. *J Eukaryot Microbiol.* 2003;50:77-85.

**Figure 14.36**
Licensed to the Armed Forces Institute of Pathology.
Vavra J, Yachnis AT, Shadduck JA, Orenstein JM. Microsporidia of the genus *Trachipleistophora*-causative agents of human microsporidiosis: description of *Trachipleistophora anthropophthera* n. sp. (Protozoa: Microsporidia). *J Eukaryot Microbiol.* 1998;45:273-283.

**Fig 14 41, 14.42.**
Cali A, Owen RL. Intracellular development of *Enterocytozoon*, a unique microsporidian found in the intestine of AIDS patients. *J Protozool.* 1990;37:145:155.

**Figure 14.48.**
Cali A, Takvorian PM, Lewin S, et al. Identification of a new Nosema-like microsporidian associated with myositis in an AIDS patient. *J Eukaryot Microbiol.* 1996;43:108S.

**Figure 14.50**
Cali A, Kotler DP, Orenstein JM. *Septata intestinalis*, n. g, n. sp, an intestinal microsporidian associated with chronic diarrhea and dissemination in AIDS patients. *J Eukaryot Microbiol.* 1993;40:101-112.

### The following figures are used by permission, "Massachussets Medical Society © 2010."

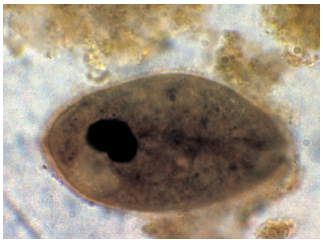
**Figure 14.24, 14.25a,b**
Coyle C, Weiss LM, Rhodes LV, et al. Fatal myositis due to the microsporidian *Brachiola algerae*, a mosquito pathogen. *N Engl J Med*. 2004;351:42-47.

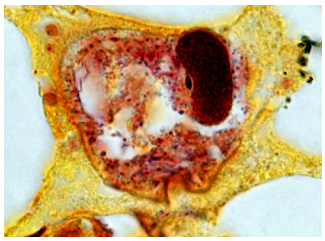
### The following figures are used by permission, "Copyright © American Journal of Tropical Medicine and Hygiene."

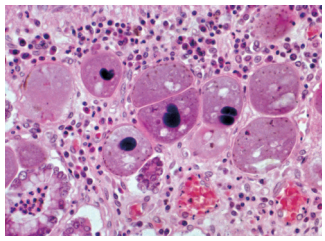
**Figures 14.47, 14.49**
Cali A, Meisler DM, Rutherford I, et al. Corneal microsporidiosis in a patient with AIDS. *Am J Trop Med Hyg.* 1991;44:463-468.

### The following figure used by permission.

**Figure 14.58**
Compliments of Govinda S. Visvesvara, Ph.D. Centers for Disease Control and Prevention.







15

# Balantidiasis

*Ronald C. Neafie, Ellen M. Andersen, and Mary K. Klassen-Fischer*

## *Introduction*

### Definition

Balantidiasis is infection by *Balantidium coli*, the largest protozoan parasite and the only ciliate parasite known to infect humans. Malmsten first described the organism in 1857 in 2 patients with severe diarrhea; one of these infections was fatal.[1]

### Synonyms

Balantidiasis is also known as balantidiosis, balantidial dysentery, and ciliary dysentery.

## *Epidemiology*

*Balantidium coli* is endemic worldwide. It is most prevalent in temperate and tropical regions, but has been reported in Norway, Sweden, Finland, and northern Russia.[2] This ciliate parasite inhabits a variety of hosts, especially primates.[3] Humans are most commonly infected by contact with infected pigs.[4] In some pig-raising areas of New Guinea, human infection rates are as high as 28%.[5,6] An outbreak of balantidiasis on the Pacific island of Truk in 1971 led to 110 human infections.[7] Human-to-human transmission can occur when personal hygiene is poor, especially among institutionalized populations.[8] Nonhuman primates are another source of infection. *Balantidium coli* has been reported in numerous primate species, including orangutans, chimpanzees, gorillas, and Old and New World monkeys.[3,9,10] Other hosts for *B. coli* include rats, fowl, turtles, and cockroaches. Humans have been reported to be asymptomatic carriers of *B. coli*.[4]

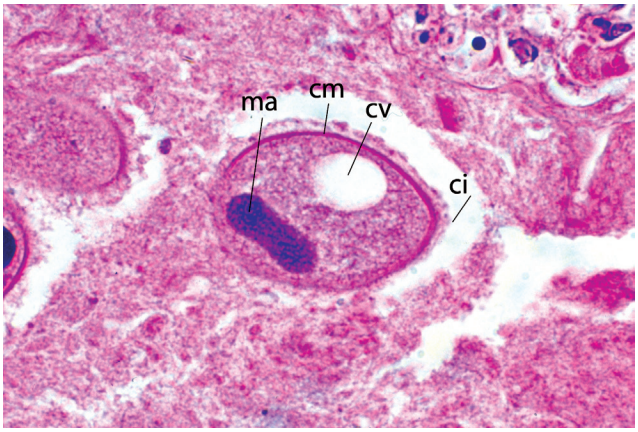



**Figure 15.1**
*Balantidium coli* trophozoite in colon. Note cilia (ci), cell membrane (cm), large macronucleus (ma), and large contractile vacuole (cv). x570

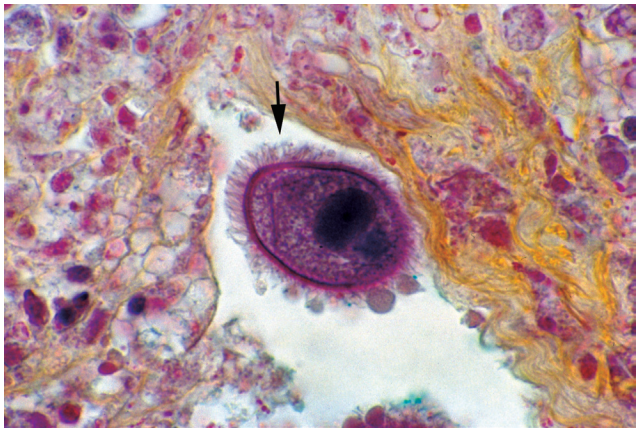


**Figure 15.2**
*Balantidium coli* trophozoite in colon. Note prominent cilia (arrow), cell membrane, and large macronucleus. Movat x570

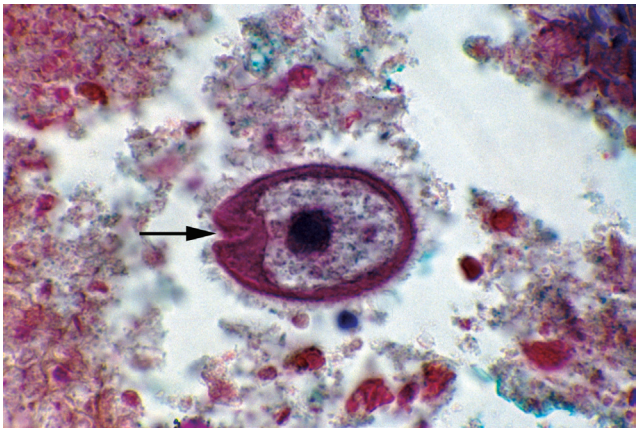


**Figure 15.3**
*Balantidium coli* in colonic ulcer. Note cilia-lined peristome (arrow) at anterior end. Movat x610

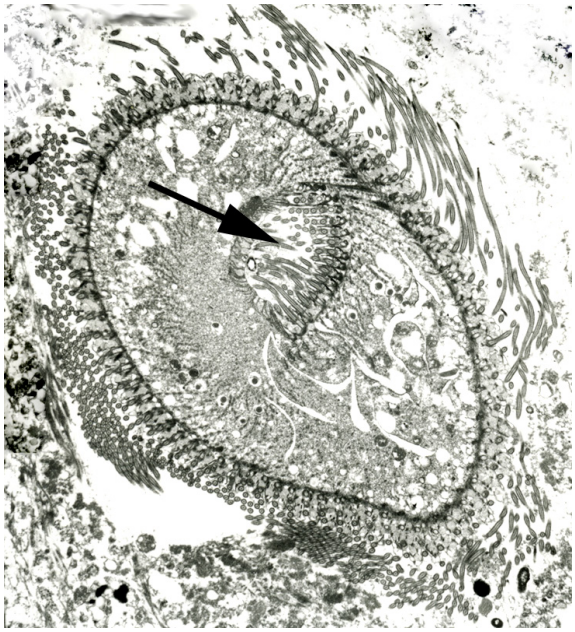


**Figure15.4**
Electron micrograph of *Balantidium Coli* trophozoite in colon depicting ciliated cell membrane and cilia-lined peristome (arrow) surrounding cytostome. x1350

## *Infectious Agent*

### Morphologic Description

The trophozoite of *B. coli* is 50 µm to 200 µm by 40 µm to 70 µm; in tissue sections most are 40 µm to 80 µm by 25 µm to 45 µm. They are ovoid, with a cell membrane covered with uniform cilia (Figs 15.1 and 15.2). Near the anterior end is the funnel-shaped peristome, a ciliated area surrounding the cytostome (mouth) (Figs 15.3 and 15.4). Residual products are eliminated through the cytopyge, a small triangular opening at the posterior end. The granular cytoplasm contains food and usually 1 or 2 contractile vacuoles (Fig 15.1). The most obvious structure within the cytoplasm is the large, often kidney-shaped macronucleus (Fig 15.5). The tiny micronucleus lies within the concave depression of the macronucleus (Fig 15.6). The micronucleus is not observed in hematoxylin and eosin stained sections, but may be identified using special stains such as Brown-Hopps, Movat, and Masson. Unusual forms, possibly undergoing division, conjugation, or apoptosis, may rarely be seen (Figs 15.7 and 15.8). Precysts are round, ciliated, and have a peristome (Fig 15.9). Cysts, which are not observed in histologic sections of colon, are spherical and vary from 45 µm to 75 µm in diameter. They have a large macronu-

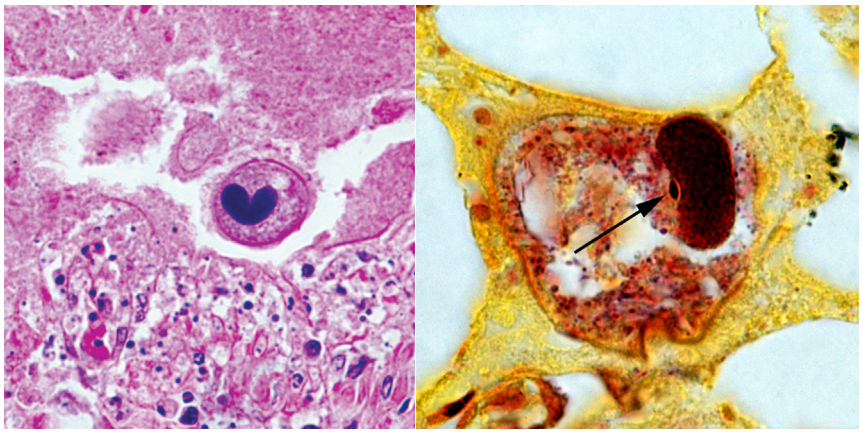
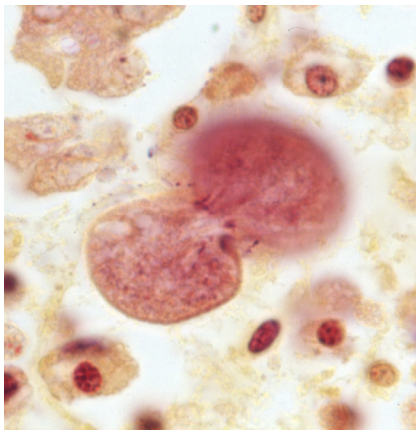


**Figure 15.5 (left) and 15.6 (right)**
Left, *Balantidium coli* trophozoite in colon demonstrating kidney-shaped macronucleus. x380 and right, the tiny micronucleus (arrow) adjacent to the macronucleus. BH x835



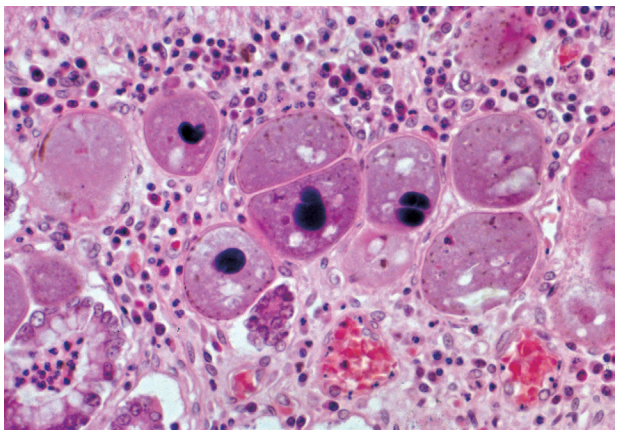


**Figure 15.7 (Left)**
Unusual appearance of *Balantidium coli* trophozoite in colonic mucosa. H x1000

**Figure 15.8 (Right)**
Multiple *Balantidium coli* trophozoites in wall of colon. x240

cleus (Fig 15.10) and a tiny micronucleus which is rarely observed (Fig 15.6). Cysts may also contain cytoplasmic inclusions, cellular debris, mucus, and food vacuoles (Fig 15.11). The ultrastructural and molecular characterization of *B. coli* have been reported but the molecular nature needs more study to be a useful tool for identification.[11]

### Life Cycle and Transmission

Trophozoites of *B. coli* usually inhabit the colon of the host. They divide asexually by transverse binary fission of the micronucleus, the macronucleus, and finally the cytoplasm. Rarely, they reproduce sexually by conjugation. Trophozoites encyst during transport through the intestine or externally in soft stool (Fig 15.12). In this process, a trophozoite becomes round, partially retracts its cilia, and secretes a cyst wall. Cysts can remain viable for several days in stool. The parasite excysts after it is ingested by another suitable host. Humans are infected by ingesting cysts, the infective stage of *B. coli*, in contaminated water or food. Pigs and rats are the most important reservoir hosts for *B. coli*.

## *Clinical Features and Pathogenesis*

*Balantidium coli* may inhabit the bowel lumen without invading tissue or provoking clinical symptoms. Parasites that invade tissue do so by mechanical action of the cilia and by lytic action, particularly in patients weakened by underlying factors such as malnutrition or immunosuppresion.[12]

Balantidiasis can mimic intestinal amebiasis. The acute form of the disease is marked by rapid onset of diarrhea or dysentery, with 20 bowel movements or more per day.[13] Other frequent complaints are abdominal colic, tenesmus, nausea, and vomiting. Chronic balantidiasis produces intermittent diarrheal episodes alternating with normal bowel movements or constipation. Patients may occasionally have headache, insomnia, anorexia, weight loss, or muscular weakness. *Balantidium coli* may cause appendicitis and lung involvement, and has been attributed to urinary tract disease.[14-17] Extra-abdominal balantidiasis occasionally develops in patients with cancer or post-organ transplantation.[18-20] Peripheral eosinophilia is not a feature of balantidiasis.

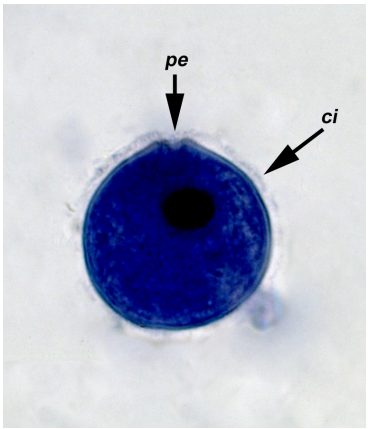



**Figure 15.9**
*Balantidium coli* trophozoite in colon demonstrating kidney-shaped macronucleus. Iron-hematoxylin x380

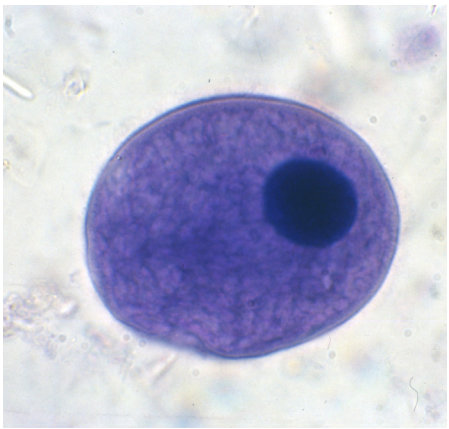


**Figure 15.10**
*Balantidium coli* cyst in stained stool specimen illustrating cyst wall and single large macronucleus. Iron-hematoxylin x860

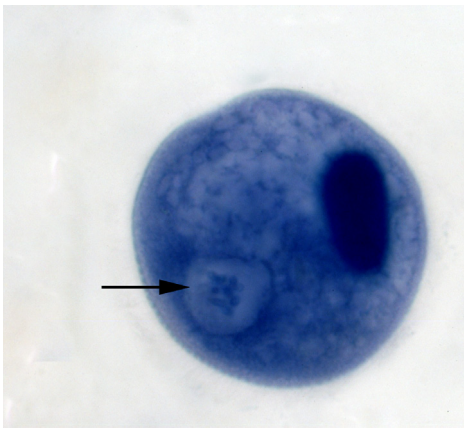


**Figure 15.11**
*Balantidium coli* cyst in stained stool specimen showing single large macronucleus and food vacuole (arrow) containing bacteria. Iron-hematoxylin x900

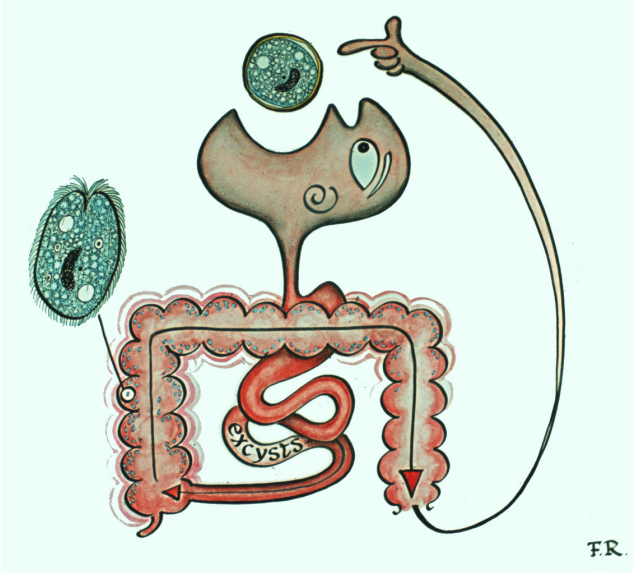



**Figure 15.12**
Life cycle of *Balantidium coli*. Humans usually acquire balantidiasis from infected pigs, although human-to-human transmission takes place. Ingested cysts excyst in the intestine to become trophozoites. Drawing by Frank O. Raasch.

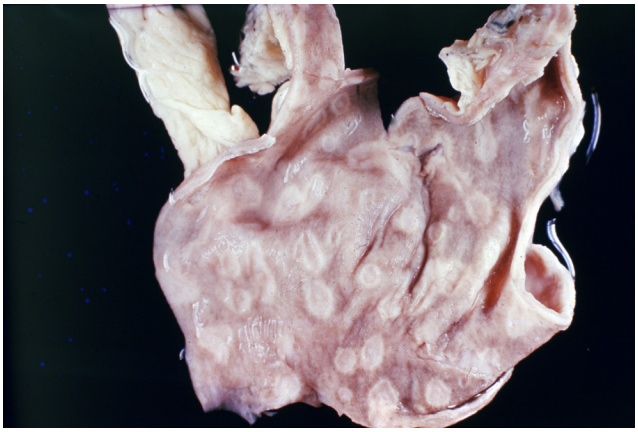


**Figure 15.13**
Numerous ulcers in colon of patient with balantidiasis. x1

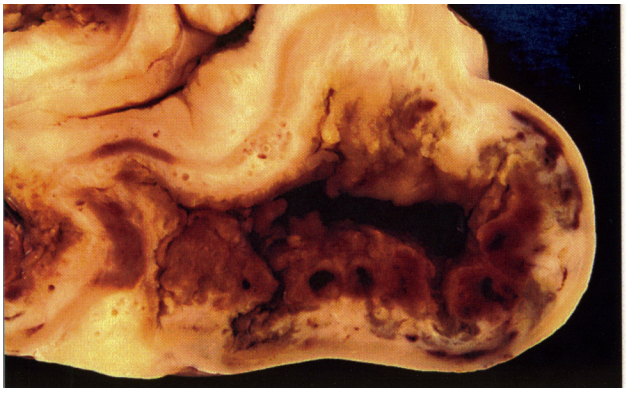


**Figure 15.14**
Necrotic lesion of large intestine caused by *Balantidium coli*. x60

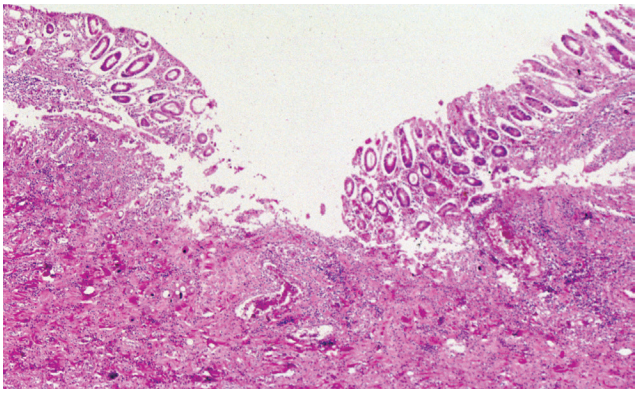


**Figure 15.15**
Flask-shaped ulcer in colon of patient with balantidiasis. x25

## Pathologic Features

Parasites usually invade the colon and appendix. Invasion of the ileum however, has been reported. Early lesions appear as flask-shaped ulcers a few millimeters in diameter, similar to those seen in intestinal amebiasis. Ulcer borders are frayed, swollen, and undermined (Fig 15.13). The surface is covered with a thick, friable, adherent mucous layer. Ulcers may be superficial or may perforate the intestinal wall (Fig 15.14), releasing parasites into the peritoneal cavity and causing peritonitis, and sometimes death.[21] Extraintestinal infections involving the liver, vagina, ureter, bladder, and lung have been reported but are extremely rare.[22,23]

Microscopically, coagulation necrosis containing trophozoites of *B. coli* forms the base of the ulcer (Fig 15.15). Trophozoites stain well with hematoxylin and eosin and are readily seen within the ulcer (Figs 15.16 to 15.19). The macronucleus stains black and, although it may vary considerably in shape, a kidney-shaped configuration is diagnostic (Fig 15.5). Trophozoites are usually more numerous at the periphery of the ulcer than in the necrotic center. There is edema of adjacent tissues, with infiltrates of chronic inflammatory cells, primarily lymphocytes and plasma cells (Fig 15.20). Neutrophils are insignificant unless there is secondary bacterial infection (Fig 15.21). Eosinophils have been reported, but are not a common finding.[2,24]

## Diagnosis

Diagnosis is established by identifying *B. coli* trophozoites or cysts in feces or scrapings from intestinal lesions. Only trophozoites are seen in biopsy specimens of infected tissues (Fig 15.1). Trophozoites usually appear in diarrheic stools; cysts appear in more solid stools. Trophozoites are actively motile in wet mounts of fresh feces. The macro-

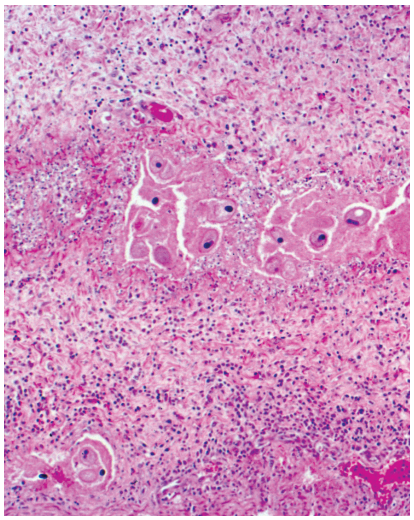


**Figure 15.16**
Several *Balantidium coli* trophozoites in necrotic area of colon. x60

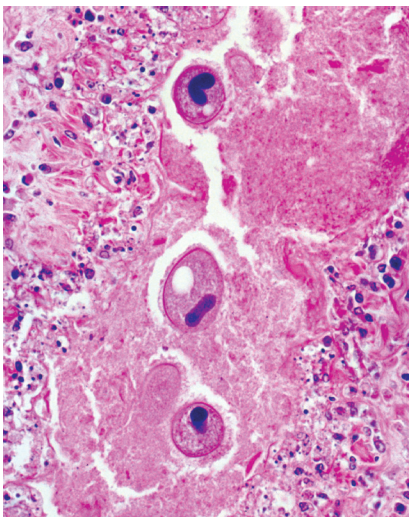


**Figure 15.17**
Higher magnification of *Balantidium coli* trophozoites shown in Figure 15.16. x235

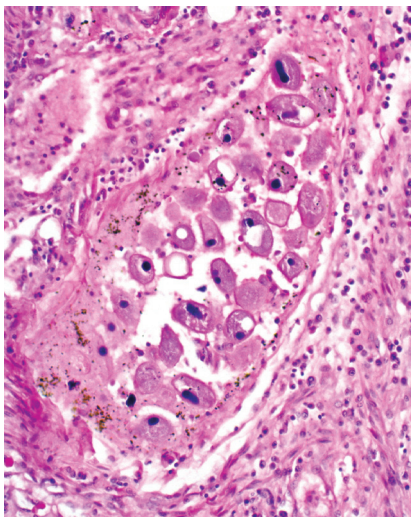


**Figure 15.18**
Cluster of *Balantidium coli* trophozoites in wall of colon. Note readily identifiable macronuclei. x120

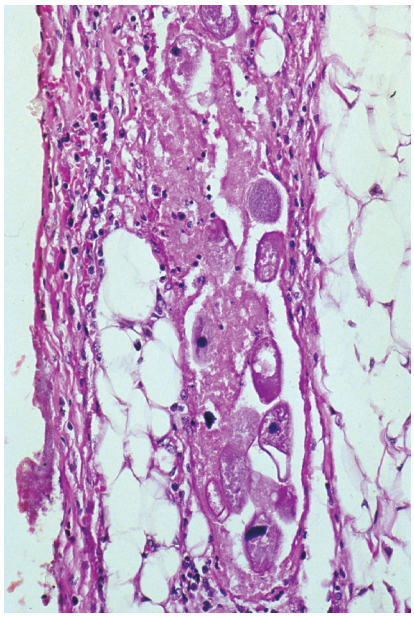


**Figure 15.19**
Trophozoites of *Balantidium coli* in inflamed, necrotic serosa of patient with peritonitis. x160

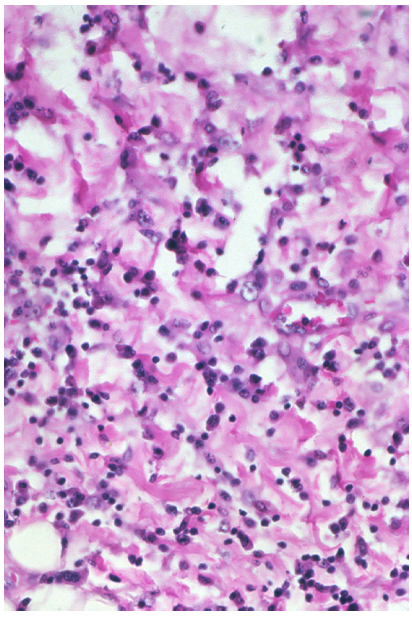


**Figure 15.20**
Inflammatory infiltrate adjacent to ulcer in wall of colon of patient with balantidiasis. Infiltrate is composed of plasma cells and lymphocytes. x245

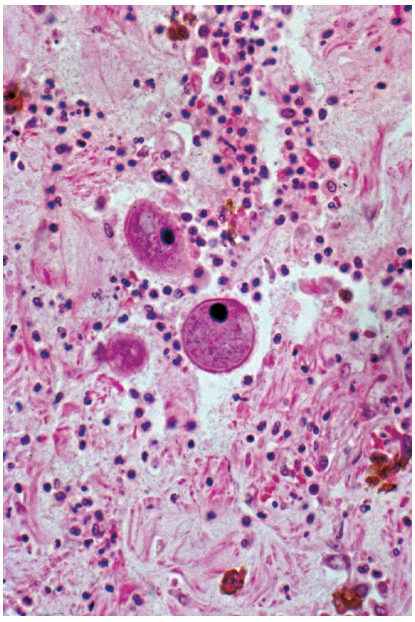


**Figure 15.21**
Trophozoites of *Balantidium coli* in colonic exudate composed primarily of neutrophils. Neutrophils suggest secondary bacterial infection. x235

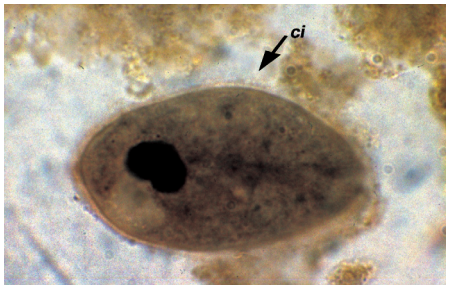



**Figure 15.22**
Trophozoite of *Balantidium coli* in feces. Note oval configuration, kidney-shaped macronucleus, vacuole in cytoplasm, and cilia (ci). Iron-hematoxylin. x590

nucleus stains well with iron-hematoxylin on smears from fresh stool (Fig 15.22). Diagnosis can also be made by identifying trophozoites in surgical, cytological,[25] and autopsy specimens (Figs 15.16 and 15.17). Special care must be taken in differentiating *B. coli* from ciliocytophthoria in nasopharyngeal specimens.[26]

## Treatment and Prevention

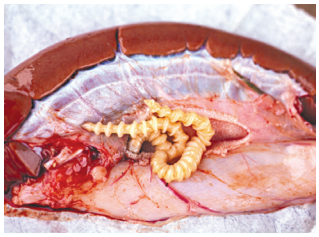
The drugs of choice for balantidiasis are tetracycline (for adults: 500 mg 4 times/day for 10 days), or iodoquinol (650 mg 3 times/day for 20 days), metronidazole (500 mg 2 times/day for 5 days); other drugs such as ampicillin, carbasone, diodoquin, nitrimidazine, and paromomycin have been used with varying results.[22,27,28] Effective sanitation and use of water from protected sources are the most useful measures of protection. Limiting exposure to pigs is helpful but often impractical.[29-32]

## References

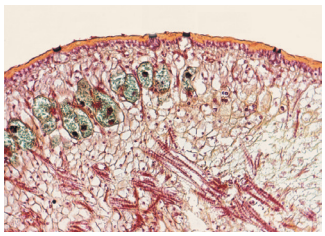

1. Kean BH, Mott KE, Russell AJ, eds. *Tropical Medicine and Parasitology Classic Investigations.* Vol 1. Ithaca, NY: Cornell University Press; 1978:173-177.
2. Arean VM, Koppisch E. Balantidiasis: a review and report of cases. *Am J Pathol.* 1956;32:1089-1115.
3. Nakauchi K. The prevalence of *Balantidium coli* infection in fifty-six mammalian species. *J Vet Med Sci.* 1999;61:63-65.
4. Esteban JG, Aguirre C, Angles R, Ash LR, Mas-Coma S. Balantidiasis in Aymara children from the northern Bolivian Altiplano. *Am J Trop Med Hyg.* 1998;59:922-927.
5. Ewers WH. Parasites of man in Papua-New Guinea. *Southeast Asian J Trop Med Public Health.* 1972;3:79-86.
6. Radford AJ. Balantidiasis in Papua New Guinea. *Med J Aust.* 1973;1:238-241.
7. Walzer PD, Judson FN, Murphy KB, Healy GR, English DK, Schultz MG. Balantidiasis outbreak in Truk. *Am J Trop Med Hyg.* 1973;22:33-41.
8. Giacometti A, Cirioni O, Balducci M, et al. Epidemiologic features of intestinal parasitic infections in Italian mental institutions. *Eur J Epidemiol.* 1997;13:825-830.
9. Labes EM, Hegglin D, Grimm F, et al. Intestinal parasites of endangered orangutans (*Pongo pygmaeus*) in Central and East Kalimantan, Borneo, Indonesia. *Parasitology.* 2010;137:123-135.
10. Toft JD 2d. The pathoparasitology of the alimentary tract and pancreas of nonhuman primates: a review. *Vet Pathol Suppl.* 1982;7:44-92.
11. Nilles-Bije ML, Rivera WL. Ultrastructural and molecular characterization of *Balantidium coli* isolated in the Philippines. *Parasitol Res.* 2010;106:387-394.
12. Vasilakopoulou A, Dimarongona K, Samakovli A, Papadimitris K, Avlami A. *Balantidium coli* pneumonia in an immunocompromised patient. *Scand J Infect Dis.* 2003;35:144-146.
13. Castro J, Vazquez-Iglesias JL, Arnal-Monreal F. Dysentery caused by *Balantidium coli*—report of two cases. *Endoscopy.* 1983;15:272-274.
14. Dodd LG. *Balantidium coli* infestation as a cause of acute appendicitis. *J Infect Dis.* 1991;163:1392.
15. Sharma S, Harding G. Necrotizing lung infection caused by the protozoan *Balantidium coli*. *Can J Infect Dis.* 2003;14:163-166.
16. Koopowitz A, Smith P, van Rensburg N, Rudman A. *Balantidium coli*-induced pulmonary haemorrhage with iron deficiency. *S Afr Med J.* 2010;100:534-536.
17. Maino A, Garigali G, Grande R, Messa P, Fogazzi GB. Urinary balantidiasis: diagnosis at a glance by urine sediment examination. *J Nephrol.* 2010;23:732-737.
18. Anargyrou K, Petrikkos GL, Suller MT, et al. Pulmonary *Balantidium coli* infection in a leukemic patient. *Am J Hematol.* 2003;73:180-183.
19. Yazar S, Altuntas F, Sahin I, Atambay M. Dysentery caused by *Balantidium coli* in a patient with non-Hodgkin's lymphoma from Turkey. *World J Gastroenterol.* 2004;10:458-459.
20. Barsoum RS. Parasitic infections in organ transplantation. *Exp Clin Transplant.* 2004;2:258-267.
21. Ferry T, Bouhour D, De Monbrison F, et al. Severe peritonitis due to *Balantidium coli* acquired in France. *Eur J Clin Microbiol Infect Dis.* 2004;23:393-395.
22. Garcia-Laverde A, de Bonilla L. Clinical trials with metronidazole in human balantidiasis. *Am J Trop Med Hyg.* 1975;24:781-783.
23. Ladas SD, Savva S, Frydas A, Kaloviduris A, Hatzioannou J, Raptis S. Invasive balantidiasis presented as chronic colitis and lung involvement. *Dig Dis Sci.* 1989;34:1621-1623.
24. Arean VM, Echevarria R. Balantidiasis. In: Marcial-Rojas RA, Moreno E, eds. *Pathology of Protozoal and Helminthic Diseases with Clinical Correlation.* Huntington, NY: Krieger Publishing Co; 1975:234-253.
25. Lahiri VL, Elhence BR, Agarwal BM. Balantidium peritonitis diagnosed on cytological material. *Acta Cytol.* 1977;21:123-124.
26. Hadziyannis E, Yen-Lieberman B, Hall G, Procop GW. Ciliocytophthoria in clinical virology. *Arch Pathol Lab Med.* 2000;124:1220-1223
27. Garcia LS. Flagellates and ciliates. *Clin Lab Med.* 1999;19:621-638.
28. Wolfe MS. Miscellaneous intestinal protozoa. In: Strickland GT, ed. Hunter's *Tropical Medicine and Emerging Infectious Diseases*. 8th ed. Philadelphia, Pa: WB Saunders; 2000:603-606.
29. Schuster FL, Ramirez-Avila L. Current world status of *Balantidium coli*. *Clin Microbiol Rev.* 2008;21:626-638.
30. Ogbolu DO, Alli OA, Ogunleye VF, Olusoga-Ogbolu FF, Olaosun I. The presence of intestinal parasites in selected vegetables from open markets in south western Nigeria. *Afr J Med Med Sci.* 2009;38:319-324.
31. Karanis P, Kourenti C, Smith H. Waterborne transmission of protozoan parasites: a worldwide review of outbreaks and lessons learnt. *J Water Health.* 2007;5:1-38.
32. Schuster FL, Visvesvara GS. Amebae and ciliated protozoa as causal agents of waterborne zoonotic disease. *Vet Parasitol.* 2004;126:91-120.


## Acknowledgement

**15.12**
Drawing by Frank O. Raasch







16

# Pentastomiasis

*Wayne M. Meyers and Ronald C. Neafie*

## *Introduction*

### Definition

Pentastomiasis is infection by pentastomes, which are organisms in the phylum Pentastomida (the approximately 95 species of the phylum, most correctly called pentastomids, are commonly known as pentastomes and will be so termed in this chapter). The single class within the phylum, Pentastomata, comprises 7 families in 2 orders, Porocephalida and Cephalobaenida. In the order Cephalobaenida, infections in humans by *Raillietiella hemidactyli* and *Raillietiella gehyrae* have been reported. Two families of the order Porocephalida—Porocephalidae and Linguatulidae—afflict humans. Infections by *Armillifer moniliformis, Armillifer grandis, Armillifer agkistrodontis, Armillifer najae, Leiperia cincinnalis,* and *Sebekia* sp are known[1,2] however, 2 species of porocephalida, *Armillifer armillatus* and *Linguatula serrata*, account for nearly all infections in humans.

### Synonyms

Pentastomiasis is also known as porocephaliasis. Infection by *L. serrata* is sometimes called linguatuliasis, but is more commonly known as tongue worm infection. Colloquial names for pentastomiasis include golf caddy's disease (Democratic Republic of the Congo (DRC)), halzoun (Middle East), and marrara (Sudan, Southwest Asia).

### General Considerations

Adult pentastomes are bloodsucking endoparasites of terrestrial vertebrates, almost exclusively reptiles, birds, and mammals (Figs 16.1 to 16.3). The name pentastome derives from an ancient misidentification of the 4 hooks and 1 mouth on the anterior end of the organism as 5 mouths.

The phylogeny of pentastomes has long been a puzzle. Various interpretations of the natural history of the Pen-



**Figure 16.1**
Rock python, a common definitive host of *Armillifer armillatus* in Africa.



**Figure 16.2**
Autopsy of rock python in Bas-Congo, DRC. Lung, digestive tract, and liver are being removed.



**Figure 16.4**
Adult female of *Armillifer armillatus* (10 by 0.8 cm) attached to respiratory epithelium of rock python shown in Figures 16.2 and 16.4. Note short cephalothorax (arrow) and long annulated abdomen.

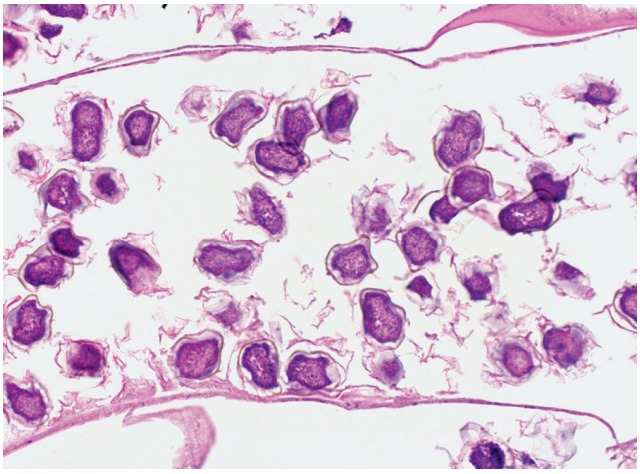


**Figure 16.5**
Eggs in section of oviduct of adult pentastomes in snake lung. X120

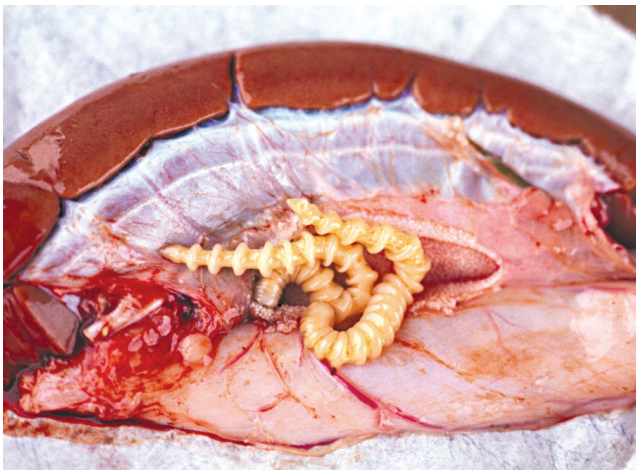


**Figure 16.3**
Two adult *Armillifer armillatus* attached to respiratory epithelium of rock python shown in Figure 16.2. Lung has been incised to reveal adult pentastomes.

tastomida place their possible divergence during the Cambrian explosion of multicellular organisms. Taxonomists initially placed them in either the phylum Annelida or the phylum Arthropoda.[3] Recent evidence, including molecular biologic findings, strongly suggests that pentastomes are closely related to crustacean arthropods, but most authorities today retain the unique minor phylum Pentastomida for these organisms.[4,5,6] A more comprehensive phylum called Lobopodia, which would include the closest relatives of the Arthropoda, such as pentastomes and related fossil forms, is under consideration.[7,8,9]

Pentastomiasis was among the earliest zoonotic parasitic diseases to be described. Pruner first described the infection in humans in Egypt in 1847. A year later, in Africa, Wyman discovered adult pentastomes in pythons.

## Epidemiology

Pentastomiasis is widespread, with most infections in humans occurring in Asia and tropical Africa. In Africa, infection is commonly by *A. armillatus*. In Asia, North Africa, Europe, and the Western Hemisphere, *L. serrata* is usually the infecting species, although rare imported *A. armillatus* infections have been reported.[10,11] *Porocephalus taiwana* infects humans in China.[2,12,13] Estimates of minimal prevalences have been established by detection of calcified, C-shaped, encysted larvae in radiologic films of the abdomen.[14] This method revealed a prevalence of 40% in midwestern Nigeria.[15] Autopsy series probably produce more accurate data. In Malaysia, larval pentastomes were found in over 45% of a series of consecutive autopsies from an aboriginal population.[16] A study in the DRC found an autopsy prevalence of 23%.[17] Seroepidemiologic surveys have so far yielded prevalences lower than those derived from autopsy.[18] However, advances in the serologic detection of pentastomiasis may provide more accurate data.[19,20]

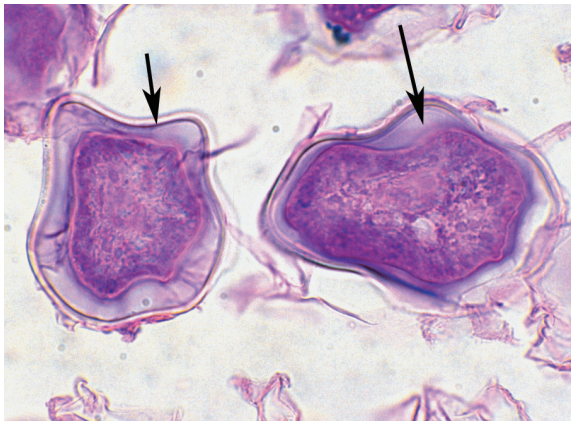


**Figure 16.6**
Higher magnification of unembryonated eggs in Figure 5, demonstrating thin outer shell (short arrow) and thick inner shell (long arrow). X600



**Figure 16.7**
Third-stage infective (nonencysted) larva of *Armillifer armillatus* attached to peritoneal surface of diaphragm, found at autopsy in Congolese patient. X3

## *Infectious Agent*

### Morphologic Description

Adult pentastomes are elongate and cylindrical or flat. In many species, the body is divided into 2 distinct regions: a short cephalothorax and a long abdomen (Fig 16.4). The cephalothorax is crowned by a mouth and 2 pairs of chitinized hooks. In some species (especially *A. armillatus*), pseudoannulations encircle the abdomen, but the body is not segmented. The number of annuli is a useful identifying feature—for example, 18 to 22 annuli in *A. armillatus*; 30 in *A. moniliformis*. Adults are a few millimeters to 15 cm long, depending on the species, and males are generally much smaller than females. Pentastomes have an extensive reproductive system and a primitive digestive tract, but no circulatory or respiratory system. Paired frontal glands lie alongside the gut for much of its length. Ducts from these glands open to the cuticular surface on the cephalothorax.[20,21] In the female, the genital pore is located on either the anterior (Cephalobaenida) or posterior (Porocephalida) end.

Pentastome eggs are ovoid and double-shelled (Figs 16.5 and 16.6). Eggs vary considerably in size according to species (average 105 by 125µm) and are embryonated when deposited. The embryo emerges as a first-stage larva with rudimentary appendages (see life cycle). The larva molts twice, loses its appendages, and develops into a third-stage larva, the infective form commonly found in humans (Fig 16.7). The larva attaches to host tissue by hooks on its anterior end (Fig 16.8). Although smaller, infective third-stage larvae are morphologically similar to adult pentastomes. The cuticle of the third-stage larva is smooth (Fig 16.9) in all species infecting humans except *L. serrata*, which has a spiny cuticle (Figs 16.10 and 16.11).

In tissue sections, larvae display several distinctive histologic anatomic features.[22] In cross section, the frontal glands, also called acidophilic glands, appear as red aggregates of cells and matrix around the digestive tube (Fig 16.12). The cuticle is 5 to 10 µm thick and has sclerotized openings (Figs 16.9 and 16.13). The subcuticular area contains subcutaneous glands, and striated muscle fibers are arranged in circular and longitudinal patterns in the organism's parenchyma (Fig 16.9).[23]

### Life Cycle and Transmission

Each stage in the life cycle of a pentastome is parasitic. Adult Porocephalidae inhabit the respiratory passages of reptiles, and adult Linguatulidae the nasal passages of mammals. Numerous species of vertebrates serve as intermediate hosts, including humans, nonhuman primates,dogs and, most commonly, rodents.[13,24-26] Direct infection that bypassed the intermediate host has been seen in stressed captive lizards, but in such instances the infective larvae did not develop into adults.[27] Occasionally, both adults and third-stage larvae have been found in infected snakes, representing true autoinfection.[28]

The life cycle of *A. armillatus* typifies the stages of a common porocephalida pentastome in the definitive (snake) and intermediate (usually rodent) host (Fig 16.14). Using their anterior hooks, male and female adults attach to the respiratory epithelium of snakes such as the rock python (*Python sebae*) and some cobras and vipers (Fig 16.3). Copulation takes place 3 to 4 months after infection of a definitive host. Approximately 4 to 8 months later, fertilized females begin to deposit embryonated eggs. The eggs are carried by respiratory secretions to the snake's oral cavity, where they are either discharged or swallowed and ejected in the feces.[29,30] Vegetation and water contaminated with these eggs are sources of infection for intermediate rodent hosts.

In rodents, ingested eggs hatch, releasing first-stage larvae in the digestive tract. Larvae apparently use a stylet ex-

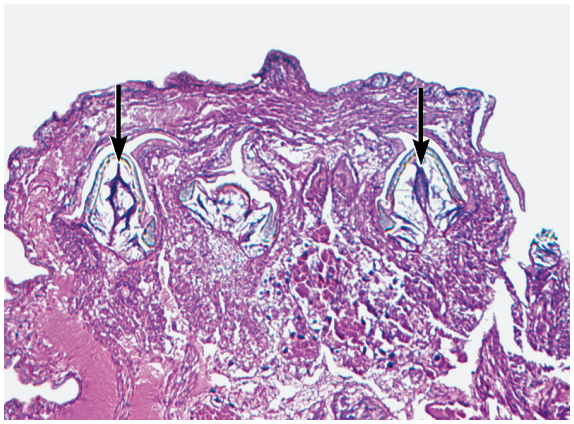


**Figure 16.8**
Section of anterior end of pentastome larva removed from human gut wall, showing 2 of 4 hooks (arrows). X57

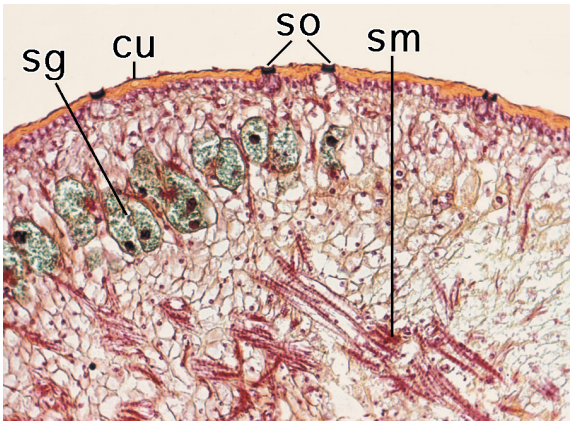



**Figure 16.9**
Section of *Armillifer armillatus* removed from human liver. Cuticle (cu) is smooth but punctuated by sclerotized openings (so). Subcuticular glands (sg) and striated muscle (sm) are prominent. Movat X60

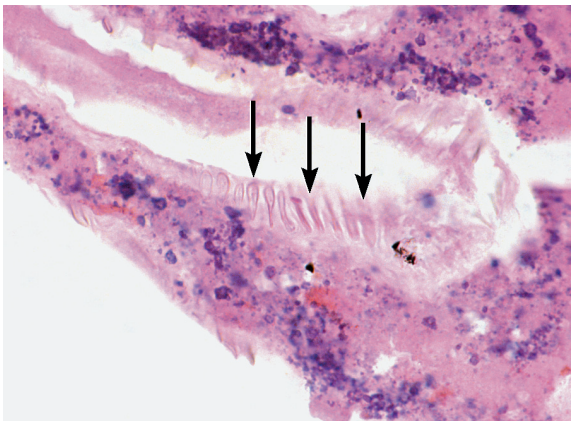


**Figure 16.10**
Cuticle of degenerated *Linguatula serrata* in liver, showing numerous spines (arrows). X380

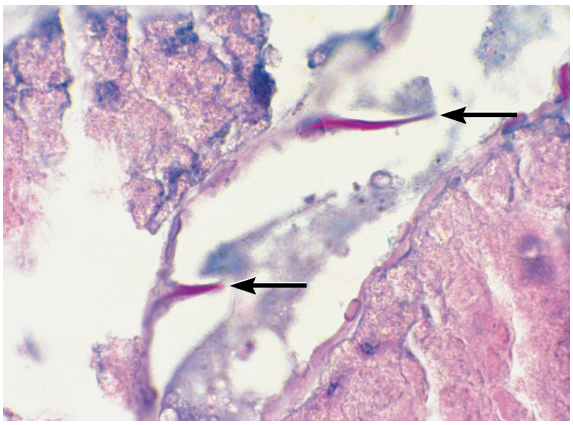


**Figure 16.11**
Spines (arrows) on degenerated cuticle of *Linguatula serrata* are acid-fast with Ziehl-Neelsen stain. X600

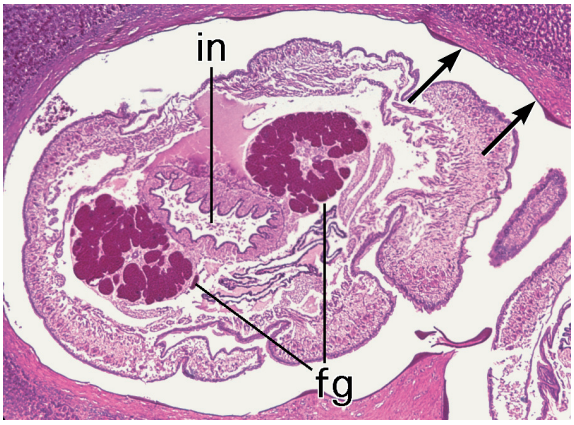



**Figure 16.12**
Encysted *Armillifer armillatus* larva in liver. Shed cuticle from previous molt lines cyst wall (arrows). Acidophilic frontal glands (fg) lie along intestine (in). X21

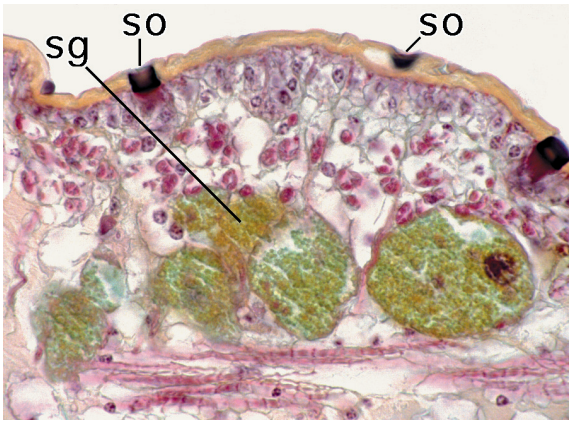



**Figure 16.13**
Detail of encysted infective larva in lung. Black cylindrical sclerotized openings (so) in cuticle and green subclavicular glands (sg) are prominent in Movat-stained section. X425

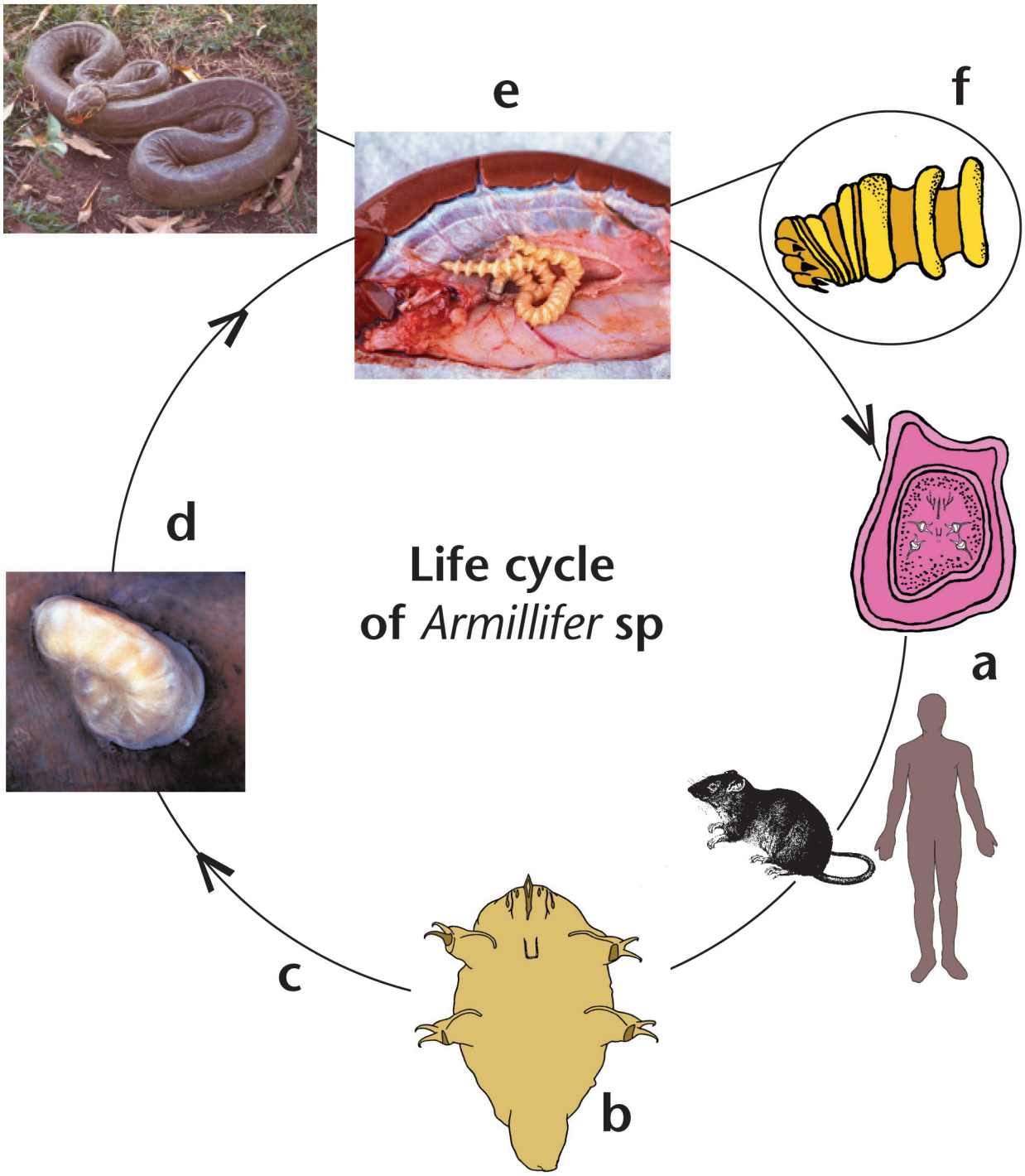



**Figure 16.14**
Life cycle of *Armillifer* sp. **a**) Eggs (usually embryonate and passed in respiratory secretions, saliva, or feces are ingested by secondary host—usually a rodent. **b**) 1st stage larva emerge, penetrate gut of secondary host, migrate, and encyst in various host tissues. In humans, invasion by 1st-stage larvae is asymptomatic. **c**) Larvae molt twice. **d)** 3rd-stage larvae in tissues of animal or human secondary host can excyst and migrate. In natural infection, encysted and free larvae ingested by definitive host migrate to respiratory tract to complete development. Photo shows encysted larva. e**)** Adults inhabit respiratory tract of definitive host (African rock python shown). **f**) Head of adult *Armillifer* sp has 4 hooks for attaching to host tissue.



**Figure 16.15**
Encysted *Armillifer armillatus* larva on liver of Congolese adult. Cyst is 0.6 by 1 cm and characteristically C-shaped.

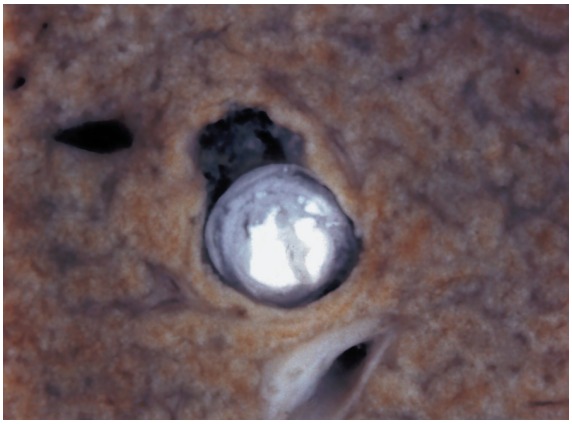


**Figure 16.16**
Cut surface of liver from patient described in Figure 16.15, showing encysted *Armillifer armillatus*. Cyst is 3 mm in diameter.

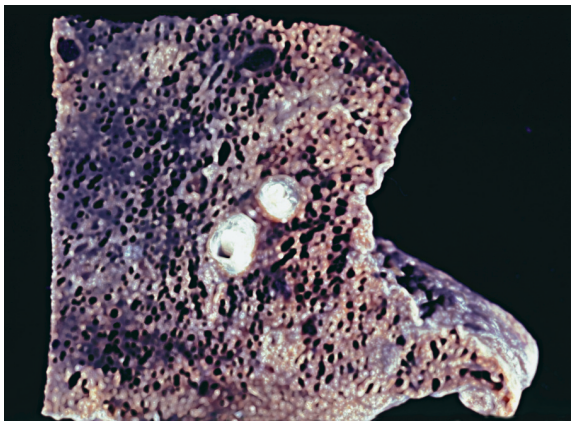


**Figure 16.17**
Two encysted *Armillifer armillatus* larvae in cut surface of lung of patient described in Figure 16.15. Larvae are 3 mm in diameter.

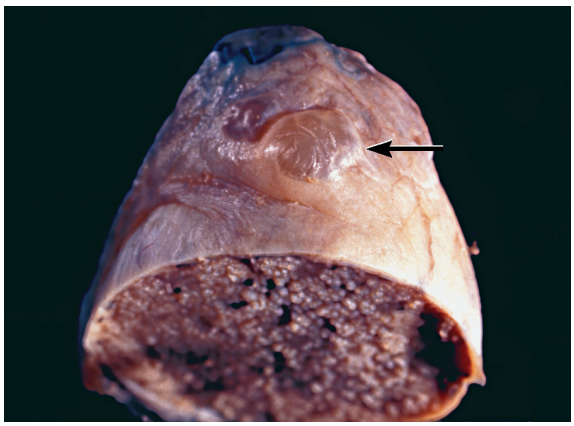


**Figure 16.18**
Encysted *Armillifer armillatus* larva (arrow) in tunica of testis of patient described in Figure 16.15. Cyst is 1.5 by 1 cm.

tending from their anterior end to penetrate the rodent's gut wall, although enzymatic activity of the frontal gland secretions may play a role in tissue invasion.[20] From observations on a pentastome of alligators (*Sebekia mississippiensis*), Boyce and Kazacos showed that larval pentastomes could breech the gut wall of experimentally infected hamsters, a potential paratenic host for this parasite, in 1 to 3 days.[31] First-stage larvae may migrate by passing through the entire thickness of the gut wall and entering the abdominal cavity, or by invading a blood or lymphatic vessel in the gut wall, mesentery, omentum, or other intra-abdominal site, and spreading hematogenously.[23] By whichever route, larvae can disseminate rapidly and widely in an intermediate host. At this stage, larvae lose their appendages, molt, and encyst in or on virtually any organ or structure (Figs 16.15 to 16.18). Whether or not all larvae encyst is controversial. A series of several molts results in infective third-stage larvae, often called nymphs. The cycle is maintained when a definitive snake host devours an infected intermediate host, usually a rodent. In the snake, infective larvae migrate from the stomach up the esophagus and into the lung, where they mature into adults and complete the life cycle. In aberrant intermediate hosts (humans or other large mammals), larvae eventually die, interrupting the life cycle.

The life cycles of all the pentastomes that infect humans vary in ways too numerous to describe here, but the life cycle of *L. serrata* deserves brief mention. Adult *L. serrata* inhabit the nasopharynx of mammalian carnivores such as dogs, foxes, or wolves. Embryonated eggs exit in nasal secretions of these definitive hosts. Herbivorous animals (intermediate hosts, typically sheep and goats) ingest the embryonated eggs. Eggs hatch, releasing first-stage larvae that penetrate the gut and develop and encyst in a manner similar to *A. armillatus*. When humans ingest first-stage *L. serrata* larvae, the larvae likewise penetrate the gut and encyst in various tissues (Fig 16.19). The normal life cycle is completed when a carnivorous definitive host devours the

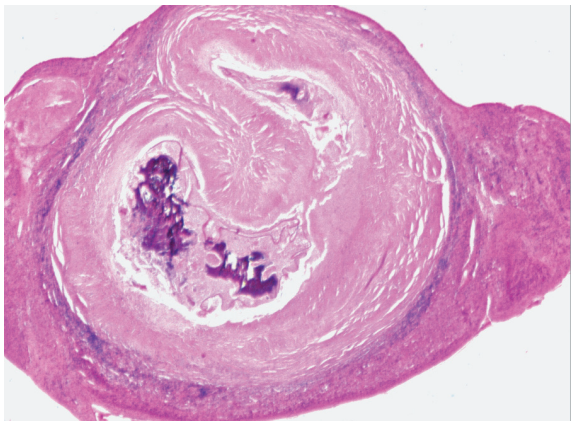


**Figure 16.19**
Section of degenerating *Linguatula serrata* larva in human liver. Note mineralization, which appears in radiographs as C-shaped opacity. X15



**Figure 16.20**
Larva of *Armillifer armillatus* extracted from inflammatory mass in conjunctiva of adult Congolese.

flesh of an intermediate host. When humans eat improperly cooked or raw flesh of an intermediate host, infective larvae migrate to the throat, where they attach and provoke the halzoun or marrara syndromes. Larvae of *L. serrata* have rarely developed into adults in the nasal cavity of humans.

## Clinical Features and Pathogenesis

Humans are usually highly tolerant of infection by pentastomes. Some authorities attribute this tolerance to the immunomodulatory effect of the frontal gland secretions that coat the larvae's cuticle and facilitate evasion of the host immune response.[20] The initial phase of pentastomiasis in all intermediate hosts is probably the penetration of the gut wall by first-stage larvae, after embryonated eggs have been ingested in contaminated meat, water, or vegetation. This asymptomatic phase has been described in animals but never directly observed in human tissue. In the abdomen, first-stage larvae molt twice and develop into infective third-stage larvae. Most, but not all, third-stage larvae encyst and lodge in various sites, showing a predilection for the mesentery and peritoneum, and on or within parenchymatous abdominal organs. First-stage larvae that enter the lymphatic or blood system in the gut wall frequently invade the lungs and occasionally the brain, but may appear in virtually any site.

Even when infection involves numerous third-stage larvae, pentastomiasis is usually asymptomatic. However, as the developing larvae gradually enlarge, they may exert pressure on surrounding structures, causing complications such as biliary obstruction. In the eye, pentastomes may cause multiple lesions, including iritis, subluxation of the lens, secondary glaucoma, conjunctivitis, and invasion of lacrimal caruncles.[32,33,34] Figures 16.20 to 16.23 depict a larva of *A. armillatus* extracted from a conjunctival mass near the lacrimal caruncle of a Congolese patient. When excised, the mass, which had developed over the course

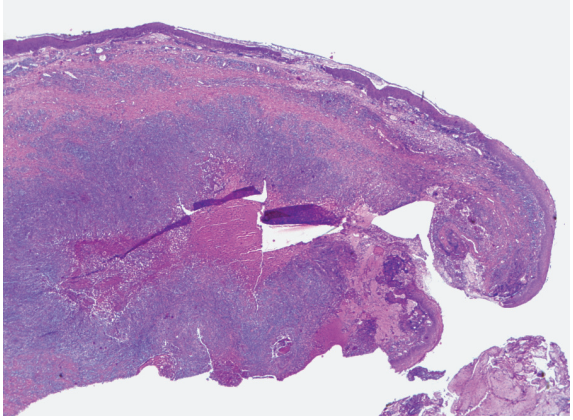


**Figure 16.21**
Section of inflammatory mass in conjunctiva of patient described in Figure 16.20. X110

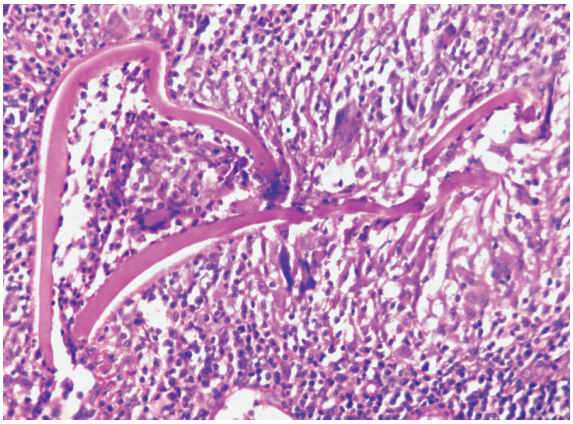


**Figure 16.22**
Detail of Figure 21 showing cuticular fragments from earlier molt of pentastome larva depicted in Figure 20. X 175



**Figure 16.23**
Movat pentachrome stain reveals black cylindrical sclerotized openings (arrows) in cuticular fragment shown in Figure 16.22. X430



**Figure 16.24**
Encysted *Armillifer armillatus* larva in human lung demonstrating typically slight tissue reaction in intermediate host. Movat x11

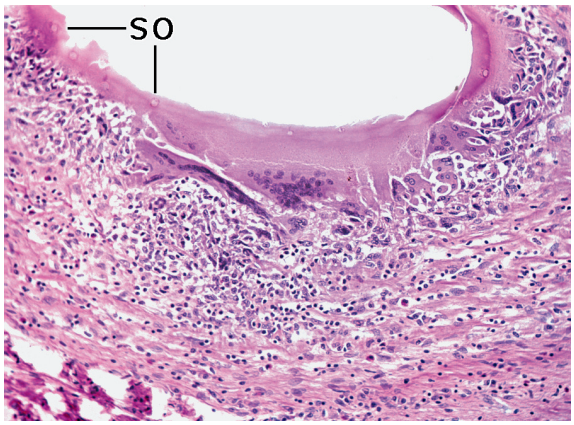



**Figure 16.25**
Degenerating cyst of *Armillifer armillatus* larva in intra-abdominal lymph node. Sclerotized openings (so) confirm diagnosis of pentastomiasis. X100

of a year and caused marked chronic irritation, had areas of extensive inflammation in which there were identifiable cuticular elements of a pentastome, such as the diagnostic sclerotized openings. Although numerous other conditions have been attributed to pentastomes, including pneumonitis, collapsed lung, peritonitis, nephritis, meningitis, and pericarditis, in most cases only a tenuous causal relationship has been established.[35,36,37]

Patients sometimes present with acute abdominal symptoms, and intestinal obstruction has been observed. Most often, however, laparotomy findings reveal only variable numbers of encysted larvae[38] or nonencysted free or attached larvae. Intestinal adhesions are sometimes associated with pentastomiasis.[39] Pentastomiasis may mimmic hepatoma clinically.[40] Pentastomiasis has resulted in 2 reported fatalities. One patient died of fulminant septicemia.[36] The other, a 5-year-old girl, had a massive *A. grandis* infection that produced generalized disease, with large numbers of larvae in the lung and brain. It was suggested that the patient had ingested a gravid pentastome.[5,41] In 1989, Mairena et al described a dermatitis caused by a *Sebekia* sp larva in Costa Rica.[42] The patient presented with marked peripheral eosinophilia and a pruritic serpiginous burrow on the abdomen, from which a 1 cm long larva was removed. Some researchers speculate that pentastomes provoke malignancies.[43] Based on our own observations and those of Fain[44] and Hopps et al,[28] we consider the association of pentastomiasis and cancer to be tenuous.

The halzoun and marrara syndromes are characterized by discomfort in the nasopharynx and throat, accompanied by paroxysmal coughing, sneezing, and sometimes dysphagia and vomiting.[45] These syndromes result when third-stage larvae ingested in raw flesh of an intermediate host migrate from the upper gastrointestinal tract to the throat and nasopharynx. Halzoun and marrara are most common in the Middle East and the Sudan. Hypersensitivity reactions may lead to dyspnea or even fatal asphyxia. Rarely, infective larvae in the nasopharynx develop into adults.

## Pathologic Features

In a definitive host, adult pentastomes do not provoke significant tissue reaction (Figs 16.3 and 16.4).[28] Flach et al depict a primary larva of a *Sambonia* sp pentastome in the intestinal wall of a monitor lizard (*Varanus exanthematicus*) provoking only slight cellular response.[27] In an intermediate host, tissue reaction to pentastome larvae varies[31] but is usually slight (Fig 16.24), suggesting to some authorities that the excretory/secretory proteins coating the cuticle of pentastomes may have immunomodulatory properties.[20,46] Inflammatory response around larvae can nevertheless be marked (Fig 16.21). In animals, the route of invasion has been described. In humans, although it has not been observed, the gastrointestinal tract is the presumed route of

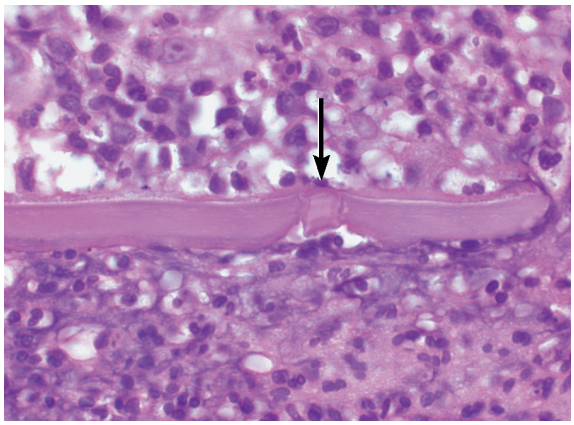


**Figure 16.26**
Conjunctival lesion containing fragment of cuticle of *Armillifer armillatus* larva. Sclerotized opening (arrow) is readily seen in H&E-stained section. X590

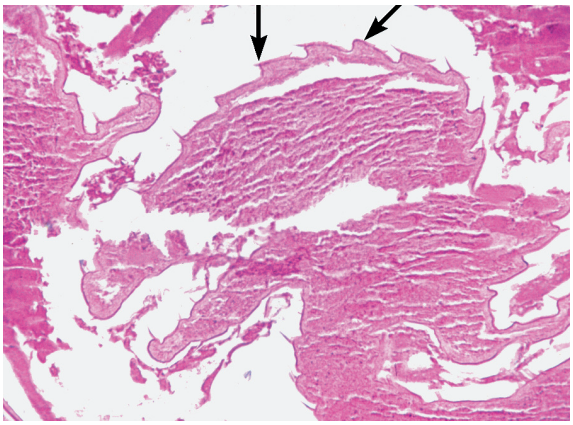


**Figure 16.27**
Cuticular fragments of *Linguatula serrata* with numerous cuticular spines (arrows). X135

invasion. Within the intestinal wall, or soon after breeching it, larvae develop into advanced forms within the abdominal cavity, or enter lymphatic or blood vessels and disseminate.[5,12,47] Following a series of molts, third-stage larvae usually encyst on or within abdominal organs or the peritoneum.[48] We have observed numerous infective larvae of *A. armillatus* at autopsies in the DRC. In the abdominal cavity of a single cadaver, we have observed encysted, nonencysted-free, and nonencysted-attached infective larvae (Figs 16.7, and 16.15 to 16.18). It is possible that the free forms had excysted after the death of the host, but since no sites consistent with recently evacuated cysts were identified, it is more likely that the free forms had never encysted.

Typically, a cyst encases a larva in a thin fibrous wall (Figs 16.12 and 16.24). As the larva molts, cuticular material merges with the lining of the cyst wall, preserving in these layers the pentastome's sclerotized cuticular openings (Fig 16.25). The same process preserves the spines of an *L. serrata* larva. After a few years, the encysted larva dies, and a granuloma may develop in response to the antigenic products of degeneration.[49] A degenerating larva can be identified by the sclerotized openings in cuticular elements—usually the longest-lasting remnants. A hyalinized calcified nodule is the final stage of an encysted pentastome (Fig 16.19).

## Diagnosis

Calcified encysted third-stage larvae are usually an incidental finding in radiographs of the abdomen or at surgery or autopsy. Histopathologic diagnosis can usually be readily made by demonstrating typical morphologic features in well-preserved larvae. Even in highly degenerated larvae, the unique sclerotized openings in the cuticle are often detectable in H&E-stained sections (Fig 16.26); however, the Movat pentachrome stain demonstrates these structures best (Fig 16.13). Cuticular spines, that may be acid-fast, distinguish *L. serrata* larvae from *A. armillatus* larvae (Figs 16.10, 16.11, and 16.27). Serologic tests using immunofluorescence, gel diffusion, and immunoelectrophoresis are available but not highly sensitive.[18] An ELISA based on the 48 kDa frontal gland metalloproteinase of pentastomes may increase the efficacy of serologic testing.[19] Molecular methods are available for some species.[13]

In tissue sections, pentastomes can be mistaken for any parasitic metazoan, especially cysticerci, spargana, nematodes, and fly larvae. However, none of these organisms has sclerotized openings in the cuticle, and cysticerci, spargana, and nematodes do not have striated muscle. Fly larvae do have striated muscle, but they also have numerous tracheal tracts which pentastomes do not have.

## Treatment and Prevention

Pentastomiasis in humans does not usually require treatment. However, patients who become symptomatic, such as those with halzoun or marrara, may require surgical removal of free or encysted parasites in the eye, throat, or nasal passages. Hypersensitivity reactions brought on by these syndromes may be treated with antihistamines and/or corticosteroids. Exploratory surgery may be warranted for patients with acute abdominal symptoms or those with radiologic or serologic evidence of pentastomiasis. Infected mammals, snakes, and captive monitor lizards have been successfully treated with ivermectin, sometimes combined with corticosteroids to reduce inflammation and surgery to remove dead pentastomes.[27,50] There are no reports of humans being treated with ivermectin, but the drug's efficacy in humans should be investigated. Diethylcarbamizine has been suggested as a treatment for linguatuliasis, but its usefulness has not been established.

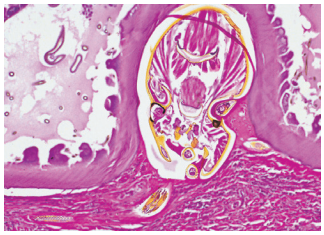
In general, pentastome infections in humans can be pre-

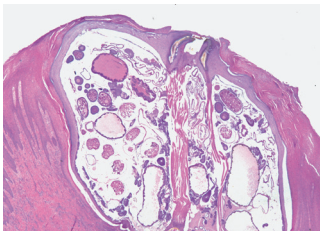
vented by adequate sanitary precautions and by avoiding the consumption of raw snake and other exotic meats.

## References


1. Warrell DA. Pentastomiasis (porocephalosis, linguatulosis/linguatuliasis). In: Warrell DA, Cox TM, Firth JD, eds. *Oxford Textbook of Medicine*. Vol 1. Oxford, UK: Oxford University Press; 2010:1237-1240.
2. Qiu MH, Ma KC, Fan PC, Lu SS. [Discovery of a new species of the pentastomid genus Porocephalus (Humboldt, 1811) from Taiwan, China and its pathogenic features] [Article in Chinese] Zhongguo Ji Sheng Chong Xue Yu Ji Sheng Chong Bing Za Zhi. 2005;23:69-72.
3. Self JT. Biological relationships of the pentastomida: a bibliography on the pentastomida. *Exp Parasitol.* 1969;24:63-119.
4. Abele LG, Kim W, Felgenhauer BE. Molecular evidence for the inclusion of the phylum Pentastomida in the Crustacea. *Mol Biochem Evol*. 1989;6:685-691.
5. Cagnard V, Nicolas-Randegger J, Dago Akribi A, et al. Generalized and lethal pentastomiasis due to *Armillifer grandis* (Hett, 1915) [in French]. *Bull Soc Pathol Exot Filiales*. 1979;72:345-352.
6. Gould SJ. Of tongue worms, velvet worms, and water bears. *Nat Hist.* 1995;104:6-15.
7. Palmer AR. Whither Pentastomida? *Nature*. 1993;361:214.
8. Ramskold L, Xianguang H. New early Cambrian animal and onychophoran affinities of enigmatic metazoans. *Nature*. 1991;351:225-228.
9. Shear WA. End of the 'Uniramia' taxon. *Nature*. 1992;359:477-478.
10. Guardia SN, Sepp H, Scholten T, Morava-Protzner I. Pentastomiasis in Canada. *Arch Pathol Lab Med*. 1991;115:515-517.
11. Dakubo JC, Etwire VK, Kumoji R, Naaeder SB. Human-pentastomiasis: a case report. *West Afr J Med*. 2006;25:166-168.
12. Min Hua Yao, Fang Wu, Lan Fang Tang. Human pentastomiasis in China: Case report and literature review. *J Parasitol.* 2008;94:1295-1298.
13. Brookings MD, Wellehan JF, Roberts JF, et al. Massive visceral pantastomiasis caused by *Porocephalus crotali* in a dog. *Vet Pathol*. 2009;46:460-463.
14. Lindner RR. Retrospective x-ray survey for porocephalosis. *J Trop Med Hyg.* 1965;68:155. .
15. Azinge NO, Ogidi-Gbegbaje EG, Osunde JA, Oduah D. *Armillifer armillatus* in Bendel State (Midwest) Nigeria (a village study in Ayogwiri Village, near Auchi, 120 kilometres from Benin City) phase I. *J Trop Med Hyg*. 1978;81:76-79.
16. Prathap K, Lau KS, Bolton JM. Pentastomiasis: a common finding at autopsy among Malaysian aborigines. *Am J Trop Med Hyg*. 1969;18:20-27.
17. Mouchet R. A note on *Porocephalus moniliformis* [in French]. *Bull Soc Pathol Exot.* 1914;7:497-501.
18. Nozais JP, Cagnard V, Doucet J. Pentastomosis. A serological study of 193 Ivorians [in French]. *Med Trop (Mars).* 1982;42:497-499.
19. Jones DA, Riley J. An ELISA for the detection of pentastomid infections in the rat. *Parasitology*. 1991;103:331-337.
20. Jones DA, Riley J, Kerby NW, Knox DP. Isolation and preliminary characterization of a 48-kilodalton metalloproteinase from the excretory/secretory components of the frontal glands of Porocephalus pentastomids. *Mol Biochem Parasitol*. 1991;46:61-72.
21. Brusca RC, Brusca GJ. *Invertebrates*. Sunderland, Mass: Sinauer Associates; 1990:680-694.
22. Tappe D, Büttner DZ. Diagnosis of human visceral pentastomiais. *PLoS Negl Trop Dis*. 2009;3:e320.
23. Chitwood MB, Lichtenfels JR. Identification of parasitic metazoa in tissue sections. *Exp Parasitol*. 1972;32:407-519.
24. Field KJ, Griffin HE, Sigler RE. Diagnostic exercise: abdominal parasites in an Asian macaque. *Lab Anim Sci.* 1991;41:504-505.
25. Lok JB, Kirkpatrick CE. Pentastomiasis in captive monkeys. *Lab Anim Sci.* 1987;37:494-496.
26. Ogunsusi RA, Mohammed AN. The chimpanzee (*Pan troglodytes*), a new host for nymphal *Armillifer armillatus* (Pentastomida: Porocephalida) in West Africa. *Rev Elev Med Vet Pays Trop.* 1978;31:361-362.
27. Flach EJ, Riley J, Mutlow AG, McCandlish IA. Pentastomiasis in Bosc's monitor lizards (*Varanus exanthematicus*) caused by an undescribed Sambonia species. *J Zoo Wildl Med*. 2000;31:91-95.
28. Hopps HC, Keegan HL, Price DL, Self JT. Pentastomiasis. In: Marcial-Rojas RA, ed. *Pathology of Protozoal and Helminthic Diseases*. Baltimore, Md: Williams & Wilkins; 1971:970-989.
29. Dakubo J, Naaeder S, Kumoji R. Totemis, and the transmission of human pentastomiasis. *Ghana Med J*. 2008;42:165-168.
30. Riley J. The biology of the pentastomids. *Adv Parasitol.* 1986;25:45-128.
31. Boyce WM, Kazacos EA. Histopathology of nymphal pentastomid infections (*Sebekia mississippiensis*) in paratenic hosts. *J Parasitol.* 1991;77:104-110.
32. Lang Y, Garzozi H, Epstein Z, Barkay S, Gold D, Lengy J. Intraocular pentastomiasis causing unilateral glaucoma. *Br J Ophthalmol.* 1987;71:391-395.
33. Lazar M, Traub Z. *Armillifer armillatus* in a human eye. *Am J Ophthalmol.* 1967;63:1799-1800.
34. Polderman AM, Manschot WA. *Armillifer armillatus* located within the lacrimal caruncle. *Acta Leiden*. 1979;47:71-77.
35. Drabick JJ. Pentastomiasis. *Rev Infect Dis*. 1987;9:1087-1094.
36. Tiendrebeogo H, Levy D, Schmidt D. Human pentastomiasis in Abidjan. A report on 29 cases [in French]. *Rev Fr Mal Respir.* 1982;10:351-358.
37. Yapo Ette H, Fanton L, Adou Bryn KD, Botti K, Malicier D. Human pentastomiasis discovered postmortem. *Forensic Sci Int*. 2003;52-54.
38. Herzog U, Marty P, Zak F. Pentastomiasis: case report of an acute abdominal emergency. *Acta Trop*. 1985;42:261-271.
39. Fisch A, Leport J, Bloch F, Sebag A, Frija J, Petite JP. Human pentastomiasis: clinical, radiological and x-ray computed tomographic study of a case [in French]. *Gastroenterol Clin Biol.* 1985;9:263-265.
40. Machado MS, Makdissi FF, Canedo LF, et al. Unusual case of pentastomiasis mimicking liver tumor. *J Gastroenterol Hepatol*. 2006; 21:1218-1220.
41. Magnino S, Colin P, Dei-Cas E, et al. Biological risks associated with consumption of reptile products. *Int J Food Microbiol*. 2009;134:163-175.
42. Mairena H, Solano M, Venegas W. Human dermatitis caused by a nymph of Sebekia. *Am J Trop Med Hyg*. 1989;41:352-354.
43. Smith JA, Oladiran B, Lagundoye SB, Lawson EA, Francis TI. Pentastomiasis and malignancy. *Ann Trop Med Parasitol.* 1975;69:503-512.
44. Fain A. Pentastomiasis in humans [in French]. *Bull Acad R Med Belg.* 1960;25:516-532.
45. Khalil GM, Schacher JF. *Linguatula serrata* in relation to halzoun and the marrara syndrome. *Am J Trop Med Hyg*. 1965;14:736-746.
46. Ambrose NC, Riley J. Further evidence for the protective role of sub-parietal cell membranous secretory product on the cuticle of a pentastomid arthropod parasite developing in its rodent intermediate host. *Tissue Cell.* 1989;21:699-722.
47. Ong HC. An unusual case of pentastomiasis of the fallopian tube in an Aborigine woman. *J Trop Med Hyg*. 1974;77:187-189.
48. Latrive JP, Trinh Dinh Hy, Ho Thi Sang, Huguier M, Le Quintrec Y. Liver abscess and visceral linguatulosis with *Linguatula serrata*. A case report with radiologic and histologic studies (author's transl) [in French]. *Sem Hop*. 1980;56:567-569.
49. Gardiner CH, Dyke JW, Shirley SF. Hepatic granuloma due to a nymph of *Linguatula serrata* in a woman from Michigan: a case report and review of the literature. *Am J Trop Med Hyg*. 1984;33:187-189.
50. Haugerud RE, Nilssen AC, Rognmo A. On the efficacy of ivermectin against the reindeer sinus worm *Linguatula arctica* (Pentastomida), with a review of ivermectin treatment in reindeer. *Rangifer*. 1993;13:157-162.







17

# Tungiasis

*J. Kevin Baird, Ronald C. Neafie, and Wayne M. Meyers*

## Introduction

### Definition

Tungiasis is infection by the flea *Tunga penetrans.* Infection in humans is acquired when the female *T. penetrans* penetrates the outer layers of skin. After copulating and taking a blood meal, the gravid flea grows within the superficial layers of the skin causing a painful, pea-sized nodule.[1] While the disease is usually limited to one or several lesions, one of the authors (WMM) has treated patients in Africa with tungiasis that involved up to 30% of the body surface. Typically, these individuals were severely debilitated and malnourished, such as patients with advanced untreated lepromatous leprosy who had been abandoned to the earthen floors of isolated village huts.

### Synonyms

*Tunga penetrans* is known by many other names, such as *Sarcopsylla penetrans, Dermatophilus penetrans, Rhynchoprion penetrans, Pulex penetrans,* chigoe, chigger, chique, jigger, sand flea, nigua, and pique. Jigger is the most common synonym, possibly derived from an African Woolof language of a Senegambia word, "jiga," for insect, or the French word "chique," based on a word of a Cariban Indian language of South and Central America and the Lesser Antilles. Tungiasis is also called dermatophiliasis. Chigger(s) is an erroneous synonym for *T. penetrans*. This term is accurately reserved for larvae of mites of the Trombiculidae family and the allergic reaction the mites provoke in human skin.

### General Considerations

Tungiasis was first described in 1526 in Oviedo's account of the crew of Columbus's *Santa Maria,* shipwrecked on Haiti in 1493.[2] Aleixo de Abreu, a Portuguese physician in Brazil may have been the first to describe the medical aspects of tungiasis, in 1623.[3] Subsequently, many European military expeditions to the New World suffered debilitating outbreaks of tungiasis. In the Abyssinian campaign of World War I, entire British military garrisons were rendered unfit for service as a result of epidemic tungiasis.[4] (For a detailed exposition of early observations on tungiasis, see the publications by D.H. Connor referenced in this chapter.)[5,6]

## Epidemiology

Multiple species of Tunga are distributed over much of the world.[7,8] *Tunga penetrans* is indigenous to Central and South America and the West Indies. Tungiasis is prevalent throughout Central America and across South America to

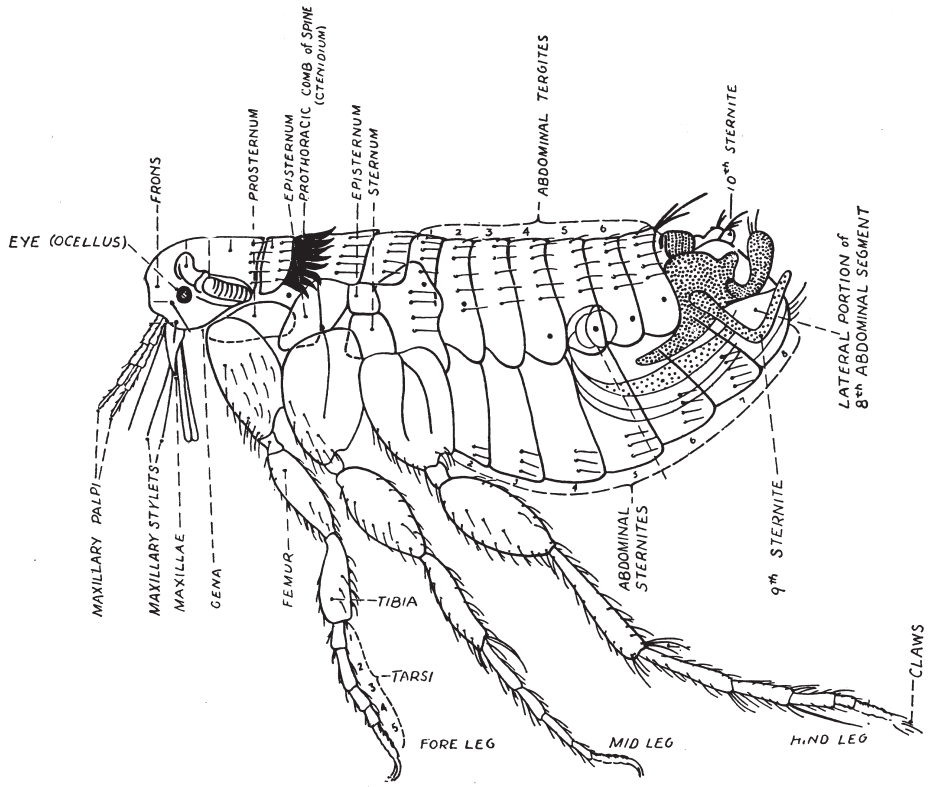



**Figure 17.1**
External morphologic features of male flea (*Nosopsyllus fasciatus*).

northern Chile and Argentina, and is common among the Popolucas people of Veracruz in southern Mexico.[9] Tungiasis may have been introduced into the Old World in 1872 when a British ship out of Brazil illegally unloaded sand ballast onto the Angolan shore.[10] The disease then spread rapidly along the Angolan coast. Many consider Stanley's treks through the African interior in the late 1800s to be the vehicle for tungiasis's rapid spread across the continent. *Tunga penetrans* is now found throughout most of Africa and Madagascar, as well as Pakistan and India.[5] There are multiple reports of imported infections in the United States, Australia, Europe, the United Kingdom, and other nonendemic regions.[11-18] Some investigators express concern that the disease may become established in environmentally favorable areas of currently nonendemic countries. The first reported autochthonous infection in Europe was in a lifeguard on the Italian shore of the Tyrrhenian Sea.[19]

*Tunga penetrans* thrives best in dry, sandy soil and high humidity. Patients seeking medical attention for tungiasis, usually recent travelers to endemic areas, often recall visits to the beach. A variety of wild and domesticated animals host the flea, including dogs, cats, mice, and swine.[20] Epidemic outbreaks of tungiasis can be devastating, especially where the flea has been previously unknown. The African tungiasis epidemic of 1873 to 1920 ravaged countless villages, causing death from tetanus, gangrene, and starvation due to incapacitated field workers. In endemic areas, children, especially boys, usually have a higher incidence of infection than adults.[21] A report in 1981 found that tungiasis afflicted 49.5% of 5595 schoolchildren in Lagos State, Nigeria.[22] In a detailed study in Trinidad, the overall prevalence of active disease was 20.5%, with a male/female ratio of 31%:13%. The average number of fleas per infected person was 5.4 in males and 2.4 in females.[23] Simple methods for community assessment have been described.[24]

## *Infectious Agent*

### Morphologic Description

Fleas are bloodsucking ectoparasites of the order Siphonaptera. Although 1800 species have been described, only about a dozen are medically important to humans. Fleas are small, brown, wingless insects with laterally compressed and highly sclerotized bodies. The adult flea is 1 to 6 mm long and has a distinct head, thorax, and abdomen (Fig 17.1). The head is divided into a dorsal portion (frons) and a ventral portion (gena). In some species, the gena has a row of stout teeth called the genal comb. Eyes are simple when present and mouthparts are adapted for piercing and sucking. The thorax is composed of 3 distinct segments, each with a pair of legs modified for clinging and jumping. In some species, the anterior thoracic segment (pronotum)



**Figure 17.2**
Nongravid adult *Tunga penetrans* are small, laterally compressed, and wingless, with long legs modified for clinging and jumping. x85

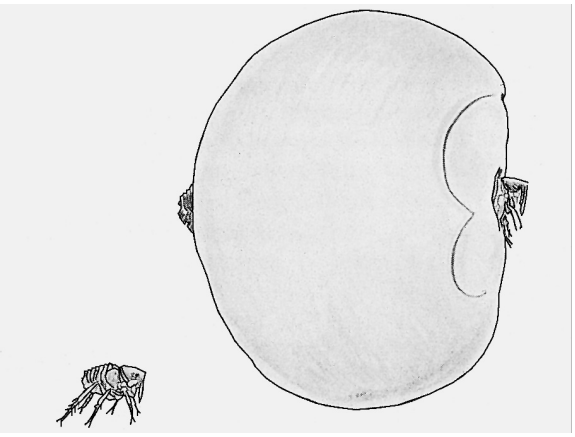


**Figure 17.3**
Comparative sizes of nongravid and gravid *Tunga penetrans*.

also has a row of teeth called the pronotal comb. The abdomen consists of 10 segments, the last 2 of which are highly modified for mating purposes in both males and females. A large, sharply angled frons, shortened thorax, and lack of combs distinguish *T. penetrans* from other species of fleas.

The male *T. penetrans* shares many basic morphologic features with the female, but only the female burrows into human skin and is observed in biopsy specimens. Therefore, the following description pertains only to the female. The unfed, nongravid *T. penetrans* is approximately 1 mm long and barely visible to the naked eye (Fig 17.2). When engorged, it increases vastly in volume (Fig 17.3).[25] Most fleas in tissue sections are swollen with numerous eggs and with various amounts of host blood (Fig 17.4). The thorax and abdomen of the flea are protected by a translucent cuticle that varies in thickness from 20 to 140 µm (Figs 17.4 and 17.5). The cuticle has spines, but these are not readily observed in tissue sections. The hypodermis is one cell layer thick and lies beneath the cuticle (Fig 17.5). A thick band of striated muscle extends from the head to the posterior end of the flea (Fig 17.4). Internally, there is an extensive respiratory system composed of variously sized branching tubules (tracheae) (Figs 17.4 and 17.6). There is a complete digestive tract with a conspicuous midgut (Figs 17.4 and 17.7).

The female has salivary glands, malpighian tubules, and fat body cells, but the reproductive organs predominate. Ovaries and oviducts are paired and usually contain eggs in various stages of maturation (Figs 17.4 and 17.8). At times virtually the entire body cavity is filled with eggs (Fig 17.9). Mature *T. penetrans* eggs are white, oval, and 480 to 650 µm by 280 to 330 µm (Figs 17.4, 17.8, and 17.9). They have a smooth, 3 µm thick shell and contain yolk and yolk droplets (Figs 17.8 and 17.10). Occasionally, the flea's head is observed in the dermis. The head is approximately 500 by 250 µm and does not swell during feeding and egg production. The cuticle of the head is 5 µm thick and stains yellow with hematoxylin and eosin (Figs 17.4 and 17.11). The head has laterally placed simple eyes lined with a heavily pigmented layer (Fig 17.12) and contains the brain and abundant striated muscle. Mouthparts are rarely observed probing a dermal capillary (Fig 17.11). A central channel for passing down saliva and sucking up blood is formed by the close proximity of the paired maxillae or cutting blades. Maxillae are 30 µm in diameter, stain yellow with hematoxylin and eosin, and are heavily serrated by sharply pointed teeth 6 µm apart (Figs 17.13 and 17.14). Legs occasionally appear in tissue sections (Fig 17.15). The cuticle of the legs has spines and stains yellow with hematoxylin and eosin. Endobacteria of the genus *Wolbachia* have been detected in female *T. penetrans*,[26,27] including in eggs and ovaries, and in free-living males.

## Life Cycle and Transmission

*Tunga penetrans* undergoes complete metamorphosis from egg through larva, pupa, and adult (Fig 17.16). The adult female *T. penetrans* burrows head first into human skin until its head lies within the dermis. The rest of its body is enclosed by the epidermis. A small hole in the keratin remains open, allowing the flea to breathe and discharge feces and eggs to the outside, and making its posterior end available to the male for mating. The adult male copulates with the embedded female and simultaneously takes a blood meal.[28] The female takes a blood meal before copulation, which lasts about 20 minutes, and then begins to produce fertile eggs. When approximately 200 eggs have been discharged, the female flea dies. Eggs that reach soil in favorable temperature and humidity hatch in 3 or 4 days.

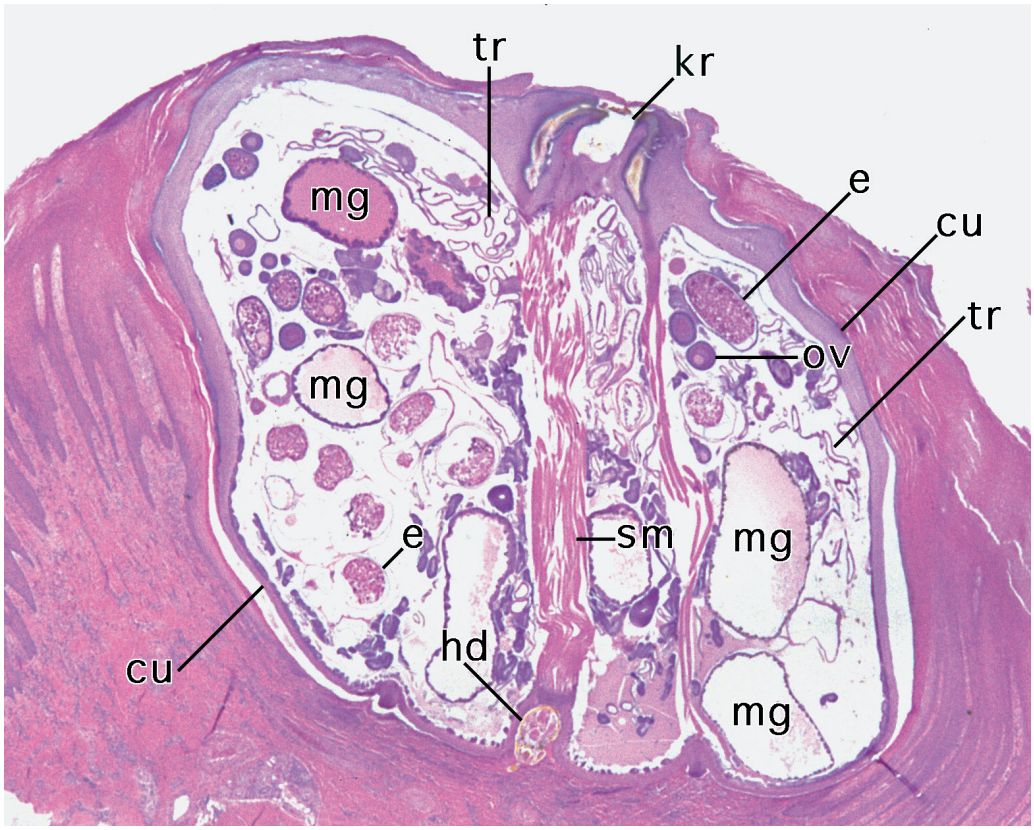



**Figure 17.4**
Vertical section through long axis of gravid *Tunga penetrans* showing small opening in keratin (kr) through which eggs, feces, and air pass. The flea is surrounded by epidermis except for the head (hd), which has penetrated the dermis and is dwarfed by the swollen abdomen. Note variably thick cuticle (cu), multiple sections of midgut (mg), striated muscle (sm), tracheae (tr), ovary (ov), and eggs (e). x21

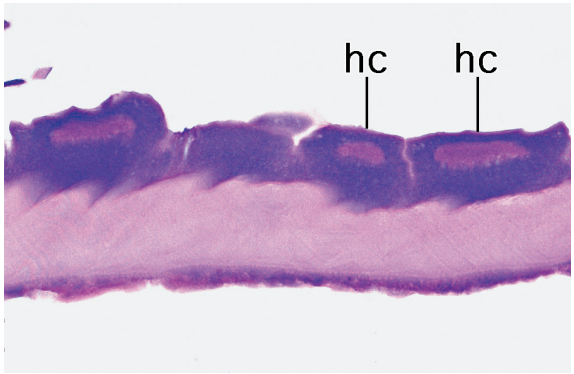



**Figure 17.5**
Section through thick cuticle and hypodermal cells (hc) of *Tunga penetrans*. x255

*Tunga penetrans* has 2 larval instars.[2] Larvae have no legs, measure 1.4 to 3.1 µm by 0.17 to 0.4 µm, and are scavengers, feeding on dust, debris, and dried blood passed per rectum of the adult. Ten to 18 days after eggs are laid, the second instar pupates, enclosing itself in a thin-walled cocoon. The adult emerges from the pupa in approximately 7 days. The complete life cycle takes approximately 3 weeks. However, it has been suggested that, as with other fleas, *T. penetrans* may remain in the pupal stage indefinitely until aroused by environmental stimuli such as vibration, sound, or odors. For example, outbreaks of tungiasis have been reported among new residents of long-abandoned villages and military garrisons. In such cases, dormant pupae may have molted into adult fleas in response to stimuli from the new occupants, or they may have survived in infected animals until new human hosts arrived.

## Clinical Features and Pathogenesis

According to observations of one of the authors (WMM), in patients naive to *T. penetrans*, the penetration of the flea produces no initial symptoms. The expanding flea, however, creates a painful erythematous nodule. If improperly treated, tungiasis can lead to ulceration, sepsis, tetanus, or gangrene. Some authors suggest that the sailor's oath, "I'll be jiggered," reflects the itching and discomfort associated with tungiasis; however this seems highly conjectural. Fleas can attack any part of the body, including arm, hand, trunk, head, face, and eyelid. Lesions usually appear on the feet because *T. penetrans* is a relatively poor jumper, able to reach only a few centimeters above the ground. Nodules under a toenail or near some other pressure-bearing portion of the foot are particularly painful. Depending upon the number and location of nodules, walking may be difficult. Usually 1 or 2 nodules form on the body at a time, but sometimes hundreds may be present (Figs 17.17 to 17.23). Massive, debilitating infection in travelers is extremely rare, but is

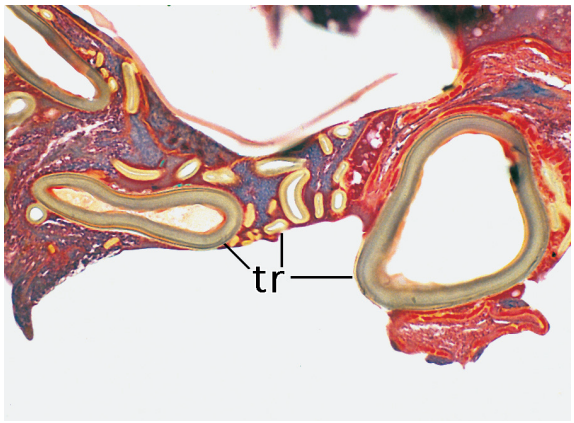



**Figure 17.6**
Tracheae (tr) within flea's body are thick-walled and vary considerably in size. Movat x240

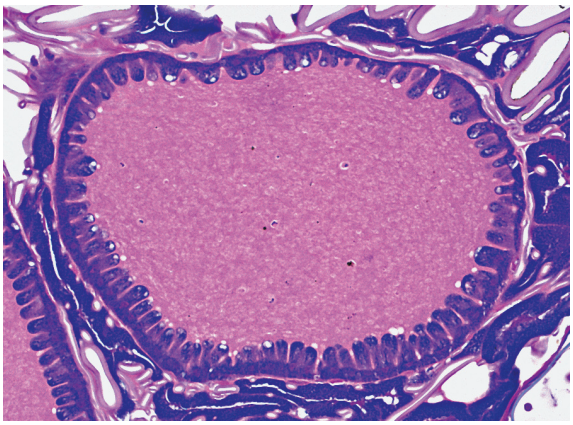


**Figure 17.7**
Section through midgut of *Tunga penetrans* containing partially digested blood. Epithelium is composed of tall columnar cells. x125

common among residents of areas experiencing an outbreak of tungiasis for the first time and in the malnourished and enfeebled. In one reported patient with epilepsy 870 jiggers were counted. [29] We are not aware of reports on possible relationships between HIV infection and tungiasis. Secondary bacterial infection and ulceration of nodules are common complications. In one study of 268 tungiasis patients, 16 (6%) had associated septicemias caused by a variety of gram-positive cocci and gram-positive and -negative bacilli. Untreated tungiasis can lead to infection by *Clostridium perfringens* or *Clostridium tetani*. In a report of 44 patients with tetanus, 11 cases were attributed to tungiasis.[30] Because of their often insensitive feet, the risk of complicated tungiasis is especially high for patients with leprosy.

## *Pathologic Features*

The burrowing flea initially appears as a minute black spot in the skin. As it enlarges, an erythematous papule develops. The epidermis proliferates and virtually engulfs the enlarging flea (Fig 17.4), resulting in hyperkeratosis, parakeratosis, and acanthosis (Fig 17.24). Ragged surfaces at the interface of the flea's cuticle and the host's keratin interlock, probably helping to hold the flea in place (Fig 17.25). The dermis becomes hyperemic and infiltrated with chronic inflammatory cells, including lymphocytes, plasma cells, and eosinophils (Figs 17.26 to 17.28). The flea exploits the inflammatory response by consuming cells migrating into the surrounding area.[31] Occasionally the flea provokes an intra-epidermal abscess (Fig 17.29). When all its eggs have been discharged, the gravid flea disintegrates. The carcass collapses and a crusting, fibrinopurulent exudate forms across the base of the crater (Fig 17.30). Ultimately the

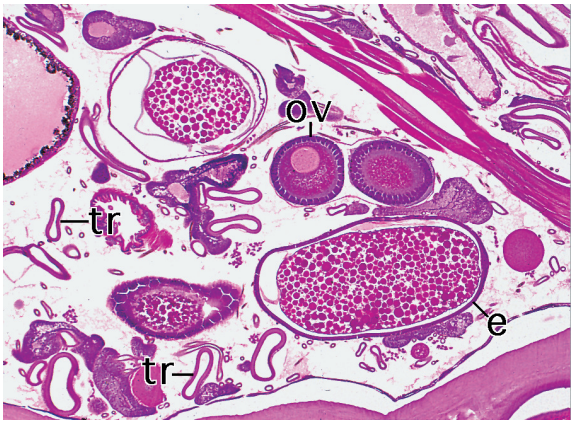



**Figure 17.8**
Section through abdomen of gravid *Tunga penetrans* demonstrating tracheae (tr), mature egg (e), and developing oocyte in ovary (ov). x60

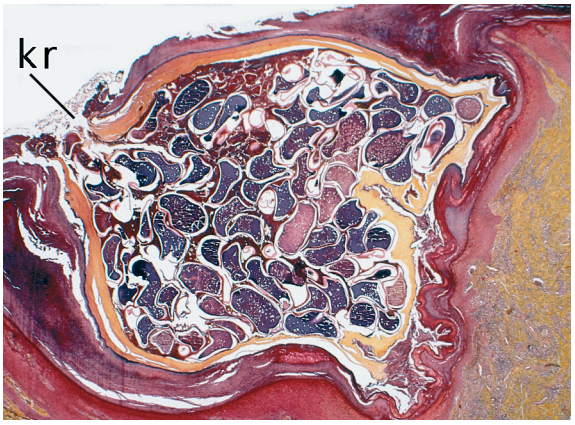



**Figure 17.9**
Section through flea's egg-filled abdomen. Note eggs exiting through small hole in keratin (kr). Movat x15

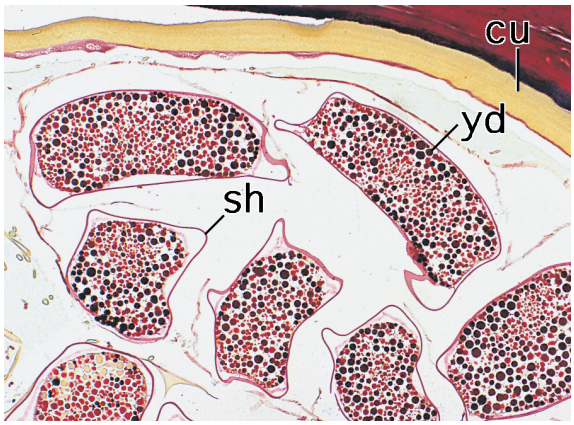



**Figure 17.10**
Section through gravid *Tunga penetrans* depicting cuticle (cu) and eggs. Eggs have smooth, 3 µm thick shell (sh) and contain yolk and yolk droplets (yd). Movat x60

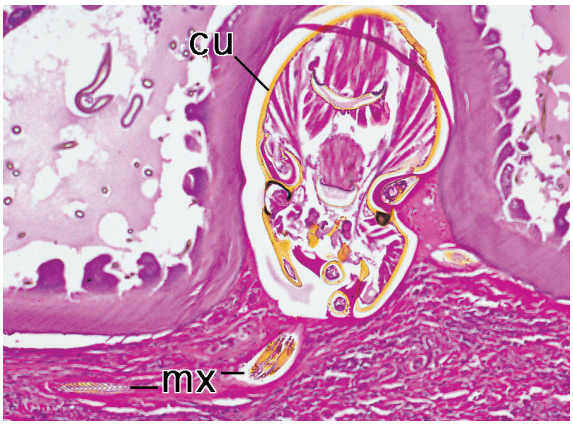



**Figure 17.11**
Tiny head and maxillae (mx) of flea penetrating the dermis. Note thin yellow cuticle (cu), 1 of 2 eyes, and striated muscle. x115

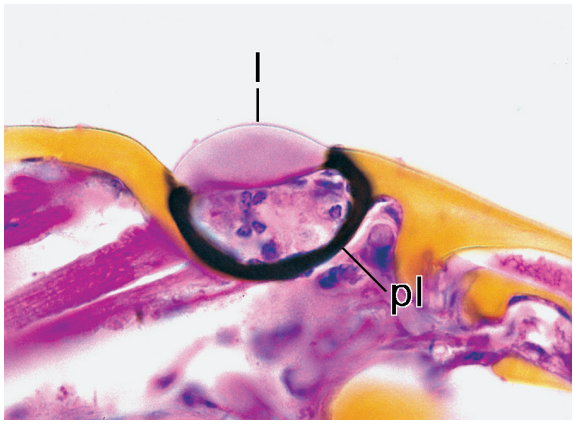



**Figure 17.12**
Higher magnification of flea's eye depicting lens (l), neurons, and glial cells, and heavily pigmented layer (pl). x645

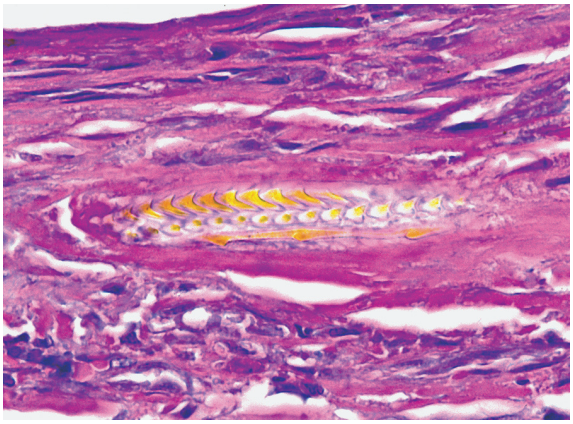


**Figure 17.13**
*Tunga penetrans* maxillae penetrating dermis. Maxillae stain yellow with H&E and are heavily serrated by sharply pointed teeth. x575

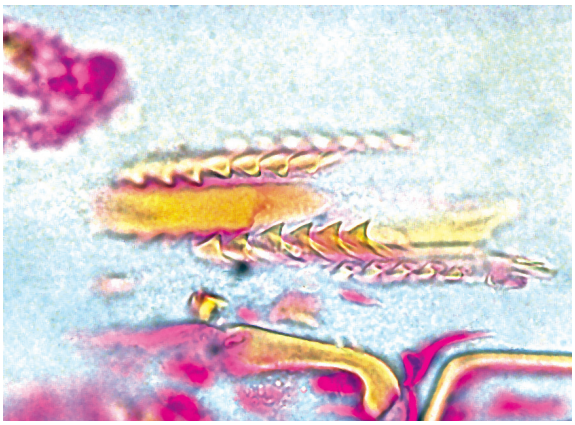


**Figure 17.14**
Sharply pointed teeth 6 µm apart in *Tunga penetrans* maxillae. x585

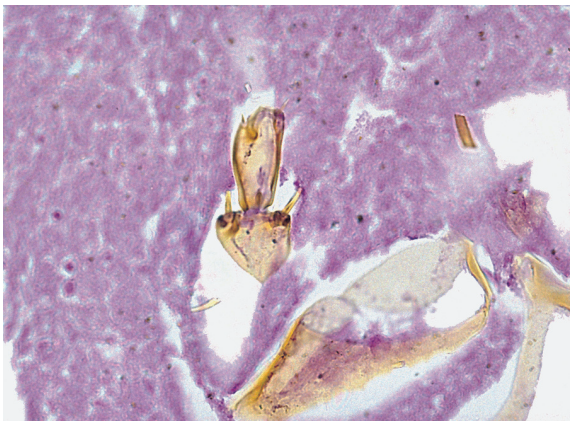


**Figure 17.15**
Section through joint of flea's leg in skin. Note cuticular spines and yellow staining of cuticle with H&E. x270

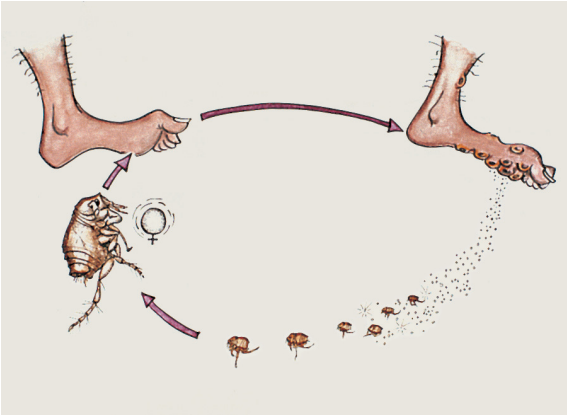


**Figure 17.16**
Simplified life cycle of *Tunga penetrans*. Eggs usually hatch in sandy soil and pass through larval and pupal stages before developing into adult fleas. Only the female flea penetrates human skin.



**Figure 17.18**
Several healing craters of tungiasis lesions along side of foot. Gravid flea either died spontaneously or was extracted by patient.

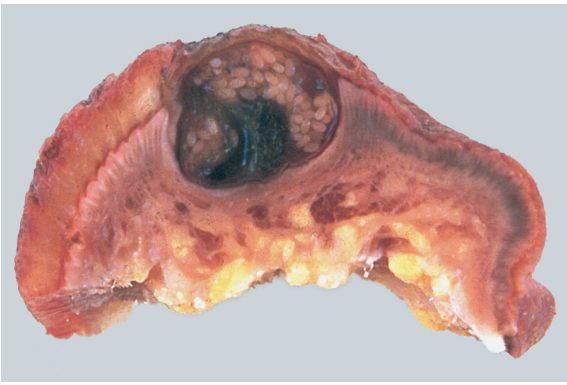


**Figure 17.20**
Vertical section through single gravid flea depicting many oval, white eggs. Epidermis surrounds all but upper portion of flea, which is covered by thin layer of keratin. x6.5



**Figure 17.17**
Fully developed single nodule at base of great toe, a classic presentation of uncomplicated tungiasis.



**Figure 17.19**
Foot of patient who died of tetanus, probably originating in multiple lesions of tungiasis on lesser pressure-bearing areas of foot. All lesions are healing and crusted.

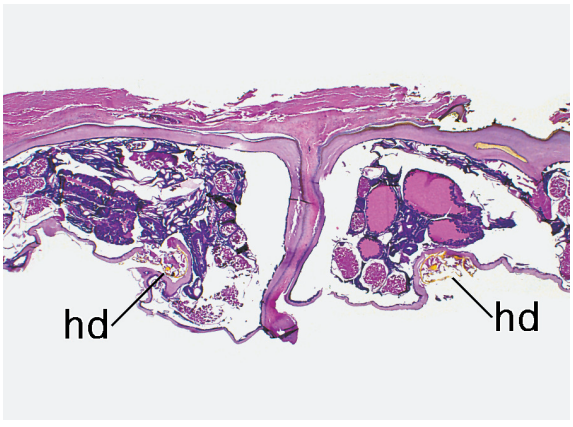



**Figure 17.21**
Section of skin containing 2 adjacent fleas. Cuticles of both heads (hd) stain yellow with H&E. x15



**Figure 17.22**
Vertical sections of skin from sole of patient described in Figure 17.19 showing multiple crusting craters of healing tungiasis. x1.3

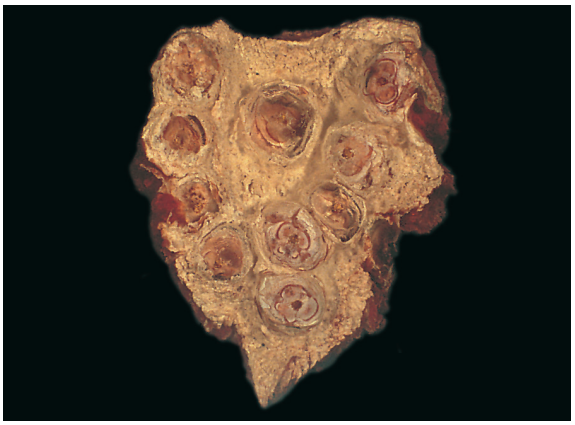


**Figure 17.23**
Surface of skin containing multiple fleas. Craters are discrete, and each opening in keratin is exit vent of single flea. x2

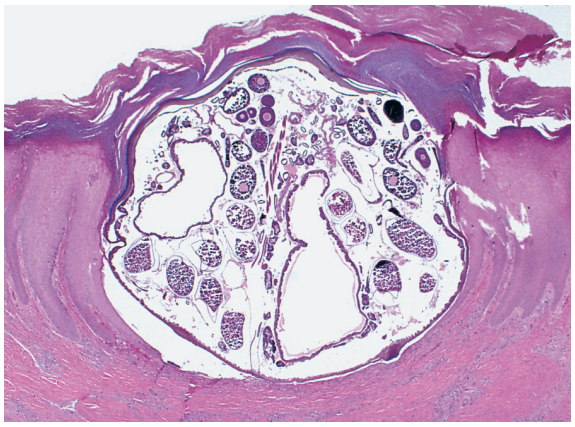


**Figure 17.24**
Section through gravid flea surrounded by hyperkeratotic, parakeratotic, and acanthotic epidermis. x65

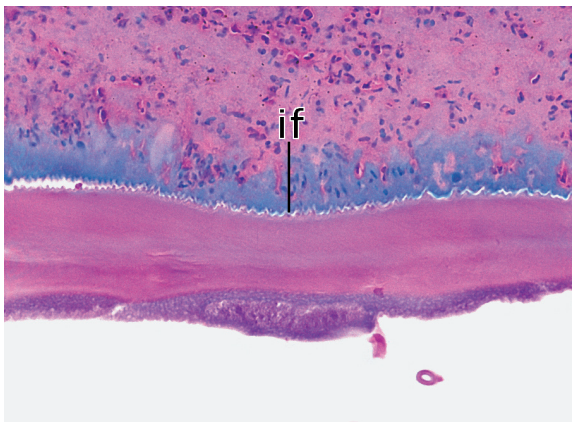



**Figure 17.25**
Section at interface (if) of ragged interlocking edges of flea cuticle and human keratin. x260

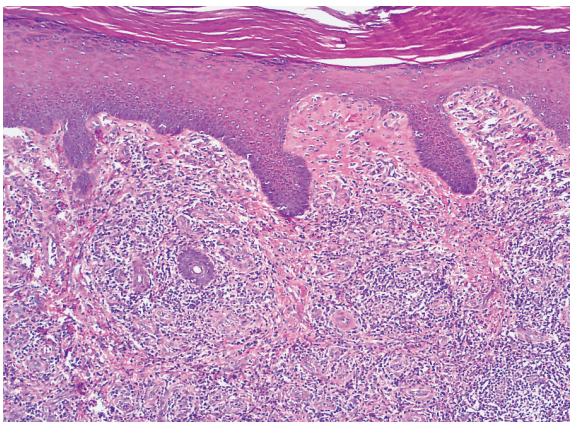


**Figure 17.26**
Section of skin adjacent to *Tunga penetrans* showing acanthosis, elongated rete ridges, and infiltration of lymphocytes, plasma cells, and occasional eosinophils. x60

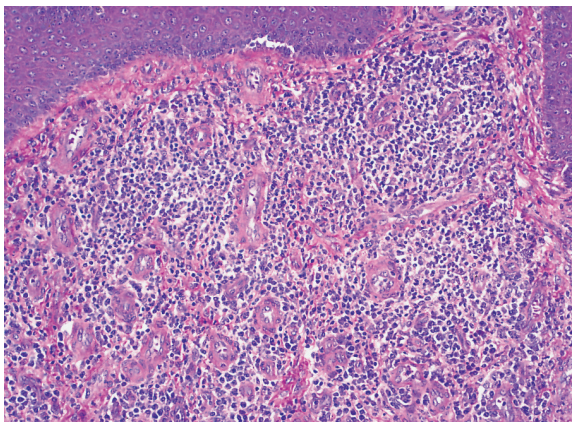


**Figure 17.27**
Section of skin in tungiasis lesion demonstrating chronic inflammation containing primarily lymphocytes and plasma cells. x145

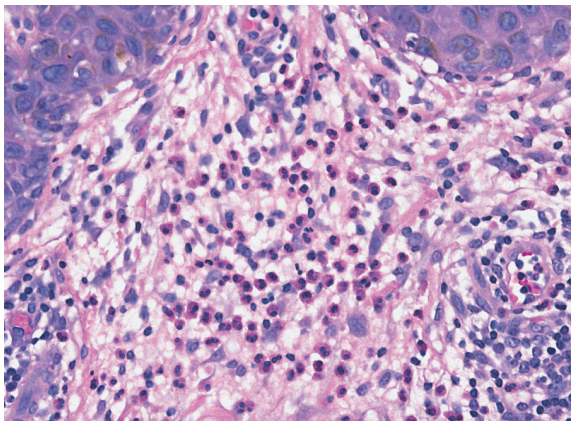


**Figure 17.28**
Section of skin from tungiasis lesion showing prominent tissue eosinophilia. x235

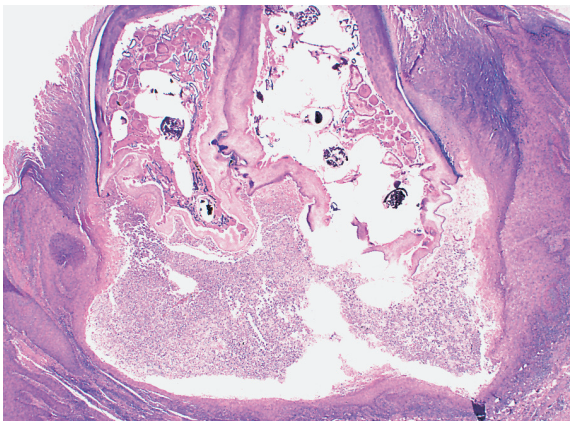


**Figure 17.29**
Section through skin depicting 2 adjacent ruptured fleas provoking intraepidermal abscess. x12

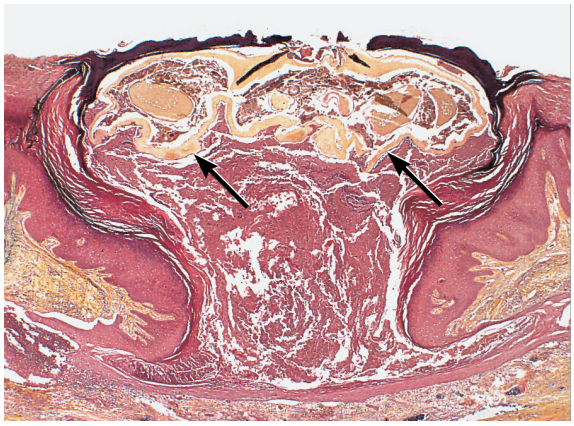


**Figure 17.30**
Collapsed, degenerated carcass of *Tunga penetrans* (arrows) in fibrinopurulent dermal exudate. x17



**Figure 17.31**
Single unstained *Tunga penetrans* egg recovered from lesion on foot of American returned from Brazil. Oval, thin-shelled egg is 650 by 420 $\mu$m and contains yolk droplets. x90

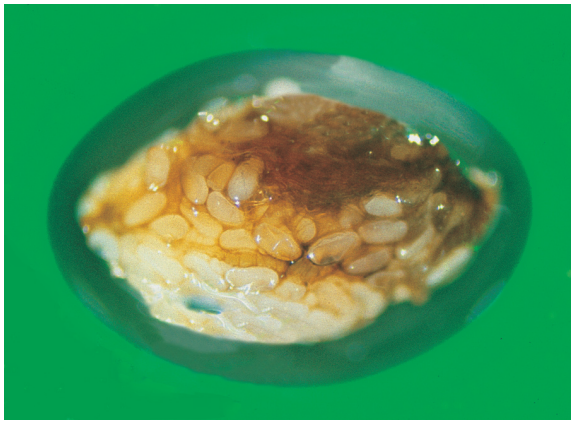


**Figure 17.32**
Mass of unstained *Tunga penetrans* eggs dissected by needle from lesion on toe of right foot. Patient had returned to Canada from Tanzania when toe became inflamed and swollen. x12

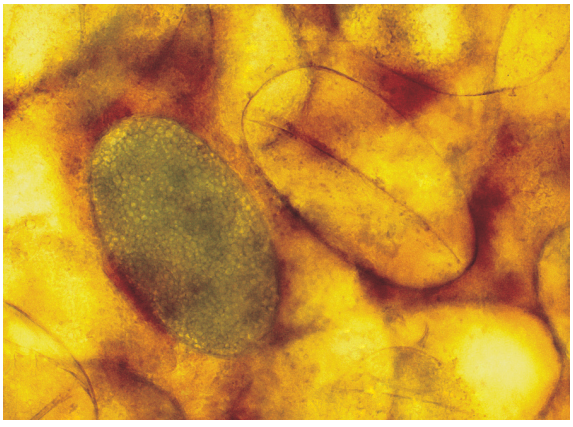


**Figure 17.33**
Higher magnification of unstained *Tunga penetrans* eggs seen in Figure 17.32. Oval, thin-shelled eggs are 600 $\mu$m long and contain yolk droplets. x60



**Figure 17.34**
Portion of gravid *Tunga penetrans* taken from toe of patient described in Figure 17.32. Eggs are fragmented but diagnostic. x25

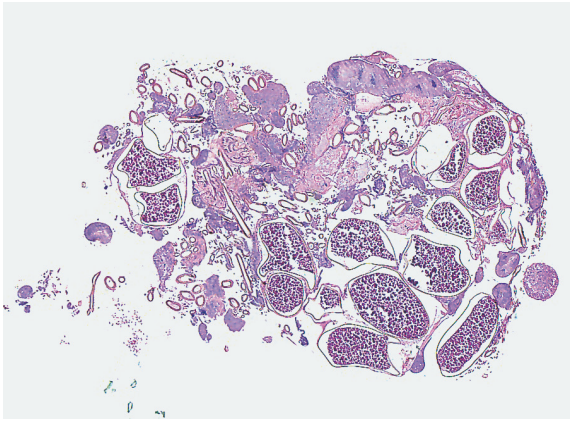


**Figure 17.35**
Biopsy of tungiasis nodule from skin of hand revealing readily identifiable *Tunga penetrans* eggs. Lesions on back and hand developed after patient returned to Canada from Uganda. Prior to biopsy, lesions were clinically diagnosed as sebaceous cysts. x25

carcass and surrounding keratin are sloughed.

In experimental infections in rats TNF-alpha to IL-10 ratios were decreased suggesting that anti-inflammatory cytokines were diminished in tungiasis.[32]

## Diagnosis

Location of the lesion is a significant factor in the diagnosis of tungiasis. A patient from an endemic area presenting with a recently acquired nodule on the foot probably has tungiasis. However, because lesions can occur on parts of the body other than the foot, definitive diagnosis depends upon identifying the parasite or its eggs from the nodule. A biopsy specimen of the lesion usually reveals a viable, gravid *T. penetrans* (Figs 17.4 and 17.24) or *T. penetrans* eggs (Figs 17.31 to 17.33). Even a small portion of the flea will usually contain identifiable eggs with characteristic yolk droplets (Fig 17.34 and 17.35).

Tungiasis is sometimes misdiagnosed as creeping eruption, dracunculiasis, tick bite, scabies, or myiasis. The scabies mite, its eggs, and its feces appear in tunnels within the epidermis. The mite is discoid and smaller than the fully developed, globose *T. penetrans* (< 0.5 mm vs > 7 mm). The furuncular nodule of *Dermatobia hominis* in South America is very similar to a tungiasis nodule, but *D. hominis* rarely infects the foot and is usually associated with a feeding mosquito. In Africa, myiasis of the foot is fairly common and could be mistaken for tungiasis. Histologically, a carefully excised *T. penetrans* is distinguished from a dipteran larva by its lack of cuticular spines and the presence of eggs. *Tunga penetrans* is rarely found in the dermis, but most dipteran larvae infecting humans penetrate to the dermis, where they are surrounded by acute inflammatory cells and then by a thin epithelium.

## Treatment and Prevention

Removing the flea by careful dissection as soon as the lesion is apparent is the best treatment for tungiasis. The tiny, visible opening on the skin surface over the flea's posterior end is gradually enlarged with a needle or other pointed instrument. The swollen body of the flea is exposed and carefully extracted from the skin with forceps. This process requires patience and skill. If the body of the flea ruptures, a painful inflammatory response may develop. The cavity left by the flea should be cleansed and dressed. Treating massive *T. penetrans* infections by removing all the fleas may not be practical. In such cases, orally administered thiabendazole (50 mg/kg body weight/day for 15 days) is usually successful.[33] Niridazole is also effective (30 mg/kg body weight weekly for 2 weeks).[34] Results on the use of Ivermentin have been variable: up to 64 per cent cure rates have been reported.[35,36]

Routinely wearing closed shoes is the most effective way to prevent tungiasis, but is often not feasible in endemic areas. The best control is to aggressively treat infected domestic animals[37] and routinely inspect feet for fleas. Repellent–based control programs may prove effective, but probably impractical in most endemic communities.[38]

## References


1. Kettle DS. *Medical and Veterinary Entomology*. 2nd ed. New York, NY: Oxford University Press; 1995:305.
2. Hicks EP. Early stages of the jigger, *Tunga penetrans*. *Ann Trop Med.* 1930;24:575-586.
3. Guerra F. Aleixo de Abreu [1568-1630], author of the earliest book on tropical medicine describing amoebiasis, malaria, typhoid fever, scurvy, yellow fever, dracontiasis, trichuriasis and tungiasis in 1623. see *J Trop Med Hyg.*1968;71:55-69.
4. Jolly GG. An entomological episode of the East African campaign. *Indian Med Gaz.* 1926;61:164-165.
5. Connor DH. Tungiasis. In: Binford CH, Connor DH, eds. *Pathology of Tropical and Extraordinary Diseases*. Vol 2. Washington, DC: AFIP; 1976:610-614.
6. Connor DH. Tungiasis. In: Connor DH, Chandler FW, Manz HJ, Schwartz DA, Lack EE, eds. *Pathology of Infectious Diseases*. Vol 2. Stamford, Conn: Appleton and Lange; 1997:1699-1707.
7. Barnes AM, Radovsky FJ. A new Tunga (*siphonaptera*) from the Nearctic region with description of all stages. *J Med Entomol.* 1969;6:19-36.
8. Pampiglione S, Trentini M, Fioravanti ML, Onore G, Rivasi F. [On a new species of sand flea from Ecuador and tungiasis, a problem of Public Health in many developing countries]. *Ann Ig.* 2003;15:747-752.
9. Macias PC, Sashida PM. Cutaneous infestation by *Tunga penetrans. Int J Dermatol.* 2000;39:296-298.
10. Hoeppli R. Early references to the occurrence of *Tunga penetrans* in tropical Africa. *Acta Trop* (Basel). 1963;20:143-153.
11. Basler EA, Stephens JH, Tschen JA. *Tunga penetrans*. *Cutis.* 1988;42:47-48.
12. Lowry MA, Ownbey JL, McEvoy PL. A case of tungiasis. *Mil Med.* 1996;161:128-129.
13. Ott AK, Charters AD, Bowman RA. Tungiasis: imported disease. *Med J Aust.* 1980;2:623-624.
14. Sanusi ID, Brown EB, Shepard TG, Grafton WD. Tungiasis: report of one case and review of the 14 reported cases in the United States. *J Am Acad Dermatol.* 1989;20:941-944.
15. Wardhaugh AD, Norris JF. A case of imported tungiasis in Scotland initially mimicking verrucae vulgaris. *Scott Med J.* 1994;39:146-147.
16. Hager J, Jacobs A, Orengo IF, Rosen T. Tungiasis in the United States: a travel souvenir. *Dermatol Online J*. 2008;14:3.
17. Davis RF, Johnston GA, Sladden MJ. Recognition and management of common ectoparasitic diseases in travelers. *Am J Clin Dermatol.* 2009;10:1-8.
18. Hakeem MJ, Morris AK, Bhattacharyya DN, Fox C. Tungiasis–a cause of painful feet in a tropical traveller. *Travel Med Infect Dis.* 2010;8:29-32.
19. Veraldi S, Carrera C, Schianchi R. Tungiasis has reached Europe. *Dermatology.* 2000;201:382.
20. Ugbomoiko US, Ariza L, Heukelbach J. Pigs are the most important animal reservoir for *Tunga penetrans* (jigger flea) in rural Nigeria. *Trop Doct.* 2008;38:226-227
21. Ade-Serrano MA, Ejezie GC. Prevalence of tungiasis in Oto-Ijanikin village, Badagry, Lagos State, Nigeria. *Ann Trop Med Parasitol.* 1981;75:471-472.
22. Ejezie GC. The parasitic diseases of school children in Lagos State, Nigeria. *Acta Trop.* 1981;38:79-84.
23. Chadee DD. Tungiasis among five communities in south-western Trinidad, West Indies. *Ann Trop Med Parasitol.* 1998;92:107-113.
24. Ariza L, Wilcke T, Jackson A, et al. A simple method for rapid community assessment of tungiasis. *Trop Med Int Health.* 2010;15:856-864.
25. Geigy R, Herbig A. Hypertrophy of the organs of the female *Tunga penetrans* [in German]. *Acta Trop* (Basel). 1949;6:246-261.
26. Fischer P, Schmetz C, Bandi C, et al. *Tunga penetrans*: molecular identification of *Wolbachia endobacteria* and their recognition by antibodies against proteins of endobacteria from filarial parasites. *Exp Parasitol.* 2002;102:201-211.
27. Heukelbach J, Bonow I, Witt L, Feldmeier H, Fischer P. High infection rate of *Wolbachia endobacteria* in the sand flea *Tunga penetrans* from Brazil. *Acta Trop.* 2004;92:225-230.
28. Geigy R, Suter P. On the mating of fleas [in German]. *Rev Suisse Zool.* 1960;67:206-210.
29. Mazigo HD, Behamana E, Zinga M, Heukelbach J. Tungiasis infestation in Tanzania. *J Infect Dev Ctries.* 2010;4:187-189.
30. Obengui. Tungiasis and tetanus at the University Hospital Center in Brazzaville [in French]. *Dakar Med.* 1989;34:44-48.
31. Lavoipierre MM, Radovsky FJ, Budwiser PD. The feeding process of a tungid flea, *Tunga monositus,* and its relationship to the host inflammatory and repair response. *J Med Entomol.* 1979;15:187-217.
32. Feldmeier H, Witt LH, Schwalfenberg S, et al. Investigations on the biology, epidemiology, pathology and control of *Tunga penetrans* in Brazil. V. Cytokine concentrations in experimentally infected Wistar rats. *Parasitol Res.* 2004;94:371-376.
33. Cardoso A. Generalized tungiasis treated with thiabendazole [letter]. *Arch Dermatol.* 1981;117:127.
34. Ade-Serrano MA, Olomolehin OG, Adewunmi A. Treatment of human tungiasis with niridazole (Ambilhar): a double-blind placebo-controlled trial. *Ann Trop Med Parasitol.* 1982;76:89-92.
35. Heukelbach J, Wilcke T, Winter B, et al. Efficacy of ivermectin in a patient population concomitantly infected with intestinal helminths and ectoparasites. *Arzneimittelforschung.* 2004;54:416-421.
36. Heukelbach J, Franck S, Feldmeier H. Therapy of tungiasis: a double-blinded randomized controlled trial with oral ivermectin. *Mem Inst Oswaldo Cruz.* 2004;99:873-876
37. Cooper JE. An outbreak of *Tunga penetrans* in a pig herd. *Vet Rec.* 1967;80:365-366.


## Acknowledgements


**Figure 17.1**
Adapted from Stitt, Clough, and Clough. Practical Bacteriology, Hematology and Animal Parasitology. 1938. The Blakiston Company

**Figure 17.3**
Originally published by Geigy and Herbig in *Acta Tropica,* 1949;6:246

**Figure 17.16**
Drawing by Frank O. Raasch







18

# Myiasis

*J. Kevin Baird, Ronald C. Neafie, Mary K. Klassen-Fischer, Wayne M. Meyers, and Douglas J. Wear*

## *Introduction*

### Definition

Myiasis is infection by fly larvae (order Diptera) that feed upon living or dead tissues of higher animals, including humans. It causes significant disease in wild and domesticated animals. In humans, myiasis has a range of manifestations, from minor irritation to life-threatening disease. Myiasis usually affects the skin, but can involve almost any organ of the body.[1]

### Synonyms

The term myiasis comes from *myia*, the Greek word for fly. The disease is known by a variety of vernacular names, reflecting the many species of fly larvae that infect humans, the organs that may be involved, and the geographic region where infection is acquired. Synonyms for particular genera and species are listed below under Infectious Agents. The common term for fly larvae is maggots.

### Classification

We have classified human myiases into 3 broad categories based on mode of infection: 1) invasive myiasis, 2) wound myiasis, and 3) passive myiasis.

### General Considerations

Fly larvae that are obligate parasites invade or consume healthy tissue. Anatomic and behavioral characteristics of the larvae permit infection of and development within an otherwise healthy host.

## *Infectious Agents, Clinical Features and Pathogenesis of Myiasis*

Most of this chapter deals with aspects of invasive myiasis and this emphasis will be reflected in the general organization of the contents and the discussion that follows.



**Figure 18.1**
*Dermatobia hominis* larva (probably early third stage) removed from leg of patient who had traveled to South America. Broad posterior half of larva tapers to narrow anterior half.

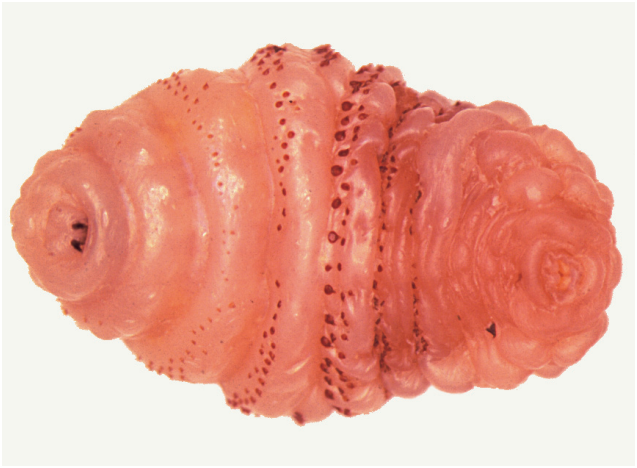


**Figure 18.2**
Mature, uniformly cylindrical third-stage *Dermatobia hominis* larva demonstrating paired mouth hooks (left).



**Figure 18.3**
Creamy white *Dermatobia hominis* larva with circumferential rows of prominent black spines. See also Figures 18.4, 18.13 and 18.18.



**Figure 18.4**
*Dermatobia hominis* larva removed from skin, showing paired mouth hooks. Same larva is pictured in Figures 18.3, 18.13 and 18.18.

## *Invasive Myiasis*

Invasive myiasis is sometimes called obligatory myiasis because larval development within living tissue is obligatory for some flies. These species have evolved elaborate behavioral and mechanical means of actively invading healthy tissue. Unlike passive and wound myiases, where many species cause the same type of disease in the same manner, the etiology of invasive myiasis tends to be species-specific. Larvae of some flies, such as *Cochliomyia hominivorax* and *Dermatobia hominis*, can penetrate a living host through almost any break in the skin, even an opening as small as a mosquito bite. We consider the exploitation of trivial wounds by fly larvae to be invasive myiasis rather than wound myiasis. Species that commonly cause invasive myiasis in humans are summarized in Table 18.1 and described in the section below.

All flies undergo a complete metamorphosis through the stages of egg, several larval instars (stages), pupa, and adult. Identification of dipteran flies is usually based upon morphologic features of the adult. However, dipteran larvae cause myiasis in humans, and rearing them to the adult stage is difficult and rarely successful. Thus, identification is usually based on examination of intact larvae. These should be carefully extracted from lesions, preferably with forceps to avoid damage to the parasites.

The flies that cause myiasis typically have 3 developmental stages. Because they are small and short-lived, first-stage larvae are rarely extracted from human skin. Identification is best accomplished by examining intact mature third-stage larvae. These are cylindrical, headless, legless, and composed of 11 to 13 body segments. *Dermatobia hominis* is shown as an example (Figs 18.1 to 18.3). The cuticle of some segments has a characteristic pattern of spines (Figs 18.1 to 18.7). The first, or cephalic, segment is short and armed with a pair of mouth hooks (Figs 18.4 and 18.7).

The structure of posterior spiracles (the breathing orifices of arthropods) is taxonomically significant (Figs 18.8 to 18.10). Respiratory openings, or slits, usually indicate the larval stage: 1 slit in the first stage, 2 in the second, and 3 in the third. Respiratory slits may be straight, curved, or sinuous. Variations in the outer sclerotized area called the peritreme and the rounded structure called the button are described for each species below.[1,2] (See James[3] for comprehensive details and further study.)

Often, intact larvae or the biopsy specimen containing them are processed and sectioned in the laboratory, making identification more difficult since some key characteristics such as posterior spiracles and mouth hooks are rarely seen in tissue sections (Fig 18.11). However, all species of fly larvae that cause invasive myiasis share certain morphologic features that distinguish them from other arthropods and from helminths: a typically thick cuticle with rows of spines in some areas (Fig 18.12); a complex network of internal tracheae (breathing tubes) (Fig 18.13)[4]; and abundant

| Genus and species | Geographic distribution | Usual host | Site/type of infection |
|---|---|---|---|
| **Family Oestridae** | | | |
| *Dermatobia hominis* | Central and South America | Humans | Furuncle |
| *Cuterebra* sp | North America | Rodents, rabbits, hares | Creeping eruption, furuncle |
| *Hypoderma* sp | North America, Europe, Asia | Cattle, deer | Deep creeping eruption |
| *Gasterophilus* sp | Worldwide | Horses, donkeys, zebras | Creeping eruption, stomach, eye |
| *Oestrus ovis* | North America, Europe, Asia | Sheep, goats | Eye, mouth, nose |
| *Rhinoestrus purpureus* | Eastern and southern Europe, northern Africa, Asia Minor | Cattle, horses | Eye, mouth, nose |
| **Family Calliphoridae** | | | |
| *Cordylobia anthropophaga* | Sub-Saharan Africa | Domestic animals, house rat | Furuncle |
| *Cochliomyia hominivorax* | Western hemisphere | Livestock | Orifices, furuncle, wound |
| *Chrysomyia bezzian*a | Africa, India, southern China, Indonesia, New Guinea | Livestock | Furuncle, nose, sinuses, mouth |
| **Family Sarcophagidae** | | | |
| *Wohlfahrtia vigil, W. v. opaca* | North America | Humans, young animals | Furuncle |

**Table 18.1**
Dipteran flies whose larvae cause invasive myiasis in humans.

striated muscle (Figs 18.12 and 18.13).

The cuticle is yellow in Movat-stained sections (Fig 18.14). Sections through salivary glands sometimes show giant chromosomes that have remained aligned after replication and have light and dark bands (Fig 18.15).

## *Dermatobia hominis* (human botfly, torsalo, gusano)

*Dermatobia hominis* is prevalent throughout Central America and in areas of South America.[5] In North America, it is the most common cause of myiasis in travelers returning from endemic areas. Less common vernacular names for *D. hominis* include berne, colmoyote, and ver macaque.[3] Larvae are creamy-white, 1 cm to 2 cm long, and have circumferential rows of prominent black spines (Figs 18.1 to 18.5). First-stage larvae are narrow posteriorly and become pyriform after the first molt. Early third-stage larvae are also pyriform and can be identified by 3 straight respiratory slits (Fig 18.8). Mature third-stage larvae are elongate to ovate. Posterior spiracles are in a sunken cavity and have 3 straight slits and no button (Fig 18.9).[6] Anterior spiracles are prominent and flowery.

A female *D. hominis* fly captures a female mosquito, deposits eggs onto the underside of the mosquito (Figs 18.16 and 18.17), and releases the mosquito unharmed. Stable flies and other Diptera may also serve as carriers of *D. hominis* eggs. The eggs remain viable for up to a month. When the mosquito feeds on a human host, first-stage fly larvae emerge from the eggs, fall to the host's skin, and penetrate the wound made by the feeding mosquito.[7]

Most patients with *D. hominis* infection present with a single furuncular nodule, or warble, containing a single larva (Figs 18.18 and 18.19). A first-stage larva is usually small, short-lived, and hardly noticeable except for some slight movement under the skin. As the larva grows and molts to the second and third stages, the furuncle may become painful and develop a discharge from the opening through which the larva breathes. Unless it is removed (Fig 18.20), a larva remains in the host for weeks to months before dropping to the ground to pupate. If the larva ruptures or dies, an intense inflammatory reaction ensues (Fig 18.21). Furuncles can arise on any part of the body, but are most common on exposed surfaces. The vast majority of *D. hominis* infections have no serious complications, but some first stages migrate into deeper tissues and cause disfiguring or crippling injury. Patients may develop secondary bacterial infections or severe allergic reactions (Fig 18.22). There is a report of external ophthalmomyiasis caused by

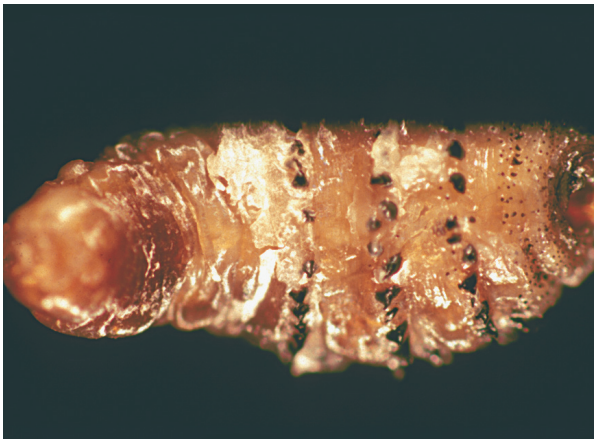


**Figure 18.5**
Larva of *Dermatobia hominis* removed from leg of patient who had visited Panama, showing 3 rows of large cuticular spines.

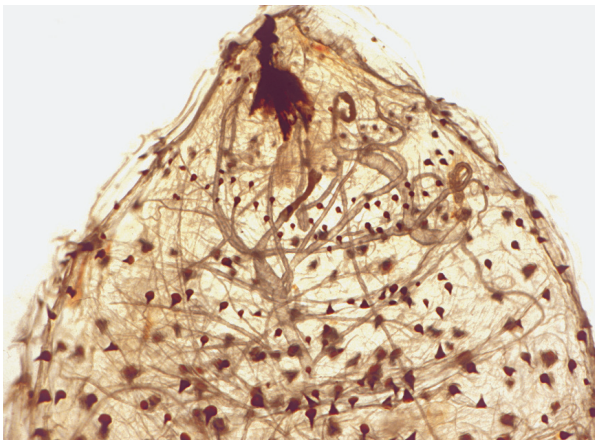


**Figure 18.6**
Various-sized cuticular spines on unstained, cleared larva of *Dermatobia* sp (probably not *hominis*) removed from back of man bitten while lying on sand in Majorca.

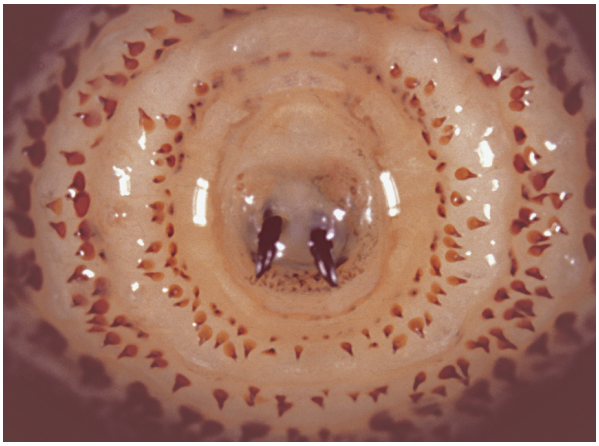


**Figure 18.7**
Cephalic view of *Dermatobia hominis* larva removed from forehead of patient who had visited Belize. Note paired mouth hooks.

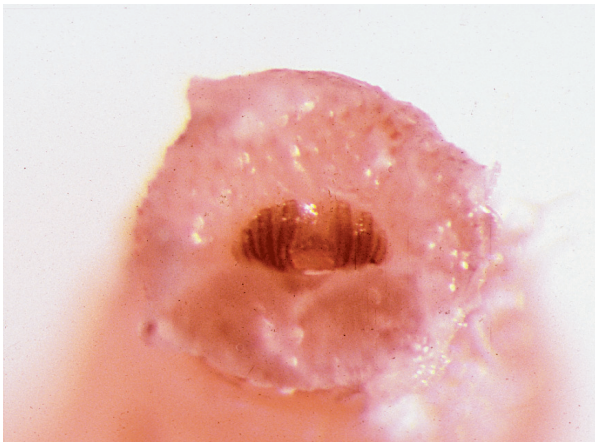


**Figure 18.8**
Three respiratory slits in each posterior spiracle of early third-stage *Dermatobia hominis* larva removed from arm of patient who had visited Panama



**Figure 18.9**
Higher magnification of posterior spiracles of early third-stage *Dermatobia hominis* larva seen in Figure 18.8. Note 3 straight respiratory slits on each spiracle, and no peritreme or button.
.

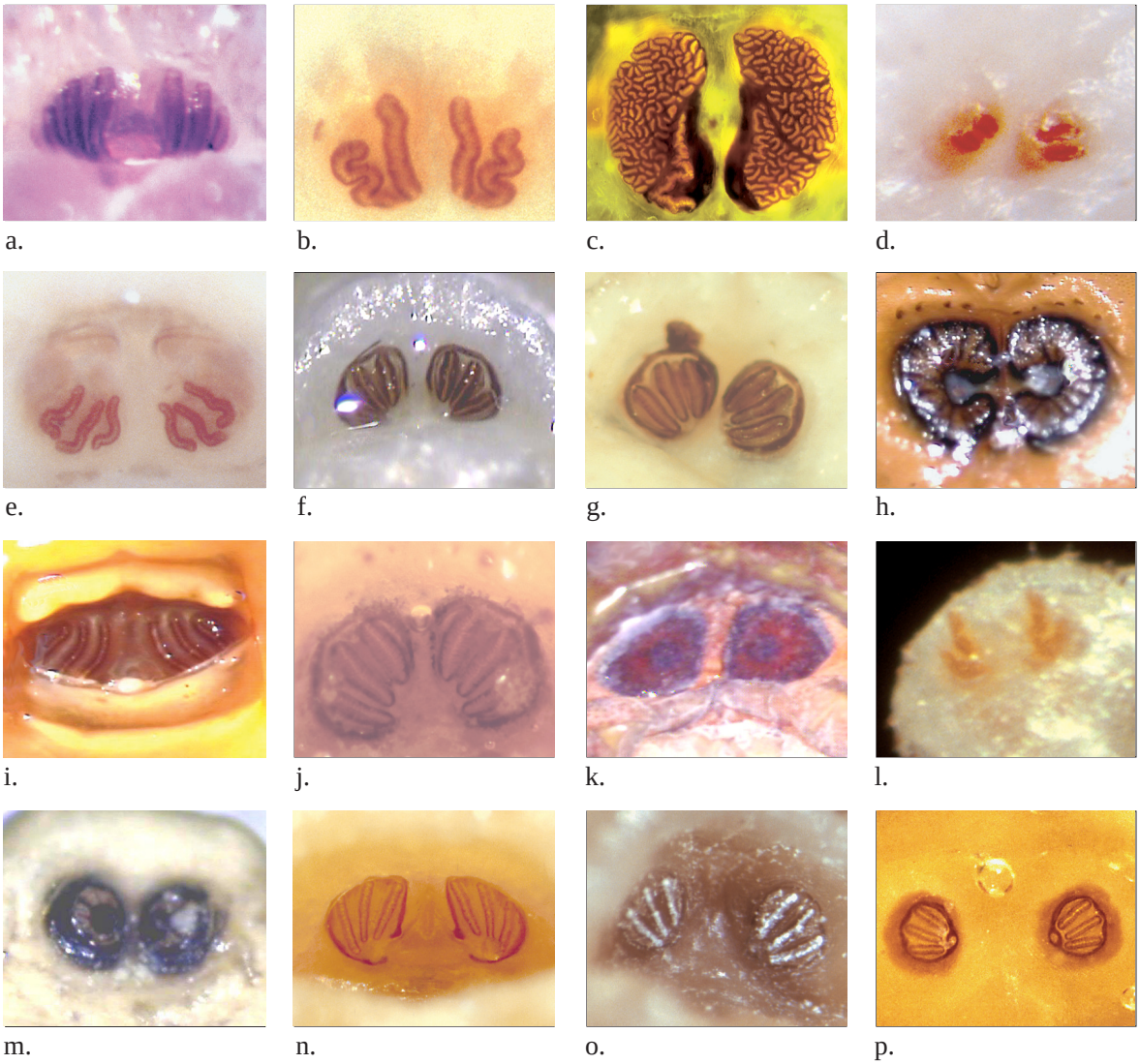



**Figure 18.10**
Posterior spiracles of 16 fly larvae associated with human infection.

a. *Dermatobia hominis*
b. *Cuterebra* sp (2nd stage)
c. *Cuterebra* sp (3rd stage)
d. *Cordylobia anthropophaga* (2nd stage)
e. *Cordylobia anthropophaga* (3rd stage)
f. *Cochliomyia hominivorax*
g. *Chrysomyia bezziana*
h. *Hypoderma bovis*
i. *Gasterophilus intestinalis*
j. *Wohlfahrtia magnifica*
k. *Oestrus ovis*
l. Family Muscidae (1st stage)
m. Family Muscidae (3rd stage)
n. *Phaenicia sericata*
o. *Calliphora vicina*
p. *Lucilia* sp

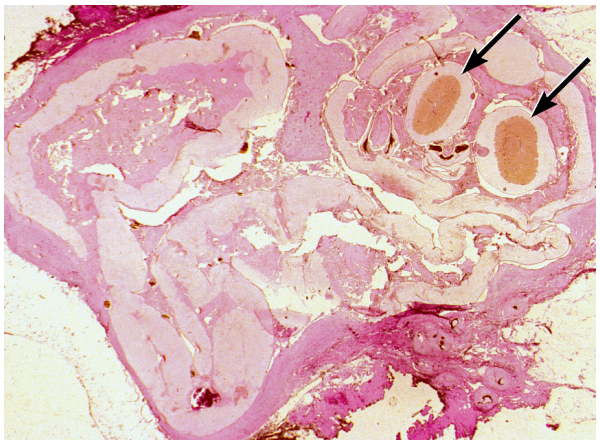


**Figure 18.11**
Posterior spiracles (arrows) of *Dermatobia hominis* larva in breast. See also Figures 18.21 and 18.36. x5.5

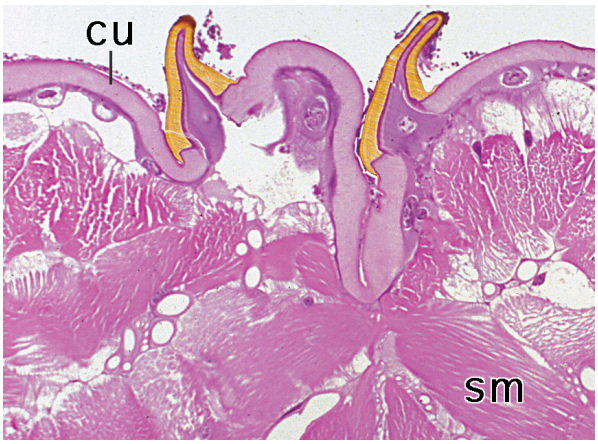



**Figure 18.12**
Thick cuticle (cu), 2 yellow, black-tipped cuticular spines, and underlying striated muscle (sm) in *Dermatobia hominis* larva described in figure 18.29. See also Figure 18.24. x65

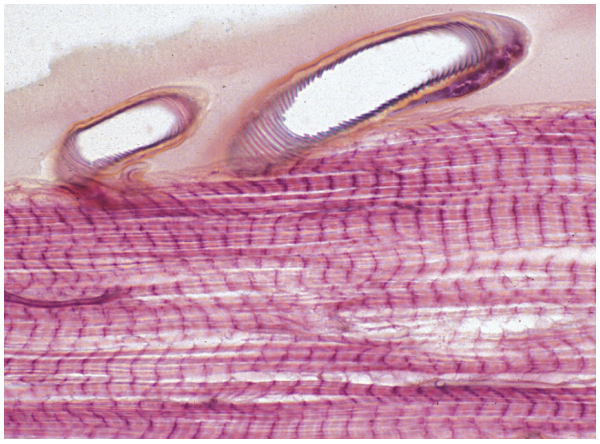


**Figure 18.13**
Striated muscle and 2 sections of tracheal tubes in *Dermatobia hominis* larva removed from skin. See also Figures 18.3, 18.4, and 18.18. x325

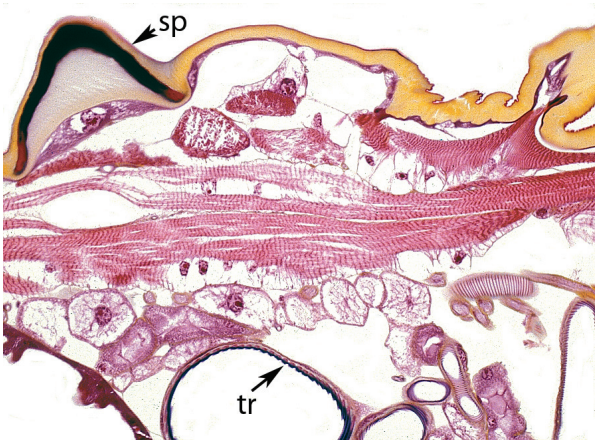



**Figure 18.14**
Cuticle of *Dermatobia hominis* staining yellow with Movat. Note pigmented spine (sp) and tracheae (tr). x130

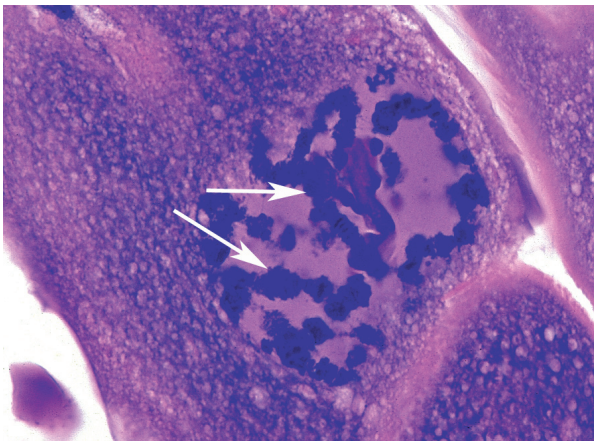


**Figure 18.15**
High power view of salivary gland showing giant chromosomes (arrows). x650



**Figure 18.16**
Adult *Dermatobia hominis.*

*D. hominis*, but no reports of orbital invasion.[8] One patient is reported to have died when a first-stage larva of *D. hominis* entered the brain through a cranial suture.[9,10] A Panamanian child who died of malaria had several warbles on the scalp. One larva had bored a 4-mm hole through the anterior fontanel and entered the cerebral cavity (Fig 18.23).

Histopathologically, larvae are readily observed in the dermis (Fig 18.24) or subcutaneous tissue (Fig 18.25). Occasionally, a larva may protrude from its burrow in the furuncle (Fig 18.26). The initial reaction is a mixed inflammatory cellular infiltrate composed of neutrophils, lymphocytes, histiocytes, and eosinophils (Fig 18.27). The larva is easily identified by its thick spiny cuticle (Figs 18.12, 18.25, 18.27, 18.28 and 18.29), numerous breathing tubes (Figs 18.13, 18.25, and 18.30 to 18.32), and abundant striated muscle (Figs 18.13, 18.30 and 18.31). Posterior spiracles are rarely seen (Figs 18.11 and 18.33 to 18.35). If a dead larva is not removed, a granuloma eventually forms (Fig 18.36). The spiny cuticle can usually be recognized even in a degenerated larva (Figs 18.36 to 18.39).

## *Cuterebra sp* (rabbit bots, rabbit warbles, rodent bots)

Infections by larvae of *Cuterebra* sp have been reported in the northeastern United States and adjacent areas of Canada among people who frequent wooded areas. Although several species are known, the particular ones that affect humans have not been established. First-stage larvae are rather slender, 1 mm to 6 mm long, and have 6 to 9 bands of spines (Fig 18.40). Second-stage larvae are plumper, and have less noticeable bands of spines (Fig 18.41) and 2 distinct respiratory slits on the posterior spiracles (Fig 18.42). Third-stage larvae are robust and up to several centimeters long (Fig 18.41). They are covered with spines that are whitish in the early third stage and later turn deep red or black (Fig 18.43). Mature third-stage larvae have prominent oval or kidney-shaped posterior spiracles that are divided into several plates, each composed of numerous respiratory slits (Fig 18.44).[6]

The large, bumblebee-like flies (Fig 18.45) of this genus do not feed. Each species appears briefly at a particular time of year and deposits eggs in or around the habitats of rodents, rabbits, and hares, their definitive hosts. When a warm-blooded animal approaches, first-stage larvae emerge, attach to the animal, then migrate to and penetrate a mucous membrane. Larvae migrate through the host's deep organs and lodge in the dermis, creating a warble. Within the warble, larvae molt twice, grow massively, and eventually drop to the ground and pupate. Pupae burrow into the ground and emerge as adult flies at the end of winter.

Humans encounter first-stage larvae of *Cuterebra* sp in the habitat of a definitive host. Larvae penetrate the mucous membranes of the eye, nose, or mouth, and sometimes cause a creeping eruption over the face. In some

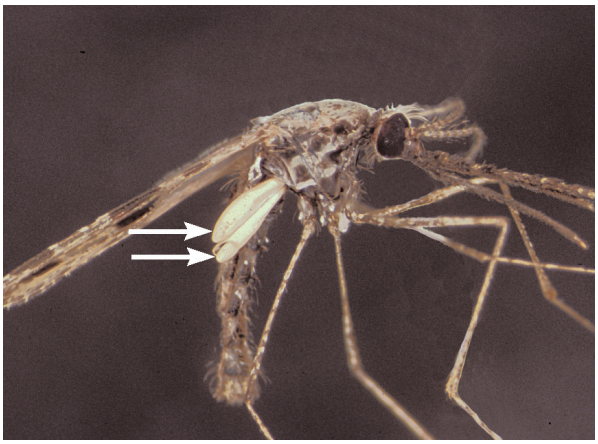


**Figure 18.17**
*Dermatobia hominis* eggs (arrows) deposited on underside of *Anopheles punctimacula* mosquito captured in Belize.

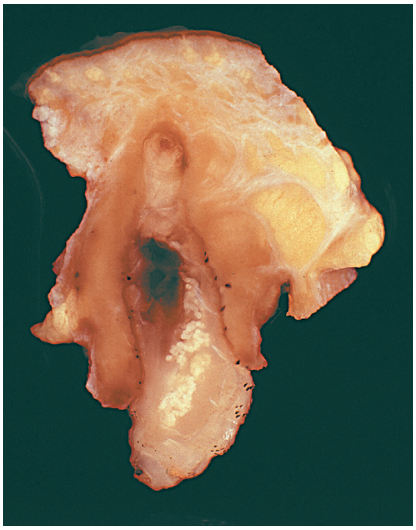


**Figure 18.18**
Cross section of skin containing larva of *Dermatobia hominis*. See also Figures 18.3, 18.4, and 18.13. x2.3



**Figure 18.19**
Posterior of *Dermatobia hominis* larva protruding (arrow) from furuncular nodule in skin.

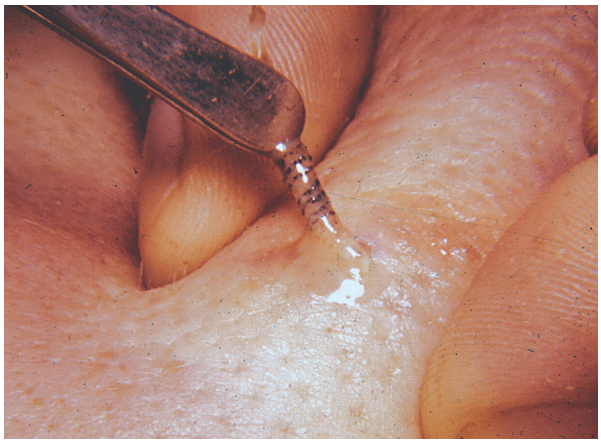


**Figure 18.20**
Forceps extraction of *Dermatobia hominis* larva seen in Figure 18.19.

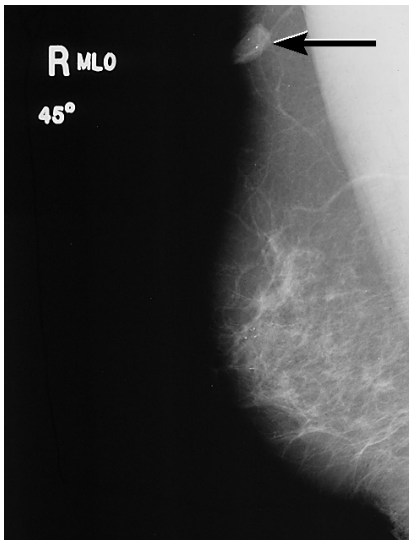



**Figure 18.21**
Mammogram showing degenerating *Dermatobia hominis* in lesion (arrow) of 2 years duration. Histologic sections of same larva are seen in Figures 18.11 and 18.36.



**Figure 18.22**
Periorbital edema resulting from severe allergic reaction to myiasis of scalp caused by *Dermatobia hominis* larva.

instances, larvae invade the dermis directly and migrate no farther. Most infections in humans consist of a single furuncular nodule (Fig 18.46) containing a second- or third-stage larva.[11] First-stage larvae of *Cuterebra* sp rarely cause myiasis. However, if observed in tissue sections, they can be identified by their small size, cuticle, and prominent spines (Figs 18.47 to 18.49). Spines are larger on later-stage larvae (Fig 18.50).

## *Cordylobia anthropophaga* (tumbu fly, ver de Cayor)

*Cordylobia anthropophaga* (family Calliphoridae) is found only in sub-Saharan Africa. Tumbu flies infect many domestic animals and rodents, and are responsible for most cases of myiasis among inhabitants of, or travelers to, tropical regions of Africa.[12] The common house rat (*Rattus*) is an important reservoir host. Club-shaped second-stage larvae of *C. anthropophaga* superficially resemble *D. hominis* larvae (2.5 mm to 5 mm long with black spines on the anterior pseudosegments) (Fig 18.51). However, the spines of *C. anthropophaga* are smaller and irregularly distributed (Figs 18.51 to 18.53). Third-stage larvae are 13 to 15 mm long, up to 5 mm wide, and sparsely covered with spines. The posterior spiracle has sinuous slits and a button (Figs 18.54 to 18.56).[3]

A female tumbu fly deposits several hundred eggs in sand contaminated with the urine and feces of humans or animals, or onto soiled clothing and linens. Humans often acquire infection from laundered clothing that has been dried in the open and left unironed. First-stage larvae are infective for 9 to 15 days.

Larvae penetrate human skin at the site of initial contact without causing pain or irritation. The patient becomes aware of infection when an erythematous, indurated papule several centimeters in diameter appears on the skin. Many patients have multiple lesions at a time (Figs 18.57 to 18.59). Deeper tissues may become involved, creating serious complications. (The histologic features of *C. anthropophaga* are shown in Figs 18.60 to 18.62.)

*Cordylobia rodhaini* (formerly *Stasisia rodhaini*), whose definitive hosts are the antelope and giant rat, rarely infects humans.[13]

## *Cochliomyia hominivorax* (primary screwworm, New World screwworm)

*Cochliomyia hominivorax* (also known as *Cochliomyia americana* and *Callitroga americana*) is a veterinary scourge with considerable economic impact. It is prevalent from the southwestern United States to Chile. Infection rates in humans correlate with those in local livestock. *Cochliomyia hominivorax*, which can also cause wound and imperceptive myiasisis, is an obligate parasite that requires larval development within a living, warm-blooded host.[3] Larvae are 2 mm to 6 mm long, with distinct bands of fine



**Figure 18.23**
Brain of child in a Panamanian hospital with malaria, measles, and numerous warbles on scalp and back. Larva of *Dermatobia hominis* bored 4-mm hole through anterior fontanel. The 4 by 6 cm cerebral cavity, discovered at autopsy, communicates with lateral ventricle. Larva is seen at the base of the cavity.

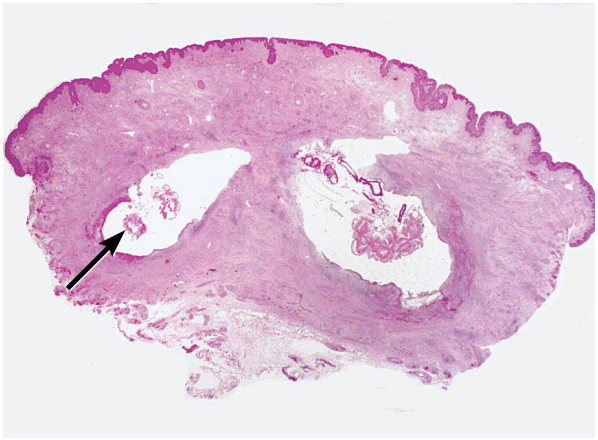


**Figure 18.24**
Larva of *Dermatobia hominis* (arrow) in dermis of scrotum. See also Figures 18.12 and 18.29. x2.8

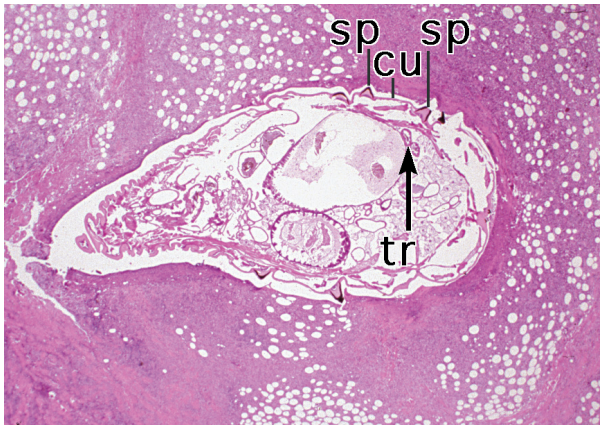



**Figure 18.25**
Cuticle (cu), spines (sp), and tracheae (tr) of *Dermatobia hominis* larva in subcutaneous tissue of back of patient bitten in Belize. x13.7

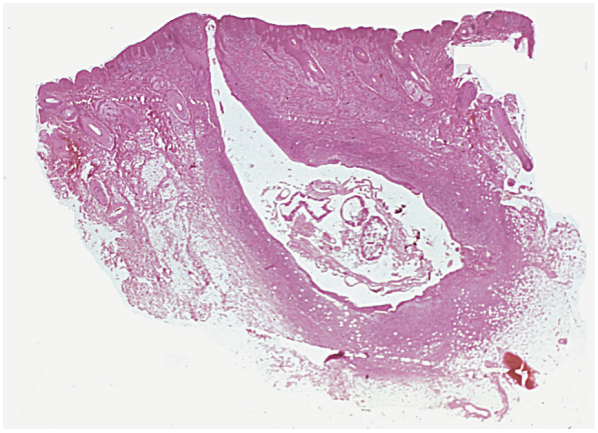


**Figure 18.26**
Larva communicating with pubic surface of patient bitten by an insect in Colombian banana grove 2 weeks previously. x15.8

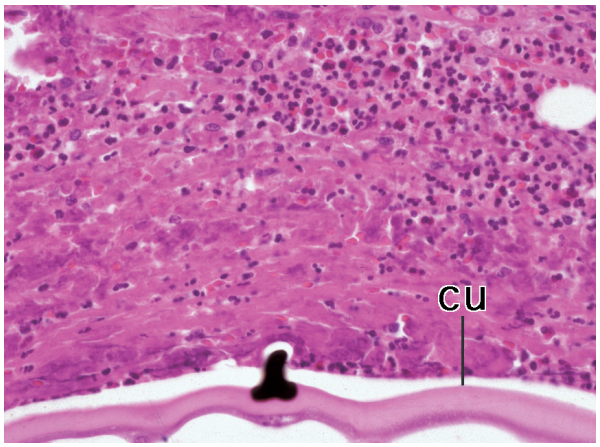



**Figure 18.27**
Neutrophils, lymphocytes, histiocytes, and eosinophils surround thick spiny cuticle (cu) of *Dermatobia hominis* larva seen in Figure 18.25. x250

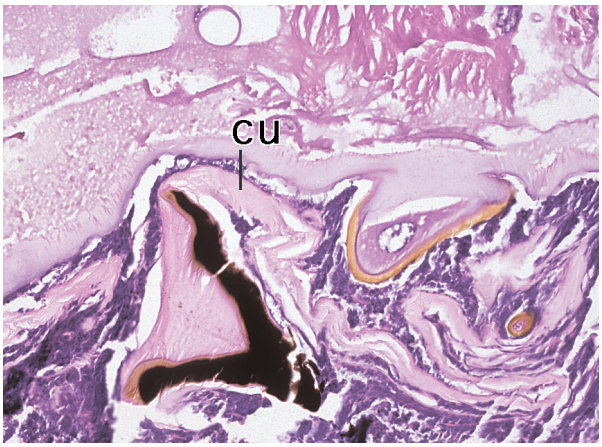



**Figure 18.28**
Thick cuticle (cu) and black and yellow spines of *Dermatobia hominis* larva. Patient bitten 6 weeks previously while visiting Costa Rica. H&E x106



**Figure 18.29**
Spine of *Dermatobia hominis* larva removed from scrotal skin of patient who had visited Colombia. See also Figures 18.12 and 18.24. Movat x300

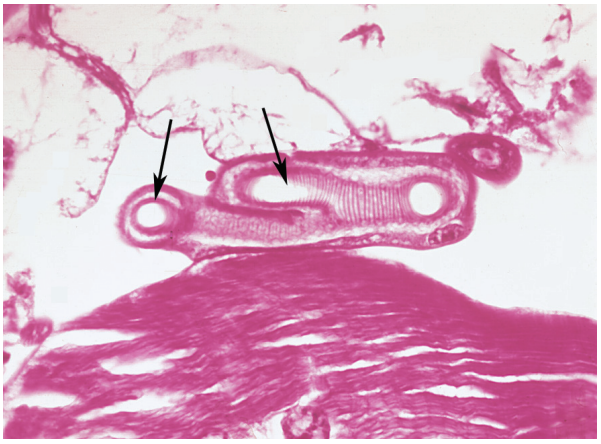


**Figure 18.30**
Tracheae (arrows) and striated muscle of *Dermatobia hominis* larva seen in Figure 18.26. x1190

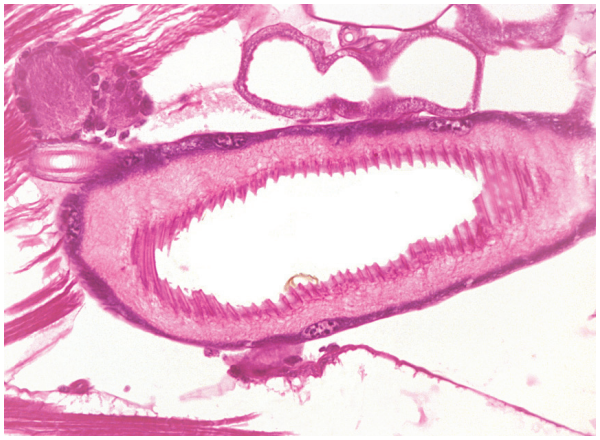


**Figure 18.31**
Tracheae and striated muscle of *Dermatobia hominis* larva seen in Figures 18.26 and 18.30. x190

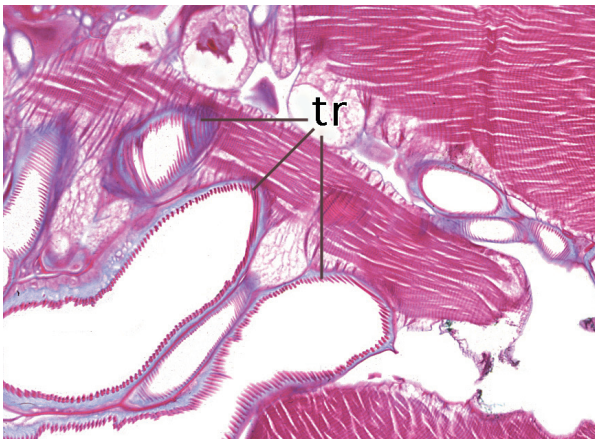



**Figure 18.32**
Tracheae and striated muscle of *Dermatobia hominis* larva. Patient was bitten 3 months previously while visiting Mexico. x130

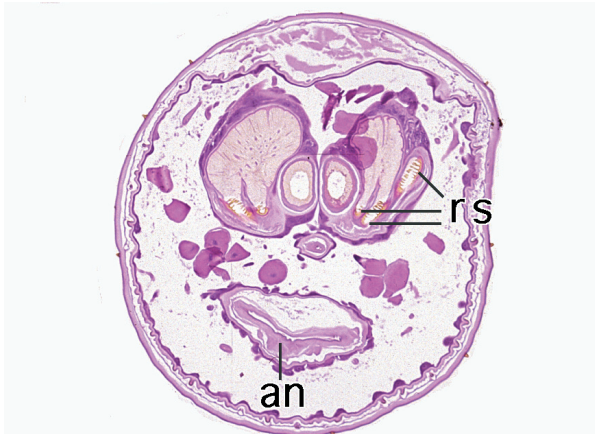
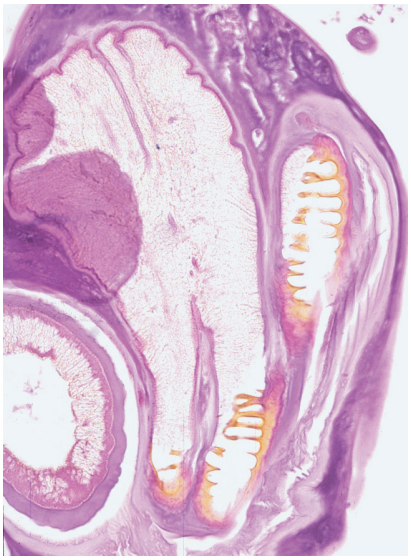



**Figure 18.33**
Cross section of posterior end of *Dermatobia hominis* larva. Respiratory slits (rs) are dorsal; anus (an) is ventral. x56

**Figure 18.34**
Higher power of left respiratory slits of *Dermatobia hominis* seen in Figure 18.33. Openings appear golden yellow. x140



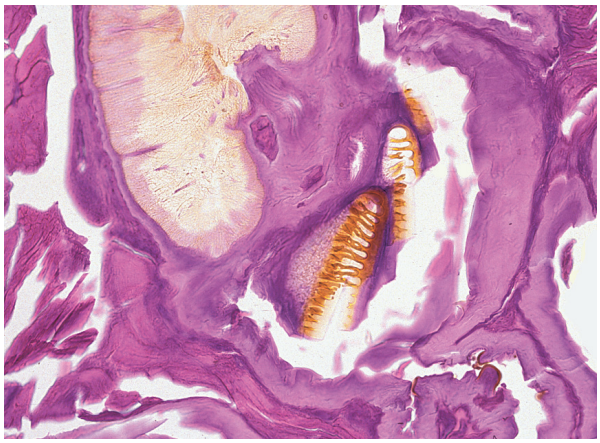


**Figure 18.35**
Portions of 3 respiratory slits of *Dermatobia hominis* larva removed from leg of patient bitten in Costa Rica. x156

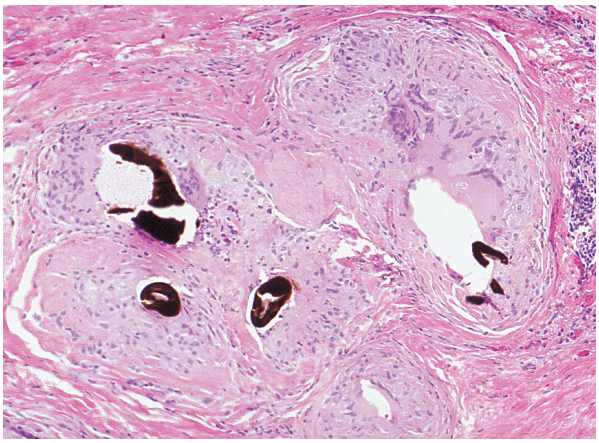


**Figure 18.36**
Black cuticular spines of *Dermatobia hominis* larva centered in granuloma of breast in patient from El Salvador. See also Figures 18.11 and 18.21. x90

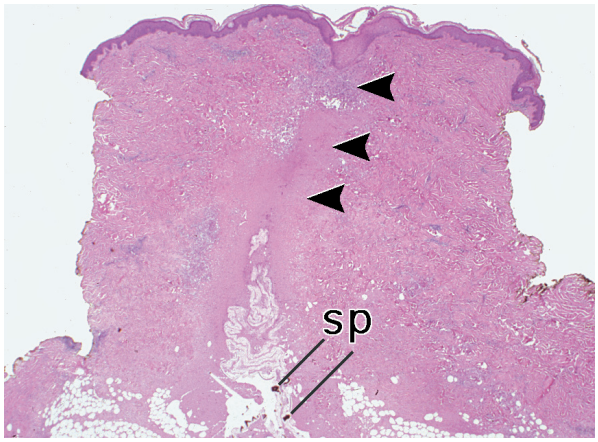



**Figure 18.37**
Degenerating *Dermatobia hominis* larva deep in skin of shoulder in patient returned from Bolivia. Necrotic tract (arrow) points toward surface and black spines (sp) are deep. x14

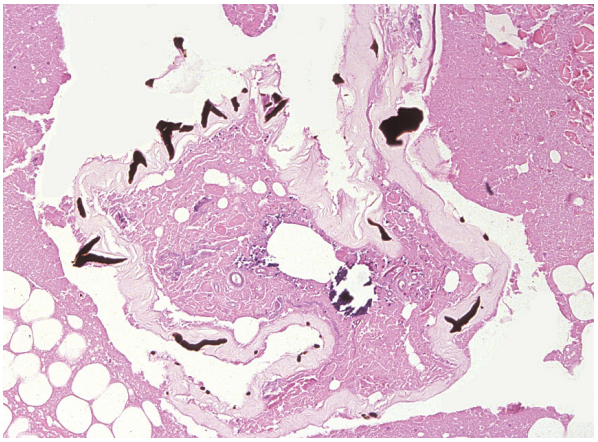


**Figure 18.38**
Higher magnification of pigmented spines of *Dermatobia hominis* larva described in figure 18.37, in panniculus. x80

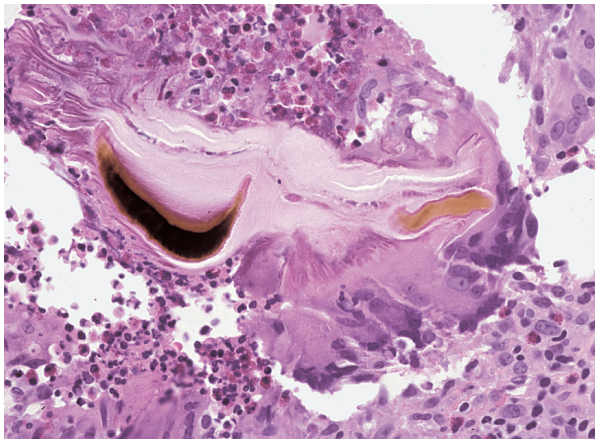


**Figure 18.39**
Pigmented spines of degenerating *Dermatobia hominis* larva in scalp of patient who visited Bolivia. x260



**Figure 18.40**
First-stage larva of *Cuterebra ruficrus* with 9 bands of spines.

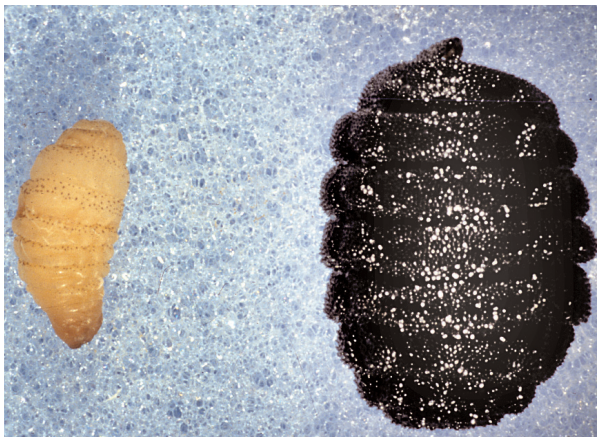


**Figure 18.41**
Second- (left) and third-stage (right) *Cuterebra* sp larvae. Second-stage larva is plumper than first-stage larva shown in Figure 18.40, and bands of spines are less noticeable. Third-stage larva is larger still.

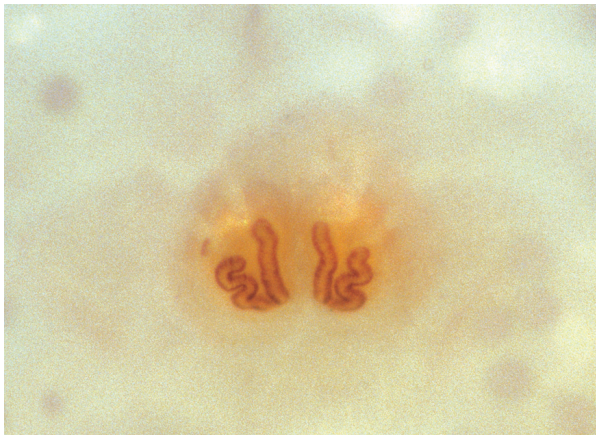


**Figure 18.42**
Posterior spiracles of second-stage *Cuterebra* sp larva have 2 respiratory slits each.

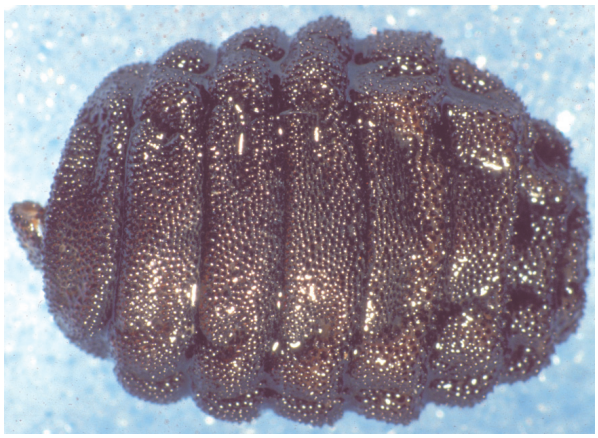


**Figure 18.43**
Early third-stage *Cuterebra* sp larva removed from scalp is covered with whitish spines.

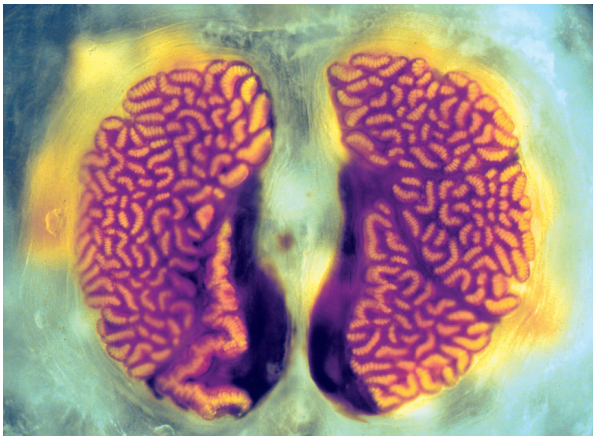


**Figure 18.44**
Kidney-shaped posterior spiracles in third-stage *Cuterebra* sp larva have numerous respiratory slits.



**Figure 18.45**
Adult *Cuterebra* sp fly resembles a bumblebee.

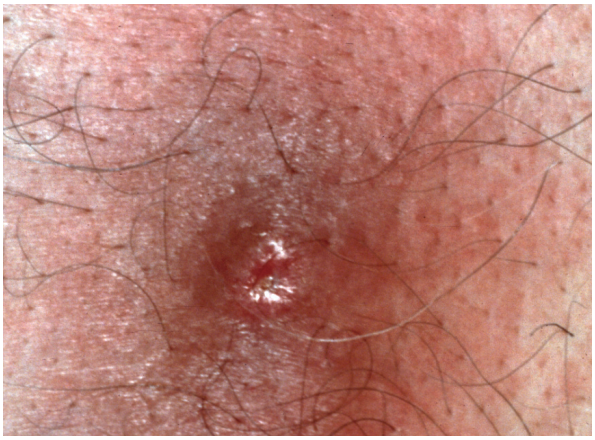


**Figure 18.46**
Single furuncular nodule containing second-stage *Cuterebra* sp larva on skin of chest.

spines around the anterior portion of each of 10 to 12 pseudo-segments (Fig 18.63). Anterior spiracles are distinctively fan-like. Posterior spiracles are elevated; slits point toward an opening in the peritreme and have lateral swellings (Fig 18.64). The button is indistinct or absent.[6] Pigmented tracheal trunks (Fig 18.63) distinguish *C. hominivorax* larvae from the noninvasive, carrion-feeding larvae of the closely related *Cochliomyia macellaria*.[3,6]

A female *C. hominivorax* fly is attracted to body orifices and minor wounds in living animals (Fig 18.65). Within minutes, it can lay 10 to 400 eggs, from which invasive first-stage larvae emerge in 11 to 22 hours. Larvae penetrate mucous membranes or wounds, migrate through underlying tissues while feeding, and emerge through the skin 3 to 5 days later. Larvae drop to the ground, pupate, and emerge as adult flies a week later. The entire life cycle is completed within a month.

In humans, infection can cause severe discomfort and disfiguring wounds.[14,15] Larvae that penetrate the head may migrate to the brain and cause death.[16]

## *Chrysomyia bezziana* (Old World screwworm)

*Chrysomyia bezziana* (synonym *Pycnosoma bezzianum*) resembles *Cochliomyia hominivorax* in life cycle and pathogenesis. It is a common parasite of livestock throughout Africa, from India to southern China, and across Indonesia to New Guinea. *Chrysomyia bezziana* flies are metallic green or blue. Larvae resemble *C. hominivorax* larvae, but are larger (4 mm to 9 mm for second-stage larvae and up to 18 mm for third-stage larvae) (Figs 18.66 to 18.68). *Chrysomyia bezziana* is an obligate parasite whose larvae must develop on living tissue, unlike its close relative, *Chrysomyia megacephalus*, a noninvasive carrion-feeder that sometimes causes passive or wound myiasis. *Chrysomyia bezziana* can also cause myiasis of the nose, mouth, and accessory sinuses,[17] a disease known as peenash in India (Figs 18.69 to 18.73).[3]

## *Hypoderma* sp (cattle grub, heel fly, deer warble)

*Hypoderma lineatum* (common cattle grub or heel fly), *Hypoderma bovis* (northern cattle grub), and *Hypoderma diana* (deer warble) infect humans, cattle, and deer throughout North America, Europe, and Asia.[3] Most infections in humans are probably caused by *H. lineatum*, but distinctions among the species are not medically important. Second-stage larvae of *Hypoderma* sp are 10 mm to 18 mm long, and have indistinct pseudosegments and approximately 16 bands of small spines on the ventral surface. The stout third-stage larvae are up to 3 cm long and are cream-colored to brown (Fig 18.74), depending on maturity. The kidney-shaped posterior spiracle has an eccentric button and many openings divided into plates (Fig 18.75).[3,6]

The bumblebee-like flies are densely covered with yellow

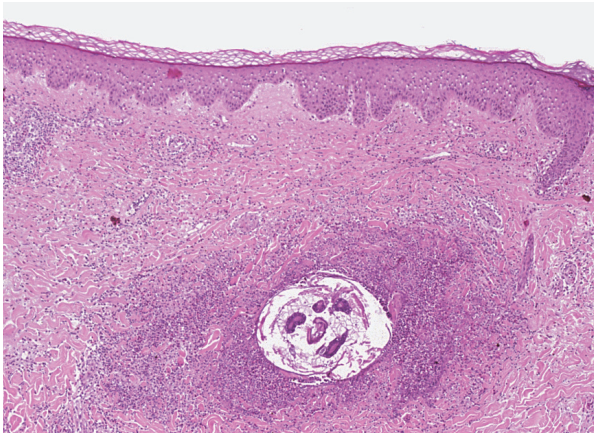


**Figure 18.47**
First-stage larva in skin of leg 13 days after invasion of *Cuterebra* sp fly. x105

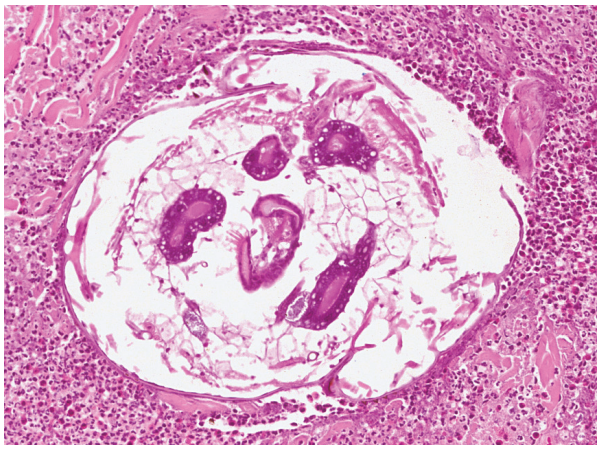


**Figure 18.48**
Higher magnification of *Cuterebra* larva seen in figure 18.46. Larva is approximately 500 $\mu$m in diameter. x140

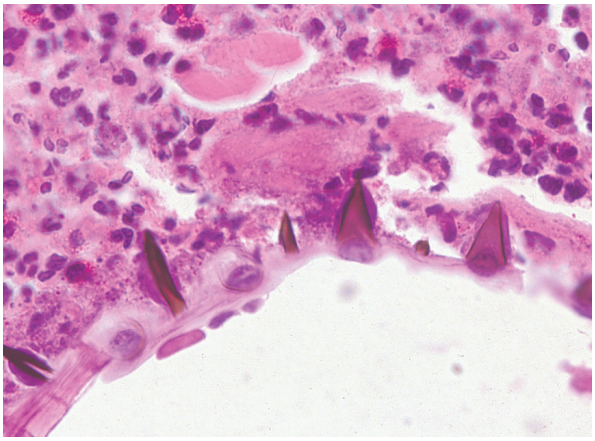


**Figure 18.49**
Sharp-pointed black spines on cuticle of first-stage *Cuterebra* sp larva in inflammatory nodule. x640

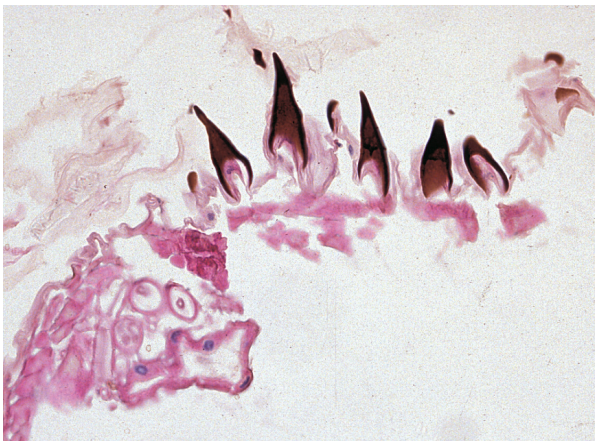


**Figure 18.50**
Black spines on later-stage *Cuterebra* sp larva, approximately 4 times larger than spines depicted in Figure 18.49. x200



**Figure 18.51**
Dorsal view of second-stage *Cordylobia anthropophaga* larva removed from thigh of expatriate in Benin.



**Figure 18.52**
Cephalic segments of *Cordylobia anthropophaga* larva described in Figure 18.51. Spines are larger and denser than those in anal segments. (See 18.53)

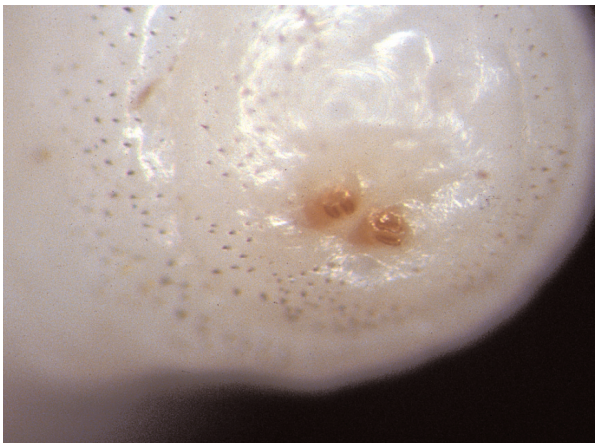


**Figure 18.53**
Posterior spiracles of *Cordylobia anthropophaga* described in Figures 18.51 and 18.52. Two respiratory slits angle dorsally and medially with no peritreme.

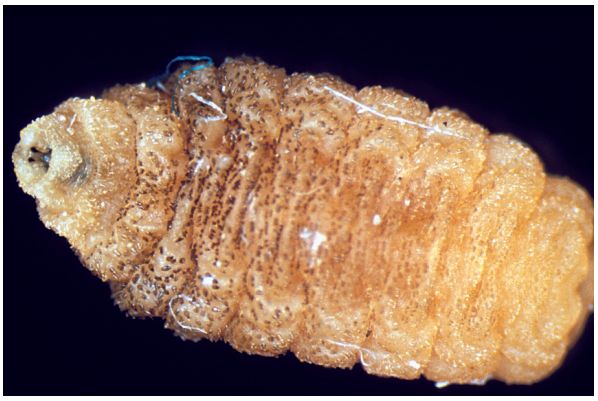


**Figure 18.54**
Ventral view of third-stage *Cordylobia anthropophaga* larva showing transversely wrinkled segments.



**Figure 18.55**
Dorsal view of *Cordylobia anthropophaga* larva seen in Figure 18.54 showing posterior spiracles.



**Figure 18.56**
Each posterior spiracle of third-stage *Cordylobia anthropophaga* larva seen in figures18.54 and 18.55 has 3 moderately sinuous slits and button. There is no sclerotized peritreme.



**Figure 18.57**
Cutaneous furuncles due to *Cordylobia anthropophaga* on left abdomen and flank. Patient sunbathed on poolside wooden cot in Ivory Coast 9 days previously.

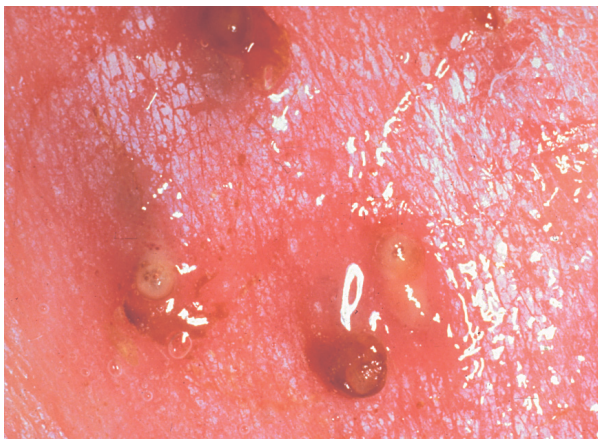


**Figure 18.58**
*Cordylobia anthropophaga* larvae migrate to surface of skin when breathing holes are covered with petroleum jelly.

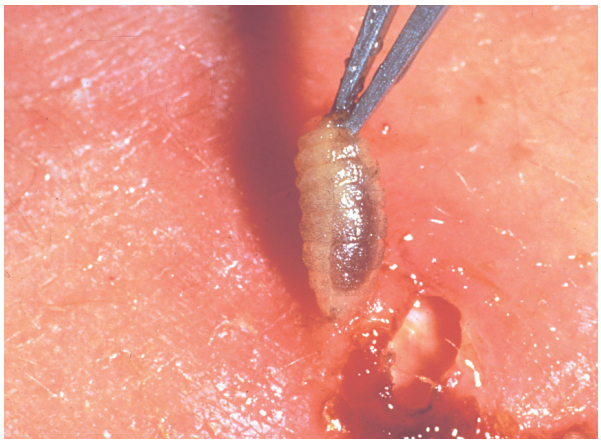


**Figure 18.59**
Fifteen minutes after application of petroleum jelly to breathing hole, *Cordylobia anthropophaga* larva is lifted from lesion.

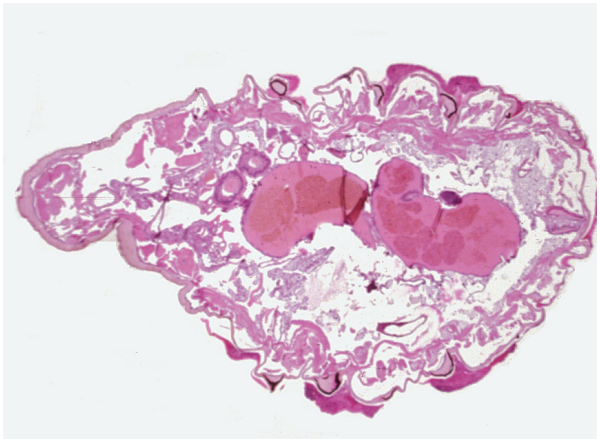


**Figure 18.60**
Cross section of *Cordylobia anthropophaga* larva removed from arm of expatriate in West Africa. x13

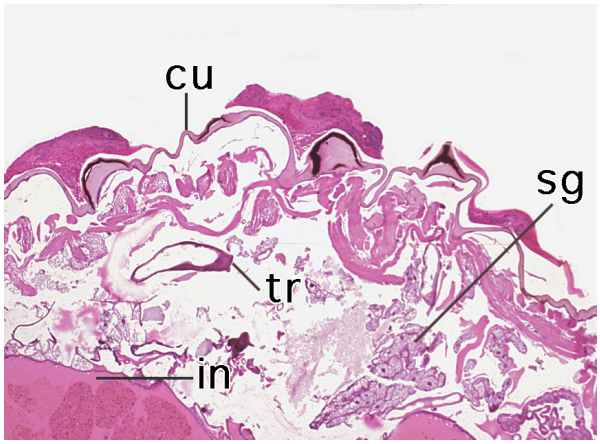



**Figure 18.61**
Chitinized cuticle (cu), black spines, salivary glands (sg), intestine (in) containing digested blood, and tracheae (tr) in *Cordylobia anthropophaga* larva seen in figure 18.60. x26

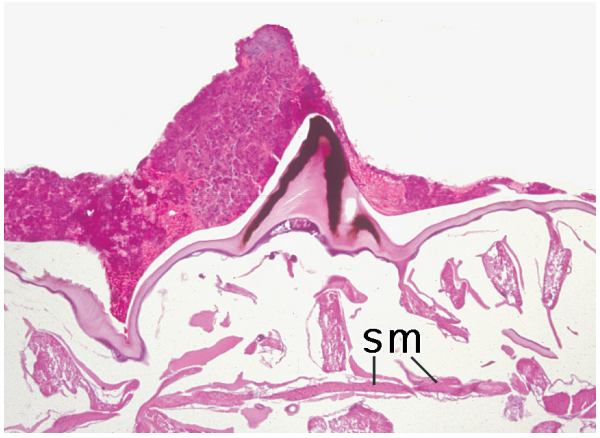



**Figure 18.62**
Black spine and striated muscle (sm) of *Cordylobia anthropophaga* larva seen in Figures 18.60 and 18.61. x218

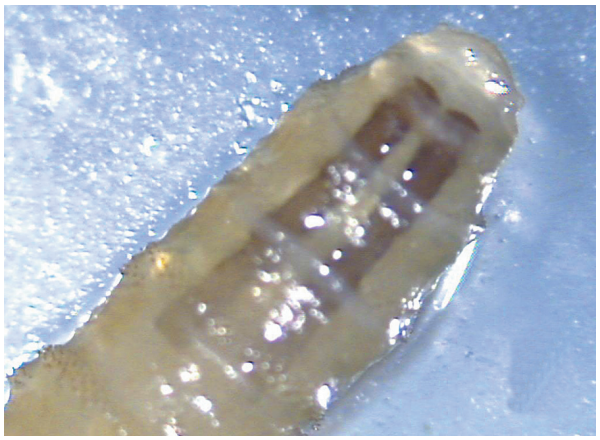


**Figure 18.63**
Dorsal view of pigmented tracheal trunks of third-stage *Cochliomyia hominivorax* larva.

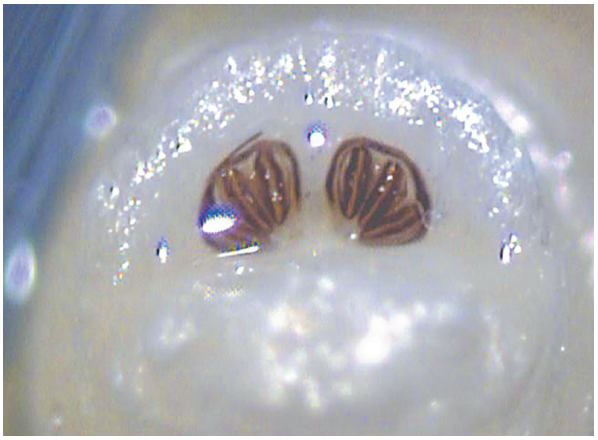


**Figure 18.64**
Posterior spiracles of third-stage *Cochliomyia hominivorax* larva. Respiratory slits point toward opening in peritreme.

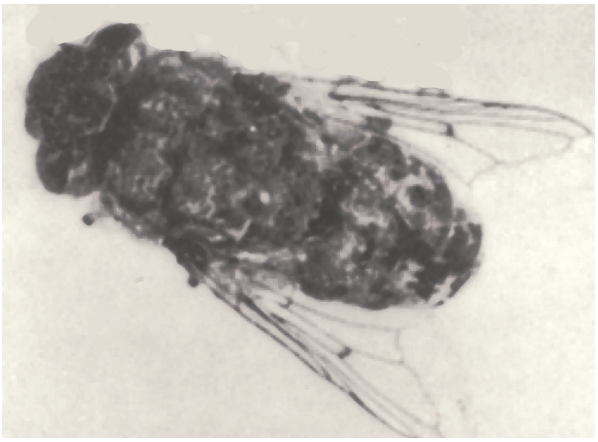


**Figure 18.65**
Adult *Cochliomyia hominivorax (screwworm).*

hair divided by 2 broad bands of black hair. Adult females, which live for only a few days, repeatedly strike an animal host, laying 1 or more eggs at each pass. Eggs adhere to the host's body hairs for 4 days, after which first-stage larvae emerge, crawl down the hairs, and penetrate the skin through hair follicles or minor breaks in the skin. Over a period of 4 months, larvae migrate along nerve trunks to the spinal cord and brain (Fig 18.76), proceed to the muscle and adipose tissue of the back, and lodge in the dermis where they create a warble (Fig 18.77). After 11 weeks, mature third-stage larvae drop to the ground and pupate. The complete life cycle in a definitive host takes 1 year.

Larvae rarely develop fully in humans. They usually create an atypical creeping eruption with swellings that appear suddenly and may persist for several weeks. The process is then repeated at a site several centimeters away. Larvae tend to migrate toward the head and neck, leaving no definite track. Before larvae develop to the third stage, they usually die, provoking an intense inflammatory response, a tender swelling, and edema involving much of the head and face. There may be peripheral eosinophilia.[18] The creeping eruption caused by *Hypoderma* sp is deeper in the subcutaneous tissue and more painful than that caused by *Gasterophilus* sp. Invasion of the orbit by first-stage *Hypoderma* sp larvae may irreversibly damage the eye.[19]

## *Gasterophilus* sp (horse bots)

Several species of *Gasterophilus* infect horses, donkeys, and zebras. Infections with *Gasterophilus intestinalis* (also known as *Gasterophilus equi*), *Gasterophilus haemorrhoidalis* (nose botfly), and other undetermined species have been reported in humans.[3,20,21] Larvae are elongate with rows of spines. The posterior spiracle is not deeply sunken and has curved slits (Fig 18.78).[6] First-stage larvae hatch from eggs laid on the host's facial hairs, penetrate the epidermis, and migrate to the mouth, where they are swallowed. Larvae

lodge in the gastric mucosal epithelium, where they mature to the third stage (Fig 18.79). They are passed in feces and pupate in the ground.

Invasive first-stage larvae occasionally infect humans, causing a creeping eruption of the skin (myiasis linearis) that is strikingly similar to the cutaneous larva migrans of *Ancylostoma braziliense*. Migrating larvae create narrow, raised, erythematous tunnels in serpentine or crisscross patterns in the skin. The eruptions are severely pruritic, but not as painful as those caused by *Hypoderma* sp. Larvae usually do not develop beyond the first stage in humans. They occasionally migrate to the stomach and cause irritation (Fig 18.79). There is a report of a patient with a pulmonary infarct caused by a larva tentatively identified as *G. intestinalis*,[20] and another report of a *G. intestinalis* larva in the posterior chamber of the eye.[21] The distinctive bands of a *Gasterophilus* sp larva are visible through well-oiled skin, making extraction with a needle possible.

### *Wohlfahrtia vigil* (Nearctic flesh fly)

*Wohlfahrtia vigil* infects humans in eastern North America; the subspecies *Wohlfahrtia vigil opaca* infects humans in western North America. A closely related obligate parasite, *Wohlfahrtia magnifica*,[22] infects wounds or body openings but cannot penetrate skin (Figs 18.80 to 18.83). A European species, *Wohlfahrtia meigenii*, closely resembles *W. vigil* but is strictly saprophytic. *Wohlfahrtia vigil* larvae are tapered anteriorly.[3] The anterior spiracle has 9 or 10 papillae. Posterior spiracles are located within a pronounced depression surrounded by 12 tubercles. The female *W. vigil* fly deposits eggs on or near a suitable host, preferring clean human flesh to filth or suppuration. First-stage larvae penetrate intact skin and lodge in the underlying dermis, creating a painful furuncular nodule that may resemble impetigo. The white posterior end of the larva is visible and sometimes mistaken for pus. Young children, especially infants, are most often infected.[23]

### *Oestrus ovis* (sheep nasal botfly, head bot)

This honeybee-like fly is found in North America, Europe, and Asia. Larvae have strong curved mouth hooks (Figs 18.84 to 18.86).[3] Single hairlike spines arise from pits (Figs 18.87 and 18.88). Posterior spiracles are barely visible and not divided into sclerotized plates. The button is central (Fig 18.89).[6] During its 28-day lifespan, the female fly aggressively strikes the eyes, nares, or mouth of sheep and goats, depositing a first-stage larva with each strike. Larvae immediately bore into the mucosa and migrate to the frontal sinuses or nasopharynx. They anchor to the epithelium using 2 prominent claws, and mature in 1 to 12 months.

Infection in humans is prevalent in areas where people live in close association with large numbers of sheep and goats. In humans, *Oestrus ovis* causes ophthalmomyiasis. Larvae deposited in or near the eye migrate to the




**Figure 18.66**
Four of 7 *Chrysomyia bezziana* larvae removed from maxillalry burrow in mouth of girl from Democratic Republic of Congo. Third-stage larvae were 13 mm long and 3 mm wide at midbody.

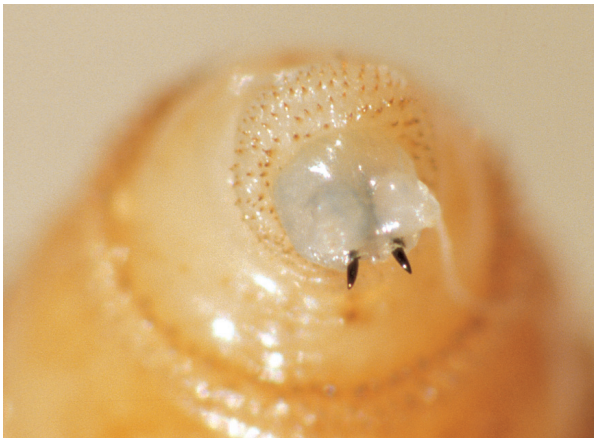


**Figure 18.67**
Mandibular sclerite with teeth of *Chrysomyia bezziana* larva is longer than width of basal portion of larva seen in Figure 18.66.

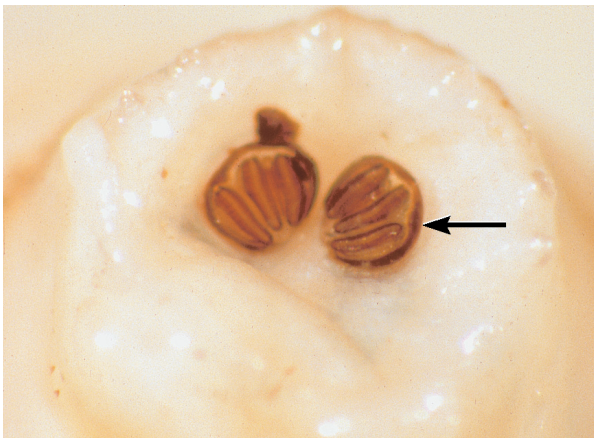


**Figure 18.68**
Posterior spiracles of *Chrysomyia bezziana* larva seen in Figures 18.66 and 18.67, showing incomplete peritreme (arrow). Respiratory slits point toward opening in peritreme.



**Figure 18.69**
*Chrysomyia bezziana* larva from oral cavity of African patient. three slits in posterior spiracle point toward ventral opening in peritreme. Note distinct button (arrow).

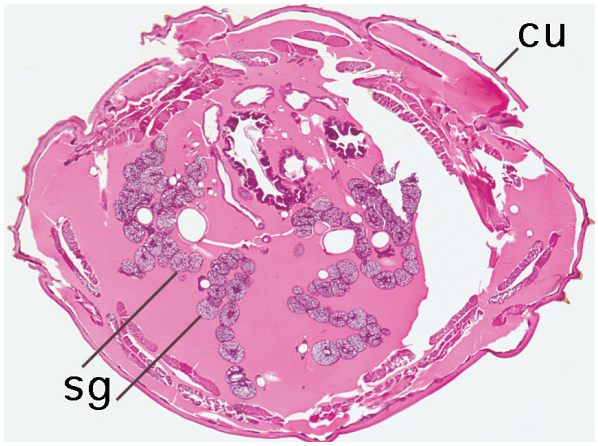



**Figure 18.70**
Higher magnification *Chrysomyia bezziana* larva showing cuticle (cu), and salivary glands (sg). x18.5

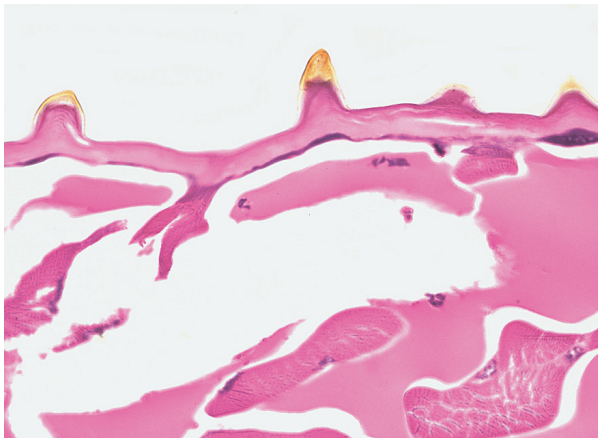


**Figure 18.71**
Black pigment in inner layer of cuticle of *Chrysomyia bezziana* larva seen in Figure 18.70. Note pointed yellow-brown tips of spines. x136

conjunctival sac, eyelid, or lachrymal duct. Symptoms resemble acute catarrhal conjunctivitis. The orbit of the eye is usually spared, and the infection is benign and self-limiting.[24] Larvae that directly penetrate the eye do not develop further, but cause pain and tissue destruction that may lead to enucleation of the eye.

### *Rhinoestrus purpureus* (Russian gadfly)

*Rhinoestrus purpureus* is found throughout eastern and southern Europe, northern Africa, and Asia Minor. Larvae infect cattle, horses, and sometimes humans. Crescent-shaped posterior spiracles partially encircle the button.[3] The postanal swelling has 2 conical lateral protuberances. Life cycle and clinical features are very similar to *O. ovis*.[25]

### *Auchmeromyia luteola* (Congo floor maggot)

*Auchmeromyia luteola* is sometimes identified as a species that causes myiasis. In tropical Africa, this unusual but medically interesting fly deposits eggs on the earthen floor of a human dwelling. The eggs hatch within 2 days. At night, larvae, known as Congo floor maggots, seek out sleeping humans, pierce their skin with oral hooklets, and feed on exuded blood. Engorged larvae return to the soil at sunrise. While an attack by the blood-feeding larvae of *A. luteola* is a nuisance, we do not believe it constitutes myiasis in the strictest sense.[26]

## *Wound (or Traumatic) Myiasis*

Eggs or larvae are deposited on traumatized or chronically diseased tissue (Figs 18.90 to 18.93). The same fly species that attack healthy tissues of sleeping or incapacitated persons also deposit eggs or larvae within traumatized or diseased tissue. Opportunistic fly larvae feed upon dead tissue, inflammatory cells, or secondary bacterial invaders.

Patients with severe wounds are usually incapacitated to some degree, even if they are conscious. They may be unable or reluctant to move or touch the injured area, or to tolerate frequent changes of dressing. From the perspective of a probing fly, wounded tissue on such a patient is carrion.[27] Invasion of the wound by fly larvae often aggravates local pain and delays healing. If the wound is not thoroughly cleansed, larvae may consume surrounding healthy tissue and cause an already traumatized patient added distress.

Some fly larvae apparently feed upon secondary bacterial invaders without inhibiting normal healing of wounds. *Phaenicia sericata*,[28] a benign fly larva that feeds on carrion, has been used to treat battlefield injuries since the American Civil War (Figs 18.94 to 18.99). Isolated peoples in China, Southeast Asia, and Australia have used carrion-feeding fly larvae to aid the healing of wounds since ancient times.



**Figure 18.72**
Tips of spines of *Chrysomyia bezziana* larva may be pointed or round. x270

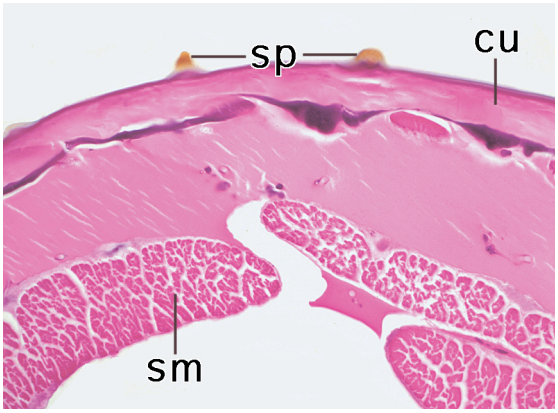



**Figure 18.73**
Higher magnification of striated muscle (sm), cuticle (cu), and pointed and round spines (sp) of *Chrysomyia bezziana* larva described in Figure 18.70. x200



**Figure 18.74**
Single stout brown third-stage larvae of *Hypoderma* sp.

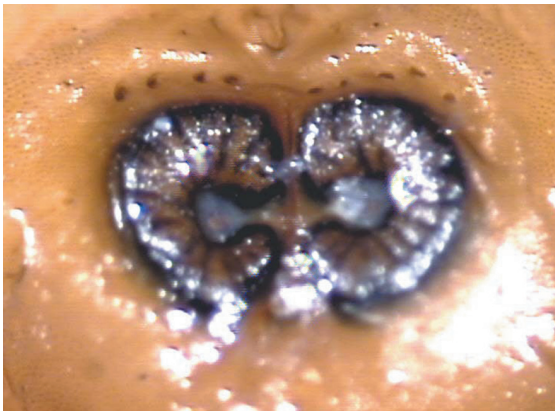


**Figure 18.75**
Kidney-shaped posterior spiracles of third-stage *Hypoderma lineatum* larva.

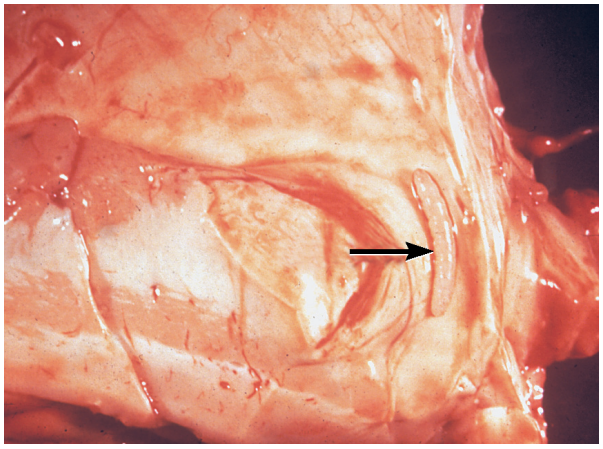


**Figure 18.76**
Long cream-colored third-stage larva of *Hypoderma bovis* (arrow) in lateral ventricle of bovine brain.

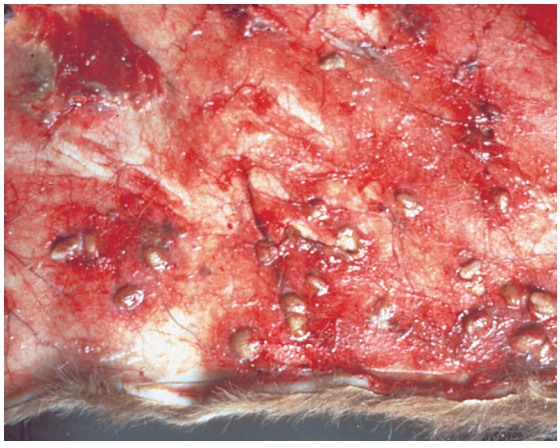


**Figure 18.77**
Single stout brown third-stage larvae of *Hypoderma bovis* on underside of oxhide.

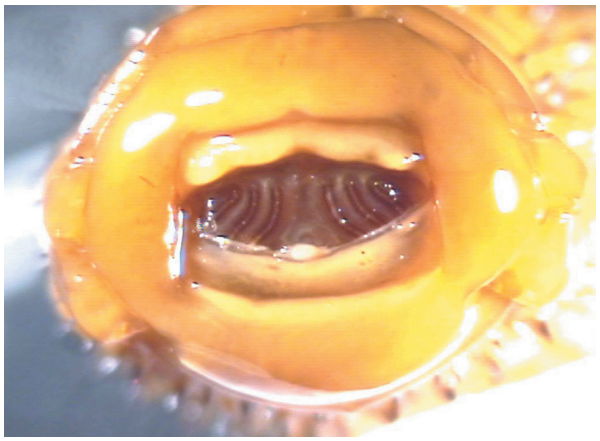


**Figure 18.78**
Posterior spiracle in third-stage *Gasterophilus intestinalis* larva has curved respiratory slits.



**Figure 18.79**
Third-stage *Gasterophilus intestinalis* larvae in stomach of horse.



**Figure 18.80**
Third-stage *Wohlfahrtia magnifica* larva removed from orbital mass (see Figure 18.83).

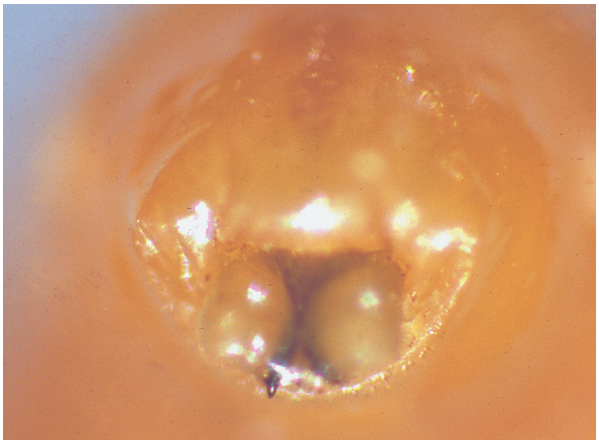


**Figure 18.81**
Anterior bucal hooks of third-stage *Wohlfahrtia magnifica* larva.

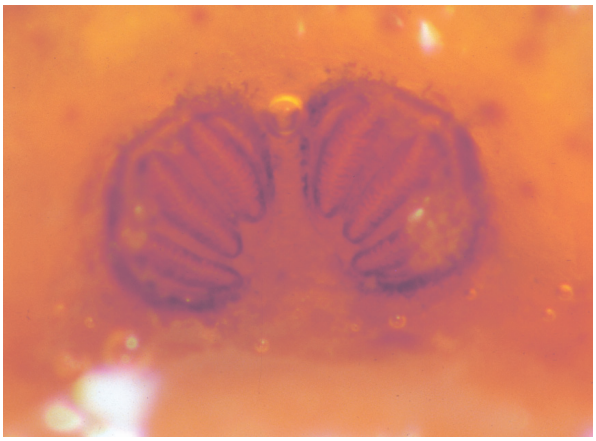


**Figure 18.82**
Posterior spiracles of third-stage *Wohlfahrtia magnifica* larva.



**Figure 18.83**
Third-stage *Wohlfahrtia magnifica* larva on retro-orbital surface of rapidly expanding squamous cell carcinoma replacing contents of eye in patient from India.

## *Passive Myiasis*

Eggs or larvae of saprophytic or house flies are deposited on incapacitated patients or incidentally ingested in food. They cause relatively little damage to healthy tissue. There are 3 distinct types of passive myiasis: 1) false enteric myiasis, 2) true enteric myiasis, and 3) imperceptive myiasis.

### False enteric myiasis

False enteric myiasis is caused by common house or storeroom flies such as *Piophila* sp,[29] whose larvae are called cheese skippers. Flies of the families Muscidae and Sarcophagidae may also cause this type of infection. Humans usually acquire false enteric myiasis, sometimes called pseudomyiasis,[30] by ingesting eggs or larvae deposited on food (Fig 18.100). In many cases, this is not a true myiasis, since the larvae's normal development on food is interrupted by incidental ingestion. Ingested larvae probably do not feed or develop while passing through the host's gastrointestinal tract. In sufficient numbers, larvae may provoke mild to severe abdominal pain, malaise, vomiting, nausea, and bloody diarrhea. With rare exceptions, larvae eventually pass without further complications.

### True enteric myiasis

True enteric myiasis is caused by fly larvae that feed and develop within the lumen of the host's bowel. In animals, *Gasterophilus* sp larvae must attach to the gastric mucosa in order to develop (Fig 18.79). In humans, *Gasterophilus* sp larvae cause a creeping eruption on the skin, not enteric myiasis. True enteric myiasis in humans is probably acquired through the rectum, where excrement-feeding larvae develop. The rat-tailed larvae of *Eristalis tenax*,[31] the drone fly, appear to be specifically adapted to this environment. They lodge in the rectum and project a stalked breathing aperture toward the anus. *Fannia* sp,[32] *Muscina* sp,[33] and *Sarcophaga* sp[34] larvae also develop in the rectum (Fig 18.101). Infection usually occurs after eggs and larvae of these flies are deposited near the anus. Paralyzed patients and people who sleep uncovered are susceptible to this type of infection.

### Imperceptive myiasis

Imperceptive myiasis is infection of the body orifices of incapacitated or sleeping persons by larvae of saprophytic flies that normally thrive on dead tissue. When a living host is unable to drive off a probing fly, the fly deposits eggs, usually in an orifice, as it would in a dead host. Most of these infections involve the mouth, nares, eyes, or ears of paralyzed or comatose patients (Figs 18.102 and 18.103). Some hospitals have reported blow flies (Calliphoridae) of the genera *Calliphora* (Figs 18.104 to 18.108),[35] *Phaenicia* (Figs 18.94 to 18.99),[28] *Lucilia* (Figs 18.109 to 18.116),[36] *Phormia*,[27] *Cochliomyia* (Figs 18.63 to 18.65),[15] *Chrysomyia* (Figs 18.66 to 18.73),[34] and *Megaselia* sp[36] as the cause of nosocomial myiasis among disabled patients.

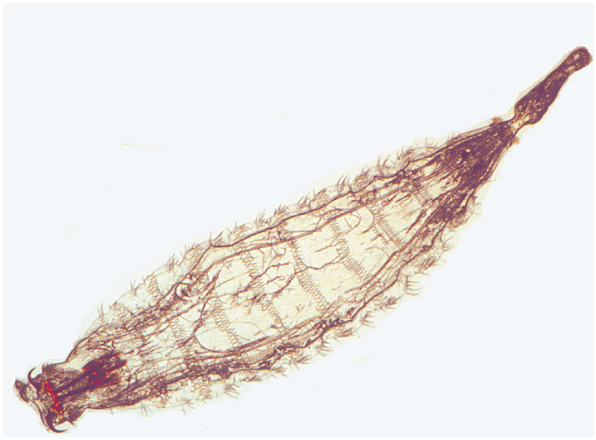


**Figure 18.84**
First-stage *Oestrus ovis* larva removed from margin of eyelid. Patient had traveled to United States from England.

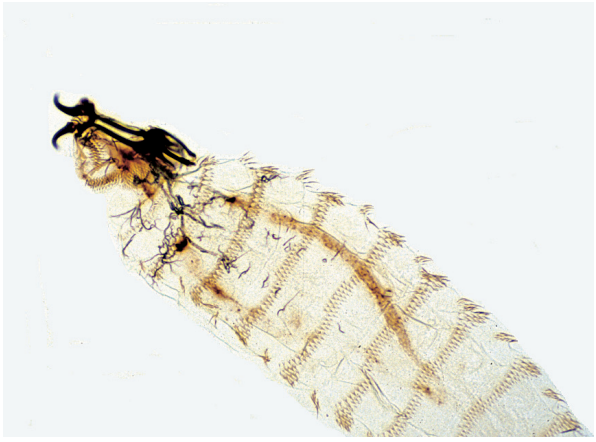


**Figure 18.85**
Transparent first-stage *Oestrus ovis* larva removed from conjunctiva of patient from United States.

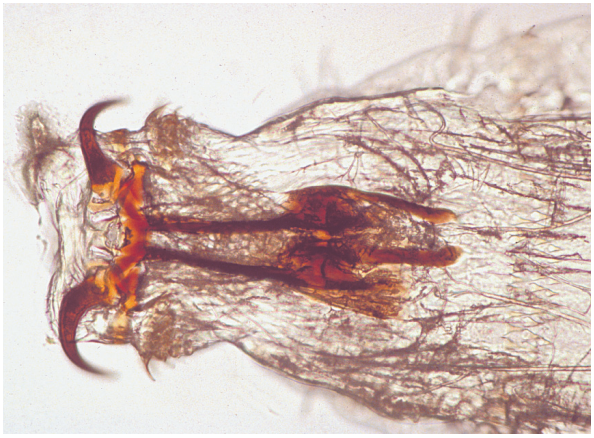


**Figure 18.86**
Strong curved mouth hooks on first-stage *Oestrus ovis* larva seen in Figure 18.84.

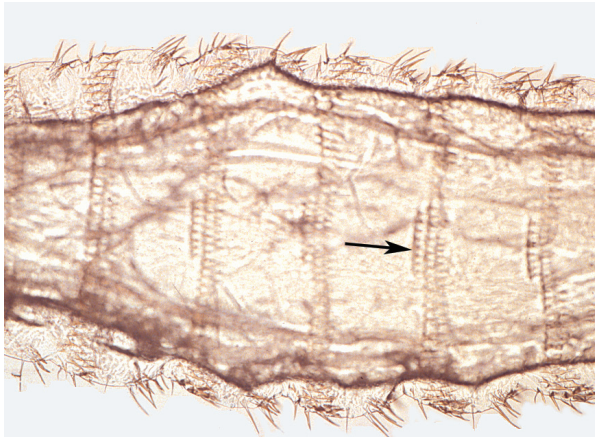


**Figure 18.87**
Single hair rises from each pock-like pit (arrow) on surface of *Oestrus ovis* larva. Transparent larva is not readily observable in situ.

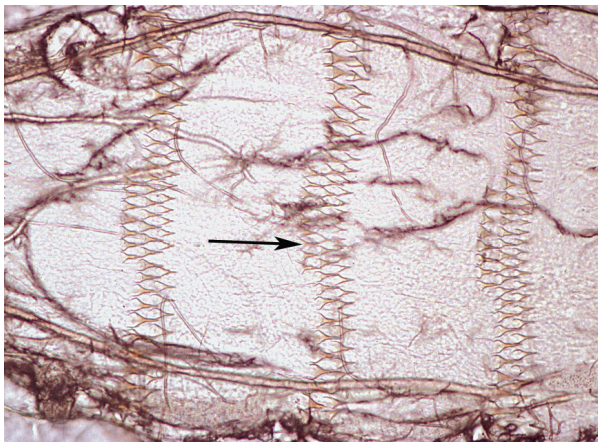


**Figure 18.88**
Higher magnification of pock-like pits (arrow) implanted with single hair on surface of *Oestrus ovis* larva.

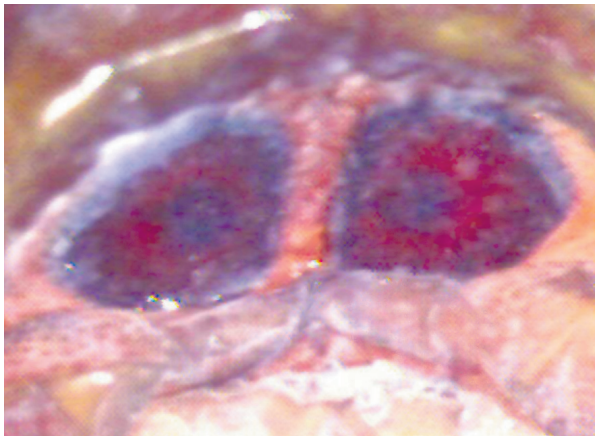


**Figure 18.89**
Posterior spiracle of *Oestrus ovis* larva has central button and is not divided into sclerotized plates.

Usually, larvae are detected and eliminated soon after infection, preventing damage to host tissue. A fly probing the face of a sleeping person will probably evoke a defensive response, but a fly around the genitalia or rectum may not. People who sleep uncovered in areas infested by flies may acquire myiasis of the rectum, penis, or vagina. An individual with periodontal disease sleeping with an open mouth may acquire dental myiasis caused by saprophytic species of *Chrysomyia*.

## Pathologic Features

In all types of myiasis, the inflammatory reaction ranges from acute eosinophilic with abscess formation, to granulomatous (Figs 18.27, 18.36 and 18.114–18.116). The surrounding inflammatory infiltrate may include lymphocytes, eosinophils, histiocytes, mast cells, and plasma cells (Fig 18.27).[4]

## Diagnosis

Diagnosis of myiasis is made by microscopic identification of larvae; gross examination of whole larvae preserved in 70% alcohol or formalin is essential for definitive identification. The patient's travel history is another useful factor in species identification, since the geographic distribution of each species that causes myiasis is well documented.

Fly larvae that cause myiasis must be differentiated from other arthropods that infect the skin, such as ticks, mites, and fleas. These latter organisms are found in the epidermis (*Tunga* fleas), keratin (scabies mites), and hair follicles (*Demodex)*, but do not penetrate to the dermis or subcutaneous tissue, as is common with fly larvae.[11] The presence of eggs would rule out fly larvae, which lack the reproductive structures of mature arthropods, but could indicate *Tunga* fleas or scabies and *Demodex* mites. *Tunga* fleas have no spines; mites lack a discernible hypodermis.[11]

## Treatment and Prevention

Whichever species is the cause of infection, myiasis is treated by extracting the larvae. There are no specific medications for dislodging larvae. Endoscopic removal is recommended for larvae in nasal passages. In wounds, surgical exposure may help to visualize the organisms and facilitate their removal with instruments. A solution of 5% chloroform and olive oil applied to the open wound may help to immobilize larvae during this procedure. Larvae can be removed from furuncular lesions surgically, or by suffocation or application of lateral pressure.[37] Repeated application of materials such as petroleum jelly or bacon fat[38] to the overlying skin blocks the spiracles, suffocating the larvae and causing them to partially or completely self-extrude. Ivermectin will kill larvae and facilitate extraction.[39,40] Alum (hydrated



**Figure 18.90**
First-stage larva (family Muscidae) removed from arm of patient with no history of travel outside United States. Note 7 rows of small cuticular spines.

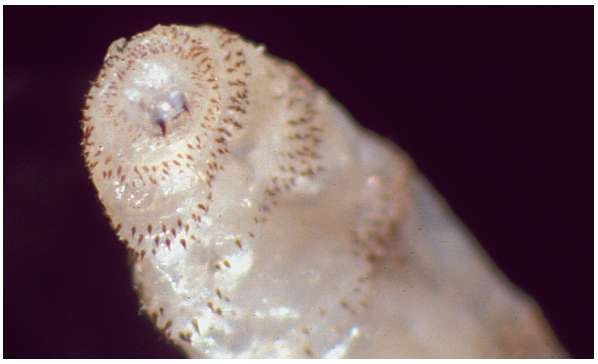


**Figure 18.91**
Cephalic segment of first-stage larva (family Muscidae) seen in Figure 18.90 showing mouth hooks. Adult fly may have deposited eggs on arm of sleeping host.



**Figure 18.92**
First-stage larva (family Muscidae) seen in Figures 18.90 and 18.91, showing posterior spiracles (arrow).



**Figure 18.93**
Wound myiasis in patient from Democratic Republic of Congo with genital herpes. Thirty larvae were removed from left labium.



**Figure 18.94**
One of 5 *Phaenicia sericata* larvae removed from ear of patient with repeated ear infections.

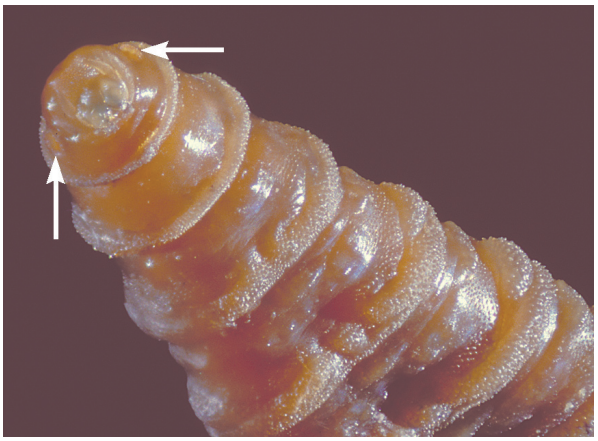


**Figure 18.95**
Cephalic end of *Phaenicia sericata* larva showing mouth hooks. Eye-like structures (arrows) on first thoracic segment are anterior spiracles. Note small cuticular spines.

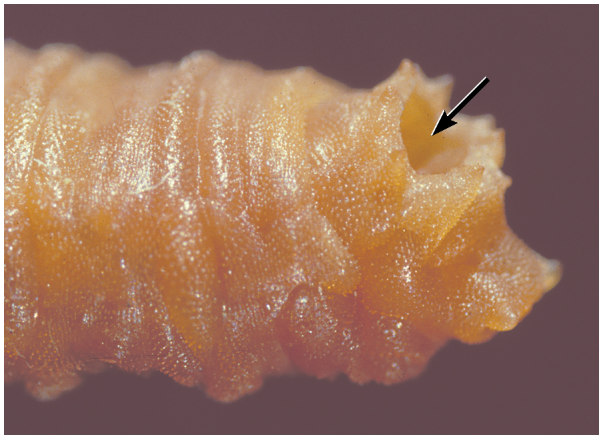


**Figure 18.96**
Lateral view of anal segment of *Phaenicia sericata*. Spiracles (arrow) are located in dorsal cavity.



**Figure 18.97**
Posterior spiracles of *Phaenicia sericata* have 3 slits each; peritreme opens ventrally. There may be 6 to 20 transverse subdivisions of slits.

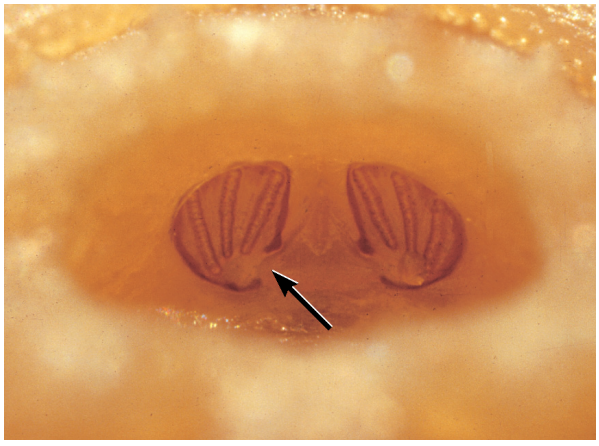


**Figure 18.98**
Third-stage larva of *Phaenicia sericata* removed from patient who had not traveled outside United States. Posterior spiracles have 3 slits; peritreme (arrow) opens ventrally.

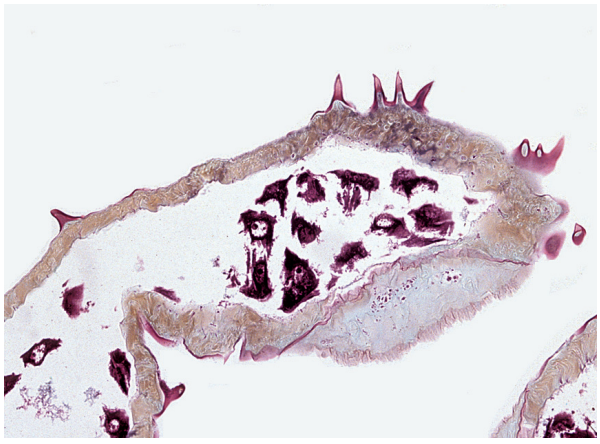


**Figure 18.99**
Cuticle and spines of *Phaenicia sericata* larva. x150



**Figure 18.100**
Larva of black soldier fly (*Hermetia illucens*) passed in feces of patient who regularly chewed tobacco.



**Figure 18.101**
Adult *Sarcophaga hemorrhoidalis.*

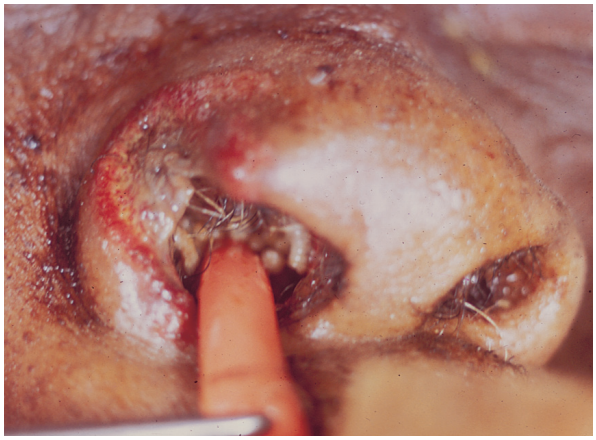


**Figure 18.102**
Myiasis of nares surrounding nasogastric tube in incapacitated patient.



**Figure 18.103**
Nonpathogenic fly larva in mucus expelled by sneeze. Two-year-old patient had rhinorrhea and mild cough for 2 days.



**Figure 18.104**
One of 3 *Calliphora vicina* larvae removed by lavage from ear.

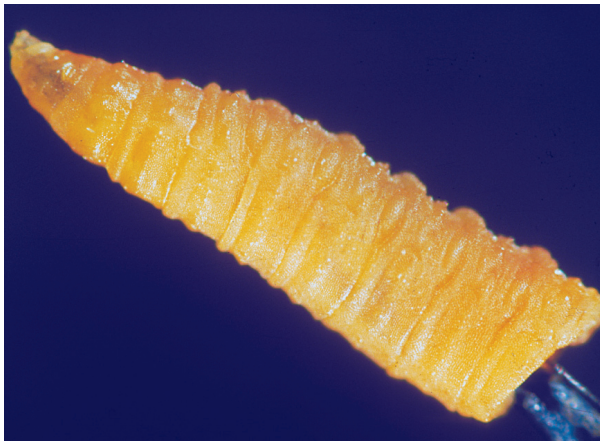


**Figure 18.105**
*Calliphora* sp larva removed from leg at site of wound.

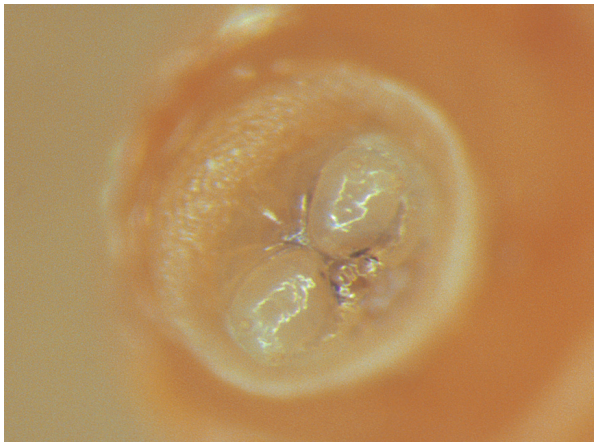


**Figure 18.106**
Cephalic end of *Calliphora vicina* larva.

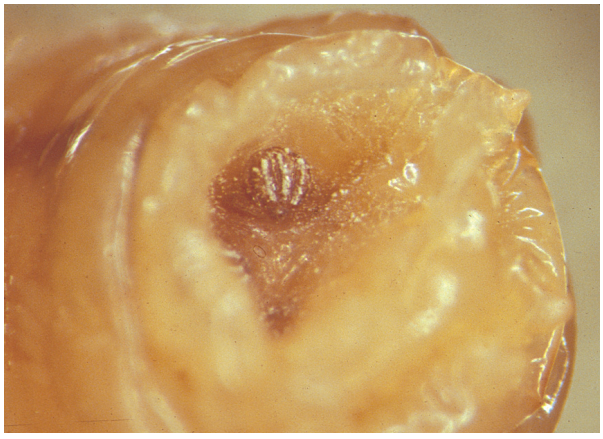


**Figure 18.107**
Posterior spiracles in shallow cavity in anal segment of third-stage *Calliphora vicina* larva.

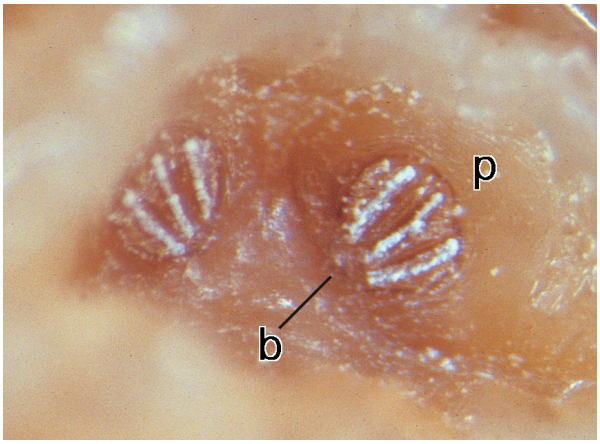



**Figure 18.108**
Six transverse subdivisions in respiratory slits of *Calliphora vicina* larva. Peritreme (p) and button (b) are heavily chitinized.



**Figure 18.109**
*Lucilia* sp larva (1.3 cm long) removed from back of patient in Africa.

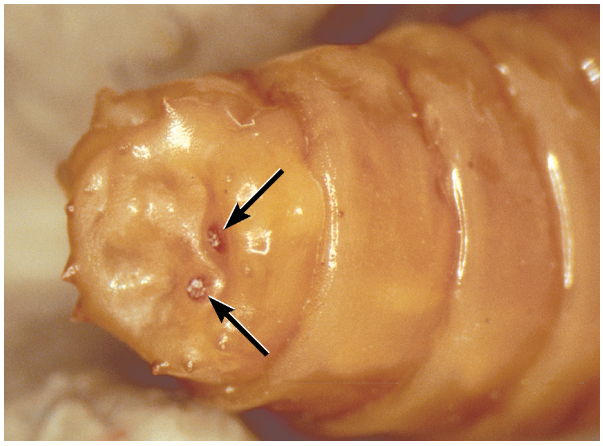


**Figure 18.110**
Posterior spiracles (arrows) located in shallow cavity of anal segment of *Lucilia* sp larva.

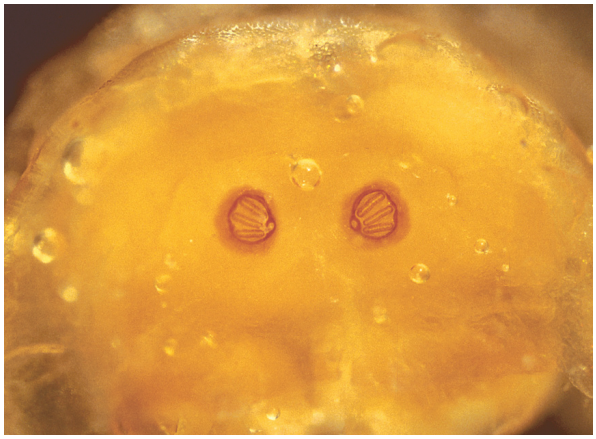


**Figure 18.111**
Caudal view of posterior spiracles of *Lucilia* sp larva.

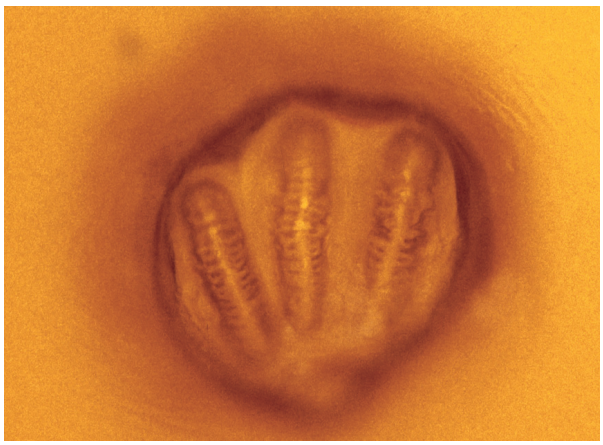


**Figure 18.112**
Posterior spiracles of *Lucilia* sp have straight slits with numerous transverse subdivisions, closed peritreme, and heavily chitinized peritreme and button.

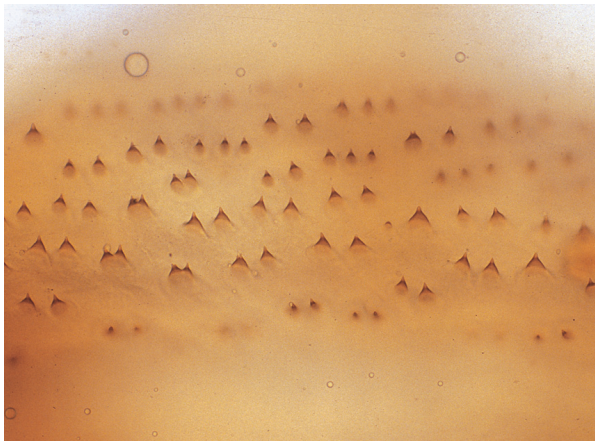


**Figure 18.113**
Pigmented spines on cuticle of *Lucilia* sp larva.

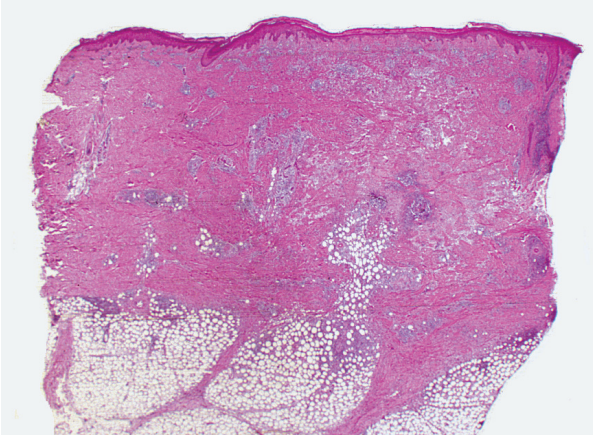


**Figure 18.114**
Dermal abscesses surround sites of degenerating *Lucilia* sp larva.

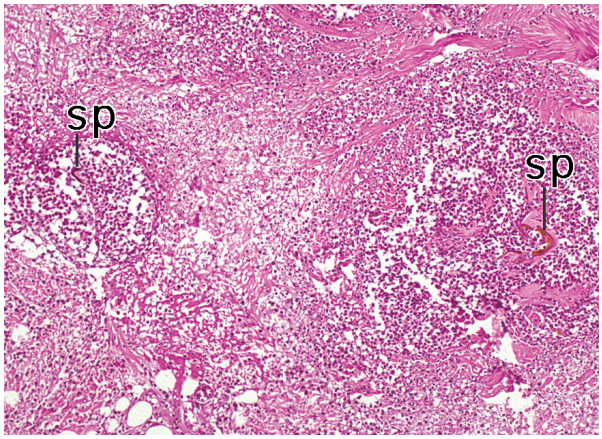



**Figure 18.115**
Two fragments of cuticle and pigmented spines (sp) of *Lucilia* sp larva centered in abscess with eosinophils and necrosis.

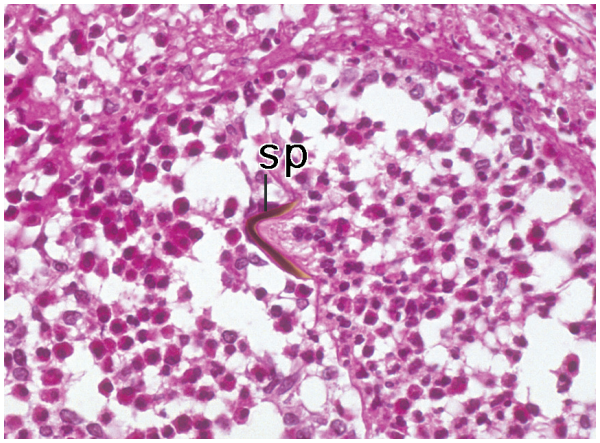



**Figure 18.116**
Pigmented spine (arrow) of *Lucilia* sp larva centered in abscess.

potassium aluminum sulfate) powder applied to skin will help expel the larvae. Local or systemic antibiotics are indicated for significant secondary bacterial infections. Preventive measures for myiasis include effective care of wounds, adequate personal hygiene, and limited exposure to flies.

## References


1. Hall MJR, Screwworm flies as agents of wound myiasis. Online FAO Corporate Document Repository. Website, 1991. Available at: http://www.fao.org/ag/aga/agap/frg/feedback/war/u4220b/u4220b07.htm. Accessed March 2011.
2. Shelton DA, Wright PK, Chaudhry I, Curry A. A persistent scalp nodule caused by the human botfly: exoskeletal larval spines are a key diagnostic feature of myiasis. *Histopathology.* 2009;54:751-752.
3. James MT. The Flies That Cause Myiasis in Man. Washington, DC: United States Government Printing Office; 1947.
4. Baker DJ, Kantor GR, Stierstorfer MB, Brady G. Furuncular myiasis from *Dermatobia hominis* infestation. Diagnosis by light microscopy. *Am J Dermatopathol.* 1995;17:389-394.
5. Bhandari R, Janos DP, Sinnis P. Furuncular myiasis caused by *Dermatobia hominis* in a returning traveler. *Am J Trop Med Hyg.* 2007;76:598-599.
6. Stojanovich CJ, Pratt HD, Bennington EE. Key to Some Full-grown Fly Larvae of Public Health Importance. Atlanta, Ga: Communicable Disease Center; 1962.
7. Curran CH. The human bot fly. In: Neider, C, ed. *The Fabulous Insects.* Manchester, NH: Ayer Pub Co; 1954: 70-79.
8. Goodman RL, Montalvo MA, Reed JB, et al. Photo essay: anterior orbital myiasis caused by human botfly (*Dermatobia hominis*). *Arch Ophthalmol.* 2000;118:1002-1003.
9. Rossi MA, Zucoloto S. Fatal cerebral myiasis caused by the tropical warble fly, *Dermatobia hominis*. *Am J Trop Med Hyg.* 1973;22:267-269.
10. Marco de Lucas E, Díez C, Gutiérrez A, et al. Unusual MRI findings in a patient with history of frontal fracture and skin infestation by fly larvae, as a possible sign of intracerebral myiasis. *Clin Neurol Neurosurg.* 2008;110:725-728.
11. Baird JK, Baird CR, Sabrosky CW. North American cuterebrid myiasis: report of 17 new infections of human beings and review of the disease. *J Am Acad Dermatol.* 1989;21:763-772.
12. Fusco FM, Nardiello S, Brancaccio G, Rossiello R, Gaeta GB. Cutaneous myiasis from *Cordylobia anthropophaga* in a traveller returning from Senegal: a case study. [in Italian]. *Infez Med*. 2005;13:109-111.
13. Tamir J, Haik J, Schwartz E. Myiasis with Lund's fly (*Cordylobia rodhaini*) in travelers. *J Travel Med*. 2003;10:293-295.
14. Mariwalla K, Langhan M, Welch KA, Kaplan DH. Cutaneous myiasis associated with scalp psoriasis. *J Am Acad Dermatol.* 2007;57(suppl 2):S51-52.
15. Trombetta L, Oliva A, Galache V, Bava J, Troncoso A. Cutaneous myiasis due to *Cochliomyia hominivorax* in a drug user. *J Infect Dev Ctries.* 2009;3:873-876.
16. Murray VI, Thompson K. Myiasis in man and other animals in Trinidad and Tobago (1972-73). *Trop Agric.* 1976;53:263-266.
17. Lui PC, Lee MK, Wong JH, et al. Myiasis by *Chrysomya bezziana* in surgical pathology. *Pathology.* 2005;37:80-82.
18. Starr J, Pruett JH, Yunginger JW, Gleich GJ. Myiasis due to *Hypoderma lineatum* infection mimicking the hypereosinophilic syndrome. *Mayo Clin Proc.* 2000;75:755-759.
19. Edwards KM, Meredith TA, Hagler WS, Healy GR. *Ophthalmomyiasis interna* causing visual loss. *Am J Ophthalmol.* 1984;97:605-610.
20. Ahmed MJ, Miller A. Pulmonary coin lesion containing a horse bot, *Gasterophilus*. Report of a case of myiasis. *Am J Clin Pathol.* 1969;52:414-419.
21. Anderson WB. Ophthalmomyiasis. *Am J Ophthalmol.* 1935;18:699-705.
22. Kokcam I, Saki CE. A case of cutaneous myiasis caused by *Wohlfahrtia magnifica*. *J Dermatol*. 2005;32:459-463.
23. Staub HP, Kimmel GC, Berglund EB, Sholler LJ. Cutaneous myiasis due to *Wohlfahrtia vigil*. *Pediatrics.* 1964;34:880-884.
24. Reingold WJ, Robin JB, Leipa D, Kondra L, Schanzlin DJ, Smith RE. *Oestrus ovis* ophthalmomyiasis externa. *Am J Ophthalmol.* 1984;97:7-10.

25. Rastegaev IuM. Myiasis in man caused by larvae of the horse botfly, *Rhinoestrus purpureus Br*.[in Russian]. *Med Parazitol (Mosk).* 1980;49:86-88.

26. Noireau F. Infestation by *Auchmeromyia senegalensis* as a consequence of the adoption of non-nomadic life by Pygmies in the Congo Republic. *Trans R Soc Trop Med Hyg.* 1992;86:329.

27. Seaquist ER, Henry TR, Cheong E, Theologides A. *Phormia regina* myiasis in a malignant wound. *Minn Med.* 1983;66:409-410.

28. Beckendorf R, Klotz SA, Hinkle N, Bartholomew W. Nasal myiasis in an intensive care unit linked to hospital-wide mouse infestation. *Arch Intern Med.* 2002;162:638-640.

29. Saleh MS, el Sibae MM. Urino-genital myiasis due to *Piophila casei*. *J Egypt Soc Parasitol.* 1993;23:737-739.

30. Zumpt F. *Myiasis in Man and Animals in the Old World. A Textbook for Physicians, Veterinarians and Zoologists*. London, England: Butterworth; 1965.

31. Fernandes LF, Pimenta FC, Fernandes FF. First report of human myiasis in Goiás state, Brazil: frequency of different types of myiasis, their various etiological agents, and associated factors. *J Parasitol.* 2009;95:32-38.

32. Perez-Eid C, Mouffok N. Human urinary myiasis caused by *Fannia canicularis* (Diptera, Muscidae) larvae in Algeria [in French]. *Presse Med.* 1999;28:580-581.

33. Shivekar S, Senthil K, Srinivasan R, et al. Intestinal myiasis caused by *Muscina stabulans*. *Indian J Med Microbiol.* 2008;26:83-85.

34. Ferraz AC, Proença B, Gadelha BQ, et al. First record of human myiasis caused by association of the species *Chrysomya megacephala* (Diptera: Callipliorida e), *Sarcophaga (Liopygia) ruficornis* (Diptera: Sarcophagidae), and *Musca domestica* (Diptera: Muscidae). *J Med Entomol.* 2010;47:487-490.

35. Balcioglu IC, Ecemis T, Ayer A, Ozbel Y. Subungual myiasis in a woman with psychiatric disturbance. *Parasitol Int.* 2008;57:509-511.

36. Hira PR, Assad RM, Okasha G, et al. Myiasis in Kuwait: nosocomial infections caused by *Lucilia sericata* and *Megaselia scalaris*. *Am J Trop Med Hyg.* 2004;70:386-389.

37. Boggild AK, Keystone JS, Kain KC. Furuncular myiasis: a simple and rapid method for extraction of intact *Dermatobia hominis* larvae. *Clin Infect Dis.* 2002;35:336-338.

38. Brewer TF, Wilson ME, Gonzalez E, Felsenstein D. Bacon therapy and furuncular myiasis. *JAMA.* 1993;270:2087-2088.

39. Osorio J, Moncada L, Molano A, Valderrama S, Gualtero S, Franco-Paredes C. Role of ivermectin in the treatment of severe orbital myiasis due to *Cochliomyia hominivorax*. *Clin Infect Dis.* 2006;43:e57-59.

40. Clyti E, Nacher M, Merrien L, et al. Myiasis owing to *Dermatobia hominis* in a HIV-infected subject: Treatment by topical ivermectin. *Int J Dermatol.* 2007;46:52-54.

## *Acknowledgements*

**Figure 18.21**
Courtesy of Douglas G. Kahn

**Figure 18.11**
Specimen contributed by Douglas G. Kahn

**Figure 18.22**
Contributed by Kathy Smith

**Figure 18.36**
Specimen contributed by Douglas G. Kahn

**Figure 18.57**
*Arch Dermatol* 1990;126:199-202. ©1990, American Medical Association. All rights reserved

**Figure 18.58**
*Arch Dermatol* 1990;126:199-202. ©1990, American Medical Association. All rights reserved

**Figure 18.59**
*Arch Dermatol* 1990;126:199-202. ©1990, American Medical Association. All rights reserved

**Figure 18.63**
Courtesy of University of Georgia, College of Veterinary Medicine

**Figure 18.64**
Courtesy of University of Georgia, College of Veterinary Medicine

**Figure 18.74**
Courtesy of University of Georgia, College of Veterinary Medicine

**Figure 18.75**
Courtesy of University of Georgia, College of Veterinary Medicine

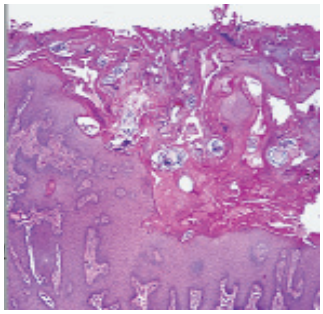
**Figure 18.78**
Courtesy of University of Georgia, College of Veterinary Medicine

**Figure 18.89**
Courtesy of University of Georgia, College of Veterinary Medicine

**Figure 18.102**
National Museum of Health and Medicine #76-12135-2







19

# Scabies and Demodicosis

*J. Kevin Baird, Ellen M. Andersen, Ronald C. Neafie, and Wayne M. Meyers*

## *Introduction*

The only species of mites that are fully adapted to humans are *Sarcoptes scabiei*, *Demodex folliculorum* and *Demodex brevis*: *S. scabiei* causes scabies and the *Demodex* sp cause demodicosis. Because both are dermatological diseases they are described together; however, due to their dissimilarities they are presented as separate topics.

## SCABIES

### Definition

Scabies is a contagious dermatitis of humans and animals caused by the mange mite *Sarcoptes scabiei*.

### Synonyms

Scabies is also known as seven-year itch, camp itch, sarcoptic mange, acariasis, and Norwegian itch.

### General Considerations

Bonomo first identified *S. scabiei* as the etiologic agent of scabies in 1687, making the organism arguably the first recognized microscopic pathogen of humans. Renucci provided the first definitive description of the disease in 1834. Various strains of *S. scabiei*, exhibiting morphologic and physiologic differences, infect a wide range of domestic and wild animals (eg, varieties suis, equi, and canis in swine, horses, and dogs, respectively). Some varieties of *S. scabiei* that usually infect animals can infect humans, but only transitorily.[1] Most *S. scabiei* infections cause only minor irritation which, at worst, may lead to secondary bacterial infection. On the other hand, crusted (Norwegian) scabies can be life-threatening. This anergic form of scabies was first described by Danielssen and Boeck in 1848 in Norwegian leprosy patients. The severity of scabies in immunocompromised patients emphasizes the importance of host immunity in controlling the parasite.

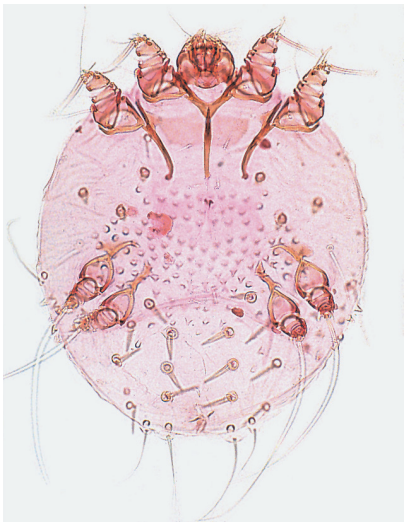


**Figure 19.1**
Ventral view of adult female *Sarcoptes scabiei* showing small head, 4 pairs of legs, and multiple bristles and spines. x135

## Epidemiology

*Sarcoptes scabiei*, a cosmopolitan parasite, is especially prevalent in temperate climates and in regions characterized by poverty, overcrowding and poor hygiene.[2] Humans confined to camps, prisons, and institutions are also at risk of infection.[3-8] Prevalence increases during colder months when bathing and laundering may be less frequent. Epidemics of scabies are often cyclic, perhaps because of fluctuation in immunity. Contact with clothing, bedding, or skin infested with viable mites leads to infection; transmission through sexual contact is incidental. Developing forms of *S. scabiei* spend several days outside of the skin, providing ample opportunity for transmission. The skin of patients with anergic scabies (crusted or Norwegian) harbors enormous numbers of mites and may be the source of epidemic scabies in hospitals or institutions.[9-11]

## Infectious Agent

### Morphologic Description

Female *S. scabiei* are discoid and measure 350 to 450 µm by 250 to 350 µm (Fig 19.1). Males are ovoid and approximately half the size of females. There are 2 anterior pairs of legs and 2 posterior pairs extending from the ventral surface at mid-body. The head, containing mouthparts, extends from the anterior edge of the carapace. The anterior pairs of legs in both sexes end in delicately stalked discs. Each of the posterior legs of the female has a single long bristle. The male has stalked discs on the fourth pair of legs as an aid in mating. The numerous ridges, spines, hairs, and bristles that cover the body surface (especially dorsally), are taxonomically useful.

In tissue sections, adult *S. scabiei* are around 350 µm in greatest dimension. They have a 3 µm thick exoskeleton with transverse striations, spines, and hairs (Fig 19.2). Transverse striations are 3 to 8 µm apart (Fig 19.3). Spines are up to 7 µm wide at the base and 10 µm long, and have pointed ends (Fig 19.3). Hairs are 3 µm wide and vary

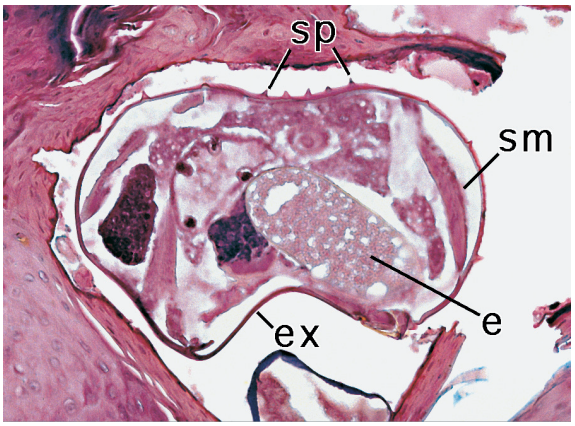



**Figure 19.2**
Adult female *Sarcoptes scabiei* in keratin. Note thin exoskeleton (ex), dorsal spines (sp), striated muscle (sm), and egg (e) measuring 165 by 65 µm. Movat x180

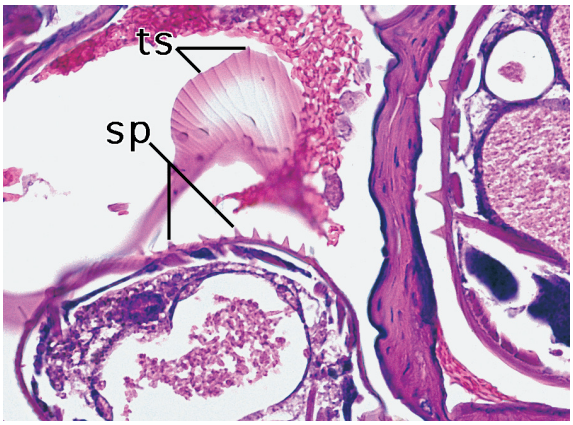



**Figure 19.3**
Section through *Sarcoptes scabiei* depicting dorsal spines (sp) and transverse striations (ts) on exoskeleton. x250




**Figure 19.4**
Section through *Sarcoptes scabiei* demonstrating dorsal spines (sp), hairs (hr), and 2 legs (lg). x260

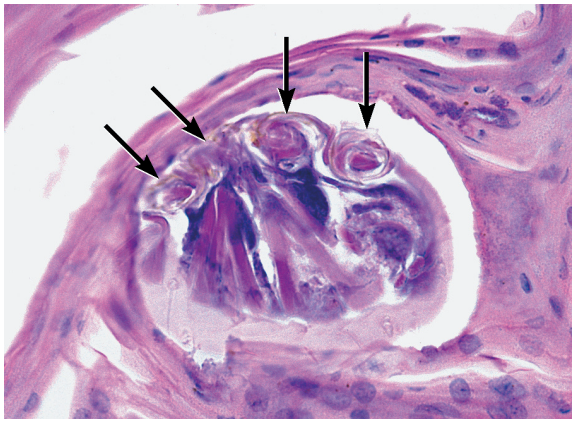


**Figure 19.5**
Section through *Sarcoptes scabiei* showing 4 legs (arrows). x370

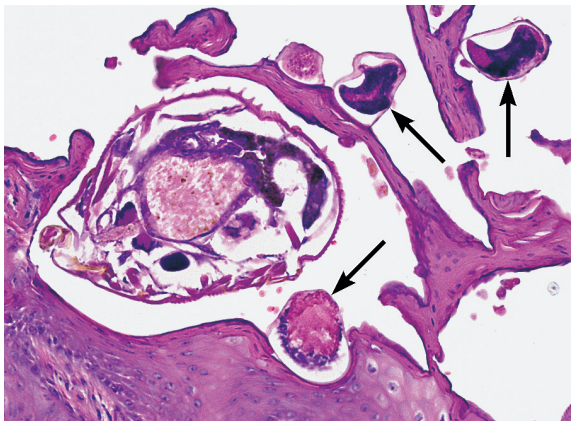


**Figure 19.6**
Section showing adult *Sarcoptes scabiei* and several eggs (arrows) in keratin. x120

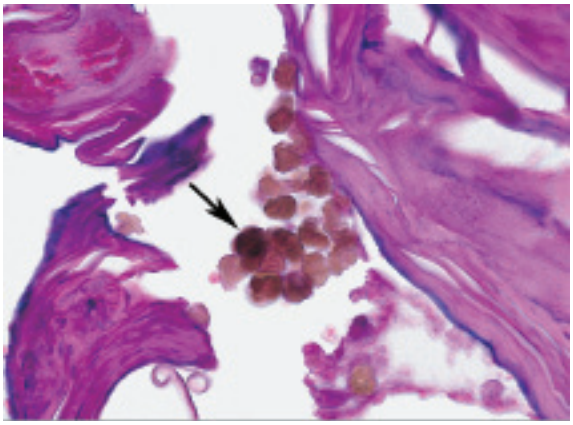


**Figure 19.7**
Brown fecal pellets (arrow) of *Sarcoptes scabiei* free in keratin. x280

in length (Fig 19.4). Spines and hairs are unequally distributed over the body. Like all arthropods, mites have striated muscle (Fig 19.2). Portions of the mite's short stumpy legs are frequently observed in sections (Fig 19.5). Eggs measure up to 150 by 65 µm and have a shell 1 to 2 µm thick. They may be observed in various stages of development within the adult female and free in the keratin where they are deposited (Figs 19.2 and 19.6). Mite fecal pellets may also be found in the keratin (Fig 19.7).

### Life Cycle

All stages of the life cycle of *S. scabiei* can take place in or on skin, where the mites can maintain themselves indefinitely in a single host. Adult *S. scabiei* live primarily in the stratum corneum of human skin, and can burrow at a rate of 0.5 to 5 mm per day. Gravid mites lay 1 or 2 eggs daily for up to 2 months. Six-legged larvae emerge from the eggs in 2 to 3 days and molt 3 times, first into protonymphs, then tritonymphs, and finally into adults. Development from egg to adult takes approximately 2 weeks.

## *Clinical Features and Pathogenesis*

In primary scabies infections, the first symptoms appear approximately 1 month after infection. Infants as young as 30 days may have lesions of scabies.[12] Itching is most intense at night. *Sarcoptes scabiei* prefer lightly keratinized skin with few pilosebaceous units. The sinuous, dirty-reddish burrow of *S. scabiei* is usually up to 3 cm long, with a terminal vesicle harboring the parasite. Burrows usually appear in the folds of hands and wrists, or on nipples, penis, scrotum, and lower buttocks (Figs 19.8 to 19.11). Involvement of the penis is often severe, with papules, nodules, ulcers, and pyoderma (Fig 19.10). Extracts of scabies mites downregulate IL-8 secretion and modulate cytokine secretion of keratinocytes influencing multiple proinflammatory



**Figure 19.8**
Scabies of the hands on a Brazilian adult. There are multiple burrows and papules with a weeping eczematous dermatitis.

factors that favor invasion of the mites into the skin of the host.[13,14]

Most scabies infections involve fewer than 20 adult mites. With adequate personal hygiene, these infections usually self-resolve. Hypersensitivity produces itching, but eventually seems to inhibit proliferation of the mites. Chronic scabies with attendant itching and scratching may lead to secondary bacterial infection causing eczematous dermatitis with pustules and impetigo (Fig 19.8).[15]

Crusted scabies is the uncontrolled proliferation of *S. scabiei* that occurs almost exclusively in immunocompromised patients. Loss of the immune process that ordinarily restricts the parasite allows the mites to proliferate unchecked. Patients typically have lymphadenopathy, eosinophilia, elevated IgE, and diminished IgA.[16] The presence of cytotoxic T-cells and lack of B-cells contribute to uncontrolled growth of scabies mites.[17] Patients present with a psoriasiform dermatitis that includes large hyperkeratotic plaques (Fig 19.12). Frequently, large areas of the skin are involved, markedly stigmatizing the patient. Itching in crusted scabies



**Figure 19.9**
Scabies of the groin. Note multiple short burrows and several mildly inflamed papules.



**Figure 19.10**
Scabies of the glans penis. Note inflamed papules in this lightly keratinized area.



**Figure 19.11**
Scabies over the buttocks of a Brazilian child. Papules are inflamed and secondarily infected.



**Figure 19.12**
Crusted scabies over buttocks, trunk, thighs, elbow, and hand of a 19-year-old Congolese man. Patient was chronically ill, suggesting immuno–suppression. Lesions are papulosquamous and excoriated.

is minimal, but painful fissures can develop in large crusting lesions, and secondary bacterial infection may lead to sepsis.[18] Crusted scabies can also be an opportunistic infection of AIDS or transplant patients.[10,12,19-21] Many closely related *Sarcoptes* sp are found in foodstuffs and house dust, causing dermatitis or allergic reactions in hypersensitive people.

## Pathologic Features

Burrows of *S. scabiei* are usually restricted to the stratum corneum (Fig 19.13). In classic scabies, adult mites are frequently difficult to find in histologic sections. The upper dermal layer below the burrow is edematous and may contain a lymphocytic infiltrate (Fig 19.13). Fecal material and eggs in the burrow (Fig 19.7 ) are often the only clues for the histopathologic diagnosis of scabies. Mite feces may be the major factor stimulating the hypersensitivity and pruritis in scabies. The most remarkable histologic feature of crusted scabies is the vast number of burrows, mites, eggs, and feces in the hyperkeratotic area (Figs 19.14 and 19.15). The epidermis may be spongiotic (Fig 19.16). In the papillary dermis and upper dermis there may be heavy infiltrations of chronic inflammatory cells and moderate numbers of eosinophils. This response may be relatively diminished in patients with AIDS (Fig 19.15). Persistent itching nodules sometimes follow scabies, resembling prurigo nodularis, in which there is a chronic inflammatory response with eosinophils, most prominently around vessels and skin appendages. No parasites are present.

## Diagnosis

Scrapings of skin from affected areas can be treated with 10% potassium hydroxide or mineral oil as clearing agents and examined microscopically for mites. Crusted scabies usually yields mites with a single scraping. In ordinary

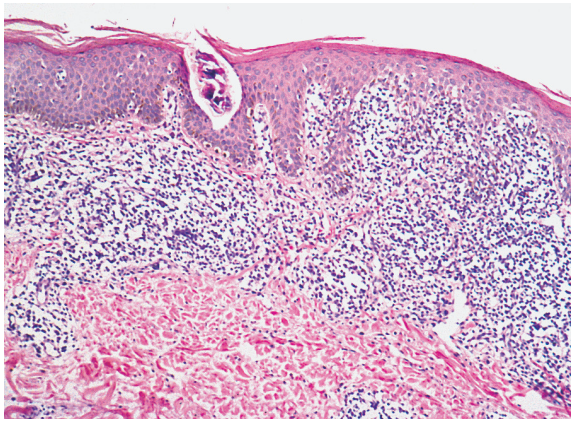


**Figure 19.13**
Classic scabies with single *Sarcoptes scabiei* in stratum corneum. Note chronic inflammation of upper dermis. x70

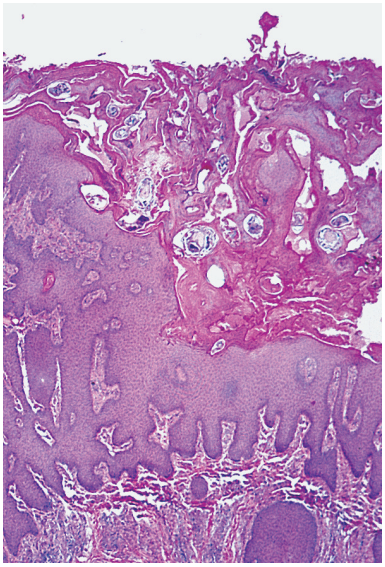


**Figure 19.14**
Section of skin from right buttock of Congolese patient with crusted scabies depicted in Figure 19.12. Note acanthosis, hyperkeratosis, parakeratosis, and many *Sarcoptes scabiei*. x19

scabies, several scrapings may be required to locate the scarce mites. Alternatively, an adult mite can be located and extracted with the aid of a magnifying glass and a needle. The mite will appear as a glistening white speck, often in a vesicle at the terminus of a burrow.

In histologic sections, mites must be differentiated from other parasites that infect the skin. *Sarcoptes scabiei* can be differentiated from *Demodex* sp by anatomic location, morphology, and size. The presence of striated muscle (Fig 19.2) rules out infection by helminths. The absence of a hypodermis rules out dipteran larvae (maggots or bots) and ticks. The presence of cuticular spines and hairs (Fig 19.4) rules out *Tunga penetrans*, the chigoe flea.

## Treatment

Patients with scabies should bathe in hot soapy water before applying any medications. A 5% suspension of permethrin applied topically has been the treatment of choice, but oral ivermectin is increasingly used to treat severe cases of scabies.[10,22-25] Some authorities find benzyl benzoate (25% lotion) preferable.[26,27] Permethrin should not be used in infants under 2 months old or in women who are pregnant or nursing. A 1% lindane (gamma benzene hexachloride) lotion may be used, although there is some concern about lindane's potential toxicity to humans, especially children and pregnant or nursing women.[28,29] Topical applications of 10% crotamiton or bathing in a 5% suspension of flowers of sulfur in lanolin are alternative therapies. Clothing and linens should be washed in very hot water, and other household members should be examined for infection. Control strategies for childhood scabies have been described.[30]

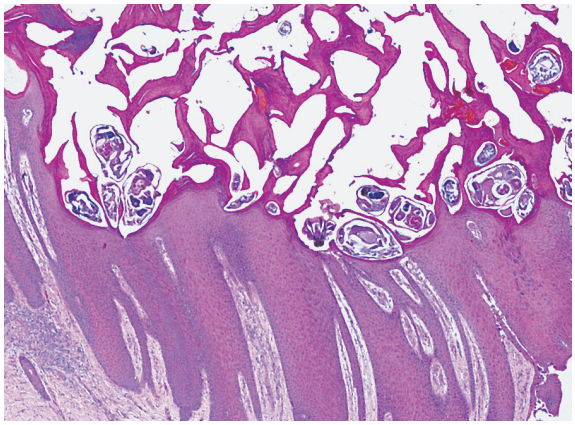


**Figure 19.15**
Section of skin from 40-year-old male AIDS patient from Maryland, demonstrating features of crusted scabies. Note acanthosis and numerous *Sarcoptes scabiei* within burrows of hyperkeratotic horny layer, and mild chronic inflammation of upper dermis. x25

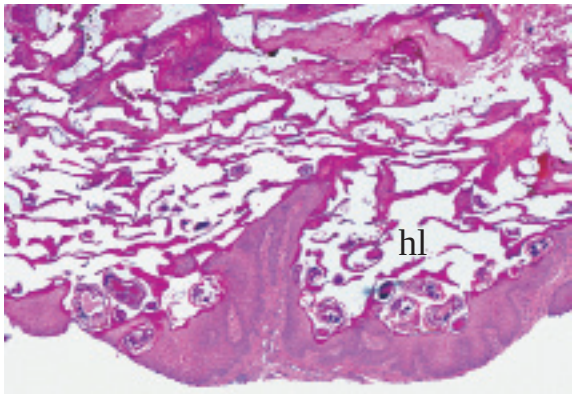



**Figure 19.16**
Biopsy of skin from right shoulder of 81-year-old woman from California who had recently been treated for lymphoma. Section shows features of crusted scabies with numerous burrows containing mites, eggs, and feces in hyperkeratotic layer (hl). x25

# DEMODICOSIS

## Definition

Demodicosis (also called demodicidosis) is a folliculitis caused by *Demodex folliculorum* or *Demodex brevis*, the hair follicle mites.

## Synonyms

Synonyms for demodicosis include acarus folliculorum, demodectic blepharitis, pityriasis folliculorum, and acne rosacea demodes.

## General Considerations

Demodicosis was recognized by Henle and Berger in 1841.[31] Akbulatova reported the involvement of 2 types of *Demodex* in 1963, which were described in 1972 by Desch and Nutting as 2 distinct species, *D. folliculorum* and *D. brevis*.[32]

## *Epidemiology*

*Demodex* sp are found worldwide. In one study,[31] prevalence of the organism in skin biopsies varied with the tissue biopsied (4% from the back to 45% from the temple) and the age of the patient (0% among children under 10 years of age to 35% in patients over 80). Prevalence at autopsy, where multiple sections of numerous specimens were evaluated, was nearly 100%.[33] Men are more often infected than women; infection in young children is rare but has been reported.[34] Status of *Demodex* sp in the pilosebaceous complex may provide a tool in forensic studies.[35]

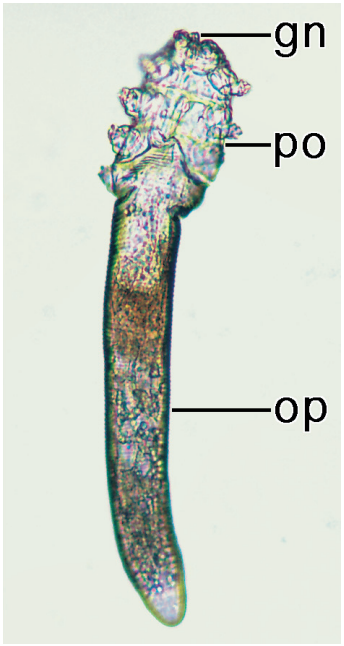



**Figure 19.17**
Adult female *Demodex folliculorum* expressed from human skin. Note 3 body divisions: gnathosoma (gn), podosoma (po), and opisthosoma (op). x50

## *Infectious Agent*

### Morphologic Description

*Demodex folliculorum* and *D. brevis* are obligate parasites that live in hair follicles and sebaceous glands (Figs 19.17 to 19.19). In tissue sections, it is very difficult to identify the species of *Demodex* on the basis of morphology. Adults of both species are tiny, elongate, and vermiform, and have 3 body divisions: gnathosoma, podosoma, and opisthosoma (Fig 19.17). The gnathosoma is the short anterior region that contains the mouthparts. The podosoma, immediately posterior to the gnathosoma, has 4 pairs of short stumpy legs (Figs 19.18 and 19.20). The opisthosoma, the long posterior half of the body, tapers to a rounded end. Its transverse striations give the appearance of segmentation (Fig 19.21). *Demodex* sp have striated muscle and are protected by a 1 µm thick exoskeleton (Fig 19.22).

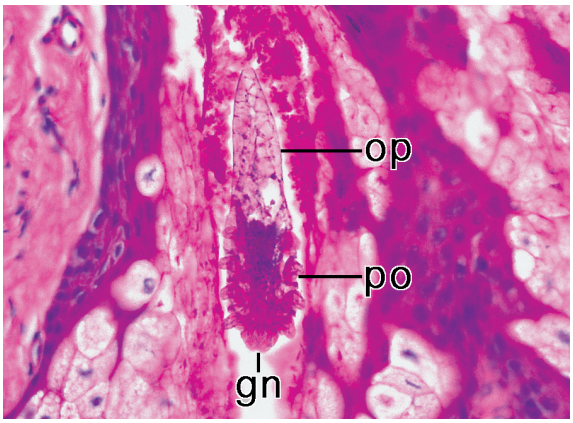



**Figure 19.18**
Section of sebaceous gland through *Demodex* sp in hair follicle. Note short anterior gnathosoma (gn), podosoma with 4 pairs of legs (po), and long posterior opisthosoma (op). x265

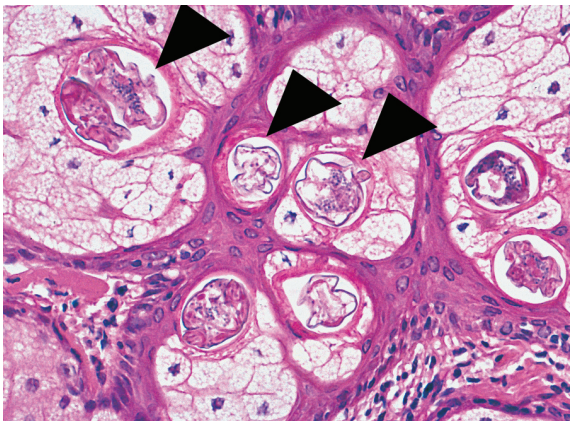


**Figure 19.19**
Several *Demodex* sp (arrow heads) in sebaceous glands. x245

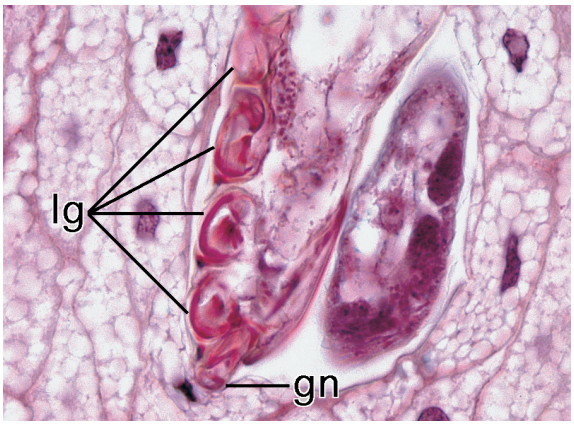



**Figure 19.20**
Section depicting 2 *Demodex* sp in sebaceous gland. Note short gnathosoma (gn) at anterior end and 4 legs (lg) on mite at left. Movat x645

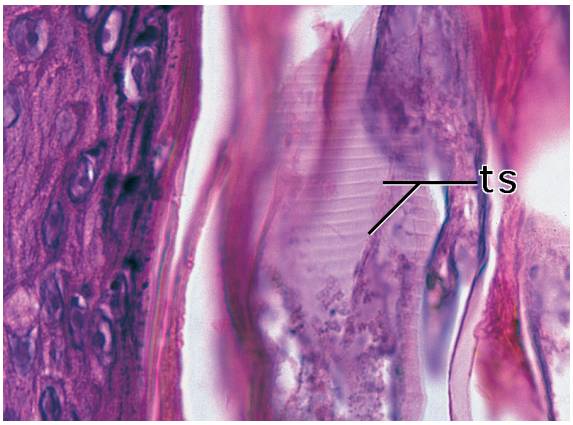



**Figure 19.21**
Transverse striations on long posterior of *Demodex* sp give an appearance of segmentation. x640

Adult female *D. folliculorum* are 294 µm long (average) and 55 µm wide (maximum).[32] Adult males are 280 µm long (average) and 47 µm wide (maximum). *Demodex folliculorum* eggs are arrowhead-shaped and approximately 105 by 42 µm.

Adult female *D. brevis* are 208 µm long (average) and 54 µm wide (maximum).[32] Adult males are 166 µm long (average) and 50 µm wide (maximum). *Demodex brevis* eggs are oval and approximately 60 by 34 µm.

Some species of *Demodex* cause serious disease in animals, resulting in significant economic loss. *Demodex phyllorides*, for example, causes mange in pigs (Figs 19.23 and 19.24).

### Life Cycle

The sequential stages of the life cycle of *Demodex* sp are adult, egg, larva, protonymph, and nymph.[32] The adult stage lasts just a few days, and the entire life cycle is completed in approximately 2 weeks.

## Clinical Features and Pathogenesis

Demodicosis is generally asymptomatic, although many symptomatic cases have been reported.[36,37] *Demodex* sp have been associated with folliculitis,[38] pityriasis rosacea, blepharitis, and seborrheic dermatitis. Many authorities consider these associations to be incidental; however, there is growing agreement that demodicosis is a disease that can complicate or cause all of these lesions. Topical steriods may promote lesions related to *Demodex* sp.[39] Immunosuppressed patients may develop extensive cutaneous demodicosis.[40]

## Pathologic Features

*Demodex* sp may provoke perifollicular inflammation.[31,38]

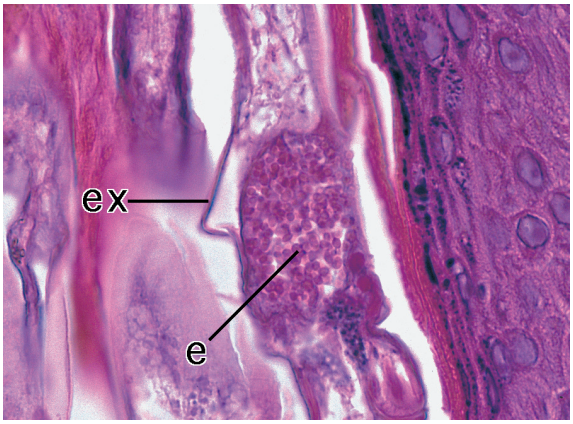



**Figure 19.22**
Section of *Demodex* sp in hair follicle demonstrating thin exoskeleton (ex) and developing egg (e). x640

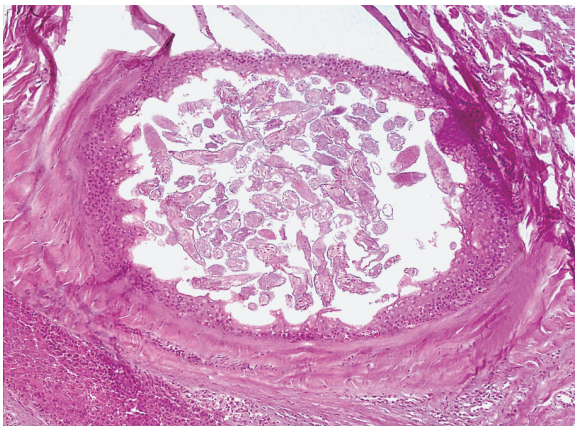


**Figure 19.23**
Massive infestation of pig's ear by *Demodex phyllorides*. Numerous mites are observed at this level. x60




**Figure 19.24**
Higher magnification of *Demodex phyllorides* pictured in Figure 19.17, illustrating anteriormost pair of legs (lg) and short gnathosoma (gn) with mouthparts. x585

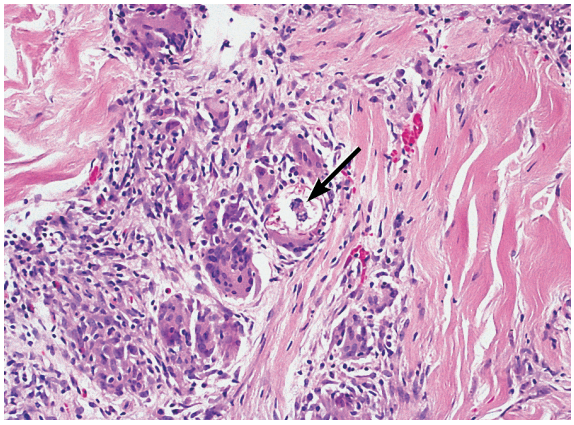


**Figure 19.26**
Section of skin from patient with *Demodex* sp (arrow) in granulomatous lesion outside of follicles. x125

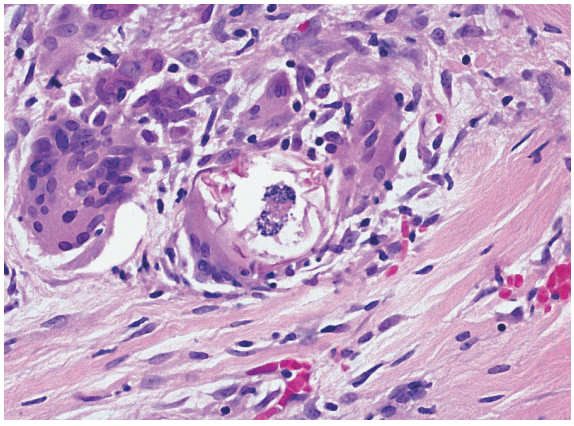


**Figure 19.27**
Higher magnification of Figure 19.27 showing *Demodex* sp engulfed by giant cell. x270

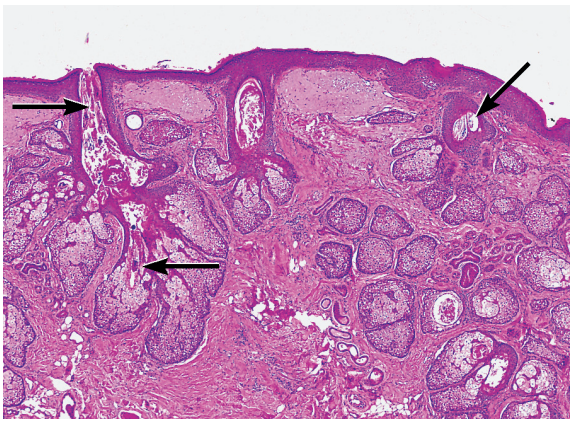


**Figure 19.25**
Section of skin showing *Demodex* sp (arrows) in pilosebaceous unit. x25

The follicular epithelium is spongiotic. *Demodex* sp are usually in the pilosebaceous units (Fig 19.25); *Demodex folliculorum* usually inhabits the follicle and *D. brevis* the sebaceous glands. However, either or both may be found in the follicle or the sebaceous gland. In one study, almost a third of the follicles examined was surrounded and occasionally breached by lymphocytes and histiocytes.[31] Sometimes there are granulomatous reactions around pilosebaceous units in specimens containing *Demodex* sp, especially the more heavily infected units. Occasionally, *Demodex* sp are found in granulomas outside of follicles (Figs 19.26 and 19.27). We believe this is strong evidence that *Demodex* sp are pathogens and cause the disease entity demodicosis.

## Diagnosis

Scrapings of skin from affected areas can be treated with 10% potassium hydroxide or mineral oil as clearing agents and examined microscopically for mites. Demodecid mites are found in hair follicles (Fig 19.18), and can be expressed in contents of the follicles. Microscopic analysis of standardized skin biopsy specimens offers a quantitative evaluation.[41-42]

In histologic sections, mites must be differentiated from other parasites that infect the skin. *Demodex* sp can be differentiated from *S. scabiei* by anatomic location, morphology, and size. The presence of striated muscle rules out infection by helminths. The absence of a hypodermis rules out dipteran larvae (maggots or bots) and ticks.

## Treatment

Patients with demodicosis should bathe in hot soapy water before applying any medications. An ophthalmologist observing *Demodex* sp in the eyelid can remove the mite mechanically or by using tea tree oil scrubs.[42,43]

## References


1. Fain A. Study of the variability of *Sarcoptes scabiei* with a review of the Sarcoptidae [in French]. *Acta Zool Pathol Antverp*. 1968;47:1-196.
2. Holt DC, McCarthy JS, Carapetis JR. Parasitic diseases of remote indigenous communities in Australia. *Int J Parasitol*. 2010;40:1119-1126.
3. Holness DL, DeKoven JG, Nethercott JR. Scabies in chronic health care institutions. *Arch Dermatol*. 1992;128:1257-1260.
4. Marshall R, Barkess-Jones L, Sivayoham S. An outbreak of scabies in a school for children with learning disabilities. *Commun Dis Rep CDR Rev.* 1995;5:R90-R92.
5. Parish LC, Witkowski JA, Millikan LE. Scabies in the extended care facility. *Int J Dermatol*. 1991;30:703-706.
6. Utsumi M, Makimoto K, Quroshi N, Ashida N. Types of infectious outbreaks and their impact in elderly care facilities: a review of the literature. *Age Ageing*. 2010;39:299-305.
7. Raza N, Qadir SN, Agha H. Risk factors for scabies among male soldiers in Pakistan: case-control study. *East Mediterr Health J*. 2009;15:1105-1110.
8. Alsamarai AM. Frequency of scabies in Iraq: survey in a dermatology clinic. *J Infect Dev Ctries.* 2009;3:789-793.
9. Fain A. Epidemiological problems of scabies. *Int J Dermatol*. 1978;17:20-30.
10. Guggisberg D, de Viragh PA, Constantin C, Panizzon RG. Norwegian scabies in a patient with acquired immunodeficiency syndrome. *Dermatology*. 1998;197:306-308.
11. Portu JJ, Santamaria JM, Zuberto Z, et al. Atypical scabies in HIV-positive patients. *J Am Acad Dermatol.* 1996;34:915-917.
12. Guerci S, Cappellaro E, Contratti M, et al. [A sign of the changing times: neonatal scabies.]. *Minerva Pediatr.* 2010;62:329-332.
13. Mullins JS, Arlian LG, Morgan MS. Extracts of *Sarcoptes scabiei* De Geer downmodulate secretion of IL-8 by skin keratinocytes and fibroblasts and of GM-CSF by fibroblasts in the presence of proinflammatory cytokines. *J Med Entomol.* 2009;46:845-851.
14. Elder BL, Arlian LG, Morgan MS. Modulation of human dermal microvascular endothelial cells by Sarcoptes scabiei in combination with proinflammatory cytokines, histamine, and lipid-derived biologic mediators. *Cytokine*. 2009; 47:103-111.
15. Steer AC, Jenney AW, Kado J, et al. High burden of impetigo and scabies in a tropical country. *PLoS Negl Trop Dis.* 2009;3:e467.
16. Hancock BW, Ward AM. Serum immunoglobulin in scabies. *J Invest Dermatol.* 1974;63:482-484.
17. Walton SF, Beroukas D, Roberts-Thomson P, Currie BJ. New insights into disease pathogenesis in crusted (Norwegian) scabies: the skin immune response in crusted scabies. *Br J Dermatol*. 2008;158:1247-1255.
18. Glover A, Young L, Goltz AW. Norwegian scabies in acquired immunodeficiency syndrome: report of a case resulting in death from associated sepsis. *J Am Acad Dermatol.* 1987;16:396-399.
19. Magee KL, Hebert AA, Rapini RP. Crusted scabies in a patient with chronic graft-versus-host disease. *J Am Acad Dermatol*. 1991;25:889-891.
20. Moss VA, Salisbury J. Scabies in an AIDS hospice unit. *Br J Clin Pract.* 1991;45:35-36.
21. Van de Welde K, Spach DH, Turbyfill D, Aboulafia DM. AIDS-associated Norwegian scabies. *AIDS Reader*. 1994;May/June:88-96.
22. Dourmishev AL, Serafimova DK, Dourmishev LA, Mualla MA, Papaharalambous V, Malchevsky T. Crusted scabies of the scalp in dermatomyositis patients: three cases treated with oral ivermectin. *Int J Dermatol*. 1998;37:231-234.
23. Huffam SE, Currie BJ. Ivermectin for *Sarcoptes scabiei* hyperinfestation. *Int J Infect Dis.* 1998;2:152-154.
24. Orkin M, Maibach HI. Scabies and pediculosis. In: Freedberg IM, Eisen AZ, Wolff K, et al, eds. *Fitzpatrick's Dermatology in General Medicine*. Vol 2. 5th ed. New York, NY: McGraw-Hill; 1999:2677-2684.
25. Yeruham I, Hadani A. Control of human scabies by topical application of ivermectin. *Ann Trop Med Parasitol*. 1998;92:627-629.
26. Bachewar NP, Thawani VR, Mali SN, Gharpure KJ, Shingade VP, Dakhale GN. Comparison of safety, efficacy, and cost effectiveness of benzyl benzoate, permethrin, and ivermectin in patients of scabies. *Indian J Pharmacol.* 2009;41:9-14.
27. Ly F, Caumes E, Ndaw CA, Ndiaye B, Mahe A. Ivermectin versus benzyl benzoate applied once or twice to treat human scabies in Dakar, Senegal: a randomized controlled trial. *Bull World Health Organ.* 2009;87:424-430.
28. Franz TJ, Lehman PA, Franz SF, Guin JD. Comparative percutaneous absorption of lindane and permethrin. Arch Dermatol. 1996;132:901-905.
29. Meinking TL, Taplin D. Safety of permethrin vs lindane for the treatment of scabies. Arch Dermatol. 1996;132:959-962.
30. Gilmore SJ. Control strategies for endemic childhood scabies. *PLoS One*. 2011;6:e15990.
31. Aylesworth R, Vance JC. *Demodex folliculorum* and *Demodex brevis* incutaneous biopsies. *J Am Acad Dermatol*. 1982;7:583-589.
32. Desch C, Nutting WB. *Demodex folliculorum* (Simon) and *D. brevis akbulatova* of man: redescription and reevaluation. *J Parasitol*. 1972;58:169-177.
33. Rufli T, Mumcuoglu Y. The hair follicle mites *Demodex folliculorum* and *Demodex brevis*: biology and medical importance. A review. *Dermatologica*. 1981;162:1-11.
34. Patrizi A, Neri I, Chieregato C, Misciali M. Demodicidosis in immunocompetent young children: report of eight cases. *Dermatology*. 1997;195:239-242.
35. Desch CE. Human hair follicle mites and forensic acarology. *Exp Appl Acarol*. 2009; 49:143-146.
36. Nutting WB. Pathogenesis associated with hair follicle mites (Acari: Demodicidae). Acarologia. 1976;17:493-507.
37. Pallotta S, Cianchini G, Martelloni E, et al. Unilateral demodicidosis. *Eur J Dermatol.* 1998;8:191-192.
38. Vollmer RT. Demodex-associated folliculitis. *Am J Dermatopathol*. 1996;18:589-591.
39. Karincaoglu Y, Tepe B, Kalayci B, Seyhan M. Is *Demodex folliculorum* an aetiological factor in seborrheic dermatitis? *Clin Exp Dermatol.* 2009;34:e516-520.
40. Damian D, Rogers M. Demodex infestation in a child with leukaemia: treatment with ivermectin and permethrin. *Int J Dermatol.* 2003;42:724-726.
41. Askin U, Seckin D. Comparison of the two techniques for measurement of the density of *Demodex folliculorum*: standardized skin surface biopsy and direct microscopic examination. *Br J Dermatol.* 2010;162:1124-1126.
42. Kojima T, Ishida R, Sato EA, et al. In vivo evaluation of ocular demodicosis using laser scanning confocal microscopy. *Invest Ophthalmol Vis Sci.* 2011;52:565-569.
43. Liang L, Safran S, Gao Y, Sheha H, Raju VK, Tseng SC. Ocular demodicosis as a potential cause of pediatric blepharoconjunctivitis. *Cornea*. 2010;29:1386-1391.


## Acknowledgements


**Figure 19.12**
Contributed by AD Askew

**Figure 19.17**
Contributed by LR Ash